

RITA M RAPP

510 pgs  
17 foldouts  
MSC-PA-R-69-2

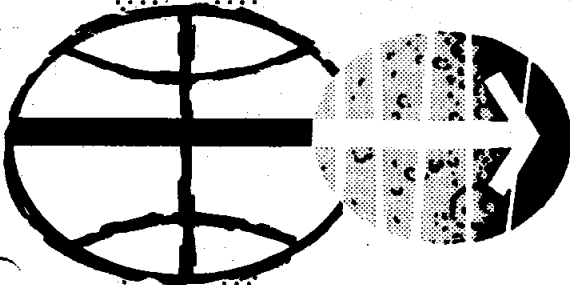


NATIONAL AERONAUTICS AND SPACE ADMINISTRATION

APOLLO 9 MISSION REPORT

DISTRIBUTION AND REFERENCING

This paper is not suitable for general distribution or referencing. It may be referenced only in other working correspondence and documents by participating organizations.



MANNED SPACECRAFT CENTER

HOUSTON, TEXAS

MAY 1969

APOLLO SPACECRAFT FLIGHT HISTORY

<u>Mission</u>	<u>Spacecraft</u>	<u>Description</u>	<u>Launch date</u>	<u>Launch site</u>
PA-1	BP-6	First pad abort	Nov. 7, 1963	White Sands Missile Range, N. Mex.
A-001	BP-12	Transonic abort	May 13, 1964	White Sands Missile Range, N. Mex.
AS-101	BP-13	Nominal launch and exit environment	May 28, 1964	Cape Kennedy, Fla.
AS-102	BP-15	Nominal launch and exit environment	Sept. 18, 1964	Cape Kennedy, Fla.
A-002	BP-23	Maximum dynamic pressure abort	Dec. 8, 1964	White Sands Missile Range, N. Mex.
AS-103	BP-16	Micrometeoroid experiment	Feb. 16, 1965	Cape Kennedy, Fla.
A-003	BP-22	Low-altitude abort (planned high- altitude abort)	May 19, 1965	White Sands Missile Range, N. Mex.
AS-104	BP-26	Micrometeoroid experiment and service module RCS launch environment	May 25, 1965	Cape Kennedy, Fla.
PA-2	BP-23A	Second pad abort	June 29, 1965	White Sands Missile Range, N. Mex.
AS-105	BP-9A	Micrometeoroid experiment and service module RCS launch environment	July 30, 1965	Cape Kennedy, Fla.
A-004	SC-002	Power-on tumbling boundary abort	Jan. 20, 1966	White Sands Missile Range, N. Mex.
AS-201	SC-009	Supercircular entry with high heat rate	Feb. 26, 1966	Cape Kennedy, Fla.
AS-202	SC-011	Supercircular entry with high heat load	Aug. 25, 1966	Cape Kennedy, Fla.

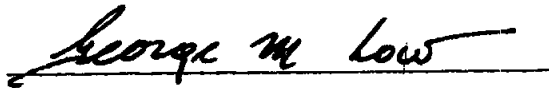
(Continued inside back cover)

APOLLO 9 MISSION REPORT

PREPARED BY

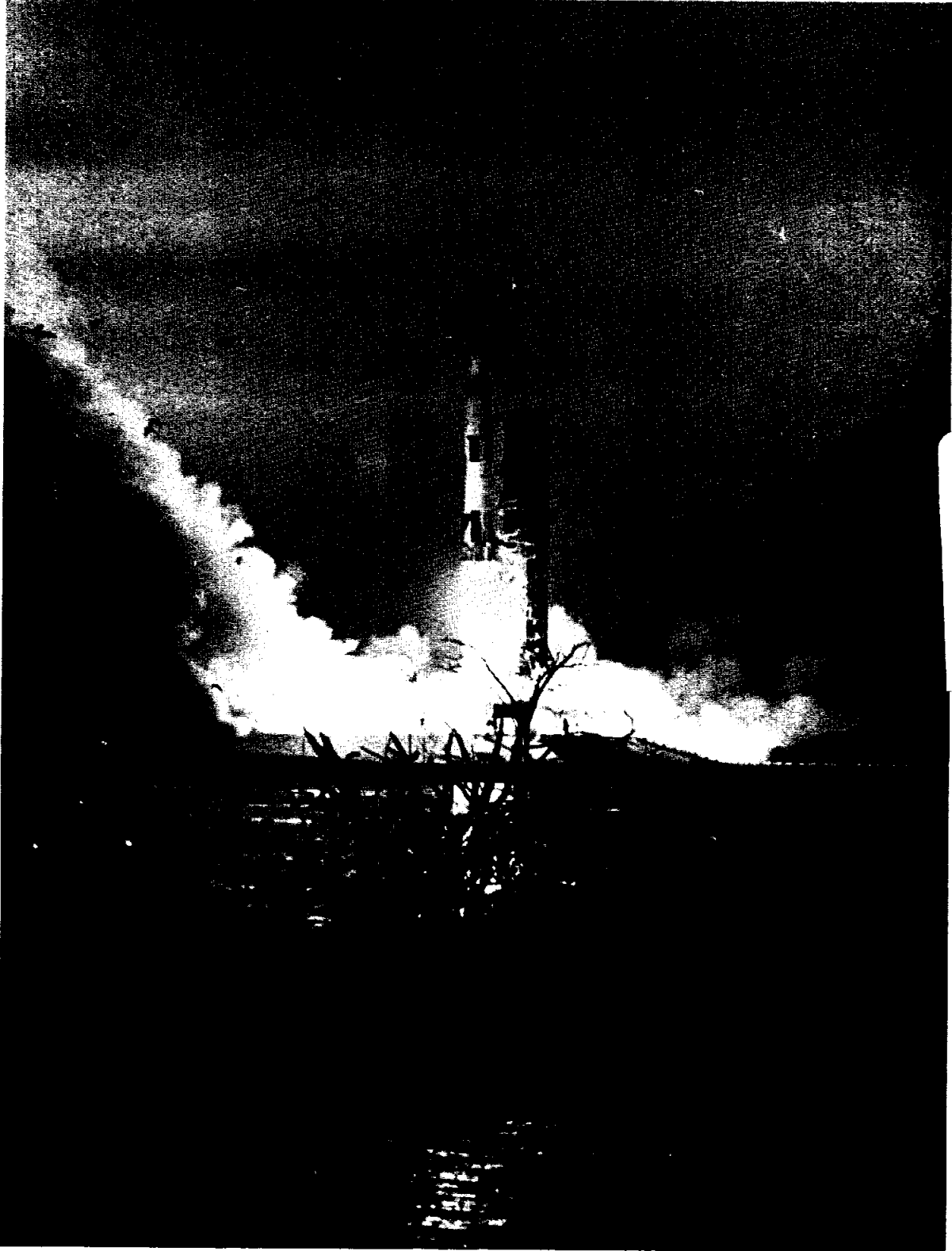
Mission Evaluation Team

APPROVED BY

A handwritten signature in black ink that reads "George M. Low". The signature is written in a cursive style and is positioned above a solid horizontal line.

George M. Low  
Manager, Apollo Spacecraft Program

NATIONAL AERONAUTICS AND SPACE ADMINISTRATION  
MANNED SPACECRAFT CENTER  
HOUSTON, TEXAS  
May 1969



RITA M RAPP

Apollo 9 lift-off.

## CONTENTS

Section		Page
1.0	<u>SUMMARY</u> . . . . .	1-1
2.0	<u>INTRODUCTION</u> . . . . .	2-1
3.0	<u>MISSION DESCRIPTION</u> . . . . .	3-1
4.0	<u>EXTRAVEHICULAR ACTIVITY</u> . . . . .	4-1
4.1	FLIGHT PLAN . . . . .	4-1
4.2	ACTUAL TIMELINE . . . . .	4-2
4.3	FLIGHT CREW ACTIVITIES . . . . .	4-2
4.4	EXTRAVEHICULAR MOBILITY UNIT . . . . .	4-5
4.5	SPACECRAFT INTERFACES . . . . .	4-7
5.0	<u>RENDEZVOUS AND DOCKING OPERATIONS</u> . . . . .	5-1
5.1	MISSION PLANNING ASPECTS . . . . .	5-2
5.2	TRAJECTORY DETERMINATION . . . . .	5-4
5.3	CREW PROCEDURES . . . . .	5-7
5.4	GUIDANCE, NAVIGATION, AND CONTROL . . . . .	5-15
5.5	VISIBILITY . . . . .	5-16
5.6	DOCKING OPERATIONS . . . . .	5-16
5.7	GROUND SUPPORT OPERATIONS . . . . .	5-17
6.0	<u>COMMUNICATIONS</u> . . . . .	6-1
7.0	<u>TRAJECTORY</u> . . . . .	7-1
7.1	LAUNCH PHASE . . . . .	7-1
7.2	SPACECRAFT/S-IVB SEPARATION . . . . .	7-1
7.3	ORBITAL FIRINGS . . . . .	7-2
7.4	ENTRY . . . . .	7-4
7.5	TRACKING ANALYSIS . . . . .	7-5
8.0	<u>COMMAND AND SERVICE MODULE PERFORMANCE</u> . . . . .	8-1
8.1	STRUCTURAL AND MECHANICAL . . . . .	8-1
8.2	ELECTRICAL POWER . . . . .	8-13
8.3	CRYOGENIC STORAGE . . . . .	8-18
8.4	COMMUNICATIONS EQUIPMENT . . . . .	8-18

Section		Page
8.5	INSTRUMENTATION . . . . .	8-20
8.6	GUIDANCE, NAVIGATION, AND CONTROL . . . . .	8-22
8.7	REACTION CONTROL SYSTEMS . . . . .	8-76
8.8	SERVICE PROPULSION . . . . .	8-83
8.9	ENVIRONMENTAL CONTROL SYSTEM . . . . .	8-88
8.10	CREW STATION . . . . .	8-92
8.11	CONSUMABLES . . . . .	8-95
9.0	<u>LUNAR MODULE PERFORMANCE</u> . . . . .	9-1
9.1	STRUCTURAL AND MECHANICAL SYSTEMS . . . . .	9-1
9.2	THERMAL CONTROL . . . . .	9-6
9.3	ELECTRICAL POWER . . . . .	9-7
9.4	COMMUNICATIONS . . . . .	9-8
9.5	INSTRUMENTATION . . . . .	9-22
9.6	GUIDANCE AND CONTROL . . . . .	9-24
9.7	REACTION CONTROL SYSTEM . . . . .	9-50
9.8	DESCENT PROPULSION . . . . .	9-60
9.9	ASCENT PROPULSION . . . . .	9-69
9.10	ENVIRONMENTAL CONTROL SYSTEM . . . . .	9-77
9.11	CREW STATIONS . . . . .	9-88
9.12	RADAR . . . . .	9-89
9.13	CONSUMABLES . . . . .	9-90
10.0	<u>FLIGHT CREW</u> . . . . .	10-1
10.1	FLIGHT CREW PERFORMANCE SUMMARY . . . . .	10-1
10.2	PILOTS' REPORT . . . . .	10-2
11.0	<u>BIOMEDICAL EVALUATION</u> . . . . .	11-1
11.1	BIOINSTRUMENTATION PERFORMANCE . . . . .	11-1
11.2	PHYSIOLOGICAL DATA . . . . .	11-2
11.3	MEDICAL OBSERVATIONS . . . . .	11-2
11.4	PHYSICAL EXAMINATIONS . . . . .	11-7

Section	Page
12.0	<u>FOOD AND WATER</u> . . . . . 12-1
	12.2 WATER . . . . . 12-4
13.0	<u>PHOTOGRAPHY</u> . . . . . 13-1
	13.1 OPERATIONAL PHOTOGRAPHY . . . . . 13-1
	13.2 MULTISPECTRAL TERRAIN EXPERIMENT . . . . . 13-2
14.0	<u>MISSION SUPPORT PERFORMANCE</u> . . . . . 14-1
	14.1 FLIGHT CONTROL . . . . . 14-1
	14.2 NETWORK PERFORMANCE . . . . . 14-6
	14.3 RECOVERY OPERATIONS . . . . . 14-8
15.0	<u>ASSESSMENT OF MISSION OBJECTIVES</u> . . . . . 15-1
	15.1 LUNAR MODULE S-BAND COMMUNICATIONS PERFORMANCE . . 15-1
	15.2 SPACECRAFT/NETWORK S-BAND/VHF COMPATIBILITY . . . 15-2
	15.3 EXTRAVEHICULAR ACTIVITY . . . . . 15-2
16.0	<u>LAUNCH VEHICLE SUMMARY</u> . . . . . 16-1
17.0	<u>ANOMALY SUMMARY</u> . . . . . 17-1
	17.1 COMMAND AND SERVICE MODULES . . . . . 17-1
	17.2 LUNAR MODULE . . . . . 17-27
	17.3 GOVERNMENT-FURNISHED EQUIPMENT . . . . . 17-57
18.0	<u>CONCLUSIONS</u> . . . . . 18-1
APPENDIX A - <u>VEHICLE DESCRIPTIONS</u> . . . . . A-1	
	A.1 COMMAND AND SERVICE MODULES . . . . . A-1
	A.2 LUNAR MODULE . . . . . A-12
	A.3 SPACECRAFT/LAUNCH-VEHICLE ADAPTER . . . . . A-58
	A.4 LAUNCH VEHICLE DESCRIPTION . . . . . A-59
	A.5 MASS PROPERTIES . . . . . A-60
APPENDIX B - <u>SPACECRAFT HISTORIES</u> . . . . . B-1	
APPENDIX C - <u>POSTFLIGHT TESTING</u> . . . . . C-1	
APPENDIX D - <u>DATA AVAILABILITY</u> . . . . . D-1	
APPENDIX E - <u>SUPPLEMENTAL REPORTS</u> . . . . . E-1	

## 1.0 SUMMARY

Apollo 9 was the first manned flight of the lunar module and was conducted to qualify this portion of the spacecraft for lunar operations. The crew members were James A. McDivitt, Commander; David R. Scott, Command Module Pilot; and Russell L. Schweikart, Lunar Module Pilot.

The primary objectives of the mission were to evaluate crew operation of the lunar module and to demonstrate docked vehicle functions in an earth orbital mission, thereby qualifying the combined spacecraft for lunar flight. Lunar module operations included a descent engine firing while docked with the command module, a complete rendezvous and docking profile, and, with the vehicle unmanned, an ascent engine firing to proppellant depletion. Combined spacecraft functions included command module docking with the lunar module (after transposition), spacecraft ejection from the launch vehicle, five service propulsion firings while docked, a docked descent engine firing, and extravehicular crew operations from both the lunar and command modules. These primary objectives were all satisfied.

All spacecraft systems operated satisfactorily in performing the mission as planned. The thermal response of both spacecraft remained within expected ranges for an earth orbital flight, and consumable usages were maintained within acceptable limits. Management of the many complex systems of both spacecraft by the crew was very effective, and communications quality was generally satisfactory.

The space vehicle was launched from the Kennedy Space Center, Florida, at 11:00:00 a.m. e.s.t., on March 3, 1969. Following a normal launch phase, the S-IVB stage inserted the spacecraft into an orbit of 102.3 by 103.9 nautical miles. After the post-insertion checkout was completed, the command and service modules were separated from the S-IVB, transposed, and docked with the lunar module. The docked spacecraft were ejected from the S-IVB at 4:08:06.

One firing of the descent engine and five service propulsion firings were performed while the spacecraft were in the docked configuration. The dynamics and stability of the spacecraft during these firings was excellent. Stroking tests (engine gimbaling) were also performed during the second and third firings to further evaluate the docked vehicle dynamics and the docking interfaces of the two spacecraft. These tests showed the dynamics and interfaces to be very satisfactory with responses to the stroking inputs being lower than predicted.

At approximately 70 hours, the Commander and Lunar Module Pilot entered the lunar module and began preparations for extravehicular activity. Both spacecraft were depressurized and their respective hatches opened at

approximately 73 hours. The Lunar Module Pilot egressed and evaluated the handrails, obtained many excellent and valuable engineering photographs, and retrieved the thermal sample from the exterior of the lunar module. Also, the Command Module Pilot moved his upper torso outside the command module side hatch and retrieved three thermal samples from the exterior of the service module. The extravehicular activity lasted 47-minutes and was abbreviated from the planned 2-hour 15-minute operation because of the inflight illness of the Lunar Module Pilot during the previous day. The performance of all of the extravehicular mobility unit systems was excellent throughout the operation.

The two crewmen again transferred to the lunar module at about 89 hours to perform a lunar-module-active rendezvous. The lunar module primary guidance system was used throughout the rendezvous; however, mirror-image back-up maneuver computations were also made in the command module. The descent propulsion system was used to perform the phasing and insertion maneuvers, and the ascent engine was used to establish a constant differential height after the coelliptic sequence had been initiated. The terminal phase was nominal, and lunar module docking was completed at approximately 99 hours. The rendezvous and docking were completed satisfactorily, and propellant usage by the lunar module reaction control system was about 30 percent less than predicted. The ascent stage was jettisoned about 2.5 hours later, and a 362.3-second firing of the ascent engine to oxidizer depletion was performed.

The final 5 days of the mission were spent in completing the photography experiment, performing three service propulsion firings, plus performing numerous landmark tracking exercises. The sixth service propulsion firing was made to lower the apogee. It was delayed one revolution because the translation maneuver that was to precede the firing was not properly configured in the autopilot. After properly configuring the autopilot, the firing was successfully completed at about 123.5 hours. The seventh service propulsion firing was made to raise the apogee, and the firing time was increased to a nominal 25 seconds to permit an evaluation of the propellant quantity and gaging system, which had exhibited anomalous behavior during earlier service propulsion firings. A total of 584 frames of film were exposed for the multispectral photography experiment during this period.

As a result of unfavorable weather in the planned landing area, the deorbit maneuver was delayed for one revolution to accommodate repositioning of the landing point. As determined from the onboard computer solution, the spacecraft landed within 2.7 nautical miles of the target point at 241 hours 54 seconds.

## 2.0 INTRODUCTION

The Apollo 9 mission was the ninth in a series of flights using specification Apollo hardware and the first manned flight of the lunar module. This mission was the third manned flight of block II command and service modules and the second manned flight using a Saturn V launch vehicle.

Because of the excellent performance of the command and service modules during the Apollo 7 and 8 missions, only the command and service module performance that significantly differed from that of the previous two missions will be reported. This report concentrates on lunar module flight results and those activities involving combined vehicle operations. Numerous systems in both vehicles were involved in the extravehicular activity, lunar module rendezvous, and communications, and these subjects are reported separately in sections 4, 5, and 6, respectively.

A complete analysis of certain flight data is not possible within the time frame for preparation of this report. Therefore, report supplements will be published for the guidance, navigation, and control system performance; the biomedical evaluation; the multispectral terrain photography; and the trajectory analysis. Other supplements will be published as necessary. A list of all supplements is contained in Appendix E.

In this report all times are elapsed time from range zero, established as the integral second before lift-off. Range zero for this mission was 16:00:00 G.m.t., March 3, 1969. Also, all references to mileage distance are in nautical miles.

### 3.0 MISSION DESCRIPTION

The Apollo 9 mission was a 10-day flight to qualify the lunar module and to demonstrate certain combined spacecraft functions for manned lunar flight. The primary flight objectives were to verify the ability of the lunar module and the spacecraft/launch-vehicle adapter to sustain Saturn V launch loads, to complete docked and undocked propulsion maneuvers, to perform a lunar-module-active rendezvous with the command module, to demonstrate extravehicular activity from both spacecraft, and to operate lunar module systems in earth orbit for periods of time comparable to the lunar mission profile. To meet these objectives and to operate within the constraints of necessary crew activity, station coverage, trajectory, and consumables, the lunar module was evaluated during three separate periods of manning, which required multiple activation and deactivation of systems, a situation unique to this mission. The flight plan actually followed (fig. 3-1) is very close to that established prior to flight, and the few deviations from this plan are discussed in the following paragraphs.

The space vehicle was launched at 11:00:00 a.m. e.s.t., March 3, 1969, and the insertion orbit was 102.3 by 103.9 miles. After post-insertion checkout, the command and service modules were separated from the S-IVB, transposed, and docked with the lunar module. At about 4 hours, an ejection mechanism, used for the first time on this mission, ejected the docked spacecraft from the S-IVB. After a separation maneuver, the S-IVB engine was fired twice, with the final maneuver placing the spent stage into a solar orbit. At about 6 hours, the first docked service propulsion maneuver was performed and lasted 5 seconds.

Crew activity on the second day was devoted to systems checks and three docked service propulsion maneuvers, made at approximately 22, 25, and 28.5 hours. The firing durations for these maneuvers were 110, 280, 28 seconds, respectively.

On the third day, the Commander and Lunar Module Pilot initially entered the lunar module to activate and check out the systems and to perform the docked descent engine firing. This maneuver was conducted at 50 hours and lasted 372 seconds. Both digital-autopilot attitude control and manual throttling of the descent engine to full thrust were demonstrated. After the two crewmen returned to the command module, preparations were made for the fifth docked service propulsion maneuver, conducted at approximately 54.5 hours to circularize the orbit for the lunar-module active rendezvous.

The fourth day of activity was highlighted by a two-vehicle extravehicular operation, which was abbreviated from the flight plan because

of a minor inflight illness previously experienced by the Lunar Module Pilot and because of the many activities required for rendezvous preparation. The Lunar Module Pilot, wearing the extravehicular mobility unit, egressed the depressurized lunar module at approximately 73 hours and remained in the vicinity of the forward platform for about 47 minutes. During this same time, the Command Module Pilot, dependent on spacecraft life support, partially exited through the command module hatch for observation, photography, and retrieval of thermal samples. The Lunar Module Pilot also retrieved thermal samples from the spacecraft exterior. Although the planned transfer from the lunar module to the command module was not conducted because of the abbreviated operation, an evaluation of the lunar module handrails that would have been used was conducted.

On the fifth day, the lunar module rendezvous operation was performed, beginning with undocking at approximately 92.5 hours. After a small service module reaction-control-system separation maneuver for initial separation and system verification, the descent propulsion system was used to perform a phasing maneuver. At about 95.5 hours, after a proximity pass with the command and service modules, the descent engine was again used to perform the insertion maneuver and to provide the planned separation distance of 75 miles required for rendezvous initiation. After the lunar module was staged, the reaction control system was used to effect the co-elliptic sequence initiation, which positioned the lunar module 10 miles below and 82 miles behind the command module. The ascent engine was then used for the first time and performed a constant-delta-height maneuver. The terminal phase began at about 98 hours with a reaction control system maneuver to provide final closing. Final braking maneuvers were performed as scheduled to bring the two vehicles to within 100 feet, and station-keeping was instituted to permit photography from both spacecraft. The spacecraft docked at approximately 99 hours, the crew transferred to the command module and the ascent stage was jettisoned about 3 hours later. The ascent engine was then fired to oxidizer depletion, as planned, and the 362.4-second maneuver placed the ascent stage in a 3760.9- by 126.6-mile orbit.

During the sixth day, the sixth service propulsion maneuver, which was intended to lower the perigee, was postponed for one revolution because the reaction-control translation required prior to ignition for propellant settling was improperly programmed. The maneuver was performed successfully at approximately 123.5 hours.

In the final 4 days, a series of landmark tracking exercises and a multispectral photography experiment were performed. The duration of the seventh service propulsion maneuver, performed at about 169.5 hours, was increased to 25 seconds to permit a test of the propellant gaging system. The eighth service propulsion maneuver (deorbit) was performed at 240.5 hours, one revolution later than planned because of unfavorable weather in the planned recovery area. Following a normal entry profile

using the primary guidance system, the command module landed close to the target point in the Atlantic Ocean at 241:00:54. The parachutes were released after landing, and the spacecraft remained in the stable I (upright) attitude. The crew were recovered by helicopter and taken to the primary recovery ship.

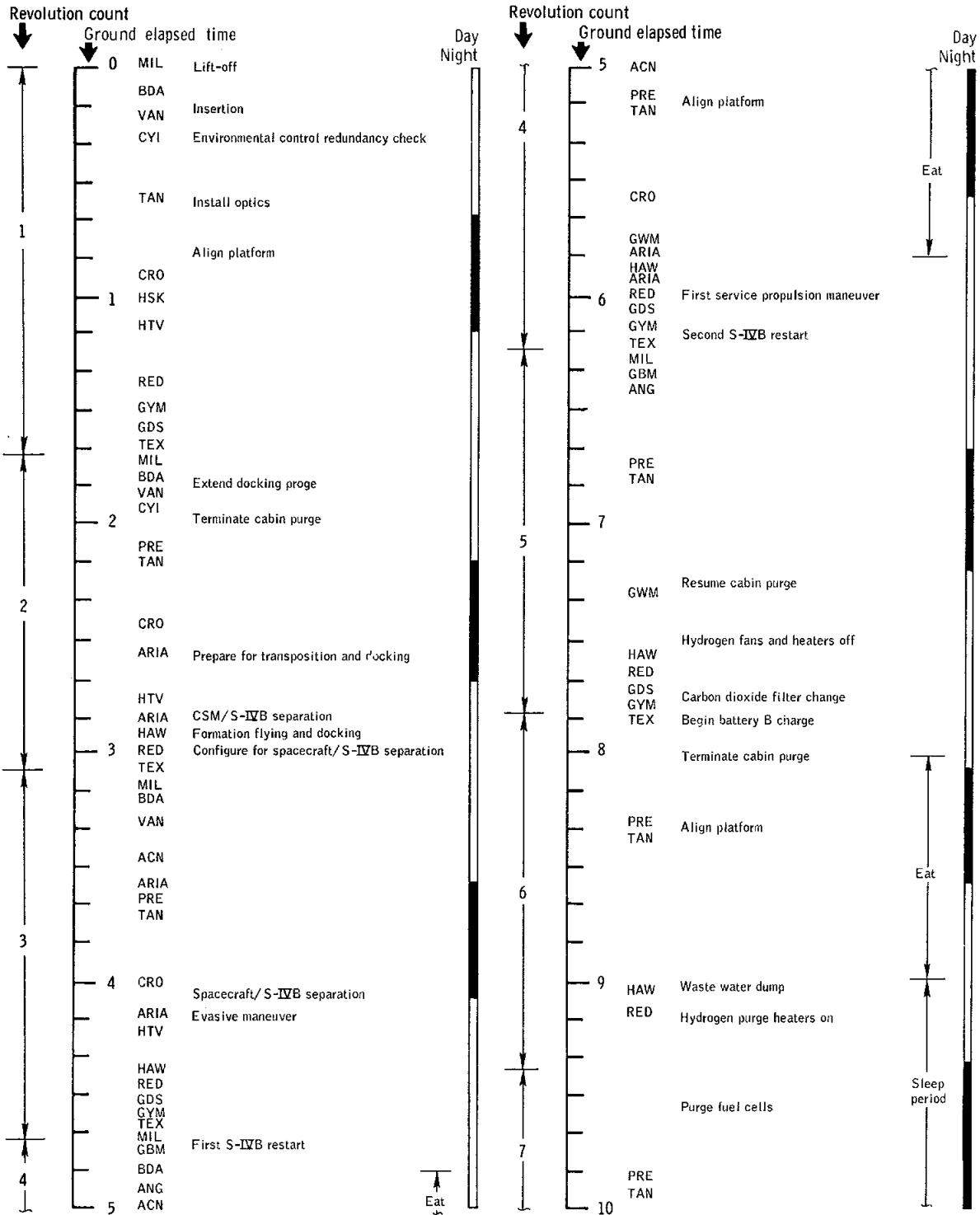
TABLE 3-I.- SEQUENCE OF EVENTS

Event	Time, hr:min:sec
Launch Phase	
Range zero (16:00:00 G.m.t.)	
Lift-off	0:00:00.7
Maximum dynamic pressure	0:01:25.5
S-IC inboard engine cutoff	0:02:14.3
S-IC outboard engine cutoff	0:02:42.8
S-IC/S-II separation	0:02:43.5
S-II engine ignition commanded	0:02:44.2
Interstage jettison	0:03:13.5
Launch escape tower jettison	0:03:18.3
S-II engine cutoff	0:08:56.2
S-II/S-IVB separation	0:08:57.2
S-IVB engine ignition	0:09:00.8
S-IVB engine cutoff	0:11:04.7
Orbital Phase	
Orbital insertion	0:11:14.7
Command and service module/S-IVB separation command	2:41:16
Docking	3:01:59.3
Spacecraft ejection from S-IVB	4:08:06
First service propulsion maneuver	5:59:01.1
Second service propulsion maneuver	22:12:04.1
Third service propulsion maneuver	25:17:39.3
Fourth service propulsion maneuver	28:24:41.4
First descent propulsion maneuver	49:41:34.5
Fifth service propulsion maneuver	54:26:12.3
Lunar module hatch open for extravehicular activity	72:53:00
Lunar module hatch closed after extravehicular activity	73:49:00

TABLE 3-I.- SEQUENCE OF EVENTS - Concluded

Event	Time, hr:min:sec
Orbital Phase - concluded	
First undocking	92:39:36
Command and service module/lunar module separation	93:02:54
Descent propulsion phasing maneuver	93:47:35.4
Descent propulsion insertion maneuver	95:39:08.1
Coelliptic sequence initiation maneuver	96:16:06.5
Constant delta height maneuver (first ascent propulsion)	96:58:15
Terminal phase initiation	97:57:59
Docking	99:02:26
Lunar module jettison	101:22:45
Ascent propulsion firing to depletion	101:53:15.4
Sixth service propulsion maneuver	123:25:07
Seventh service propulsion maneuver	169:39:00.4
Eighth service propulsion maneuver (deorbit)	240:31:14.9
Entry Phase	
Command module/service module separation	240:36:03.8
Entry interface (400 000 feet altitude)	240:44:10.2
Begin blackout	240:47:01
End blackout	240:50:43
Drogue deployment	240:55:07.8
Main parachute deployment	240:55:59.0
Landing	241:00:54

NASA-S-69-1930

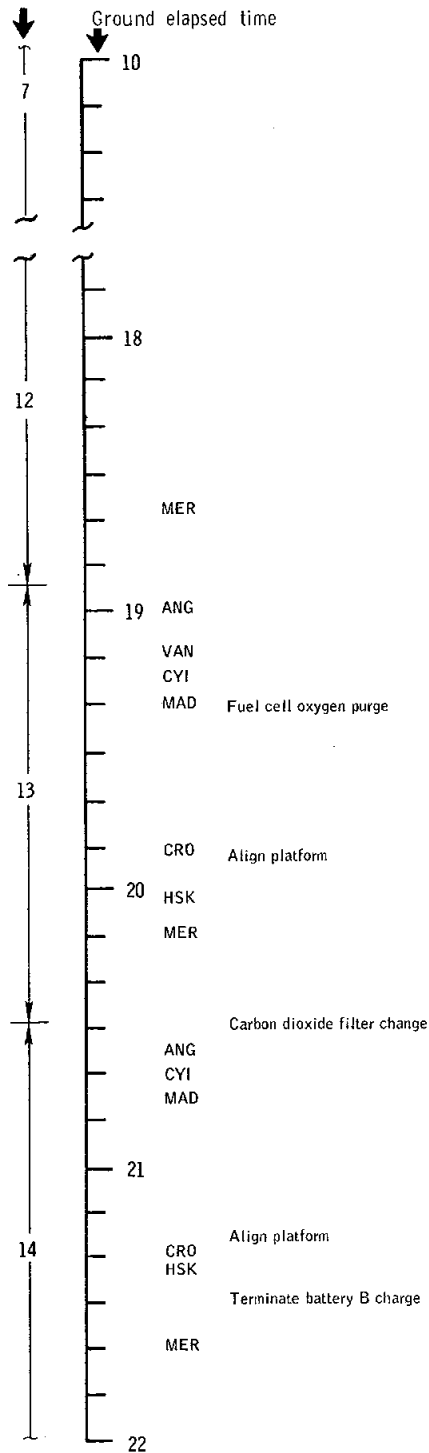


(a) 0 to 10 hours.

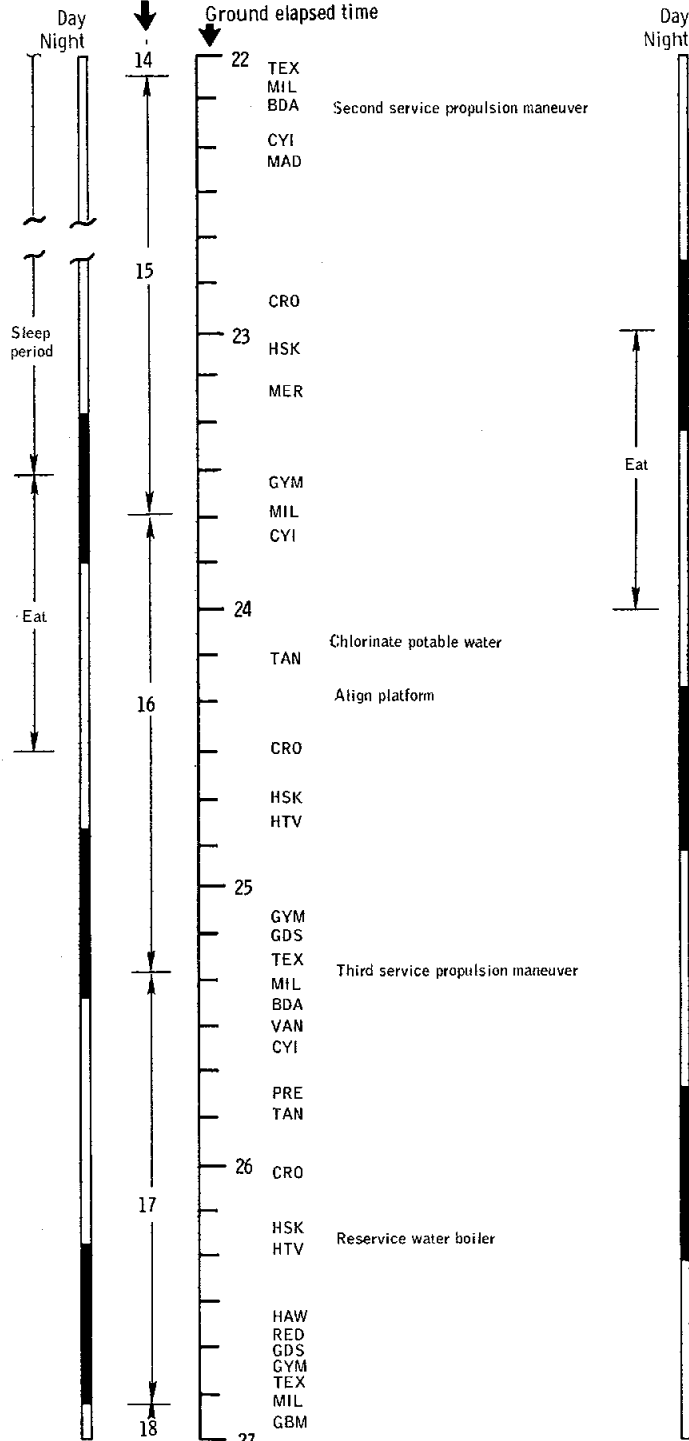
Figure 3-1. - Flight plan activities.

NASA-S-69-1931

Revolution count



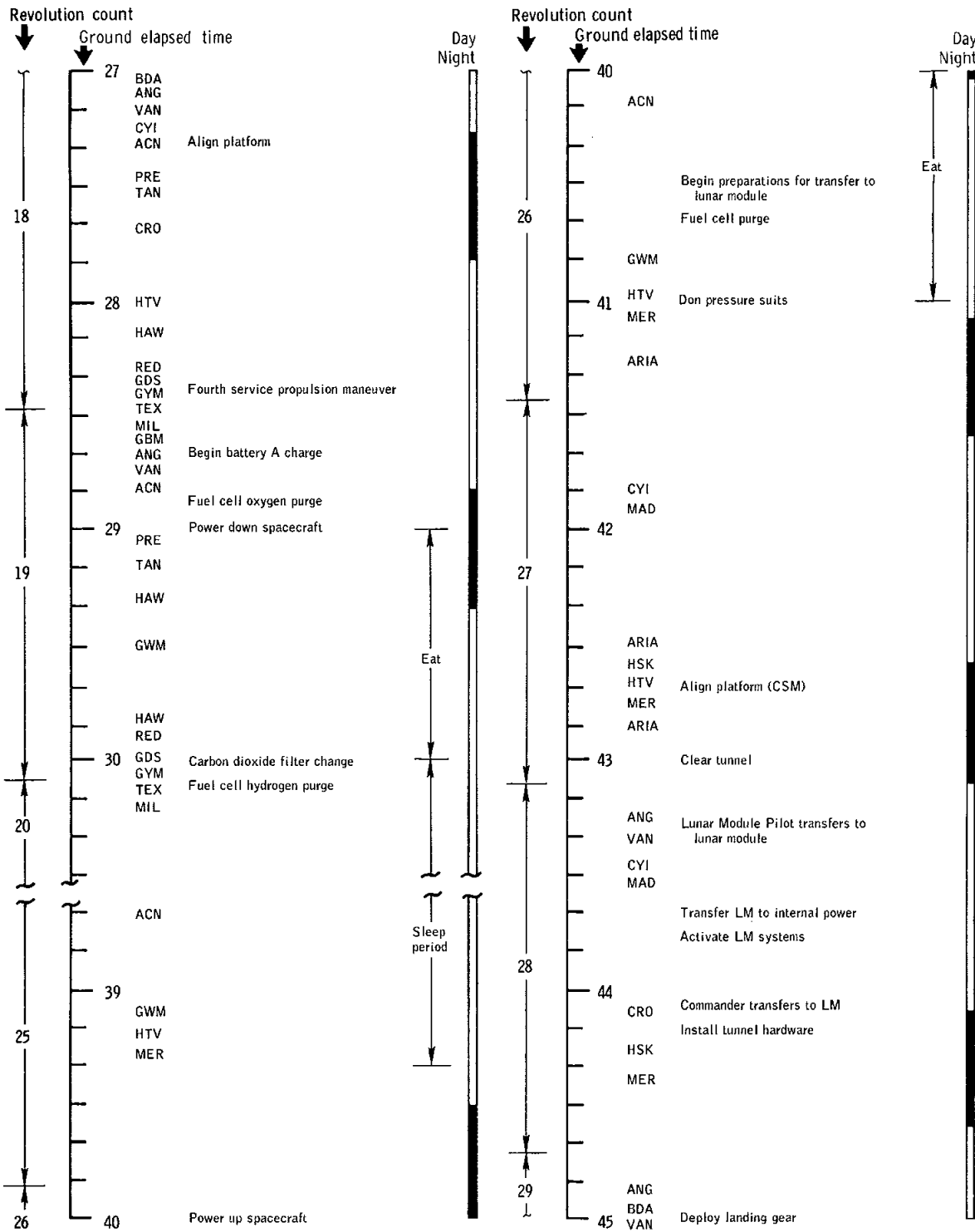
Revolution count



(b) 10 to 27 hours.

Figure 3-1. - Continued.

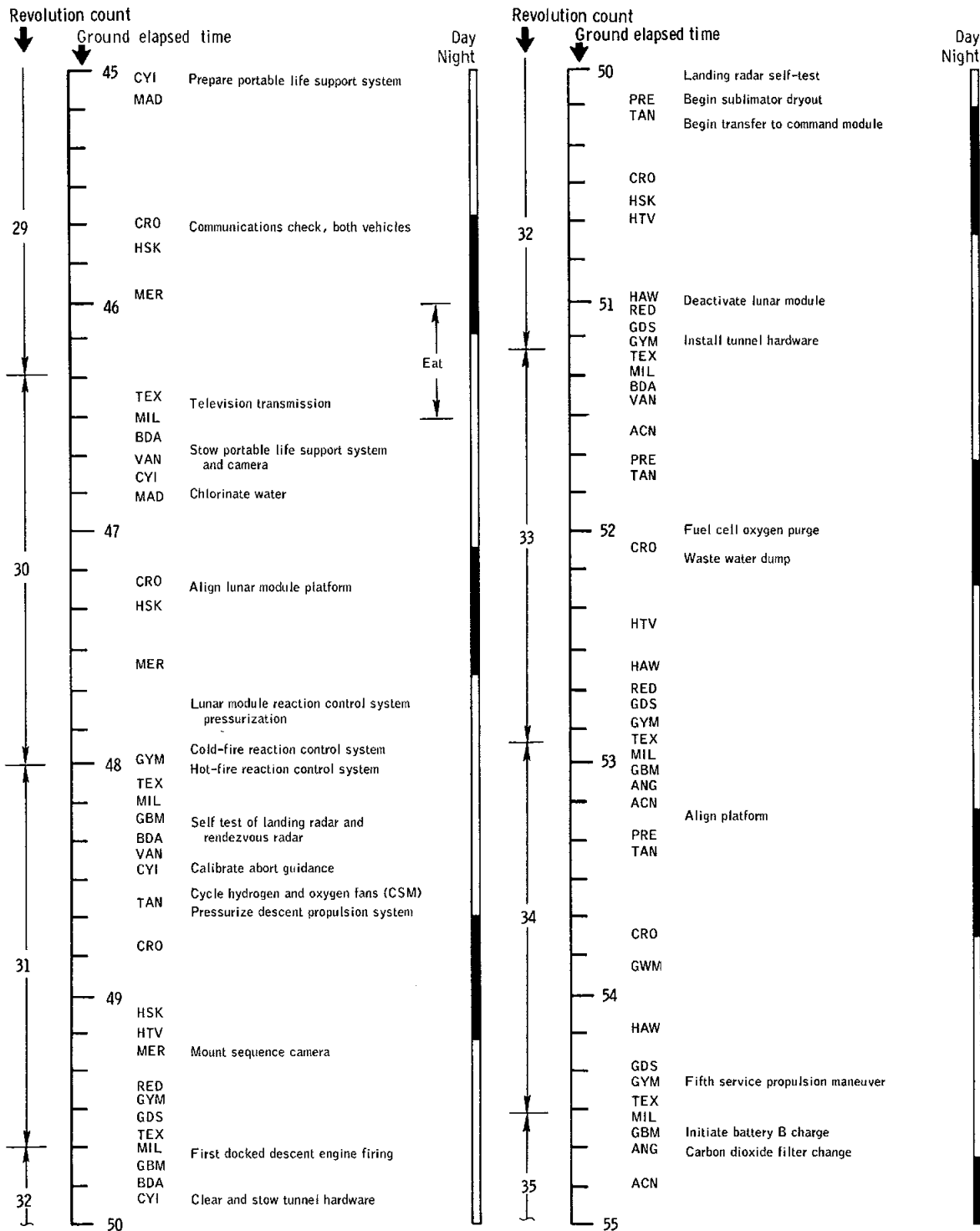
NASA-S-69-1932



(c) 27 to 45 hours.

Figure 3-1. - Continued.

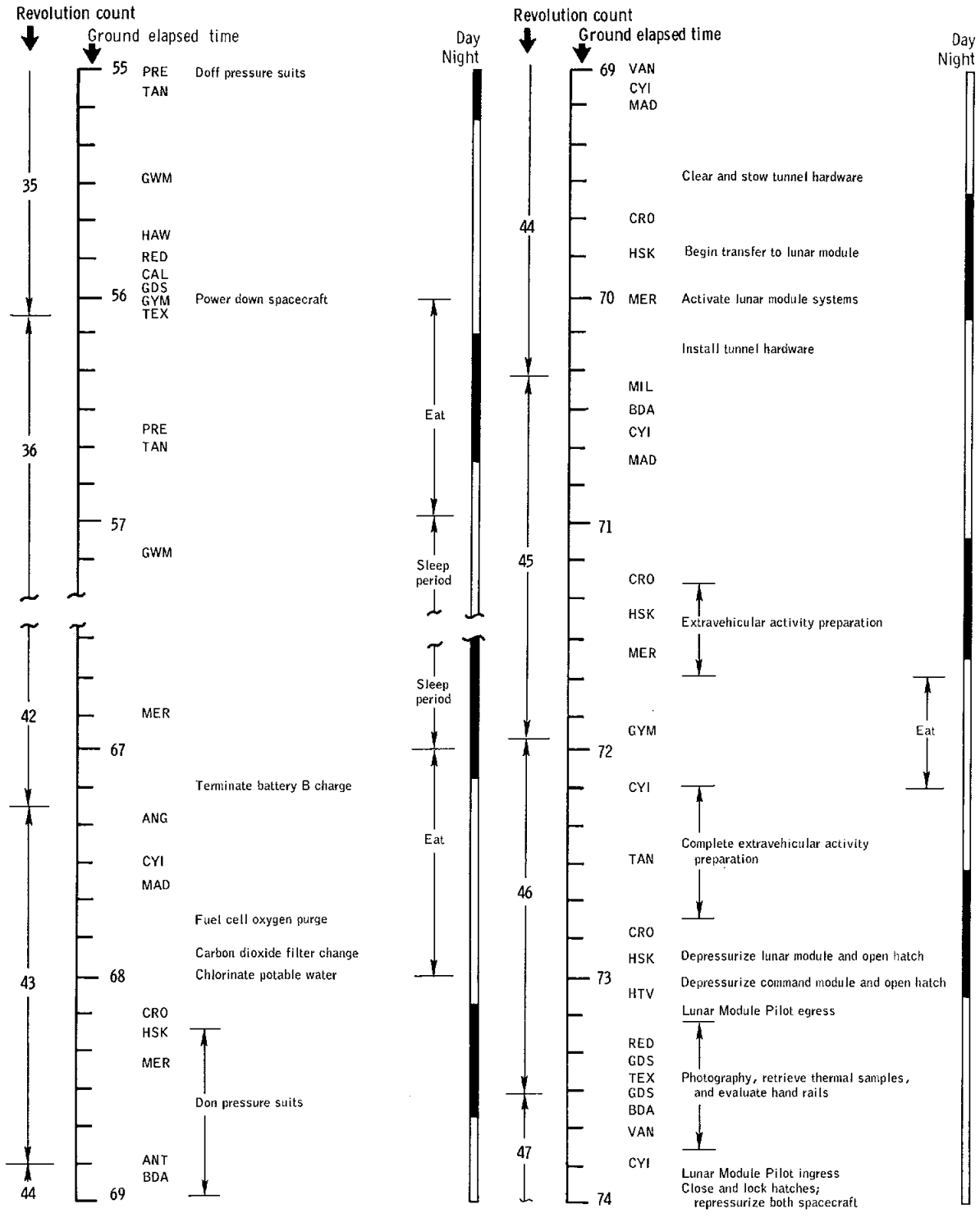
NASA-S-69-1933



(d) 45 to 55 hours.

Figure 3-1. - Continued.

NASA-S-69-1934

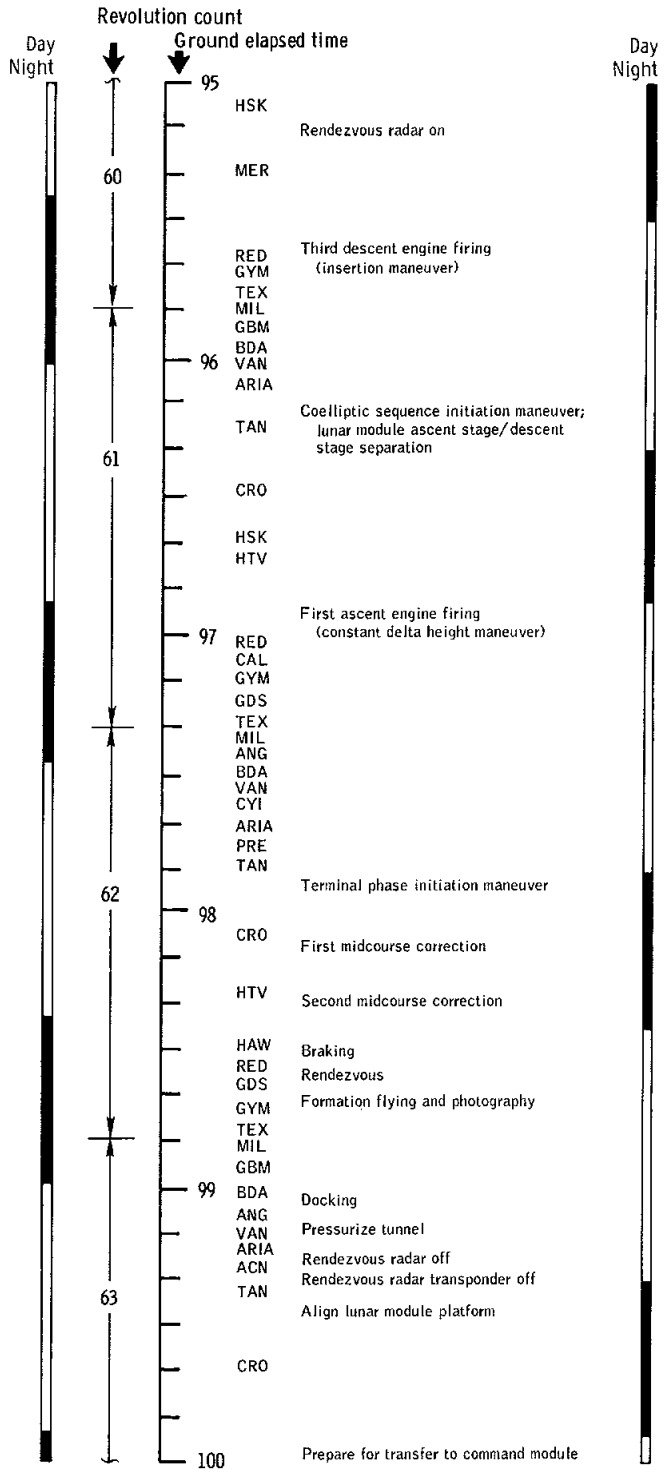
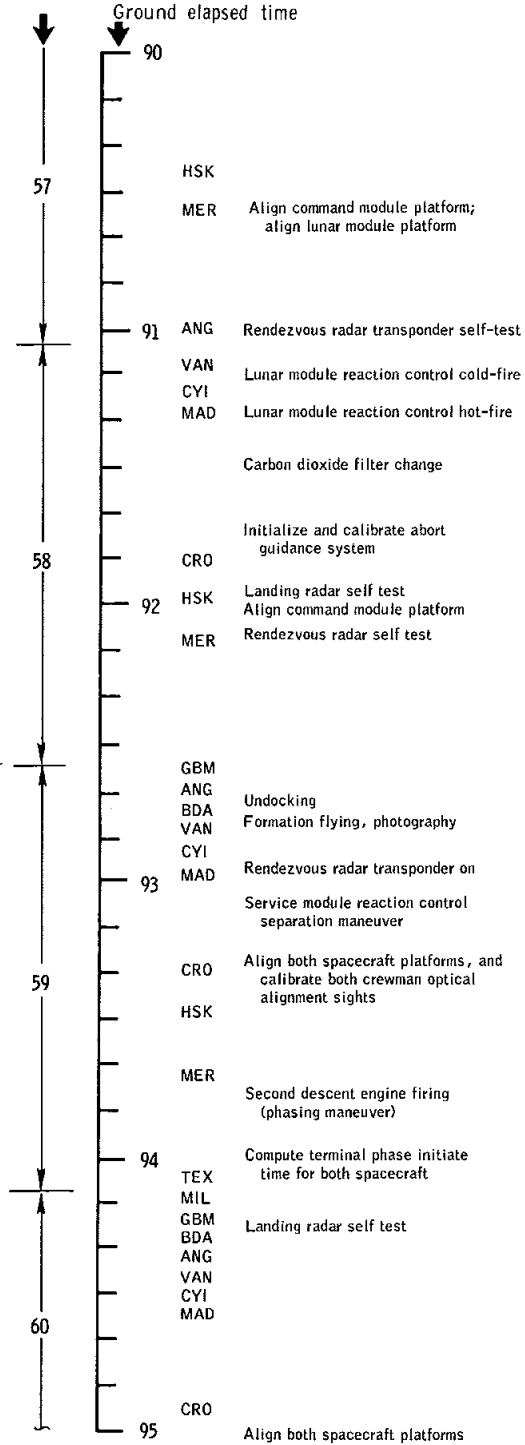


(e) 55 to 74 hours.

Figure 3-1. - Continued.



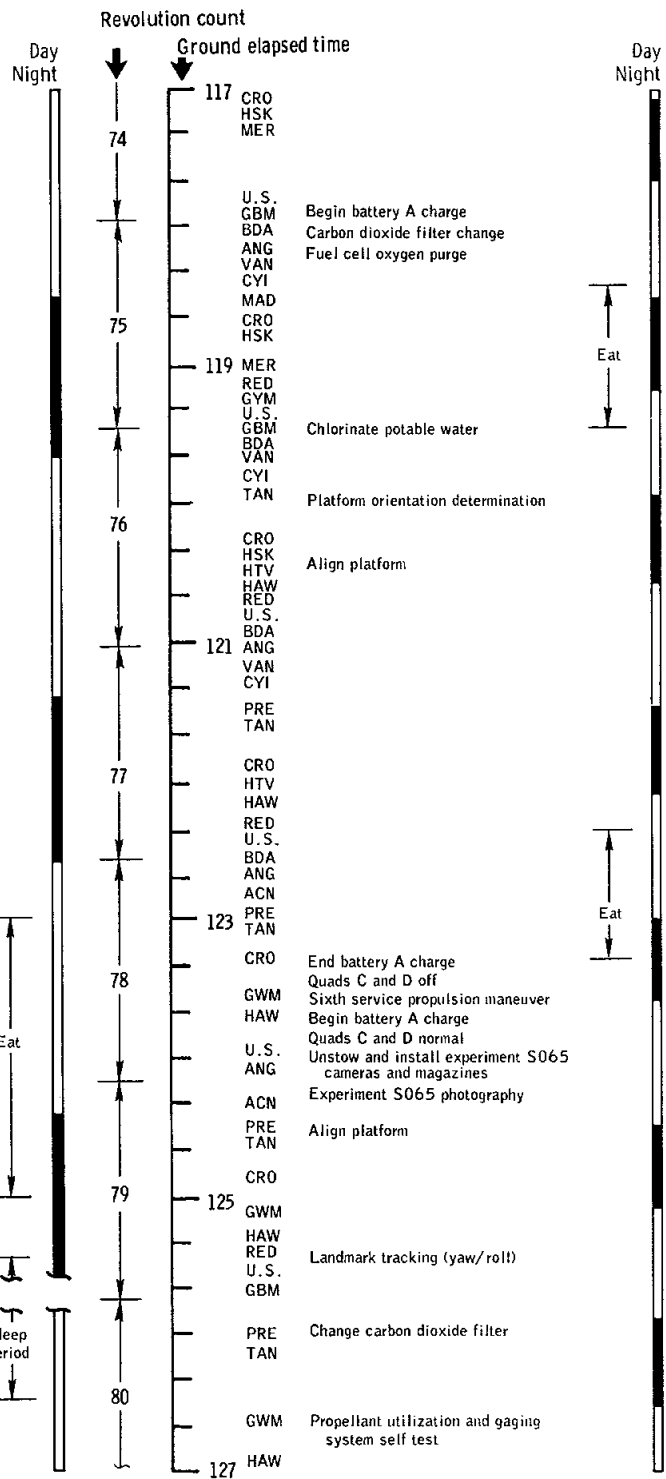
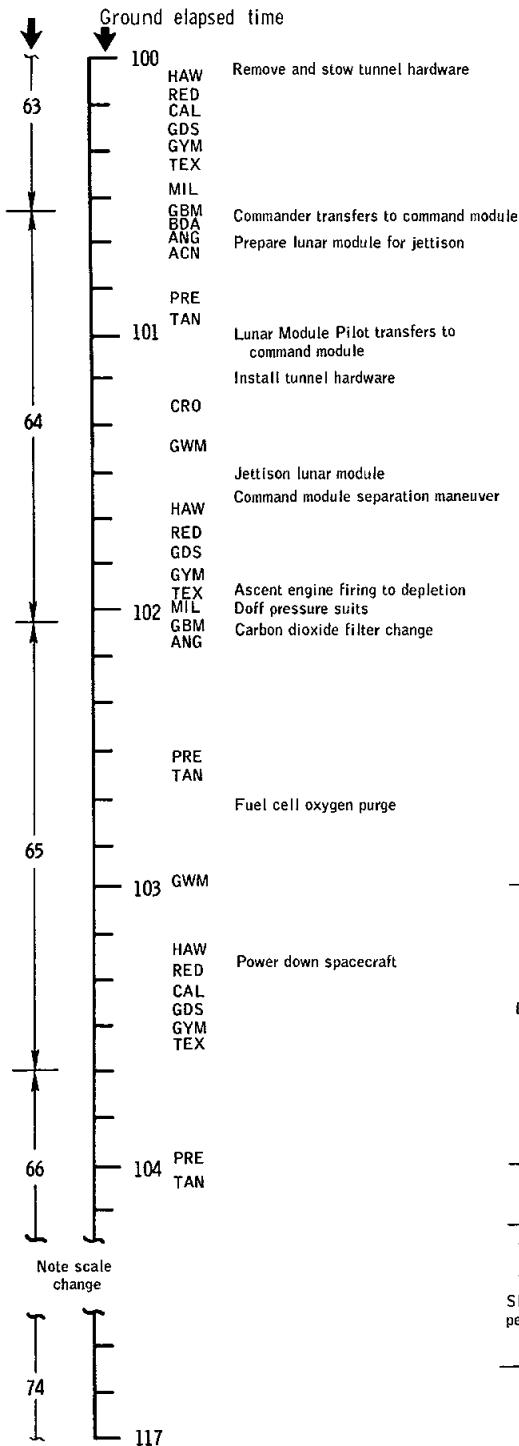
NASA-S-69-1936  
Revolution count



(g) 90 to 100 hours.

Figure 3-1. - Continued.

NASA-S-69-1937  
 Revolution count

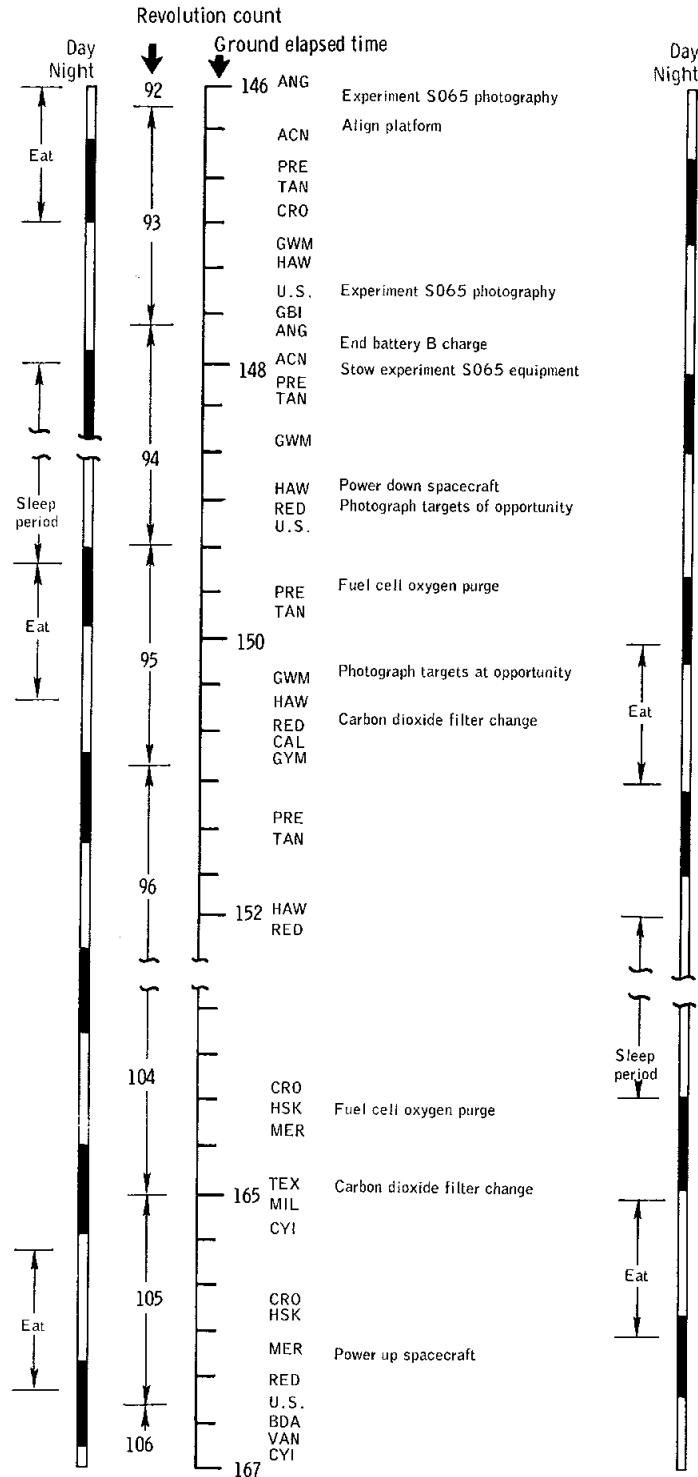
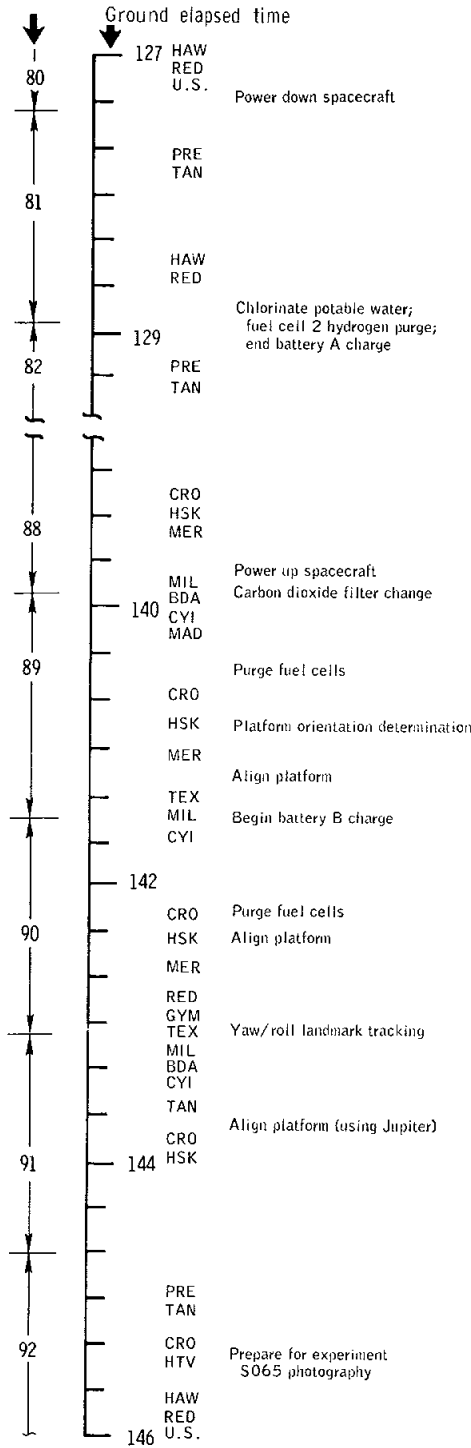


(h) 100 to 127 hours.

Figure 3-1. - Continued.

NASA-S-69-1938

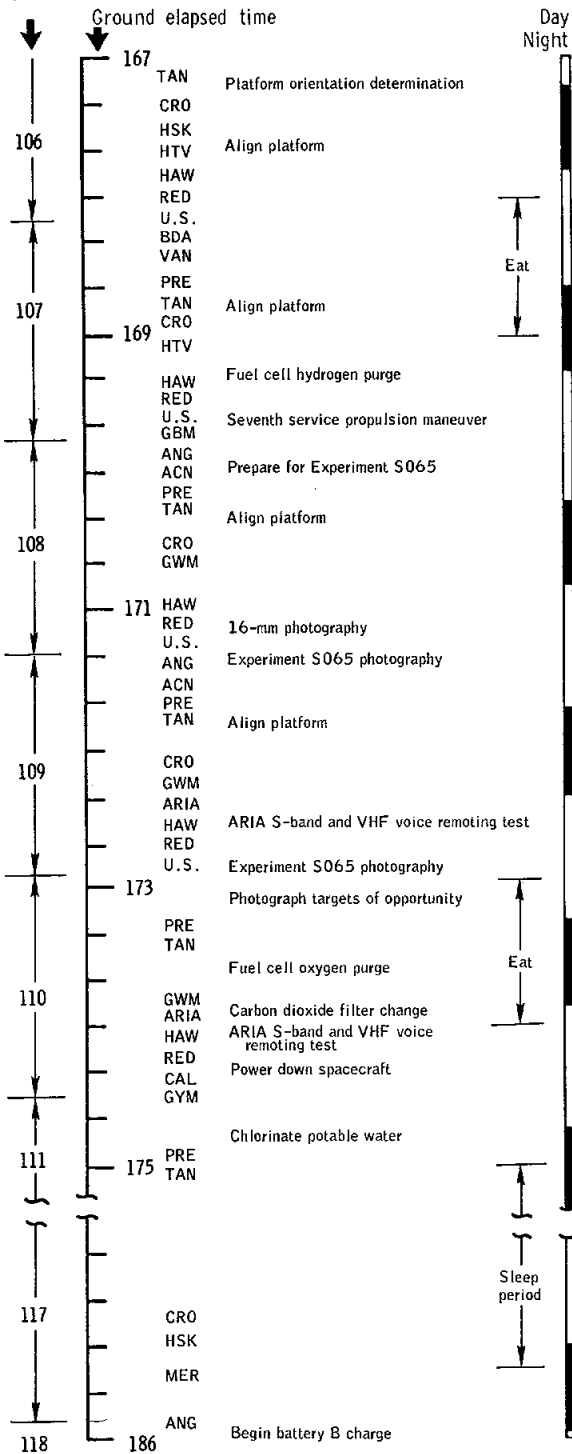
Revolution count



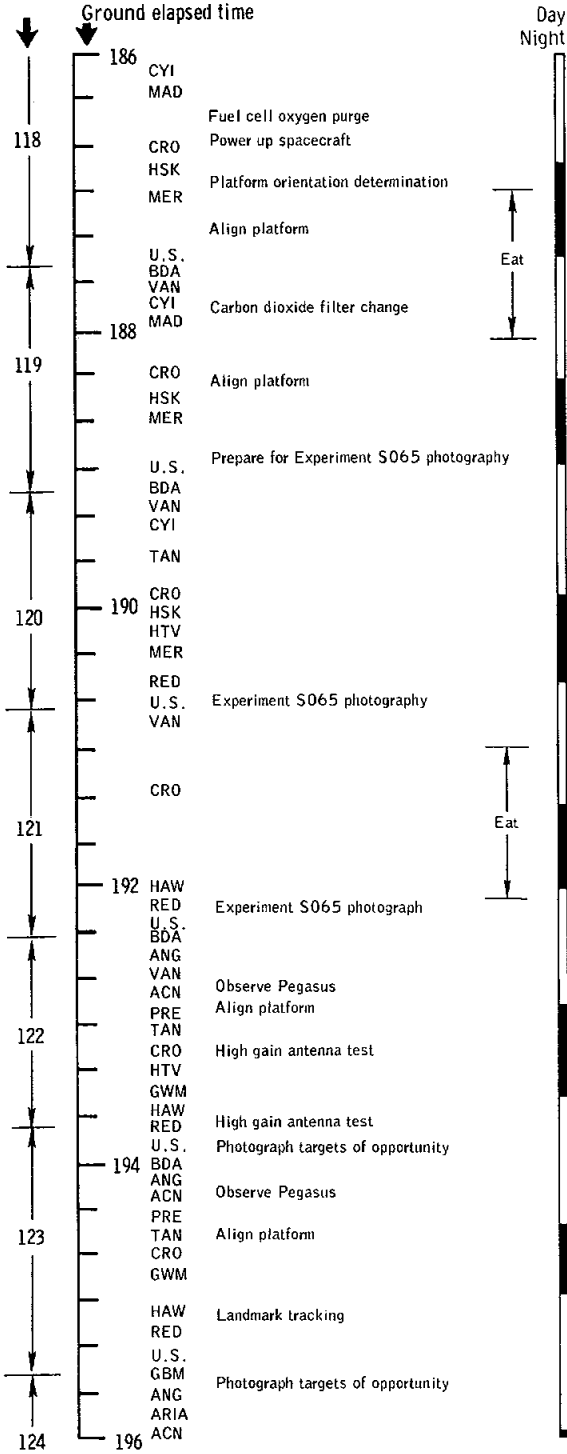
(i) 127 to 167 hours.

Figure 3-1. - Continued.

NASA-S-69-1939  
 Revolution count



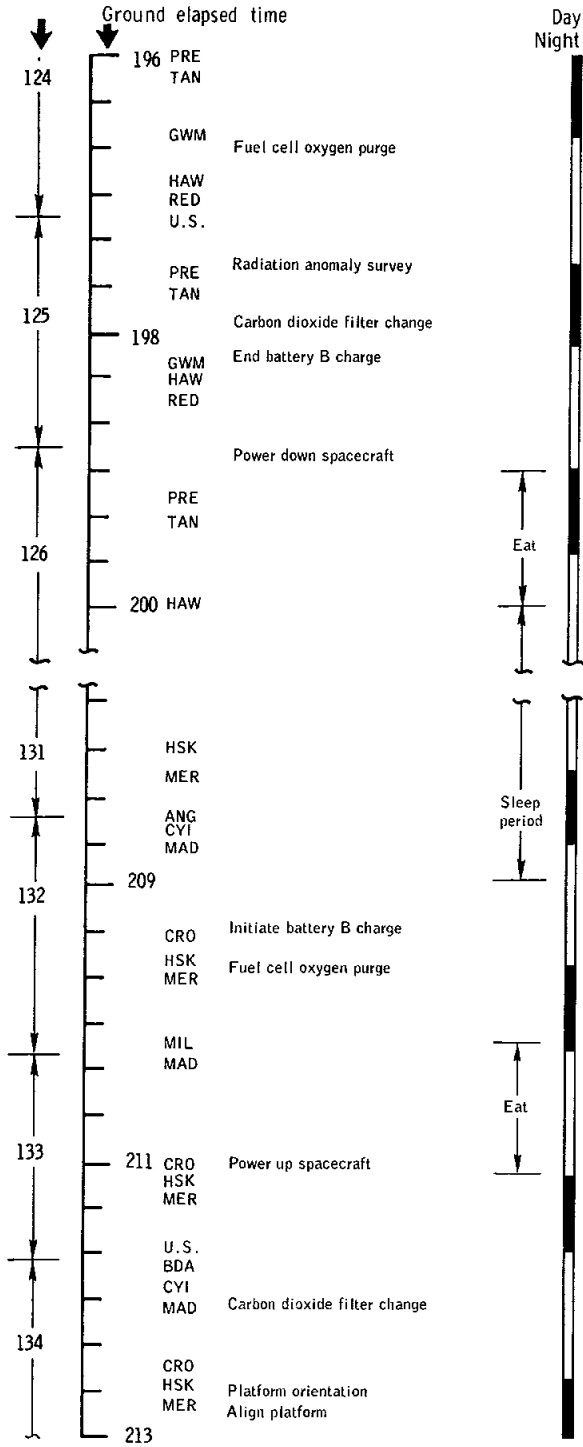
Revolution count



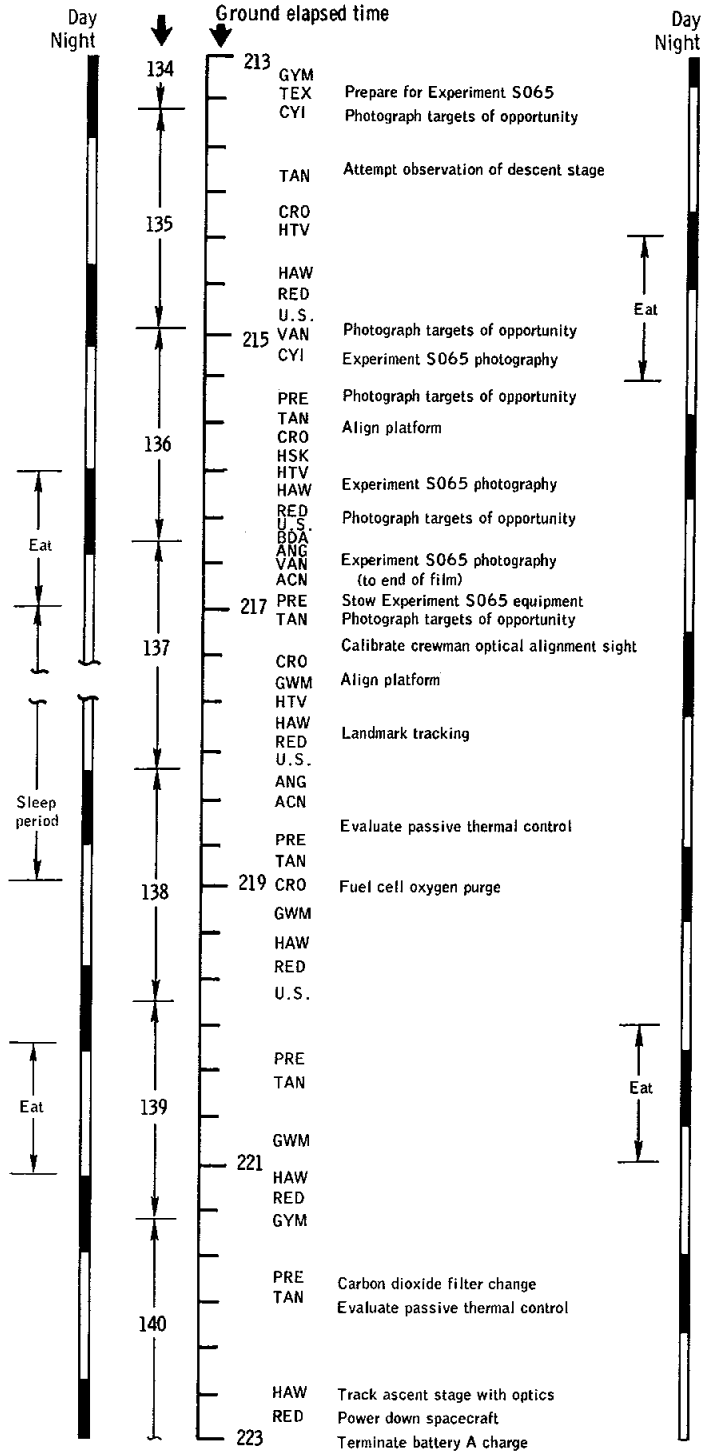
(j) 167 to 196 hours.

Figure 3-1. - Continued.

Revolution count



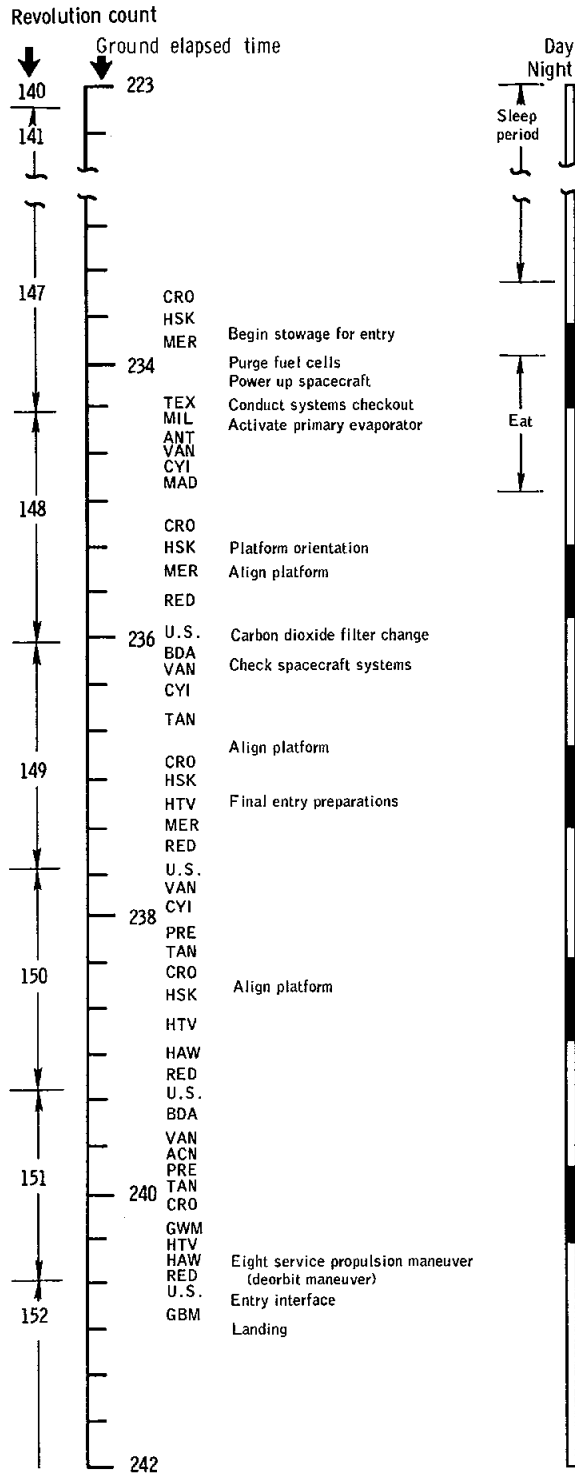
Revolution count



(k) 196 to 223 hours.

Figure 3-1. - Continued.

NASA-S-69-1941



(I) 223 to 242 hours.  
Figure 3-1. - Concluded.

#### 4.0 EXTRAVEHICULAR ACTIVITY

The planned use of two vehicles for the lunar landing mission requires development of hardware and procedures for extravehicular transfer from the lunar module to the command module in the event the transfer tunnel becomes unusable. Demonstration of this capability was at one time an Apollo 9 objective, and since the hardware was the same as that for lunar surface exploration, evaluation of its operation was included in the transfer demonstration.

The planned extravehicular operation provided the opportunity to support other developmental objectives, such as photographing the exterior of both vehicles and retrieval of thermal samples. It was originally intended that the Lunar Module Pilot egress from the lunar module, transfer to the open hatch in the command module, then return to the lunar module. However, the plan was abbreviated because of a minor in-flight illness experienced by the Lunar Module Pilot on the day preceding the extravehicular operation as well as concern for the crowded timeline required for rendezvous the following day.

As a result of the extravehicular activity performed during the Apollo 9 mission, the extravehicular transfer capability was demonstrated and is considered satisfactory for future missions. Further, successful operational experience with the procedures and equipment has provided additional confidence in the capability to perform successful lunar surface operations. The guidelines for planning and conduct of extravehicular activity as defined in the "Summary of Gemini Extravehicular Activity," NASA SP-149, continue to be valid.

#### 4.1 FLIGHT PLAN

The plan called for the Lunar Module Pilot to egress, mount the 16-mm camera on the lunar module forward platform, transfer to and partially ingress the command module, retrieve thermal samples, transfer back to the lunar module, evaluate lighting aids during a dark side pass, obtain 70-mm still photography from the platform area, provide television transmission from the platform area, retrieve lunar module thermal sample, and ingress the lunar module. The entire operation was planned for 2 hours 15 minutes outside the spacecraft.

The vehicle attitude during extravehicular activity was constrained primarily by the limitation that no direct solar illumination could impinge on the command module interior through the open hatch. The lunar module had a less stringent thermal requirement in that the forward hatch

could remain open up to 45 degrees for any sun position for the entire activity. The plan was to start with the command module minus Z axis pointed at the sun, pitch down 15 degrees, and roll left 80 degrees. This attitude would satisfy the command module thermal constraint and provide good lighting for command module photography.

## 4.2 ACTUAL TIMELINE

The Lunar Module Pilot donned and checked the extravehicular mobility unit, depressurized the lunar module, and began his egress to the forward platform at 72:59:02. Egress was completed at 73:07:00. The command module was depressurized and the side hatch opened at 73:02:00.

During the first 20 minutes, the Lunar Module Pilot and Command Module Pilot photographed each other's activities. The Command Module Pilot discovered the thermal sample was missing from the side of the command module, but at 73:26:00 he retrieved the service module thermal samples. The Lunar Module Pilot retrieved the lunar module thermal sample at 73:39:00, and 3 minutes later, began an abbreviated evaluation of translation and body-attitude-control capability using the extravehicular transfer handrails.

The Lunar Module Pilot began his ingress at 73:45:00 and completed it at 73:46:03. The command module hatch was closed and locked at 73:49:00, and the lunar module hatch was locked a minute later. Both vehicles were repressurized, and the two crewmen in the lunar module returned to the command module.

## 4.3 FLIGHT CREW ACTIVITIES

### 4.3.1 Preflight Preparation

There are specific advantages to each of the three types of crew training. These types of training are: one-g mockup training, zero-gravity training, and altitude chamber training.

The one-g mockups are high fidelity representations of the flight vehicles without operational subsystems. One-g mockup training enables a detailed review of procedures and equipment interfaces with emphasis on the operations during the preparation and post-extravehicular activity periods. One-g mockup training accomplished was: Commander, 4 exercises, 15 hours; Command Module Pilot, 7 exercises, 18.5 hours; Lunar Module Pilot, 7 exercises, 19.5 hours.

Zero-gravity training was conducted in the Water Immersion Facility and in the zero-gravity aircraft. Neutral buoyancy simulations in the Water Immersion Facility training were used for total extravehicular activity timeline evaluations. The Water Immersion Facility training accomplished was: Commander, 5 exercises, 5 hours; Command Module Pilot, 1 exercise, 1 hour; Lunar Module Pilot, 11 exercises, 12.5 hours.

Further refinement of specific tasks was accomplished in the true zero-gravity field provided by the zero-gravity aircraft. The training accomplished was: Commander, 59 parabolas; Command Module Pilot, 27 parabolas; Lunar Module Pilot, 71 parabolas. Each parabola provided about 30 seconds of zero-gravity.

Altitude chamber familiarization included testing of the portable life support system and the oxygen purge system with the Lunar Module Pilot and of the oxygen purge system with the Commander, as well as testing of the intravehicular pressure garment assembly with the Command Module Pilot. Testing for the Lunar Module Pilot and Command Module Pilot included one run each at thermal vacuum conditions. The testing for the Commander and for two additional Lunar Module Pilot chamber runs were conducted in an 8-foot altitude chamber. The Lunar Module Pilot spent a total of 9 hours, the Commander 2 hours, and the Command Module Pilot 1 hour training in the altitude chamber. First-time flight usage of equipment required additional chamber test time on the part of the Lunar Module Pilot and the Commander.

Additional information on the extravehicular mobility unit was obtained from formal briefings and informal discussions, the Apollo Operations Handbook, and briefings in support of altitude-chamber testing.

#### 4.3.2 Procedures

The nominal extravehicular activity plan called for the Lunar Module Pilot to spend 2 hours 15 minutes outside the spacecraft during the fourth mission day. However, the minor sickness experienced by this pilot on the third day required a revised extravehicular activity plan that would accomplish only those items that had the greatest priority: donning and checkout of the extravehicular mobility units, cabin depressurization and hatch opening for both the command module and the lunar module. While the command module side hatch was open, the Command Module Pilot was to retrieve the thermal samples from the command module. The Lunar Module Pilot was not to egress but was to remain connected to the lunar module support hoses even though using the portable life support system. The condition of the Lunar Module Pilot just prior to extravehicular activity was sufficiently improved to permit further modification of the plan to more nearly approach the preflight plan (fig. 4-1). Returning entirely to the preflight timeline was considered in view of the pilot's improved

condition, but was rejected in favor of terminating the activity at the end of one daylight pass to provide adequate preparation time for the next day's rendezvous activities.

After the Lunar Module Pilot donned the portable life support system and oxygen purge system and connected the extravehicular lifeline to the lunar module cabin interior, he egressed and moved to the foot restraints (fig. 4-2) on the forward platform. While restrained, he retrieved the lunar module thermal sample and performed 16-mm and 70-mm photography of the Command Module Pilot's activities and the exterior of both spacecraft.

The initial extravehicular activities by the Lunar Module Pilot were recorded by the Command Module Pilot on both 16-mm and 70-mm film (see figure 4-3). The Command Module Pilot retrieved thermal samples from the service module but the command module sample was missing. The Command Module Pilot's life support came from the spacecraft environmental control system hoses, which also served as his restraint during partial egress to retrieve the samples (fig. 4-4). The Command Module Pilot was wearing an intravehicular suit with minimal thermal insulation; however, he had participated in a thermal vacuum test of this suit and was familiar with its reaction to the space environment. The upper part of his body, down to slightly above his waist, was exposed to the extravehicular environment for about 70 percent of the hatch-open time, and he experienced no thermal extremes.

The Lunar Module Pilot conducted an evaluation of the extravehicular transfer handrails by translating along the lunar module rail to the point where the rail turned and crossed the top surface of the lunar module (fig. 4-5). Translation capability and body attitude control were both evaluated as excellent. After the handrail evaluation, the Lunar Module Pilot returned to the forward hatch and ingressed the lunar module. The hatches of both spacecraft were closed and the spacecraft were repressurized. The post-extravehicular activity procedures were conducted according to plan.

Both oxygen purge systems were checked at the start of each day of lunar module activity. A check of the Commander's oxygen purge system heater showed it to be intermittent on the day of extravehicular activity, and the unit was not operable on the rendezvous day. A discussion of this failure is contained in section 17.

### 4.3.3 Crew Performance

The modified extravehicular plan accomplished all the principal extravehicular test objectives; however, extravehicular transfer between the two spacecraft and various communications checks were not performed. No problems were encountered in performing any of the planned tasks.

Body control by the extravehicular crewman was excellent in the foot restraints and on the handrail. All translations, lunar module egress and ingress, and stability evaluation were performed satisfactorily with a minimum of effort. Inflight capabilities were found to be similar to that experienced during reduced gravity training. The primary difference was that some tasks were easier to perform inflight. These differences are attributed to the external perturbing forces occasionally experienced in the Water Immersion Facility and zero-gravity aircraft. Data from the extravehicular mobility unit show a very low metabolic expenditure during extravehicular activity. The extravehicular crewman's heart rate ranged from 66 to 88 beats/minute during the period outside the spacecraft. The spacecraft and crew performance during extravehicular activity was sufficiently good that the crew stated that extravehicular transfer from one spacecraft to the other would pose no problem.

### 4.4 EXTRAVEHICULAR MOBILITY UNIT

The extravehicular mobility unit used for Apollo 9 is described in Appendix A. The performance of the extravehicular mobility unit was nominal, and most telemetry data closely paralleled that obtained during crew training. The extravehicular mobility unit could not be evaluated under design heat loads and work-rate conditions because of time limitations on the extravehicular activity. Both the Lunar Module Pilot and the Command Module Pilot reported they were comfortable and experienced no visual problems with the extravehicular visor assembly. The Command Module Pilot wore one extravehicular glove and one intravehicular glove. The hand with the intravehicular glove became warm but was not uncomfortable. After the extravehicular activity, the portable life support system was successfully recharged with oxygen and water for possible contingency reuse.

There were three minor discrepancies in the operation of the extravehicular mobility unit. As indicated in figure 4-6, the liquid cooling garment inlet temperature did not reach equilibrium. Equilibrium of the inlet temperature was reached during ground tests under similar workload conditions. Several conditions, either separately or combined, could have caused this deficiency. The extravehicular activity was performed at a low metabolic rate; therefore, the portable life support

system was operating with the diverter valve set in the minimum-cool position at the low end of the performance range. In this idling state, system performance was difficult to evaluate and normal telemetry inaccuracies preclude detection of small performance shifts. The Lunar Module Pilot had donned the liquid cooling garment on the third day and left it on for the extravehicular activity on the fourth day.

The crewman stated that the liquid cooling garment kept him cool and operated satisfactorily at all times during extravehicular activity, however, the garment was saturated with air after it was used. The cooling garment differential temperature indicated that performance of the sublimator was degraded. This is attributed to the entrapped air in the system. Previous tests indicate that air would pocket in the sublimator when the diverter valve is in the minimum position which restricts the liquid flow through the sublimator.

If the extravehicular activity had been accomplished as planned, it was anticipated that the diverter valve would be in minimum position at startup and would be moved to intermediate and then cycled to either minimum or maximum depending upon the crewman comfort. However, because the Lunar Module Pilot did work at a very low rate for the complete time, the minimum position would be expected.

The second problem concerned the portable life support system feed-water pressure transducer which normally indicates sublimator startup by a tone to the crewman and sublimator performance through telemetry. The transducer indicated a 17-percent downward shift on the third day, but on the fourth day just prior to extravehicular activity, the level had risen to a downward shift of only 8 percent. Data during the extravehicular activity, however, were normal, and no shift was evidenced.

The third discrepancy was an indicated failure of one of the two heater circuits in the oxygen purge system during checkout on the fifth day. It had been intermittent during checkout on the fourth day. The problem most likely resulted from a failed-open power switch which was cam-operated and controlled by an actuator and cable mechanism on the crewman's chest. See section 17 for further details.

A plot of performance parameters for the portable life support system is shown in figure 4-6. The oxygen supply pressure decreased from 960 to approximately 830 psia during system operation, indicating a usage of about 0.2 pound. A rate of 900 to 1000 Btu/hr was originally predicted for the extravehicular activity; however, the readjusted plan did not require the crewman to be as active as originally planned. During the 47-minute extravehicular activity, the Lunar Module Pilot produced approximately 500 Btu which indicates a rate of about 600 Btu/hr. This determination was based on heart rate, oxygen consumption, and liquid cooling

garment thermodynamics. Based on a postflight analysis of the lithium hydroxide element, a total of 90.6 grams of carbon dioxide, corresponding to 1170 Btu, were produced during the 28-minute preparation time for extravehicular activity, the 47 minutes of extravehicular activity, and the 34-minute period after extravehicular activity when returning to the normal spacecraft oxygen environment. However, the 1170-Btu determination could have been compromised to some degree because the lithium hydroxide container was not sealed for the postflight return to the Manned Spacecraft Center. Figure 4-7 shows inflight oxygen usage compared with preflight predictions.

#### 4.5 SPACECRAFT INTERFACES

The extravehicular transfer subsystem consisted of a series of handrails leading from the lunar module forward hatch to the command module side hatch. Lighting was provided by a deployable extravehicular pole lamp at the vehicle interface, the service module docking spotlight, and radioluminescent discs imbedded in the handrails (fig. 4-2). The lunar module handrail was rigid and continuous from near the forward hatch to near the docking interface. The command module handrails were rigid but discontinuous because of constraints imposed by vehicle structure. All handrails and lighting aids were adequate for the extravehicular activity. Photographs taken during flight verified proper deployment of the extravehicular pole lamp and the uppermost handrail on the command module; both were spring-loaded to deploy at escape tower jettison.

The crew reported that when the lunar module forward hatch was opened for extravehicular activity, it tended to bind on top and had to be pushed downward to be opened. Additionally, the forward hatch had a tendency to close during extravehicular activity, and the hatch friction device had no noticeable effect. See section 17 for a discussion of the hatch problems. A slight delay between closing and locking the forward hatch occurred when the Commander had difficulty in getting into position to operate the handle. Closing and locking of the command module side hatch took only 23 seconds, and this hatch operated without incident. Communications were excellent between the command module/lunar module/extravehicular crewmen and the network during most of the extravehicular activity. The communication configuration used was command module one-way relay with the portable life support system mode-select in position 1.

A preflight analysis indicated that with the portable life support system operating inside the lunar module cabin, relay of the portable life support system data to the Manned Space Flight Network through the command module might not be possible. During the flight, however, excellent data and voice were received at the Manned Space Flight Network

when the portable life support system antenna was erected inside the lunar module and also between the command module and lunar module during the extravehicular activity. Therefore, it was shown that radio frequency radiation leakage from the closed lunar module cabin to the closed command module cabin is sufficient to establish a good communication link.

A ground test of a lunar module test article (LTA-8) and the portable life support system in the anechoic chamber demonstrated that during extravehicular activity, the Lunar Module Pilot's electrocardiograph data would be degraded if the Lunar Module Pilot was within 4 feet of the antenna when the development flight instrumentation B-transmitter was operating. Examination of the flight data shows that the transmitter was on but did not degrade the electrocardiogram. The reason for the lack of interference is unknown. However, on future flights no development flight instrumentation will be installed.

The extravehicular lifeline secured the crewman to the lunar module at all times. The vehicle end of the lifeline was attached to the minus Y overhead attach point and the crewman end to the lunar module left restraint attach point on the pressure garment assembly. The lifeline was fabricated of Polybenzimidazole webbing 1-inch wide and 1/16-inch thick (fig. 4-8). Three hooks were provided, one permanently attached at each end and one positionable to any point along the 25-foot length of the tether for transfer of cameras and thermal samples. Each hook was provided with a locking-type keeper, which a crewman in a pressurized suit could easily operate. The entire assembly was designed for an ultimate tensile strength of 600 pounds and was packed in a Teflon-coated beta cloth bag that provided for orderly management of the webbing as the lifeline was deployed for use.

The thermal sample tether (fig. 4-9) was fabricated from the same material as the lifeline assembly. Two hooks were provided, one permanently attached to the end of the webbing and the other adjustable to any point along the 14-foot length of the tether. One hook was identical in design to the nonadjustable lifeline hook, and the other was a basic waist tether hook. The assembly was packed in a Teflon-coated beta cloth bag which acted as a container while the assembly was stowed and provided a means of managing the webbing during deployment and use. This tether could also have been used as an aid in closing the command module side hatch, if necessary.

NASA-S-69-1942

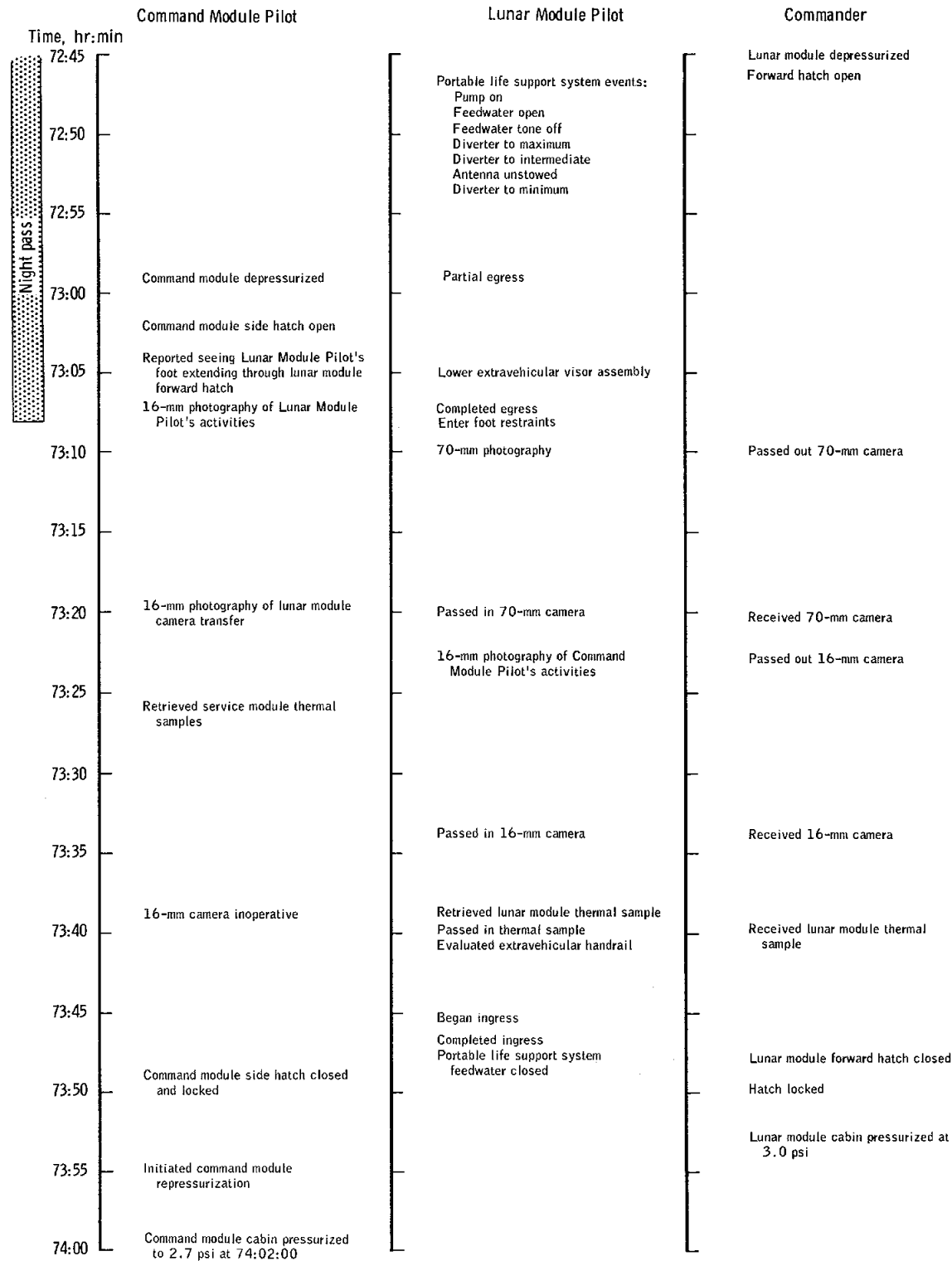


Figure 4-1. - Timeline for extravehicular activity.

NASA-S-69-1943

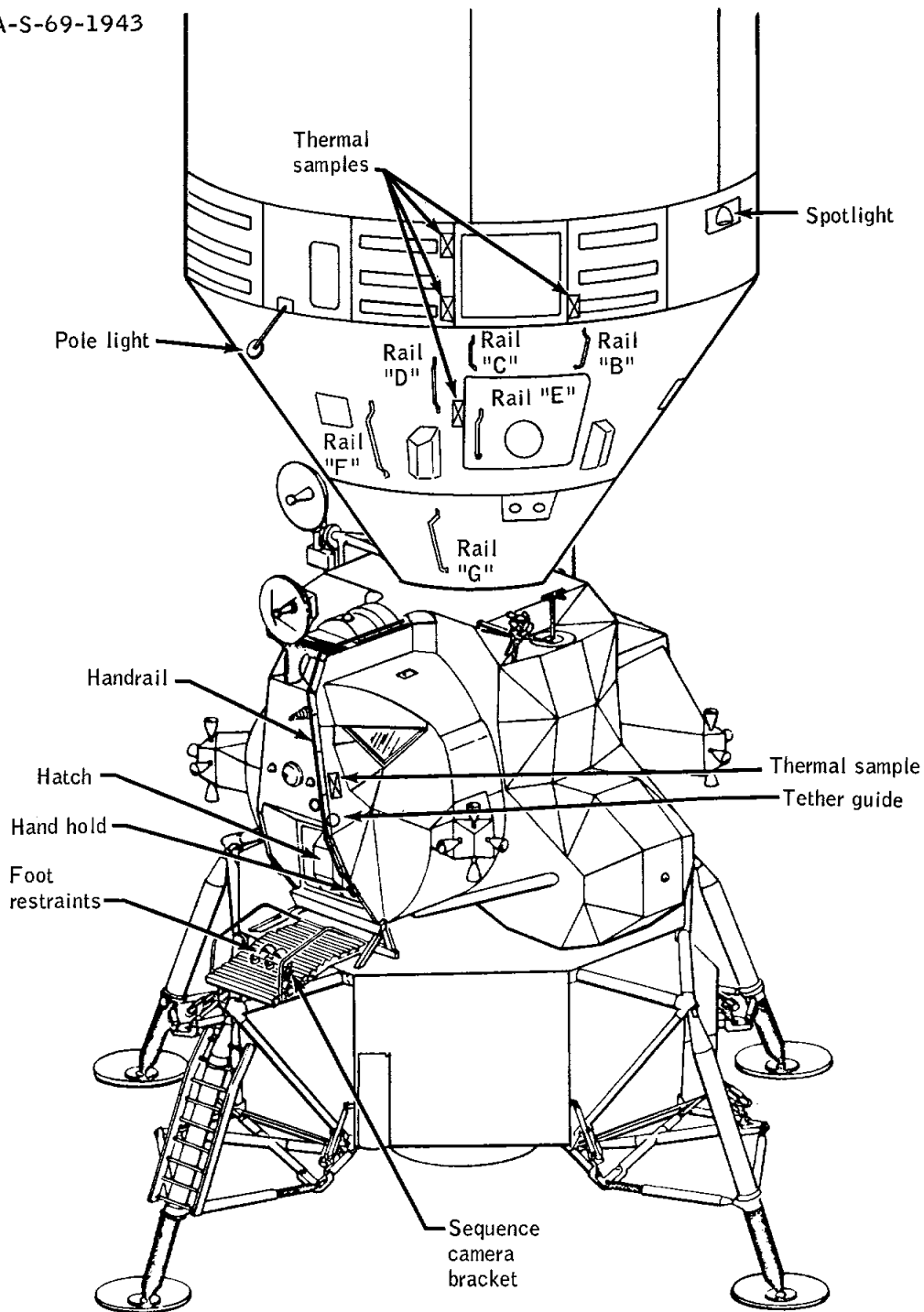


Figure 4-2.- Relative spacecraft positions and location of handrails and thermal samples.



Figure 4-3.- Lunar Module Pilot on forward platform.



Figure 4-4.- Command Module Pilot retrieving thermal samples.

NASA-S-69-1946



Figure 4-5.- Lunar Module Pilot evaluating handrails.

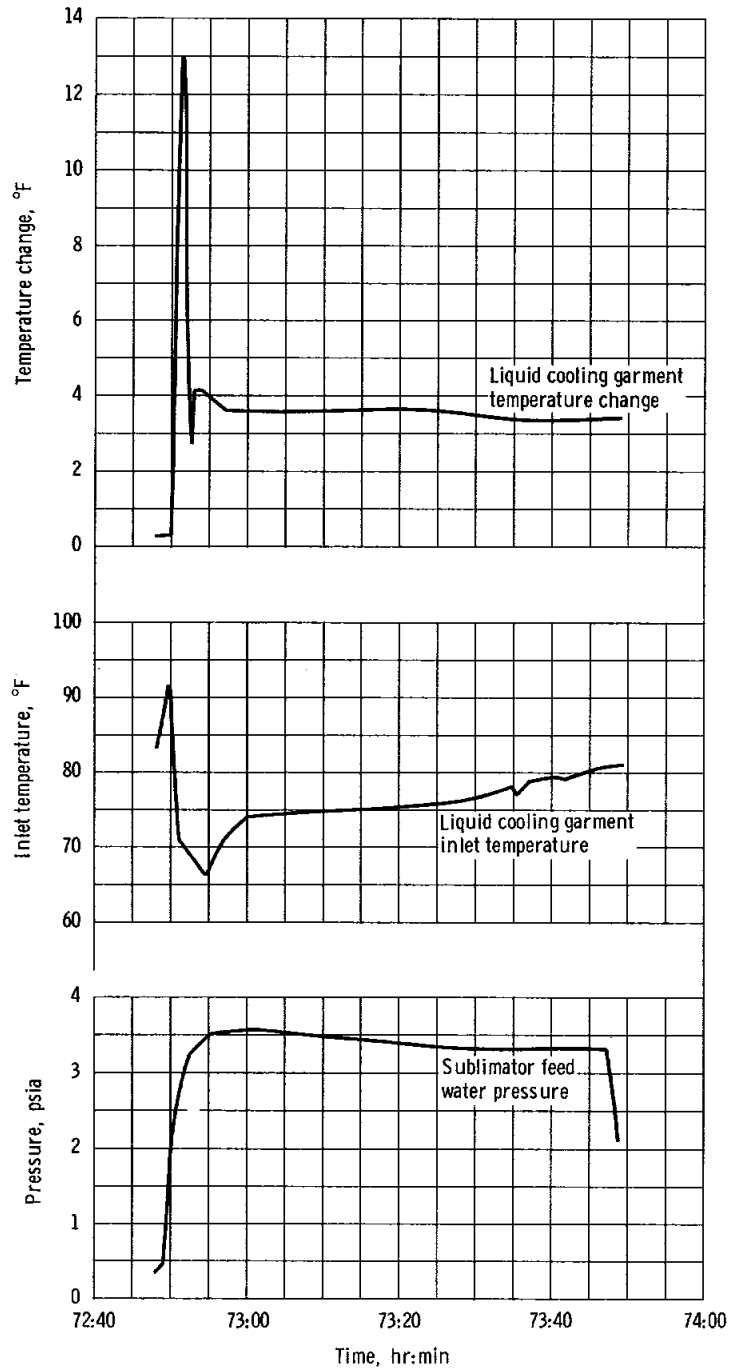


Figure 4-6. - Portable life support system operational parameters.

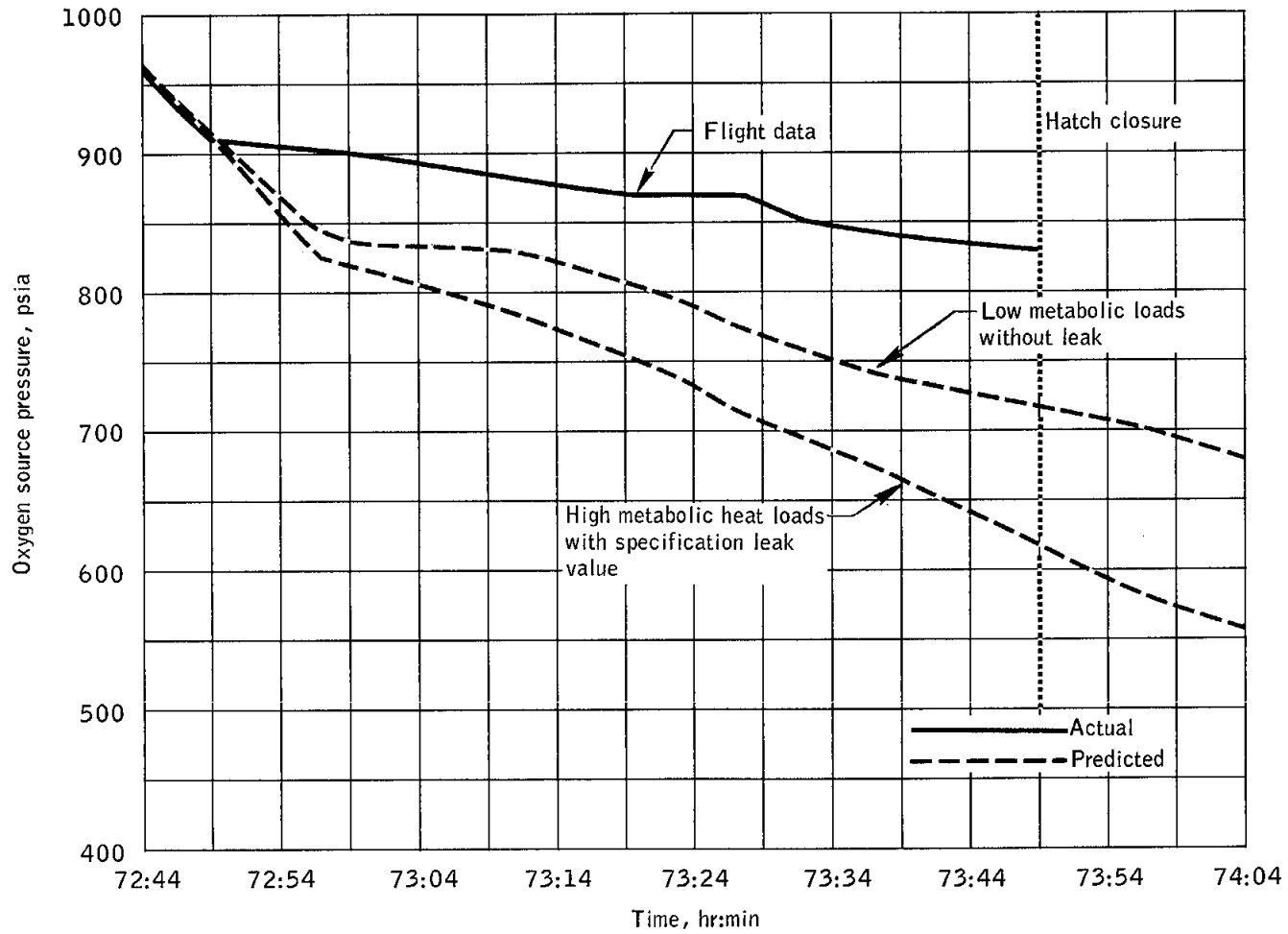


Figure 4-7.- Oxygen usage during extravehicular activity.



Figure 4-8.- Extravehicular lifeline.

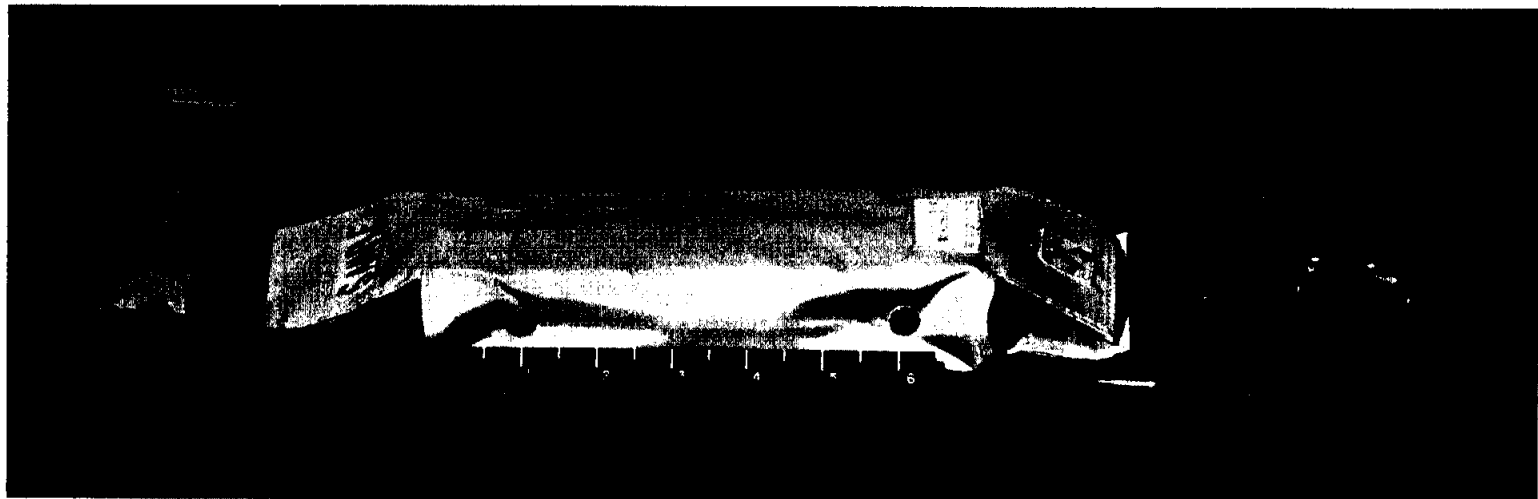


Figure 4-9.- Thermal sample tether.

## 5.0 RENDEZVOUS AND DOCKING OPERATIONS

All aspects of the rendezvous and docking operations have been evaluated and are discussed in detail in this section.

The rendezvous operation planned for Apollo 9 was to verify lunar module hardware, software, and procedures in earth orbit as preliminary qualification for operations in lunar orbit. The rendezvous flight plan consisted of a series of translational maneuvers that progressively increased the separation distance between the command and service modules and the lunar module through several decision points and culminated in execution of the coelliptic flight plan. The orbit prior to undocking was intended to be 130 miles circular, but was actually 122 by 127 miles. This variation presented no problems for either systems or procedures; however, an adjustment in the bias time for the terminal phase initiation time from 3 minutes to 4 minutes was made before starting the rendezvous. Computer solution times used in this section are based on Real Time Computer Complex time, which was 1.07 seconds earlier than range zero.

Flight plans and procedures generated prior to the mission were followed closely by the crew throughout the rendezvous. Overall mission planning, procedures development, and crew training for the Apollo 9 mission resulted in a well integrated flight plan that was executed proficiently by the crew and ground support teams. The implications of all decisions required during the mission had been thoroughly considered prior to flight, resulting in a definite set of guidelines for priority of solutions to be used for each maneuver. The guidance and navigation systems performed as planned, and all first priority maneuver solutions were used.

Apollo rendezvous plans have evolved from principles and experience gained during the Gemini Program, in which 10 rendezvous operations were performed to investigate effects of mission variables and to develop ground and onboard procedures (see references 1 and 2). Although Apollo systems and mission profiles differ from those of Gemini, the concepts of coelliptical approach to the terminal phase, terminal phase maneuver logic, and manual backup procedures are all applicable. The primary difference between the Gemini and Apollo rendezvous plans is in the maneuver logic prior to the terminal phase (see figure 5-1). Gemini used a two-impulse maneuver sequence to reach a fixed point, whereas Apollo uses a horizontal phasing maneuver followed by a coelliptical maneuver prior to the terminal phase. These maneuvers could not be computed by Gemini onboard equipment as they are in Apollo.

## 5.1 MISSION PLANNING ASPECTS

The major requirements imposed on the rendezvous flight plan were as follows:

(a) After undocking, the command and service modules were to be inserted into a small (maximum range 2.8 miles) equiperiod orbit similar to that planned for the lunar landing prior to descent orbit insertion.

(b) One-half orbit after initiation of the small equiperiod orbit, a descent engine insertion maneuver was to be made to place the lunar module into a larger equiperiod orbit. A return to the command module was possible from this orbit by a terminal phase initiation maneuver with an equivalent differential altitude of 10 miles.

(c) Sufficient network tracking was required prior to each maneuver to permit a ground solution to be computed and sent to the crew.

(d) Use of coelliptic flight plan maneuver logic was required for the lunar-module-active rendezvous. The coelliptic flight plan is defined as a series of four basic maneuvers: coelliptic sequence initiation, constant differential height, terminal phase initiation, and terminal phase final. The coelliptic sequence initiation maneuver is constrained to be horizontal at a fixed time so as to arrive at a desired line-of-sight elevation angle at a preselected time. The constant differential height maneuver for Apollo 9 was planned to occur at the first apsidal crossing after coelliptic sequence initiation. Terminal phase initiation is targeted to occur at a fixed line-of-sight elevation angle, which was 27.5 degrees for Apollo 9. The terminal phase initiation maneuver was planned to occur 25 minutes prior to sunrise to meet lighting constraints (reference 3). The terminal phase final maneuver is the impulsive braking at the intercept point located 130 degrees of target-orbit travel after initiation of the terminal phase.

It was intended that the Apollo 9 rendezvous verify in earth orbit many of the maneuvers, computer programs, control modes, and procedures planned for lunar missions. The sequence of events for the coelliptic flight plan in earth and lunar orbits are quite similar, as shown in table 5-1 and figure 5-2, which compare the Apollo 9 trajectories and events with a lunar profile.

The mission planning rationale for each of the major Apollo 9 rendezvous maneuvers between undocking and final braking is summarized in the following paragraphs.

### 5.1.1 Initial Separation

The initial separation of the vehicles was to be achieved by a 5-ft/sec impulse directed radially downward using the service module reaction control system. This maneuver provided additional time for alignment of the inertial measuring units in both vehicles and for systems checks without requiring the crewmen to devote their attention to formation flying. The separation distance chosen was large enough to permit adequate verification of rendezvous radar operation but small enough to permit return to the command module, if required, without additional guidance information. A decision point was established before committing to the larger separation distance inherent in the phasing orbit.

### 5.1.2 Phasing Orbit

The purpose of the phasing orbit was to produce a vertical separation distance from which either the full coelliptic flight plan or a safe return to the command module could be made following checkout of the descent propulsion system, abort guidance system control, and rendezvous navigation. The phasing maneuver was to be targeted from the ground and performed radially upward to produce an equiperiod orbit from which either the insertion maneuver or a terminal phase abort maneuver could be made.

### 5.1.3 Insertion Maneuver

The insertion maneuver was designed to produce a coelliptical orbit with the lunar module above and going away from the command module. It was to be computed on the ground to provide sufficient separation distance for execution of the coelliptic flight plan. Following the insertion maneuver, no further decision points were defined, since the easiest return was to complete the primary mission.

### 5.1.4 Coelliptic Sequence Initiation

The coelliptic sequence initiation maneuver is computed both onboard the lunar module using stored navigation state vectors and by the ground. The maneuver logic is to determine the horizontal velocity increment required at a preselected time to bring the lunar module at the desired conditions for transfer to an intercept trajectory.

### 5.1.5 Constant Differential Height Maneuver

The constant differential height maneuver is computed by the lunar module and by the ground. The maneuver logic is to determine the horizontal and vertical velocity increments required to make the orbits coelliptic at the first apsidal crossing after coelliptic sequence initiation.

This maneuver aligns the semi-major axes of the orbits and equalizes the differential altitudes at perigee and apogee. The nominal value of the differential altitude for Apollo 9 was selected to be 10 miles.

### 5.1.6 Terminal Phase

The terminal phase is defined as the period between the terminal phase initiation maneuver and final braking. The terminal phase initiation maneuver is the first point in the coelliptic flight plan that attempts to place the lunar module on an intercept trajectory. Although the coelliptic sequence initiation maneuver is targeted to provide a line-of-sight elevation angle to the command module of 27.5 degrees at a preselected time, trajectory dispersions and uncertainties will cause shifts in the time of arrival. The onboard programs provide the capability to initiate the terminal phase on either time or elevation angle. However, the elevation angle option is selected so as to more nearly standardize the time histories of range, closing velocity, and line-of-sight angular drift during the terminal phase. The maneuver logic computes the incremental velocity required to intercept the target in a specified length (130 degrees) of orbital travel.

Midcourse corrections are planned following navigation updating of onboard state vectors. These corrections are included to remove trajectory dispersions and guarantee a fixed arrival time of intercept.

## 5.2 TRAJECTORY DETERMINATION

Several hours prior to undocking for rendezvous, a maneuver plan was generated based on the actual orbit to meet the required lighting conditions at terminal phase. The lighting constraint on the terminal phase initiation maneuver was that it should occur 25 minutes prior to sunrise. In the preflight operational trajectory (reference 4), this point occurred at 97:59:53, but in real time occurred at 97:56:23. Hence, the timeline was advanced by about 3 minutes and maneuvers were retargeted to place terminal phase initiation in the correct position.

Along with the planning for a nominal rendezvous, the abort and rescue procedures were verified, the rendezvous maneuver biases were recomputed, and a simulation of the onboard computation of the coelliptic flight plan was performed. As a result, the onboard terminal phase initiation bias time was changed from 3 to 4 minutes.

Table 5-II shows the maneuvers for the nominal plan, as well as the ground, onboard, actual, and best-estimated trajectory solutions. Figure 5-3 shows the relative motion between the lunar module and command module. Figure 5-4 shows the ground track during the rendezvous.

At 93:02:54, the first maneuver of the rendezvous profile was executed with the service module reaction control system so that 45 minutes later the lunar module would be trailing the command module by 2.8 miles. However, the best estimated trajectory shows this trailing distance was only 2 miles, indicating that some small dispersions were acquired either during station-keeping or as a result of the separation maneuver.

The first lunar module rendezvous maneuver was executed at 93:47:35 with the descent propulsion system under abort guidance control. This maneuver placed the lunar module in a near equiperiod orbit with apogee and perigee altitudes approximately 12.2 miles above and below that of the command and service modules orbit. The phasing maneuver was ground computed prior to the rendezvous.

The next maneuver was not applied, since it was to be used only in case of a contingency requiring a lunar module abort. The computation of this maneuver, however, provided verification of the trajectory and the performance of the onboard guidance system. The rendezvous was designed so that an elevation angle of 27.5 degrees existed between the lunar module and command module at the time of abort (94:57:53) in the phasing orbit. The lunar module computer solution showed an elevation angle of 28.85 degrees compared with the ground solution of 29.9 degrees. This difference, as well as the differences between the velocity components of this maneuver (table 5-II), were well within permission tolerances, indicating the systems were performing as expected.

The third rendezvous maneuver was executed at 95:39:08 and resulted in a lunar module orbit of 138.9 by 133.9 miles. The maneuver was executed with the descent propulsion system under primary guidance control and from all indications was nearly perfect. This insertion maneuver established coelliptic orbits providing a height differential of about 12.2 miles.

Following insertion, the coelliptic flight plan was computed both onboard and by the ground. At this time, some doubt existed as to the correct apsidal crossing number to use for onboard execution because of

a misread display on the ground. The solution computed onboard using the first apsidal crossing provided the correct maneuver values, whereas the solution for the second crossing recommended by the ground required a rendezvous from above with a height differential of about 12 miles, instead of the nominal 10 miles below the target. The crew elected to use the first apsidal solution, in accordance with the flight plan, and figure 5-5 shows the relative motion for both of these solutions. See section 5.3.1 for further discussion.

Table 5-II indicates the differences in the predicted time of the constant differential height maneuver between the ground, onboard, and best estimated trajectory. Because of a tolerance constraint on eccentricity, the ground procedures were to compute a solution for this maneuver prior to coelliptic sequence initiation based on a time corresponding to a position 180 degrees after coelliptic sequence initiation. The onboard solution and the best estimated trajectory are based upon a constant differential height maneuver occurring at the first apsis after coelliptic sequence initiation. Since the onboard and ground solutions for coelliptic sequence initiation agreed within the preflight tolerances, the onboard solution was used. A bias of 0.7 ft/sec was added to the Z-axis component of the maneuver to account for the effects of reduced weight after staging on the firing duration.

Following coelliptic sequence initiation, the crew passed their constant differential height maneuver time to the ground, and this solution was used for comparison checks. Table 5-II shows the solutions obtained based upon the onboard constant differential height maneuver time. It should be noted in considering the validity of these solutions that very little ground coverage existed between the coelliptic sequence initiation and constant differential height maneuvers. The onboard solution was verified to have been used for the latter maneuver.

The flight crew and ground controllers computed the terminal phase initiation solution (table 5-II) based upon a 27.5-degree elevation angle. All solutions agreed within 15 seconds, and the best estimated trajectory and guidance computer solutions exactly agree, indicating onboard systems were performing as expected. The actual terminal phase initiation time was 1 minute 36 seconds later than the nominal time. This difference could have resulted from errors in either the coelliptic sequence initiation or constant differential height maneuvers, or both. For example, either a horizontal error of about 0.6 ft/sec in the constant differential height maneuver or an error of about 0.3 ft/sec at coelliptic sequence initiation could cause this time difference.

The onboard solution for terminal phase initiation was executed at 97:57:59, creating a lunar module orbit of about 126 by 113 miles. At 10 minutes after terminal phase initiation, the first midcourse correction

of less than 1 ft/sec in each axis was executed. The second midcourse correction was performed about 22 minutes after terminal phase initiation and was also a very small maneuver.

Following the midcourse maneuvers, the lunar module entered the braking phase. Because of scant network coverage during the terminal phase, a best estimated trajectory is not available for a thorough evaluation of the braking. However, based on the theoretical velocity changes and propellant used, braking was satisfactory.

### 5.3 CREW PROCEDURES

#### 5.3.1 Lunar Module

The lunar module rendezvous procedures began immediately following undocking and ended at the initiation of station keeping. These procedures are contained in reference 5 and were followed very closely throughout the rendezvous.

Separation.- Undocking was attempted at 92:38:00, with the Command Module Pilot reporting that the capture latches had not released. (See section 17 for a discussion of this problem.) Since the undocking was to be performed without attitude control in either vehicle, the combined spacecraft drifted away from the desired undocking attitude while the Command Module Pilot was troubleshooting. At 92:39:36, undocking was accomplished; however, the spacecraft were approximately 10 degrees per axis away from the planned attitude.

After receiving clearance from the command module to maneuver, the lunar module was to have initiated a 120-degree right yaw designed to place the lunar module X-Z axes in the plane of the command module X-Z axes. This plan was altered by the Commander, who terminated the yawing maneuver when the lunar module X-Z axes were in the orbital plane. The command module was then maneuvered to the correct relative position with respect to the lunar module. Because of the extra time consumed by these unplanned activities, the 180-degree pitch maneuver to point the lunar module minus X axis toward the command module for descent engine photography was reduced to a 90-degree maneuver to place both spacecraft "eye-to-eye." Attitudes during this period had been selected to provide proper lighting during the lunar module inspection. From the "eye-to-eye" position, the lunar module initiated a 360-degree yaw maneuver for landing gear inspection. At that point, the timeline and procedures returned to nominal. At 93:02:54 the command module performed a 5-ft/sec maneuver directed radially downward to achieve a safe separation distance.

Phasing.- After rendezvous radar operation was verified, the antenna was positioned clear of the alignment optical telescope field of view and turned off. While awaiting sunset, external delta V (program 30) was loaded with the phasing maneuver and the event timer set counting down.

An inertial measurement unit alignment (program 52) was initiated just prior to sunset using the center forward detent position and stars Sirius and Acrux. Before terminating program 52, the crewman optical alignment sight was calibrated and found to be pointing 0.5 degree to the left of the plus Z axis. Rendezvous radar acquisition was then performed manually, and an update and alignment of the abort guidance system was accomplished in preparation for the phasing maneuver.

The guidance mode was switched to abort-guidance-system control about 3 minutes prior to ignition. At 93:47:35, preceded by an 8-second propellant settling maneuver, the descent engine firing was initiated for the phasing maneuver. After 4 seconds at 10-percent thrust, the throttle was advanced toward 40 percent. At about 27 percent, the engine was reported to be rough and throttle changes were terminated until smooth operation was achieved. (See section 17 for a discussion of this problem.) The throttling to 40 percent was then completed, and the remainder of the firing was smooth. The primary navigation and guidance system velocity residuals were nulled with the reaction control system without difficulty after descent propulsion system shutdown.

Terminal phase initiation for abort.- When the range had increased to 19 000 feet, rendezvous navigation (program 20) and terminal phase targeting (program 34) were initiated. The first two marks taken by program 20 resulted in the 3-degree alarm. Beyond this point, no additional alarms occurred throughout the rendezvous. Terminal phase initiation targeting used the time option of program 34, and the resulting solutions were very close to nominal. This maneuver was not planned to be performed in the nominal mission, but solutions were obtained to verify guidance system operation and to provide the information required for the lunar module to return to the command module if an abort during the phasing orbit had been necessary.

Insertion.- After receiving approval at 95:20:00 to continue with insertion, final computations in program 34 were made, and the inertial measurement unit realignment was completed within the allotted time. A reacquisition of the rendezvous radar in program 20 was accomplished, followed by the incorporation of three marks into the state vector prior to reaching a separation distance of 19 000 feet.

Updating was then terminated until past the closest approach, which was reported to be 16 000 feet. An additional three marks were taken after the range had increased to 19 000 feet prior to the insertion maneuver. Insertion was executed at 95:39:08 following a standard use of the program-30/program-40 sequence.

Coelliptic sequence initiation.- Onboard computation of the coelliptic flight plan sequence (program 32) was initiated following the insertion maneuver, with input times of 96:16:03 for the time of coelliptic sequence initiation and 98:00:23 for the time of terminal phase initiation. This latter time was biased 4 minutes later than nominal to compensate for guidance computer conic advancement and impulsive thrust (instantaneous velocity change) assumptions in the coelliptic flight plan software. The biasing was necessary because the onboard software used Keplerian orbits (conic) and instantaneous velocity changes to simplify and expedite maneuver targeting. The elevation input at terminal phase initiation was a nominal 27.5 degrees.

The weighting matrix initialization and first recycle in program 32, scheduled to take place after four rendezvous-radar updates, were overlooked by the crew. Approximately 3 minutes later, ground controllers advised the crew of the oversight, and the initialization was performed after seven updates. Subsequently, following a request from the crew for the correct apsidal crossing to use in the coelliptic sequence initiation program, the ground recommended the second rather than the preplanned first crossing because of an oversight in reading a ground display. The oversight was soon corrected, but after the spacecraft had passed out of station coverage. On the final computation cycle in program 32 using the second apsidal crossing, the solution obtained was 85 ft/sec in both the primary and abort guidance systems, compared with a prior ground estimate of 39.3 ft/sec.

Based on this information, program 32 was retargeted using the first apsidal crossing, and the proper solution was obtained. Because of the time used in the retargeting, the crew was unable to enter the backup chart for coelliptic sequence initiation or to retarget the abort guidance system for the chosen first apsidal crossing. However, all the data required for the chart were logged, and postflight examination showed the chart solution to be 40.7 ft/sec, which compared quite closely with the 40.0-ft/sec solution obtained by the primary navigation and guidance system. Although the ground error in recommending an apsidal crossing parameter would have been of little consequence other than deviating from the preflight plan, the rapid and perceptive response by the crew in diagnosing and correcting the oversight indicates a high level of preparation and proficiency. As shown in figure 5-5 use of the second apsidal crossing would technically have resulted in a successful rendezvous, but from above rather than below. Table 5-III contains a summary of all solutions computed onboard the lunar module during the rendezvous.

After various pre-staging checks were completed, coelliptic sequence initiation was performed at 96:16:06, with the descent stage being jettisoned immediately after the start of reaction control system thrusting.

The ascent propulsion system interconnects were opened during the coelliptic sequence initiation maneuver, as planned, to conserve reaction control system propellant. The crew reported that a stuck indicator caused some concern when the ascent propulsion system interconnects were closed. Based on ground test experience, sticking of indicators was known to be a potential problem.

Constant differential height maneuver.- After coelliptic sequence initiation, rendezvous radar tracking was re-established, but the command module was unable to acquire the lunar module tracking light. (See section 17 for a discussion of this problem.) The constant differential height time computed in program 22 was 96:56:29, which was then biased late by 1 minute 45 seconds to 96:58:14 as an additional compensation for the conic assumption. Solutions in the constant differential height program (program 33) confirmed the differential height to be near 10 miles and terminal phase initiation time to be only about 30 seconds later than nominal (97:56:23). Agreement between all solutions for this maneuver was within about 1 ft/sec.

Midway in time between coelliptic sequence initiation and the constant differential height maneuvers, the maximum range of 98 miles was observed. The constant differential height maneuver was performed on time using the ascent propulsion system. All velocity residuals were nulled to zero with reaction control thrusting.

Terminal phase initiation.- Following the constant differential height maneuver, the radar reacquired the command module, and the terminal phase initiation program (34) was entered. As the mission developed in real time, the coelliptic phase was about 4 minutes longer than planned, causing slight deviations from the nominal procedures.

Updating of the abort guidance system with radar information proved to be easier than anticipated. However, the crew reported much more variation in the abort guidance system solutions than expected, with deviations of up to  $\pm 3$  ft/sec about the mean.

Solutions from the primary guidance system indicated a trend in the time of terminal phase initiation to increase; the final solution was given as 97:57:59, or 1 minute 36 seconds later than nominal. All other solution sources checked within expected limits. After maneuvering to the terminal phase initiation attitude, the crew noticed the signal strength of the radar decreasing rapidly. After reaching a low point, the signal strength then began to increase steadily to the value previously indicated. This behavior was subsequently determined to be the result of the command module maneuvering to its inertial firing attitude which placed the line-of-sight to the lunar module approximately 20 degrees above the command module plus X axis, a position in which the transponder return signal is greatly reduced.

Terminal phase initiation was executed using the reaction control system with the lunar module Z-axis pointing toward the command module. All velocity components were then nulled to zero.

Midcourse corrections.- All procedures after the terminal phase initiation maneuver were carried out exactly as planned, with the midcourse corrections occurring 10 and 22 minutes afterwards. These maneuvers were less than 2 ft/sec in any axis and were within expected values.

Braking.- Braking was executed following the planned schedule. At 6000 feet, no maneuver was required as the closing rate was less than the imposed maximum of 30 ft/sec. At a range of 3000 feet, the closing velocity was reduced to 20 ft/sec using the minus-Z thrusters. At 1500 feet, the closing velocity was further reduced to 10 ft/sec, and at 500 feet to 5 ft/sec. Very small corrections normal to the line-of-sight were also required. The lunar module then coasted to within 100 feet of the command module, and the relative velocities were nulled in preparation for docking.

Propellant consumption.- Reaction control system propellant consumption during rendezvous, presented in figure 9.7-5, was approximately 280 pounds, as compared to the budgeted value of 400 pounds. Most of this difference can be attributed to three factors:

- a. The mission was close to nominal during the terminal phase and the midcourse maneuvers were very small and little line-of-sight control was required. Therefore, about 100 pounds were used compared to 160 pounds budgeted.
- b. Extensive use by the Commander of minimum-impulse attitude control, particularly during the phasing orbit, resulted in less than 10 pounds of propellant required, compared with 22 pounds predicted.
- c. Lower-than-expected thruster activity during the two descent engine firings resulted in a consumption approximately 25 pounds less than expected.

### 5.3.2 Command Module Procedures

Command module power-up procedures began prior to undocking with completion of a checklist for guidance and control switch positions, which included activation of the computer and inertial measurement unit. A ground uplink was made of state vectors, computer clock synchronization, and a reference matrix, which provides a nominal platform orientation at terminal phase initiation.

Alignments.- Prior to undocking, the orientation determination program (51) for the inertial measurement unit was executed. A fine alignment to the preferred orientation was performed using the realign program (52). The automatic star-selection and optics-positioning routines were used for each fine alignment, and a fine-align check using a third star was also made. Following the initial alignment, the Command Module Pilot aligned the gyro display coupler to the inertial measurement unit, and initialized the orbital rate drive to the local vertical using altitude and angle information. The command module was maneuvered to the inertial undocking attitude at 92:22:00. Subsequent to undocking and the separation maneuver, a realignment to the reference stable-member matrix, using program 52, was completed at 93:14:00 in daylight. After sunset, the crewman optical alignment sight was calibrated using Aldebaran, which was about 10 degrees from the lunar module. During darkness, another realignment to the reference stable member matrix was accomplished, subsequent to phasing, at 94:54:00.

Separation.- The vehicle was maneuvered automatically to the pre-determined undocking attitude using the digital autopilot. The spacecraft were undocked at 92:39:36, and the required station keeping maneuvers were performed for an inspection of the lunar module.

The targeting for the separation maneuver using the reaction control system was performed by loading the desired incremental velocities into the computer. The maneuver was made using four thrusters, and the delta V counter indicated that 5.2 ft/sec had been applied.

Phasing monitor.- The crew-defined maneuver was executed to orient the preferred tracking axis at the lunar module for radar checks at close-range. Automatic tracking was initiated at 93:20:00 and was performed within 1 degree of the center of the optical alignment sight. The elapsed time from separation was recorded at 10 degrees before the horizontal crossing. Nominally, the 10-degree point should have occurred at separation plus 35 minutes, but it occurred 3 minutes 7 seconds earlier than expected. An analysis of arrival time versus errors at separation indicates that a 0.38-ft/sec posigrade velocity error can cause this early arrival time as shown in figure 5-6. The horizontal adjustment chart solution to put the command module back on an intercept trajectory was 0.85 ft/sec vertically up and 0.4 ft/sec horizontal posigrade.

The descent propulsion system phasing maneuver was initiated at 93:47:35. The command module lined up on the local horizontal, and in the event of failure of the phasing maneuver, the horizontal adjustment chart solution was to be applied using the reaction control system.

Terminal phase initiation for abort.- Automatic preferred-attitude tracking was initiated, and eight sextant navigation marks were taken. All navigation marks were used to update the lunar module state vector.

The terminal phase initiation pre-thrust program was executed and the nominal terminal phase initiation abort time was loaded. The program was recycled, and four solutions were obtained for comparison of solutions (table 5-IV.) The solutions from the command module and lunar module guidance computers compared within 0.1 degree in elevation angle, less than 0.5 ft/sec in X-axis velocity, and about 1.5 ft/sec in Z-axis velocity.

Insertion monitor.- The decision was made to proceed with insertion, and the platform was realigned to the reference matrix. The command module was maneuvered for tracking of the lunar module to monitor the flyby. The lunar module was maintained within 1 degree of the center of the optical alignment sight. The closest approach occurred at a ground elapsed time of 95:17:00.

Coelliptic sequence initiation monitor.- After the insertion maneuver, the Command Module Pilot selected the rendezvous navigation program (20) and initiated an automatic maneuver to the preferred attitude for pointing the sextant at the lunar module. The sextant navigation process was performed according to the checklist, with no problems. Data were taken to compute the onboard coelliptic sequence initiation backup solution. This solution, if it had been computed, was 40.3 ft/sec, as compared with the lunar module solution of 40.0 ft/sec. A mirror image maneuver was targeted and would have been performed if the lunar module had been unable to execute the coelliptic sequence initiation maneuver. It was scheduled to occur 1 minute after the lunar module execution time of 96:16:06.5.

Constant delta height maneuver monitor.- An automatic attitude maneuver of approximately 180 degrees was made to track the lunar module. However, there was no light visible in the sextant, and the lunar module crew reported no flash from their reaction control quads. The Command Module Pilot maintained the preferred tracking axis pointed at the lunar module to hold radar transponder coverage. The range and range-rate data were compared with the lunar module data at the horizontal crossing, and agreement was very good. Two backup pads for the constant differential height maneuver were received. The service-propulsion-system thrust program was selected, and an automatic maneuver to the thrust attitude was made. The command module was targeted with the mirror image maneuver for 1 minute later.

Terminal phase initiation targeting.- Following the constant differential height maneuver, the rendezvous navigation program was selected to provide preferred attitude tracking for sextant navigation. An automatic attitude maneuver of approximately 180 degrees was made, and the lunar module appeared about 1/2 degree from the center of the reticle. After about an hour, the first three sextant marks were made, and the weighting matrix was reinitialized for five additional marks. At the

conclusion of the first mark period, the state vector comparison was very good. The terminal phase initiation targeting program was selected after taking the marks, and a solution was computed based upon a terminal phase initiation elevation angle of 207.5 degrees. Two additional scheduled marking periods of five marks were accomplished, and two extra marking periods were taken. The terminal phase initiation was monitored by targeting a mirror-image maneuver. The lunar module state vector was updated with the terminal phase initiation data. The solutions obtained by the command module computer are presented in table 5-IV.

Midcourse maneuver backup.- The command module procedures from terminal phase initiation to terminal phase final were modified from nominal because the lunar module tracking light was not working. This failure prevented the Command Module Pilot from taking navigation marks to update the state vector. Even though no marks were taken, the terminal phase maneuver pre-thrust program was selected, and a midcourse solution was calculated to check program operation. The computer obtained a small correction comparable in magnitude to the lunar module solution. At a range of 3 miles and again at 1.5 miles, the command module and lunar module values of range and range rate compared favorably, indicating the state vectors were in close agreement. An automatic maneuver was made in the rendezvous navigation program to point the X-axis of the command module at the lunar module. When the lunar module appeared in daylight, it was visible all the way to station-keeping, even against the earth background.

Braking monitor.- Lunar module braking was monitored, and velocity corrections normal to the line of sight were monitored using the thrust-monitor program. After sunrise, the lunar module was tracked by the Command Module Pilot using the diastimeter.

The diastimeter (fig. 5-7) is an optical device used to measure the distance to a target of known dimensions, such as the lunar module. The device is mounted in the command module window and uses a split image to determine range in terms of the angle subtended by the target. It was carried on this mission as a backup ranging device to the rendezvous radar for the last 3 miles of the terminal phase. The crew reported performance of the diastimeter was as predicted.

Propellant consumption.- Utilization of service module reaction control system propellant was somewhat higher than expected, as illustrated in figure 8.7-2. Approximately 100 pounds of propellant was used between lunar module undocking and docking, as compared with the predicted value of 50 pounds. The difference results primarily from the preflight assumption of minimum-impulse attitude control utilization during the lunar module tracking; whereas automatic tracking in the lunar module minimum deadband mode was used inflight, as specified by actual flight procedures. The digital autopilot was used in the automatic mode throughout rendezvous for all attitude changes, including those for lunar module tracking, to minimize the workload and facilitate use of the sextant. Attitude con-

trol propellant estimates for subsequent missions should therefore be based on using the automatic control modes.

#### 5.4 GUIDANCE, NAVIGATION, AND CONTROL

Onboard navigation throughout the rendezvous was performed autonomously, with no state vector updates required from the ground. A final comparison of the onboard vectors with those from the best estimated trajectory is not yet available; however, preliminary indications are that the state vector update process in both vehicles was satisfactory. The lunar module radar and command module sextant sighting histories are shown in figure 5-8. The periods of ground coverage are also indicated. The loss of the lunar module tracking light during the coelliptic sequence initiation maneuver prevented sextant updates until after the constant differential height maneuver.

The sensor/computer interface, data incorporation routines, and the recursive navigation process were thoroughly demonstrated in both vehicles. Table 5-V contains the results of a preliminary analysis showing the effect of radar data incorporation on the onboard state vector. The comparison was made between the two coelliptic flight plan maneuvers during a 30-minute period in which 17 radar marks were incorporated. The lunar module onboard state vectors for both vehicles at the beginning of the period were integrated forward, without radar updates, to the time of the last available downlink state vector prior to the constant differential height maneuver. The relative range and range rate were then computed for the improved and unimproved state vectors and compared to those from the best estimated trajectory. The result shown in table 5-V indicates that the radar data causes the relative state vector to approach that from the best estimated trajectory.

Figure 5-9 contains time histories of the relative range and range rate from the rendezvous radar, the command module computer, and the best estimated trajectory. Command module data are transmitted on the downlink only when requested by the crew; therefore, only a few points are available. The comparisons from both systems appear satisfactory, however.

Guidance and control system support of the rendezvous was nominal for both vehicles, and all necessary capability was available. Inertial component stabilities in the platforms of both spacecraft and in the lunar module abort sensor assembly were well within the required limits. The various attitude reference alignments were sufficiently accurate to have no measurable effect on the targeting. All computer programs and routines performed properly and provided the necessary capability to the crew.

The digital autopilot was used in both vehicles throughout the rendezvous sequence for attitude and translation maneuver control. Automatic attitude control for pointing of the radar and optics was utilized extensively and operated satisfactorily.

## 5.5 VISIBILITY

Successful rendezvous and docking depended upon several types of visual sightings from both vehicles. The relative positions of the vehicles during some of the more important sighting events are shown in figure 5-10. All required visual sightings were performed satisfactorily with the two following exceptions.

Failure of the lunar module tracking light during the coelliptic sequence initiation prevented the command module navigation update between this maneuver and the constant differential height maneuver. Subsequent to the latter maneuver, daylight sextant marks were taken to reduce sufficiently the state vector uncertainties and obtain a valid terminal phase initiation solution. This failure was not critical, because the lunar module guidance systems performed adequately and command module maneuvers were not required. Therefore, the primary effect of the light failure was to prevent command module verification of acquisition and track in darkness at ranges up to 100 miles.

The lunar-module-active docking required use of the crewman optical alignment sight, mounted in the overhead window, for alignment with the docking target. Because the docking was conducted in daylight, reflection from the command module obscured the reticle pattern, even at the maximum brightness setting (see section 17 for further discussion). This deficiency substantially increased the time required for docking; however, the Commander was able to complete the maneuver.

## 5.6 DOCKING OPERATIONS

The command module performed initial docking to the lunar module after transposition, and all operations were performed as expected. Lunar module docking was performed after rendezvous and is discussed below.

The rendezvous terminal phase was completed, and formation flying was begun at about 98:33:00, soon after sunrise. The crew decided to dock as soon as possible after rendezvous to provide longer daylight in event of a docking difficulty. During preparation for docking, the docking probe EXTEND/RELEASE switch was placed to the RETRACT position, but the probe position indicators did not read properly, so the crew recycled the switch to obtain proper indications (see section 17 for further discussion). Because of this discrepancy, confidence in the probe configuration was reduced, and the crew decided to perform probe retraction manually, rather than automatically as specified in the checklist. As discussed previously, the reticle of the crewman optical alignment sight

was washed out by sunlight reflection from the command module; however, the Commander performed an excellent docking aided by position reports from the Command Module Pilot.

Capture and retraction were nominal at 99:02:26, and all docking latches engaged properly with only a 0.2-degree ring angle error. The extend latch did not engage the roller on the probe piston, as was indicated by the extend latch indicator. This is a normal condition for the second docking. Four strokes on the preload handle were necessary to completely engage the extend latch. The requirement to manually engage the extend latch is specified in the docking tunnel checklist.

The docking system performed as required for the command module and lunar module docking events. Although the docking hardware was not instrumented, the indicated initial contact conditions would result in minimal loading of the probe and drogue. The following information concerning the two dockings is based on an analysis of onboard film and crew comments.

	Transposition docking	Lunar-module- active docking
Axial velocity at contact, ft/sec . . . . .	0.3	<0.1
Lateral velocity at contact, ft/sec . . . . .	0	--
Angular velocity at contact, ft/sec . . . . .	0	--
Angular alignment at contact, deg . . . . .	0	--
Miss distance at contact, in. . . . .	3.2	--
Initial contact to capture time, sec . . . . .	<1	7
Retract time, sec . . . . .	10	5
Ring contact velocity, ft/sec . . . . .	0.07	--

## 5.7 GROUND SUPPORT OPERATIONS

Ground support during the rendezvous centered around acquisition and processing of network tracking data to obtain maneuver solutions and monitoring the status of onboard systems from telemetry data. A nominal maneuver table was obtained before undocking for the spacecraft orbit that existed at the start of rendezvous. In addition to the nominal mission, all rendezvous abort maneuvers and resulting trajectories were determined. The initial orbit was off nominal at 122 by 127 miles and required another computation of the bias times for use in the onboard

program used to calculate the coelliptic sequence initiation maneuver. The new bias was computed to be 4 minutes, instead of the 3-minute value corresponding to the preplanned 130-mile circular orbit.

During the rendezvous, network tracking data were incorporated into the ground state vectors, and all maneuvers through terminal phase initiation were computed and sent to the crew. The ground solutions for the phasing and insertion maneuvers were executed, since no onboard targeting capability exists. The range at closest approach in the phasing orbit was determined in real time to be 1.3 miles after the phasing maneuver, 1.9 miles with half the data from the pass over the continental United States, and 2.7 miles following incorporation of all tracking data. The insertion maneuver was computed while the vehicle was in the phasing orbit and included all stateside tracking data. After the insertion maneuver, the coelliptic-flight-plan maneuvers were computed and transmitted to the crew. The computed time of coelliptic sequence initiation was 96:16:03.6, compared with the nominal time of 96:17:01. The ground then computed maneuvers for the command module in the event a lunar module rescue became necessary. Ground computation of the coelliptic sequence initiation maneuver yielded 39.3 ft/sec, as compared with 40 ft/sec computed onboard the lunar module. The onboard solution was entered into the ground vector as the actual maneuver, and the time of the constant differential height maneuver agreed with the lunar module computation of 96:58:14. The ground-computed velocity components of the constant differential height maneuver agreed within 1.4 ft/sec in each axis. The final ground support was to determine a backup solution for the terminal phase initiation maneuver during the coelliptical orbit phase. The maneuver information transmitted to the crew was in close agreement with that calculated onboard.

TABLE 5-I.- APOLLO 9 AND LUNAR MISSION PROFILE COMPARISON

Mission	Coelliptic sequence initiation velocity, ft/sec	Constant differential height		Terminal phase initiation			Terminal phase orbital travel, deg	Terminal phase theoretical intercept velocity, ft/sec
		Horizontal velocity, ft/sec	Vertical velocity, ft/sec	Elevation angle, deg	Horizontal velocity, ft/sec	Vertical velocity, ft/sec		
Apollo 9	28.1	-39.2	-13.7	27.5	19.4	-9.7	130	40.0
Lunar mission profile	31.2	0.0	0.0	26.6	22.7	-10.6	130	50.5

TABLE 5-II.- SUMMARY OF RENDEZVOUS MANEUVERS

Parameters <sup>a</sup>	Lunar module guidance onboard solution	Command module guidance onboard solution	Ground	Pre-rendezvous nominal	Best-estimated trajectory	Actual target solution
Separation maneuver (service module reaction control system)						
Velocity change, ft/sec - X			0.0	0.0	0.0	0.0
- Y			0.0	0.0	0.0	0.0
- Z			5.0	5.0	5.0	5.0
Ignition time, hr:min:sec			93:02:53	93:02:53	93:02:54	93:02:53
Resultant apogee/perigee altitudes, miles			127/122	127/122		
Maximum horizontal trailing distance, miles				2.8	2.0	
Phasing maneuver (descent propulsion system, abort guidance control)						
Velocity change, ft/sec - X	-90.9		0.9	0.8		0.9
- Y	-1.2		0.0	0.0		0.0
- Z	-0.9		-90.7	-90.7		-90.7
Ignition time, hr:min:sec			93:47:36	93:47:36	93:47:35.4	93:47:36
Residual velocities, ft/sec - X						-0.9 <sup>b</sup>
- Y						-0.8 <sup>b</sup>
- Z						-0.6 <sup>b</sup>
Resultant apogee/perigee altitudes, miles			137/112	137/112	137/112	
Point of closest approach, miles			1.9	2.8	2.7	
Terminal phase initiation for abort						
Velocity change, ft/sec - X	-20.1	19.6	-20.2	-19.3	-20.0	
- Y	0.0	0.6	0.4	0.1	2.7	
- Z	1.8	-3.3	-1.5	7.0	3.4	
Time of abort maneuver, hr:min:sec	94:57:53	94:57:53	94:57:53	94:57:53	94:57:53	
Elevation angle, deg	28.85	28.75	29.9	27.5	28.3	
Abort time lighting, min before daylight	25	25	25	25	25	

<sup>a</sup>Velocity changes are shown in a local vertical coordinate system with X measured along the velocity vector, Z measured radially downward, and Y orthogonal to these.

<sup>b</sup>These velocities reflect values before residuals were trimmed.

TABLE 5-II.- SUMMARY OF RENDEZVOUS MANEUVERS - Continued

Parameters <sup>a</sup>	Lunar module guidance onboard solution	Command module guidance onboard solution	Ground	Pre-rendezvous nominal	Best-estimated trajectory	Actual target solution
Insertion maneuver (descent propulsion system, primary guidance control)						
Velocity change, ft/sec - X			43.1	42.7	43.7	43.1
- Y			0.0	0.0	0.0	0.0
- Z			0.8	-0.3	0.8	
Ignition time, hr:min:sec			95:39:07	95:39:07	95:39:08.1	
Residual velocities, ft/sec - X						-0.9
- Y						-0.8
- Z						-0.6
Resultant apogee/perigee altitudes, miles			139/134	139/134	139/134	
Differential altitude at insertion, miles			12.2	12.1	12.1	
Variation in differential altitude, miles				0.1	0.1	
Concentric sequence initiation (lunar module reaction control system with interconnect)						
Velocity change, ft/sec - X	-40.0		-39.3	-39.4	-40.0	-40.0
- Y	0.0		0.6	0.0	0.0	0.0
- Z	0.0		0.0	0.0	0.0	0.0
Ignition time, hr:min:sec	96:16:03		96:16:03	96:15:52	96:16:06.5	96:16:03
Resultant apogee/perigee altitudes, miles			138/113	138/113	138/113	
Differential altitude at ignition, miles				12.0	12.2	
Predicted time for constant differential height maneuver	96:58:14		97:00:32	96:57:44	96:57:55	
Constant differential height maneuver (ascent propulsion system)						
Velocity change, ft/sec - X	-39.2		-38.2	38.9	-39.9	-39.2
- Y	0.1		-0.9	0.0	0.0	0.1
- Z	-13.7		-15.1	-15.1	-14.4	-13.7
Ignition time, hr:min:sec	96:58:14		96:58:14	96:57:44	96:58:15	96:58:14
Residual velocities, ft/sec - X						-2.4
- Y						0.8
- Z						0.0
Resultant apogee/perigee altitudes, miles			117/113	117/111	116/111	
Differential altitude, miles			9.7	10.0	10.0	
Variation in differential altitude, miles			0.2	0.2	0.0	

<sup>a</sup>Velocity changes are shown in a local vertical coordinate system with X measured along the velocity vector, Z measured radially downward, and Y orthogonal to these.

TABLE 5-II.- SUMMARY OF RENDEZVOUS MANEUVERS - Concluded

Parameters <sup>a</sup>	Lunar module guidance onboard solution	Command module guidance onboard solution	Ground	Pre-rendezvous nominal	Best-estimated trajectory	Actual target solution
Terminal phase initiation (lunar module reaction control system)						
Velocity change, ft/sec - X	19.4	-19.5	19.6	20.0	19.5	19.4
- Y	0.4	-0.5	0.1	0.0	2.3	0.4
- Z	-9.7	9.0	-10.5	-10.6	-10.9	-9.7
Ignition time, hr:min:sec	97:57:59	97:58:08	97:57:45	97:56:23	97:57:59	97:57:59
Resultant apogee/perigee altitudes, miles			129/113	125/113	126/113	
Differential altitude, miles			9.8	10.2	10.0	
Elevation angle, deg	27.5	27.5	27.5	27.5	27.5	
Lighting at time of ignition, min:sec until day	23:24	23:15	23:29		23:24	
Targeted time of ignition, hr:min:sec	97:56:23	97:56:23	97:56:23	97:56:23		
Time slip of ignition, min:sec	1:36	1:42	1:22		1:36	
First midcourse correction (reaction control system)						
Velocity change, ft/sec - X	-1.0	-0.6				-1.0
- Y	-0.3	0.5				-0.3
- Z	0.9	-2.3				0.9
Ignition time, hr:min:sec	98:08:00					98:08:00
Second midcourse correction (reaction control system)						
Velocity change, ft/sec - X	0.2					0.2
- Y	0.9					0.9
- Z	-1.8					-1.8
Ignition time, hr:min:sec	98:20:03					98:20:20
Terminal phase braking (reaction control system)						
Theoretical velocity change, ft/sec - X			16.8	16.6	16.5	
- Y			-1.1	0.6	0.5	
- Z			23.2	23.7	22.8	
Total	27.8	29.3	28.7	28.9	28.1	
Time of theoretical intercept, hr:min:sec			98:29:51	98:28:59	98:30:03	
End of braking, hr:min:sec	98:33:50					
Time between theoretical intercept and end of braking, min:sec			3.59		3.47	

<sup>a</sup>Velocity changes are shown in a local vertical coordinate system with X measured along the velocity vector, Z measured radially downward, and Y orthogonal to these.

TABLE 5-III.- LUNAR MODULE SOLUTIONS

Maneuver	Solution, ft/sec		
	Primary guidance	Abort guidance	Backup charts
Coelliptic sequence initiation	40.0 horizontal, retrograde	(a)	<sup>b</sup> 40.7 horizontal, retrograde
Constant differential height	39.2 horizontal, retrograde 13.7 vertical, up	40.0 horizontal, retrograde 14.0 vertical, up	39.5 horizontal, retrograde 14.5 vertical, up
Terminal phase initiation	21.7 forward 0.3 down 0.5 right	20 at elevation angle of 23.46 deg	20 forward 1 down (c)
First midcourse correction	1.4 aft 0.1 up 0.4 left	(c) (c) (c)	6 aft 0.0 (c)
Second midcourse correction	1.8 forward 0.0 0.9 left	(c) (c) (c)	1 forward 0.0 (c)

<sup>a</sup>System not targeted for first apsidal crossing at coelliptic sequence initiation because of lack of time.

<sup>b</sup>Solution computed postflight with data taken by crew during mission.

<sup>c</sup>No solution computed.

TABLE 5-IV.- COMMAND MODULE SOLUTIONS

(a) Abort from phasing orbit

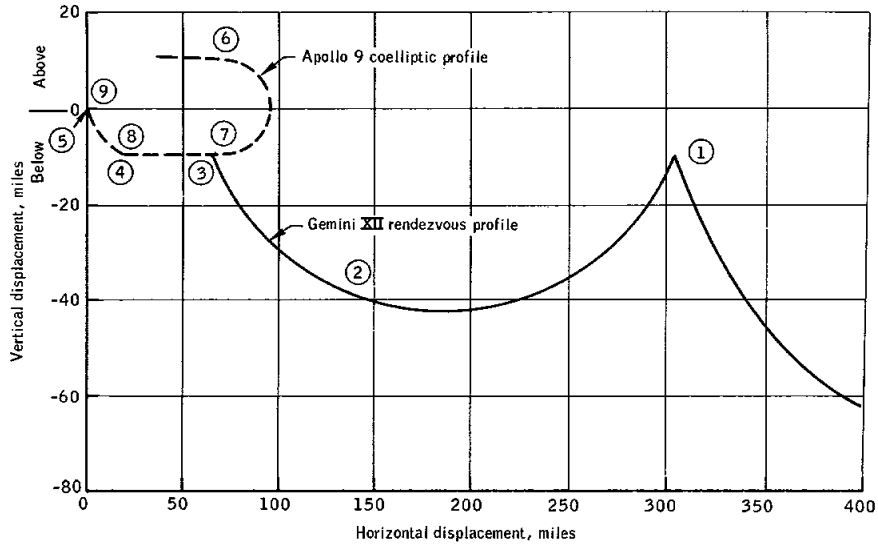
Parameter	Solution			
	First	Second	Third	Fourth
Ignition time, hr:min:sec	94:57:53	94:57:53	94:57:53	94:57:53
Velocity change, ft/sec - X	20.7	18.7	19.5	19.6
Y	0.0	0.0	-0.8	0.6
Z	2.5	-6.6	-1.8	-3.3
Elevation angle, deg	211.49	207.26	209.19	208.75
No. of navigation updates	8	13	21	26

(b) Terminal phase initiation

Parameter	Solution				
	First	Second	Third	Fourth	Using lunar module ignition time
Ignition time, hr:min:sec	98:03:09.33	98:04:30.21	97:58:19.12	97:58:08.17	97:57:59
Velocity change, ft/sec - X	-20.2	-19.0	-19.3	-19.5	-19.4
Y	-0.3	-0.1	-0.2	-0.5	0.0
Z	9.5	11.7	8.8	9.0	8.8
Elevation angle, deg	207.0	207.5	207.5	207.5	207.3
No. of navigation updates	5	10	20	26	--

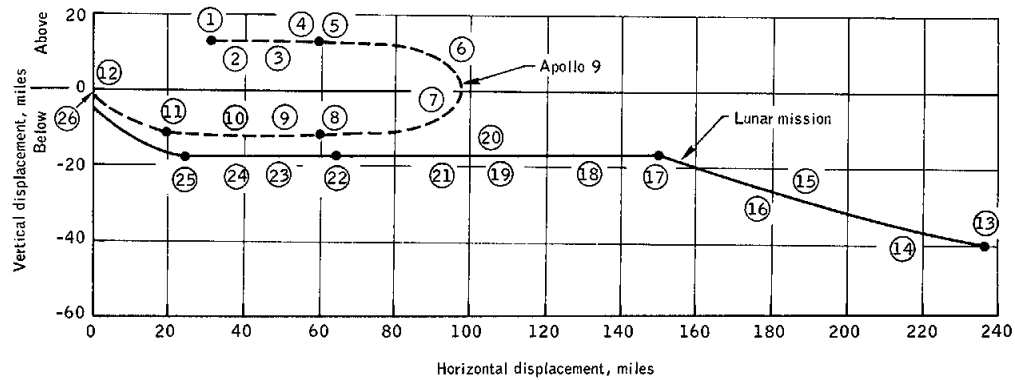
TABLE 5-V.- LUNAR MODULE NAVIGATION

Conditions	Range, ft	Range rate, ft/sec
A. Lunar module computer integration (no updates)	598 737	-43.0
B. Lunar module computer integration (17 updates - 96:17:06.7 to 96:43:55.94)	594 826	-47.1
C. Best-estimated trajectory	593 381	-49.9
Condition A minus Condition B	3 911	4.1
Condition B minus Condition C	1 445	2.8



Gemini XII			Apollo 9		
No.	Maneuver	Velocity, ft/sec	No.	Maneuver	Velocity, ft/sec
1	Phase adjust	58.2	6	Coelliptic sequence initiation	40.0
2	Corrective combination	1.6	7	Constant differential height	41.6
3	Coelliptic maneuver	56.7	8	Terminal phase initiation	21.6
4	Terminal phase initiation	21.4	9	Terminal phase final	28.1
5	Terminal phase final	27.9			

Figure 5-1.- Comparison of Gemini XII and Apollo 9 rendezvous profiles.



Apollo 9			Lunar Mission		
No.	Event	Time from insertion, hr:min	No.	Event	Time from insertion, hr:min
1	Insertion maneuver	0:00	13	Insertion maneuver	0:00
2	Navigation updates (18 marks)	0:08 to 0:30	14	Alignment	0:05
3	Abort guidance system update	0:33	15	Navigation updates (18 marks)	0:19 to 0:39
4	Staging	0:40	16	Abort guidance system update	0:44
5	Coelliptic sequence initiation	0:40	17	Coelliptic sequence initiation	0:51
6	Navigation updates (20 marks)	0:48 to 1:12	18	Navigation updates (14 marks)	0:55 to 1:10
7	Abort guidance system update	1:15	19	Ptane change maneuver	1:19
8	Constant differential height maneuver	1:24	20	Navigation updates (16 marks)	1:20 to 1:37
9	Navigation updates (26 marks)	1:32 to 2:06	21	Abort guidance system update	1:42
10	Abort guidance system update	2:08	22	Constant differential height maneuver	1:49
11	Terminal phase initiation	2:17	23	Navigatation updates (20 marks)	1:51 to 2:14
12	Final braking	2:53	24	Abort guidance update	2:11
			25	Terminal phase initiation	2:26
			26	Final braking	3:14

Figure 5-2.- Comparison of major events for Apollo 9 and the lunar mission.

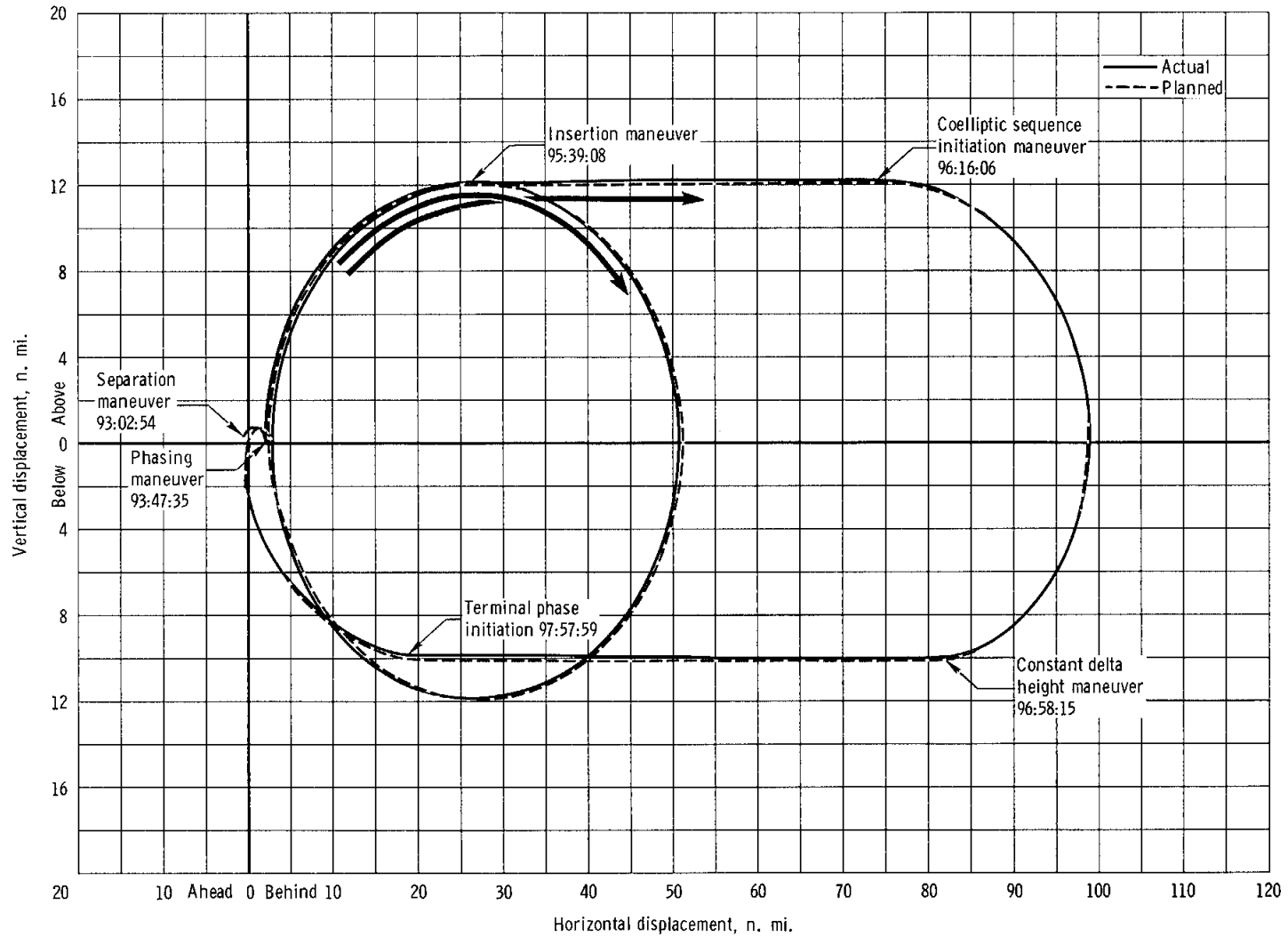


Figure 5-3. - Relative motion between command and service modules and lunar module during rendezvous.

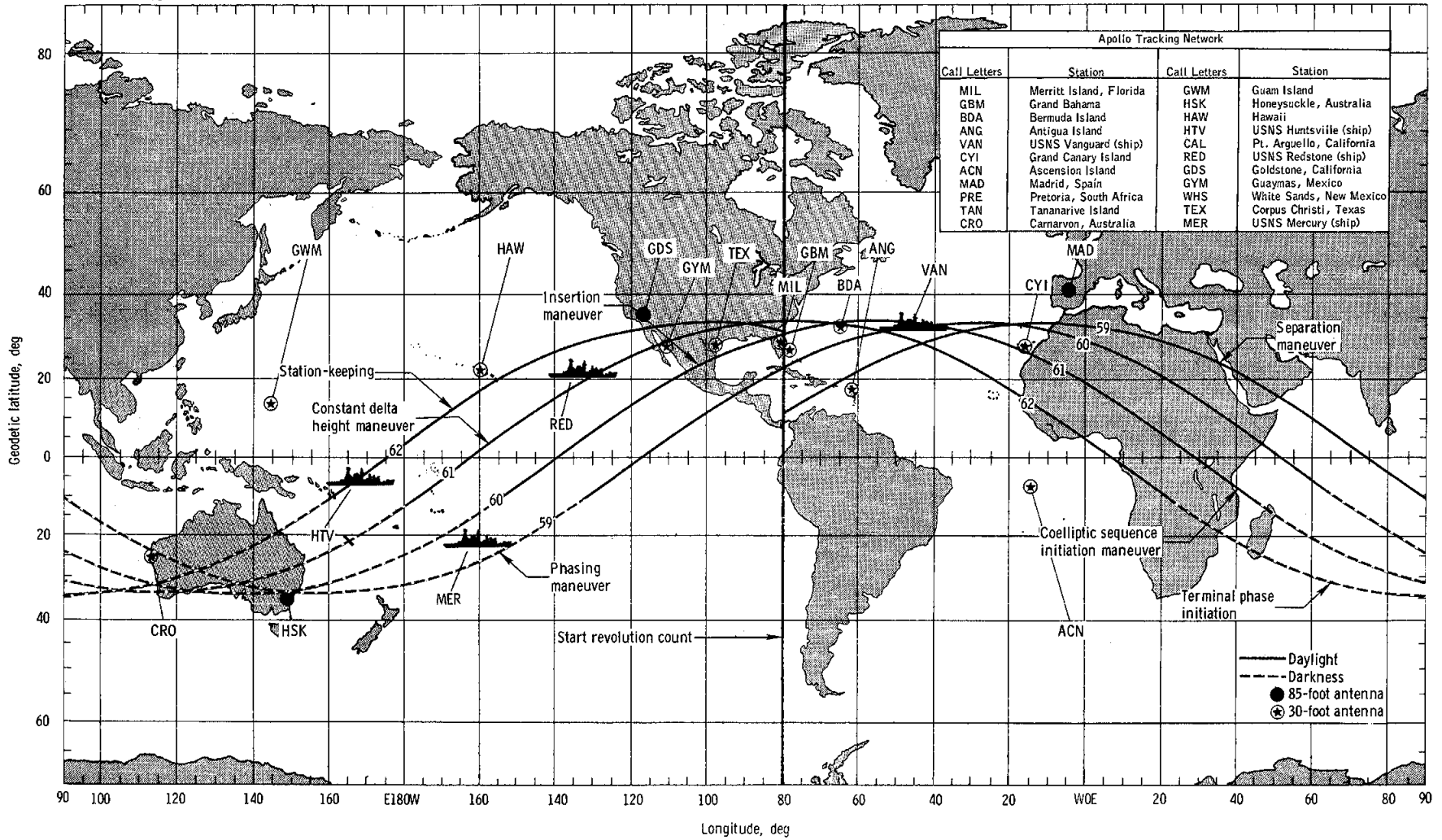


Figure 5-4. - Ground track for rendezvous.

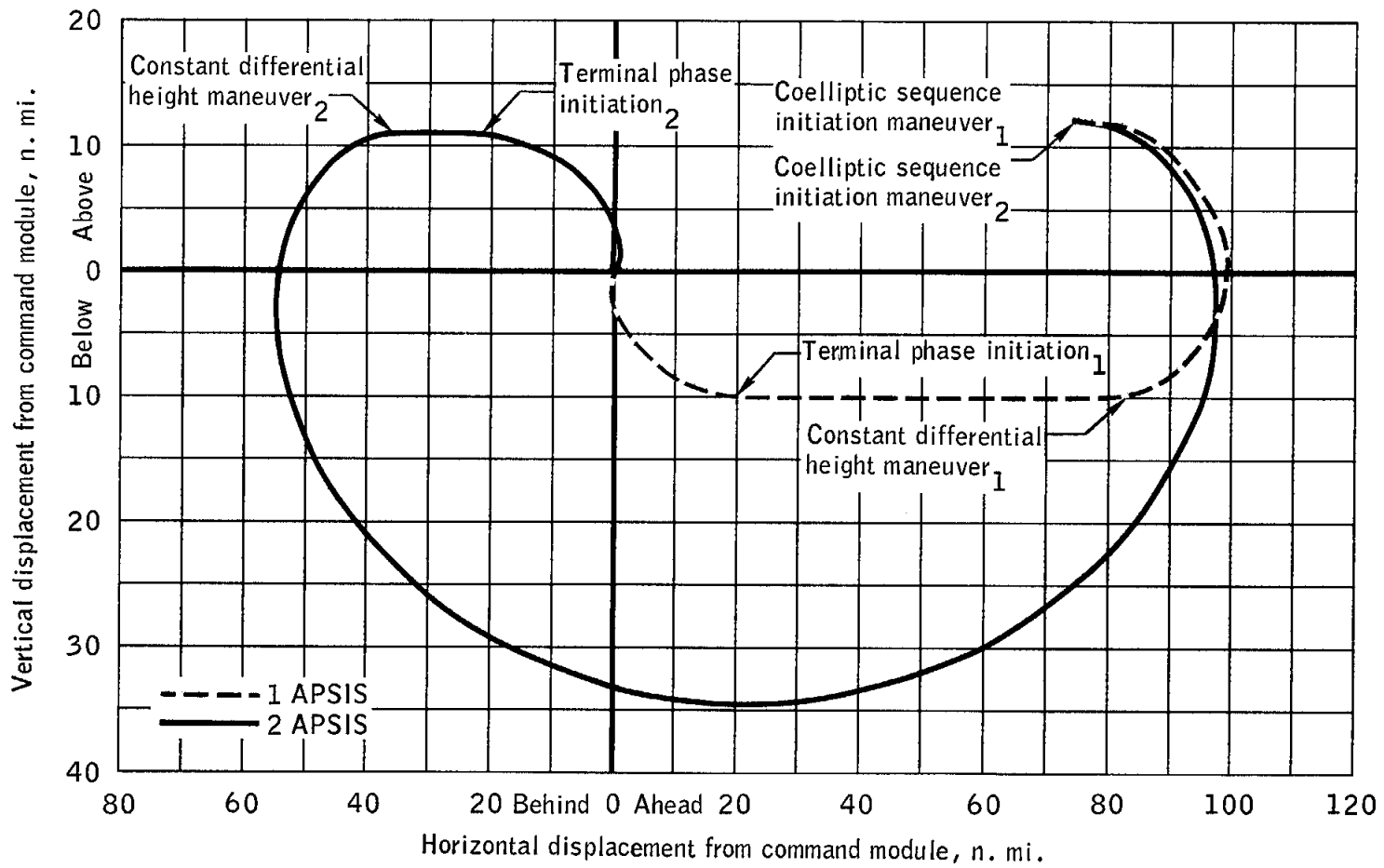


Figure 5-5.- Relative spacecraft motion for first and second apsidal solutions.

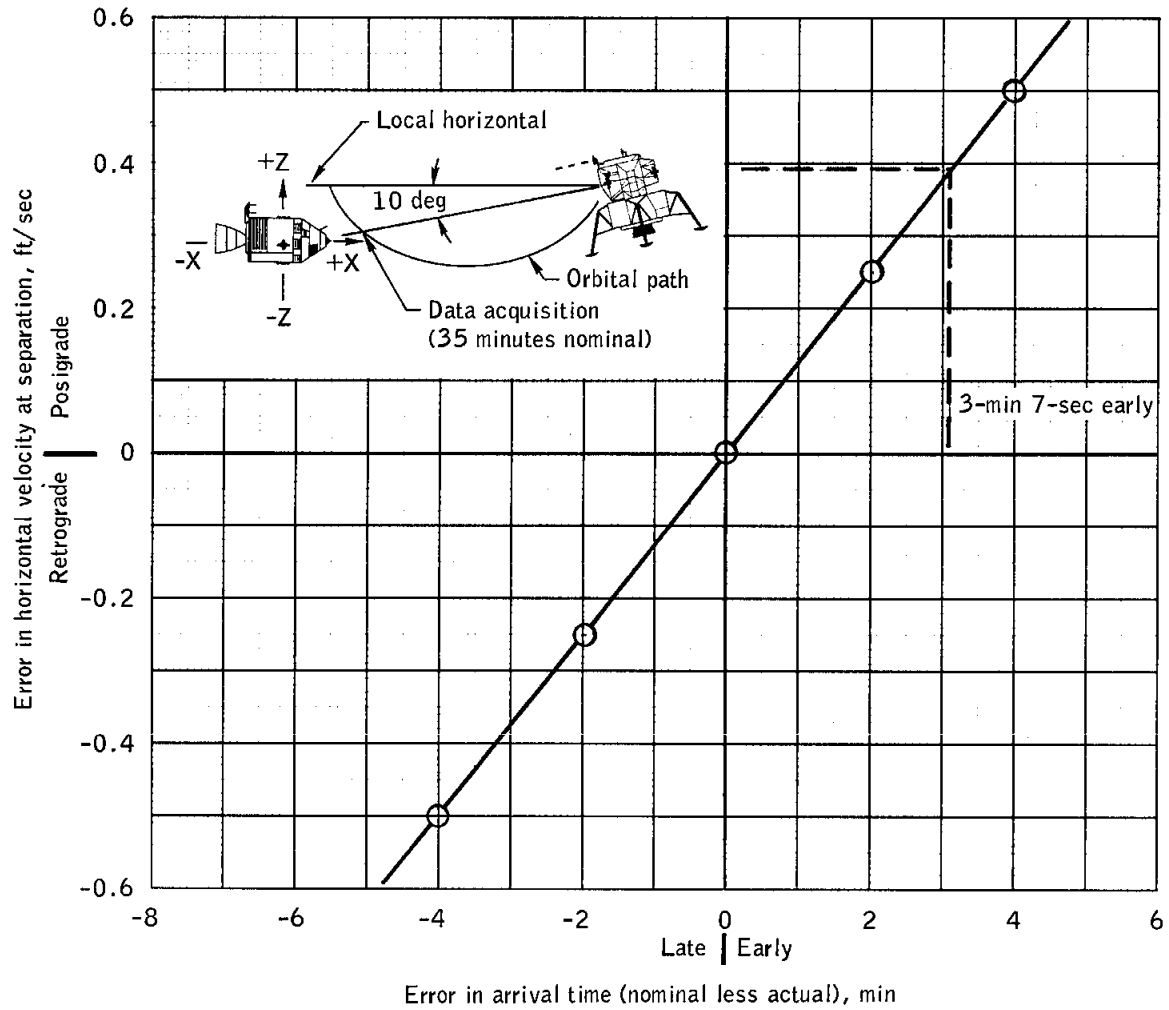


Figure 5.6- .- Effect of separation maneuver errors.

5-32

NASA-S-69-1956

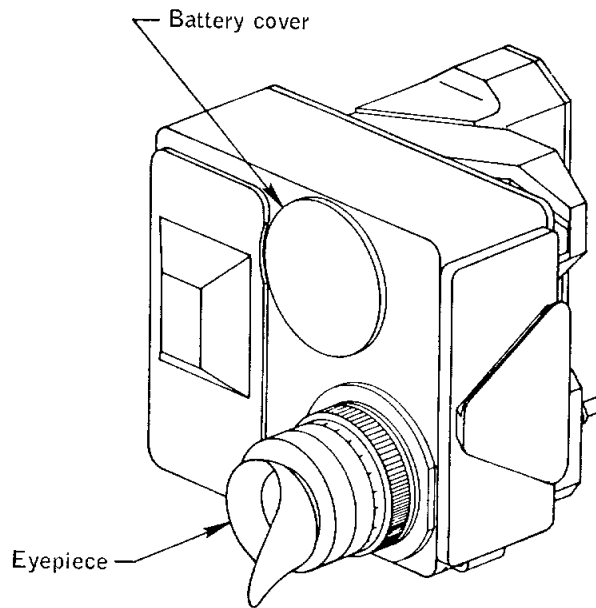
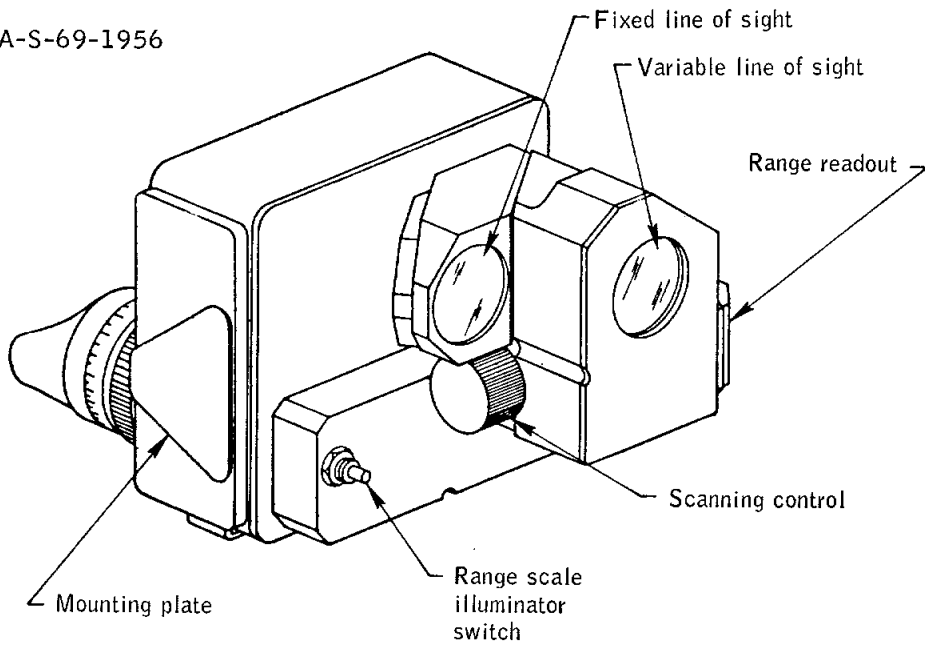
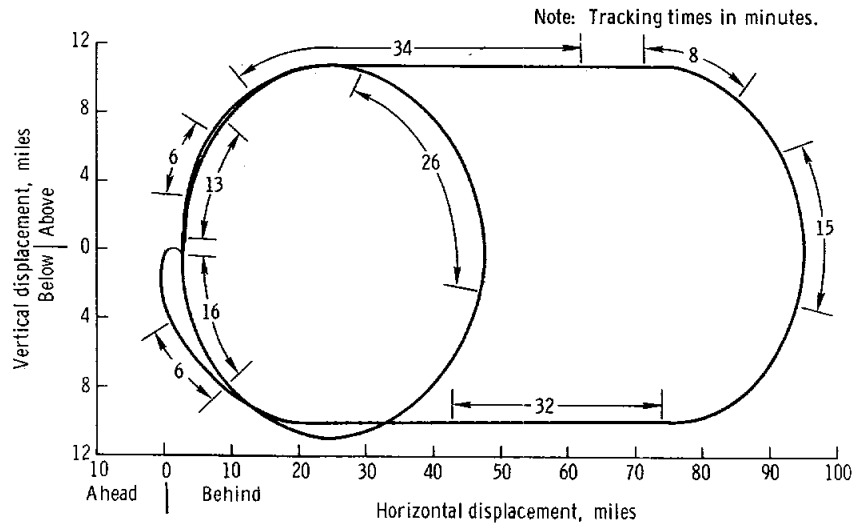


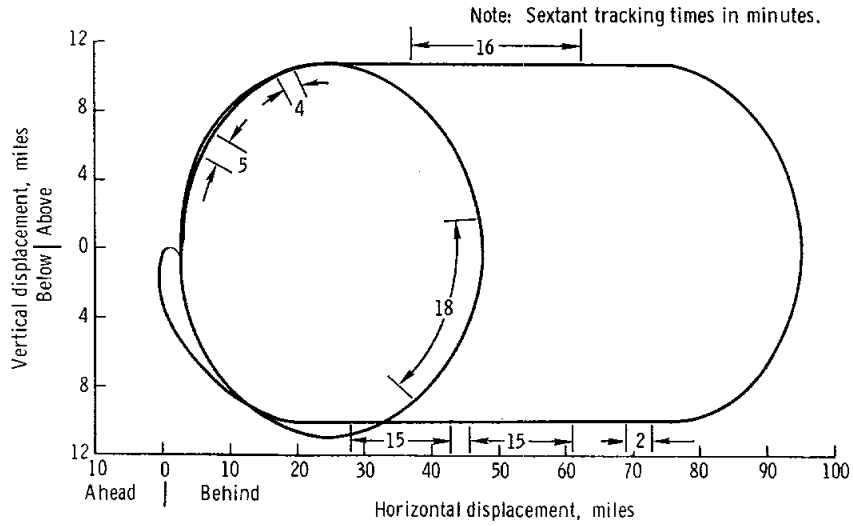
Figure 5-7.- Diastimeter.

NASA-S-69-1957

(a) Ground-station tracking coverage.



(b) Sextant updates.



(c) Lunar module radar inputs to guidance computer.

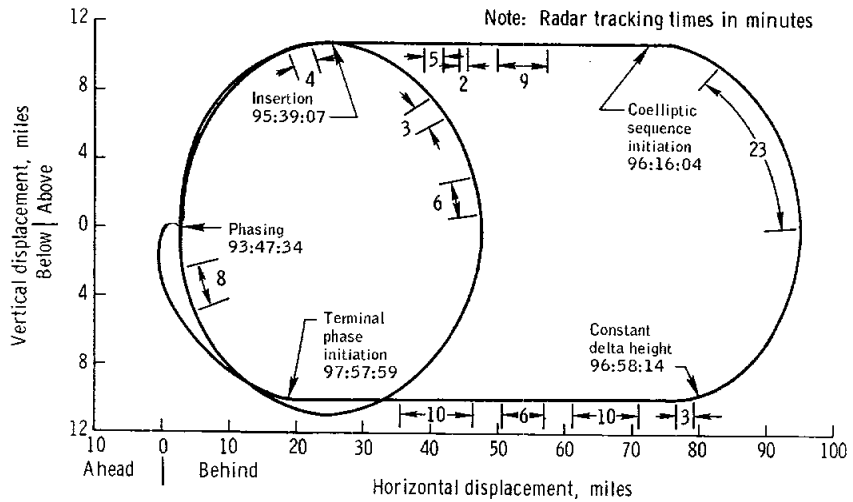
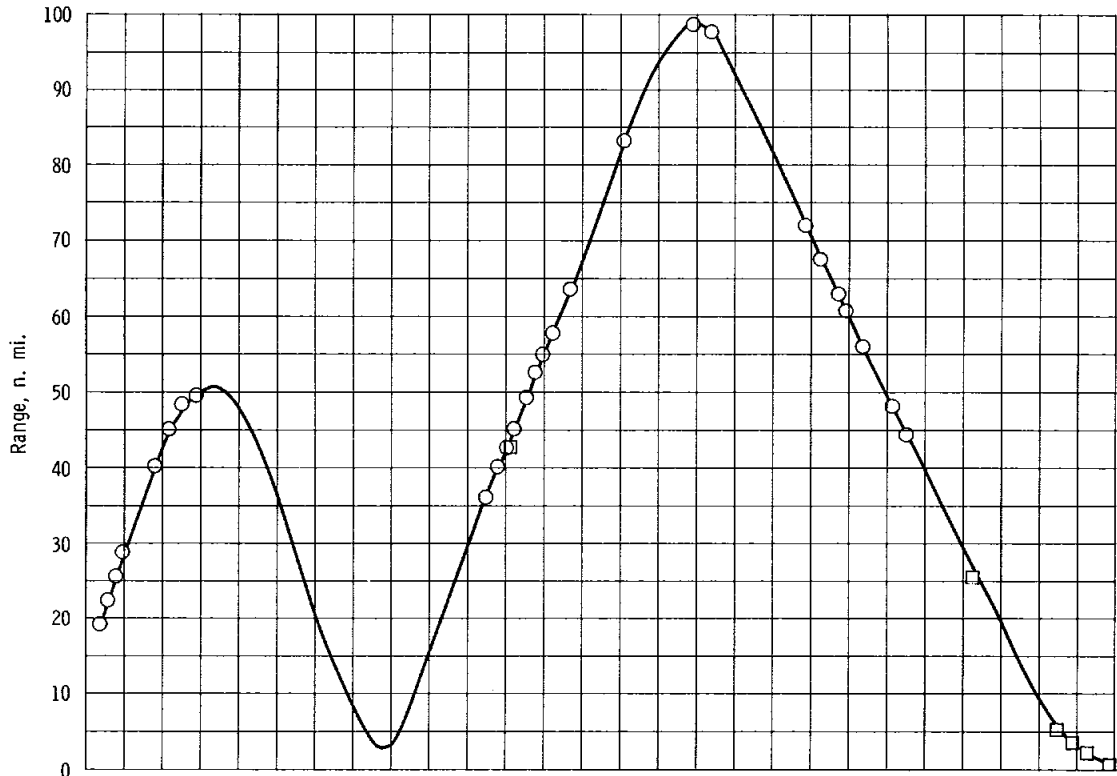
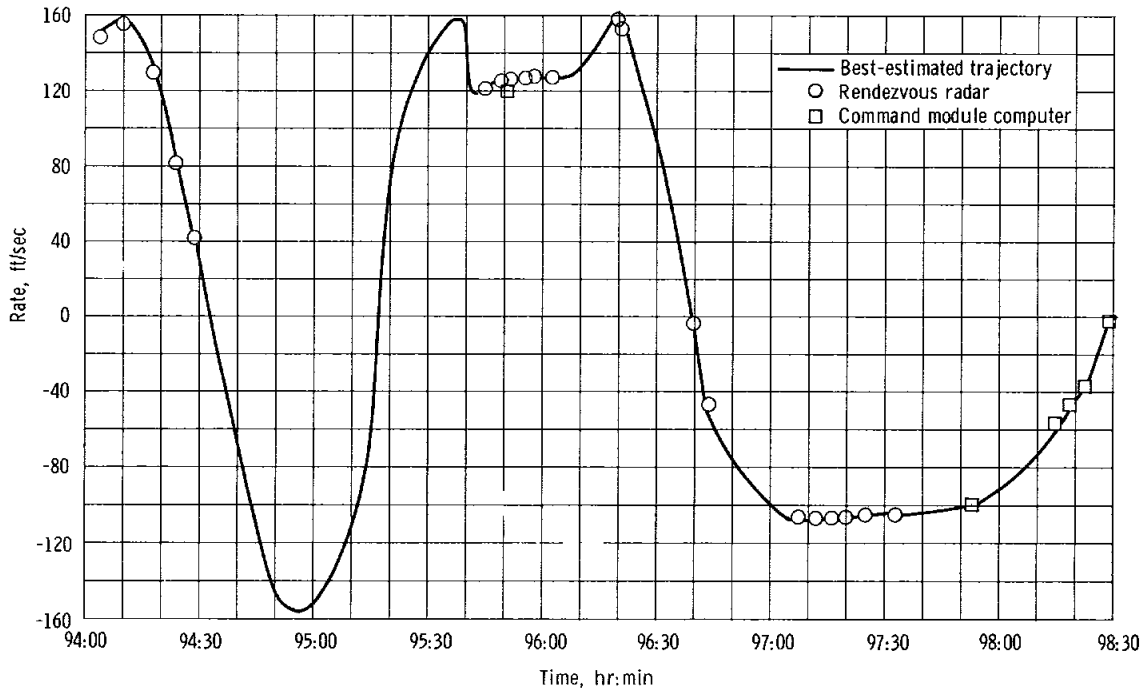


Figure 5-8. - Command module and lunar module sighting history.



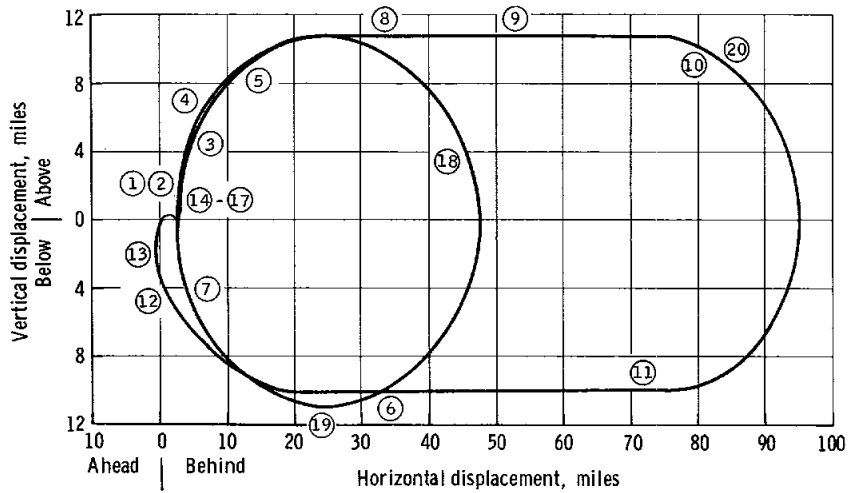
(a) Range.



(b) Range rate.

Figure 5-9. - Time history of range and range rate during rendezvous.

NASA-S-69-1959



No.	Device	Command module sightings	No.	Device	Lunar module sightings
1	Sextant	Stars in daylight	14	Crewman optical alignment sight	Command module visible as silver object against clouds and earth in daylight
2	Sextant	Flashing light daylight and darkness			
3	Sextant	Lunar module reaction control jets			
4	Telescope	Sun reflection in optics obscured lunar module	15	Alignment optical telescope	Sirius visible immediately prior to sunset. Gradually able to see Canus Major and Orion. Eyepatch on for one minute prior to sightings.
5	Sextant	Flashing light visible at night	16	Crewman optical alignment sight	Spica dim but visible with moon and bright planet in field of view
6	Sextant	Stars in darkness	17	Crewman optical alignment sight	Command module visible
7	Crewman optical alignment sight	Lunar module visible during closest approach			
8	Sextant	Lunar module in daylight	18	Crewman optical alignment sight	Command module visible all around phasing orbit day and night. Disappeared after insertion maneuver.
9	Sextant	Lunar module landing gear pads discernable in daylight			
10	Sextant	Flashing light not visible in darkness	19	Alignment optical telescope	Stars visible at night
11	Sextant	Lunar module resolved as object in daylight			
12	Crewman optical alignment sight	Lunar module visible at dawn against earth background	20	Crewman optical alignment sight	Command module not visible after sunset
13	Diastimeter	Lunar module visible at dawn against earth background			

Figure 5-10. - Sighting events.

## 6.0 COMMUNICATIONS

This section discusses the overall evaluation of Apollo 9 communications performance for the various links between the command module, the lunar module, the extravehicular crewman, and the Manned Space Flight Network. The communications capabilities evaluated are voice, telemetry, tracking, command, and television.

Performance of the communication systems, including the command module and lunar module equipment (sections 8.4 and 9.4, respectively), was generally satisfactory. However, several problems degraded the overall system performance and temporarily inhibited voice, telemetry, command, or tracking capability.

Pictures of excellent quality were received during the two television transmissions from the lunar module. Voice quality was good throughout the rendezvous phase and during most of the mission. However, on several occasions, procedural errors or improper equipment configurations prevented communications between the Mission Control Center and the spacecraft. A communications check utilizing the backup S-band voice signal combinations was performed over the Carnarvon station during the first revolution. Good quality voice was received by both the spacecraft and the station; however, the downlink voice was not remoted to the Mission Control Center.

The first communications problem was a procedural error that occurred during the launch phase. As shown in figure 6-1, procedural errors at the Grand Bahama Island station caused degraded S-band system performance between 0:02:00 and 0:02:32, when the ground receiver locked on to a 51.2-kHz spurious signal in the downlink spectrum, and between 0:02:32 and 0:03:17, when the antenna tracked a sidelobe. A complete loss of S-band communications was encountered between 0:05:01 and 0:06:00 because the operator of the ground transmitter interrupted transmissions 30 seconds early. At 0:05:12, the operator recognized the error and energized the transmitter, but he was unsuccessful in reestablishing two-way phase lock. At 0:05:30 the Bermuda station initiated uplink transmissions as scheduled. The spacecraft transponder immediately locked to the Bermuda signal; however, solid two-way phase lock was not established until 0:06:00. See section 14 for further details.

During the first television transmission, no voice was received at the Mission Control Center until the Merritt Island station was requested to remote VHF voice instead of S-band. Subsequent investigations showed that good quality S-band voice was received and recorded at Merritt Island, but that transmission to the Mission Control Center was inhibited by improper equipment operation or configuration within the station (see section 14).

Excellent quality voice transmissions were received from each of the crewmen during the extravehicular activity. However, the crew did not receive Mission Control Center transmissions relayed through the Texas, Merritt Island, Bermuda, and USNS Vanguard stations. Only one of the transmissions relayed through the Guaymas station was received by the crew. As a result of improper configurations at the Guaymas, Texas, Merritt Island, and USNS Vanguard stations, all voice transmissions, except one, were on the S-band uplink only. Reception of the S-band transmissions was inhibited, as planned, by the spacecraft volume-control settings being at full decrease. Voice transmissions through Bermuda were unsuccessful as they occurred during periods of intervehicular communications when the VHF receivers were captured. Good quality uplink voice was received by each of the crewmen during transmissions through the USNS Huntsville, USNS Redstone, and Canary Island stations.

Telemetry data and voice were recorded onboard when the command module was outside the network coverage area. Solid frame synchronization was provided by the telemetry decommutation system during most of the data playbacks. The quality of the recorded voice was dependent on the play-to-record speed ratio of the data storage equipment and on the type of network station which received the playbacks. Several single S-band stations reported high-level tone interference in the received voice with a play-to-record ratio of 32. These stations were using a new receiver installed to provide capability to support a dual-vehicle earth orbital mission. Data indicate that the interference was caused by use of an intermediate-frequency amplifier with insufficient bandwidth to accommodate the combination of the modulation spectrum, Doppler, spacecraft transmitter frequency offset, and spacecraft transmitter short-term frequency stability.

The transceiver and power amplifier switching associated with lunar-module secondary S-band checks caused several signal dropouts during the Antigua and Carnarvon coverage of revolutions 29 and 32, respectively. Since Antigua is a single S-band station and was attempting to support both vehicles, some data were lost.

Invalid S-band range-code acquisitions were reported by the Goldstone, Honeysuckle, and Texas stations during their coverage of lunar module operations. The range-code acquisition problems during Goldstone coverage of revolutions 31 and 32 were caused by false uplink phase locks. The inability of the Texas station to achieve a valid range-code acquisition during the ascent engine firing to depletion was caused by use of an incorrect uplink range-code modulation index. Discussion and analyses of the Honeysuckle problem will be included in a supplemental report.

The performance of the lunar module UHF command system was good throughout lunar module operations. The performance of the command and

service modules S-band command system was satisfactory, except for the time period from 109:21:50 to 118:46:53. Verification of spacecraft acceptance of real-time commands was not detected by the ground stations during the above period. Data indicate that the commands were being properly encoded and transmitted. Subsequently, the crew was able to correct the problem (see section 17). The lunar module S-band steerable antenna was not functionally tested during the mission.

The service-module high-gain antenna was acquired and tracked successfully for S-band communications during the Carnarvon and Hawaii station coverage during revolution 122. The received uplink and downlink carrier power levels during both passes corresponded with preflight predictions.

NASA-S-69-1960

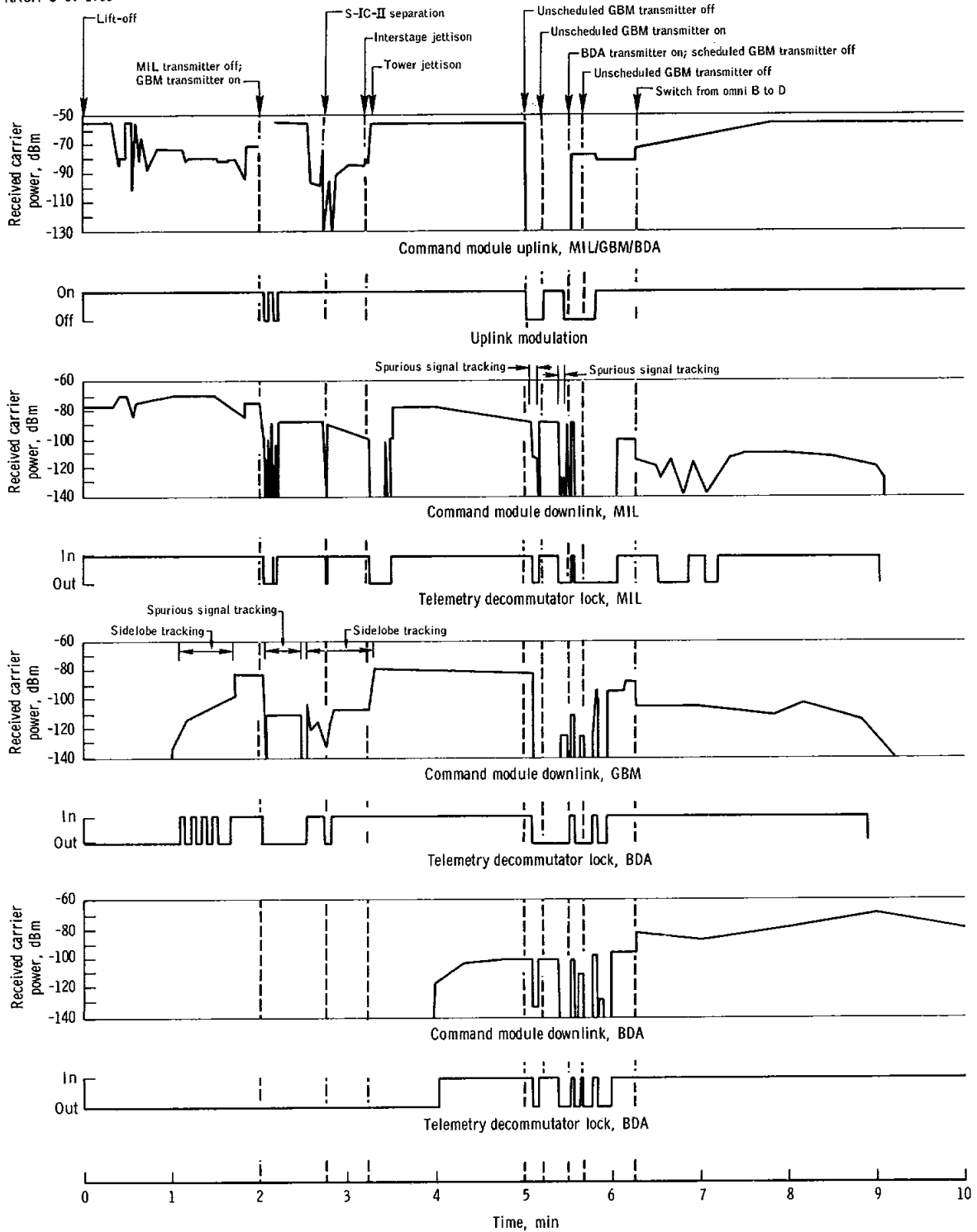


Figure 6-1. - S-band communications during launch.

## 7.0 TRAJECTORY

The trajectory data for the phase from lift-off to spacecraft separation from the S-IVB were provided by the Marshall Space Flight Center, and a detailed analysis of these data is presented in reference 6. All spacecraft trajectory information is based on the reduction and post-flight analysis of data from the Manned Space Flight Network. This section includes analysis of firings performed by the service propulsion system, descent propulsion system, and ascent propulsion system during all mission phases except rendezvous. Trajectory analysis for the rendezvous maneuvers is presented in section 5.0.

The earth model contains geodetic and gravitational constants representing the Fisher ellipsoid. The state vectors and orbital parameters are presented in the geographic coordinate system defined in table 7-I. Table 7-II presents the trajectory conditions for all flight events. The ground track during launch and the initial revolutions is shown in figure 7-1.

### 7.1 LAUNCH PHASE

First stage (S-IC) cutoff was 3 seconds later than planned, and the corresponding altitude, velocity, and flight-path angle were low by 9501 feet, 96 ft/sec, and 1.1 degrees, respectively. The trajectory for the launch phase is plotted in figure 7-2.

Second stage (S-II) cutoff was 2.3 seconds later than planned, and altitude, velocity, and flight-path angle were low by 8158 feet, 268 ft/sec, and 0.45 degree, respectively. The degraded performance of the first and second stages resulted from the planned trajectory not being adjusted for the off-nominal engine performance, the increase in propellant temperature, and the 3-day lift-off postponement (see section 16.0). A nominal orbit insertion (figure 7-2) was achieved by the first S-IVB firing, which lasted 10.8 seconds longer than planned. At orbital insertion, the altitude, velocity, and flight-path angle were 1052 feet low, 3 ft/sec high, and 0.005 degree high, respectively.

### 7.2 SPACECRAFT/S-IVB SEPARATION

The command and service modules remained attached to the S-IVB until 2:41:16, when the transposition and docking phase began. This operation was completed successfully at 3:01:59.3. At 4:08:06, the docked spacecraft were separated from the S-IVB. Following a small separation maneuver, the

S-IVB performed two restart maneuvers, the second of which placed it in a heliocentric orbit. The resulting aphelion, perihelion, and period were 80 093 617 miles, 44 832 845 miles, and 245 days, respectively.

### 7.3 ORBITAL FIRINGS

During the 4 days prior to rendezvous, one descent propulsion and five service propulsion firings were performed by the docked spacecraft. No translation maneuvers were required to effect propellant settling prior to the first three service propulsion firings. After rendezvous, an ascent engine firing to propellant depletion and three undocked service propulsion firings were performed. The trajectory parameters at ignition and cutoff for each orbital firings are shown in table 7-II. The maneuver summary presented in table 7-III includes the firing times, velocity changes, and resultant orbits for each maneuver.

#### 7.3.1 Docked Firings

The first docked service propulsion firing was performed at about 6 hours and was conducted approximately 1.5 minutes earlier than planned to optimize Hawaii station coverage. This firing, including the shutdown, was controlled by the primary guidance system using external-velocity logic. The platform was aligned normally, and the posigrade velocity increment was applied in-plane.

At approximately 22 hours, the second docked service propulsion firing was performed. This firing was also external-velocity targeted and controlled by primary guidance. The velocity change was applied largely out-of-plane.

Approximately two revolutions after the second service propulsion firing, the longest docked service propulsion system firing was conducted as planned. This firing also was conducted largely out-of-plane, but with sufficient in-plane velocity to raise the apogee to 275 miles. Following this firing, the command and service module rescue capability for the lunar module rendezvous was established. The full-amplitude stroking test was conducted during the initial portion of the firing and manual thrust vector control during the final 45 seconds of the firing.

Approximately two revolutions after the third service propulsion firing, the fourth service propulsion firing was made, targeted out-of-plane such that the resulting apogee and perigee values did not change significantly.

Following power-up and systems checks in the lunar module, the docked descent engine firing was performed at approximately 50 hours. This firing lasted 372 seconds and was manually terminated. Attitudes were controlled by the primary guidance system.

Approximately three revolutions after the docked descent engine firing, the service propulsion system was activated for the final docked firing, which resulted in an orbit of 129.2 by 123.8 miles as compared with the planned circular orbit of 130.0 miles. Although large velocity residuals were expected, no provisions had been made to null these errors. The time of terminal phase initiation during the rendezvous occurred 4 minutes earlier because of the dispersions in this firing, but the orbit following this final docked firing was acceptable for the rendezvous sequence.

### 7.3.2 Undocked Firings

During rendezvous operations (see section 5.0), the descent stage had been left in earth orbit. Subsequently, it entered the earth's atmosphere on March 22, 1969, at 0345 G.m.t., impacting in the Indian Ocean off the coast of North Africa.

At approximately 101.5 hours, the ascent stage was jettisoned, and a separation maneuver was performed by the command and service modules. At approximately 102 hours, the ascent stage was ignited for a 362.4-second firing to propellant depletion. The ascent propellant interconnect remained open throughout the firing. As a guarantee that a guidance cut-off would not be sent prematurely, the firing was targeted with a velocity increment in excess of that required to deplete propellants. The final orbit for the ascent stage was 3760.9 by 126.6 miles, with a lifetime of 5 years.

The sixth service propulsion firing was conducted at 123:25:07, one revolution later than planned because the propellant-settling maneuver was unsuccessful during the first attempt. The firing was performed retrograde to lower the perigee so the reaction control system deorbit capability would be enhanced in the event of a contingency. The total velocity change during the sixth service propulsion firing was less than planned because the fifth firing had resulted in a lower-than-planned orbit.

Approximately 2 days later, the service propulsion system was activated for the seventh time, and a gaging system test had been added to the firing objectives. The test required a firing time of approximately 25 seconds, which was 15 seconds longer than planned prior to flight. The firing was largely out-of-plane; however, a small in-plane velocity

component raised the apogee to 253.2 miles to establish the desired conditions at the nominal deorbit point. If the service propulsion system had failed at deorbit, the reaction control system could have conducted a deorbit maneuver from this apogee condition and still landed near the primary recovery area.

The final maneuver (deorbit) occurred at 240:31:114.9 over Hawaii. The ignition was delayed approximately one revolution to effect a landing south of the planned recovery area because of unfavorable weather conditions. The firing was nominal.

#### 7.4 ENTRY

The entry trajectory (fig. 7-3) was generated by correcting the guidance and navigation accelerometer data for known errors in the inertial platform.

Command module/service module separation occurred at 240:36:04. The entry interface velocity was 3 ft/sec lower and the flight-path angle 0.007 degree higher than predicted. The peak entry load factor was 3.35g. Section 8.6 contains the discussion of entry guidance. At drogue deployment, the guidance and navigation system indicated a 0.7-mile undershoot while the postflight reconstructed trajectory indicates a 2.7-mile overshoot. The entry data are listed in table 7-IV. After separation, the service module reaction control system was expected to fire for 118 seconds. The finite duration of this firing was dependent upon fuel cell capability and was calculated to be as short as 94 seconds and as long as 124 seconds. The firing was performed in order to place the service module on a trajectory which would prevent recontact by providing adequate downrange and crossrange separation. The service module structure cannot survive entry intact, however, impact predictions assume that structural integrity is maintained. The impact point corresponding to a 118-second firing was computed to be 22.4 degrees north latitude and 66.2 degrees west longitude, or 99 miles downrange from the command module. Radar tracking data predicted an impact at 22.0 degrees north latitude and 65.3 degrees west longitude, or 175 miles downrange from the command module. Differences in the impact point predictions, with the attendant dispersions, would be expected in light of the gross uncertainties existing in the required finite values for ballistic coefficient, vehicle attitude, drag coefficient, length of engine firing, and radar tracking accuracy.

## 7.5 TRACKING ANALYSIS

Few problems were encountered in processing radar tracking data. In general, data quality was consistent with that of previous earth-orbit missions. Minor operational errors persisted but did not degrade orbit determination efforts. A consistent bias in the Madrid station range measurements and a bias in angle data from the Carnarvon station existed. Both problems are being examined.

In general, tracker performance was excellent, and no significant problems were encountered. The S-band system performed well, and orbit determination results showed excellent agreement between C-band and S-band solutions.

TABLE 7-I.- DEFINITION OF TRAJECTORY AND ORBITAL PARAMETERS

<u>Trajectory parameter</u>	<u>Definition</u>
Geodetic latitude	Spacecraft position measured north or south from the earth equator to the local vertical vector, deg
Longitude	Spacecraft position measured east or west from the Greenwich meridian to the local vertical vector, deg
Altitude	Perpendicular distance from the reference ellipsoid to the point of orbit intersect, ft
Space-fixed velocity	Magnitude of the inertial velocity vector referenced to the earth-centered, inertial reference coordinate system, ft/sec
Space-fixed flight-path angle	Flight-path angle measured positive upward from the geocentric local horizontal plane to the inertial velocity vector, deg
Space-fixed heading angle	Angle of the projection of the inertial velocity vector onto the local geocentric horizontal plane, measured positive eastward from north, deg
Apogee	Maximum altitude above the oblate earth model, miles
Perigee	Minimum altitude above the oblate earth model, miles
Period	Time required for spacecraft to complete 360 degrees of orbit rotation, min
Inclination	Angle between the orbit plane and the equator, deg

TABLE 7-II.- TRAJECTORY PARAMETERS

Event	Time, hr:min:sec	Latitude, deg	Longitude, deg	Altitude, miles	Space-fixed velocity, ft/sec	Space-fixed flight-path angle, deg	Space-fixed heading angle, deg E of N
Launch Phase							
S-IC inboard engine cutoff	0:02:14.3	28.73N	80.16W	22.4	6 329.5	22.58	72.42
S-IC outboard engine cutoff	0:02:42.8	28.87N	79.67W	34.8	9 014	18.54	75.34
S-II engine cutoff	0:08:56.2	31.79N	65.04W	100.7	22 754	0.92	81.87
S-IVB engine cutoff	0:11:04.7	32.60N	55.93W	103.1	25 564	-0.01	86.98
Parking Orbit							
Orbital insertion	0:11:14.7	32.63N	55.17W	103.1	25 570	-0.01	87.41
Command module/S-IVB-lunar module separation	2:41:16	11.92S	162.91E	107.0	25 553	0.02	59.26
Command module/lunar module docking	3:01:59.3	28.83N	124.36W	108.8	25 549	-0.02	73.90
Command module-lunar module/S-IVB separation	4:08:06	14.32S	135.62E	105.2	25 565	0.03	60.37
Pre-Rendezvous Maneuvers							
First service propulsion maneuver Ignition	5:59:01.1	29.46N	167.82W	108.7	25 549.8	0.000	75.15
Cutoff	5:59:06.3	29.53N	167.53W	108.7	25 583.8	0.001	75.29
Second service propulsion maneuver Ignition	22:12:04.1	27.54N	64.13W	107.9	25 588.2	-0.034	71.66
Cutoff	22:13:54.4	29.78N	56.43W	108.0	25 701.7	-0.020	73.68
Third service propulsion maneuver Ignition	25:17:39.3	33.13N	83.93W	109.7	25 692.4	0.158	83.89
Cutoff	25:22:19.2	33.98N	62.22W	115.7	25 794.3	0.456	90.86
Fourth service propulsion maneuver Ignition	28:24:41.4	33.99N	111.19W	114.3	25 807.7	0.388	89.52
Cutoff	28:25:09.3	33.99N	109.00W	115.0	25 798.9	0.434	90.14
First descent propulsion maneuver (docked) Ignition	49:41:34.5	33.16N	89.64W	110.0	25 832.7	-0.020	82.09
Cutoff	49:47:46.0	33.80N	60.76W	117.0	25 783.0	0.530	95.18
Fifth service propulsion maneuver Ignition	54:26:12.3	30.43N	111.20W	128.2	25 700.8	0.826	106.23
Cutoff	54:26:55.6	29.60N	108.14W	129.3	25 473.2	0.010	107.01
Rendezvous Maneuvers							
Separation maneuver (service module) Ignition	93:02:54	24.29N	35.15E	126.4	25 480.5	0.020	114.13
Cutoff	93:03:03.5	23.98N	35.85E	126.5	25 480.5	0.003	114.44
Second descent propulsion maneuver (phasing) Ignition	93:47:35.4	23.89S	155.44W	121.1	25 518.9	0.002	65.48
Cutoff	93:47:54.1	23.36S	154.27W	121.1	25 518.2	0.206	64.98

TABLE 7-II.- TRAJECTORY PARAMETERS - Concluded

7-8

Event	Time, hr:min:sec	Latitude, deg	Longitude, deg	Altitude, miles	Space-fixed velocity, ft/sec	Space-fixed flight-path angle, deg	Space-fixed heading angle, deg E of N
Rendezvous Maneuvers - Concluded							
Third descent propulsion maneuver (insertion)							
Ignition	95:39:08.1	23.09N	102.77W	136.7	25 412.6	0.036	65.74
Cutoff	95:39:30.4	23.42N	102.08W	136.7	25 453.0	0.031	65.35
Coelliptic sequence initiation maneuver (lunar module reaction control system)							
Ignition	96:16:06.5	7.54S	40.10E	137.9	25 452.0	-0.042	122.91
Cutoff	96:16:38.2	8.72S	41.27E	137.9	25 412.0	-0.048	122.63
Constant delta height maneuver (first ascent propulsion firing)							
Ignition	96:58:15	2.42N	159.23W	112.7	25 592.0	-0.002	56.44
Cutoff	96:58:17.9	3.26N	157.98W	112.7	25 550.6	-0.030	56.44
Terminal phase initiation (lunar module reaction control system)							
Ignition	97:57:59	30.86S	65.38E	113.0	25 540.8	-0.044	104.42
Cutoff	97:58:36.6	31.49S	68.27E	113.0	25 560.5	-0.013	102.85
Station-keeping	98:30:51.2	11.42N	168.72W	123.5	25 509.9	0.030	58.13
Post-Rendezvous Maneuvers							
Ascent propulsion firing to depletion							
Ignition	101:53:15.4	28.56N	112.57W	126.5	25 480.3	-0.017	108.77
Cutoff	101:59:17.7	19.59N	88.22W	134.4	29 415.4	2.230	111.85
Sixth service propulsion maneuver							
Ignition	123:25:07.0	23.89S	110.00E	119.6	25 522.2	0.017	65.47
Cutoff	123:25:08.4	23.86S	110.07E	119.5	25 489.0	0.020	65.44
Seventh service propulsion maneuver							
Ignition	169:39:00.4	33.66N	102.88W	103.8	25 589.6	-0.067	92.97
Cutoff	169:39:25.3	33.57N	100.95W	103.3	25 825.9	-0.414	92.79
Eighth service propulsion maneuver							
Ignition	240:31:14.9	25.89N	155.88W	171.9	25 318.4	-1.158	67.75
Cutoff	240:31:26.6	26.17N	155.13W	170.5	25 142.8	-1.753	68.10

TABLE 7-III.- MANEUVER SUMMARY

Maneuver	Ignition time, hr:min:sec	Firing time, sec*	Velocity change, ft/sec*	Resultant orbit			
				Apogee, miles	Perigee, miles	Period, min	Inclination, deg
First service propulsion maneuver	5:59:01.1	5.2	36.6	127.6	111.3	88.8	32.56
Second service propulsion maneuver	22:12:04.1	110.3	850.5	192.5	110.7	90.0	33.46
Third service propulsion maneuver	25:17:39.3	279.9	2567.9	274.9	112.6	91.6	33.82
Fourth service propulsion maneuver	28:24:41.4	27.9	300.5	275.0	112.4	91.6	33.82
First descent propulsion maneuver (docked)	49:41:34.5	371.5	1737.5	274.6	112.1	91.5	33.97
Fifth service propulsion maneuver	54:26:12.3	43.3	572.5	131.0	125.9	89.2	33.61
Ascent propulsion firing to depletion	101:53:15.4	362.3	5373.4	3760.9	126.6	165.3	28.95
Sixth service propulsion maneuver	123:25:07.0	1.4	33.7	123.1	108.5	88.7	33.62
Seventh service propulsion maneuver	169:39:00.4	24.9	650.1	253.2	100.7	90.9	33.51
Eighth service propulsion maneuver	240:31:14.9	11.7	322.7	240.0	-4.2	88.8	33.52

NOTE: Apogee and perigee values are referenced to an oblate earth.

\*Firing times and velocity changes do not include the plus-X translation maneuver for propellant settling.

TABLE 7-IV.- ENTRY TRAJECTORY PARAMETERS

Entry interface (400 000 feet altitude)	
Time, hr:min:sec . . . . .	240:44:10.2
Geodetic latitude, deg north . . . . .	33.52
Longitude, deg west . . . . .	99.05
Altitude, miles . . . . .	65.90
Space-fixed velocity, ft/sec . . . . .	25 894
Space-fixed flight-path angle, deg . . . . .	-1.74
'Space-fixed heading angle, deg east of north . . . . .	99.26
Maximum conditions	
Velocity, ft/sec . . . . .	25 989
Acceleration, g . . . . .	3.35
Drogue deployment	
Time, hr:min:sec . . . . .	240:55:07.8
Geodetic latitude, deg north	
Recovery ship report . . . . .	23.21
Best-estimate trajectory . . . . .	23.22
Onboard guidance . . . . .	23.26
Target . . . . .	23.25
Longitude, deg west	
Recovery ship report . . . . .	67.94
Best-estimate trajectory . . . . .	67.98
Onboard guidance . . . . .	68.01
Target . . . . .	68.00

NASA-S-69-1961

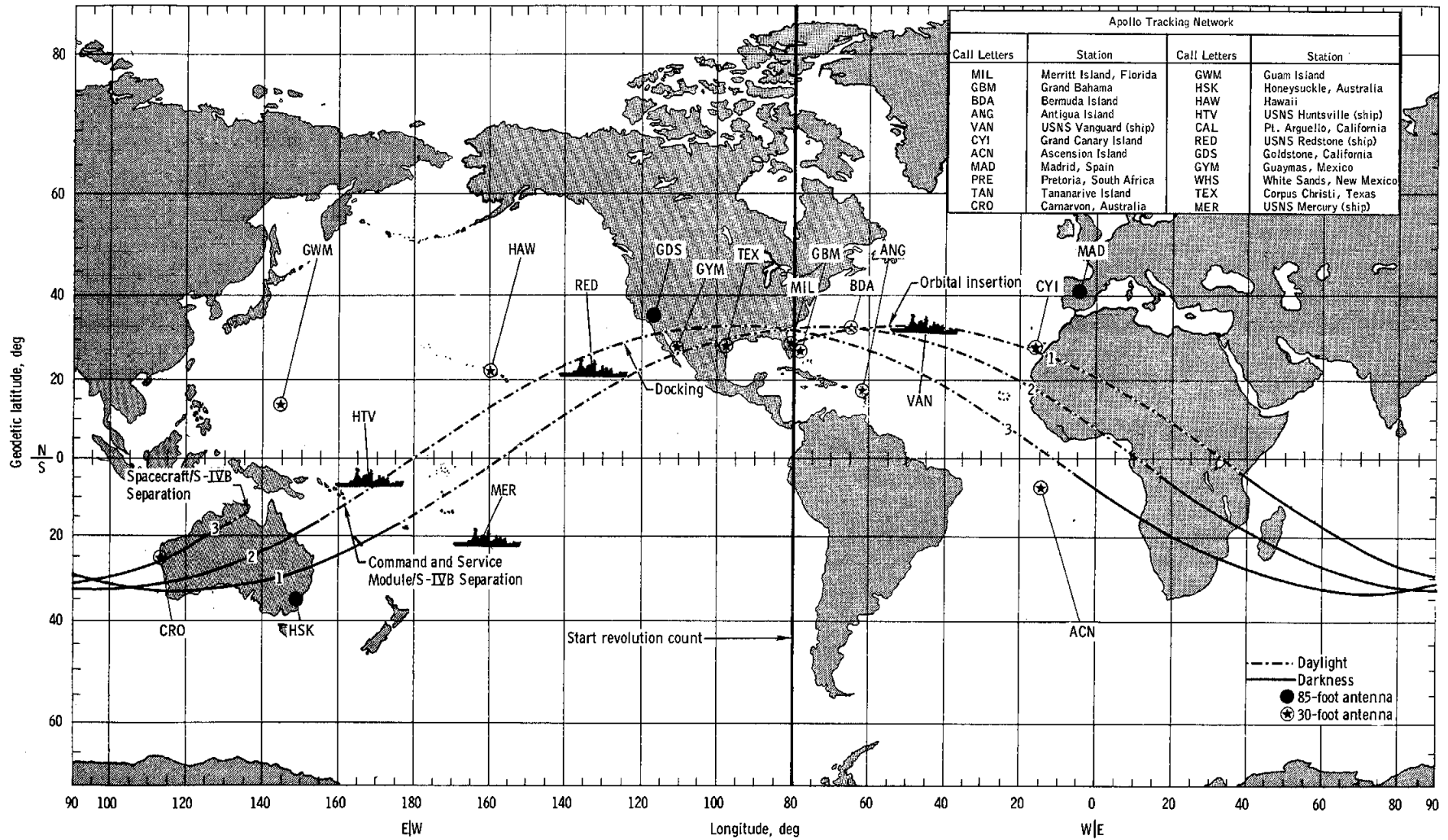
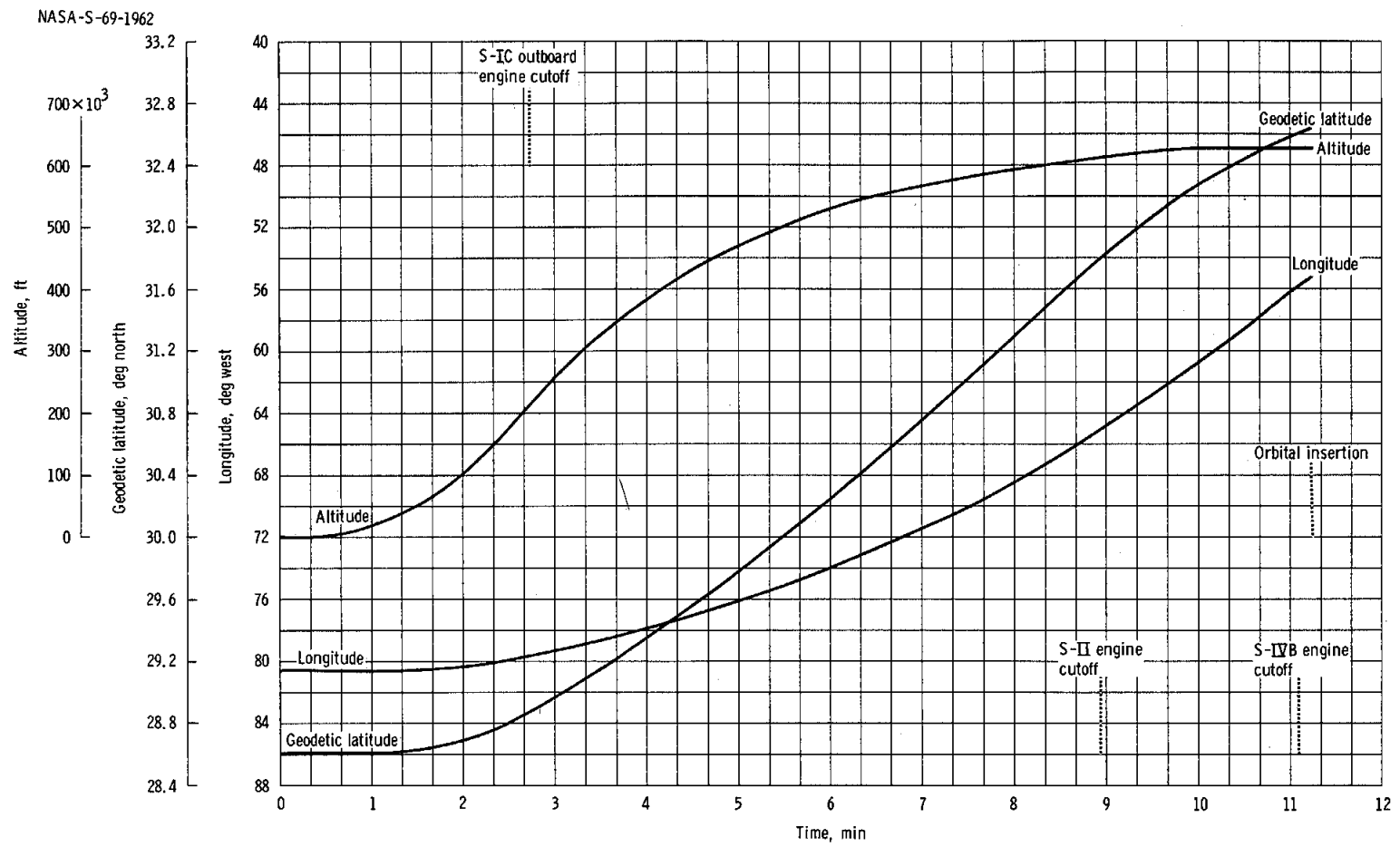
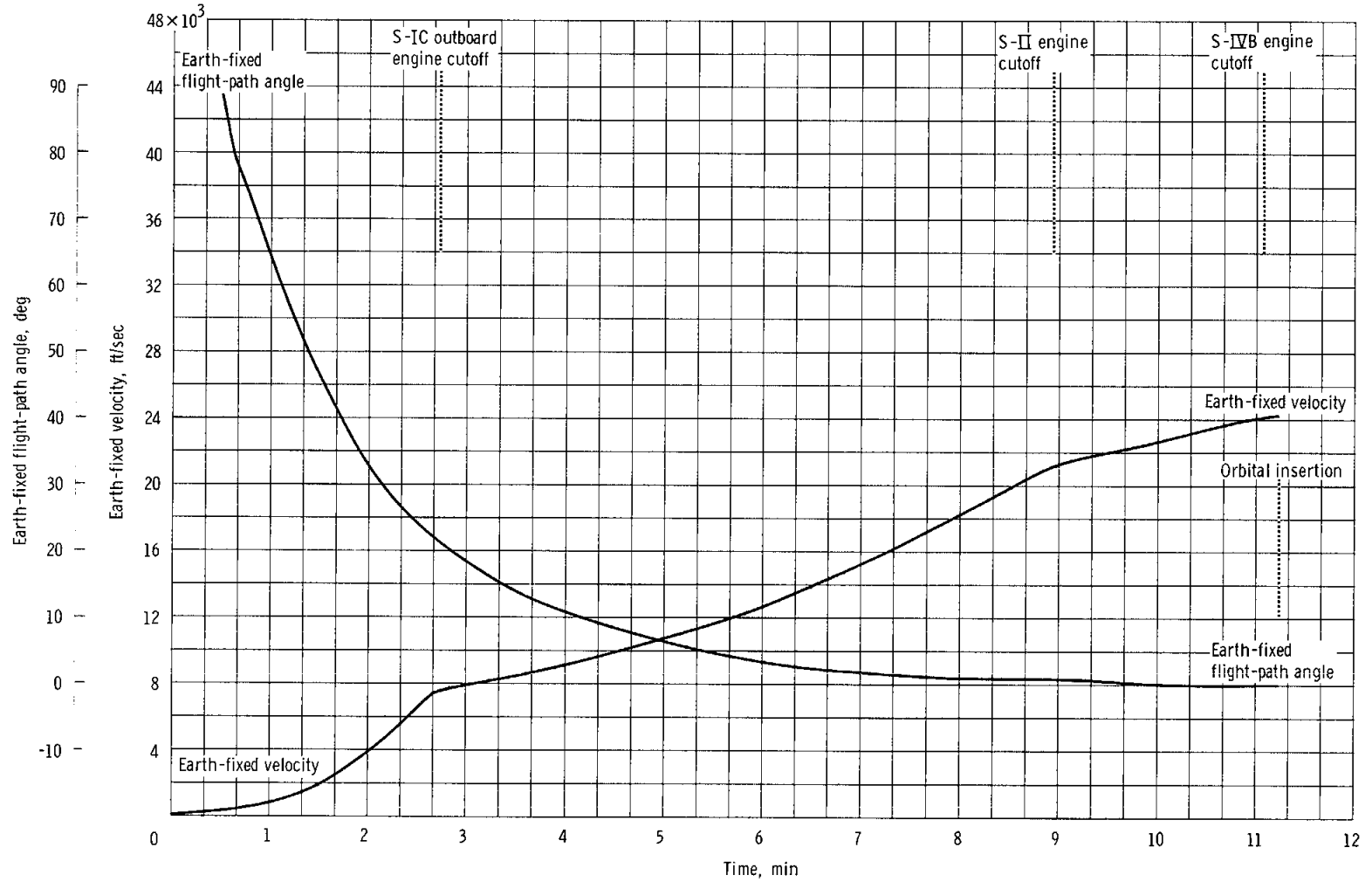


Figure 7-1. - Ground track during launch and parking orbits.



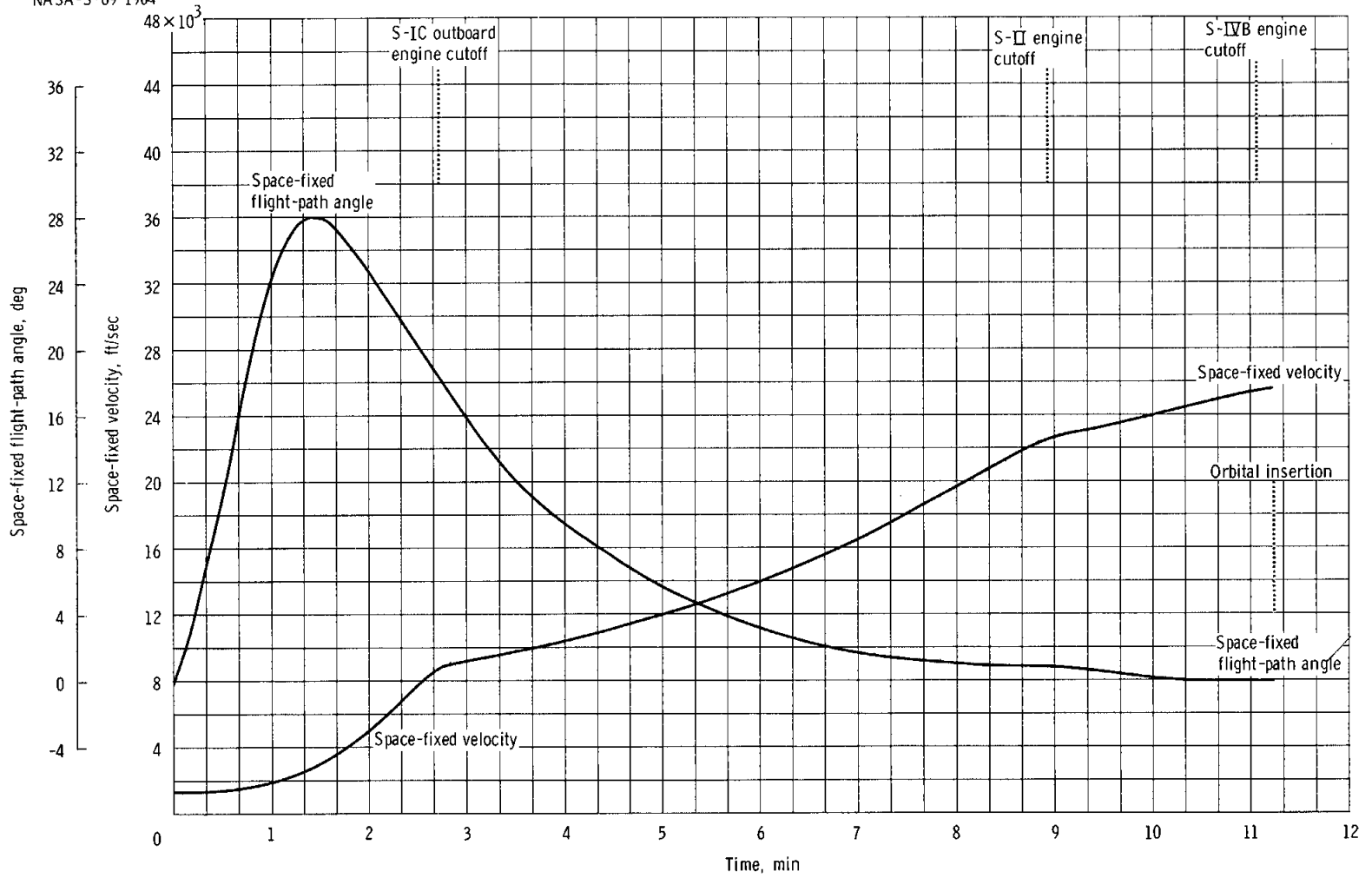
(a) Altitude, latitude, and longitude.

Figure 7-2. - Trajectory parameters during launch phase.



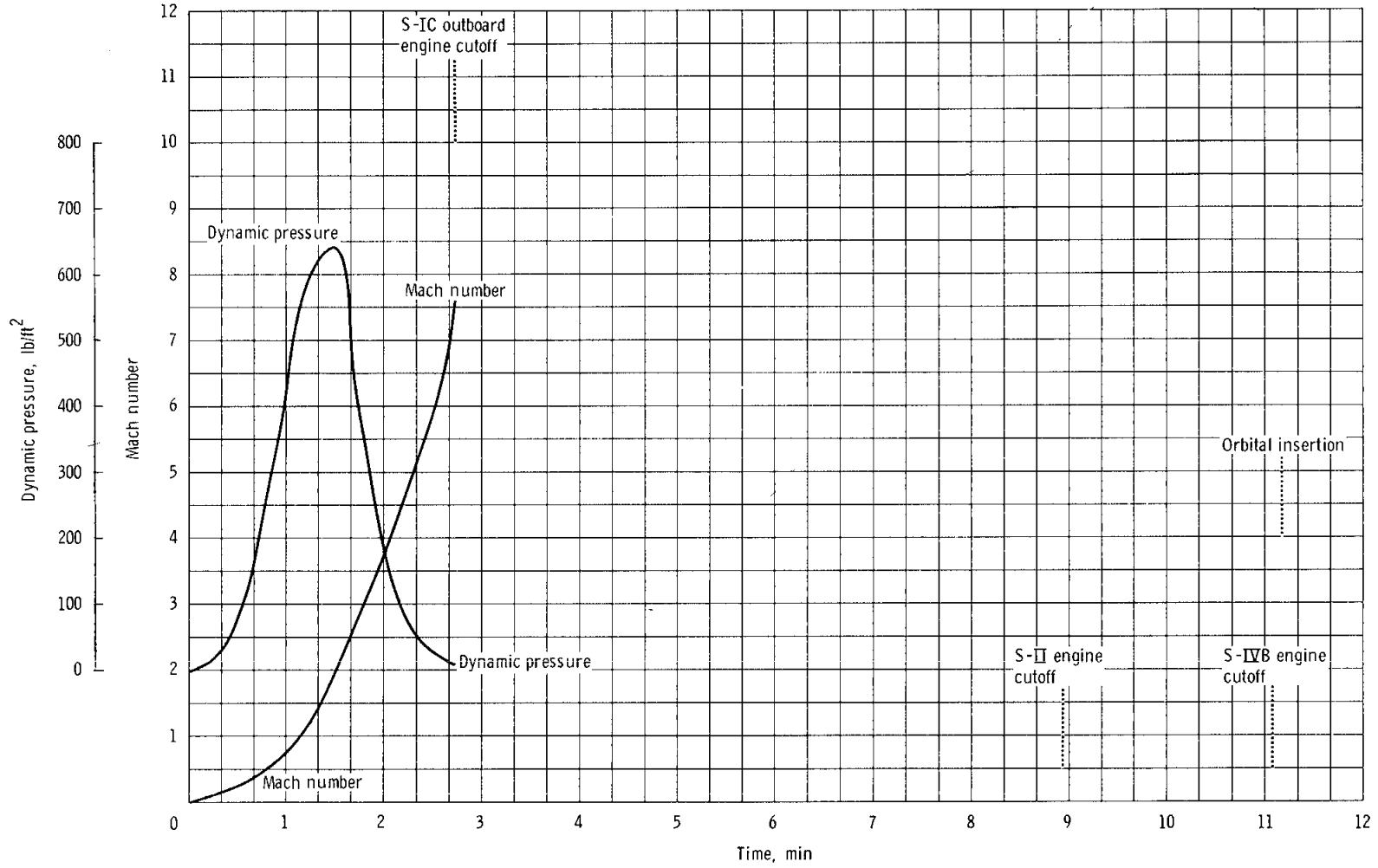
(b) Earth-fixed flight-path angle and velocity.

Figure 7-2. - Continued.



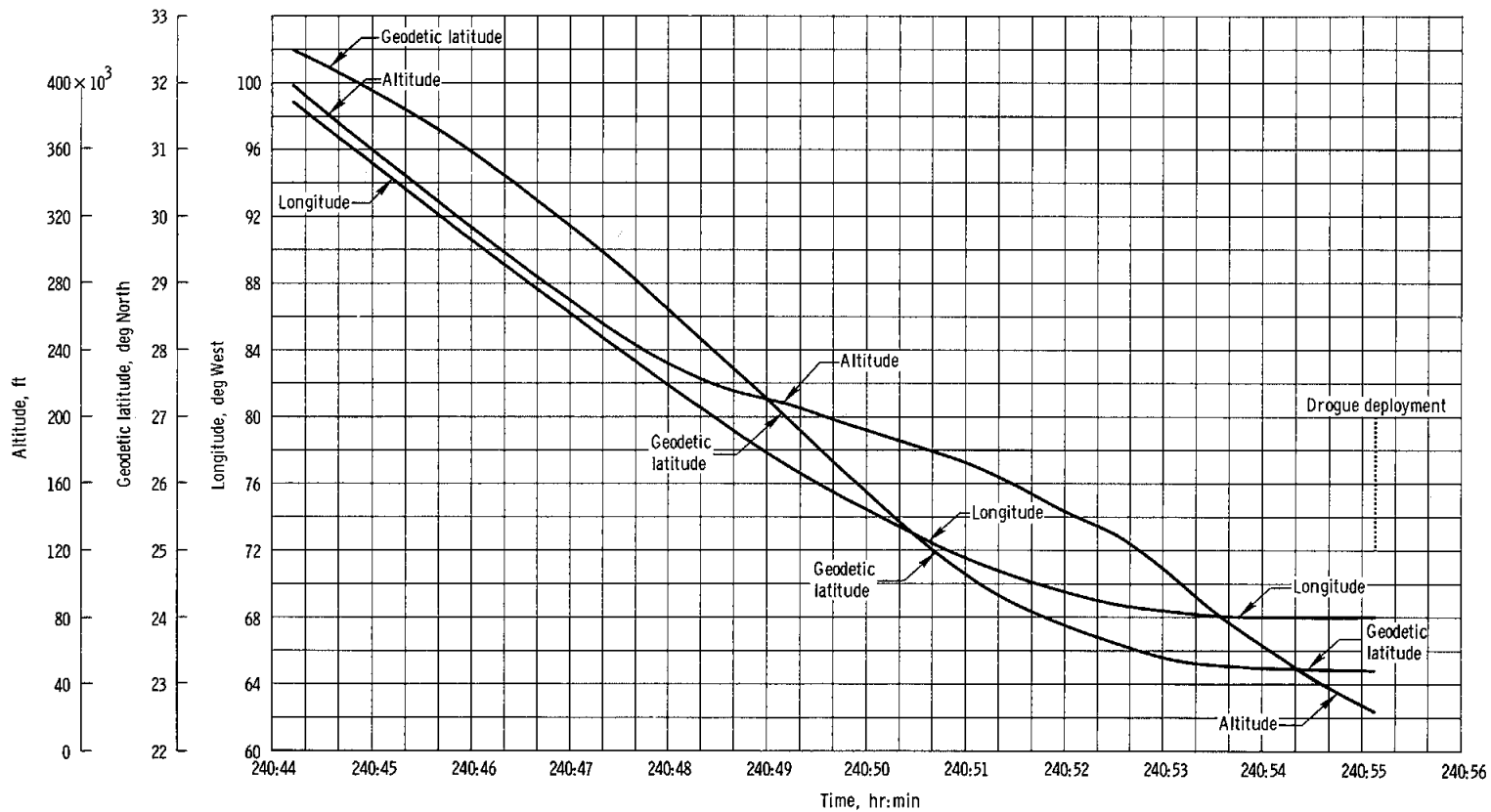
(c) Space-fixed flight-path angle and velocity.

Figure 7-2. - Continued.



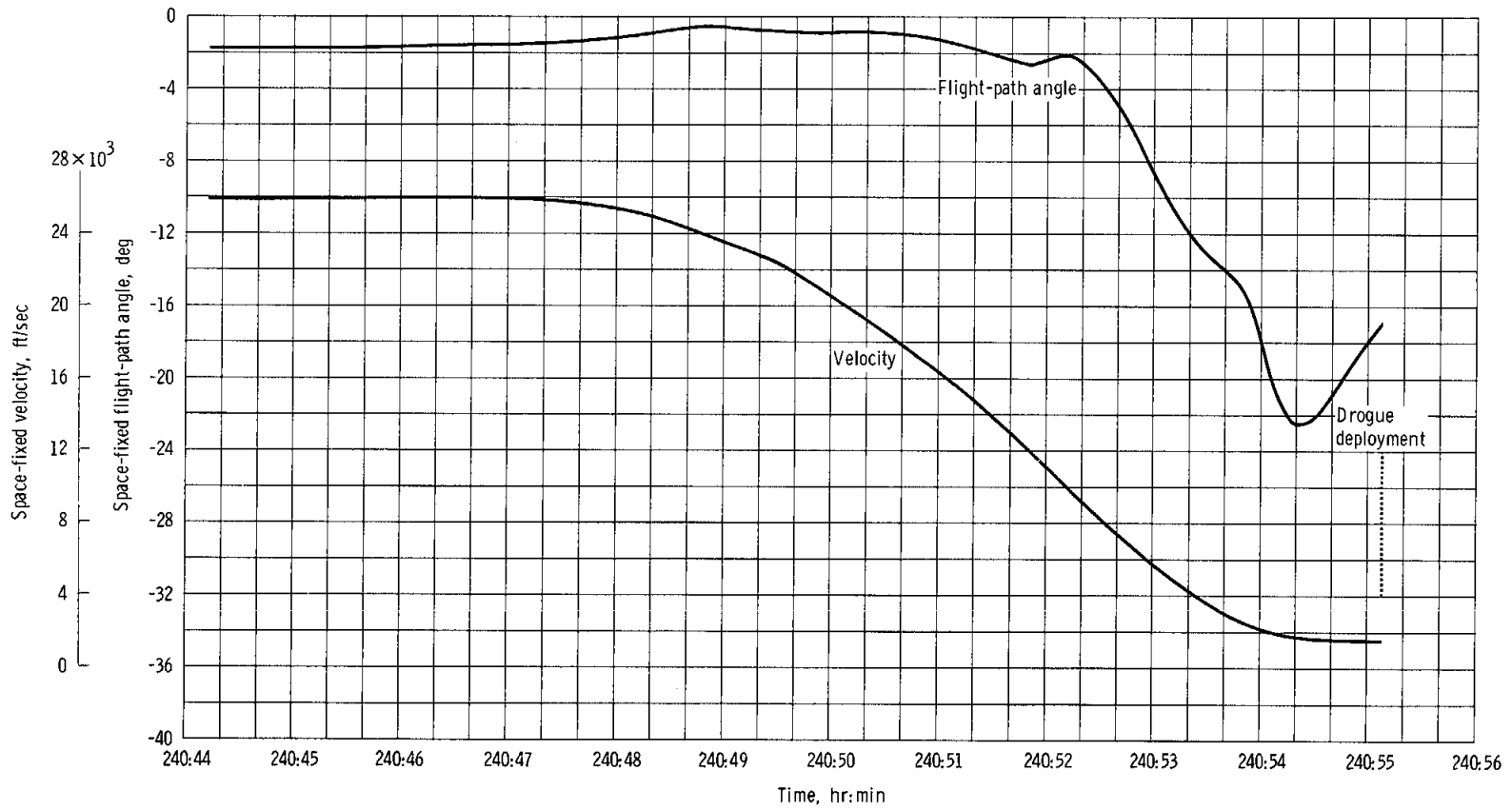
(d) Dynamic pressure and Mach number.

Figure 7-2. - Concluded.



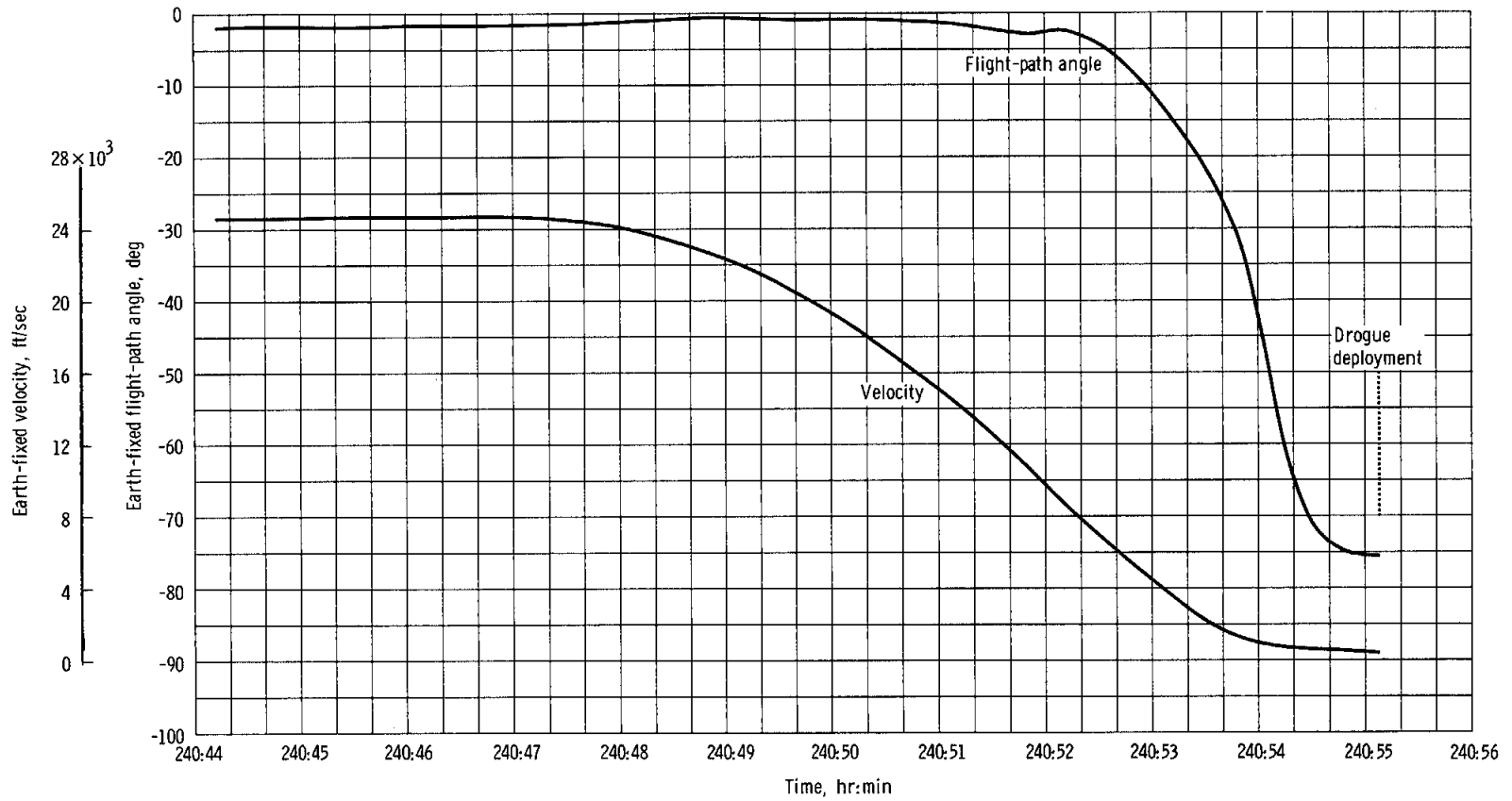
(a) Geodetic latitude, longitude, and altitude.

Figure 7-3. - Trajectory parameters during entry.



(b) Space-fixed velocity and flight-path angle.

Figure 7-3. - Continued.



(c) Earth-fixed velocity and flight-path angle.

Figure 7-3. - Concluded.

## 8.0 COMMAND AND SERVICE MODULE PERFORMANCE

This section presents the specific performance of major system groups in the command and service modules. No separate sections are included for the launch escape system and the spacecraft/launch-vehicle adapter, both of which performed as expected. All command and service module systems performed satisfactorily; only those systems for which performance significantly differs from previous flights or for which results are considered pertinent to future flights will be discussed. The sequential, pyrotechnic, thermal protection, power distribution, and emergency detection systems operated exactly as intended and are not documented. Specific discrepancies and anomalies in other systems are mentioned in this section but are discussed in greater detail in section 17, Anomaly Summary. Detailed analyses of system performance related to the Apollo 9 extravehicular and rendezvous operations are contained in sections 4 and 5, respectively, and are not presented here. A compilation of liquid consumable quantities is presented at the end of this section.

### 8.1 STRUCTURAL AND MECHANICAL

#### 8.1.1 Structural Loads Analysis

Analysis of spacecraft structural loads was based on measured acceleration, aerodynamic, and engine data, all of which indicate that the loads were less than design values for all phases of flight.

Launch phase.- Peak ground winds at launch were 14.4 knots, compared to the launch restriction of 30 knots. The calculated and predicted loads at the various interfaces at lift-off are compared in table 8.1-I. The highest spacecraft loads, also shown in the table, occurred in the region of maximum dynamic pressure and were caused primarily by the angle of attack induced by wind shear. Maximum axial acceleration of the spacecraft occurred immediately prior to first-stage outboard-engine cutoff (table 8.1-I).

The crew reported experiencing a negative longitudinal acceleration during shutdown and separation of the first stage; the maximum negative acceleration recorded was minus 0.8g at 0:02:43.6. This negative acceleration is greater than any measured in the three previous Saturn V missions (fig. 8.1-1), but it was still less than the design value. This negative acceleration is attributed to a more rapid thrust decay of the first-stage engines from the 30-percent thrust level. The command module accelerations during this period are shown in figure 8.1-2. The measured and predicted maximum tension loads at separation are compared in table 8.1-I.

The crew reported low-level longitudinal oscillations near the end of second-stage flight. The maximum longitudinal oscillation measured at the command module forward bulkhead was 0.05g at 9 Hz, which is within the acceptable structural levels.

Docked spacecraft.- The maximum accelerations for the docked spacecraft were measured during the start transient of the first service propulsion firing (table 8.1-II and fig. 8.1-3). The calculated and allowable loads at the docking interface are compared in table 8.1-III. The stroking (engine gimbaling) test during the third service propulsion firing was to have a maximum gimbal angle of  $\pm 0.02$  radians, but only 80 percent of this amplitude was obtained. The rates for this stroking test are shown in figure 8.1-4, and the measured and allowable loads are compared in table 8.1-III.

The crew reported a low-frequency bending motion when the service module reaction control system was operated in the docked configuration (see section 8.6). Peak rates measured during these operations were less than 0.1 deg/sec in pitch and yaw. All of the docked spacecraft interface loads were within design limits.

Command and service module accelerations.- The maximum command and service module accelerations were experienced during the eighth service propulsion firing, which involved the lowest spacecraft weight; these accelerations are shown in table 8.1-II. A time history of the acceleration for the start of the firing is shown in figure 8.1-5, and is representative of the normal response to start transients experienced on previous flights. During entry, the maximum X-axis acceleration was 3.35g.

### 8.1.2 Mechanical Systems

The mechanical systems of particular interest for Apollo 9 are the docking mechanism, the side hatch, and the earth landing system. The docking mechanism is discussed in section 5, and operation of the side hatch is discussed in sections 4 and 10.2.

All entry events, from forward heat shield jettison through main parachute deployment, were accomplished automatically, as planned. The forward heat shield was recovered after landing and appeared to have functioned properly. The two drogues and three pilot parachutes deployed properly and without apparent damage. After the main parachutes were inflated, the flight crew noted that several individual sails were damaged in the lower skirt area of at least one of the canopies; the damage included one broken suspension line (see fig. 8.1-6). Parachute damage caused by contact of the deployment bag with an adjacent canopy is characterized by torn or friction-burned sails in a localized area in the lower

skirt, with suspension-line break near the canopy. The parachute system is designed to sustain this type of minor damage, which is of a relatively low-probability and does not jeopardize the inflation or performance characteristics of the main parachutes. Recontact was observed on 22 of 27 boilerplate tests, but in only 7 of these cases was any damage found, and this was similar to that observed in Apollo 9. There was no indication that the reaction control system propellant depletion firing and purge caused any significant damage to the main parachutes.

### 8.1.3 Thermal Control

The temperature response for all passively controlled elements of the command and service modules remained within normal operating limits and was consistent with Apollo 7 data. Temperatures for the service propulsion and reaction control system tanks remained within a range of 57° to 77° F, except during rendezvous, and exhibited a slight cooling trend. During the rendezvous (92 to 101 hours), the temperature of the quad-C helium tank increased to 82° F because the spacecraft was maintained at a sun-oriented attitude that would cause this increase. The quad-B helium tank was also sun-oriented and exhibited a similar temperature increase but at a lower range. The temperatures of the service propulsion feedlines, the command module reaction-control helium tanks, and the command module ablator remained within expected ranges.

### 8.1.4 Thermal Samples

A group of thermal-control-coating and window-glass specimens were selected for placement on both vehicles for retrieval and postflight evaluation to determine the degradation in thermal absorptance and emittance resulting from the launch, staging, and induced and natural environments. Four of the five thermal samples were retrieved; one thermal sample was missing. These specimens were located on the spacecraft as shown in figure 4-2.

Preflight and postflight absorptance and emittance measurements of the samples were made. The visual appearance of the service module specimens indicated degradation, and measurements over the thermally significant wavelength spectrum (0.28 to 2.5 microns) confirmed the degradation to be predominantly in the visual range (approximately 0.38 to 0.76 microns). However, the total degradation was within the allowable limits for acceptable performance. Results of chemical analyses identifying the degradation sources will be included in a supplemental report. Table 8.1-IV contains the results of the analyses conducted to the time of publication of this report.

TABLE 8.1-I.- MAXIMUM SPACECRAFT LOADS DURING LAUNCH PHASE

Interface	Load	Lift-off		Maximum q <sub>a</sub>		End of first-stage boost		Staging	
		Calculated <sup>a</sup>	Predicted <sup>b</sup>	Calculated <sup>a</sup>	Predicted <sup>b</sup>	Calculated <sup>a</sup>	Predicted <sup>b</sup>	Calculated <sup>a</sup>	Predicted <sup>b</sup>
Launch escape system/command module	Bending moment, in-lb . . .	370 000	2 173 000	708 900	1 390 000	31 100	113 000	46 000	960 000
	Axial force, lb . . . . .	-9 760	-11 000	-21 200	-27 300	-35 000	-36 100	6 970	5 000
Command module/service module	Bending moment, in-lb . . .	514 000	2 810 000	884 100	1 827 000	257 000	504 000	137 000	1 260 000
	Axial force, lb . . . . .	-23 310	-36 000	-82 500	-91 000	-83 700	-90 500	17 565	12 400
Service module/adapter	Bending moment, in-lb . . .			3 074 000	5 390 000	2 700 000	2 496 000	1 279 000	1 780 000
	Axial force, lb . . . . .			-176 300	-194 000	-265 500	-299 000	55 190	38 600
Adapter/instrument unit	Bending moment, in-lb . . .			9 637 500	16 300 000	1 740 000	3 919 000	1 874 000	3 630 000
	Axial force, lb . . . . .			-269 500	-297 000	-406 000	-445 000	85 690	59 000

NOTE: Negative axial force indicates compression.

The flight conditions at maximum q<sub>a</sub> were:

Condition	Measured	Predicted <sup>b</sup>
Flight time, sec . . . . .	79	75.4
Mach no. . . . .	1.42	1.35
Dynamic pressure, psf . . .	633	685.7
Angle of attack, deg . . . .	4.13	6.35
Maximum q <sub>a</sub> , psf-deg . . . .	2614	4354

The accelerations at the end of first-stage boost were:

Acceleration	Measured	Predicted <sup>b</sup>
Longitudinal, g . . . . .	3.9	4.04
Lateral, g . . . . .	0	0.05

<sup>a</sup>Calculated from flight data.

<sup>b</sup>Predicted Apollo 9 loads for Saturn V, block II design conditions.

TABLE 8.1-II.- MEASURED ACCELERATIONS DURING TWO MANEUVERS

Maneuver	Acceleration, g		
	X	Y	Z
First service propulsion firing (docked)	0.08	0.08	0.05
Eighth service propulsion firing (deorbit)	0.5	0.15	0.1

TABLE 8.1-III.- CALCULATED SPACECRAFT INTERFACE LOADS  
DURING TWO DOCKED SERVICE PROPULSION MANEUVERS

Maneuver	Load	Calculated*	Limit capability**
First firing	Bending moment, in-lb . . .	19 000	220 000
	Axial force, lb . . . . .	-18 600	-18 600
100 percent stroking test (third firing)	Bending moment, lb . . . .	30 000	320 000
	Axial force, lb . . . . .	8 400	8 400

\*Based on flight data.

\*\*For factor of safety of 1.5.

TABLE 8.1-IV.- THERMAL SAMPLE DEGRADATION SUMMARY

Material	Sample <sup>a</sup>	Absorptance				Emittance		
		Allowable	Preflight	Postflight	Change, percent	Preflight	Postflight	Change, percent
Service module: radiator thermal control coating	1	0.50	0.20	0.28	40.0	0.93	0.93	0
	2	0.50	0.20	0.25	25.0	0.93	0.93	0
	3	0.50	0.20	0.27	37.0	0.93	0.93	0
Service module: bay IV outer shell	1	0.50	0.25	0.37	48.0	0.86	0.88	2.3
	2	0.50	0.24	0.34	42.0	0.86	0.88	2.3
	3	0.50	0.24	0.40	67.0	0.86	0.87	1.1
Lunar module: thermal shield coating		N/A	0.70	0.73	4.3	0.73	0.70	4.3
Lunar module: glass		Approximately 2 percent decrease in transmittance						
Command module: thermal control tape		Sample was not retrieved						

<sup>a</sup>Sample 1 - located at top of radiator panel in line with minus Z forward-firing thruster; sample 2 - located at top of radiator panel but not in line with minus Z forward-firing thruster; sample 3 - located at bottom of radiator panel directly below sample 2.

NASA-S-69-1969

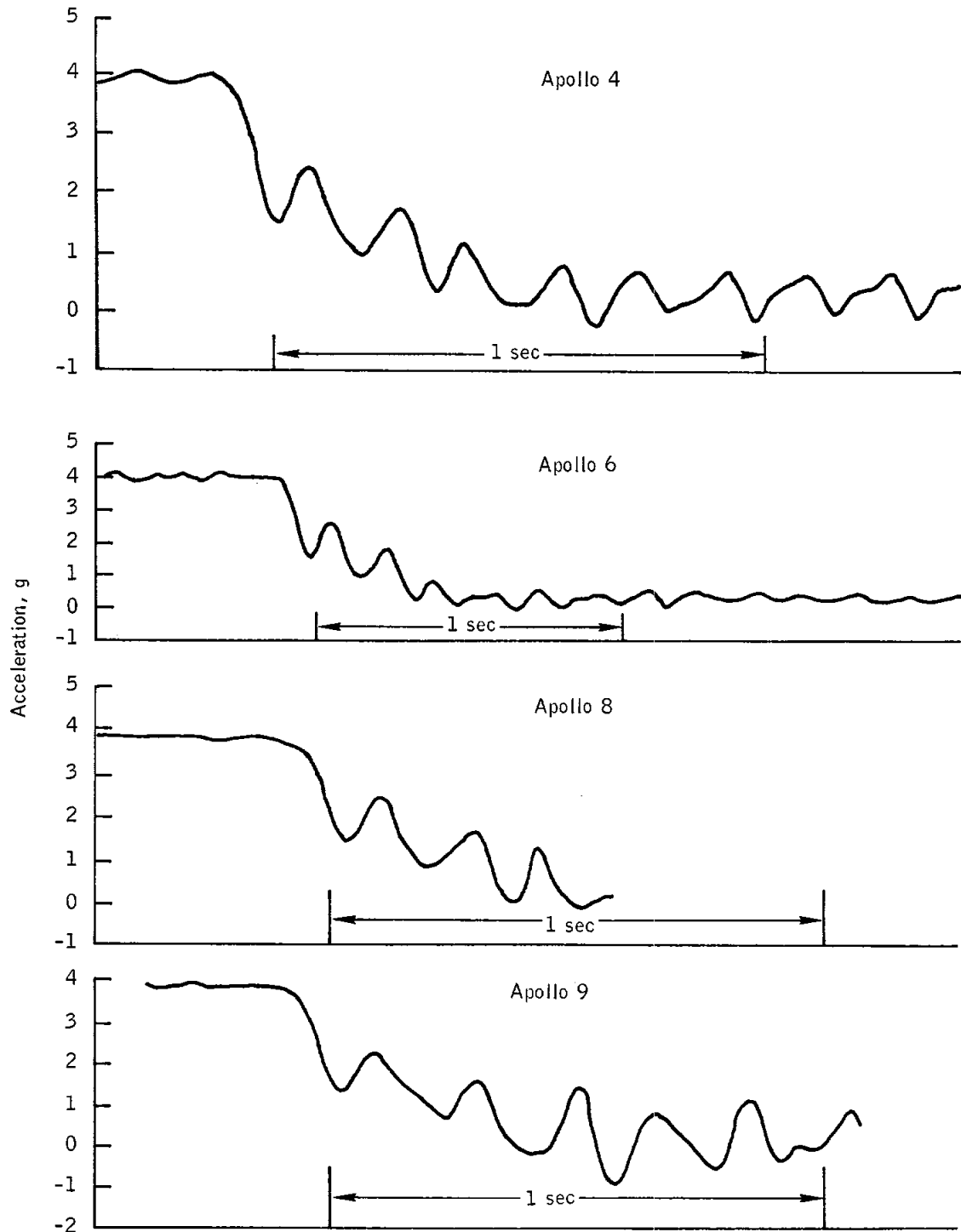


Figure 8.1-1.- Comparison of command module X-axis acceleration at S-IC outboard engine cutoff.

NASA-S-69-1970

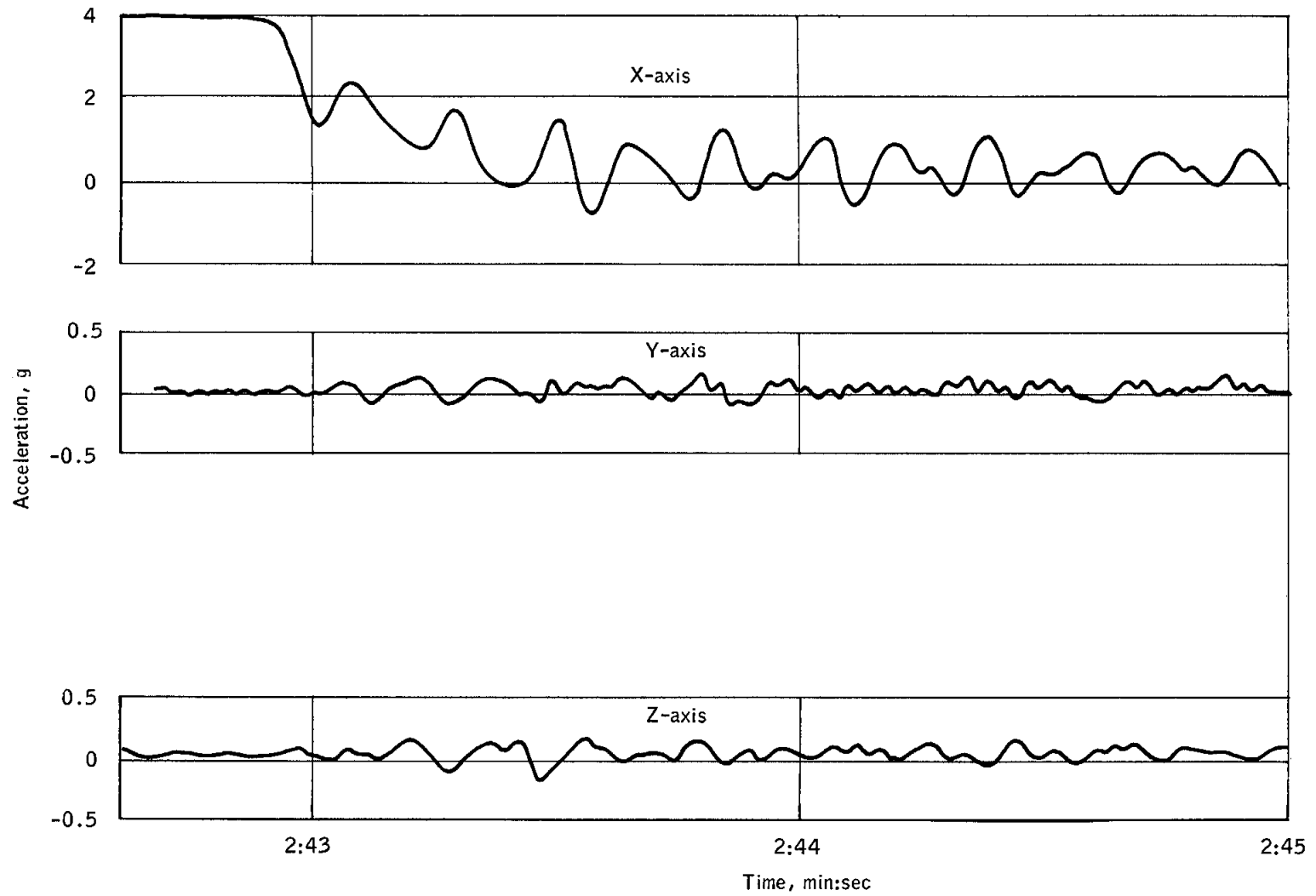


Figure 8.1-2.- Command module accelerations at S-IC outboard engine cutoff.

NASA-S-69-1971

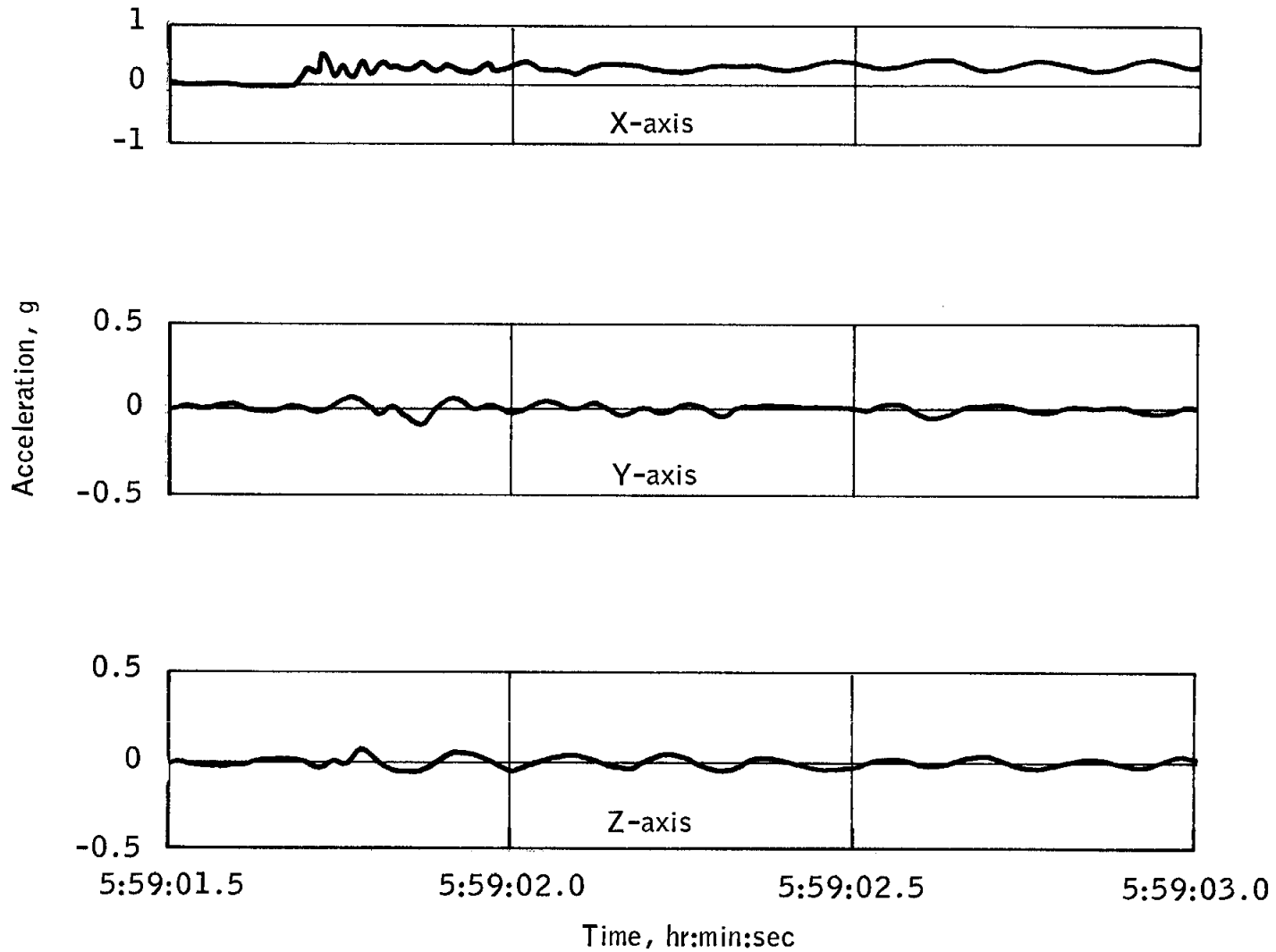


Figure 8.1-3.- Command module linear accelerations during first service propulsion firing.

NASA-S-69-1972

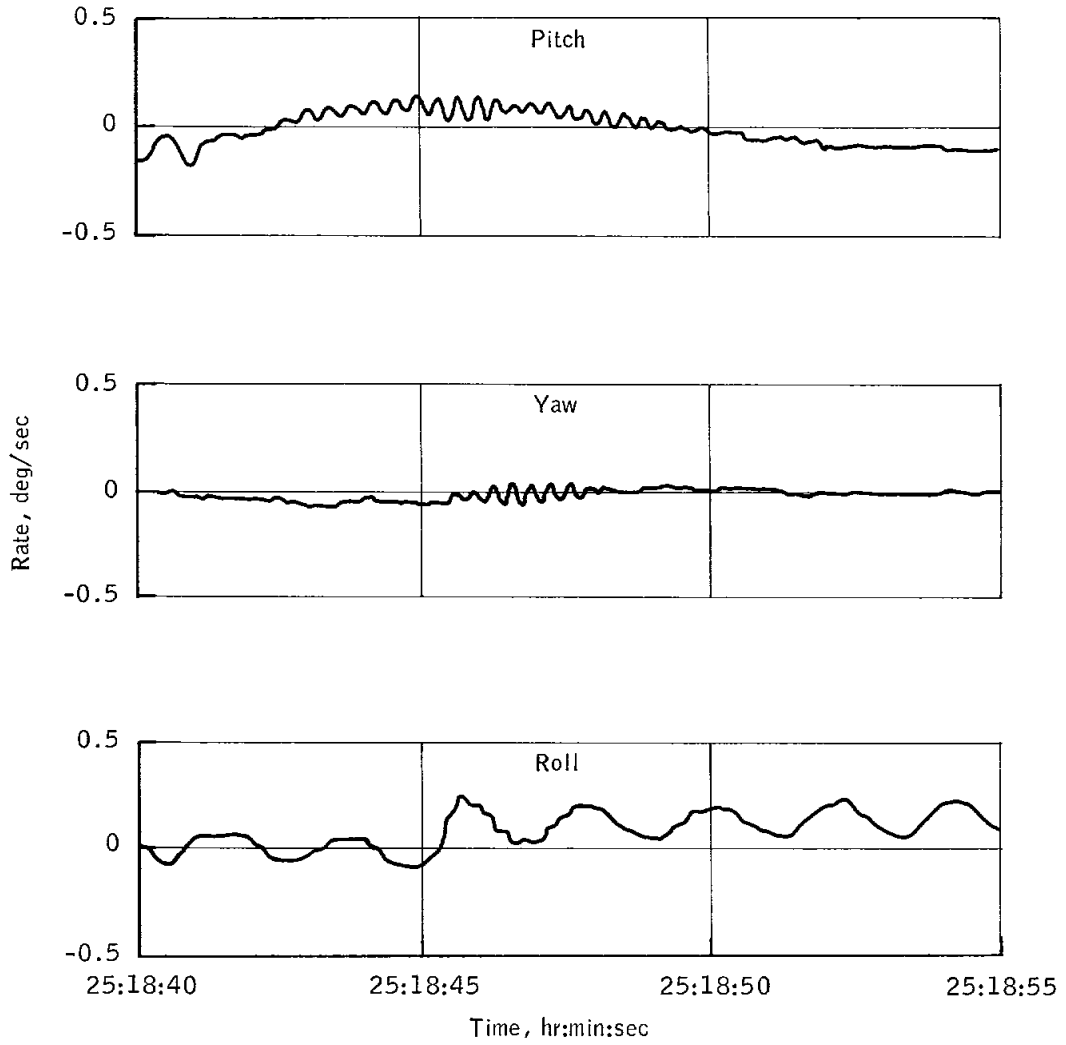


Figure 8.1-4.- Command module rates during stroking test, third service propulsion firing.

NASA-S-69-1973

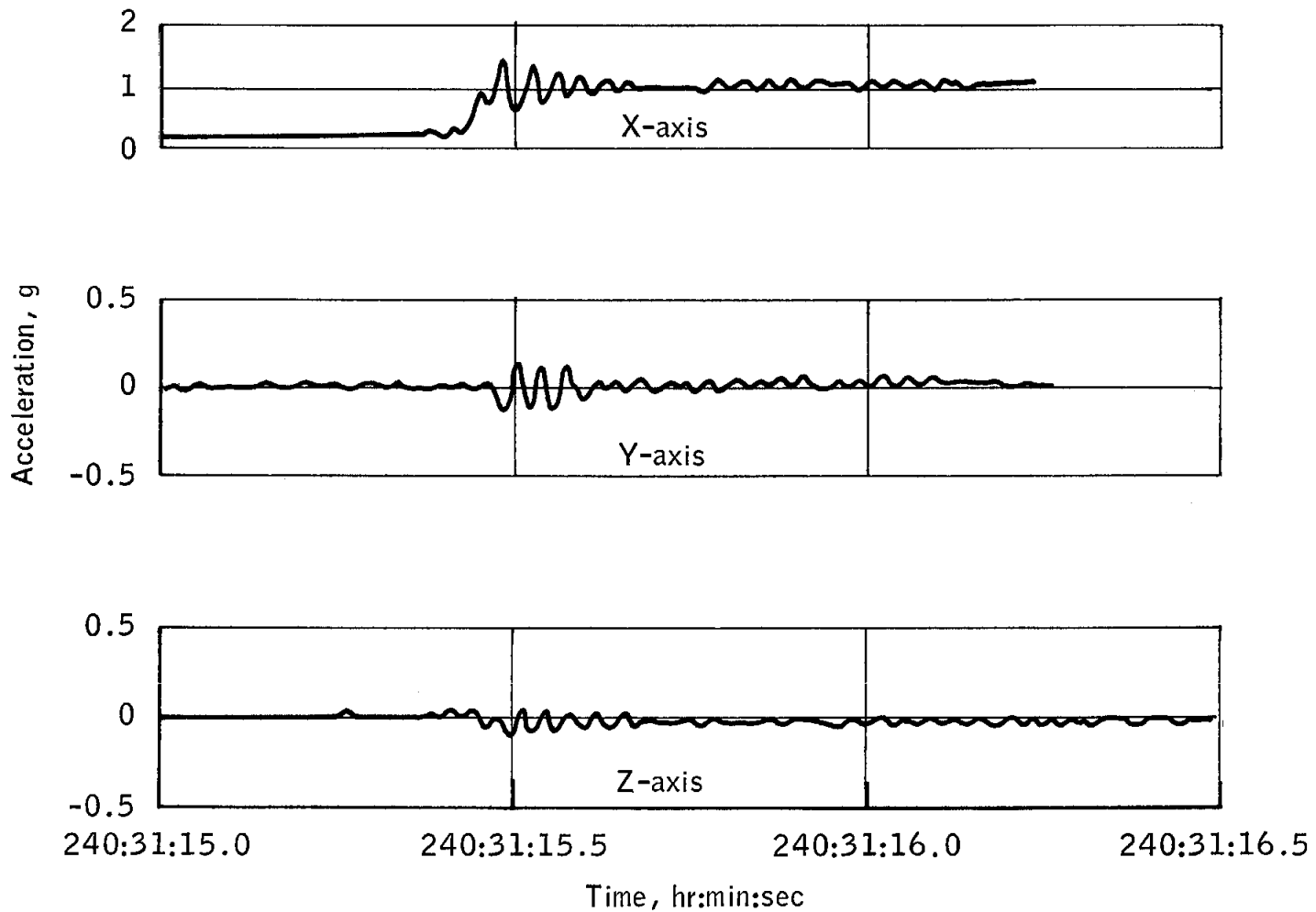


Figure 8.1-5.- Command module linear accelerations during eighth service propulsion firing (deorbit maneuver).



Figure 8.1-6.- Main parachute damage.

## 8.2 ELECTRICAL POWER

### 8.2.1 Fuel Cells

The fuel cells and radiators performed satisfactorily during pre-launch operations and the mission. The fuel cells were activated 206 hours prior to launch and shared the spacecraft electrical loads with ground support equipment until 2 hours prior to launch, when they assumed the entire spacecraft electrical load.

After lift-off, the fuel cells had provided approximately 455 kWh of energy at an average current of 21.5 amperes per fuel cell at an average command module bus voltage of 29.3 V dc. Bus voltages were maintained between 28.1 and 30.4 V dc during all mission phases when fuel cell power was being used. The maximum deviation from equal load sharing between fuel cells was an acceptable 2.5 amperes.

The thermal performance under a current load for fuel cells 1 and 3 was within the normal range throughout the flight. The condenser exit temperature for fuel cell 2 was outside the nominal range during power-up and power-down phases between 88 hours to 191 hours, as shown in figure 8.2-1. The minimum condenser exit temperature observed for fuel cell 2 was 148° F at 110 hours with an average current of 15 amperes per fuel cell; the maximum value observed was 184° F at approximately 147 hours with an average current of 27.8 amperes per fuel cell. These and other excursions resulted in low and high caution and warning indications. Fuel cell behavior during this period was very similar to that observed during Apollo 7. The valve travel in the secondary coolant regenerator bypass was restricted between approximately 4 percent and 10 percent bypass during the period from 88 to 191 hours; however, modulation was achieved between these points (fig. 8.2-1). Fuel cell 2 condenser exit temperature returned to normal operating limits after 191 hours under relatively high current conditions. The corresponding bypass valve modulation was normal, between 8 and 19 percent. Section 17 contains a detailed discussion of this anomaly.

Little or no performance increase followed hydrogen or oxygen purging during the flight, indicating that high-purity reactants were being supplied to the fuel cells from the cryogenic tanks.

Calculations based on total ampere-hours generated by the fuel cells indicate a total consumption of 40 pounds of hydrogen and 316 pounds of oxygen, not including purges. These quantities agree well with measured cryogenic quantities and the estimated oxygen usage by the environmental control system. Based on total ampere-hours, the fuel cells produced 356 pounds of water during the mission.

### 8.2.2 Batteries

The entry and pyrotechnic batteries performed satisfactorily in support of mission requirements. A plot of bus A and B voltages during the mission is shown in figure 8.2-2. Entry batteries A and B were fully recharged just prior to lift-off. During flight, batteries A and B received four recharges. The charging characteristics of battery B were different from those anticipated. Each time battery B was recharged, the established end cutoff current level of 0.4 ampere was reached before a full battery recharge was achieved. Battery A responded as expected, achieving the fully recharged condition prior to reaching the cutoff current level.

Postflight testing showed that battery B had a higher internal resistance than the majority of batteries of this configuration. To insure a higher charge return on future missions, charging will proceed below the formerly established 0.4 ampere so long as a 39.5-volt level is not exceeded and the charge return does not exceed 100 percent of the previous discharge. Additionally, for Apollo 11 and subsequent, the charger output voltage has been raised significantly, such that a full charge will be returned even though the impedance of individual batteries may differ slightly. A plot of total ampere-hours remaining throughout the mission is shown in figure 8.2-3. Battery C was not recharged after installation in the spacecraft. Charging times were similar to charging times on Apollo 8.

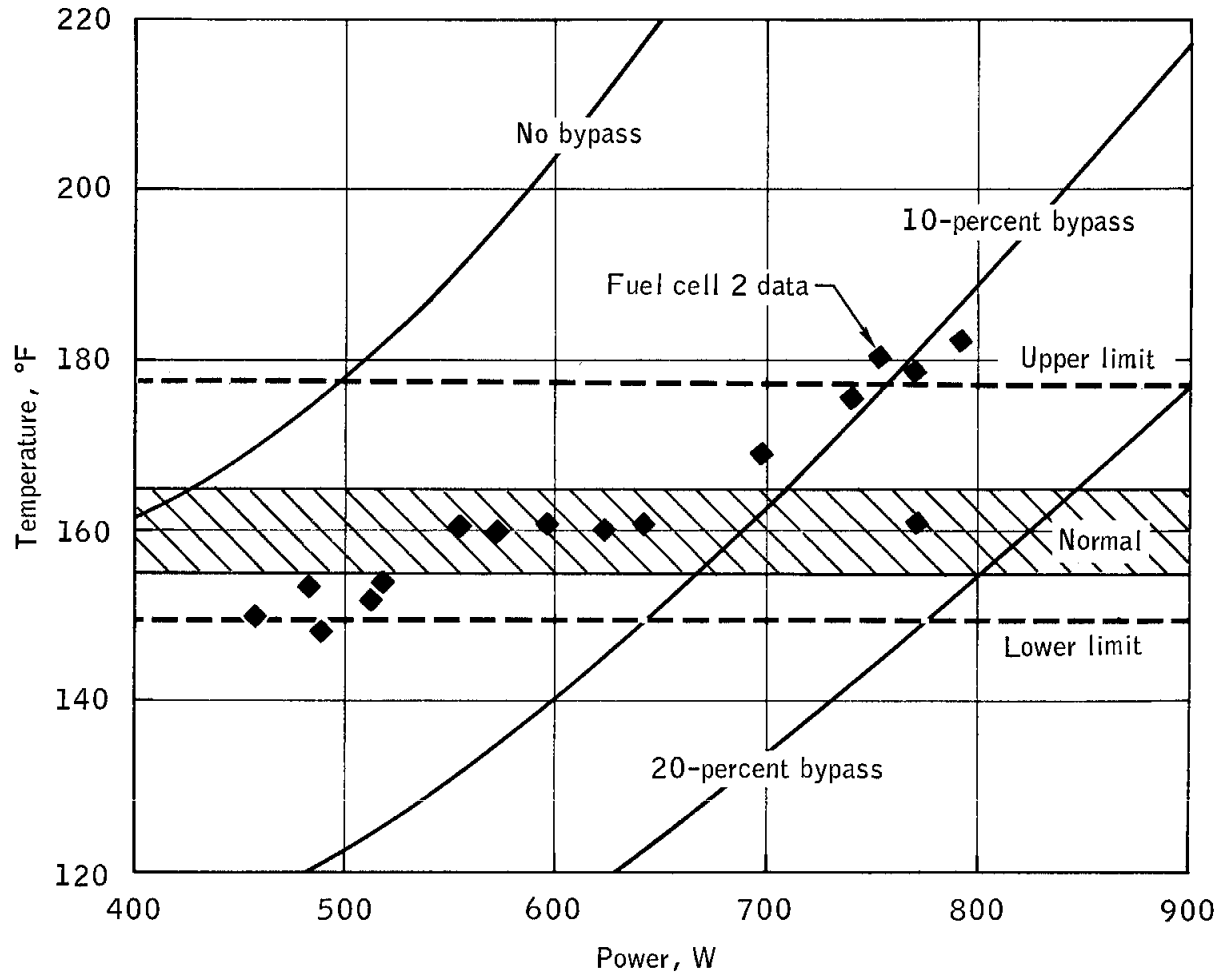


Figure 8.2-1.- Fuel cell 2 condenser exit temperature compared with power output.

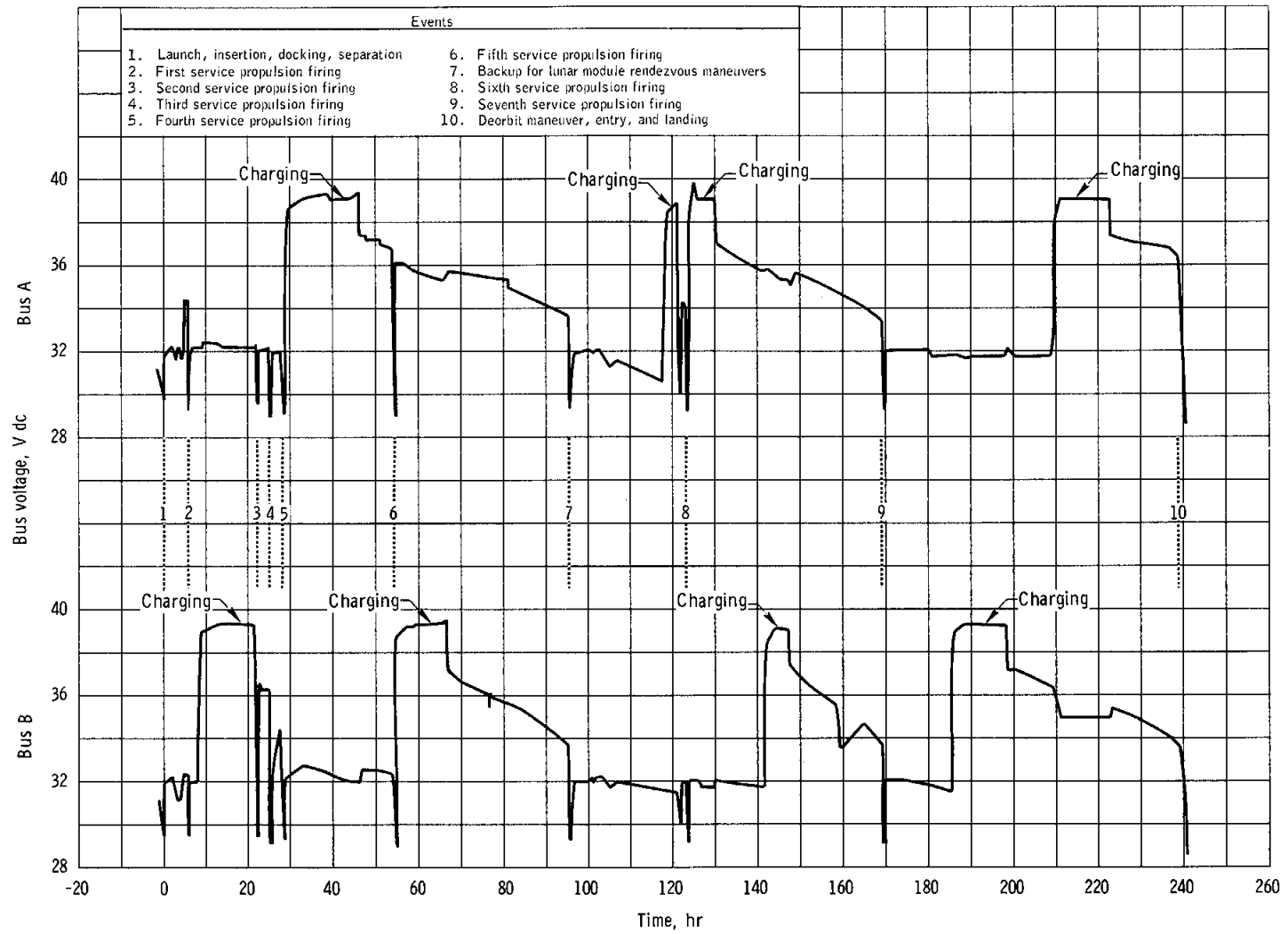


Figure 8.2-2. - Battery bus voltages during the mission.

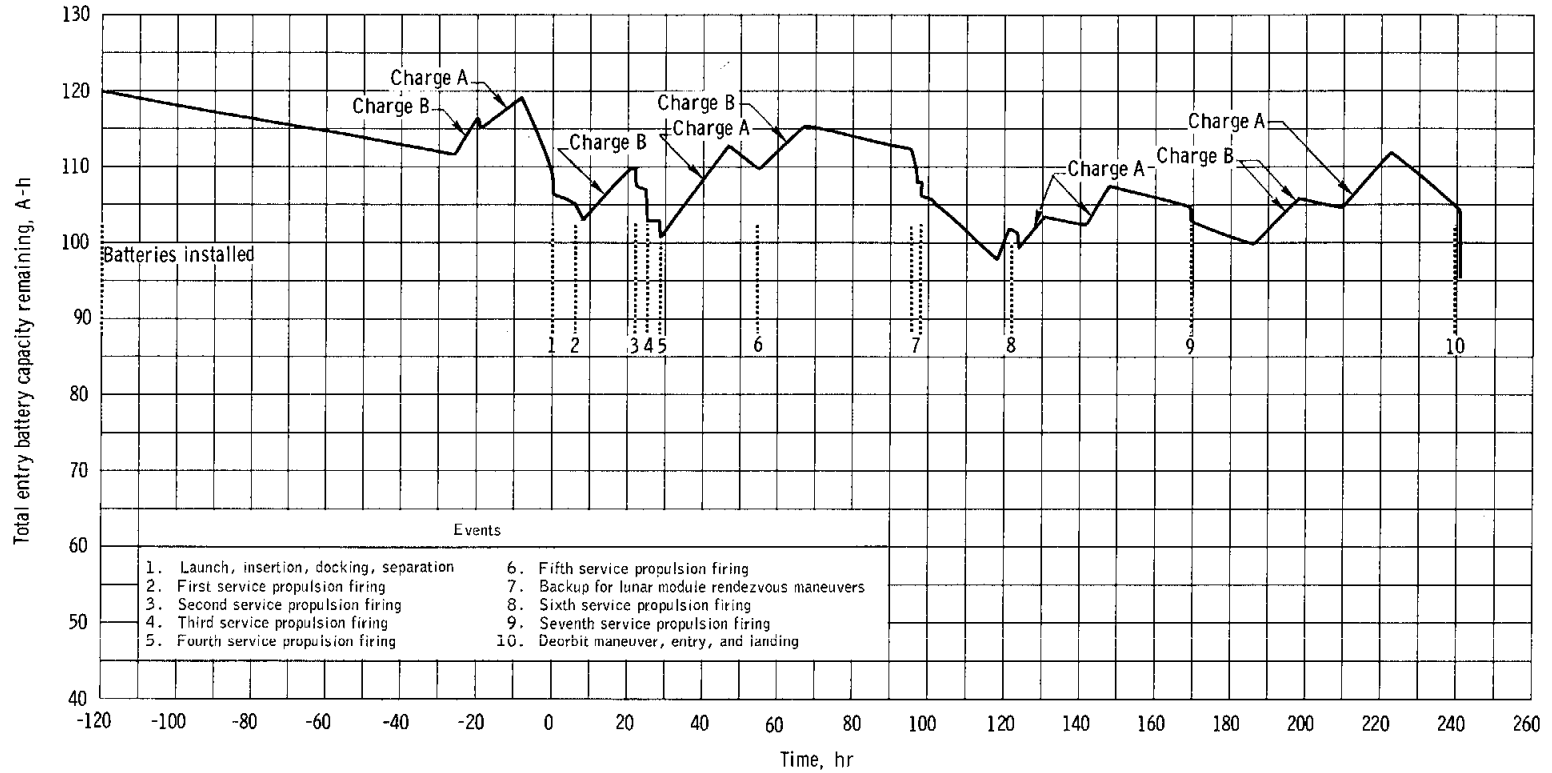


Figure 8.2-3. - Battery capacity remaining.

### 8.3 CRYOGENIC STORAGE

The cryogenic storage system satisfactorily supplied reactants to the fuel cells and metabolic oxygen to the environmental control system. At launch, the total oxygen quantity was 614.2 pounds (125.5 pounds above minimum requirements) and the total hydrogen quantity was 52.9 pounds (7.6 pounds above the minimum requirements). Consumption from the system was nominal during the flight.

The oxygen and hydrogen usage rate throughout the mission was as predicted and corresponded to an average fuel-cell current of 67.3 amperes and an average environmental control system oxygen flow rate of 0.35 lb/hr.

During the flight, the hydrogen-tank automatic pressure control system failed, and this anomaly is discussed in section 17. As a result of this failure, the hydrogen system pressure was controlled with the fans in a manual mode. This procedure caused no constraints to the mission.

Near the beginning of the fourth revolution, a caution and warning alarm was actuated by a low-pressure indication at 228 psia for hydrogen tank 1. The allowable pressure range for the hydrogen system is 225 psia to 260 psia; therefore, it was concluded that the caution and warning system was set too close to tank 1 lower limit. To prevent the alarm from actuating during rest periods, one of two methods was used, depending on which would allow the greatest length of time between alarms. Either the pressure was allowed to decay to 190 psia and the fans in one tank were turned on prior to the rest period, or the pressure was raised to 270 psia and the fans were turned off in both tanks. When either of these procedures were used, the rise or decay rate was slow enough to prevent early awakening of the crew in all except the first rest period. Because of the high fluid density at that time, the pressure decay rate was greater than could be tolerated for the full rest period.

### 8.4 COMMUNICATIONS EQUIPMENT

The onboard equipment operated satisfactorily except for a malfunction at 109 hours. During a 10-hour period following 109 hours, the spacecraft system would not process uplink command functions. The crew cycled the up-telemetry command-reset switch and restored normal operation. See section 17 for further discussion of this anomaly.

The overall quality of the VHF voice communications was very good. The VHF system was used as the primary ground-to-air link for voice communications, except over stations having only the S-band capability. The VHF relay through S-band to the network during the extravehicular activities was very good.

The crew reported some difficulty with voice communications between the lunar module and the command module when using the voice-operated transmitter (VOX) mode. The designed release times for VOX in the command module was 2.2 seconds and in the lunar module was 0.8 second. The Commander, in the lunar module, was aware of an audible "click", which he associated with the noise accompanying normal VOX dropout at the end of a transmission. Assuming that all other conversation had ceased, the Commander would speak. In a number of instances, the Command Module Pilot, not having completed his transmission, would also be speaking. The dual transmission was accompanied by a loud high-pitched tone in the Command Module Pilot's and Lunar Module Pilot's headset. The tone was not audible to the Commander. The VOX mode was a normal mode of operation for extravehicular activity, but was not exercised extensively during simulator training due to lack of trainer communications fidelity. A post-flight check was made of the command module audio center release times and these were found to be within specification.

After landing, the swimmers were unable to establish communications with the crew through the swimmer interphone. Postflight testing of the swimmers' equipment has verified proper operation. During the recovery operations, the spacecraft umbilical was severely damaged, preventing a complete test of the circuits. The swimmers' umbilical interphone is a secondary requirement, with VHF being prime for the crew/swimmer communications link.

The flight crew reported that use of the lightweight headset was satisfactory. However, one microphone electrically failed after 2 days. This anomaly is discussed in detail in section 17.

During the entire flight, the Lunar Module Pilot used a modified version of the communications carrier adapter tubes (bare tubes inserted into his ear canals), which effectively increases the volume by about 10 dB. He reported excellent results and was always able to operate at lower volume control levels in both the command module and lunar module.

## 8.5 INSTRUMENTATION

The instrumentation system, consisting of 315 operational measurements, adequately supported the mission. Lunar module PCM data were successfully transmitted to the command and service modules over the VHF link for the first time. The data were recorded on the data storage equipment and subsequently transmitted to the Manned Space Flight Network using the S-band system. Instrumentation problems experienced during the mission are discussed in the following paragraphs:

a. The onboard display of helium tank pressure failed at lift-off. Postflight testing indicates that the malfunction was not located in the command module and, therefore, could have been a failure associated with the service module measuring system.

b. The carbon dioxide partial pressure measurement experienced a calibration shift before lift-off and was erratic during the flight.

c. During loading of the service propulsion fuel, several tank-level sensors failed. Previous failures of similar sensors were attributed to instrumentation wiring failures caused by fracturing of glass seals in the tank sensor tube assembly.

d. A bias error in the compensator network occurred on the oxidizer storage tank measurement at tank crossover. At the time the sensor was uncovered, a capacitance change occurred. This change resulted from the sensor changing from wet to dry and caused a bias shift of 3 percent.

e. The oxygen flow rate measurement for fuel cell 3 erroneously indicated a flow rate 6 percent greater than that for fuel cells 1 and 2. This error may be attributed to a gain shift in the transducer amplifier.

f. The service propulsion system helium tank pressure measurement exhibited approximately 3-percent noise during the flight. This has been attributed to improperly shielded return wiring in the service module. The existence of this condition was known prior to the flight.

g. The central timing equipment experienced a reset to zero at about 168 hours. This reset was attributed to electromagnetic interference and had no effect on spacecraft operation.

h. The data storage equipment did not start recording when the up-data link command reset switch was activated, approximately 30 seconds prior to ignition, for the eighth service propulsion firing (deorbit maneuver). The recorder did start approximately 20 seconds later when

the forward command was sent through the updata link. Postflight examination and tests of the forward/off/rewind switch showed the switch to be operating properly. Also, x-rays of the switch revealed no contamination.

i. The signal conditioning equipment was off for 0.04 second at 240:30:55. It is believed that this was due to inadvertent activation of the signal conditioning equipment power switch.

## 8.6 GUIDANCE, NAVIGATION, AND CONTROL

Performance of the guidance and control systems was satisfactory throughout the mission. Ascent phase monitoring functions were within nominal limits except for a larger-than-expected error in the onboard calculation of insertion apogee and perigee. The error was caused by a prelaunch shift in the platform X-axis accelerometer bias. Control system operation during command and service module separation, transposition, docking, and spacecraft/S-IVB separation was nominal, although Y-axis translation capability was inhibited for a time by inadvertent closure of propellant isolation valves.

The digital autopilot satisfactorily controlled the thrust vector during the docked and undocked service propulsion firings. Two stroking tests were performed in which the pitch gimbal of the service propulsion engine was oscillated in accordance with a preset profile, and body-bending response data were obtained. Satisfactory attitude control of both the docked and undocked configurations was demonstrated using both the digital autopilot and the stabilization and control system.

The capability for optical alignment of the inertial reference system in the docked configuration was adequately demonstrated.

Landmark tracking data for orbital navigation were obtained using the yaw/roll control technique. Inflight stability of inertial-measurement-unit components was satisfactory. The scanning telescope shaft drive mechanism exhibited a tendency to stick intermittently during the first 5 days of the mission. The cause has been identified as a press-fit pin which came loose from a mechanical counter and interfered with the gear train. The sextant, which is mechanically independent of the telescope, operated properly.

A nominal entry was performed using the automatic modes for both guidance and control. The entry monitor system performed properly when monitoring service propulsion maneuvers and correctly shut down the engine on the third firing. During entry, however, the stylus failed to scribe properly, although performance of the acceleration/velocity drive mechanism was correct. The scribing problem has been attributed to a leak in the hermetic seal of the scroll assembly, which allowed the scroll emulsion to harden during the period when the cabin was evacuated.

Detailed evaluation beyond the scope of those described in this document, will be published as supplemental reports, as listed in appendix E.

## 8.6.1 Mission-Related Performance

Launch and insertion.- The inertial measurement unit was released from gyrocompassing and was fixed inertially at 1.07 seconds, after the computer received and processed the lift-off discrete signal from the launch-vehicle instrument unit. System monitoring parameters during the ascent phase were nominal and representative of those on previous flights. The orbital parameters calculated onboard and displayed to the crew at insertion differed to a greater extent than on previous missions from those obtained from real-time ground trajectory determination. The onboard calculation was in error because of an incorrectly compensated X-axis accelerometer bias, discussed in section 8.6.2. The respective parameters were as follows:

	Onboard	Real-time ground determination	Best estimate trajectory
Apogee, mi. . . . .	103.0	103.9	100.7
Perigee, mi. . . . .	89.5	102.3	99.7

Separation from S-IVB.- Separation of the command and service modules from the S-IVB, the plus-X translation, and the pitch-axis turn-around maneuver were nominal. Figure 8.6-1 contains a composite of spacecraft dynamic parameters during periods of interest for which data were available. Initial attempts at Y-axis translation were unsuccessful because of inadvertent closure of propellant isolation valves. Figure 8.6-2 shows the sequence of control modes exercised during diagnosis of the problem. The initial docking transients were small, as shown in figure 8.6-1; however, oscillations of 1 deg/sec maximum at 0.95 Hz occurred for approximately 30 seconds in the pitch and yaw axes when the latching mechanism was activated. No dynamic analysis of spacecraft separation can be performed because telemetry data are too limited in the low-bit-rate mode used at that time; however, the maneuver was reported to be as expected.

Attitude reference system alignments.- The inertial measurement unit was optically aligned as shown in table 8.6-I. The star-angle difference checks contained in the table indicate that docked alignments were as accurate as those performed undocked. In one case, the platform was aligned with the crewman optical alignment sight using backup alignment computer programs (P53 and P54). A subsequent alignment check made with the sextant indicated approximate backup alignment errors as follows:

Axis	Error, deg
X	0.073
Y	0.060
Z	0.085

For the first time, the feasibility of using planets for alignments was demonstrated using the planet Jupiter and the star Acrux. During the first alignment attempt, an excessively large star-angle difference was displayed because of an error in extrapolating the planet vectors, which are inserted manually into the computer. These vectors are provided to the crew in tables containing an entry approximately every 50 hours. The computer uses this information in the planet/star angle computation. The second alignment attempt was satisfactory and resulted in very small torquing angles, although a larger-than-normal star-angle difference was again measured. This difference could have been the result of small errors in the vector extrapolations or the error caused by inability to determine the center of the planet in the sextant. The small gyro-torquing angles indicate that the error was in the planet vector.

Translation maneuvers.- The significant guidance and control parameters for the eight service propulsion firings are contained in table 8.6-II. Five of the eight firings were performed in the docked configuration, and all but the third were under exclusive control of the digital autopilot. The third firing was started under digital autopilot control, but manual takeover capability was exercised after 3 minutes 55 seconds of the firing. The maneuver was completed under manual thrust vector control through the stabilization and control system with rate damping. Cutoff was controlled by the entry monitor system velocity counter.

Figures 8.6-3 to 8.6-7 contain time histories of spacecraft dynamic parameters for the docked maneuvers. Figures 8.6-8 to 8.6-10 contain similar histories for the undocked maneuvers and, with table 8.6-II, show that gimbal trim estimations for the service propulsion engine were very accurate in each case. The largest mistrim noted was 0.20 degree during the seventh maneuver. The steady-state differential clutch current of the engine-gimbal pitch actuator increased steadily with firing time through the mission. The change was caused by an increasing lateral thrust component on the engine skirt as a result of uneven ablator erosion. The net effect was an offset between the commanded and actual gimbal position proportional to the side force and increasing to 0.3 degree by the end of the mission. The thrust component equivalent to a 0.3-degree offset, which corresponds to 105 milliamperes of differential current, is approximately 420 pounds. The differential current is discussed further in section 8.6.3. The steady-state gimbal-position offset results in an effective mistrim at ignition; before ignition, there is no side force and therefore no offset. An attempt to account for the offset by biasing the pre-firing trim value for the deorbit maneuver proved undesirable in that an effective attitude error was introduced when the autopilot commanded the ignition attitude. The attitude control loop of the autopilot is much slower than the gimbal trim loop; therefore, a slight degradation in system performance occurred. However, this is not a problem to the control system.

The ability of the digital autopilot to control docked firings was thoroughly demonstrated over a wide range of propellant loadings and spacecraft weights. The vehicle weights varied as follows:

Service propulsion firing	Weight, lb		
	Command and service modules	Lunar module	Total
1	59 012	32 031	91 043
2	58 603	32 031	90 634
3	51 213	32 031	83 244
4	32 487	32 031	64 518
5	31 438	21 933	52 371

The manual takeover during the third maneuver was performed smoothly, as shown in figure 8.6-11. The only noticeable transient occurred about the roll axis. The spacecraft was riding the edge of the digital autopilot 5-degree roll attitude deadband at takeover. The stabilization and control system deadband was set to 0.2 degree. Therefore, at switch-over, an approximate 5-degree attitude change occurred. Cutoff was accurately controlled by the entry monitor system.

Figures 8.6-12 to 8.6-19 show time histories of velocity to be gained in each body axis for all firings. The only velocity residual of significance occurred in the fifth maneuver when 11.5 ft/sec remained in the Y-axis. Prior to flight, residuals of this order had been predicted as a result of the low vehicle weight and the low gain of the digital autopilot during this maneuver, combined with a rapidly moving center of mass.

The entry monitor system velocity counter was initialized to monitor all maneuvers. The post-firing residuals were very low in each case, as shown in table 8.6-II.

Stroking tests.- Stroking tests were performed during the second and third service propulsion firings. These tests were designed to obtain inflight data on structural bending and control system performance for possible digital autopilot improvements. The engine gimbal was commanded to oscillate about the pitch axis in accordance with a stored program designed to induce a constant energy level across the frequency band of interest. The commanded wave form was triangular with a maximum amplitude of 1.12 degrees. Figures 8.6-20 and 8.6-21 are expanded time histories of spacecraft dynamics during the two stroking tests. The

first test was performed at 40-percent amplitude to allow examination of the response at this level before proceeding with the second test. There was no detectable response in the rate data. However, the engine gimbal response was proper, and the characteristic rigid body response was detectable in vehicle attitude. For a fully loaded vehicle at 40-percent amplitude stroking, preflight simulations predicted a peak-to-peak bending response of 0.32 deg/sec, which would have been above the rate-gyro threshold and telemetry quantization. Hence, the lack of any detectable bending response during the 40-percent amplitude test gave confidence in proceeding with the second test at full amplitude.

The full amplitude test was initiated approximately 60 seconds after ignition (fig. 8.6-21). Preflight analyses and simulations had predicted an actual peak-to-peak bending oscillation in the rate data ranging from 0.2 to 0.5 deg/sec, depending on the value assumed for the structural damping factor. The observed rate was approximately 0.1 deg/sec. This comparison may be misleading, because the amplitudes are so small that the quality of the rate information is most likely masked by small signal nonlinearities. However, by compensating for all known telemetry effects, the rate response amplitude is still expected to be smaller than preflight predictions, which implies the actual control system stability margins are larger than predicted. This preliminary conclusion will be confirmed by further reduction and analysis of the data and be reported in a supplemental report.

Attitude control.- The ability of the digital autopilot and the stabilization and control system to provide all required attitude control functions in the docked configuration was thoroughly demonstrated.

Figure 8.6-22 contains the desired and actual platform gimbal angles during a representative automatic digital-autopilot attitude maneuver. Figure 8.6-23 is a representative phase-plane plot for the pitch axis prior to a service propulsion engine firing. This figure shows attitude-hold performance in coasting flight, as well as during a period of plus-X translation. The buildup of a negative 0.62-degree attitude error experienced during the translation is the normal result of a disturbance torque resulting from a center-of-gravity offset.

An extensive search was made of the available data for evidence of the body bending reported by the crew when thrusters were fired. Only two occurrences were found, and in both cases the oscillation amplitudes were less than 0.05 deg/sec peak-to-peak at a frequency of approximately 3.5 Hz. These oscillations were of the same order as those produced during the gimbal drive test, as shown in figure 8.6-24.

The reported tendency of the spacecraft to seek an in-plane attitude is to be expected in earth orbit. The approximate predicted torque from

aerodynamic drag for the docked spacecraft is 2 ft-lb at 100 miles altitude with the X-axis oriented out-of-plane. The corresponding torque on the command and service module under similar circumstances would be 0.5 ft-lb.

Orbital navigation.- Onboard orbital navigation techniques using the landmark tracking program (P22) were exercised four times while the spacecraft were undocked (table 8.6-III). The yaw/roll technique with the spacecraft oriented out-of-plane was utilized throughout each exercise and was proved feasible.

A problem with the telescope drive impeded landmark acquisition during the first attempt (see section 17 for further discussion). Thereafter, the landmark was acquired successfully with the telescope and then tracked with the sextant. Automatic positioning of the optics was utilized, and the optics drive capability was satisfactory. The relatively high spacecraft body rates required in earth orbit caused the computer to generate program alarms (no. 121) during the first two tracking attempts. This alarm is produced during marking operations when the difference between successive samplings of gimbal angles is larger than a programmed value. The check was intended to guard against transients in the coupling data unit by inhibiting the affected mark data from being used in the state-vector update process. After the alarm was inhibited by an erasable memory change, no further problems were encountered.

The navigation weighting matrix was initialized to correct landmark data. These tracking data were not used to update the onboard state vector. The evaluation of tracking data accuracy will be presented in a supplemental report.

The rendezvous navigation program (P20) was utilized to position the spacecraft and optics for acquisition and tracking the lunar module ascent stage late in the mission. The range at the first sighting was 2700 miles, and six marks were taken.

Figure 8.6-25 contains a comparison of the onboard state vector with that derived postflight using precision orbital integration over a 9-hour period. The results indicate that the onboard state vector degrades in position and velocity, as expected, at rates of approximately 10 000 ft/hr and 10 ft/sec/hr, respectively.

Entry.- The planned velocity and flight-path angle at the entry interface were 25 895 ft/sec and minus 1.76 degrees, respectively, and the computer calculated values of 25 893 ft/sec and minus 1.76 degrees. These entry parameters compare favorably with the interface conditions obtained from the best-estimated radar vector following the deorbit maneuver. Altitude and range during entry are shown in figure 8.6-26.

The spacecraft reached the entry interface with the initial roll guidance program operating and the computer indicating an inertial range of 1835 miles to landing. The spacecraft was manually held at the entry trim conditions (29-degree window mark) predicted for the 0.05g level until the computer switched to the post-0.05g program. After 0.05g, the spacecraft was rate-damped in pitch and yaw, and the digital autopilot controlled the lift vector during the remainder of entry. Figure 8.6-27 contains the spacecraft dynamic history during entry, and all responses were nominal.

The computer sensed 0.2g at 240:47:22 and changed to the FINAL PHASE program. The crew conducted a systems check by comparing the displayed downrange error with the ground predicted value after the computer changed to the final phase. The difference was approximately 14 miles, well within the 100-mile tolerance for downrange error. Calculated roll commands from the guidance computer terminated at 240:53:55.

The bank angle commands calculated by the onboard computer and reconstructed from the accelerometer data are presented in figure 8.6-28 as functions of time. Comparison of the two curves indicates the commands computed onboard were proper. The slight deviation of the reconstructed commands is caused by an accumulation of errors in the trajectory simulation.

A summary of landing point data is shown in figure 8.6-29. The computer display indicated an overshoot of 2.9 miles at 67.97 degrees west longitude and 23.22 degrees north latitude. The estimate of the landing point determined by the recovery forces was 67.94 degrees west longitude and 23.21 degrees north latitude, indicating an overshoot of 4.4 miles. Adequate tracking data were not obtained after communications blackout, and no absolute navigation accuracy can be determined. However, a reconstructed trajectory has been produced by applying estimated platform errors to the accelerometer data (table 8.6-IV). The trajectory from the corrected accelerometer data indicates a landing at 67.98 degrees west longitude and 23.23 degrees north latitude. The comparison with the computer data shows a downrange navigation error at guidance termination of approximately 0.7 mile, which is within the 1-sigma landing accuracy predicted before the mission.

### 8.6.2 Guidance and Navigation System Performance

Inertial subsystem.- Inflight performance of all inertial components was excellent. All system voltages and the accelerometer temperature measurement remained stable.

The inertial component preflight test history is summarized in table 8.6-V. The values selected for computer compensation are also

shown. The ascent phase velocity comparisons with the S-IVB data (fig. 8.6-30) indicate the 1.1-cm/sec X-axis accelerometer bias error which caused the insertion apogee and perigee errors mentioned previously. Although a reference-matrix initialization error, similar to that seen in Apollo 8, precludes an accurate quick-look determination of all the error coefficients, the dominant contribution to the X- and Z-axis error propagation was the X-axis accelerometer bias error. The linear propagation error shown in the X-axis was a direct effect. The characteristic acceleration-sensitive propagation history seen in the Z-axis was an indirect effect resulting from a bias-induced misalignment about the Y-axis during prelaunch gyrocompassing. The latter effect indicates that a bias shift occurred prior to lift-off but after the final performance test 5 days before launch. Figure 8.6-31 contains a history of the X-axis accelerometer bias for the 12 months before flight. The last four data points show evidence of a negative trend, which apparently continued to the final inflight value of minus 0.53 cm/sec/sec. The cause of this shift is not known, but the instrument remained stable at the new value throughout the mission. Figures 8.6-32 and 8.6-33 show the values of accelerometer bias and gyro drift measured inflight.

Optical subsystem.- Performance of the scanning telescope and the sextant in the docked configuration was thoroughly demonstrated. Although the usable field of view of both instruments was restricted, as expected, by the lunar module, the remaining field proved sufficient for all earth orbital operational requirements. A partially successful star visibility test was performed at sunrise by counting the number of stars visible in the telescope field of view. With the shaft and trunnion positioned at 180 and 12 degrees, respectively, to provide a clear field of view, 19 stars were counted, representing a threshold star magnitude of plus 2.9. Five minutes after sunrise, reflected earth light from the steerable S-band antenna washed out all stars in the field of view. Spacecraft attitude data during this period are not available, therefore, the results cannot be extrapolated to lunar mission operational capability. If the visibility proves to be marginal (plus 4.0 magnitude is desirable for constellation recognition) and platform orientation is required, the use of the sun, moon, and planets may be necessary in cislunar operations.

Intermittent hang-ups in the telescope-shaft drive mechanism occurred during the first 5 days of the mission. The problem was caused by a press-fit pin which came loose from a mechanical counter and obstructed the drive mechanism (see section 17 for further discussion). The problem was not encountered after the fifth day. The sextant and telescope are mechanically independent; therefore, the sextant was unaffected and remained fully operational. The optics deadband or drift was reported to have increased late in the mission. The allowable drift in the manual mode is 50 arc-sec/sec in trunnion and 120 arc-sec/sec in shaft. The crew estimate (observed postflight) was 30 arc-sec/sec and is well within the required tolerance.

The diastimeter was used to measure range to the lunar module during the final stages of rendezvous and was reported to have operated satisfactorily. The diastimeter was also used to identify and view the satellite Pegasus on two occasions. A discussion of the diastimeter is contained in section 5.3.

Computer.- The computer performed all the necessary guidance, navigation, and control functions required. There were seven restarts and five program alarms recorded during the flight. All restarts were normal and occurred when the computer was changed from the standby to the operate mode. The program alarms noted in the available data and flight logs are listed in the following table. These alarms were associated with procedural techniques and did not represent equipment malfunctions. The times shown are for one case of what might have been several alarm occurrences.

Alarm code	Cause	Program	Time hr:min:sec
405	Two stars not available	P52	24:38:27
121	Coupling data unit not good at time of mark	P22	142:59:32
114	Optics mark made but not desired	P22	143:00:12
421	Weighting matrix overflow	(data not available)	
212	Accelerometer fail indication (accelerometer not being used)	P00	237:27:26

In addition to the restarts and alarms, two problems involved entry of data into the computer by the crew (see section 17).

The programs used by the computer during the mission are shown in table 8.6-VI. The computer update program (P27) was used numerous times with no recorded rejections of the ground commands by the computer. No clock updates were needed during the mission, and several erasable memory dumps were performed to facilitate the verification of ground analyses.

### 8.6.3 Stabilization and Control System Performance

All attitude and translation control modes were satisfactorily demonstrated. The gradual increase in differential clutch current with engine firing time was to be expected. The increase experienced and comparisons with the specification values and those computed from actual engine life tests are shown in table 8.6-VII.

#### 8.6.4 Entry Monitor System Performance

Entry monitor system performance during the orbital portion of flight was better than expected. The accelerometer bias measured by the crew was 0.2 to 0.3 ft/sec over 100 seconds, compared with the 10 ft/sec allowed over this time interval. The maneuver monitoring performance was nominal, as shown in table 8.6-II. The only discrepancy concerned the entry scroll, which did not scribe properly (see section 17). However, markings on the scroll indicate that the proper acceleration and velocity computations were performed by the unit.

TABLE 8.6-I.- PLATFORM ALIGNMENT SUMMARY

8-32

Time, hr:min	Program option*	Star used	Gyro torquing angle, deg			Star angle difference, deg	Gyro drift, mERU			Comments
			X	Y	Z		X	Y	Z	
-0:39	3		+0.116	-0.032	-0.108					
+5:18	1		+0.153	+0.333	-0.638					
8:24	3	14 Canopus; 16 Procyon	+0.110	+0.002	-0.108	000.01	-2.36	-0.04	02.32	
22:33	1		+0.701	-0.295	-1.010					
24:28	1	6 Acamar; 7 Menkar 22 Regulus; 24 Gienah	+0.232	-0.473	-0.841	000.00 000.00				
24:51	1		+0.006	+0.010	-0.022		-1.04	+1.75	-3.80	
27:28	1		+0.298	-0.374	-0.649					
53:18	1		+0.420	+0.044	-0.637					
90:31	1		+1.097	-0.363	+0.193					
93:14	3		+0.117	+0.035	-0.109		+2.9	+8.7	-2.7	
94:57	3		+0.083	+0.008	-0.034		+3.2	+0.3	-1.3	
120:23	1	33 Antares; 42 Peacock	+0.119	-1.277	+0.503					
124:32	2		+1.883	-0.815	+1.616					
140:50	2		+0.630	+0.557	-0.093					
142:27	2		-0.282	-0.657	-0.059					
145:24	3		+0.011	-0.015	+0.000	000.04			Jupiter alignment	
146:27	3		+0.100	-0.050	+0.006		+6.3	-3.2	+0.4 Daylight alignment	
167:33	2		-1.322	+1.073	-0.655					
187:12	3		-0.080	-0.013	+0.183				Program 54 with crewman optical alignment sight	
187:19	3		+0.073	+0.060	-0.084	000.01				
187:24	3		+0.003	-0.025	+0.002	000.01				
187:31	3		-0.070	+0.169	-0.133	000.05			Program 52 with scanning telescope; no torque	
188:30	2		+0.827	+0.098	+1.792	000.00				
188:35	2		-0.000	-0.059	-0.033					
191:21	2		-0.232	+0.509	-0.011					
212:52	2		+0.504	+0.193	+1.038	000.00				
215:40	3		+0.134	-0.017	-0.105					
217:25	3		+0.072	+0.007	-0.048		+3.2	+0.25	-2.1	
235:33	2		-0.128	-0.781	+0.917	000.00				
237:05	1		-0.395	-0.223	+0.534					
238:31			+0.039	-0.018	-0.069	000.00	+1.9	-0.86	-3.3	

\*1 - Preferred; 2 - Normal; 3 - REPSMMAT.

TABLE 8.6-II.- GUIDANCE AND CONTROL MANEUVER SUMMARY

Condition	Service propulsion maneuver							
	First	Second	Third	Fourth	Fifth	Sixth	Seventh	Eighth
Time								
Ignition, hr:min:sec	5:59:01.07	22:12:04.07	25:17:39.27	28:24:41.37	54:26:12.27	123:25:06.97	169:39:00.36	240:31:14.84
Cutoff, hr:min:sec	5:59:06.30	22:13:54.36	25:22:19.15	28:25:09.24	54:26:55.53	123:25:08.40	169:39:25.26	240:31:26.58
Duration, sec	5.23	110.29	279.88	27.87	43.26	1.43	24.90	11.74
Velocity*, ft/sec**								
X	-17.05 (-18.16)	+396.22 (+396.03)	+1387.49 (+1387.94)	+165.29 (+167.40)	+411.24 (+418.11)	+10.10 (+10.37)	+271.91 (+270.66)	+156.48 (+156.07)
Y aftertrim	-31.31 (-32.30)	-191.17 (-191.65)	-290.42 (-287.59)	-0.10 (-4.06)	+359.92 (+350.66)	-33.46 (-34.33)	-450.35 (-449.87)	-222.20 (-220.02)
Z	-8.07 (-8.28)	-727.87 (-727.88)	-2141.25 (-2144.60)	-250.85 (-249.99)	-176.67 (-177.10)	+13.58 (+14.78)	-389.57 (-388.84)	+180.76 (+179.50)
Velocity residual, ft/sec								
X	+1.5	-0.2	+2.7	+0.2	+1.9	+1.1	-1.3	-1.6
Y	+0.4	+0.6	-2.1	+3.4	+11.1	-0.3	-0.8	+1.0
Z	-0.3	+0.2	-0.2	+3.1	+3.4	-0.3	-0.3	-2.4
Entry monitor counter	0.0	0.0	-0.1	0.0	-2.0	+1.5	-1.0	-1.5
Engine gimbal position, deg								
Initial								
Pitch	+1.02	+1.02	+1.19	+1.55	+1.11	-0.61	-0.81	-0.55
Yaw	-0.22	-0.22	-0.17	-0.64	-0.77	-1.07	-1.03	-0.86
Maximum excursion								
Pitch	+0.35	+0.31	+0.35	+0.27	+0.31	+0.26	+0.68	-0.21
Yaw	-0.47	-0.39	-0.38	-0.38	-0.51	-0.34	-0.30	+0.38
Steady-state								
Pitch	+1.11	+1.11	+1.37	+1.73	+1.24	N/A	-0.77	-0.64
Yaw	-0.30	-0.26	-0.22	-0.73	-0.77	N/A	-0.81	-0.60
Cutoff								
Pitch	+1.06	+1.42	+1.64	+1.55	+1.28	-0.77	-0.64	-0.60
Yaw	-0.17	-0.26	-0.64	-0.64	-0.64	-0.73	-0.94	-0.94
Maximum rate excursion, deg/sec								
Pitch	-0.05	+0.12	+0.12	-0.44	+0.40	-0.25	+0.88	-1.07
Yaw	-0.04	+0.08	+0.08	+0.24	+0.47	+1.03	+1.78	+1.46
Roll	+0.05	+0.04	-0.10	0.00	-0.40	-0.44	-2.00	-0.14
Maximum attitude error, deg								
Pitch	-0.23	+2.79	+3.14	-1.86	+3.92	-0.36	Negligible	-1.38
Yaw	-0.35	+1.28	-4.35	+0.40	-5.0***	+3.24	+1.62	+0.68
Roll	-0.37	-5.0***	-5.0***	-2.30	-5.0***	-0.99	-5.0***	-4.29

\*Velocity in earth centered inertial coordinates.

\*\*Values in parentheses are the desired values.

\*\*\*Saturated.

NOTE: All maneuvers performed under digital autopilot thrust vector control.

TABLE 8.6-III.- LANDMARK TRACKING SUMMARY

8-34

Time, hr:min	Landmark		Number of marks	Tracking optics mode	Remarks
	No.	Name			
125:32	011	Guaymas, Mexico	0		Scanning telescope hung. Program alarm 121*.
143:02	021	Corpus Christi, Texas	5	Manual resolved	Scanning telescope hung. Program alarm 121*. Tracked with sextant.
143:20	207	Punta Dumford, Spanish Sahara	5	Manual resolved	Took marks early. Auto optics good. Roll rate was 0.6 deg/sec. Scanning telescope and sextant operated well.
144:35	010	Punta Yoyameko, Mexico	3	Manual resolved	Auto optics used. Took 3 marks with sextant. Did not proceed out of FL51 (Please Mark). Program alarm 121*.
144:50	212	Point Hunier, Guinea	2	Manual resolved	Tracked with sextant. Cloud cover. Program alarm 121*. Roll rate too high.
195:26	006	Point Lo-ma, San Diego, California	5	Manual resolved	Program alarm 121 inhibited. Good marks with sextant.
195:39	130	Guarico Dam, Venezuela	5	Manual resolved	Good marks with scanning telescope.
218:03	005	Santa Catalina, California	0	Manual resolved	Cloud cover; no landmark acquisition.
218:10	065	Tortue Island, Haiti	0	Manual resolved	Cloud cover. Took 5 marks on wrong landmark.

\*Coupling display units not good at time of mark.

TABLE 8.6-IV.-- ENTRY NAVIGATION

Parameter	Onboard computer	Reconstruction	Best-estimated trajectory
Altitude of 400 275 feet (240:44:09)			
X position, ft . . . . .	20 839 259	20 839 444	20 839 713
Y position, ft . . . . .	13 942	13 962	13 938
Z position, ft . . . . .	4 433 772	4 433 743	4 433 539
X velocity, ft/sec . . . . .	-6165.1	-6164.3	-6163.5
Y velocity, ft/sec . . . . .	25.5	25.5	25.5
Z velocity, ft/sec . . . . .	25 148.5	25 148.5	25 148.3
Program 64 (240:46:37)			
X position, ft . . . . .	19 641 215	19 641 536	19 641 916
Y position, ft . . . . .	17 786	17 832	17 815
Z position, ft . . . . .	7 968 923	7 968 898	7 968 679
X velocity, ft/sec . . . . .	-10 426	-10 424	-10 424
Y velocity, ft/sec . . . . .	27.2	27.2	27.2
Z velocity, ft/sec . . . . .	23 801.9	23 802.1	23 802.0
Program 67 (240:47:19)			
X position, ft . . . . .	19 179 369	19 179 742	19 180 158
Y position, ft . . . . .	18 832	18 902	18 887
Z position, ft . . . . .	8 956 091	8 956 067	8 955 846
X velocity, ft/sec . . . . .	-11 538.9	-11 537.7	-11 536.7
Y velocity, ft/sec . . . . .	22.0	22.0	22.0
Z velocity, ft/sec . . . . .	23 170.6	23 170.8	23 170.7
Guidance termination (240:53:54)			
X position, ft . . . . .	15 406 736	15 407 773	15 408 587
Y position, ft . . . . .	-56 302	-56 260	-56 270
Z position, ft . . . . .	14 242 084	14 242 463	14 242 193
X velocity, ft/sec . . . . .	-1003.6*	-1001.6*	
	-1878.9		-1875.8
Y velocity, ft/sec . . . . .	111.3*	111.4*	
	-492.9		-492.9
Z velocity, ft/sec . . . . .	121.3*	123.6*	
	1065.8		1067.8

\*Relative velocity components.

TABLE 8.6-V.- INERTIAL COMPONENT PREFLIGHT HISTORY - COMMAND MODULE

Error	Sample mean	Standard deviation	No. of samples	Countdown value	Flight load
Accelerometers					
X - Scale factor error, ppm . . . . .	-141.000	19.519	5	-140	-140
Bias, cm/sec <sup>2</sup> . . . . .	0.490	0.197	5	+0.25	+0.64
Y - Scale factor error, ppm . . . . .	-298.400	150.219	5	-456	-330
Bias, cm/sec <sup>2</sup> . . . . .	-0.211	0.164	5	-0.19	-0.10
Z - Scale factor error, ppm . . . . .	-239.000	31.336	5	-205	-280
Bias, cm/sec <sup>2</sup> . . . . .	0.443	0.076	5	+0.34	+0.44
Gyroscopes					
X - Null bias drift, mERU . . . . .	0.656	2.137	10	1.2	+2.4
Acceleration drift, spin reference axis, mERU/g . . . . .	6.179	2.031	5	5.7	+7.0
Acceleration drift, input axis, mERU/g . . . . .	6.528	3.163	7	2.3	+5.0
Acceleration drift, output axis, mERU/g . . . . .				2.2	N/A
Y - Null bias drift, mERU . . . . .	-1.089	1.724	10	-0.2	+0.0
Acceleration drift, spin reference axis, mERU/g . . . . .	7.585	5.279	7	11.8	+9.0
Acceleration drift, input axis, mERU/g . . . . .	3.439	2.651	5	-0.9	+8.0
Acceleration drift, output axis, mERU/g . . . . .				0.7	N/A
Z - Null bias drift, mERU . . . . .	1.544	1.561	8	0.15	+2.4
Acceleration drift, spin reference axis, mERU/g . . . . .	-2.880	3.497	5	-5.5	-4.0
Acceleration drift, input axis, mERU/g . . . . .	-11.039	8.454	5	-0.9	-18.0
Acceleration drift, output axis, mERU/g . . . . .				2.4	N/A

TABLE 8.6-VI.- COMMAND MODULE COMPUTER PROGRAMS

No.	Description
P00	Command module computer idling
P06	Computer power down
P11	Earth-orbit insertion monitor
P20	Rendezvous navigation
P21	Ground track determination
P22	Orbital navigation
P27	Computer update
P30	External delta V
P34	Transfer phase initiation
P35	Transfer phase (midcourse)
P40	Service propulsion system
P41	Reaction control system
P47	Thrust monitor
P51	Platform orientation determination
P52	Platform realign
P53	Backup platform orientation determination
P54	Backup platform realign
P61	Maneuver to command module service module separation attitude
P62	Command module/service module separation and pre-entry maneuver
P63	Entry initialization
P64	Post 0.05g-entry
P67	Final phase-entry
P76	Target delta V

TABLE 8.6-VII.- SERVICE PROPULSION SYSTEM DIFFERENTIAL CLUTCH  
CURRENTS AND LATERAL THRUST COMPONENTS, PITCH AXIS

Firing time, sec (accumulated)	Clutch current at shutdown, mA	Offset angle, deg	Lateral thrust component, lb	
			Actual	Specification
5.3	-30	-0.17	120	<250
115.6	-56	-0.12	224	<250
395.5	-56	-0.15	224	<250
423.4	-94	-0.28	376	<450
466.7	-88	-0.24	362	<450
468.1	N/A	N/A	N/A	<450
493.0	-88	-0.28	362	<450
504.7				

Solenoid 1 On  
 Solenoid 2 On

+R, +Z On  
 +R, -Z On  
 -R, +Z On  
 -R, -Z On

+R, +Y On  
 +R, -Y On  
 -R, +Y On  
 -R, -Y On

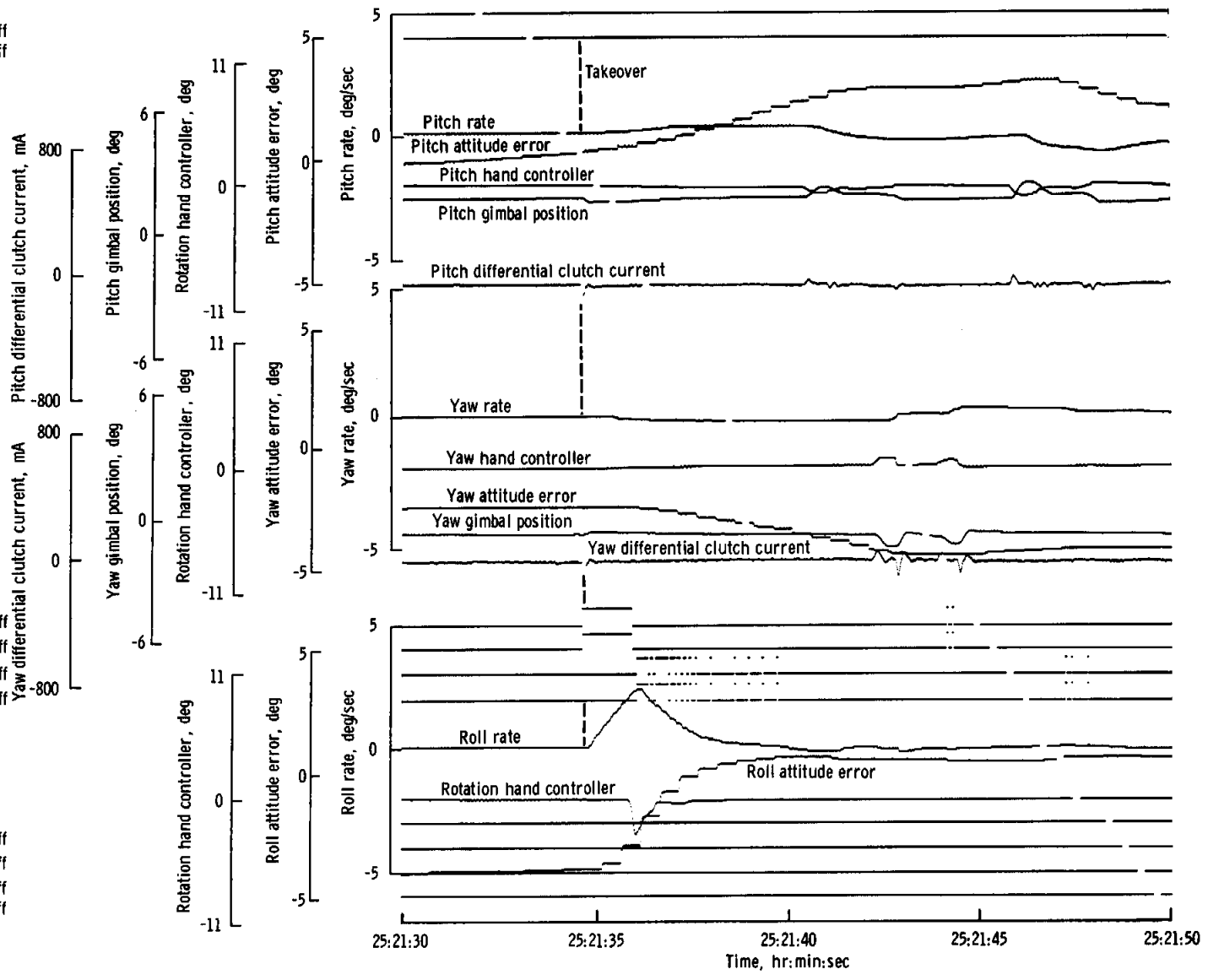


Figure 8.6-11. - Spacecraft dynamics during manual thrust vector control.

NASA-S-69-1989

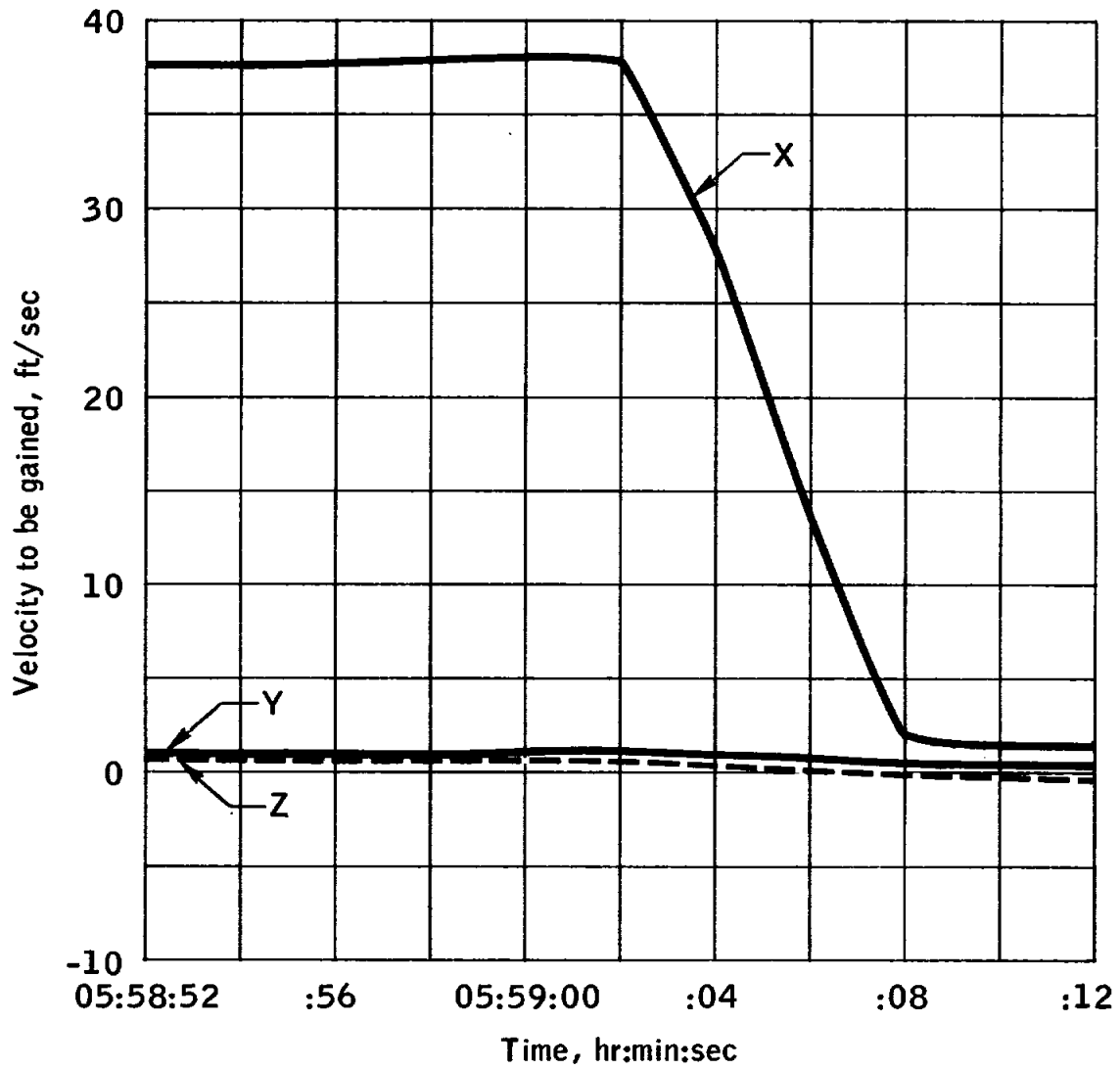


Figure 8.6-12.- Velocity to be gained during first service propulsion firing.

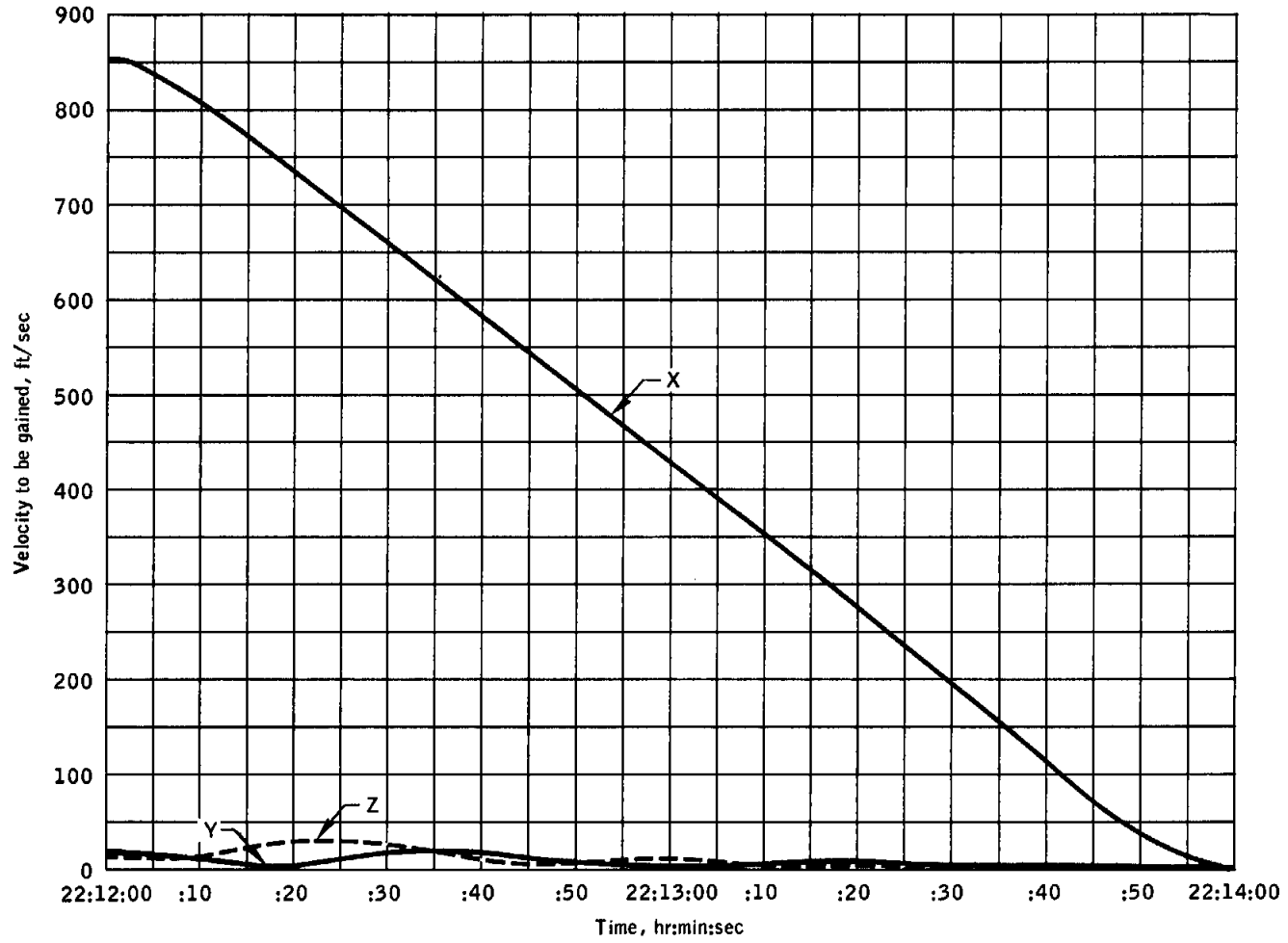


Figure 8.6-13.- Velocity to be gained during second service propulsion maneuver.

NASA-S-69-1991

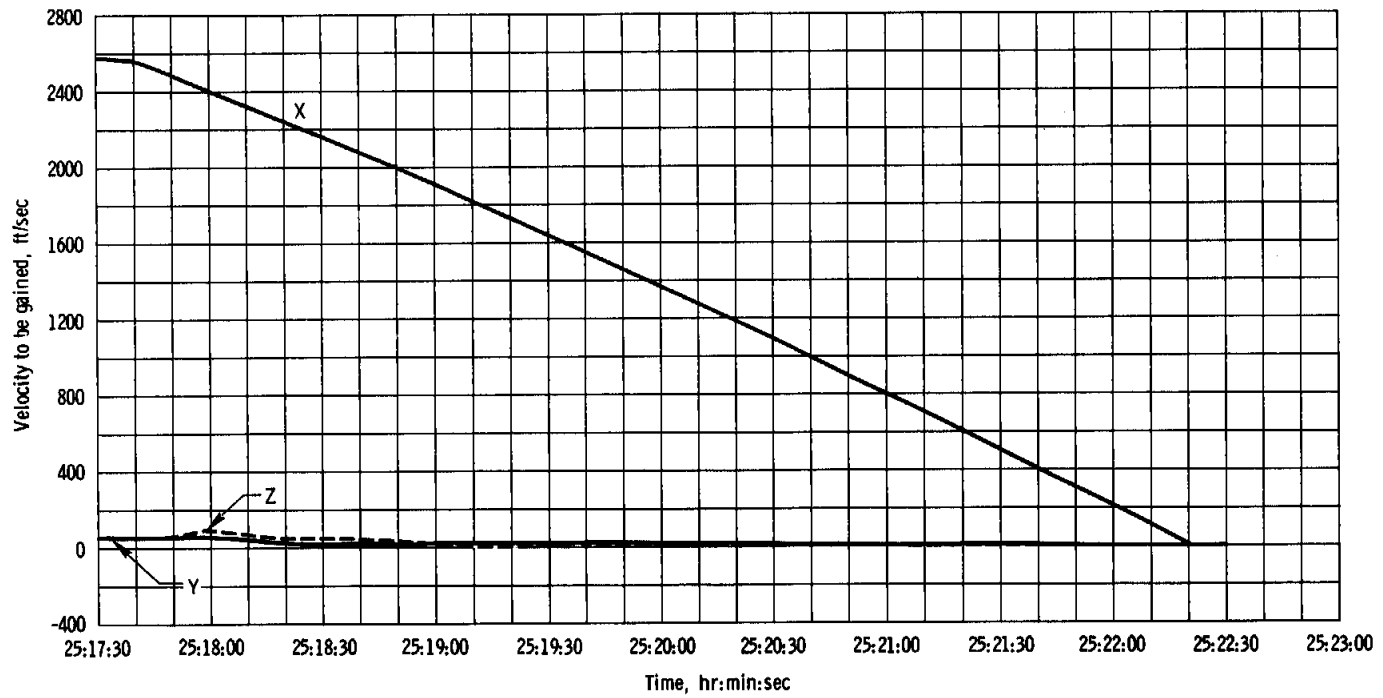


Figure 8.6-14. - Velocity to be gained during third service propulsion maneuver.

NASA-S-69-1992

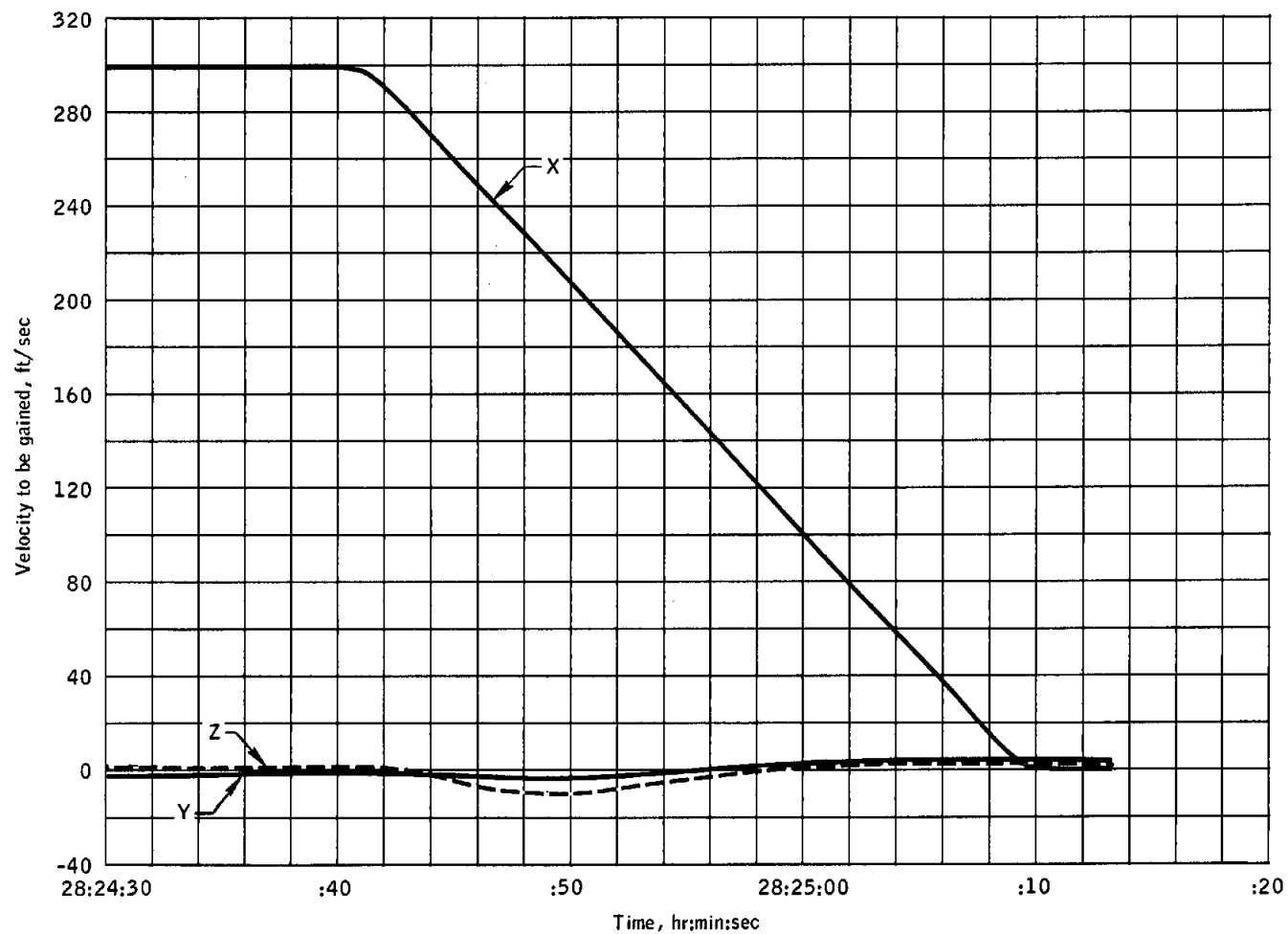


Figure 8.6-15.- Velocity to be gained during fourth service propulsion maneuver.

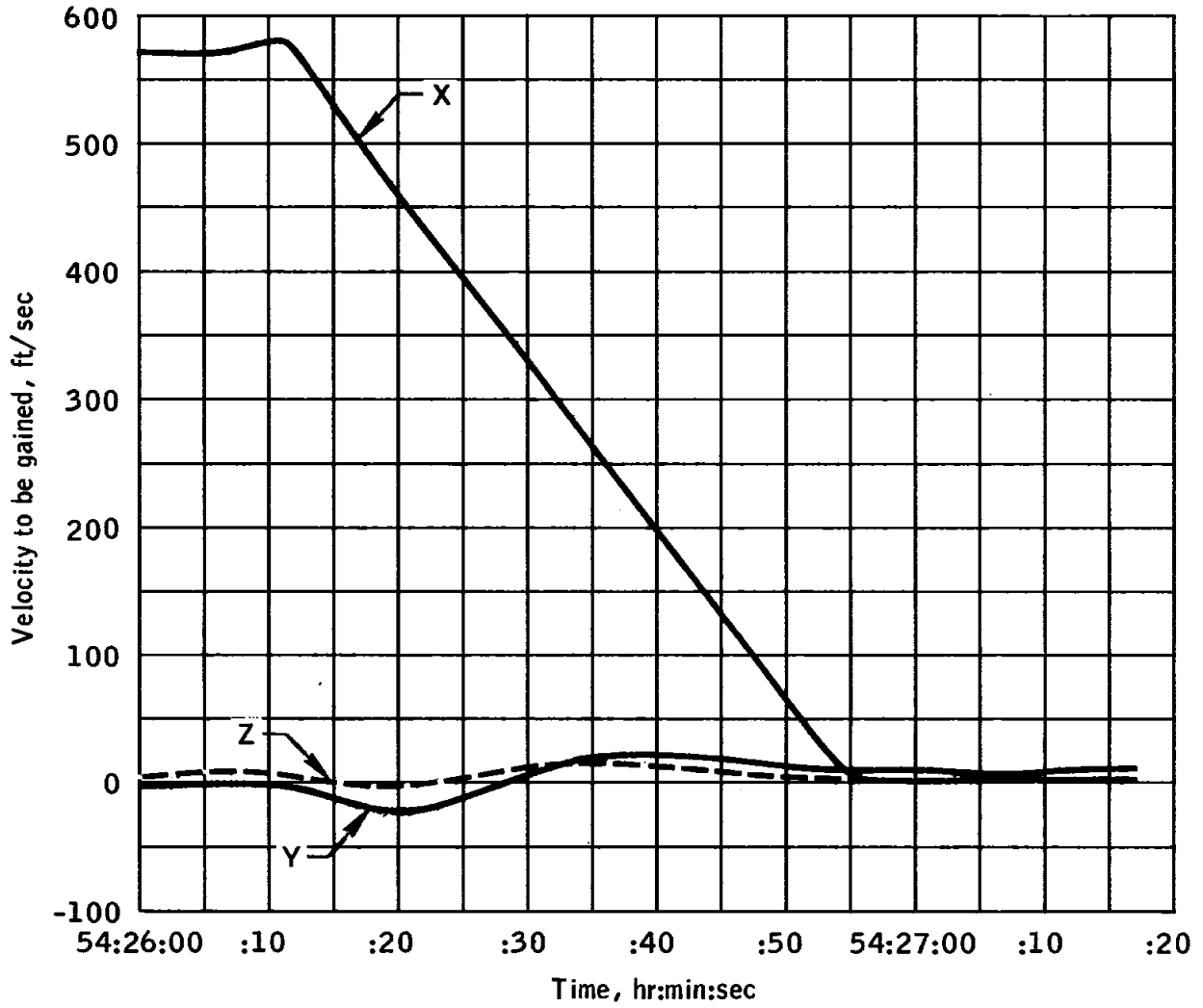


Figure 8.6-16.- Velocity to be gained during fifth service propulsion maneuver.

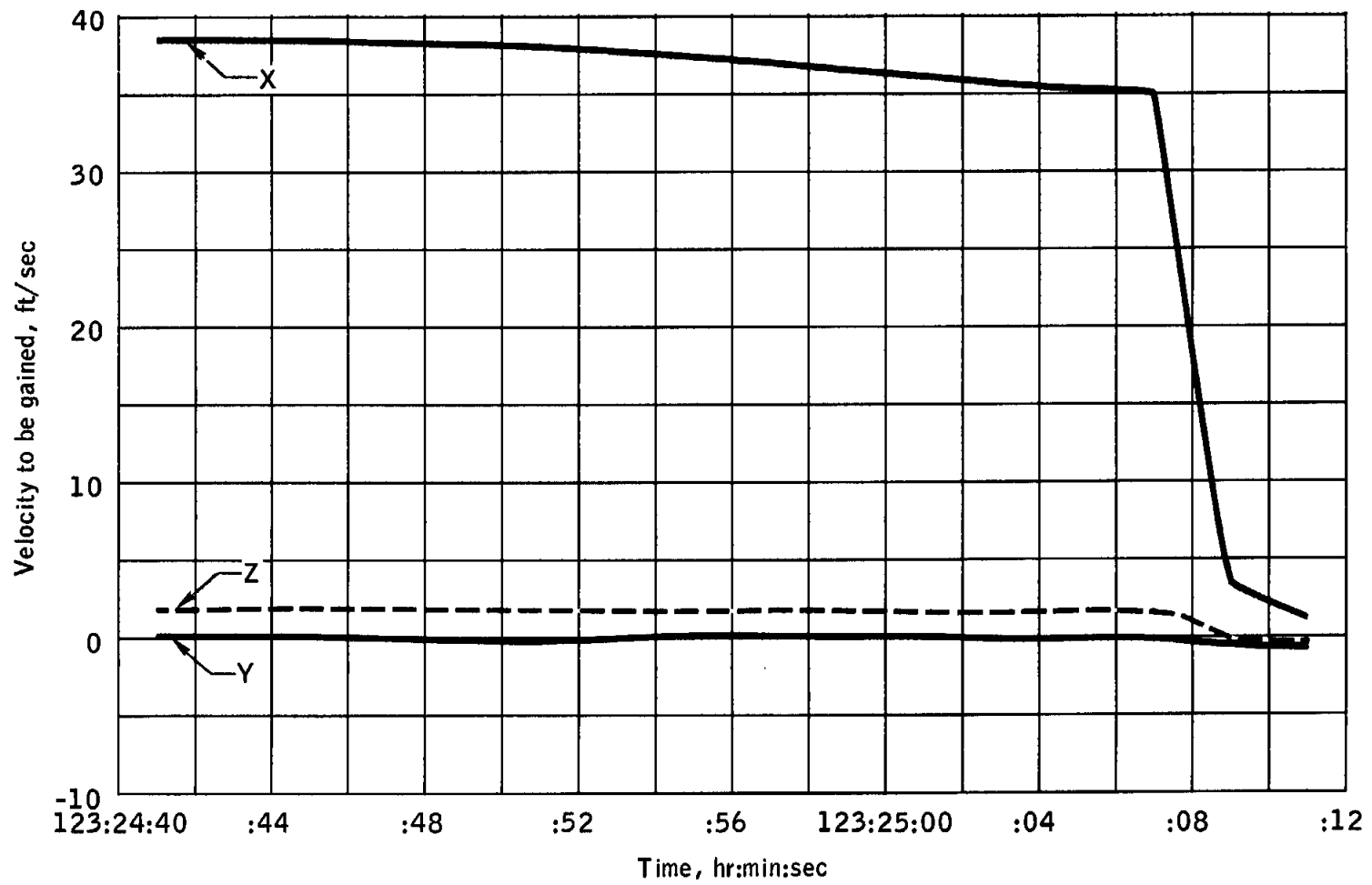


Figure 8.6-17.- Velocity to be gained during sixth service propulsion firing.

NASA-S-69-1995

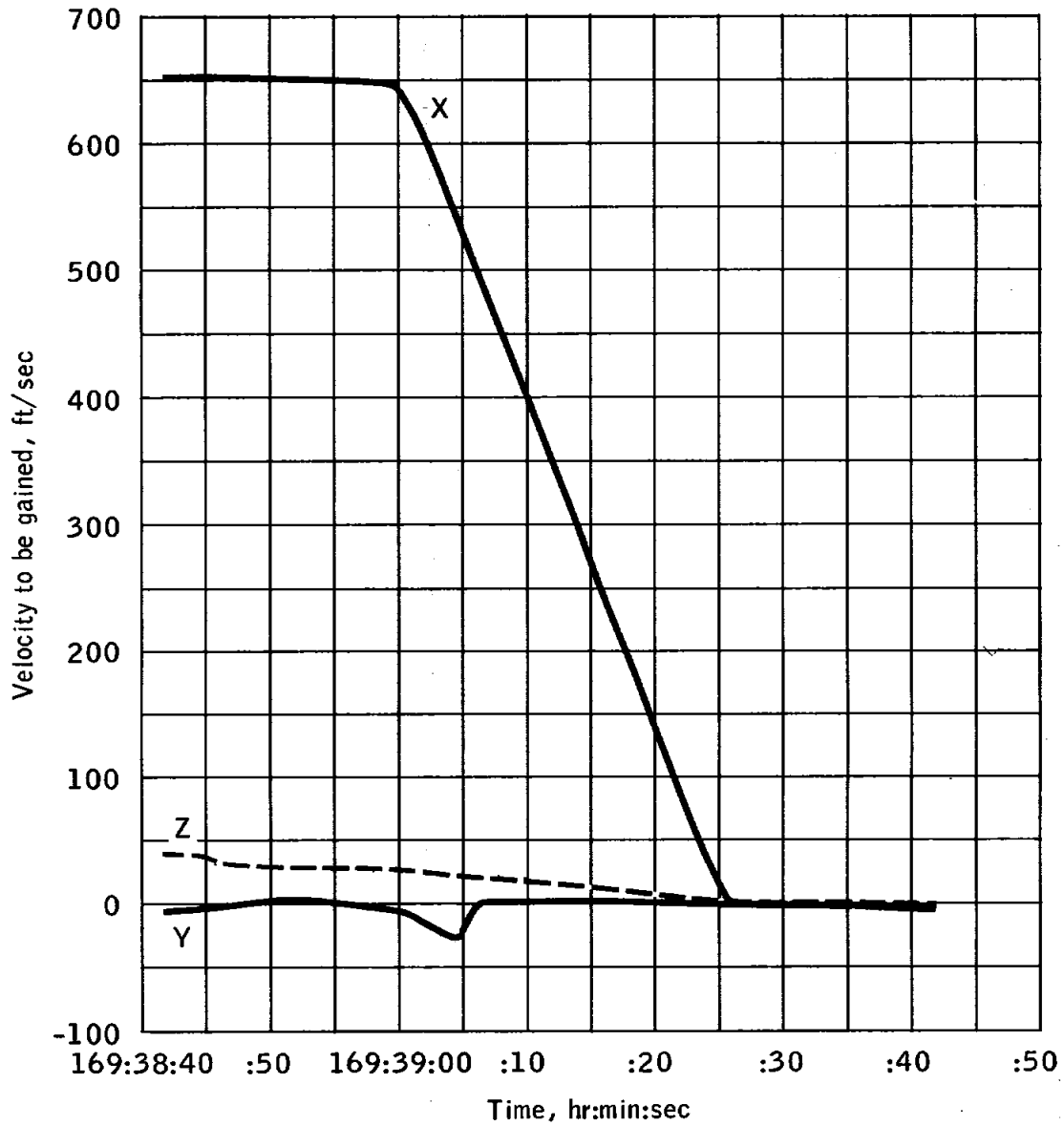


Figure 8.6-18.- Velocity to be gained during seventh service propulsion firing.



NASA-S-69-2001

+P, +X On  
 +P, -X On  
 -P, +X On  
 -P, -X On

+Y, +X On  
 +Y, -X On  
 -Y, +X On  
 -Y, -X On

+R, +Z On  
 +R, -Z On  
 +R, +Z On  
 +R, -Z On

+R, +Y On  
 +R, -Y On  
 -R, +Y On  
 -R, -Y On

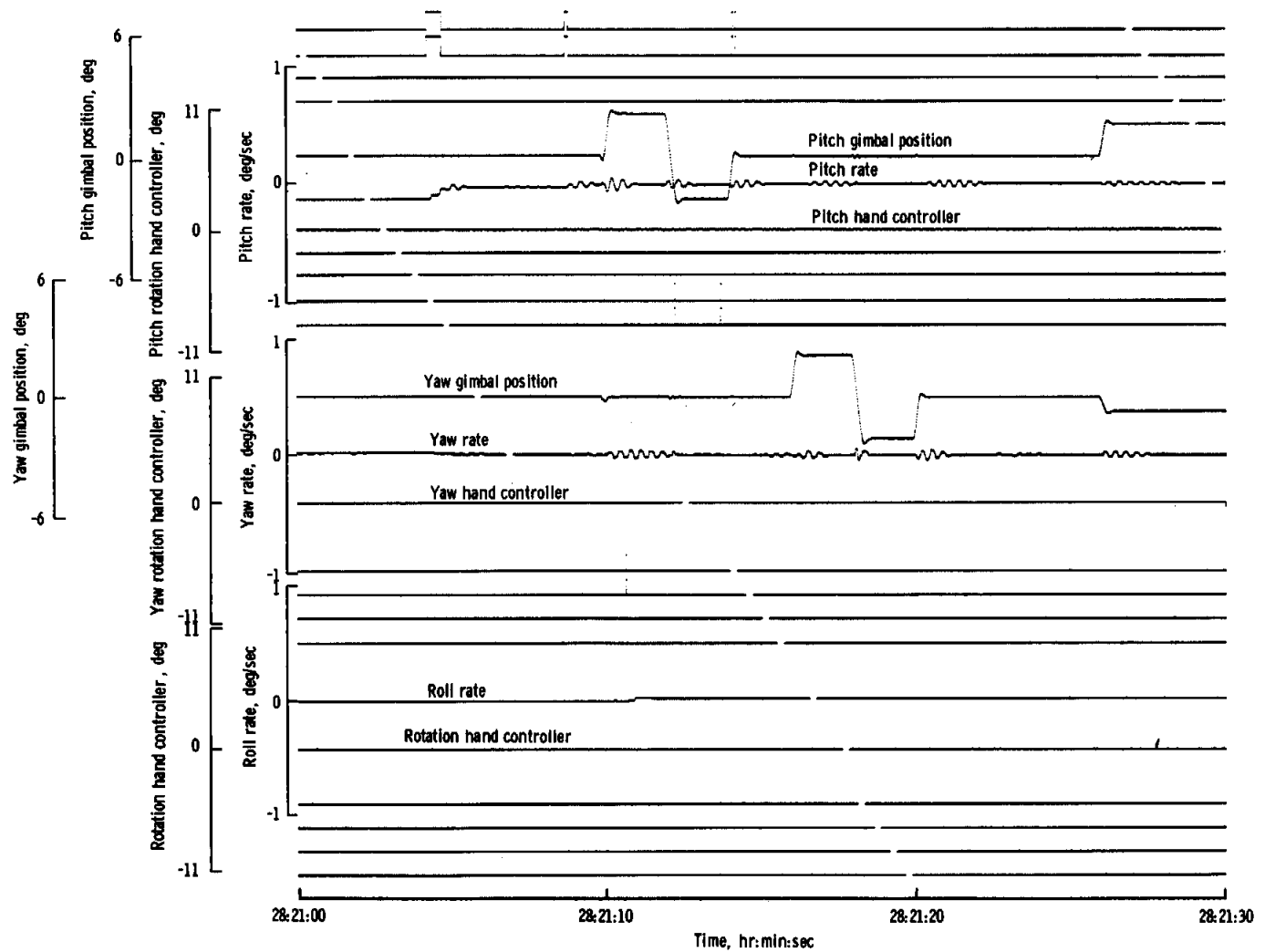


Figure 8.6-24. - Spacecraft dynamics during gimbal drive test.

NASA-S-69-2009

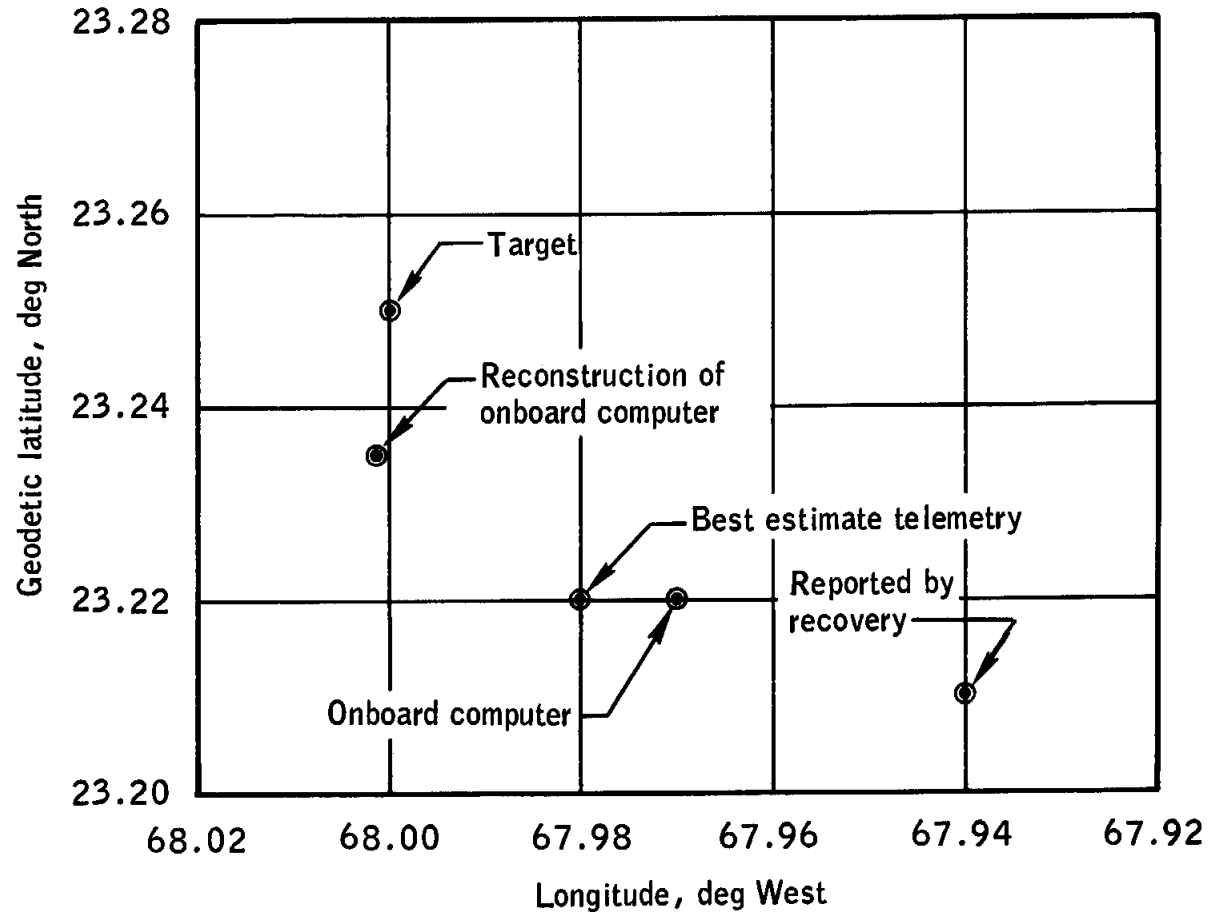


Figure 8.6-29.- Landing point data.

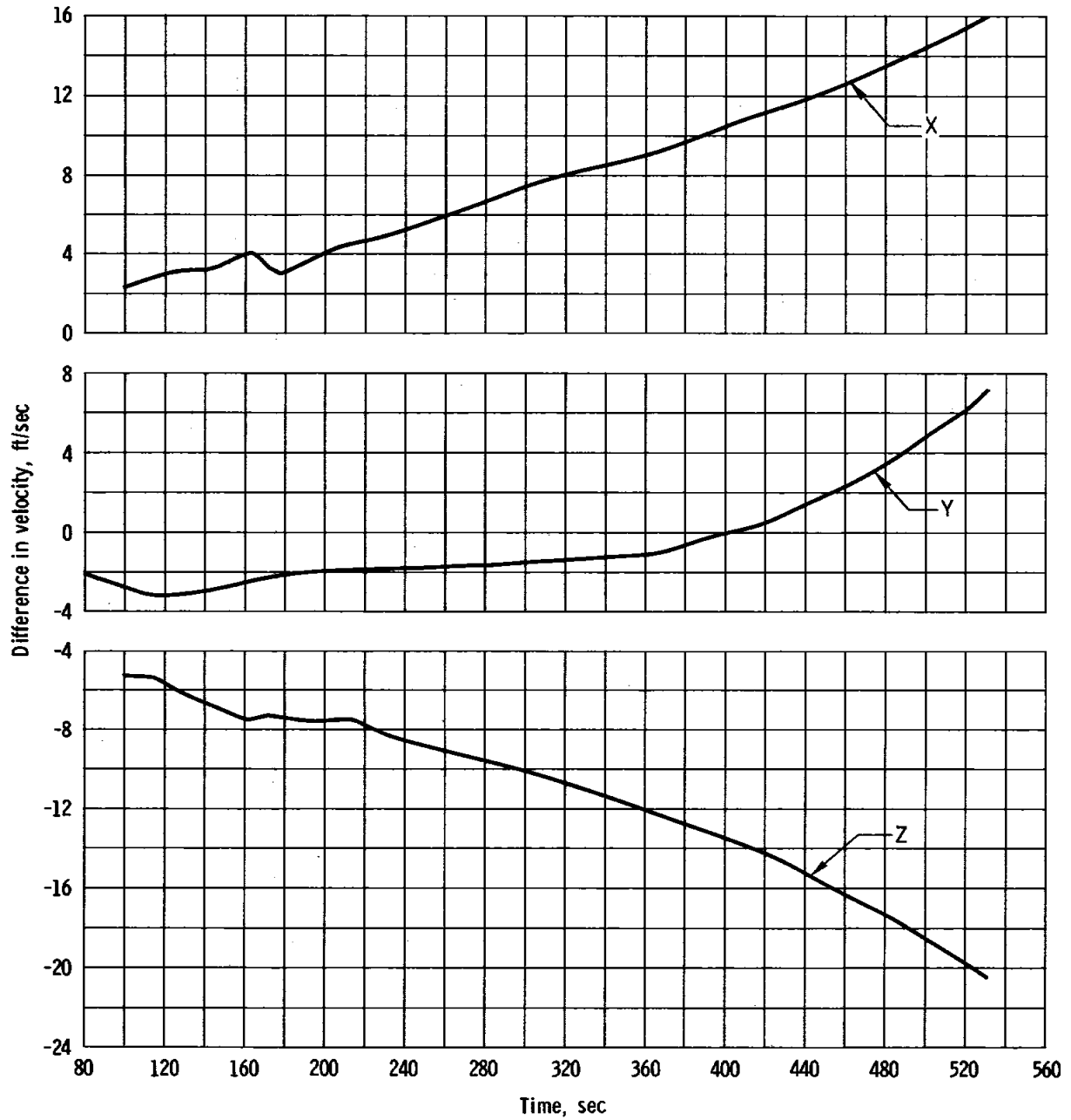


Figure 8.6-30. - Velocity comparison during ascent.

NASA-S-69-2011

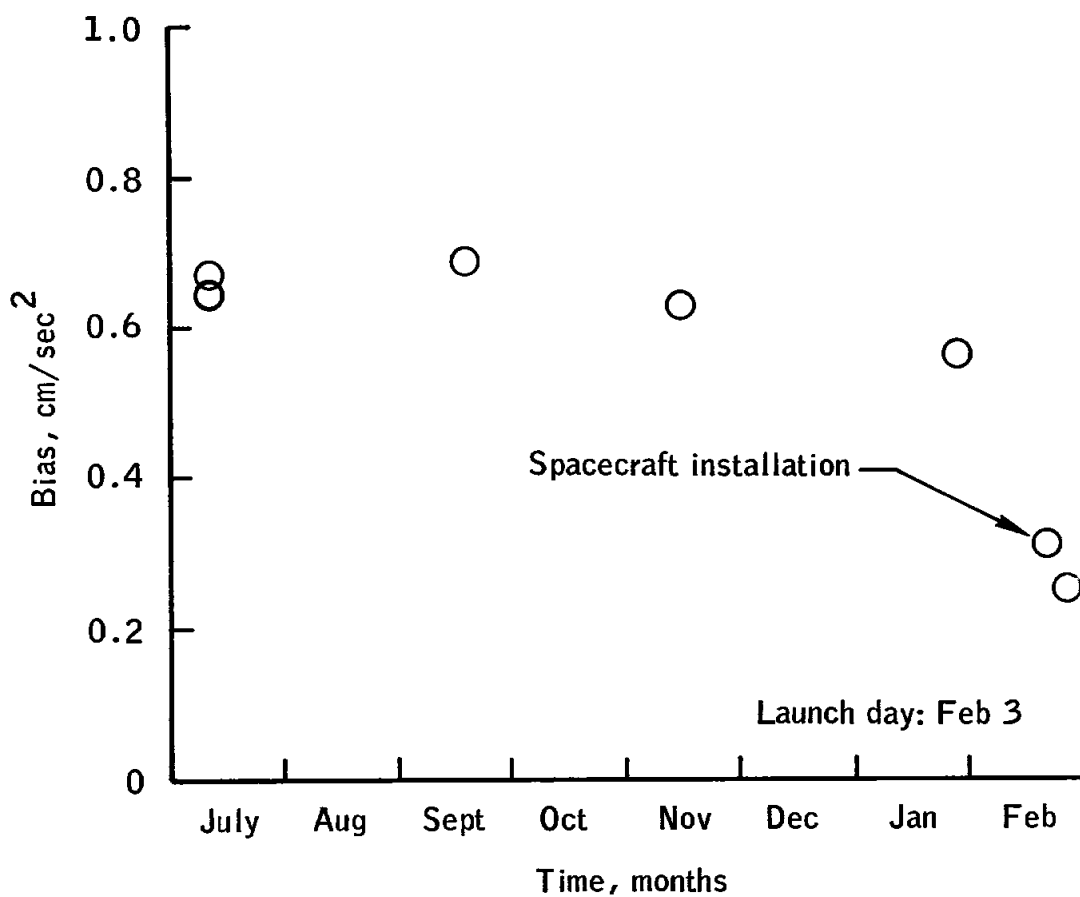


Figure 8.6-31.- Preflight history of X-axis accelerometer bias.

NASA-S-69-2012

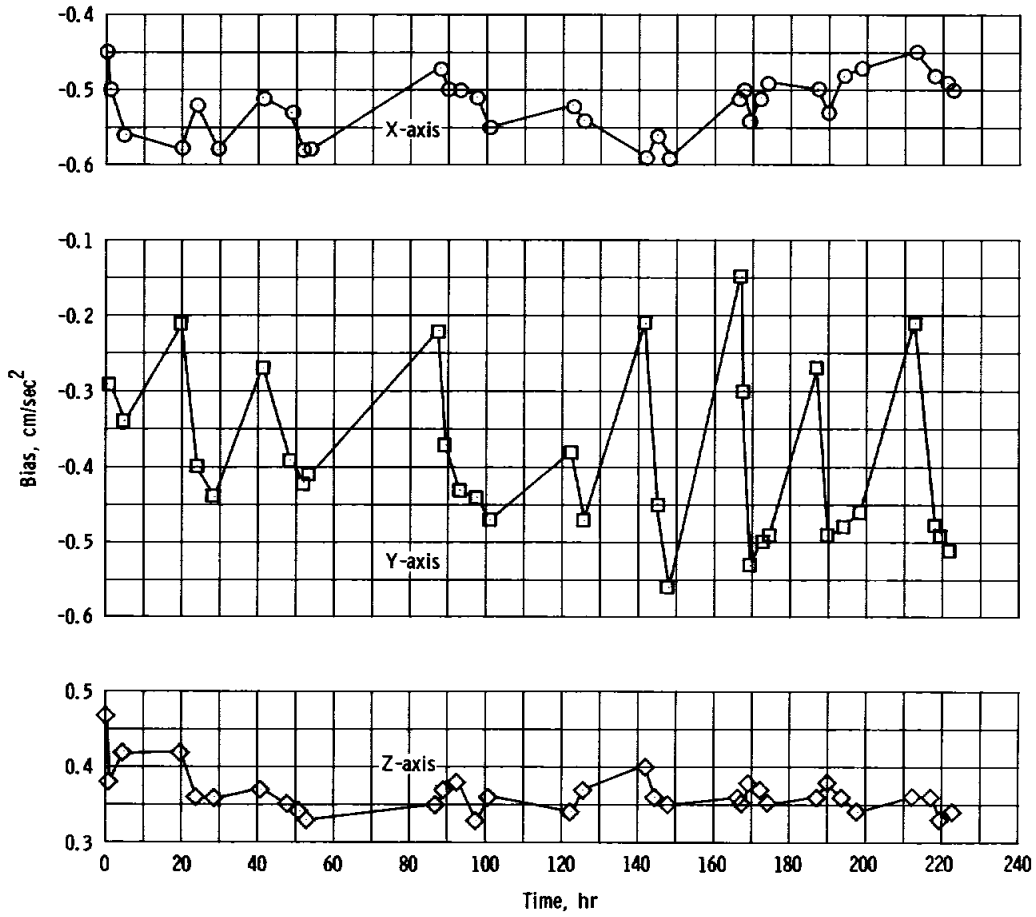


Figure 8.6-32. - Measured bias of command module accelerometers.

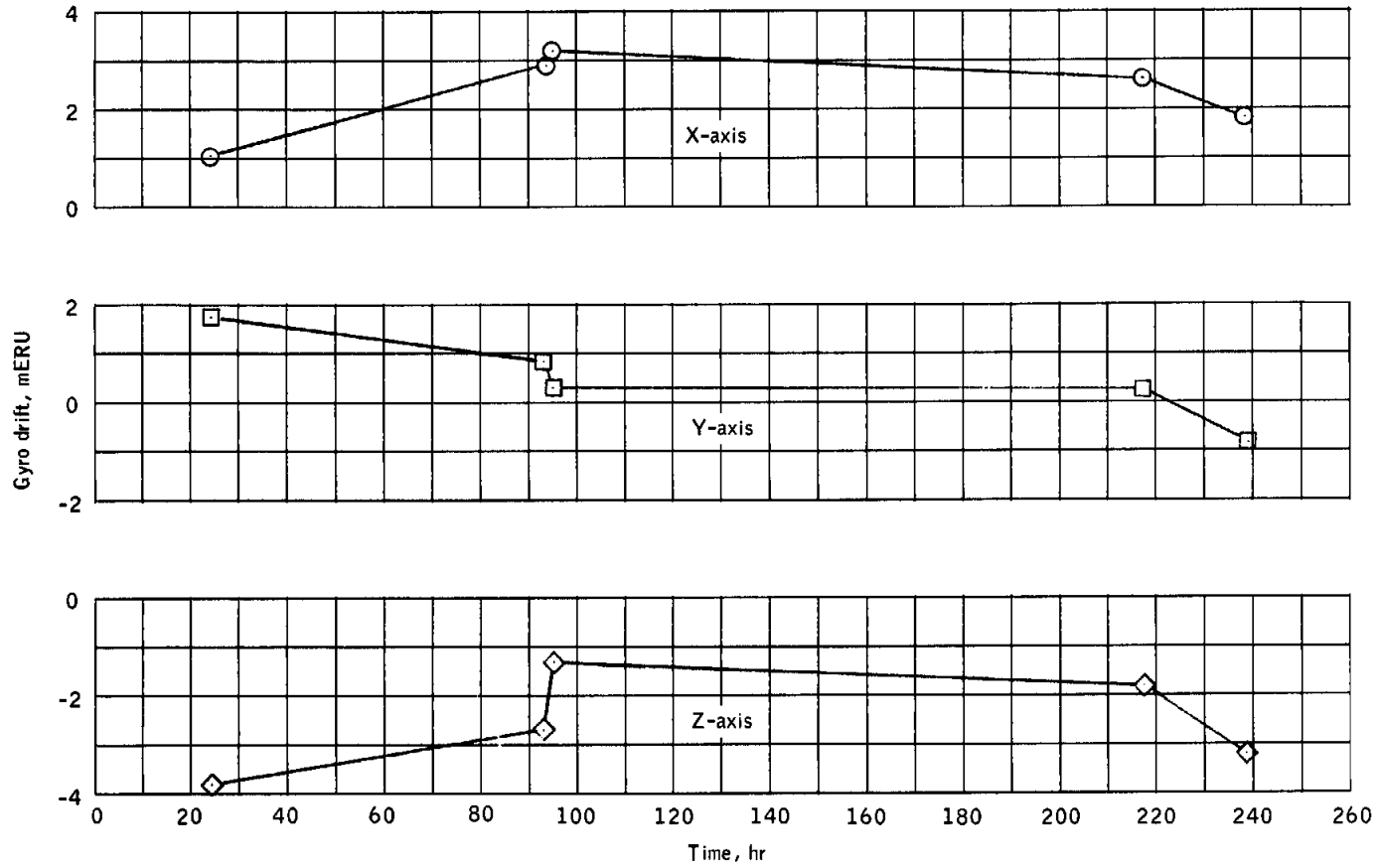


Figure 8.6-33.- Calculated bias drift or command module gyros.

## 8.7 REACTION CONTROL SYSTEMS

The service module and command module reaction control systems performed nominally.

### 8.7.1 Service Module

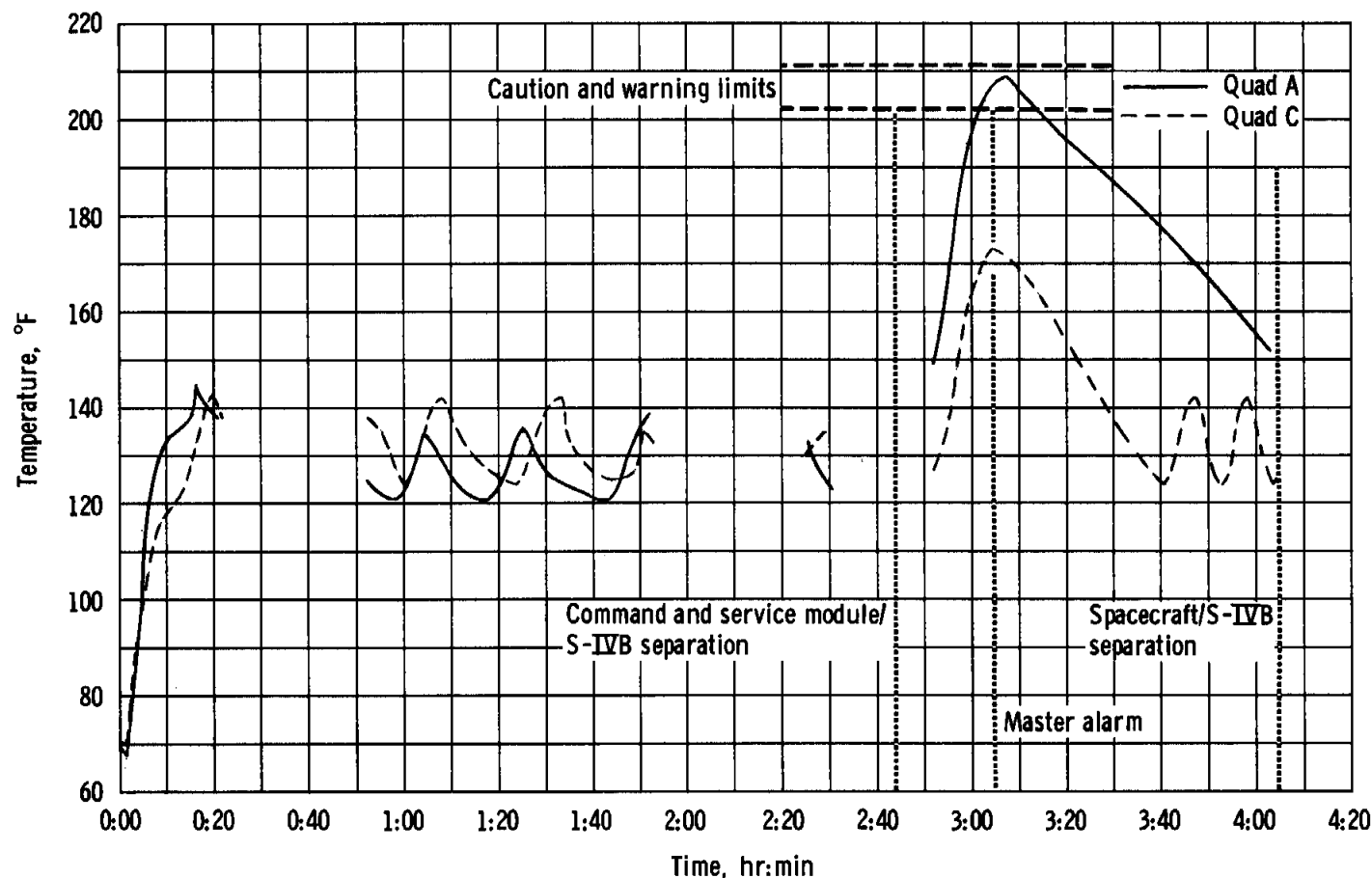
The helium pressurization components of the service module reaction control system maintained the helium and propellant manifold pressures within nominal limits. During the command and service module transposition and docking maneuvers prior to lunar module docking and extraction, the crew were unable to translate along the Y axis. The indicators for the primary and secondary propellant isolation valves on quad C and the secondary isolation valves on quad D were in the closed position. Temperature data indicate that the four valves on quad C were closed; however, it cannot be determined whether one or both secondary valves on quad D were closed. The isolation valves were opened and the docking maneuver was completed successfully. The valves remained open during the remainder of the mission. A discussion of this discrepancy is contained in section 17.

During the time that the quad C isolation valves were closed, high thruster activity was required from quad A. This resulted in a high package temperature on quad A which consequently triggered the caution and warning light. However, as shown in figure 8.7-1, the upper temperature limit of 210° F was not reached. During times of lesser thruster activity, the primary quad heaters maintained the package temperatures between 119° and 141° F.

A total of 790 pounds of propellant was used. The actual consumption for all quads is compared with the preflight predicted values, as corrected for flight plan changes, in figure 8.7-2. The total propellant consumption was 192 pounds more than predicted, partly because of the quad C isolation valves being closed but largely because of the exclusive use of the autopilot, rather than the minimum impulse mode, as indicated in section 5.3.2, during the rendezvous. With these exceptions, the actual usage rates approximated the predicted usage. A comparison of ground calculations of propellant remaining with the onboard gage readings is shown in figure 8.7-3. The telemetered gage readings have been corrected for end-point-error and converted from percent remaining to weight of propellant expended.

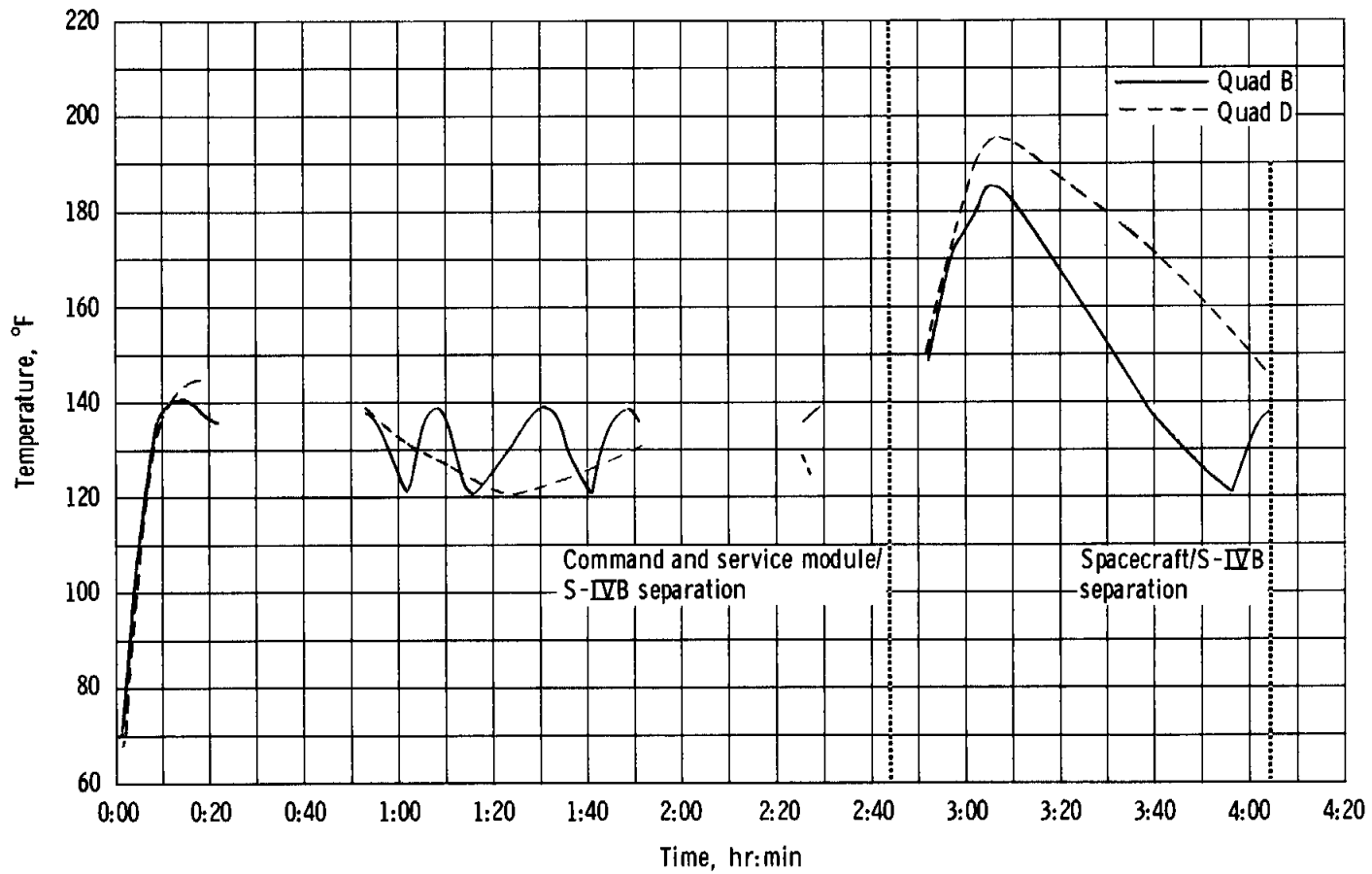
### 8.7.2 Command Module

Entry was accomplished using only system 1 of the command module reaction control system, with the exception of the first 14 seconds after command module/service module separation. Both manual and automatic control were used during entry. As indicated in figure 8.7-4, approximately 27.5 pounds of propellant was used from system 1 during entry as compared to 30 pounds predicted. The overshoot noted in three places in figure 8.7-4 results from the inability to directly measure helium bulk temperature, which together with pressure is the means of calculating propellant quantity. The temperature parameter used is helium-bottle skin temperature, which is subject to transient thermal effects and is most notable at the higher usage rates. The inherent error of this method is not large and is acceptable for system evaluation purposes. The remainder of the propellant and helium was expended during the depletion and purging operations.



(a) Quads A and C.

Figure 8.7-1. - Comparison of quad package temperatures from launch through spacecraft separation.



(b) Quads B and D.

Figure 8.7-1. - Concluded.

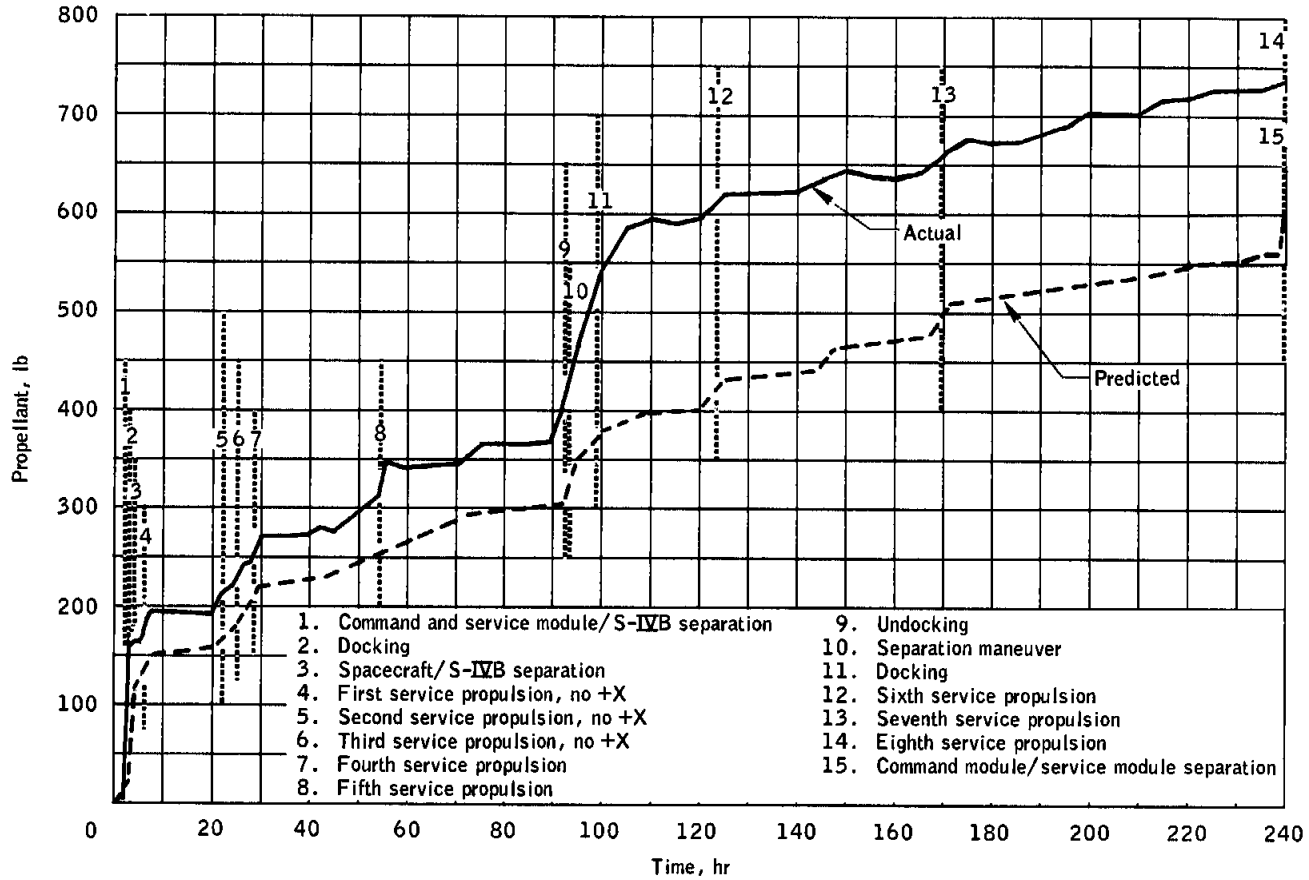


Figure 8.7-2.- Service module reaction control system propellant consumption.

## 8.8 SERVICE PROPULSION

System operation was satisfactory for the eight service propulsion firings. Ignition times and firing durations are shown in table 7-III of the trajectory section with the only discrepancy occurring with the propellant utilization and gaging system.

The duration of the longest firing, the third maneuver, was 279.9 seconds. The first three firings had ignition sequences in which a translation maneuver with the service module reaction control system was not required to effect propellant settling since the storage tanks still contained propellants. The remaining firings were preceded by a plus-X translation. The total firing time for the eight firings was approximately 505 seconds.

The fifth service propulsion firing followed a docked lunar module descent engine firing of approximately 372 seconds. Preflight analyses had indicated that when a descent engine firing was performed with the spacecraft docked, a negative acceleration greater than  $0.1 \text{ ft/sec}^2$  would result and could cause depletion of the propellant captured by the retaining screens. Although the retention reservoir would still remain full, some helium could be trapped and ingested into the engine during a subsequent service propulsion firing. However, after the docked descent engine firing, all service propulsion firings were normal and smooth, indicating that no significant quantity of helium had been ingested.

The measured steady-state pressures during the first seven firings are presented in table 8.8-I. These pressures indicate essentially nominal performance, although the oxidizer interface pressures were approximately 3 psi less than expected. A performance analysis of the second firing indicates nominal operation, with the specific impulse being within expected tolerances. Analyses also indicate that the mixture ratio was somewhat less than expected, which correlates with the reduced oxidizer interface pressures. Transient performance during all starts and shutdowns was within nominal limits.

The propellant utilization and gaging system operated normally during preflight propellant loading; however, during ground checkout, fuel point sensors 3, 8, and 15 gave failed indications. The stillwell propellant levels during the first firing and the first 25 seconds of the second and third firings were not stabilized and gave inaccurate propellant quantity readings, which resulted in erroneous unbalance meter indications and caution and warning light activations. The excessive stabilization time is attributed to stillwell capillary effects, which were more significant than on previous flights because of the increased spacecraft weight and associated lower acceleration levels; also the propellant-settling maneuver was not used.

Immediately following oxidizer storage tank depletion during the third maneuver, an excessive unbalance was indicated in the oxidizer-to-fuel ratio, and five warning light activations occurred. To verify the unbalance, the gaging system was switched from the normal to the auxiliary mode. The indicated unbalance remained within acceptable limits for a significant period of time, but then increased again, causing another warning light activation. When the gaging system was returned to the normal mode, the warning light was again activated.

Because this behavior was unexplained, the gaging system was deactivated for the fourth, fifth, and sixth firings. After a self-test indicated satisfactory operation of servo loops and the warning system, the gaging circuit was reactivated for the seventh firing. The actual unbalance at the end of the seventh firing was calculated from telemetry data to be approximately 2.2 percent (530 lbs) more oxidizer than fuel, confirming a lower-than-nominal average mixture ratio for the first seven firings.

Figure 8.8-1 shows the telemetered gaging system data for oxidizer and fuel during the third firing and figure 8.8-2 shows the indicated unbalance at selected times, as calculated from these data. The unbalance history should reflect the displayed unbalance history within the telemetry accuracy. Also shown in figure 8.8-2 are the times when a caution and warning light was activated. Additional discussion of gaging system discrepancies is contained in section 17.

TABLE 8.8-I.- STEADY-STATE PRESSURES

[All values in psia]

Parameter	Maneuver <sup>a</sup>						
	1	2	3	4	5	6	7
Oxidizer tank	174	175	175	175	175	176	175
Oxidizer interface	160	159	160	163	161	161	162
Fuel tank	174	173	175	177	174	172	174
Fuel interface	171	170	171	175	172	171	172
Engine chamber	95	101	103	106	102	99	103

<sup>a</sup>No data available for the eighth maneuver.

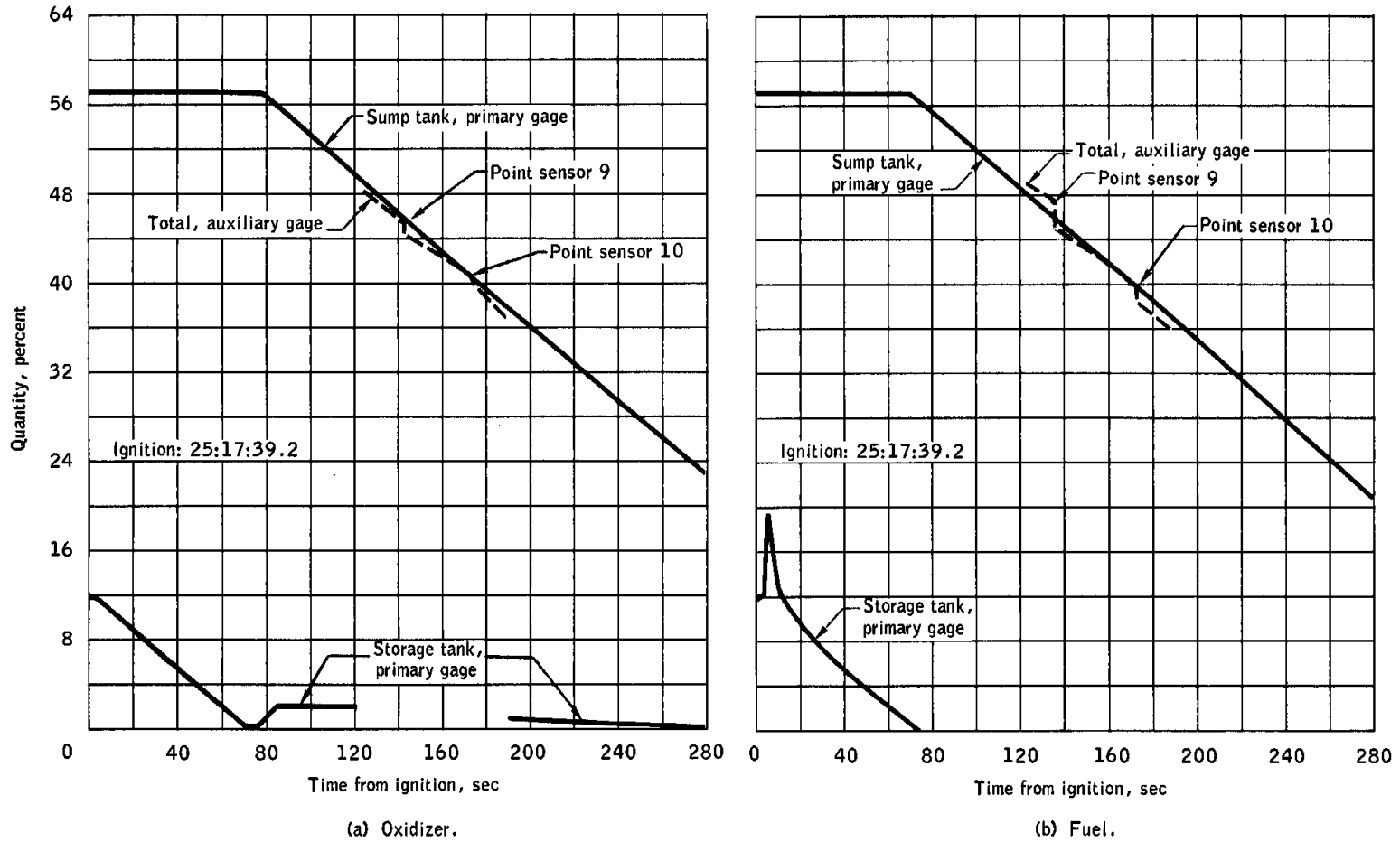


Figure 8.8-1.- Telemetered gaging quantities during third service propulsion firing.

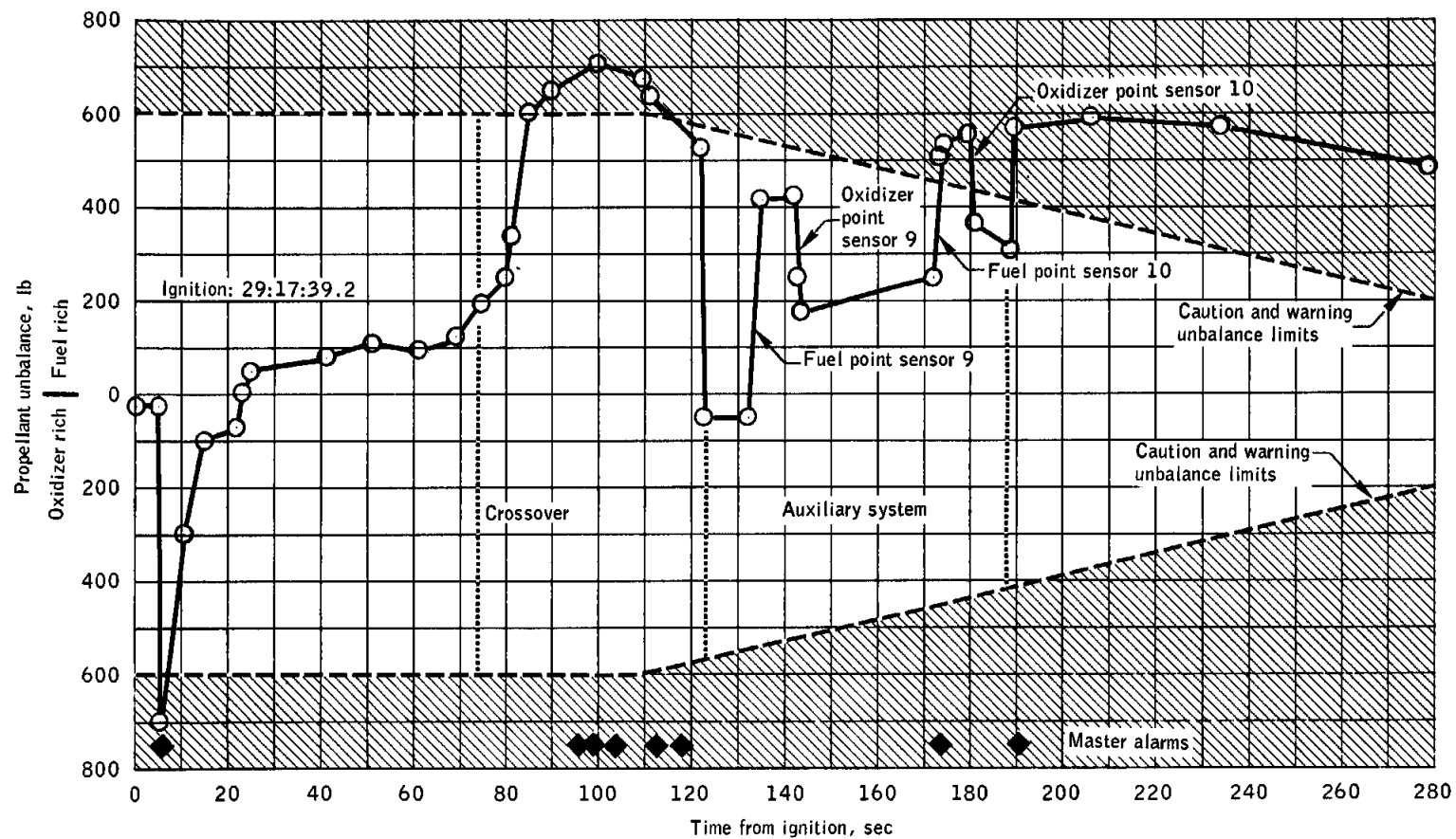


Figure 8.8-2.- Propellant balance during third service propulsion firing.

## 8.9 ENVIRONMENTAL CONTROL SYSTEM

The environmental control system performed satisfactorily throughout the mission, and system parameters were consistent with Apollo 7 results. The following paragraphs discuss those results which are pertinent to operation with the lunar module or showed discrepant performance.

### 8.9.1 Oxygen Distribution Circuits

The high- and low-pressure oxygen distribution systems operated normally during the mission. The oxygen system was used for the first time to pressurize the lunar module cabin for the initial manning. To accomplish the first pressurization, the command module cabin pressure was increased from the oxygen surge tank supply to 5.7 psia (fig. 8.9-1). After repressurization of the surge tank to 870 psi, the tunnel hatch pressurization valve was opened to permit gas flow into the lunar module until the command module cabin pressure decayed to 3.9 psia. Stored gas in the cabin repressurization package was then used to further increase cabin pressure of both vehicles to 4.6 psia. The cabin pressure regulator stabilized both cabin pressures at a normal operating level of approximately 4.9 psia.

Subsequent to pressure equalization between the two cabins, the repressurization package valve was opened and the pressures of the surge tank and the repressurization package equalized at about 550 psig. The repressurization package was then isolated, and the surge tank was re-serviced with gas from cryogenic storage supplies.

Surge tank repressurization should have been completed in 30 minutes, but after a period of 5.5 hours, the pressure had increased by only 160 psi. The crew cycled the surge tank shutoff valve several times, and the pressure increased at the anticipated rate. Postflight testing has indicated no mechanical problem, but the decal on the instrument panel was not in direct alignment with the corresponding valve detent, and apparently the valve was not initially in the full-open position.

During decompressed cabin operations for extravehicular activity, the suit circuit in the environmental control system provided pressure and temperature control for only the Command Module Pilot. The Commander and the Lunar Module Pilot were isolated from this circuit. The unused suit-supply umbilicals were turned off, with full flow directed to the Command Module Pilot's suit. System parameters during this period are given in fig. 8.9-2.

Soon after orbital insertion, the cabin fans were turned off to determine their effect on the cabin noise level. Although the noise was not objectionable when the fans were operating, they remained off for most of the mission. During the sixth day, one fan was turned on and operated for approximately 12 hours. Subsequently, the crew attempted operation of the redundant fan, but it failed to start. (After the crew opened the circuit breakers on this fan, they found the fan motor casing to be very hot to the touch.) A piece of Velcro tape was observed to be wedged in the fan impellar blade, preventing its rotation. See section 17 for a discussion of this problem. Postflight tests were conducted on the cabin fan in the stalled condition. The temperatures of the fan housing and motor stabilized after 50 minutes at 213° and 233° F, respectively.

#### 8.9.2 Thermal Control System

The thermal control system adequately controlled the environmental temperature for the crew and equipment. The primary glycol evaporator dried out at 24 hours and was deactivated until just before entry. Both coolant loops and evaporators were activated prior to entry and performed properly. The evaporator dryout was not unexpected, since a similar occurrence had been experienced during Apollo 7 and 8. Detailed discussions of this phenomenon are presented in the appropriate mission reports.

At approximately 86 hours, the radiator-system flow-proportioning valve switched to the redundant system. This switchover is not indicative of equipment failure, because no further difficulties were observed after the system was reset to the primary proportioning valve. Two similar switchover activations were observed in the Apollo 7 mission. Those activations were attributed to momentary electrical power dropouts.

During rendezvous, the inlet temperature of the secondary radiator increased to 100° F, or about 30° F above the expected range. This increase is attributed to long-duration solar heating on the area where the sensor is located and to the relatively high heat loads on the electrical power system radiator during this time. Other equipment located in the same area experienced a similar increase in temperature.

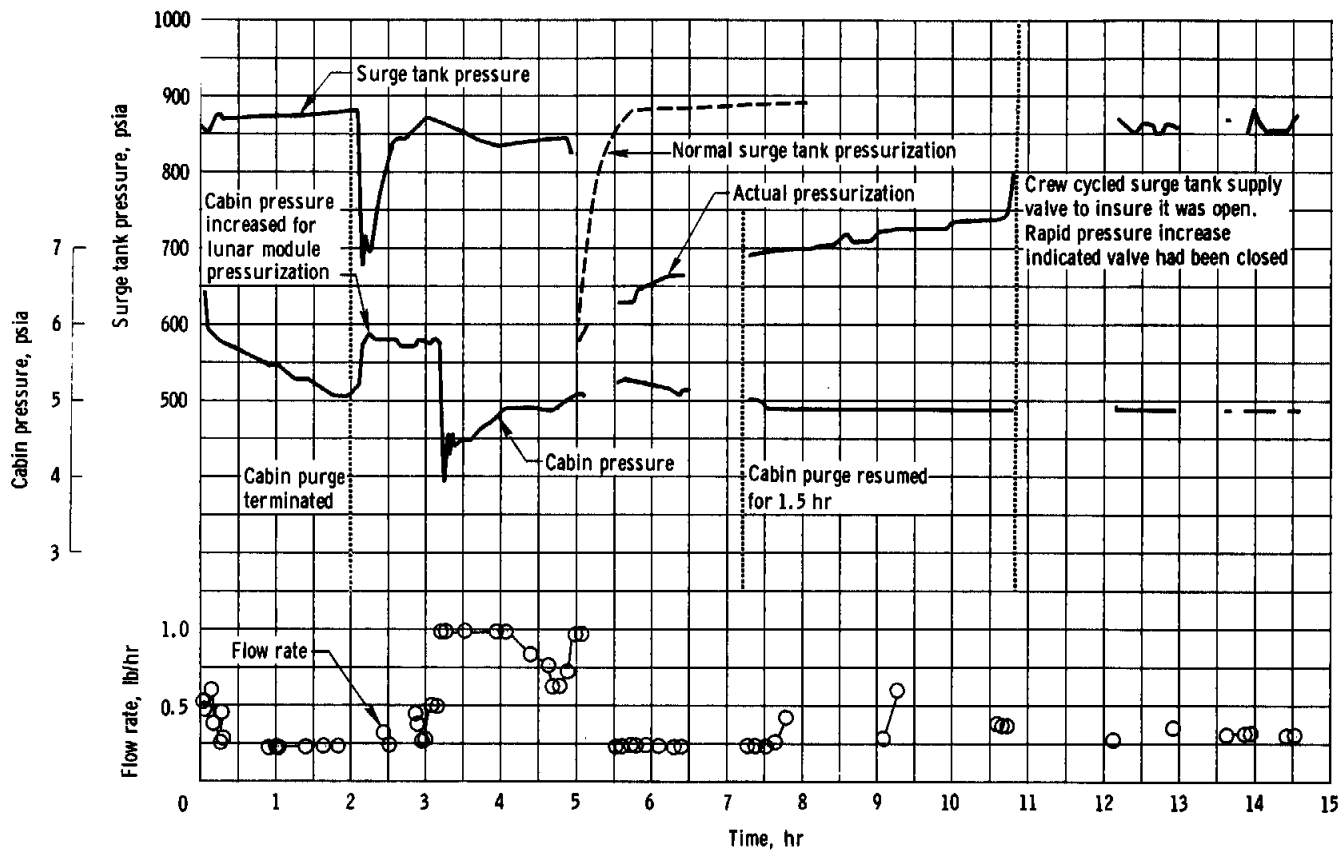


Figure 8.9-1. - Cabin and surge tank pressure and oxygen flow rate during first lunar module pressurization.

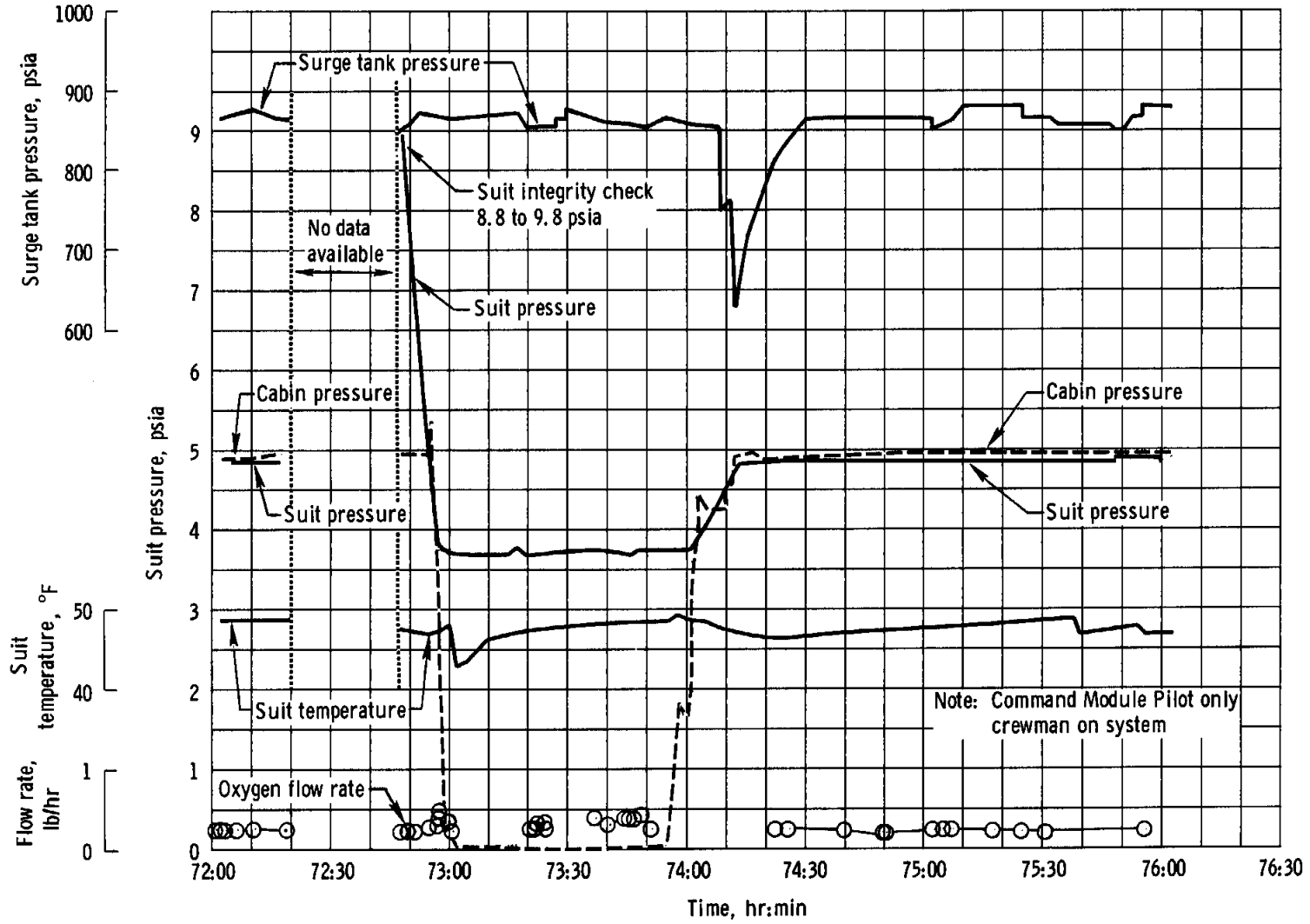


Figure 8.9-2. - Depressurized cabin operation.

## 8.10 CREW STATION

This section contains an evaluation of major crew provisions, controls and displays, and spacecraft lighting.

### 8.10.1 Crew Provisions

The inflight coverall garments were worn while the pressure suits were doffed during the first 4 days of the flight and for the last 5 days. Postflight inspection of the coverall garments indicated no excessive wear or damage. The life vests were worn during launch and entry and were successfully inflated prior to egress after landing. The heel restraint and headrest were used during entry. All eight of the constant wear garments were worn, and the defecation opening of one of the garments was ripped larger to simplify feces collection. The pressure garment assemblies were worn for approximately 47 hours of the flight, and most of that time was spent with the helmet and gloves removed. The Lunar Module Pilot wore both liquid-cooled garments; the first was worn on the third and fourth days. The Lunar Module Pilot reported many entrapped air bubbles at the completion of the fourth day. The second garment was worn on the fifth day and was never connected to the portable life support system. The helmet protective shield was worn to prevent damage to the helmet visual area when a crewman was working in the tunnel. Post-flight inspection revealed that the pressure garment assemblies had areas of excessive wear on the coverlayers and hardware.

The urine collection transfer adapter and urine transfer system were both used for urine transfer when the crew was unsuited. The Commander reported that the spare transfer assembly roll-on cuffs were too large; however, these cuffs were the same size as those provided to the Commander at launch. The Lunar Module Pilot was also provided with cuffs that were too large.

The communications carriers were worn at launch and for the suited portions of the mission. The Command Module Pilot's forehead and cheeks were affected by a skin irritation, which disappeared when the communications carrier was not worn.

The bioinstrumentation system was worn continuously, and when the electrode paste dried out, additional paste from the medical kit was applied. The electrocardiogram from the Command Module Pilot was erratic during early portions of the mission, but greatly improved when the spare sternal leads from the medical kit were substituted. Several electrode attachment tapes from the medical kit were used to reattach loose sensors.

The crew experienced a wash-out of the reticle in the command module crewman optical alignment sight during command module docking and of the lunar module crewman optical alignment sight during lunar module docking. The orientation of the sun with respect to the vehicles caused a glare from the command module that was brighter than the lunar module optics reticle pattern. For subsequent spacecraft, the brightness of the crewman optical alignment sight reticle will be increased by changing the filter in the barrel housing to a diffuser lens, and by providing a snap-on filter assembly which can be placed on the front of the barrel for viewing faint objects. See section 17.3 for a discussion of this problem.

At 192:43:00 and again at 194:13:00, the crew were successful in sighting the Pegasus II satellite, using the crewman optical alignment sight. Pointing information was provided by the Mission Control Center and the range at the time of sighting was approximately 1000 miles. Pegasus II was in the field of view for less than 1 minute during the first sighting and for approximately 2 minutes during the second sighting. Pegasus II was launched in May 1965, and has a meteoroid detection panel span of 96 feet from tip to tip, and a length of 77 feet. The cross-section while tumbling is estimated to be 2174 square feet with a mass of 22 605 pounds.

At 222:38:40 over Hawaii, a sighting was made of the lunar module ascent stage, based on pointing information provided by the Mission Control Center. Tracking was performed with the crewman optical alignment sight until 222:45:40 with a minimum slant range of 652 miles. The lunar module orbit at the time of sighting was 3761 by 127 miles and the orbit of the command and service modules was 244 by 98 miles.

The crew reported that the oxygen umbilicals were too stiff and that the umbilical portion which connected to the panel protruded into the tunnel transfer envelope. For subsequent spacecraft, the oxygen umbilicals will be fabricated from a more flexible silicone material sleeved with Teflon-coated beta cloth to meet flammability requirements. Additionally, the hoses will be relocated to provide some increase of effective length.

### 8.10.2 Displays, Controls, and Lighting

The onboard displays and controls satisfactorily supported the Apollo 9 mission except for the anomalies associated with the caution and warning system, internal floodlights, and docking spotlight.

A master alarm without an annunciator indication occurred at initial hard docking. Data during this time period do not indicate any out-of-tolerance condition that could have caused the alarm. Two unexplained

master alarms occurred during the deorbit maneuver and entry. The discussion of these three alarms is contained in section 17.

The lighting check prior to rendezvous showed the exterior spotlight was inoperative. Photographs of the service module taken during rendezvous showed that the light was not deployed. The crew later reported that the circuit breaker was open for spotlight deployment of the spotlight. The circuit breaker was closed prior to the lighting check. Section 17 contains a discussion of this problem.

Two floodlights were reported failed during the flight, and one became extremely hot, emitting a burning odor. A discussion of the floodlight discrepancy is contained in section 17.

## 8.11 CONSUMABLES

The usage of all liquid consumables, including cryogenics, is summarized in this section. Electrical power consumption is discussed in section 8.2.

## 8.11.1 Service Propulsion System Propellants

The total service propulsion system propellant loadings and consumption values were as follows. The loadings were calculated from gaging system readings and measured densities prior to lift-off.

	<u>Fuel, lb</u>	<u>Oxidizer, lb</u>
<u>Loaded</u>		
In tanks	13 803.4	22 102.3
In lines	<u>78.6</u>	<u>123.7</u>
	13 882.0	22 226.0
<u>Consumed</u>	13 125.4	20 432.2
<u>Remaining at separation</u>	756.6	1 793.8

## 8.11.2 Reaction Control System Propellants

Service module.- The propellant utilization and loading data for the service module reaction control system were as follows. Consumption was calculated from telemetered helium tank pressure histories using the relationships between pressure, volume, and temperature.

	<u>Fuel, lb</u>	<u>Oxidizer, lb</u>
<u>Loaded</u>		
Quad A	109.8	223.1
Quad B	109.3	225.4
Quad C	111.0	226.2
Quad D	<u>110.6</u>	<u>225.2</u>
	440.7	899.9

<u>Consumed</u>	270.5	519.5
<u>Remaining at separation</u>	170.2	380.4

Command module.- The propellant loading and utilization for the command module reaction control system were as follows. Consumption was calculated from pressure, volume, and temperature relationships.

	<u>Fuel, lb</u>	<u>Oxidizer, lb</u>
<u>Loaded</u>		
System 1	44.2	78.3
System 2	<u>44.2</u>	<u>78.3</u>
	88.4	156.6
<u>Consumed</u>		
System 1	9.3	17.7
System 2	<u>0.2</u>	<u>0.3</u>
	9.5	18.0
<u>Remaining at main parachute deployment</u>		
System 1	34.9	60.6
System 2	<u>44.0</u>	<u>78.0</u>
	78.9	138.6

### 8.11.3 Cryogenics

The total cryogenic hydrogen and oxygen quantities loaded at lift-off and consumed were as follows. Consumption values were based on the electrical power produced by the fuel cells.

	<u>Hydrogen, lb</u>	<u>Oxygen, lb</u>
<u>Loaded</u>		
Tank 1	26.3	305.3
Tank 2	<u>26.5</u>	<u>308.8</u>
	52.8	614.1

Consumed

Tank 1	21.2	210.6
Tank 2	<u>20.3</u>	<u>202.5</u>
	41.5	413.1

Remaining at separation

Tank 1	5.1	94.7
Tank 2	<u>6.2</u>	<u>106.3</u>
	11.3	201.0

## 9.0 LUNAR MODULE PERFORMANCE

The specific performance of the major lunar module systems is presented in this section. Performance of all lunar module systems was adequate for the Apollo 9 mission. System performance which was significantly different than planned will be discussed in detail. The pyrotechnic system operated exactly as expected and, therefore, is not included. Selected discrepancies mentioned in this section are presented in more detail in section 17, Anomaly Summary. Performance related to the extravehicular activity and rendezvous operations is contained in sections 4 and 5. A compilation of fluid and gaseous quantities is presented at the end of this section.

### 9.1 STRUCTURAL AND MECHANICAL SYSTEMS

Analyses of lunar module loads during launch and flight were based on measured acceleration, vibration, and strain data. The structural loads were less than the design values for all phases of flight.

#### 9.1.1 Launch Phase

Power spectral density analyses were prepared for 21 measurements during periods of maximum vibration at lift-off. The power spectral densities were compared to the predicted environment for each measurement location (fig. 9.1-1). During lift-off, four of the 21 measurements exceeded predictions. Figures 9.1-2 through 9.1-5 compare the level of flight vibration with the predicted flight environment for these four measurements: descent propulsion system, guidance and navigation base, landing radar antenna, and aft equipment rack.

The descent engine vibration exceeded the predicted levels during lift-off. Figure 9.1-2 shows the Y-axis vibration is greater than predicted at 21 Hz and 140 Hz. During qualification testing, a peak of  $0.3 \text{ g}^2/\text{Hz}$  occurred at 28 Hz which was the fundamental modal frequency of the engine as mounted in the test fixture. The  $0.05 \text{ g}^2/\text{Hz}$  peak at 21 Hz measured at lift-off is comparable to the qualification test data because 21 Hz is the fundamental modal frequency of the engine when mounted in the lunar module. Therefore, the engine is qualified for the 21 Hz vibration peak.

The 140 Hz peak is not considered structurally significant because it is believed to be an acoustically induced local resonance. In addition, an integration of the Y-axis analysis from 20 to 300 Hz using the

power spectral density plots yields only 1.83 g rms or a 5.5 g peak. Applying this as a load factor yields 2200 pounds for the 400-pound engine vibration qualification data yields 3520 pounds.

All descent engine components and subassemblies, with the exception of the fuel and oxidizer flow control valves, and the injector internal mechanism plumbing and wiring have been tested to levels higher than those measured on Apollo 9. In summary, the descent stage engine structure and the majority of engine components and subassemblies have been qualified to environments more severe than the Apollo 9 environment. There has been no demonstration of engine fuel and oxidizer flow control valves and the injector internal mechanism plumbing and wiring to withstand the measured 140 Hz environment with the exception of Apollo 9 and Apollo 5 flights which is considered sufficient validation for the particular environment. There is no significant increase expected in the acoustic level and resultant vibration over that experienced during Apollo 9.

Sinusoidal random vibration qualification tests were conducted on all aft equipment-rack components to levels higher than those measured during the Apollo 9 mission.

While the predicted levels were exceeded on the navigation base and the landing radar antenna, qualification tests in excess of the flight environment show an adequate factor of safety as shown in figures 9.1-4 and 9.1-5.

Lunar module linear accelerations were as predicted at lift-off, the maximum dynamic pressure/angle of attack region, and the end of first stage boost. Table 9.1-I presents a comparison of flight values and design values for these conditions.

After first stage center and outboard engine cut-off, large acceleration oscillations at 5.2 and 6.0 Hz, respectively, were measured in the lunar module. Ascent stage linear accelerations during this time period are shown in figures 9.1-6 and 9.1-7. The accelerations were approximately twice the magnitude measured on the simulated lunar modules in previous Apollo/Saturn V missions. Instrumentation locations and magnitudes of peak vibration acceleration are shown in figure 9.1-1. The acceleration vectors shown in his figure are discrete values at approximately 6.0 Hz. The descent stage oxidizer tank and aft equipment rack Z-axis measurements were transmitted on telemetry channels which were time shared with other measurements and were not operative during the period of significant oscillations at outboard engine cutoff. The Z-axis vectors shown in figure 9.1-7 are extrapolated from data obtained during inboard engine cutoff when simultaneous recordings were obtained. Y-axis responses were negligible.

Oxidizer tank dome X-axis response is shown in figure 9.1-8. The presence of the high-frequency peak superimposed on the low-frequency oscillation indicates contact between the accelerometer and the fire-in-the-hole thermal shield or between the tank helium diffuser flange and the descent stage upper deck probably due to lateral motion. Clearances between the tank and the upper deck are marginal. Relative motion between the tank and the upper deck cannot be determined; however, motion pictures of ground vibration tests show significant relative motion. Evidence indicates that there may be insufficient clearance between the tank and deck to assure no contact between the tank helium diffuser flange and the deck. (See section 17 for further details.)

The 16 outrigger struts were instrumented with strain gages calibrated to indicate load directly in pounds. The maximum strut loads occurred at the end of first-stage flight just prior to outboard engine cutoff and were well below the allowable levels. The minimum factor of safety for the outrigger struts was approximately 1.75.

The lunar module/adaptor interface loads, calculated from the measured strut forces at station 584, were well below the adaptor design loads. During outboard engine cutoff, a lateral oscillation of approximately 0.9g peak was measured at the lunar module center of gravity, and was considerably higher than those measured on previous flights. However, the ascent and descent stages were oscillating laterally approximately 180 degrees out-of-phase (fig. 9.1-1), resulting in interface loads below design levels.

### 9.1.2 Orbital Phase

The lunar module loads during the orbital phase were evaluated for the three firings of the descent engine and for the ascent engine firing to depletion. All accelerations and loads were low during these firings.

The range of lunar module vibration measurements was established for launch phase conditions and was too great for adequate data during descent engine firing.

The maximum measured load in the descent engine support struts was 3250 pounds compared with a design value of 5800 pounds. The maximum loads (fig. 9.1-9) were measured at the end of the 100-percent thrust period during the first firing.

Ascent stage accelerations, measured at the lunar module center of gravity, when thrust was increased from 40 to 100 percent during the first descent engine firing, are shown in figure 9.1-10. The acceleration history shown in this figure is typical for all descent engine firings with no low-frequency acceleration discernible.

No structural data were obtained from the first ascent engine firing, which was performed out of range of ground station acquisition. No discernible low-frequency oscillations were measured during the ascent engine firing to depletion, and the structural loads were within vehicle allowable limits.

Loads were determined at the command module/lunar module docking interface (table 8.1-II). The loads were obtained during the first service propulsion firing and during a stroking test performed in conjunction with the third service propulsion firing.

All of the mechanical systems functioned as planned except for the ingress/egress hatch, which is discussed in section 17.

TABLE 9.1-I.- LUNAR MODULE RESPONSES DURING LAUNCH

Response	Lift-off		Maximum $q\alpha$		End of first-stage boost	
	Measured	Design Limit	Measured	Design Limit	Measured	Design Limit
Longitudinal acceleration, g . . .	1.4	1.6	2.0	2.07	3.9	4.9
Lateral acceleration, g . . . . .	0.3	0.65	0.1	0.3	0.08	0.1

The flight conditions at maximum  $q\alpha$  were:

Condition	Measured	Design
Mach no. . . . .	1.42	1.29
Dynamic pressure, psf . . .	633	689
Angle of attack, deg . . .	4.13	9.6
Maximum $q\alpha$ , psf-deg . . . .	2614	6614

\*Predicted, not design.

No.	Measurement no.	Location	Range, g
1	GG6001 GG6002 GG6003	Navigation base	±2
2	GA3661 GA3662 GA3663	Tunnel equipment area	±30
3	GA3001 GA3003 GA3005	X-axis center of gravity Y-axis center of gravity Z-axis center of gravity	±10 ±2 ±2
4	GA1501 GA1502 GA1503	Ascent stage engine support strut	±30 ±30 ±30
5	GA1571 GA1572 GA1573	Ascent stage oxidizer tank	±10 ±10 ±10
6	GA3601 GA3602 GA3603	Aft equipment rack	±20
7	GQ7301 GQ7302 GQ7303	Descent stage thrust chamber	±149 ±149 ±149
8	GA2681 GA2682 GA2683	Descent stage oxidizer tank -Z axis	±10 ±10 ±10
9	GN7559	Landing radar antenna	±10

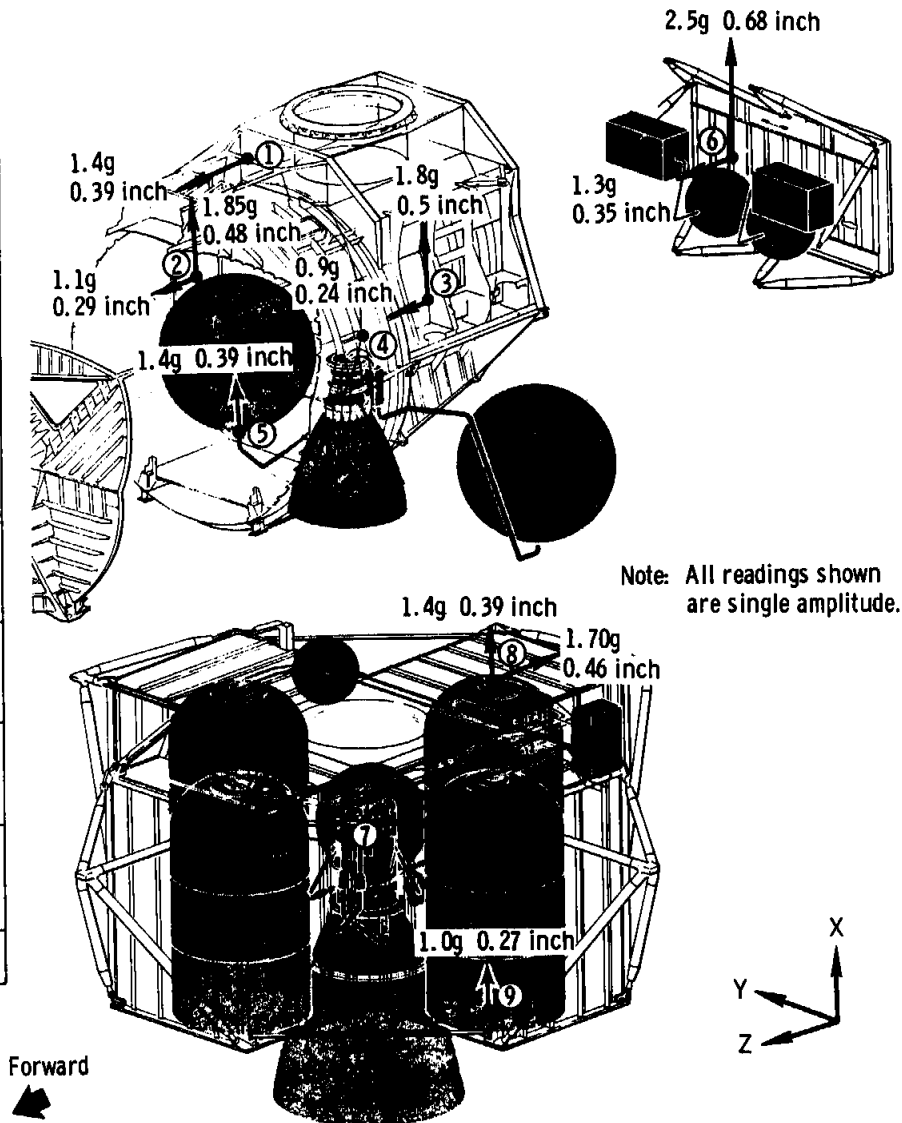


Figure 9.1-1.- Instrumentation locations and peak readings during outboard engine cutoff.

NASA-S-69-2024

Time: 0.5 to 2.5 seconds after lift-off  
Filter bandwidth: 6.0947 Hz  
RMS value: 3.153g

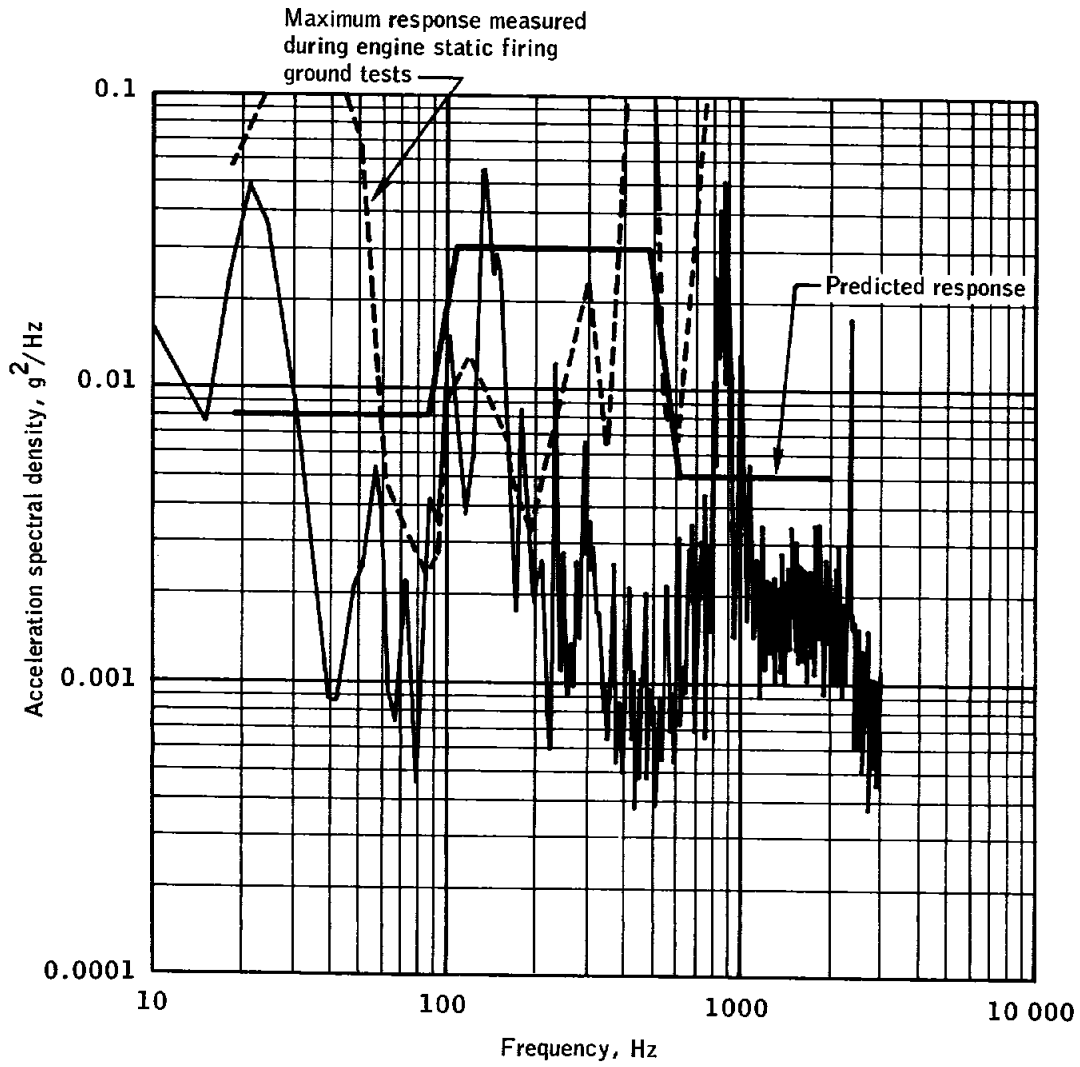


Figure 9.1-2.- Maximum vibration response in Y-axis from descent propulsion system thrust chamber.

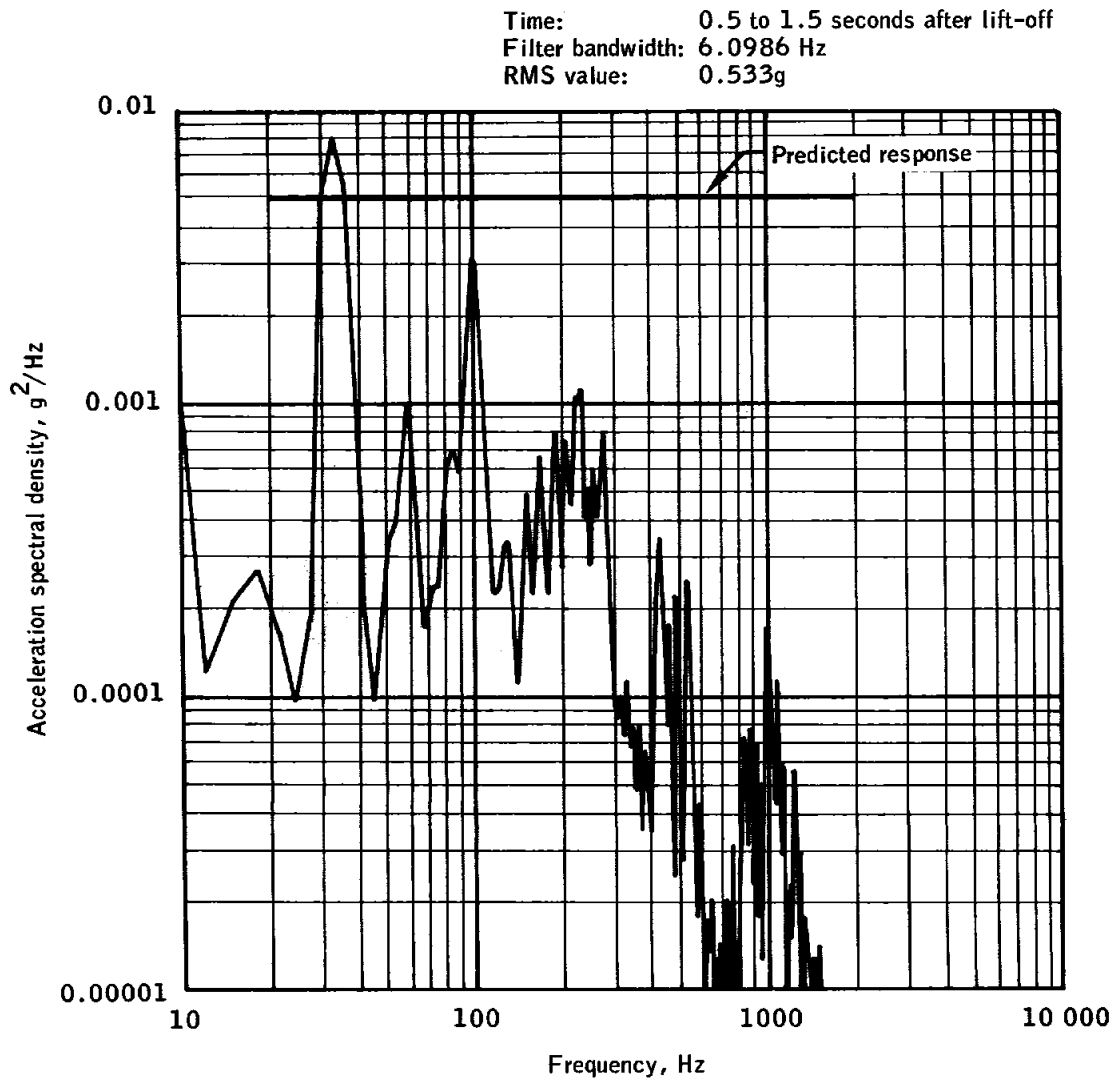


Figure 9.1-3.- Maximum vibration response in Z-axis from ascent stage aft equipment rack.

NASA-S-69-2026

Time: 0.5 to 1.5 seconds after lift-off  
 Filter bandwidth: 6.0919 Hz  
 RMS value: 0.810

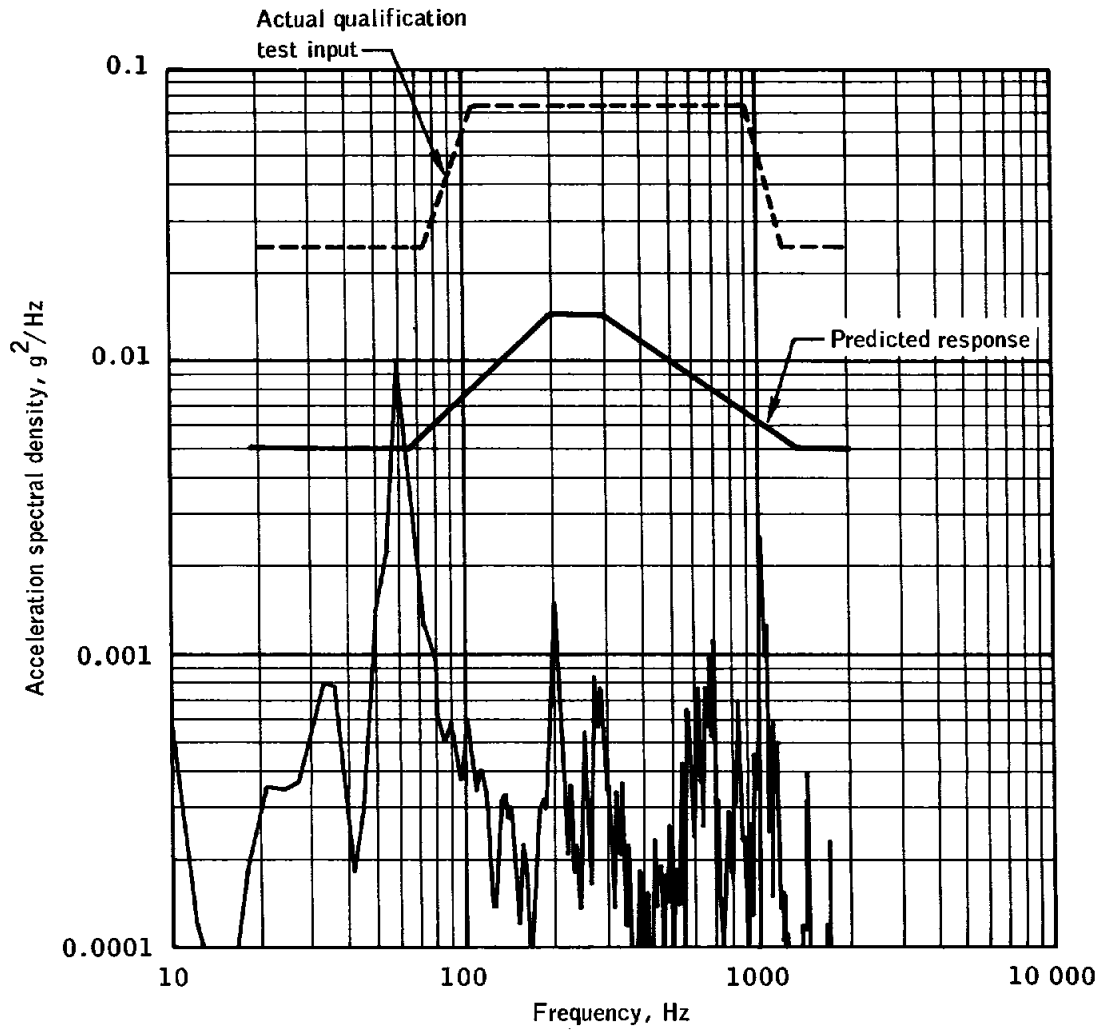


Figure 9.1-4.- Maximum vibration response in X-axis from navigation base.

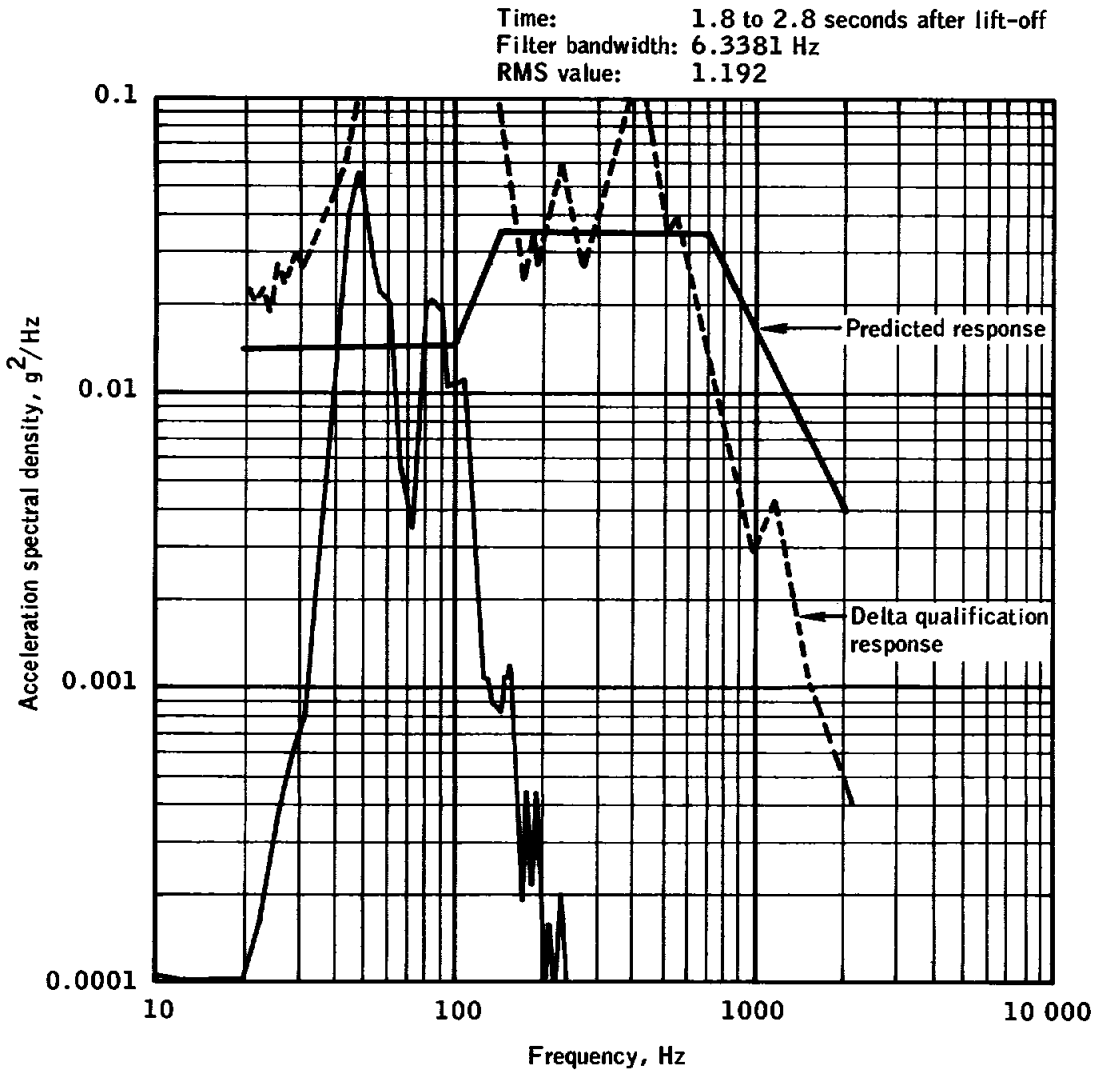


Figure 9.1-5.- Maximum vibration response in X-axis from landing radar antenna.

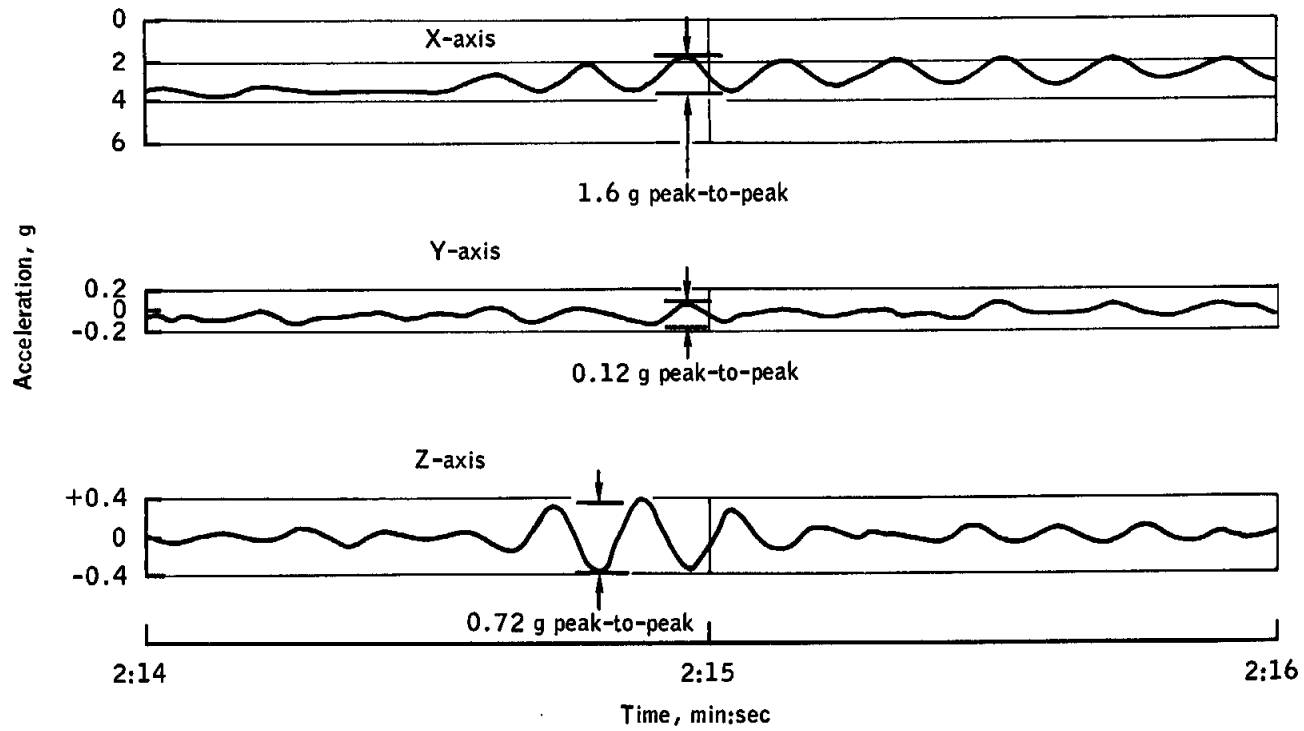


Figure 9.1-6.- Lunar module accelerations at S-IC center engine cutoff.

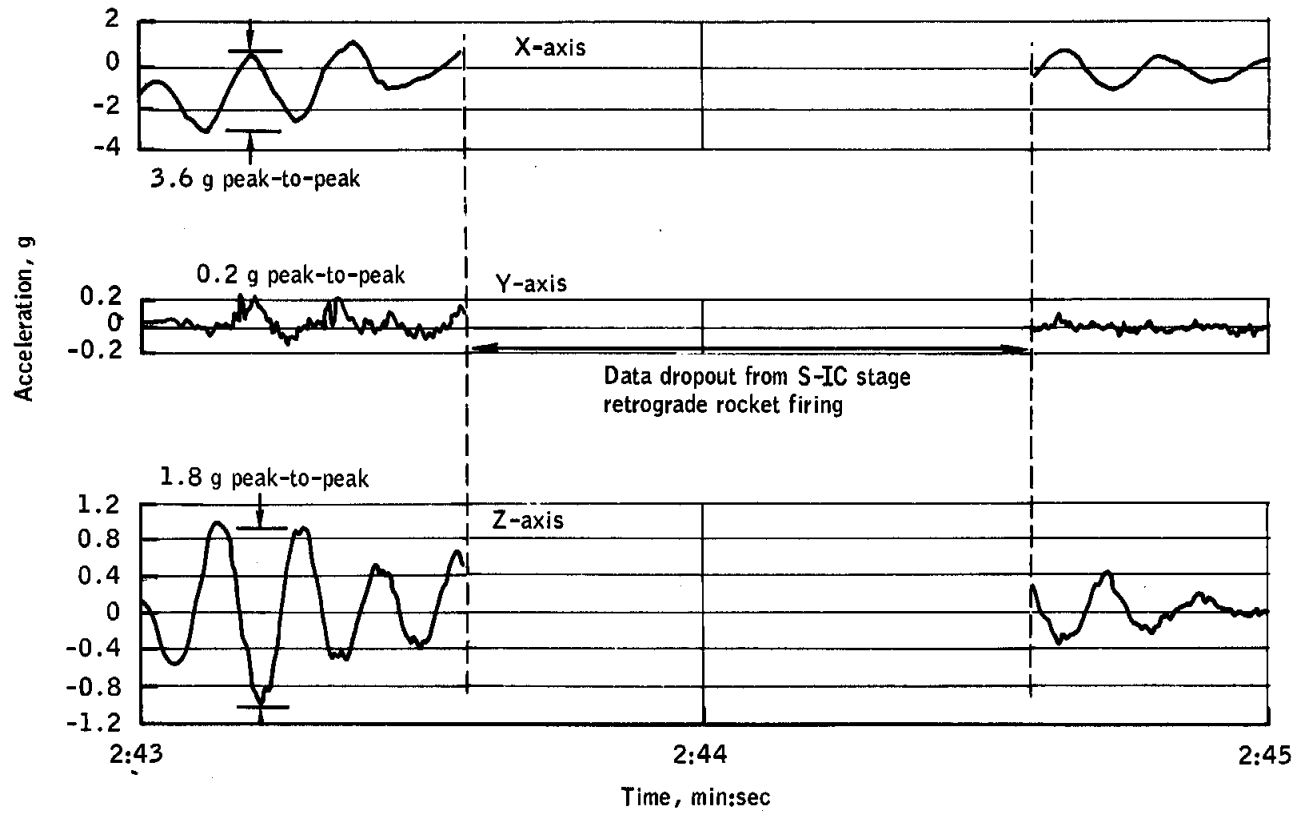


Figure 9.1-7.- Lunar module accelerations at S-IC outboard engine cutoff.

NASA-S-69-2030

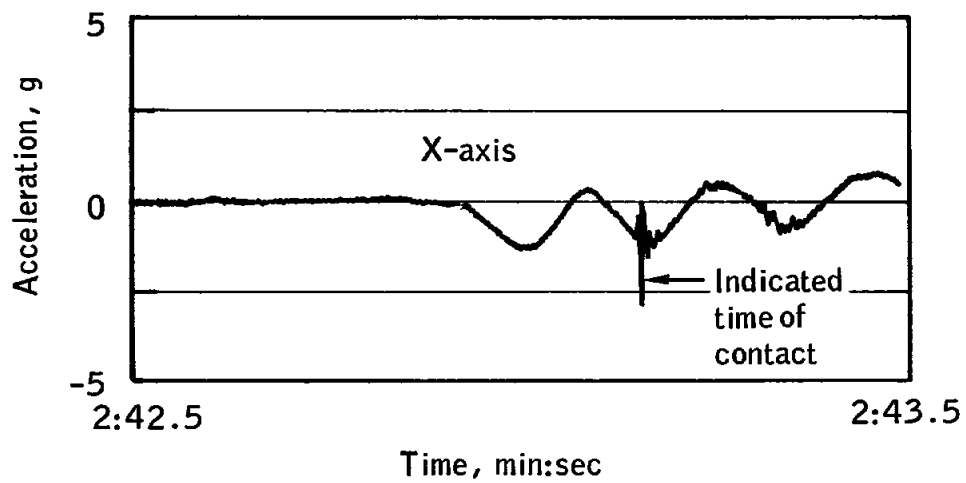


Figure 9.1-8.- Minus-Z oxidizer tank dome acceleration response.

Note: No data from strut 4.

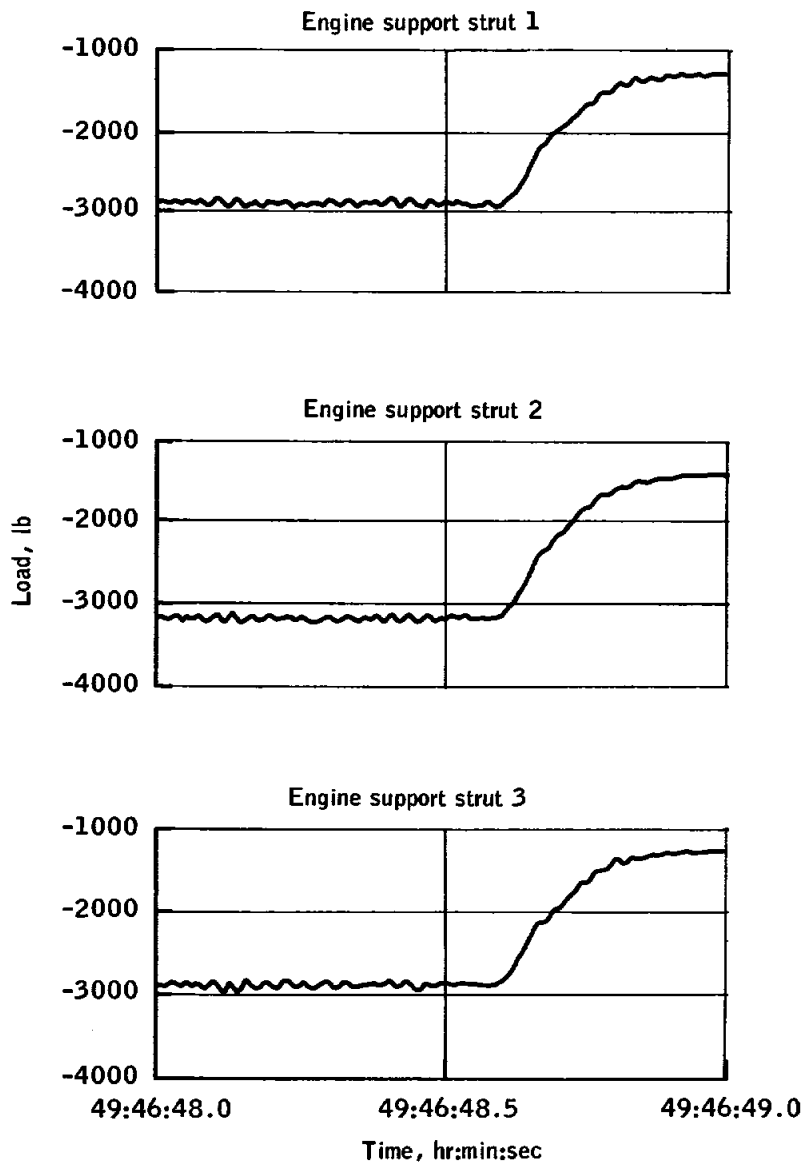


Figure 9.1-9.- Load on descent engine support struts during docked descent engine firing, 100 to 40 percent throttling.

NASA-S-69-2032

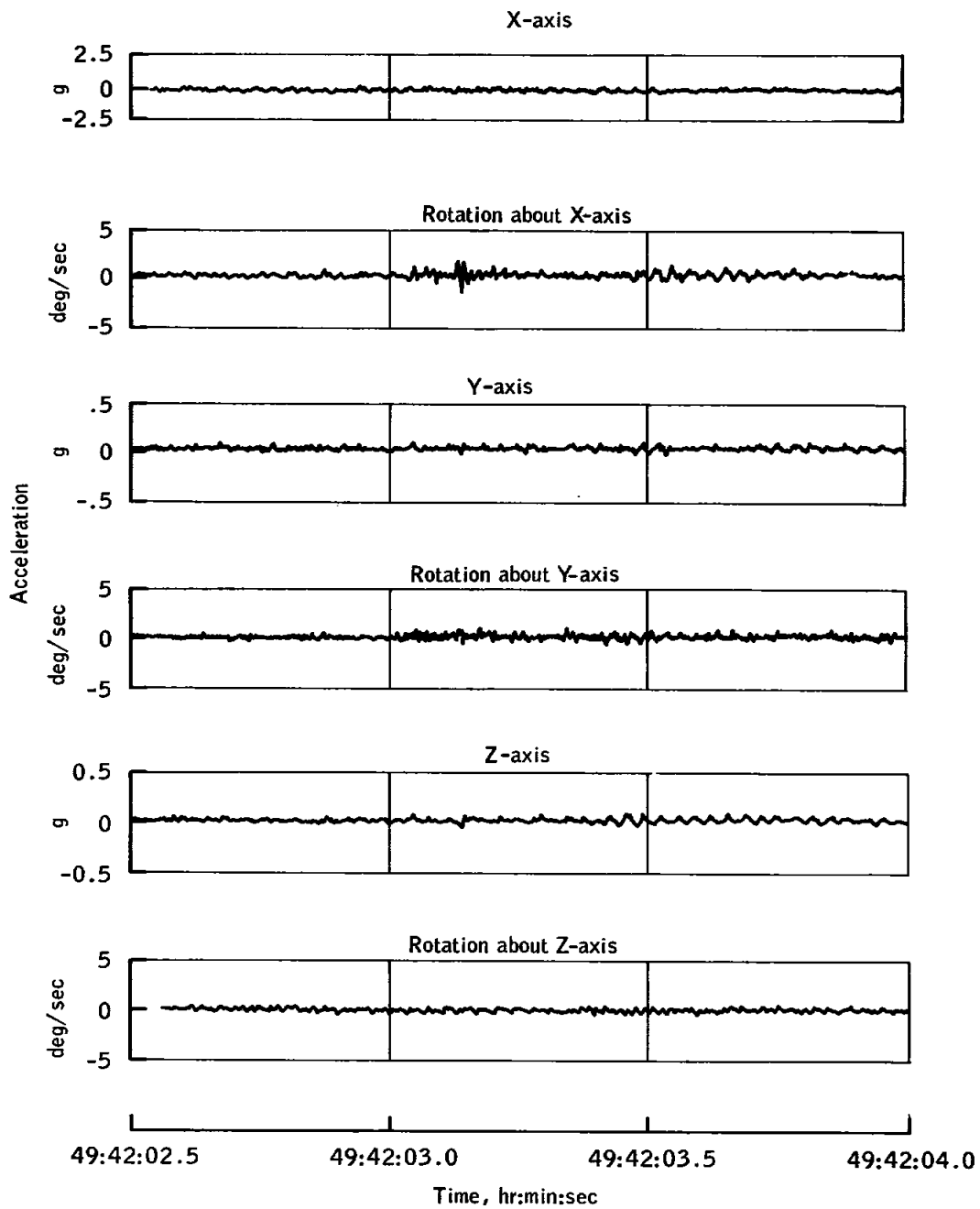


Figure 9.1-10.- Accelerations during docked descent engine firing, throttling from 40 to 100 percent.

## 9.2 THERMAL CONTROL

The thermal performance was nominal, and the response was essentially as predicted; all temperatures remained within acceptable limits. The insulation system performed satisfactorily, as is evidenced by the small change (approximately 1° to 2° F decrease) in the structural and the propellant bulk temperatures during the nonfiring periods. All tank temperatures remained within their respective fracture-mechanics limits. The most temperature-responsive elements of the lunar module were the rendezvous radar antenna, the landing radar antenna, and the descent stage base heat shield.

During the rendezvous phase, the temperature response of the rendezvous radar antenna was as predicted until about 96 hours, after which time the flight data were approximately 10° F lower than predicted (fig. 9.2-1), primarily the result of differences between the actual and predicted antenna orientation with respect to the sun.

The landing radar antenna temperature response under operating conditions was as predicted. Deviations for non-operating conditions are attributable to differences between predicted and actual antenna orientations with respect to the sun. Further, heater cycling was initiated at approximately 64° F as compared with the predicted 58° to 59° F.

The temperature response of the descent stage base heat shield was slightly lower than predicted. A comparison of peak temperature, predicted temperature range, and maximum allowable limits is shown in the figure 9.2-2.

Although the descent engine firing duration was only 371.5 seconds as compared with the 655-second firing included in the lunar landing design conditions, the outer surface temperatures were at approximately equilibrium temperatures. Consequently, only the inner facesheet surface temperatures that were affected by soakback would be appreciably higher for the lunar landing firing, but these are not predicted to exceed allowable limits.

During the docked descent engine firing, the crew reported seeing small objects flying away from the lunar module. The radiant heat from the engine will burn away the 5-mil layer of H-film taped to the exterior of the base heat shield. Charred (black) or uncharred (silver or gold) H-film may be observed drifting from the vicinity of the lunar module on future missions during initial descent engine firings.

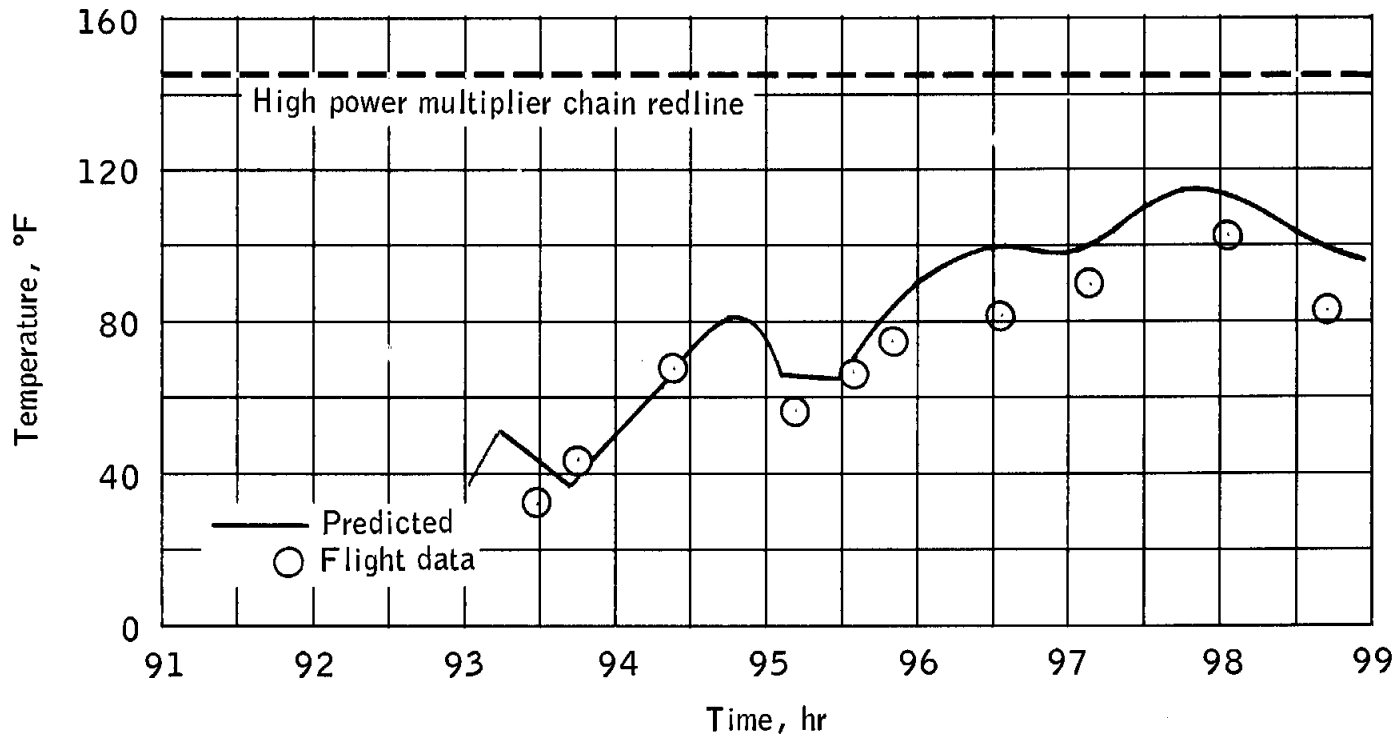


Figure 9.2-1.- Rendezvous radar temperature response.

No.	Temperature, °F			No.	Temperature, °F		
	Predicted range	Peak	Maximum allowable		Predicted range	Peak	Maximum allowable
1	1790-1930	1650	2100	6	70-550	250	1000
2	1900-2060	1860	2200	7	- -400	65	800
3	800-900	800	1000	8	70-550	275	1000
4	1300-1400	1450	1500	9	70-550	280	1000
5	1600-1700	1650	1800	10	70-550	270	1000

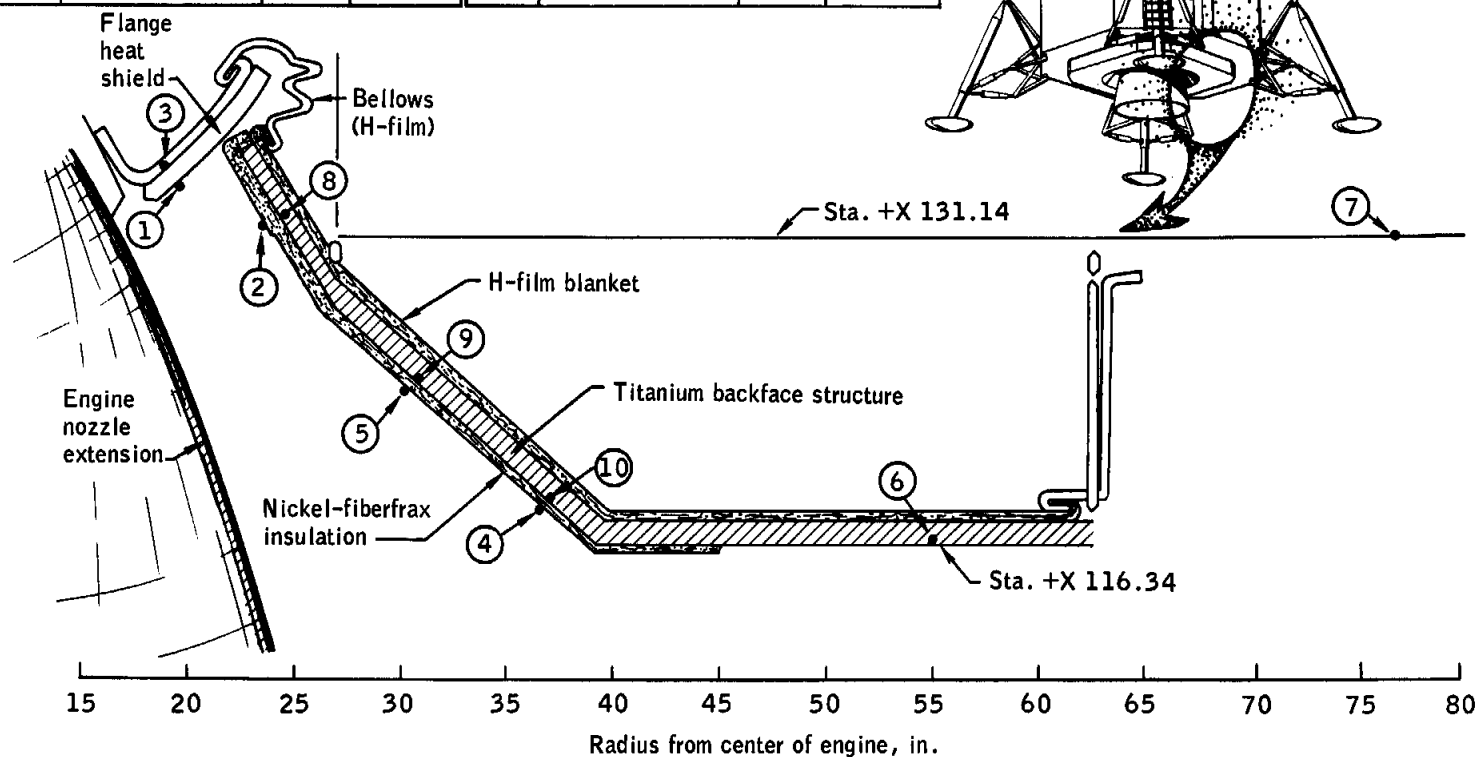


Figure 9.2-2.- Descent stage base heat shield sensor locations and peak temperature.

### 9.3 ELECTRICAL POWER

The dc bus voltage was maintained above 28.9 V dc, and the maximum observed load was 103 amperes.

The descent stage batteries provided power within the normal voltage, current, and temperature limits, delivering 1056 A-h of energy from a nominal capacity of 1600 A-h. Battery 4, located farther downstream on the glycol cooling system than the other descent stage batteries, operated from 4° to 8° F warmer and, therefore, took more of the electrical load.

The ascent stage batteries supplied 368 A-h of the nominal 620 A-h through the end of the ascent propulsion firing to depletion. The predicted usage for this period was 468 A-h. The batteries remained within normal voltage, current, and temperature limits. The large differences between the predicted and actual ampere-hour consumption for all batteries, as shown in figure 9.3-1, represents the inherent conservatism existing in the computer simulation of the cyclic electrical loads such as heaters. The Apollo 9 data are being used to update this program for Apollo 10.

The ascent stage battery data obtained 4 hours after the ascent engine firing to depletion indicated that battery 5 maintained 27 volts, or higher, until the predicted capacity of 310 A-h had been used. Battery 6 maintained greater than 30 volts until loss of signal at which time 346 A-h had been consumed. Specification capacity of the batteries is 310 A-h.

The ac bus voltage remained within normal operating limits of 115 to 118 V ac for full load and no load, respectively, at a frequency of 400 Hz.

The various backup modes of operation were demonstrated. The modes were:

- a. Ascent battery normal and alternate operation
- b. Parallel ascent/descent battery operation
- c. Inverter switching.

NASA-S-69-2035

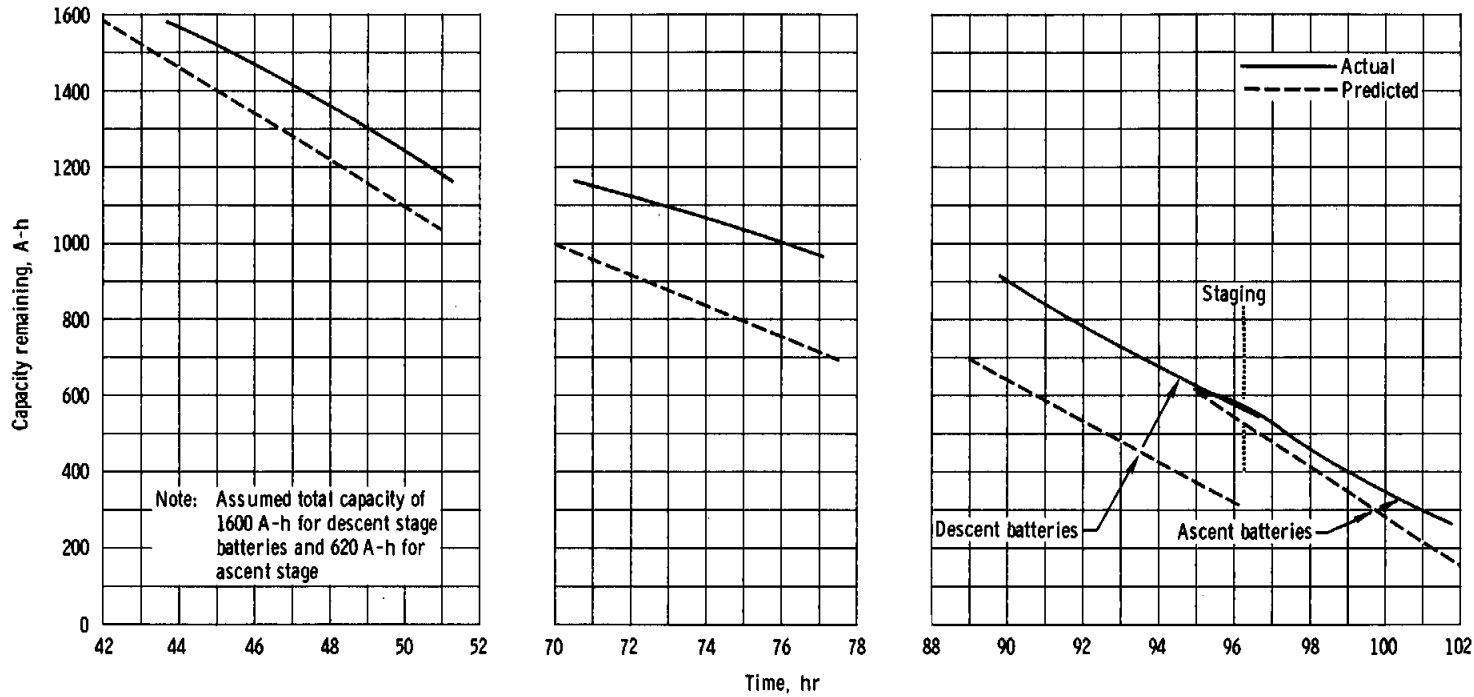


Figure 9.3-1. - Battery capacity remaining.

## 9.4 COMMUNICATIONS

The communications system operated within nominal limits. Telemetry data were provided by the S-band system in real time and by the VHF system for playback through the data storage equipment (tape recorder) in the command module.

At approximately 89 hours, the Lunar Module Pilot's push-to-talk switches (on the attitude controller assembly and on the spacecraft umbilical) failed to key the selected transmitters for the desired voice communication. At that time, the Lunar Module Pilot changed to voice-operated transmission (VOX). This anomaly is discussed in detail in section 17. Concurrent with this anomaly, the Lunar Module Pilot reported that the data storage electronic assembly (tape recorder) would not operate in the VOX mode. Analysis of the tape indicates that the Commander's audio center was configured for intercommunications ("hot microphone"), and the tape recorder was running continuously, as it should have been. Review of the voice recorded indicates that no anomaly existed.

The VHF voice communication was very good in both the A and B links; the A system provided the primary spacecraft-to-ground voice link. The primary S-band link was used throughout the mission except during the two secondary S-band checks. The secondary S-band check at Carnarvon was excellent.

Most of the planned communication system tests, including the test of the S-band steerable antenna, were eliminated from the flight plan because of lack of time.

Although the communication system adequately supported the mission, the quality of voice reception both in the spacecraft and at the ground stations was degraded by noise from cabin fans, glycol pumps, and suit compressors. When the crew had helmets off, the cabin noise was of sufficient amplitude to interfere with the normal communications and reduced transmitted and received voice intelligibility. See section 17 for further discussion.

During the extravehicular activity, the space suit communications system was used to transmit voice and portable life support system data. The voice and real-time telemetry data were good.

## 9.5 INSTRUMENTATION

## 9.5.1 Operational Instrumentation

The operational instrumentation system monitored 125 analog measurements and 111 bilevel events. The performance was satisfactory except as discussed in the following paragraphs.

a. The water quantity measuring device in ascent water tank 1 indicated a water usage rate approximately 35 percent greater than in tank 2. Data analysis indicates that the measuring device in tank 1 experienced a calibration shift prior to launch. Further discussion of this problem is contained in section 9.10.

b. The cabin display of supercritical helium pressure was intermittent; however, an independent telemetry measurement of this pressure was nominal at all times. Other measurements using the same display indicated that the meter was operating properly. The most likely cause of this discrepancy was a break in a 26-gage wire between the transducer and the meter.

c. At about 90 hours, the crew reported an abort guidance system warning light which was confirmed by telemetry. The caution and warning electronics assembly normally provides this warning if the critical operating parameters of the abort sensor assembly or abort electronics assembly are out of limits. Subsequent initialization and calibration of the abort guidance system approximately 2 hours later indicated satisfactory performance. An instrumentation anomaly is indicated because the limits of the critical operating parameters are sufficiently broad that performance degradation would have been detected had these limits been exceeded. For further details see section 17.

d. During the third firing of the descent propulsion system, a propellant low-level warning occurred (see section 9.8).

e. Operation of the measurement for the Lunar Module Pilot's suit disconnect valve in the environmental control system was intermittent during the second and third manning, (see section 17 for a detailed discussion of this problem.)

f. The reaction control system thrust chamber pressure switch on the B<sup>4</sup> up-firing engine exhibited intermittent operation and is discussed in section 9.7.

g. A number of temperature measurements, including the descent fuel and oxidizer tank temperatures, the ascent fuel and oxidizer temperatures, and the glycol temperature, indicated shifts of 2° to 5° F. The shifts

occurred when the developmental flight instrumentation system was turned on and off and at other times while this instrumentation system was operating. These fluctuations posed no operational problems during the mission. On subsequent flights, development flight instrumentation is not planned.

#### 9.5.2 Development Flight Instrumentation

The development flight instrumentation, composed of one PCM/FM and four FM/FM VHF telemetry systems, and two C-band radar systems, operated satisfactorily except for the measurement discrepancies discussed in the following paragraphs. The FM/FM system was energized for 3 minutes during the launch phase and for ten other periods during the mission, operating for a total of 10 hours.

The plus Y-axis booster strut strain measurement and the ascent oxidizer inlet measurement were both waived prior to flight but operated properly during the flight. The navigation base yaw-axis vibration measurement was intermittent during launch because of faulty vehicle wiring and failed to respond during orbital flight. The wiring at this measurement location was damaged during prelaunch checkout.

The ascent-oxidizer-tank Z-axis vibration measurement failed immediately prior to the ascent engine firing to depletion because of an open signal wire. The wiring to this measurement had been intermittent during altitude chamber testing, but subsequent trouble-shooting could not reproduce the malfunction.

The ascent engine fuel injector inlet pressure transducer failed prior to the ascent engine firing to depletion. The first recorded data of the measurement output were above 100 percent. This is indicative of a failure in the sensor strain element. The fact that the transducer was inoperative at initial data acquisition is indicative that one of the following conditions existed:

- a. The transducer became inoperative between lift-off and staging
- b. The transducer was rendered inoperative by excessive pressure during the first ascent engine firing.

This failure mode can be induced by overpressurization of the transducer. The pressure transducer has a nominal limit of 500 psia. However, satisfactory data were available prior to lift-off; therefore, it may be assumed that the transducer operated properly until engine ignition. The most probable cause of transducer failure can be attributed to pressurization transient during the first ascent engine firing. This is supported

by data from static firings which have produced transducer inlet pressures as high as 800 psia during a normal start. However, 800 psia is not indicative of the actual inlet manifold pressure during the start transient. A positive resolution to this problem cannot be determined because no ground station data are available from the firing. This transducer failure will not recur as the development flight instrumentation will not be installed on future spacecraft.

Five measurements operated improperly for short periods ranging from 3 to 20 minutes due to intermittent relay operations. The measurements are:

- a. Descent engine cavity temperature
- b. Minus Y axis descent engine strut 4 strain
- c. Descent helium primary and secondary upstream inlet pressure
- d. Descent engine oxidizer interface pressure.

The overall evaluation of the total 248 measurements indicates an average return of 98.7-percent of the data over the 10-hour period of system operation.

## 9.6 GUIDANCE AND CONTROL

Performance of the guidance and control systems was satisfactory throughout the mission. The interfaces between the primary guidance system and the abort guidance system and between the primary system and the radar systems were thoroughly exercised. The inertial measurement unit in the primary system was successfully aligned optically, and the abort guidance system was aligned several times based on angles transferred from the primary guidance system. The digital autopilot was used for control of the docked descent engine firing with satisfactory results. The digital autopilot and the abort guidance system were each used to control undocked descent engine firings. Capability for attitude control with the vehicles both docked and undocked was adequately demonstrated. The ability of the digital autopilot to control the ascent engine was demonstrated during the firing to depletion. The inertial components in the primary and the abort guidance systems exhibited excellent stability.

Detailed evaluations beyond the scope of those contained in this document will be published in supplemental reports, listed in appendix E.

### 9.6.1 Mission Related Performance

Power-up/initialization.- The lunar module guidance and control systems were powered-up for the first time on the third day, prior to the docked descent engine firing. The initial primary system power-up sequence required manual loading of a number of lunar module guidance computer erasable memory locations. The process was nominal except for an inadvertent error which required that the accelerometer bias compensations be reloaded. Procedural errors also caused difficulty in abort guidance system state vector and time initialization. Current state vectors are intercepted from the primary guidance system computer telemetry downlink by the abort guidance system upon execution of the proper primary system instructions. Computer downlink data are present only when the telemetry system is operating in the high-bit-rate mode. The first abort system updates were attempted with the telemetry system in the low-bit-rate mode and, therefore, failed. All initializations attempted in the high-bit-rate mode were successful.

The first attempts at abort guidance system time initialization were unsuccessful because the K factor, which establishes the bias between ground elapsed time and abort system absolute time, was not entered into the primary system computer. After insertion of the K factor, all time initializations were successful, with a maximum timing bias of 0.35 second.

The abort guidance system caution and warning light came on and remained on during the second power-up period. The cause was an instrumentation fault is discussed in section 17.

Attitude reference system alignments.- The primary and abort guidance systems were aligned several times with no difficulty. The initial primary system alignments while docked were performed based on a set of gimbal angles taken from the command and service module platform and corrected for structural offsets between the vehicles (X-axis only) measured both inflight and preflight. After undocking, the primary system was aligned optically three times with excellent results as shown by the star/angle difference checks contained in table 9.6-I. One of the optical alignments was performed in the docked configuration after the rendezvous. The results were comparable to the undocked alignments, although the crew indicated that the docked alignment was more difficult to perform.

The abort guidance system inertial reference was aligned many times by deriving direction cosines from gimbal angles obtained from the primary system platform. In all cases except one, the abort system was aligned within 0.02 deg/axis of the primary system. This is well within the specification value of 0.067 degree. In the excepted case, the abort system was offset 1 degree about the roll axis. The cause was a coarse

alignment being performed instead of a fine alignment. Subsequently, a fine alignment was made to the lunar module guidance computer with expected results.

Translation maneuvers.- The significant guidance and control parameters for each translation maneuver are summarized in table 9.6-II. Table 9.6-III contains velocity comparisons between the available onboard sources. Performance was always close to that predicted from preflight simulations.

Spacecraft dynamics during each maneuver for which data are available are shown in figures 9.6-1 through 9.6-3. The phasing maneuver is not included because of exceedingly noisy data. Figures 9.6-4 through 9.6-8 contain velocity-to-be-gained or velocity-sensed time histories. They were calculated by the primary and abort guidance systems for each available maneuver. Only the magnitude of the velocity-to-be-gained is shown for the abort system because this is the only value calculated that is contained in the telemetry downlink. Figure 9.6-4 also contains the command and service module guidance velocity-to-be-gained calculations.

The docked descent engine firing was performed by controlling the thrust vector of the gimballed engine with the gimbal drive actuators. The X-axis reaction control engines were inhibited to avoid plume impingement on the command module. The start transients were small, as shown in figure 9.6-1 and table 9.6-II, and the gimbal actuators responded as expected to throttle changes. Figure 9.6-9 shows the vehicle acceleration response to throttle position and the corresponding changes in time-to-go to cutoff. Fluctuations in Y- and Z-axis velocities to be gained (fig. 9.6-4) correlate with the small vehicle attitude changes during the early part of the maneuver. Figure 9.6-10 contains the command module rate data during the docked descent engine firing. The oscillations shown were caused by fuel slosh, and the magnitudes and frequencies were as predicted in preflight simulations. Similar responses were not visible in the lunar module data because of scaling. The maneuver demonstrated the feasibility of using the descent engine as a backup for the service propulsion engine when in a docked configuration.

The phasing maneuver was performed under the control of the control electronics section in the abort guidance system. Using the external velocity guidance mode, performance was nominal and backup control of the descent engine was adequately demonstrated.

The digital autopilot control of the descent engine insertion maneuver was also nominal, with small residuals and attitude excursions.

The only other rendezvous maneuver for which coverage was available was the coelliptic sequence initiation maneuver, shown in figure 9.6-7. This maneuver was performed after staging, using the four plus-X reaction control engines controlled by the digital autopilot. Response was normal, with an X-axis residual of 0.1 ft/sec.

The large velocity-to-be-gained remaining at the end of the ascent engine firing to depletion (fig. 9.6-8) is a result of the propellant depletion cutoff. The loss of acceleration was sensed by the velocity monitor routine in the computer. The routine activates when the velocity change accumulated in each of two consecutive 2-second periods is less than 10.1 ft/sec. The computer reacted properly, by recycling back to the 5-seconds-before-ignition point in the program sequence, and turned on the plus X translation after propellant depletion.

Attitude control.- The attitude control capability of the digital autopilot was exercised thoroughly in both the staged and unstaged configurations. Both the manual and automatic modes provided the necessary capability when used. Digital autopilot phase-plane plots are shown in figures 8.6-11 and 8.6-12 for attitude-hold periods in the unstaged and staged configurations, respectively. The attitude-control capability of the control electronics section in the abort guidance system was also exercised. Data are available for only a short period in the unstaged configuration, but performance was as expected.

#### 9.6.2 Primary Guidance, Navigation, and Control

Inertial measurement unit.- The preflight test history of the inertial components is summarized statistically in table 9.6-IV. All terms were stable except for the X-axis gyro drift, due to acceleration along the input axis. This term exhibited a 50 mERU shift in the last series of tests before prelaunch closeout. Because of uncertainties involved in measurements when in the launch configuration and because the term was insignificant for operational considerations, no change in the compensated value was made to account for the shift.

Figure 9.6-13 contains the accelerometer bias measurements made in-flight. All values were stable as shown.

Table 9.6-I contains the gyro drift measurements calculated from successive alignments. Again, excellent stability was demonstrated.

Platform voltage and accelerometer temperature measurements remained stable throughout the mission.

Alignment optical telescope.- The capability of the alignment optical telescope was thoroughly demonstrated. Ground tests had indicated that the telescope, with the conical sunshade attached, would provide visibility of plus-4 magnitude stars at sun angles as low as 65 degrees from the center of the field of view. The ability of the crew to distinguish the constellation Canus Major tends to confirm the ground test results. In one case, an alignment was performed at sunset using Sirius (minus-1.6 magnitude) and another star. At the time, Sirius was approximately 122 degrees from the sun.

Lunar module guidance computer.- The operation of the guidance computer was nominal. State vector updates were accomplished without incident using the update program (P27.) The programs used were:

P00 Lunar module guidance computer idling  
 P06 Primary guidance and navigation control system power down  
 P27 Lunar module guidance update  
 P30 External delta V targeting  
 P32 Concentric sequence initiation targeting  
 P33 Constant differential height targeting  
 P34 Terminal phase initiation targeting  
 P35 Terminal phase finalize targeting  
 P40 Descent engine firing program  
 P41 Reaction control firing program  
 P42 Ascent engine firing program  
 P47 Thrust monitor program

### 9.6.3 Abort Guidance System

Abort sensor assembly.- The preflight and inflight performance of the abort sensor assembly was nominal. A statistical summary of pre-installation calibration data, taken over a time period of 7 months, is shown in table 9.6-V. The compensation values selected for all terms except accelerometer scale factor correspond to the last pre-installation calibration results (within the quantization of the abort electronics assembly). The accelerometer scale factor data, which has a characteristic negative slope with time, were extrapolated to flight time using an exponential curve fit.

The results of the three inflight calibrations, as displayed to the crew, are shown in table 9.6-VI, and based on preflight calibration data, performance was as expected. The calibration data displayed to the crew are quantized to the nearest 380  $\mu\text{g}$  in earth scale flight programs (96  $\mu\text{g}$  in lunar scale flight program). However, a more precise bias calculation can be made by observing the accumulation of accelerometer velocity pulses in free fall. Two such calculations are shown in table 9.6-VI. These measurements indicate the stability experienced.

Inflight attitude reference drift values were estimated by comparing attitudes from the abort guidance system and from the primary guidance system during coasting flight. Estimates made in this manner are shown in the following table:

Channel	Relative drift, deg/hr	
	From 100:43:55 To 101:46:41	From 101:12:08 To 101:42:08
X	-0.21	-0.15
Y	-0.11	-0.16
Z	0.13	0.14

The abort sensor assembly performance during powered flight was within preflight predictions. A comparison of abort sensor assembly sensed velocities with primary guidance and navigation system sensed velocities during five maneuvers is shown in table 9.6-III. The differences in velocity values measured by the primary guidance and navigation system and the abort guidance system result from several error sources. These include misalignments (discussed in 9.6.1) as well as accelerometer, gyro, and timing biases; however, the differences were within the expected values.

Abort electronics assembly.- The abort electronics assembly flight program 3, the inflight calibration routines, and all input/output interfaces performed properly throughout the mission. Initialization, alignment, and calibration of the system were successfully completed. Guidance calculations, including the use of rendezvous radar updates, were successfully demonstrated.

Occasional premature changes of a prefiring display parameter caused a minor annoyance to the crew. The abort guidance system was targeted with external velocity components prior to each maneuver. The system is mechanized to maintain these velocity components fixed in relation to local vertical coordinate axes until initial thrust is sensed, then to "freeze" the components inertially and guide with respect to the "frozen" velocity vector. Initial thrust is sensed by the plus X accelerometer normally when plus X translation is commanded. Sensing of initial thrust is mechanized, under program control, by changing the contents of computer address 407 from 00000 to 10000. This address is identified as logic switch S07 and, prior to each firing, was displayed on the data entry and display assembly.

The S07 switch is set by the ullage counter, which, in the earth orbit scaling of flight program 3, was incremented by one velocity bit change. The switch was occasionally set before thrust initiation of this mission because of an uncompensated plus X accelerometer bias and quantization noise in the thrust acceleration computation. The characteristic was known before flight and the recommended monitoring and reset procedures were followed by the crew. The problem is not expected to occur with lunar scaled programs.

Data entry and display assembly.- Data entry and display assembly operation was normal except for frequent operator error light activations. More than one depression of the CLEAR pushbutton was often required before the light would remain extinguished. This problem is believed to be the result of a faulty pushbutton and is discussed in more detail in section 17.

#### 9.6.4 Control Electronics Section

The control electronics section was used to provide engine gimbal drive capability during the descent engine firings, to control the phasing maneuver, and also for a limited amount of attitude control. Performance during the maneuvers was satisfactory.

Null offsets of the flight director attitude indicator rate needles were reported by the crew. The offsets correlated with preflight test data and were within specification tolerances. The bias observed prior to the flight was 0.3 deg/sec. The specification tolerance is 1.0 deg/sec.

The crew also reported difficulty in establishing and maintaining a desired rate when using the rate-command capability. No data are available covering activities in this mode; however, the reported symptoms appear to be associated with the 20 deg/sec rotational hand controller scaling. A rate of 20 deg/sec is commanded when the hand controller is deflected 10 degrees. This scaling was chosen to provide proper handling characteristics near the lunar surface, not for precision control in earth orbit. The hardware responded as designed. Thus, the proportional rate-command mode would appear to be too sensitive for use in earth orbit.

TABLE 9.6-I.- PLATFORM ALIGNMENT SUMMARY

Time, hr:min	Program option*	Star used	Gyro torquing angle, deg			Star angle difference, deg	Gyro drift, mERU		
			X	Y	Z		X	Y	Z
91:05	Align to	command module gimbal angles	-0.370	-0.790	-0.310				
93:20	3	15 Sirius; 25 Acrux	+0.098	-0.076	+0.111	0.00	-3.8	-3.0	+4.3
95:02	3		+0.089	-0.055	+0.037	0.04	-3.5	-2.2	+1.4
99:46	3		+0.252	+0.008	+0.234	0.00	-3.5	0.0	+3.3

\*Option 3 - REFSMMAT.

TABLE 9.6-II.- GUIDANCE AND CONTROL MANEUVER SUMMARY

9-32

Condition	Maneuver and control mode <sup>a</sup>					
	First descent engine firing (docked)	Phasing (descent engine)	Insertion (descent engine)	Coelliptic sequence initiation (reaction control)	First midcourse correction (reaction control)	Ascent engine firing to depletion
	DAP-TVC	AGS-AUTO	DAP-TVC	DAP-RCS	DAP-RCS	DAP-TVC
Time						
Ignition, hr:min:sec	49:41:34.46	93:47:35.4	95:39:08.06	96:16:06.54	98:25:19.66	101:53:15.4
Cutoff, hr:min:sec	49:47:45.97	93:47:54.4	95:39:30.43	96:16:38.25	98:25:23.57	101:59:17.7
Duration, sec	371.51	19.0	22.37	31.71	3.91	362.3
Velocity, ft/sec <sup>b</sup>						
X planned/actual	+970.19/+967.75	66.09/66.38	-31.03/-31.64	-33.63/-32.75	-- /+2.5	+5252.55/+3813.39
Y planned/actual	-52.30/-52.06	50.62/51.51	-24.86/-25.52	-2.83/-4.08	-- /0.0	-4789.26/-3477.38
Z planned/actual	-1448.36/-1444.64	36.05/37.02	-16.63/-16.77	-21.47/-20.75	-- /0.0	-2154.52/-1576.52
Velocity residuals, ft/sec <sup>c</sup>						
X	+4.2	+0.1	0.0	+0.1	N/A	+2030.7
Y	+0.1	-0.1	-0.1	0.0	N/A	+0.5
Z	+0.1	-0.3	-0.2	0.0	N/A	+25.1
Engine gimbal position, deg						
Initial						
Pitch	+0.32	+1.38	-1.15	N/A	N/A	N/A
Roll	-1.26	-1.71	-1.18	N/A	N/A	N/A
Maximum excursion						
Pitch	+0.62	-0.76	+0.48	N/A	N/A	N/A
Roll	-0.38	+0.44	-0.30	N/A	N/A	N/A
Steady-state						
Pitch	0.00	+1.19	-1.15	N/A	N/A	N/A
Roll	-1.50	-1.23	-1.18	N/A	N/A	N/A
Cutoff						
Pitch	+0.11	+1.15	-1.23	N/A	N/A	N/A
Roll	-1.04	-1.18	-0.80	N/A	N/A	N/A
Rate excursion, deg/sec <sup>d</sup>						
Pitch	+0.4	+0.6	+1.2	+0.8	-0.8	-7.6
Roll	+0.4	+0.4	-1.8	+0.8	-0.8	-3.1
Yaw	+0.2	±0.4	Negligible	Negligible	-0.2	±0.6
Attitude error, deg <sup>d</sup>						
Pitch	+1.0	±0.2	Negligible	Negligible	Negligible	+1.9
Roll	+1.0	±0.2	-1.6	Negligible	Negligible	±0.5
Yaw	-0.8	±0.2	Negligible	Negligible	Negligible	+1.0

<sup>a</sup>DAP-TVC: digital autopilot thrust vector control; AGS-AUTO: abort guidance system automatic; RCS: reaction control.

<sup>b</sup>Earth Centered Inertial Coordinate System

<sup>c</sup>After trim

<sup>d</sup>Maximum

TABLE 9.6-III.- VELOCITY COMPARISONS

Maneuver	Axis	Sensed velocity change, ft/sec		
		Command module computer	Lunar module computer	Abort guidance system
First descent propulsion firing (docked)	X	-1738.5	+1736.6	+1739.2
	Y	+27.5	+10.6	+37.8
	Z	+37.4	+54.5	-11.2
Phasing	X	N/A	+90.0	+90.0
	Y		+1.2	+2.0
	Z		+0.9	+1.5
Insertion	X	N/A	+44.0	+43.0
	Y		0.0	-0.8
	Z		-0.8	+0.8
Coelliptic sequence initiation	X	N/A	+39.0	+39.0
	Y		+0.1	0.0
	Z		+1.5	+0.2
Second midcourse correction	X	N/A	+2.6	+2.5
	Y		0.0	0.0
	Z		0.0	0.0
Ascent propulsion firing to depletion	X	N/A	+5390.7	+5387.5
	Y		+37.7	+9.2
	Z		+126.1	+176.8

NOTE: 1. No data coverage for constant delta height maneuver, terminal phase initiation, and first midcourse correction.

2. All velocities are in spacecraft coordinates.

TABLE 9.6-IV.- INERTIAL COMPONENT PREFLIGHT HISTORY - LUNAR MODULE

Error	Sample mean	Standard deviation	No. of samples	Countdown value	Flight load
Accelerometers					
X - Scale factor error, ppm . . . . .	-932.166	44.418	6	-976	-968
Bias, cm/sec <sup>2</sup> . . . . .	0.299	0.0629	6	+0.32	+0.31
Y - Scale factor error, ppm . . . . .	-917.333	41.582	6	-965	-941
Bias, cm/sec <sup>2</sup> . . . . .	0.188	0.043	6	+0.21	+0.10
Z - Scale factor error, ppm . . . . .	-848.166	39.846	6	-878	-852
Bias, cm/sec <sup>2</sup> . . . . .	-0.040	0.031	6	-0.03	0.00
Gyroscopes					
X - Null bias drift, mERU . . . . .	3.742	0.700	4	3.0	+4.6
Acceleration drift, spin reference axis, mERU/g . . . . .	-2.775	0.655	4	-3.1	-0.5
Acceleration drift, input axis, mERU/g . . . . .	-23.950	29.536	6	-53.4	+5.4
Acceleration drift, output axis, mERU/g . . . . .	3.4250	0.2389	4	+3.1	N/A
Y - Null bias drift, mERU . . . . .	4.692	0.246	4	+4.6	+5.0
Acceleration drift, spin reference axis, mERU/g . . . . .	16.025	0.427	4	+15.9	+16.3
Acceleration drift, input axis, mERU/g . . . . .	2.399	2.307	5	+1.0	-0.3
Acceleration drift, output axis, mERU/g . . . . .	1.425	0.2801	4	+1.8	N/A
Z - Null bias drift, mERU . . . . .	6.882	0.786	4	+7.2	+4.5
Acceleration drift, spin reference axis, mERU/g . . . . .	-4.150	0.754	4	-5.0	-1.7
Acceleration drift, input axis, mERU/g . . . . .	21.175	3.735	4	+21.3	+19.6
Acceleration drift, output axis, mERU/g . . . . .	1.2825	0.3269	4	+0.8	N/A

TABLE 9.6-V.- SUMMARY OF ABORT GUIDANCE SECTION PREINSTALLATION CALIBRATION DATA

Accelerometer bias	Sample mean, $\mu\text{g}$	Standard deviation, $\mu\text{g}$	Sample size	Final calibration value, $\mu\text{g}$	Flight compensation value*, $\mu\text{g}$
X	89	37	15	124	95
Y	30	15	15	45	0
Z	169	28	15	185	190

Accelerometer scale factor	Time constant, days	Standard deviation, ppm	Sample size	Final calibration value, ppm	Flight compensation value**, ppm
X	77.6	26	10	-993	-1007
Y	93.5	25	10	-185	-206
Z	79.2	20	10	-1756	-1770

Gyro scale factor	Sample mean, ppm	Standard deviation, ppm	Sample size	Final calibration value, ppm	Flight load value, ppm
X	-2313	17	15	-2316	-2316
Y	-2441	17	15	-2440	-2440
Z	2006	19	15	2006	2005

Gyro fixed drift	Sample mean, deg/hr	Standard deviation, deg/hr	Sample size	Final calibration value, deg/hr	Flight load value, deg/hr
X	-0.28	0.031	15	-0.27	-0.269
Y	-0.47	0.014	15	-0.47	-0.471
Z	-0.05	0.141	15	-0.06	-0.056

Gyro spin axis mass unbalance	Sample mean, deg/hr/g	Standard deviation, deg/hr/g	Sample size	Final calibration value, deg/hr/g	Flight load value, deg/hr/g
X	0.82	0.119	15	0.96	0.960

\*Equivalent calibration values quantized to 95  $\mu\text{g}$ .

\*\*Extrapolated from final calibration to lift-off.

TABLE 9.6-VI.- INFLIGHT CALIBRATION MEASUREMENTS

Inflight calibration	Gyro bias, deg/hr			Accelerometer bias, $\mu\text{g}^*$		
	X	Y	Z	X	Y	Z
1	-0.21	-0.36	+0.20	0	0	+380
2	-0.07	-0.28	0.00	0	0	+380
3	-0.19	-0.13	+0.01	--	--	+380

\*Quantization for data entry and display assembly for Flight Program 3 is equivalent to 380  $\mu\text{g}$ . The expected maximum shift was 1 quantum or  $\pm 380 \mu\text{g}$ .

TABLE 9.6-VII.- COMPENSATED ACCELEROMETER BIAS

Time	Accelerometer bias, $\mu\text{g}$		
	X	Y	Z
After first inflight calibration*	22	-44	-44
After third inflight calibration**	29	-48	-48

\*Resolution of 22  $\mu\text{g}$  because of time span and velocity quantization.

\*\*Resolution of 9.7  $\mu\text{g}$  because of time span and velocity quantization.

NASA-S-69-2040

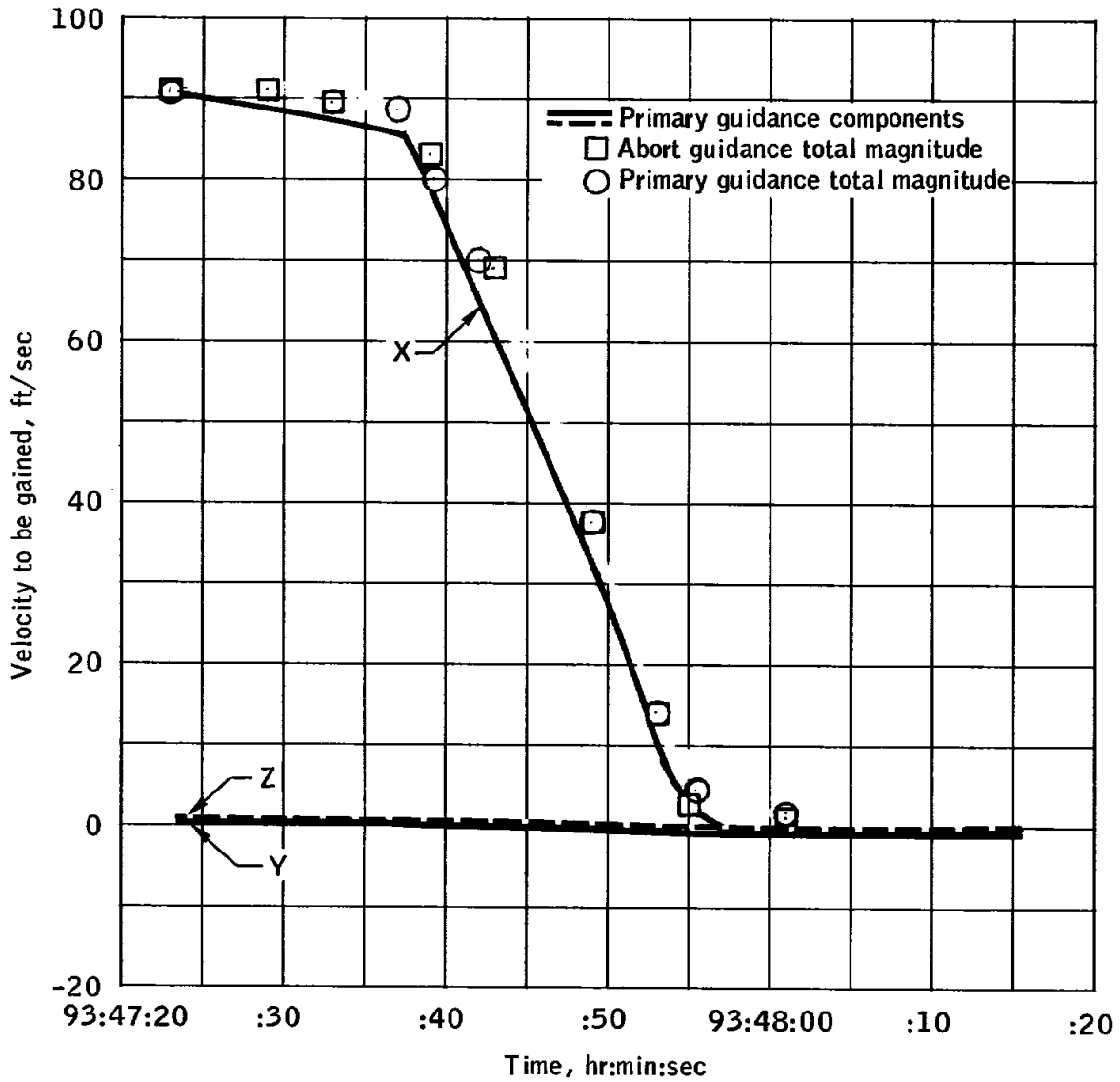


Figure 9.6-5.- Velocity to be gained during the phasing maneuver.

NASA-S-69-2041

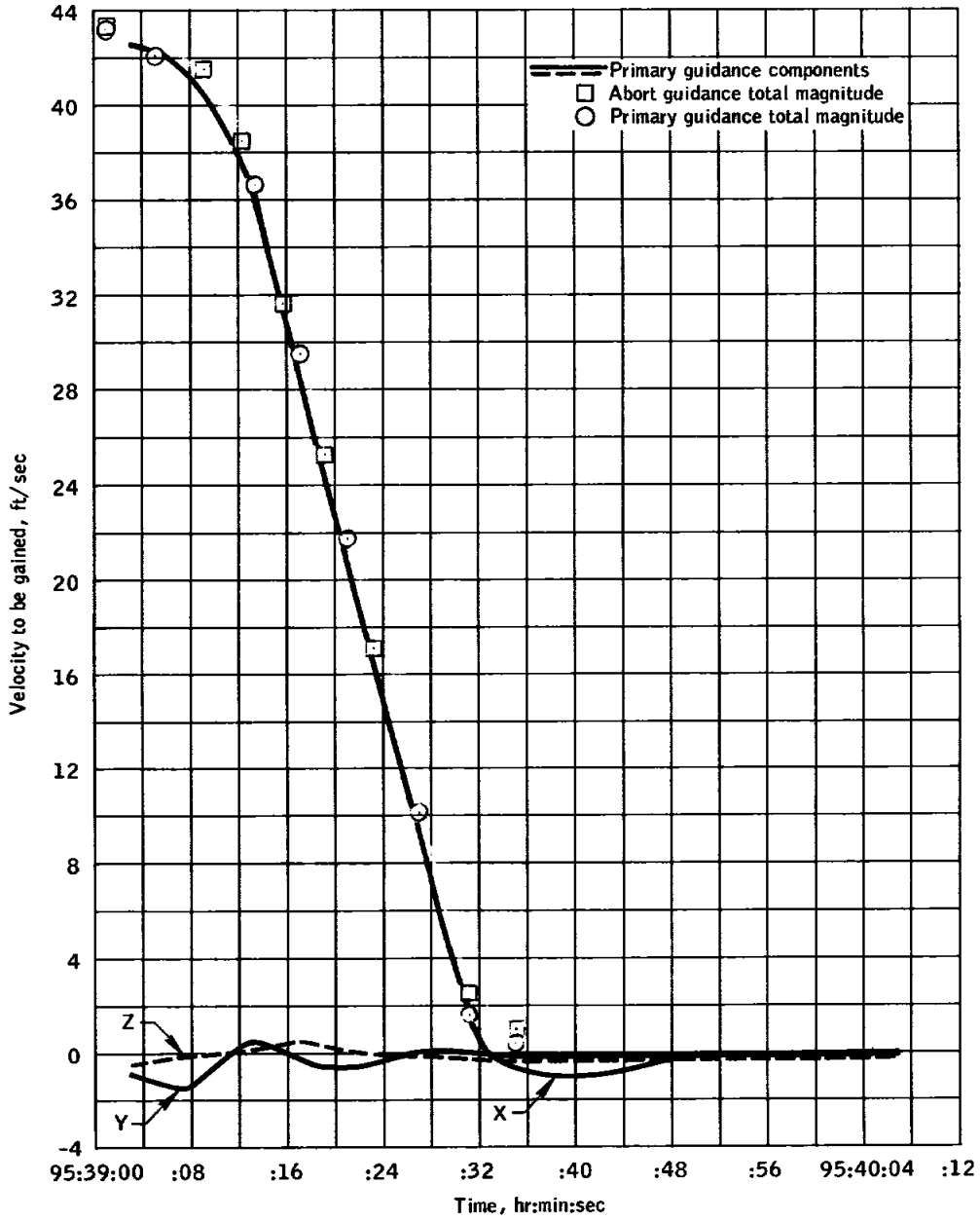


Figure 9.6-6.- Velocity-to-be-gained during insertion maneuver.

NASA-S-69-2042

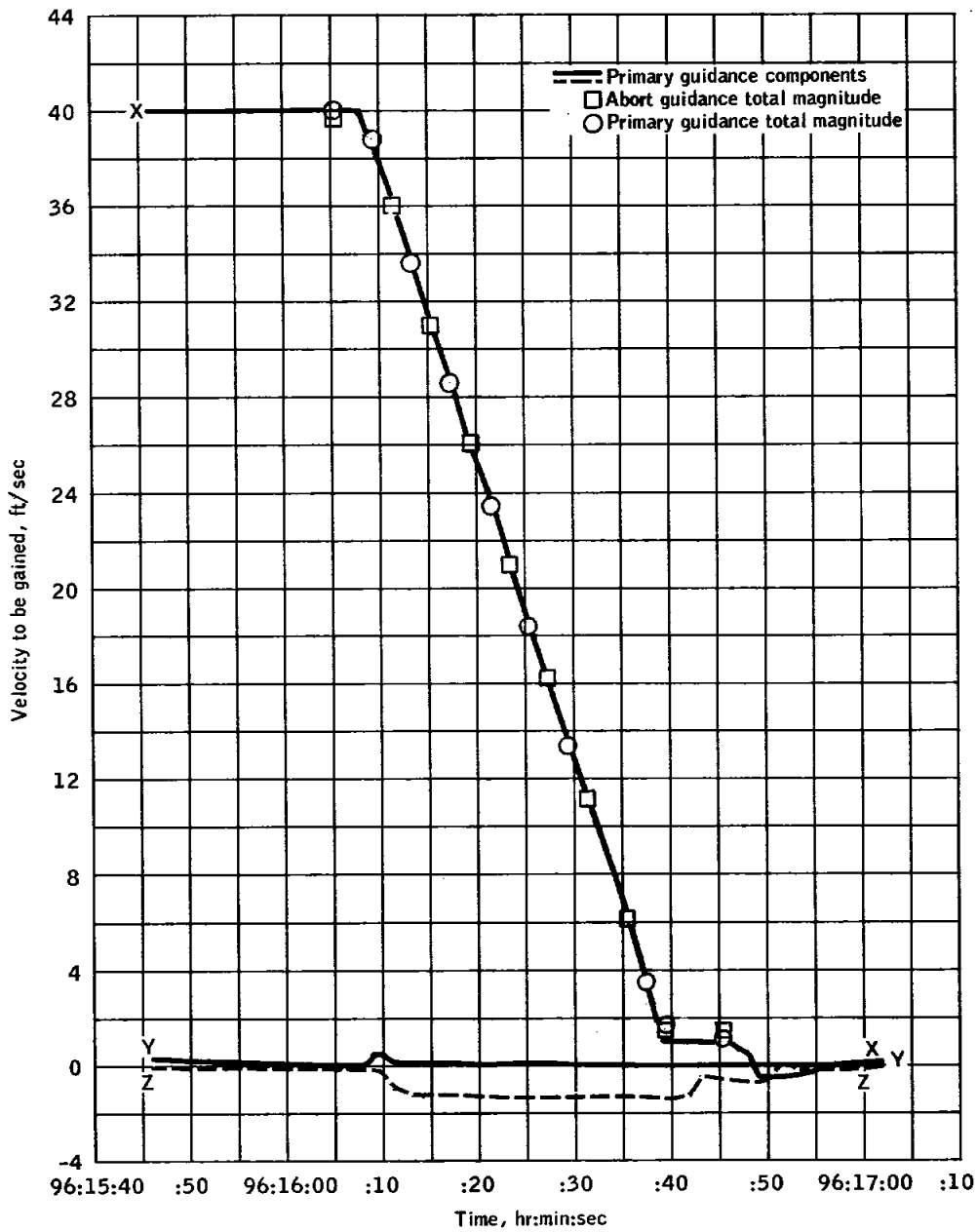


Figure 9.6-7.- Velocity to be gained during the coelliptic sequence initiation maneuver.

NASA-S-69-2043

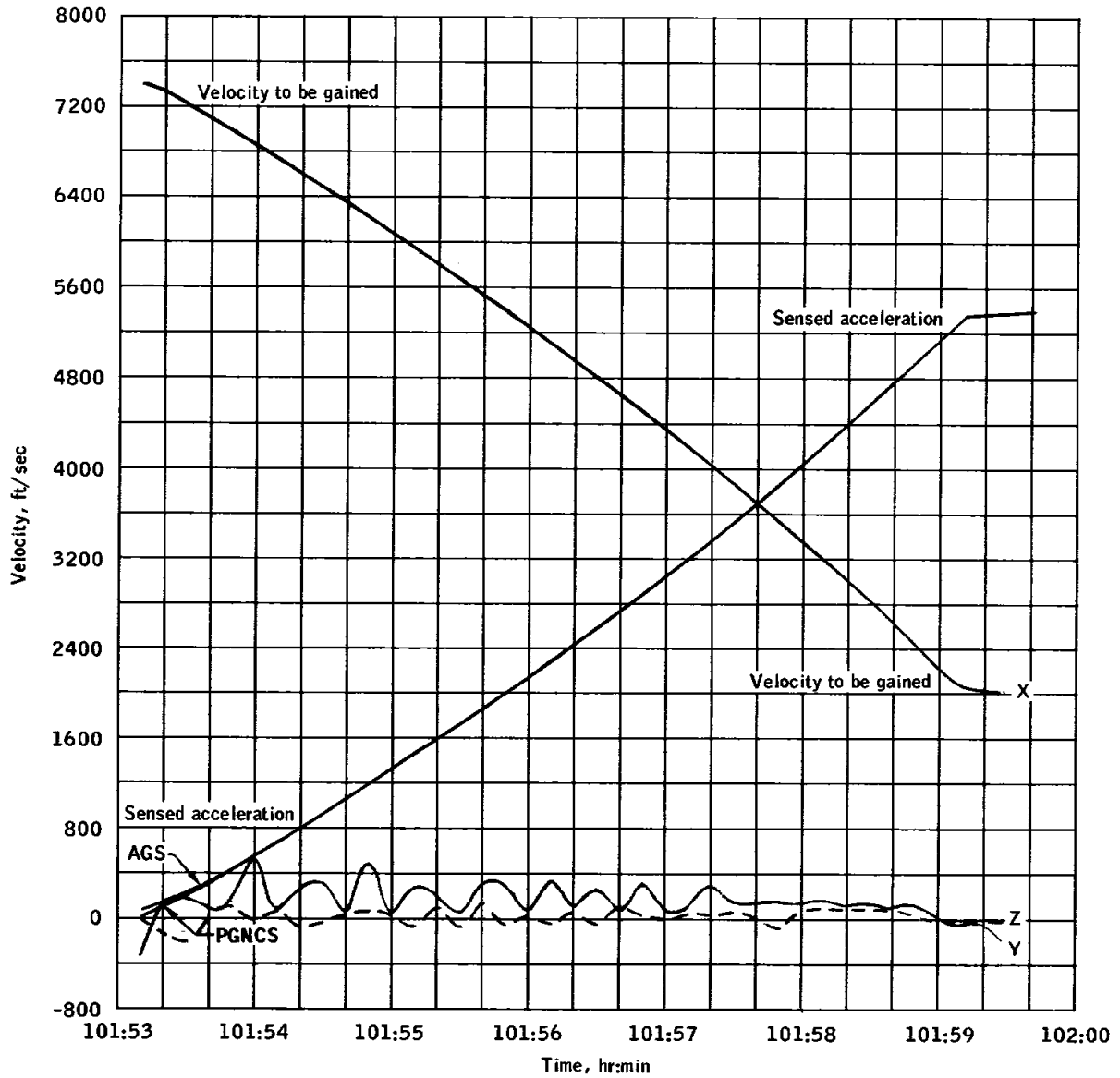


Figure 9.6-8.- Velocities during ascent engine firing to depletion.

NASA-S-69-2046

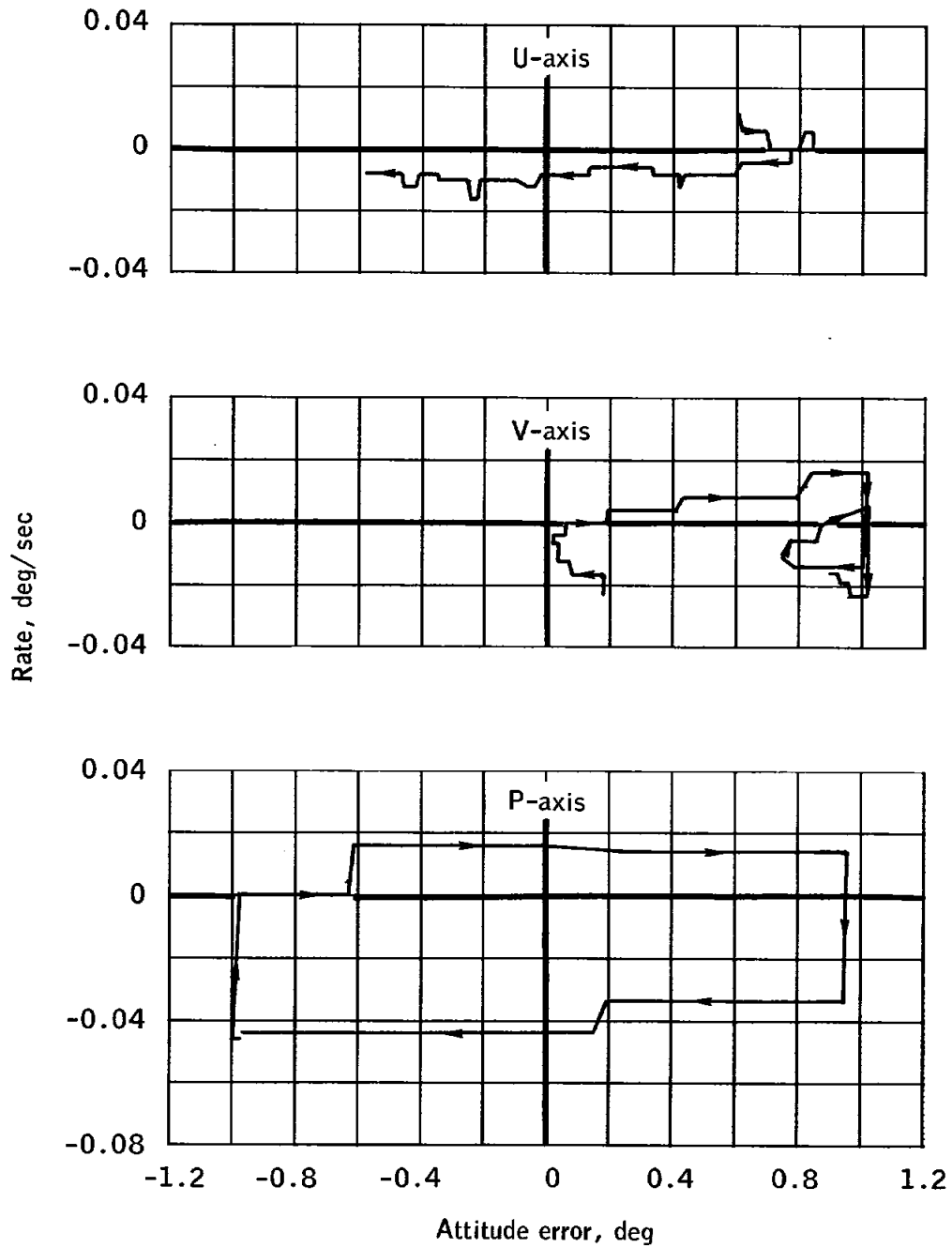
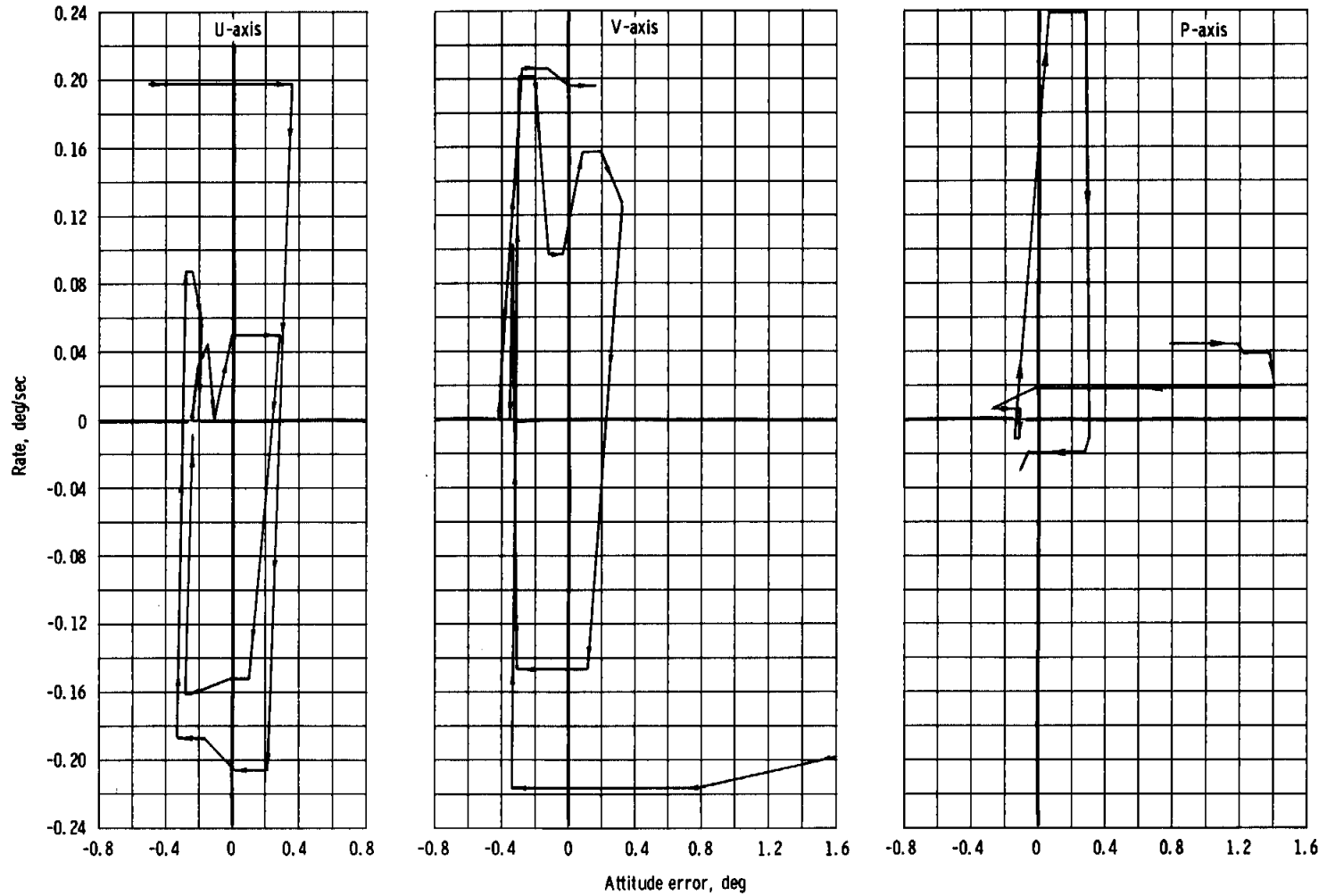


Figure 9.6-11.- Rates and attitude errors during 1-degree deadband attitude hold (unstaged vehicle).

NASA-S-69-2047



87-6

Figure 9.6-12. - Rates and attitude errors during narrow deadband attitude hold (staged vehicle).

NASA-S-69-2048

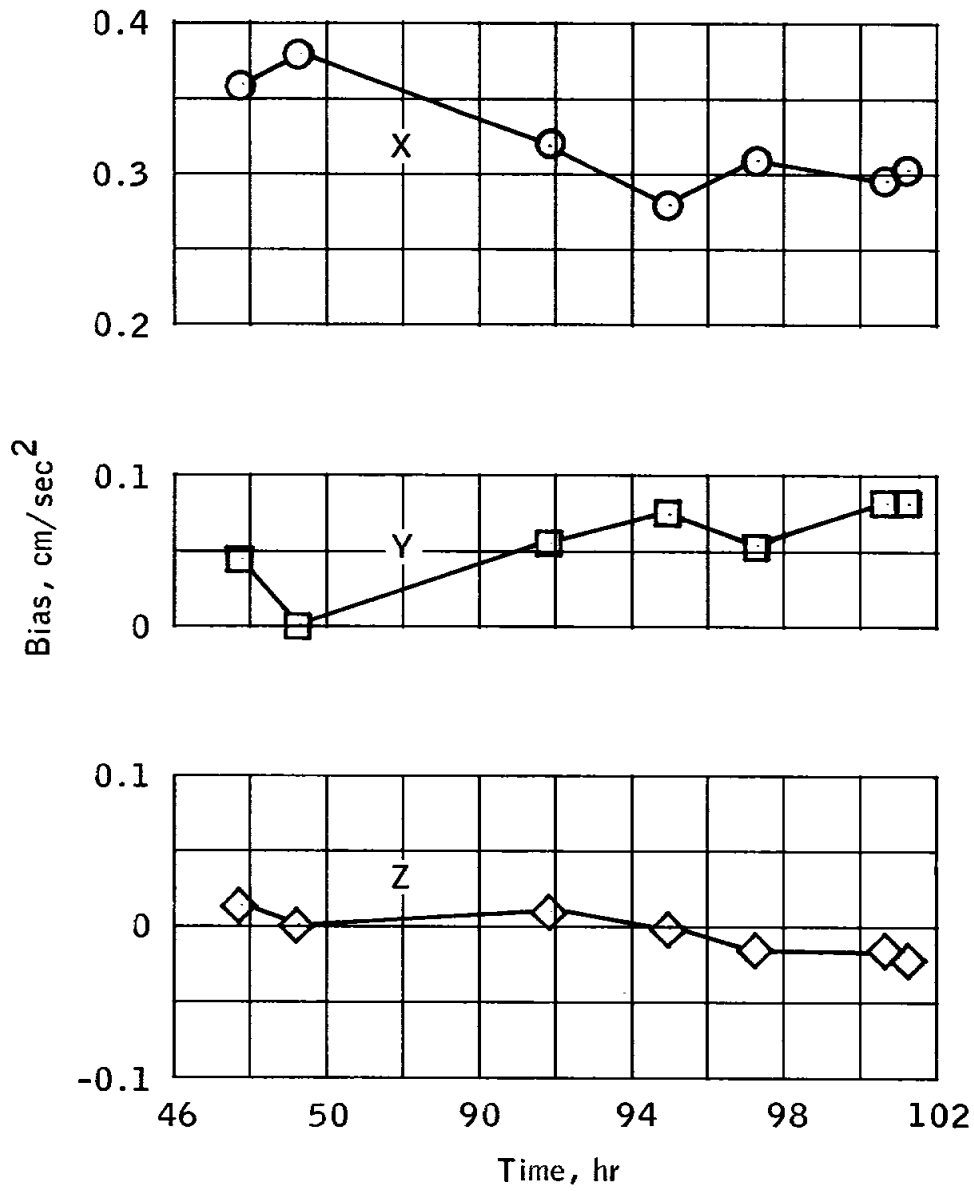


Figure 9.6-13.- Measured lunar module accelerometer bias measured during flight.

## 9.7 REACTION CONTROL SYSTEM

The performance of the reaction control system was nominal. The helium pressurization sections and the propellant feed sections operated properly. Accurate engine performance data were available for only the down-firing engines and only during the coelliptic sequence initiation maneuver and the ullage firing prior to the ascent engine firing to depletion. The calculated performance values are shown in table 9.7-I.

The thrust chamber pressure switches, with the exception of the one monitoring the quad 4 up-firing thruster, operated normally throughout the mission. The pressure switch for this engine failed closed during the first firing at about 48 hours and remained closed until about 98.5 hours when it began operating intermittently. Propellant consumption and vehicle rates indicate that the engine operation was nominal, thereby ruling out the possibility of a failed-on engine. The switch failure had no effect on the mission and the only potential problem was that the caution and warning system would have been unable to detect a failed-off condition for this engine.

Data indicate that the reaction control manifold pressure fluctuations were lower in magnitude and frequency (softer) during interconnect mode than during normal mode. In addition, system "B" manifold pressures (fig. 9.7-1) were softer during the ascent engine firing to depletion, than during the time period immediately preceding that event. During ascent engine firing to depletion, system A was in the normal mode. The cause of the softer operation could be explained by helium bubbles being flashed from the propellant solution because of manifold pressure drop during the ascent engine firing, by helium ingestion from the ascent propulsion system or by a higher saturation level of ascent propulsion propellants relative to reaction control propellants. Regardless of cause, the condition was not detrimental to reaction control system operation. Additional data concerning the performance of the lunar module reaction control system will be provided in a supplemental report.

### 9.7.1 Thermal Control

The thermal performance of the reaction control system was satisfactory, although the caution and warning system upper temperature limit of 190° F was exceeded on four occasions:

a. On quads 1 and 3 during the first descent engine firing at approximately 49 3/4 hours

b. On quad 4 after the coelliptic sequence initiation maneuver at approximately 96 1/2 hours

c. On all quads, just prior to or just after docking, at about 99 hours

d. On quads 1, 2, and 3, after the ascent engine firing to depletion at approximately 102 hours.

The caution and warning system upper temperature limit was selected so that a failed-on heater condition could be identified and was not intended to indicate high engine firing activity, which was the situation in each of the four cases. No problems resulted from the high temperatures. An example of a quad and engine component temperature profile during a period of high engine activity is shown in figure 9.7-2.

When the engine heaters were active, the quad temperatures ranged from 139° F (the lower caution and warning limit was 117° F) to above 209° F during periods of high engine activity. The maximum temperature was beyond the calibrated instrumentation range. When the engine heaters were not active, (for example, during the extravehicular activity period) quad temperatures ranged from 63° to 101° F, well above the freezing point of the propellants (18° to 21° F for the fuel and 12° F for the oxidizer). The quad temperatures during the mission are shown in figures 9.7-3 and 9.7-4. The reaction control fuel tank temperatures ranged from 66° to 70° F.

#### 9.7.2 Propellant Utilization

The actual and predicted reaction control propellant consumption profiles are compared in figure 9.7-5. The actual consumption was determined from the onboard propellant quantity measuring devices and a postflight ground-calculated pressure-volume-temperature analysis. Results of the analysis and the data from the measuring devices were in close agreement. Following periods of high thruster activity, the measuring devices showed a combined overshoot of about 6 pounds. Based on the pressure-volume-temperature analysis, the propellant consumption (fig. 9.7-5) through final docking, was approximately 280 pounds, or 30 percent less than the predicted 400 pounds. A more detailed discussion of propellant consumption during rendezvous is contained in section 5.2. Individual system propellant consumption profiles are shown in fig. 9.7-6. The maximum unbalance between the system A and B usage during rendezvous and docking was about 30 pounds and occurred after the third descent engine firing (insertion maneuver), with system B having the greater usage. After docking, the usage from system A and B had been 142 and 145 pounds, respectively. System A was used in the normal mode instead of the preplanned interconnect mode during the ascent engine firing to depletion, and the resulting propellant usage from system A was about 80 pounds.

Reaction control system propellant consumption was also calculated from thruster solenoid bilevel measurements for periods that data were available. The firing time from each solenoid was multiplied by the nominal flowrates (0.24 lb/sec of oxidizer and 0.12 lb/sec of fuel) to obtain total consumption for the period. The results compared favorably with those determined from the pressure-volume-temperature method.

### 9.7.3 System Pressurization

The reaction control system pressurization sequence was nominal. The regulators maintained acceptable outlet pressures, which varied between 178 to 184 psia.

Before reaction control system pressurization, a procedure was performed to verify that the secondary interconnect valves between the ascent propulsion system and reaction control system were closed. One of two system A panel monitors indicated an open for approximately 20 seconds instead of a normal momentary open indication. Bilevel flight data for this period indicate that the valve position indicator switches operated properly; therefore, one of the system A panel monitors was sticking. The sticky monitor persisted on subsequent secondary system A interconnect valve commands, but this had no effect on the mission.

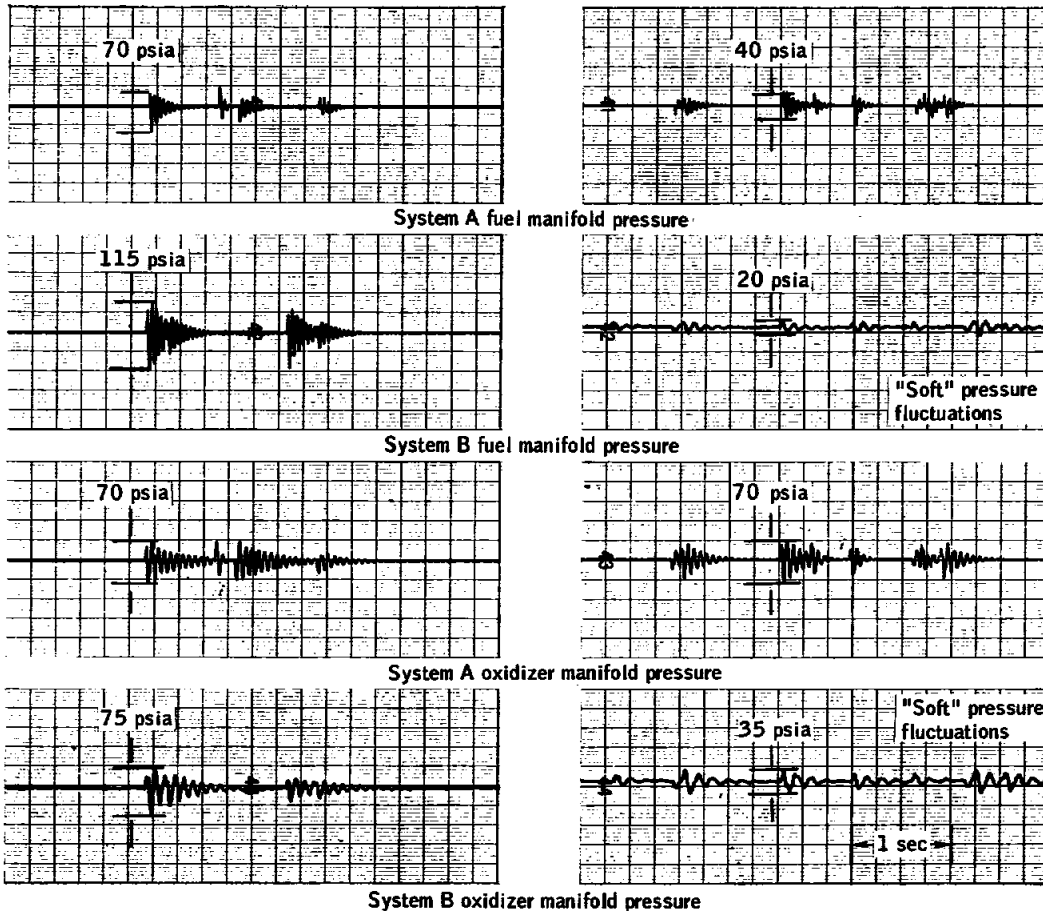
TABLE 9.7-I.- EFFECTIVE THRUST OF REACTION CONTROL ENGINES

Event	Engines	Duration, sec	Effective thrust, lb
+X translation prior to first descent engine firing	1, 3 down	9.6	79 to 96 <sup>a</sup>
+X translation prior to third descent engine firing	1, 3 down	8.5	66 to 98 <sup>a</sup>
Lunar module staging	1, 2, 3, 4 down	30.6	100.2 to 102.6
+X translation prior to final ascent engine firing (firing to depletion)	1, 3 down	34.1	103.9 to 105.2 <sup>b</sup>

<sup>a</sup>Uncertainty caused by data resolution associated with short firing and low bit rate data. Normal effective thrust for unstaged vehicle is 92 pounds, reduced from nominal 100 pounds because of plume impingement on descent stage.

<sup>b</sup>Slight increase in thrust, with firing in interconnect mode, resulted from slightly higher manifold pressure (186 psia as compared with 180 psia nominal).

NASA-S-69-2049



(a) System A and B in normal mode (98:55:20)

(b) System A in normal mode, B in interconnect mode during ascent propulsion firing to depletion (101:58:40)

Figure 9.7-1.- Manifold pressures for normal-mode operation and during ascent propulsion firing to depletion.

NASA-S-69-2050

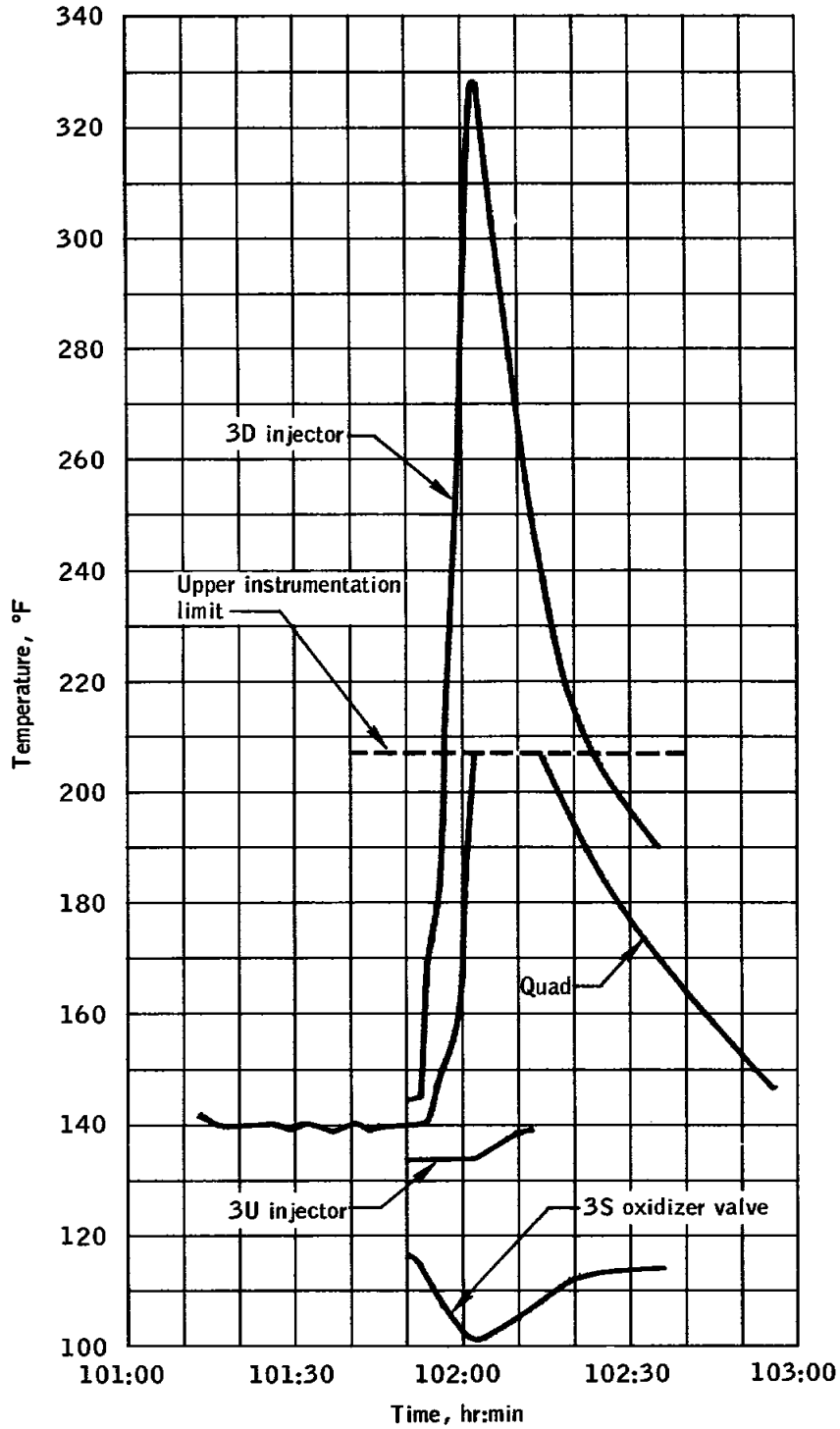


Figure 9.7-2.- Reaction control system quad 3 temperature profile during ascent engine firing to depletion.

Events	
1. Reaction control system pressurization	7. Insertion maneuver (descent engine)
2. First reaction control system hot-firing	8. Staging maneuver
3. First descent engine firing	9. Constant delta height maneuver (ascent engine)
4. Second reaction control system hot-firing	10. Terminal phase initiation
5. Undocking	11. Docking
6. Phasing maneuver (descent engine)	12. Undocking
	13. Ascent engine firing to depletion

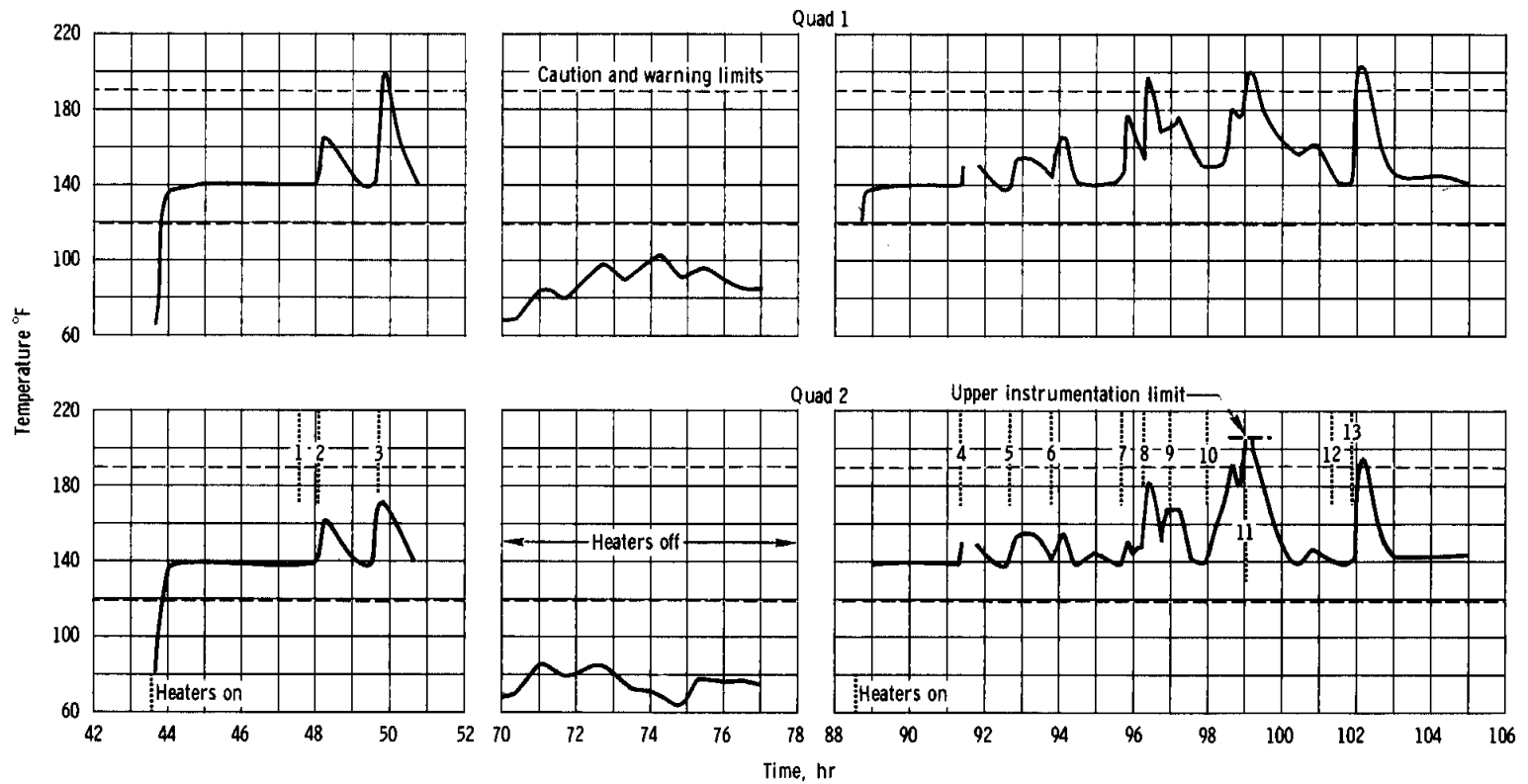


Figure 9.7-3. - Reaction control quad 1 and 2 temperature history.

Events	
1. Reaction control system pressurization	7. Insertion maneuver (descent engine)
2. First reaction control system hot-firing	8. Staging maneuver
3. First descent engine firing	9. Constant delta height maneuver (ascent engine)
4. Second reaction control system hot-firing	10. Terminal phase initiation
5. Undocking	11. Docking
6. Phasing maneuver (descent engine)	12. Undocking
	13. Ascent engine firing to depletion

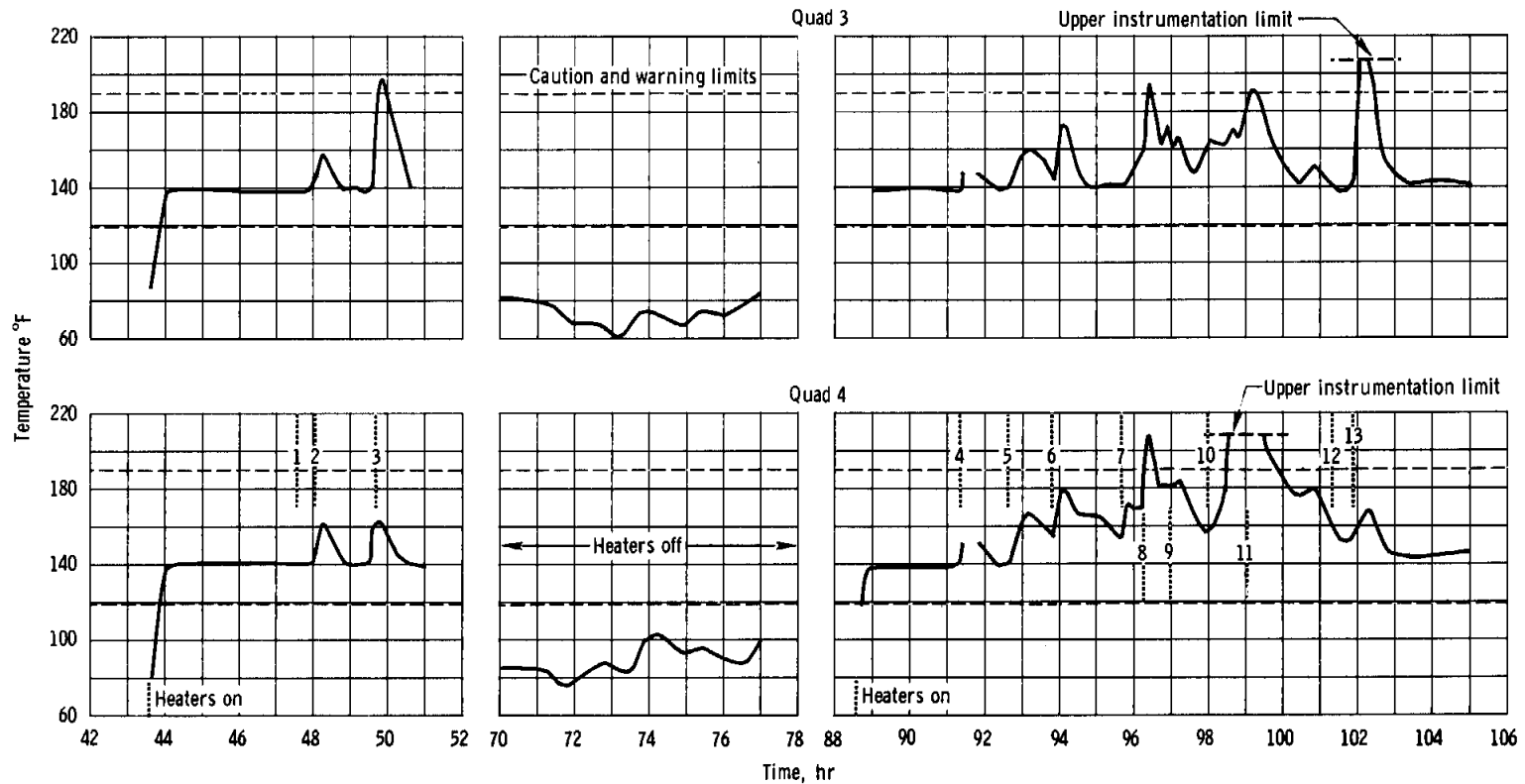


Figure 9.7-4. - Reaction control system quad 3 and 4 temperature history.

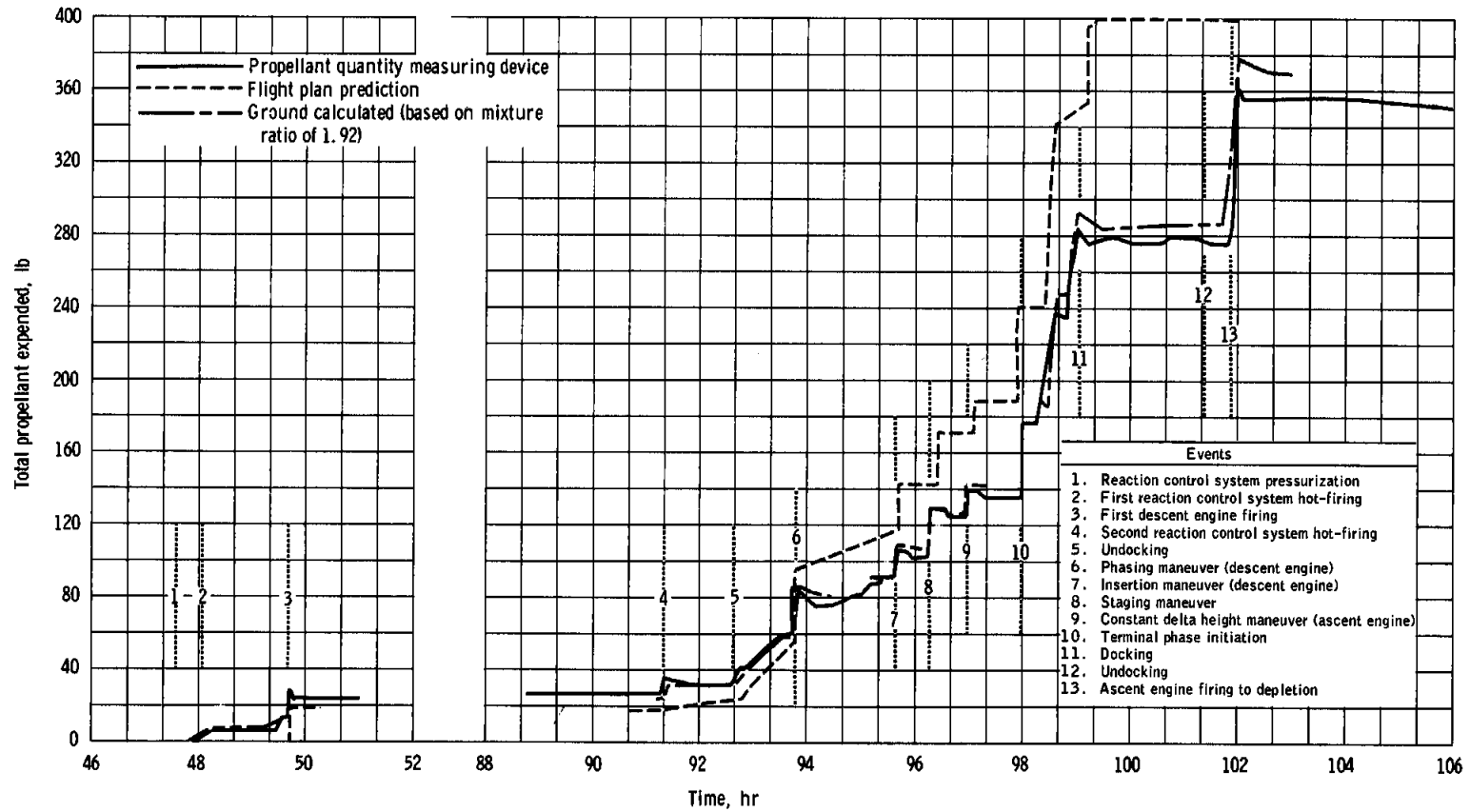


Figure 9.7-5. - Comparison of predicted and actual propellant consumption.

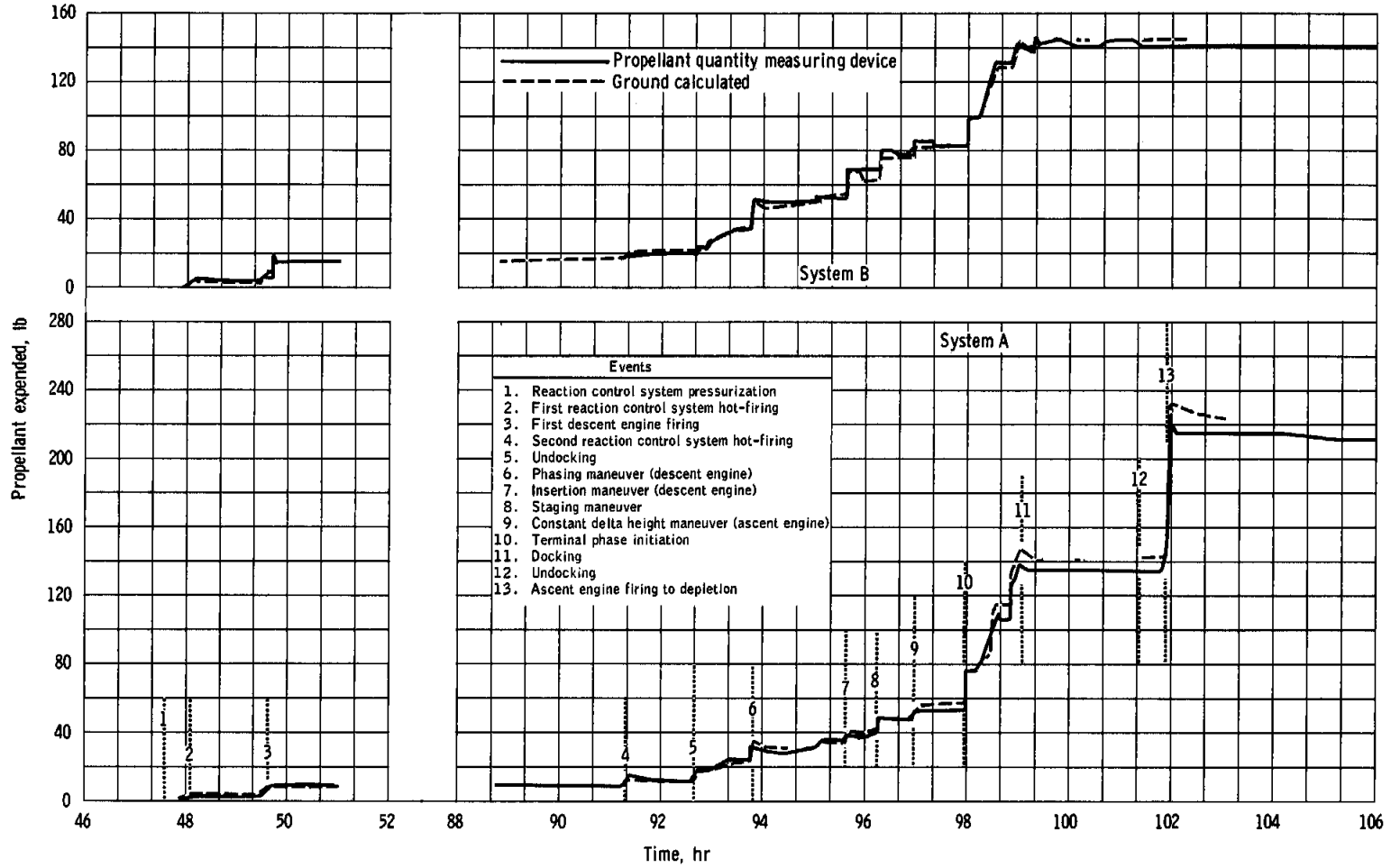


Figure 9.7-6. - Propellant usage from system A and B.

## 9.8 DESCENT PROPULSION

The descent propulsion system operated as expected, except for the following:

a. The helium regulator outlet pressure and the engine interface pressures exhibited an unexpected decay during the initial portion of the first descent engine firing.

b. An average pressure decay of 2.9 psi/hr in the supercritical helium tank was indicated between the first and second firings; during coast periods, the pressure should rise due to heat leak into the tank.

c. The crew experienced a rough engine condition while throttling from the 10- to the 37-percent setting during the second firing.

### 9.8.1 Inflight Performance

Evaluation of the steady-state performance of the descent engine at the fixed throttle position was based on a 245-second segment of the data obtained after the helium regulator outlet pressure had stabilized at 244 psia for the first firing. A comparison of the inflight predicted, measured, and calculated values are shown in table 9.8-I. The calculated values were obtained from the simulation that best matched the acceleration data from the lunar module guidance computer. Due to the possibility of a significant uncertainty in the spacecraft weight prior to the first descent engine firing, the reported values contain a degree of uncertainty. The differences between predicted and the measured and calculated performance values appears to be primarily due to the measured regulator outlet pressure of 243 psia, which was 4 psia lower than expected. Low measured interface pressures tend to substantiate the reduced regulator-outlet pressure. The predictions were based on pre-installation test regulator data. The measured chamber pressure (fig. 9.8-1) was compared with the engine acceptance test and the calculated values. The results indicate that the flight transducer may have incurred a zero shift due to thermal effects. This effect has been seen in ground tests, but to a lesser degree. The flight performance adjusted to the standard inlet conditions for full throttle position, yields a thrust of 9746 pounds, a specific impulse of 302.8 seconds, and a propellant mixture ratio of 1.59. These results compare favorably with the ground test data of 9736 pounds of thrust, 303.0 seconds of specific impulse, and a mixture ratio of 1.596.

Engine roughness was reported by the crew when the engine was throttled from the 10 to the 37 percent setting during the second descent engine system firing. The onset of roughness occurred as the throttle setting reached approximately 27 percent, at which time the setting was held

constant until the roughness ceased. This roughness is typical of that experienced with helium ingestion into the combustion chamber. The roughness lasted approximately 2.5 seconds, (see figure 9.8-2) and the remaining portion of the second firing and all of the third firing appeared nominal. See section 17 for further discussion.

### 9.8.2 System Pressurization

During the period from lift-off to first descent engine ignition, the oxidizer and fuel interface pressures decayed from approximately 144 to 107 psia and from 162 to 145 psia, respectively. This phenomenon, which was also observed during the Apollo 5 countdown and flight and during ground tests, has been attributed to helium absorption in the propellants.

Just prior to the first descent engine firing, the ambient start bottle was activated, increasing the pressures to 234 and 235 psia in the oxidizer and fuel tanks, respectively.

During the first lunar module manning, the helium system pressure was about 743 psia. During the first 33 seconds after engine ignition, the helium bottle pressure decreased to approximately 711 psia (see figure 9.8-3). At the same time, a decrease from 235 to 188 psia in the regulator-outlet manifold pressure was observed. If the system had operated correctly, sufficient helium would have passed through the regulator to maintain a constant regulator-outlet manifold pressure of about 247 psia and the heat transfer through the internal heat exchanger should have increased the pressure in the supercritical helium bottle. The data indicate that the internal heat exchanger was plugged during the initial portion of the firing. See section 17 for further discussion.

During the coast period following the first descent engine firing, the helium system pressures decreased at a rate of approximately 2.9 psi/hr. Normally, due to the absorption of heat from the engine and surrounding environment, the helium bottle pressure should continuously rise during engine shut-down periods. The pressure decrease following the first descent engine firing indicated a leak in the system. See section 17 for further discussion.

### 9.8.3 Propellant Quantity and Gaging System

Table 9.8-II presents measured data and the computed values at several points during the first firing; all measured values were within 1 percent of the calculated values. At ignition for the second and third firings, the gaging system, which uses capacitive measuring devices, was displaying erroneous quantities. This phenomenon was also noted in the

service propulsion system gaging system which also used capacitive measuring devices. In general, the displayed quantities were greater than the actual tank quantities (see figure 9.8-4). As the firings continued, the gages tended to stabilize toward correct values. The firing time for the last two maneuvers was too short for the gaging system to completely stabilize.

The data indicate that either the plus-X translation prior to ignition was not sufficient to settle the propellants or the relatively low g conditions existing during the firing caused the propellants to cling to the gaging probe and create an erroneous output.

The low-level point sensor was uncovered at the beginning of the third firing. This apparently was caused by the large ullage volume and by the inadequately settled propellants that allowed a gas bubble to pass by the point sensor after engine ignition.

Additional information concerning descent propulsion will be provided in a supplemental report.

TABLE 9.8-I.- STEADY-STATE PERFORMANCE DURING DOCKED DESCENT ENGINE FIRING

Parameter	55 seconds after ignition		300 seconds after ignition	
	Predicted	Measured	Predicted	Measured
Regulator outlet pressure, psia . . . .	247	243	247	243
Oxidizer bulk temperature °F . . . . .	66	69	66	69
Fuel bulk temperature °F . . . . .	66	69	66	69
Oxidizer interface pressure, psia . . .	225	222	225	222
Fuel interface pressure, psia . . . . .	226	223	226	223
Engine chamber pressure, psia . . . . .	106	107	102	105
Propellant mixture ratio . . . . .	1.58	1.58*	1.58	1.58*
Vacuum thrust, lb . . . . .	9847	9801*	9950	9861*
Vacuum specific impulse, sec . . . . .	303.3	302.7*	302.2	302.2*
Oxidizer flow rate, lb/sec . . . . .	19.9	19.8*	20.2	20.0*
Fuel flow rate, lb/sec . . . . .	12.6	12.5*	12.8	12.6*

\*Calculated from measured flight data.

TABLE 9.8-II.- DESCENT PROPULSION GAGING SYSTEM PERFORMANCE

Parameter	Time, hr:min:sec				
	49:42:50	49:43:50	49:44:50	49:45:50	49:46:50
Oxidizer tank 1					
Measured quantity, percent . . . .	90.7	79.8	69.1	58.1	47.3
Calculated quantity, percent . . . .	89.8	79.4	69.0	58.5	48.0
Difference, percent . . . . .	+0.9	+0.4	+0.1	-0.4	-0.7
Oxidizer tank 2					
Measured quantity, percent . . . .	91.7	81.6	71.5	60.9	50.2
Calculated quantity, percent . . . .	92.0	81.5	71.1	60.6	50.1
Difference, percent . . . . .	-0.3	+0.1	+0.4	+0.3	+0.1
Fuel tank 1					
Measured quantity, percent . . . .	91.5	80.5	69.8	59.0	48.0
Calculated quantity, percent . . . .	90.8	80.2	69.7	59.1	48.4
Difference, percent . . . . .	+0.7	+0.3	+0.1	-0.1	-0.4
Fuel tank 2					
Measured quantity, percent . . . .	90.5	79.9	69.7	59.2	48.5
Calculated quantity, percent . . . .	90.6	80.0	69.5	58.9	48.3
Difference, percent . . . . .	-0.1	-0.1	+0.2	+0.3	+0.2

NASA-S-69-2055

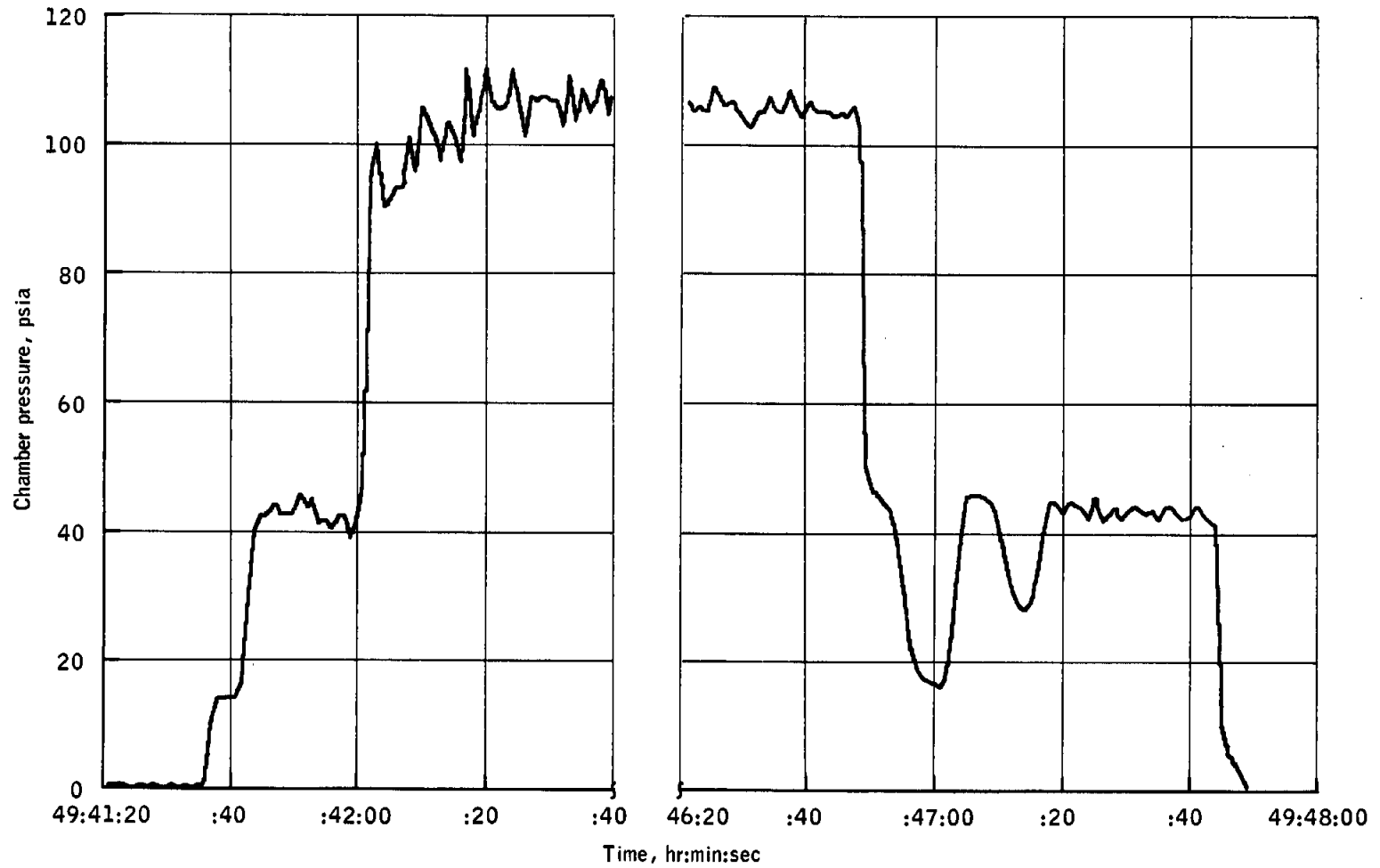


Figure 9.8-1.- Chamber pressure during docked descent engine firing.

NASA-S-69-2056

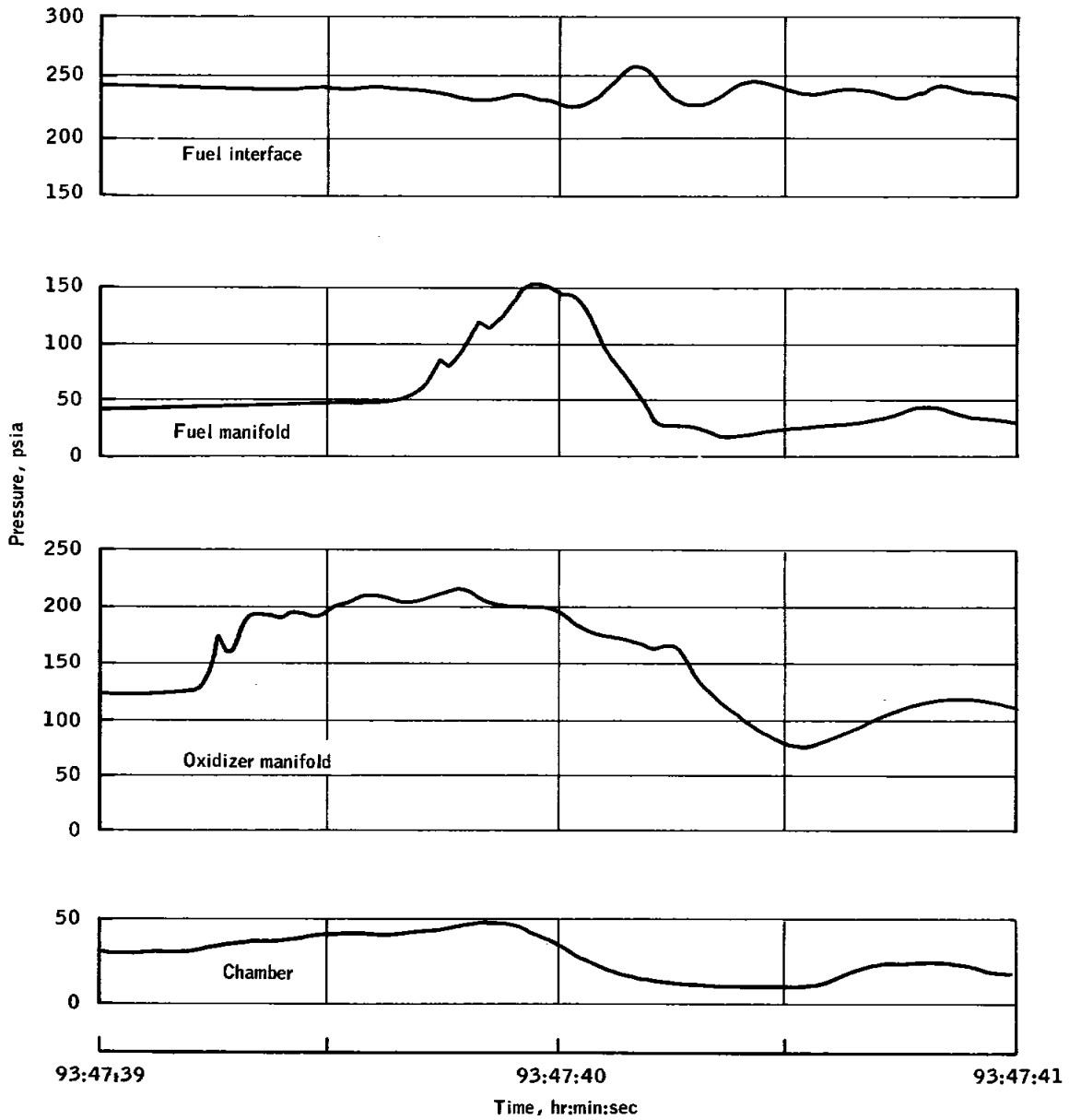


Figure 9.8-2.- Descent propulsion system pressures during second firing (phasing maneuver).

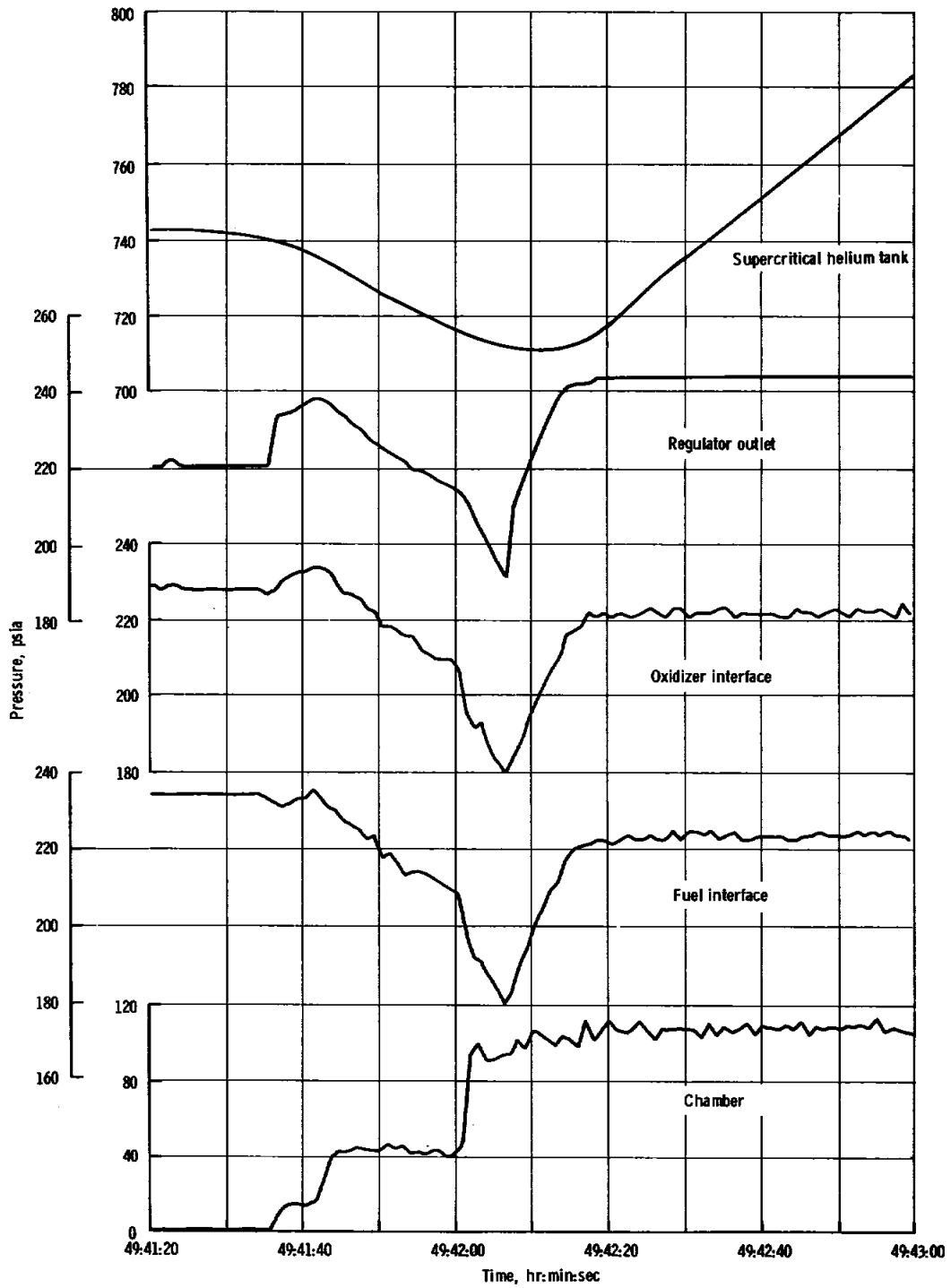


Figure 9.8-3. - Descent propulsion system pressures during start of first firing.

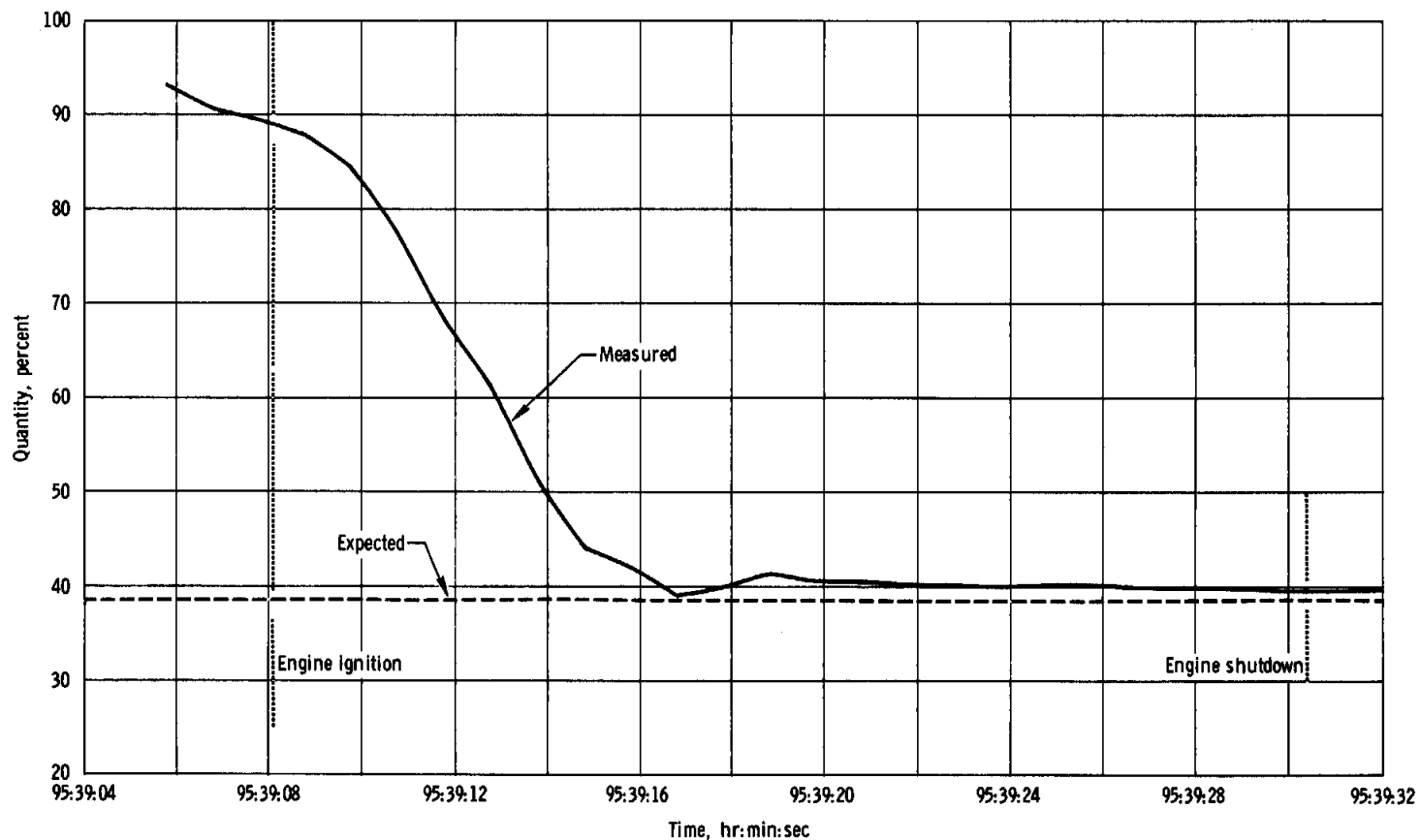


Figure 9.8-4. - Typical descent propulsion quantity gaging system operation (oxidizer tank 1).

## 9.9 ASCENT PROPULSION

The ascent propulsion system was used for two firings, a 3-second firing while the ascent stage was manned and an unmanned firing to propellant depletion. The lunar module was out of ground-tracking-station range during the first ascent engine firing; therefore, no data are available. However, when data were first acquired after the firing, system pressures and temperatures were normal. The second ascent engine firing was initiated successfully and lasted for 362.3 seconds. During the second firing, system pressures were lower than expected, thus indicating a malfunction in the class I leg of the helium regulator package. Pressure data indicate that during the firing, the helium flow rate was controlled by the class II primary helium regulator. This is an established redundant mode, and the lower operating pressures produced no undesirable effects in the system. The second ascent engine firing was terminated by the planned oxidizer depletion. The oxidizer tank low-level sensor uncovered approximately 5 seconds prior to chamber pressure decay. The engine was commanded off at about 10 seconds later. The depletion shutdown appeared nominal in all respects.

### 9.9.1 Helium Utilization

The helium storage tanks were loaded to a nominal value of 13.1 pounds. The helium tank temperatures and pressures recorded at 175 hours prior to launch were 70° F and 3020 psia for tank 1 and 70° F and 2988 psia for tank 2. The calculated helium usage during the firings agree with predicted usage.

### 9.9.2 Regulator Performance

During the initial 290 seconds of the ascent engine firing to depletion, the measured regulator outlet pressure was 176 psia as compared with the expected 184 psia. At that time, the regulator outlet pressure increased to 179 psia. A discussion of this anomaly is contained in section 17.

### 9.9.3 Feed System

Table 9.9-I presents the ascent propulsion system propellant usage prior to the firing to depletion, both by the ascent propulsion system and by the reaction control system through the interconnect. The propellant remaining at ignition for the firing to depletion is estimated to have been 1595 pounds of fuel and 2464 pounds of oxidizer.

The fuel and oxidizer interface pressures at launch were 172 and 158 psia. At approximately 43-1/2 hours, the pressures had decayed to 167 and 148 psia, respectively. The pressure drop is attributed to the absorption of helium by the propellant. The pressure predicted for maximum helium solubility was 169 and 148 psia for fuel and oxidizer, respectively.

During the ascent engine firing to depletion, reaction control system B propellants were supplied from the ascent propulsion system. The propellant usage by the reaction control system during this firing, as calculated from engine-on time, was 43.5 pounds of fuel and 21.8 pounds of oxidizer.

#### 9.9.4 Engine Performance

Table 9.9-II presents the results of an analysis of the start and shutdown transients made to determine the transient total impulse and to characterize the engine when operating in an oxidizer depletion shutdown mode.

In general, all applicable transient specification requirements were satisfied, and the flight data compared favorably with ground test data. Representative traces of the shutdown transients are presented in figure 9.9-1.

The transient characteristics that the engine demonstrated during an oxidizer depletion shutdown mode are shown in figure 9.9-2. This figure provides a comparison of flight data with ground test data. The data indicate that the characteristics of the oxidizer depletion during flight compared favorably with the ground test.

Table 9.9-III compares the actual and predicted ascent propulsion system performance during the firing to depletion. The measured flight data compared closely with the predicted values for the actual regulator pressure conditions. Figure 9.9-2 is a time history of the chamber pressure during the firing to depletion.

The oxidizer tank low-level sensor was uncovered at 347 seconds.

Ground test data indicated that the oxidizer low-level sensor would uncover with approximately 7 seconds of firing time remaining. Flight data indicates that the low-level sensor did activate approximately 6 seconds prior to oxidizer depletion. Calculations indicate that there was

approximately 90 pounds of fuel remaining at the time the oxidizer low-level sensor was uncovered, compared with a predicted value of 105 pounds. Using this information, the average propellant mixture ratio was calculated to be  $1.6 \pm 0.02$ .

A supplemental report will be issued to provide detailed evaluation data on the ascent propulsion system.

TABLE 9.9-I.- PROPELLANT USAGE FROM ASCENT PROPULSION SYSTEM

Event	Time, hr:min:sec	Used		Remaining	
		Oxidizer	Fuel	Oxidizer	Fuel
Launch	0:00:00	--	--	2524	1626
Coelliptic sequence initiate maneuver (reaction control usage through interconnect) - estimated; no data available	96:16:03	20	10	2504	1616
Constant delta height maneuver (first ascent engine firing) - usage estimated; no data available	96:58:14	23	13	2481	1603
Ullage-settling plus X translation with reaction control system through interconnect	101:52:42	17	8	2464	1595
Ignition for ascent propulsion firing to depletion	101:53:15	--	--	2464	1595

TABLE 9.9-II.- ASCENT ENGINE TRANSIENT ANALYSIS

Parameter	LM-3 ascent engine firings						White Sands test results	Class nominal values	Specification values
	Second inflight firing	Engine acceptance tests							
		First	Second	Third	Fourth	Average			
Time from ignition signal to initial thrust rise, sec . . . . .	0.146	0.280	0.270	0.275	0.200	0.256	0.145		
Time from ignition signal to 90 percent of steady-state thrust, sec . . . . .	0.221	0.320	0.296	0.307	0.264	0.297	0.256	0.265 - 0.351	<sup>a,b</sup> 0.360 max.
Time from indicated beginning of valve opening to full open, sec . . . . .	0.090	0.116	0.115	0.115	0.090	0.109	0.128		
Maximum value of chamber pressure overshoot during start, psia . . . . .	178								<sup>a</sup> 178 max.
Start transient total impulse from ignition signal to 90 percent steady-state thrust, lb-sec . . . . .	≈25	61.4	56.0	51.1	56.1	56.2	≈35.4	35 - 61	<sup>b</sup> 10 - 80
Engine run-to-run repeatability, lb-sec . . . . .						±5.1		±13	<sup>a</sup> ±35
Time from indicated chamber pressure decay to cutoff signal, sec . . . . .	11						10		
Maximum peak-to-peak chamber pressure oscillation during shutdown, psia . . . . .	35						23		
Chamber pressure decay rate from steady-state to cutoff signal, psia/sec . . . . .	10						11.6		
Chamber pressure at cutoff signal, psia . . . . .	9						8		
Shutdown transient impulse from steady-state thrust, sec . . . . .	≈14 623						≈13 230		
Nominal shutdown transient impulse from cutoff signal to 10 percent steady-state thrust, lb-sec . . . . .		364.2	337.3	350.6	319.6	342.9		231 - 367	<sup>b</sup> 240 - 390
Engine run-to-run shutdown repeatability, lb-sec . . . . .						±23.3		±73	<sup>a</sup> ±75

<sup>a</sup> Contractor's engine design requirement specification.

<sup>b</sup> Vendor's acceptance test specification.

TABLE 9.9-III.- STEADY-STATE PERFORMANCE DURING SECOND FIRING

Parameter	15 seconds after ignition			150 seconds after ignition			340 seconds after ignition		
	Predicted <sup>a</sup>	Predicted <sup>b</sup>	Measured <sup>c</sup>	Predicted <sup>a</sup>	Predicted <sup>b</sup>	Measured <sup>c</sup>	Predicted <sup>a</sup>	Predicted <sup>b</sup>	Measured <sup>c</sup>
Regulator outlet pressure, psia . . . .	186	176	176	185	176	176	185	180	180
Oxidizer bulk temperature, °F . . . . .	68	68	68	68	68	68	67	67	68
Fuel bulk temperature, °F . . . . .	68	68	68	68	68	68	68	68	68
Oxidizer interface pressure, psia . . .	172	163	163	171	162	163	169	166	164
Fuel interface pressure, psia . . . . .	172	163	163	171	163	162	170	166	164
Engine chamber pressure, psia . . . . .	125	119	122	124	119	121	123	121	122
Mixture ratio . . . . .	1.609	1.606	--	1.606	1.603	--	1.601	1.599	--
Thrust, lb . . . . .	3508	3354	--	3481	3338	--	3471	3396	--
Specific impulse, sec . . . . .	310.1	310.1	--	310.3	310.3	--	309.6	309.6	--

<sup>a</sup> Preflight prediction based on acceptance test data and assuming nominal system performance.

<sup>b</sup> Regulator outlet pressure data from flight used; all other parameters nominal.

<sup>c</sup> Actual flight data with known biases removed.

NASA-S-69-2059

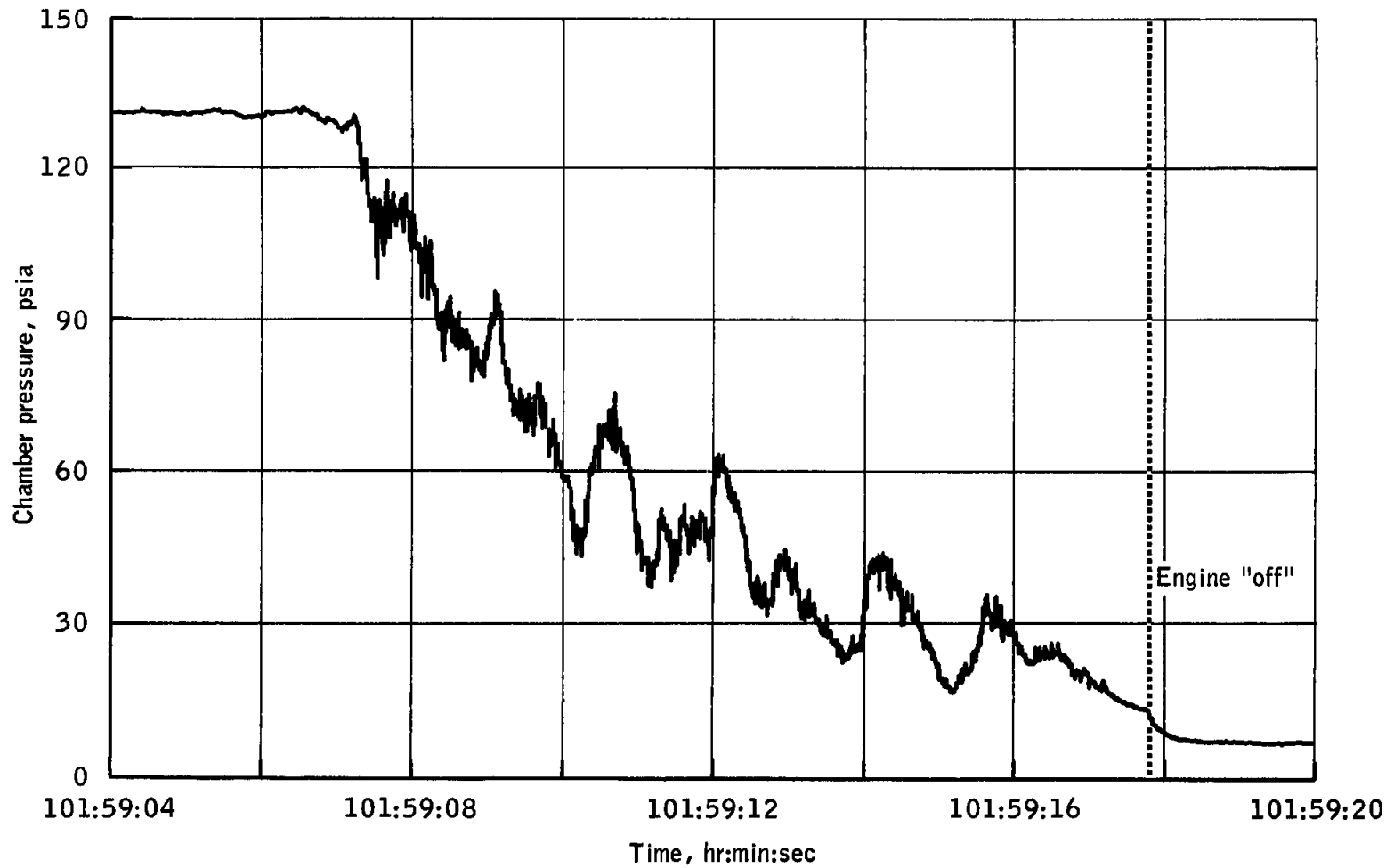


Figure 9.9-1.- Ascent engine chamber pressure during oxidizer depletion.

NASA-S-69-2060

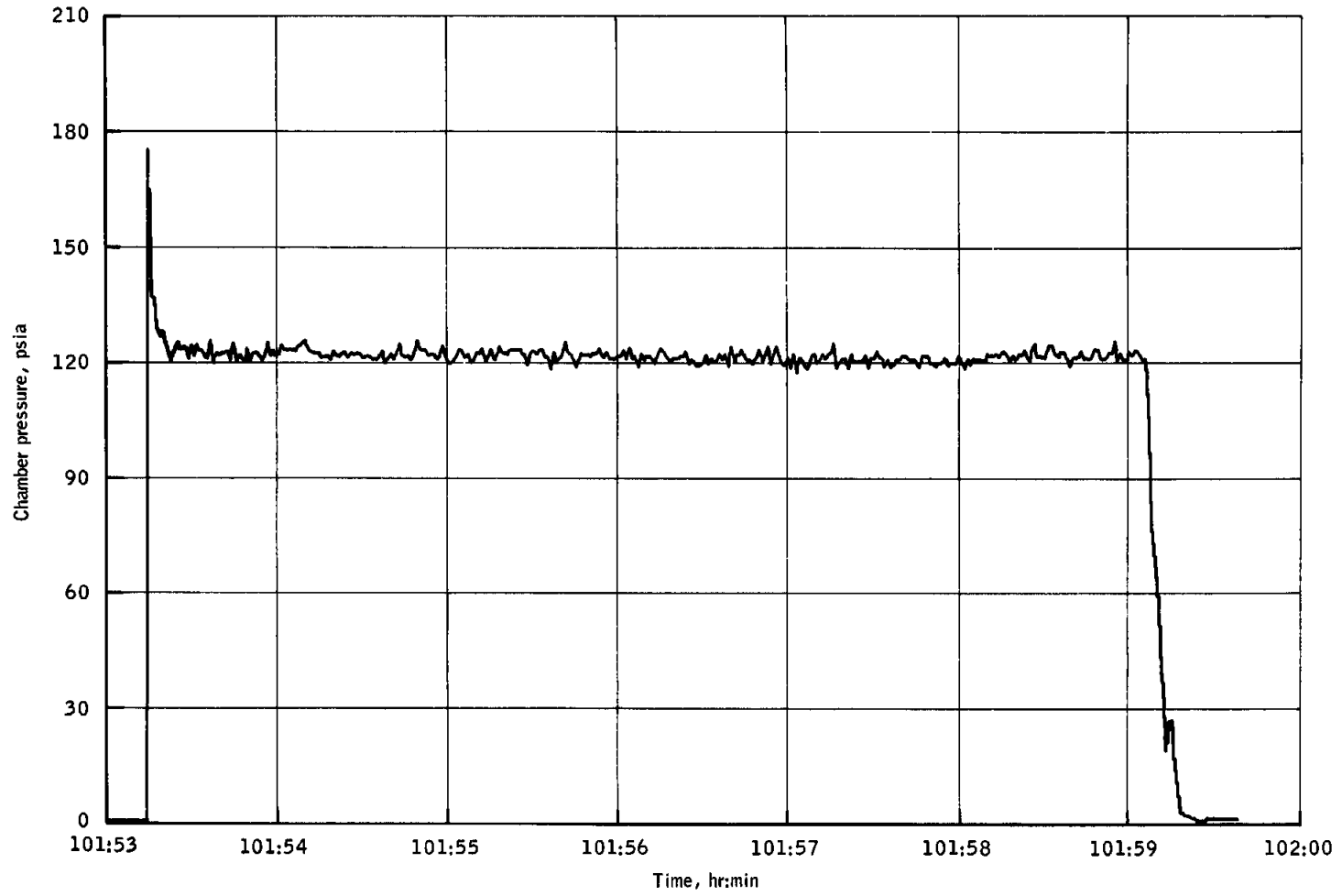


Figure 9.9-2.- Ascent engine chamber pressure during firing to depletion.

## 9.10 ENVIRONMENTAL CONTROL SYSTEM

The environmental control system was activated three times and operated normally during the 26 hours of manned operation. The system was operated in both the cabin and egress modes. The second manning included approximately 1 hour of egress mode operation with one crewman on the suit loop. The primary sublimator was activated three times and dried out twice, as required. All environmental control system operating procedures required for the lunar mission were verified; these were deliberate cabin depressurization and repressurization, portable life support system recharge, and lithium hydroxide cartridge removal and installation.

### 9.10.1 Manned Operation

First manning.- The first manning lasted approximately 7 hours. During the activation of the primary heat transport section, the environmental control system GLYCOL light came on momentarily and triggered the caution and warning system. Telemetry data indicated that the glycol temperature was decreasing normally and was just at the trigger point when the heat from the development flight instrumentation was added, triggering the caution and warning system. Thereafter, the glycol temperature was as expected.

The cabin pressure was approximately 5.1 psia, about 0.1 psi above normal, throughout the manning. The higher cabin pressure would cause higher usage of oxygen. However, there was no effect on this mission because of the available oxygen. At the end of the first manning period, the primary sublimator was successfully dried out with the crew on the suit loop for a majority of the dryout period.

During shutdown between mannings, the cabin repressurization valve was placed in the closed position, and the crew stated that this was accompanied by a loud "bang." This is a design characteristic of the valve when it is repositioned rapidly from automatic to closed. This repositioning causes both seats of the valve to be open momentarily, allowing a sudden surge of oxygen flow into the cabin; thus, a sharp report results. A caution note has been added to the Apollo Operations Handbook (May 1, 1969, issue) advising of the loud noise and procedures for minimizing the noise.

Second manning.- The second manning lasted approximately 8 hours. Telemetry data indicated that during transfer to the environmental control system, the Lunar Module Pilot's suit isolation valve was in the disconnect position; however, temperature data indicated that the valve was in the flow mode. Also, the crew confirmed the actual position of the valve to be correct. Therefore, the switch mechanism which gives the indication was most likely improperly adjusted. The glycol loop performed as expected.

During extravehicular activity, one crewman was supported by the environmental control system in the egress mode. The suit loop pressure was maintained at 4.07 psia (required range is 3.6 to 4.0 psia); however, the higher suit pressure regulation did not affect the mission because sufficient oxygen was available.

The portable life support system was successfully recharged with water and oxygen after extravehicular activity. The carbon dioxide level remained relatively low throughout the manning; however, the primary lithium hydroxide cartridge was replaced at the end of the second manning as planned. Primary sublimator dryout was accomplished as planned.

Third manning.- The third manning lasted approximately 11 hours. The environmental control system was activated without incident. After staging, the oxygen and glycol quantity and pressure data indicated that the interstage disconnects performed properly. At the completion of the third manning, the system was deactivated except for the primary sublimator and the glycol loop, which were required for the ascent engine firing to depletion.

#### 9.10.3 Unmanned Operation

The unmanned activities included the ascent engine firing to depletion through loss of signal.

The glycol pumps operated for approximately 6 hours after initiation of the ascent engine firing to depletion. The pump performance was degraded because the battery voltage was decreasing. The cabin was pressurized, but the environmental control system was not configured to maintain pressure. The cabin pressure did not decay in the 6 hours that data were available following the firing, indicating a very tight pressure vessel. The allowable leakage from the oxygen supply into the cabin was less than 0.1 lb/hr. The cabin leakage rate, therefore, can be concluded to be less than 0.1 lb/hr.

#### 9.10.4 Thermal and Atmospheric Control

The lunar module was launched with the upper dump valve in the open position so that the nitrogen-rich atmosphere would be dumped during the launch phase. Thereafter, both dump valves were operated in auto except when deliberately depressurizing the spacecraft.

The atmosphere revitalization section was operated for 26 hours. Of this time, 1 hour was with one crewman in the egress mode. After stabilization of the primary heat transport section, the suit inlet temperature was maintained between 40° and 50° F, with the suit temperature control

set at maximum cool throughout the mannings. Figure 9.10-1 shows a composite of the suit loop/cabin parameters during the first manning and is representative of each of the three mannings. The variations in the suit outlet temperature measurements (fig. 9.10-1) are indicative of helmet on or off mode for each of the crewmen. With helmet off, the suit outlet temperature would tend to approach cabin temperature. The figure also shows the response of the suit/cabin temperatures in relation to activating and deactivating the sublimator.

During sublimator dryout at the end of the first manning, the crew elected to remain on the suit loop. The disadvantage of the crew being on the suit loop during dryout, even though the additional crew heat load would shorten dryout time, is that condensate is retained in the suit loop. Depending upon the metabolic load, this could result in a substantial amount of condensate being generated in this time period and being retained in the centrifugal water separator, and being vaporized between mannings or discharged during the second manning activation. During the dryout, the separator speed dropped from about 3000 rpm to 1110 rpm, indicating that the separator was loading with water and approaching the stall point.

The heat transport section undergoes two major temperature changes at primary sublimator start-up and sublimator dryout. Figure 9.10-2 shows a typical start-up transient for a manning. Figure 9.10-3 shows the dryout transients. The primary sublimator holds 2.1 pounds of water. To preclude a possible rupture of the sublimator, this quantity of water must be dissipated before glycol flow is stopped. The sublimator is considered dry when the glycol outlet temperature undergoes a second inflection point. The first inflection occurs part way through the dryout sequence when the sublimator effectiveness begins to decrease, as indicated in figure 9.10-3.

The cabin temperature control valve was in the normal position throughout the mannings, and the cabin temperature was maintained satisfactorily between 65° and 70° F.

Oxygen usage.- The total oxygen consumption was 19.1 pounds from the descent stage tank and 0.58 pound from the ascent stage tanks as compared to predictions of 20.4 and 1.5 pounds, respectively. Figure 9.10-4 shows a pressure history of the descent stage oxygen tank. Figure 9.10-5 shows the consumption of ascent stage oxygen after staging and for the ascent engine firing to depletion. The indicated increase in oxygen quantity during the second manning and after cabin repressurization (fig. 9.10-4) was caused by the normal drop in tank temperature which occurred during cabin repressurization. After the repressurization, the rise in tank pressure results from the normal warmup of the gas following the rapid expansion.

The cabin atmosphere was dumped through the cabin bacteria filter (on the dump valve) before the extravehicular activity period. It took approximately 5 minutes for the cabin pressure to decrease so that the hatch could be opened. The required time to dump with clean air is a maximum of 5 minutes 10 seconds for a lunar surface timeline.

The glycol pump differential pressure fluctuated between 21 and 23 psid. The average of this differential pressure, coupled with the glycol pump preflight performance, resulted in an average glycol flow rate of 290 lb/hr. The average heat loads rejected were 5700 Btu/hr for the first manning, 5550 Btu/hr for the second manning, and 6930 Btu/hr for the third manning.

#### 9.10.5 Water Consumption

Water consumption was within predicted tolerances of 132 pounds for the descent tank and 37 pounds for the ascent tanks. Figure 9.10-6 shows the depletion rate from the descent stage for each of the three mannings. Figure 9.10-7 shows the ascent stage water consumption from staging to loss of telemetry data after the ascent engine firing to depletion. Ascent water tanks 1 and 2 are connected by a common manifold, and the depletion rates should be identical. However, the divergence of the two tank quantities (fig. 9.10-7) indicates that probably the water quantity measuring device in tank 1 had experienced a calibration shift.

The bacteria filter in the water dispenser was used successfully throughout the lunar module activities. The crew observed that the bacteria filter element had little effect on the flow of water through the dispenser.

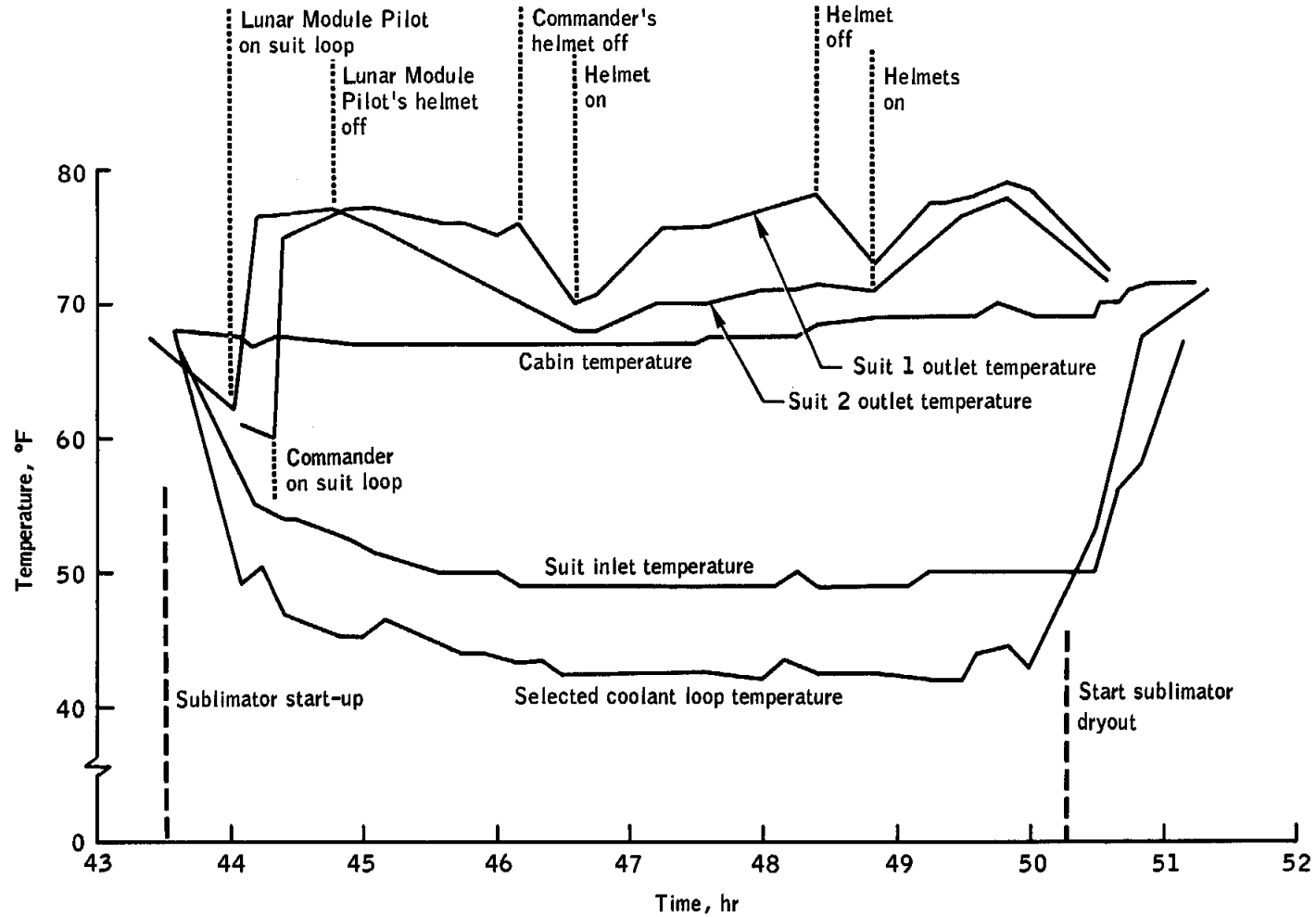


Figure 9.10-1.- Suit and cabin temperatures during first manning.

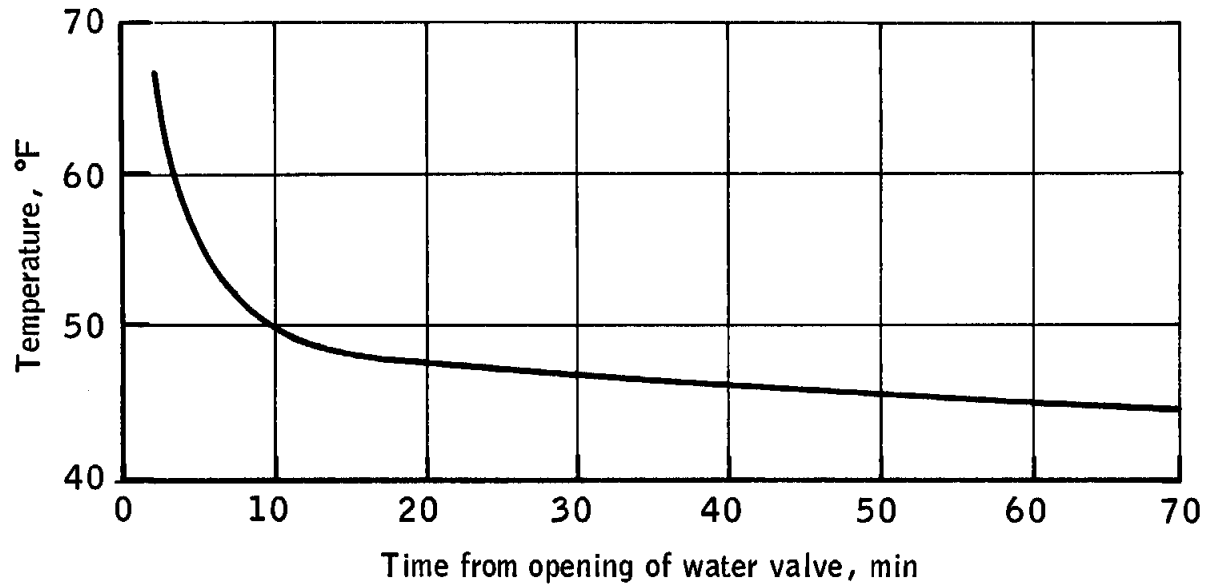
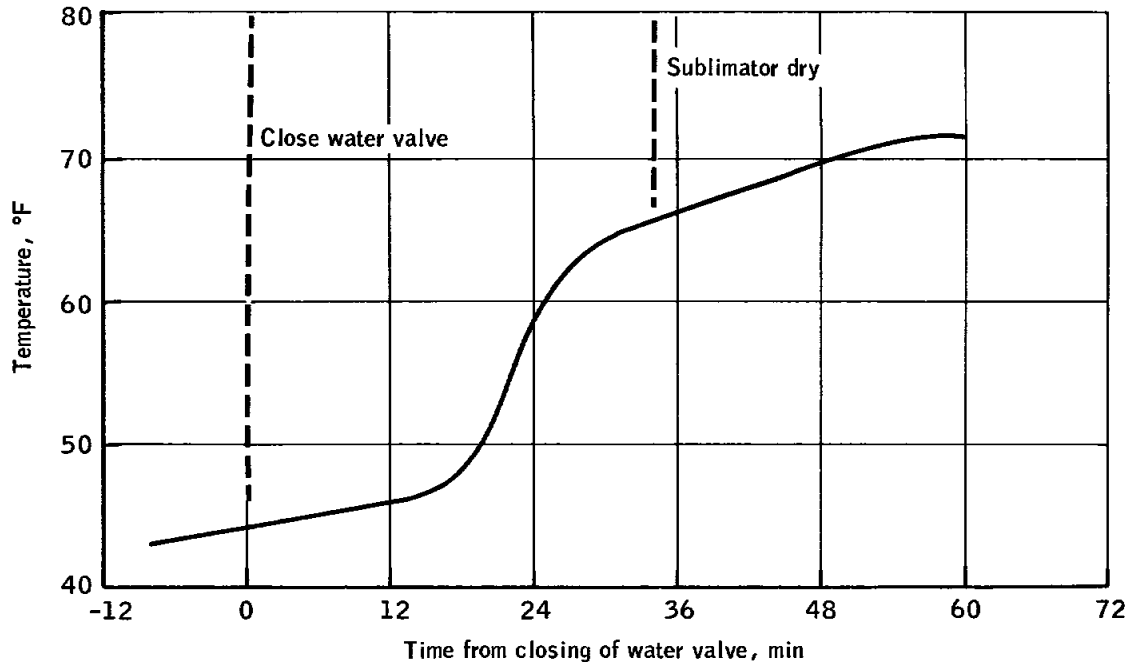
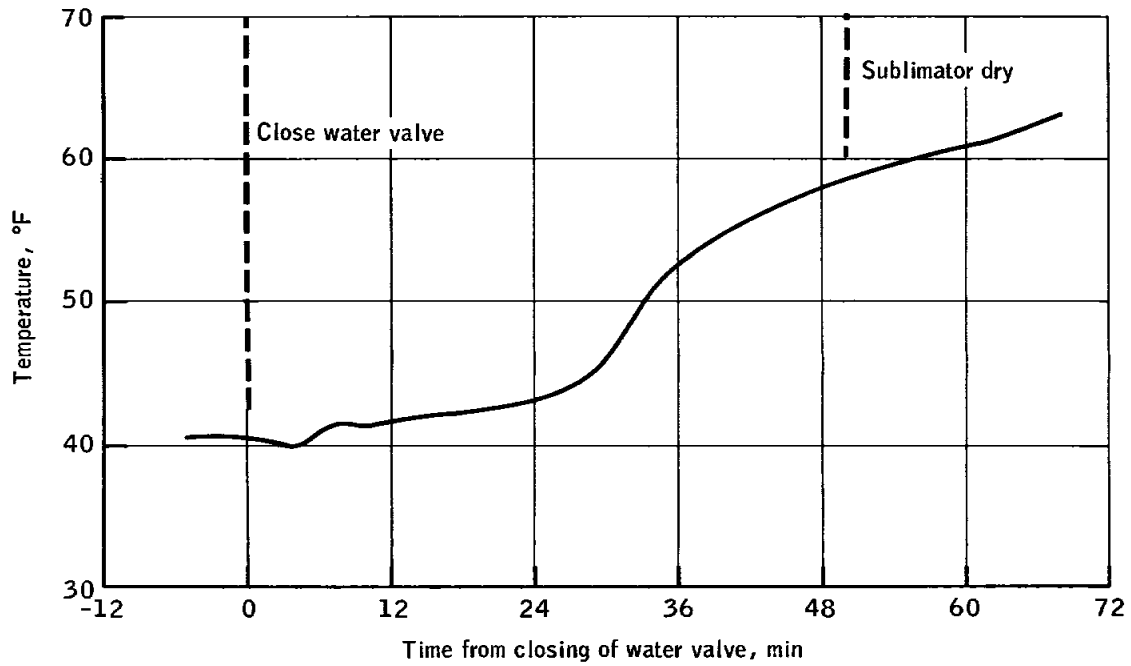


Figure 9.10-2.- Glycol temperature during sublimator start-up.

NASA-S-69-2063



(a) First manning.



(b) Second manning.

Figure 9.10-3.- Glycol temperature during sublimator dryout.

NASA-S-69-2064

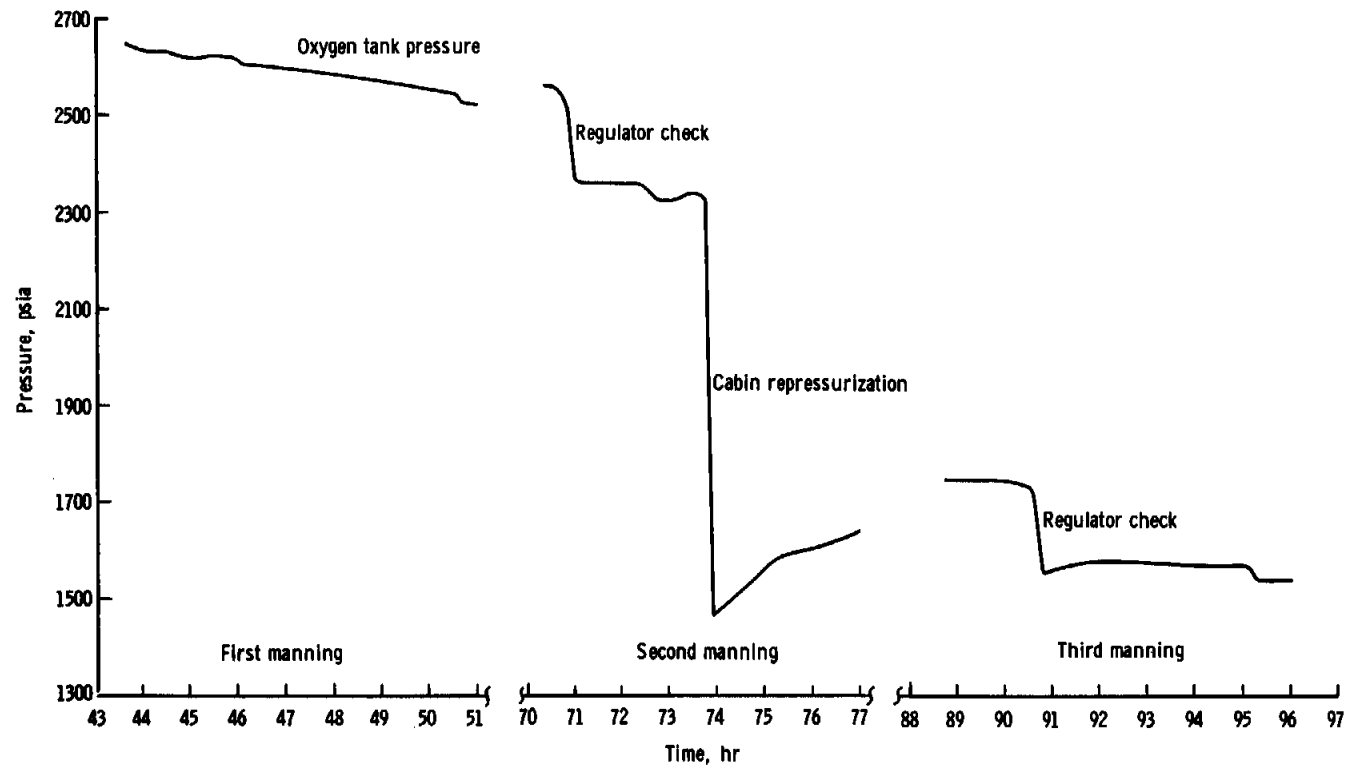


Figure 9.10-4. - Oxygen tank pressure history.

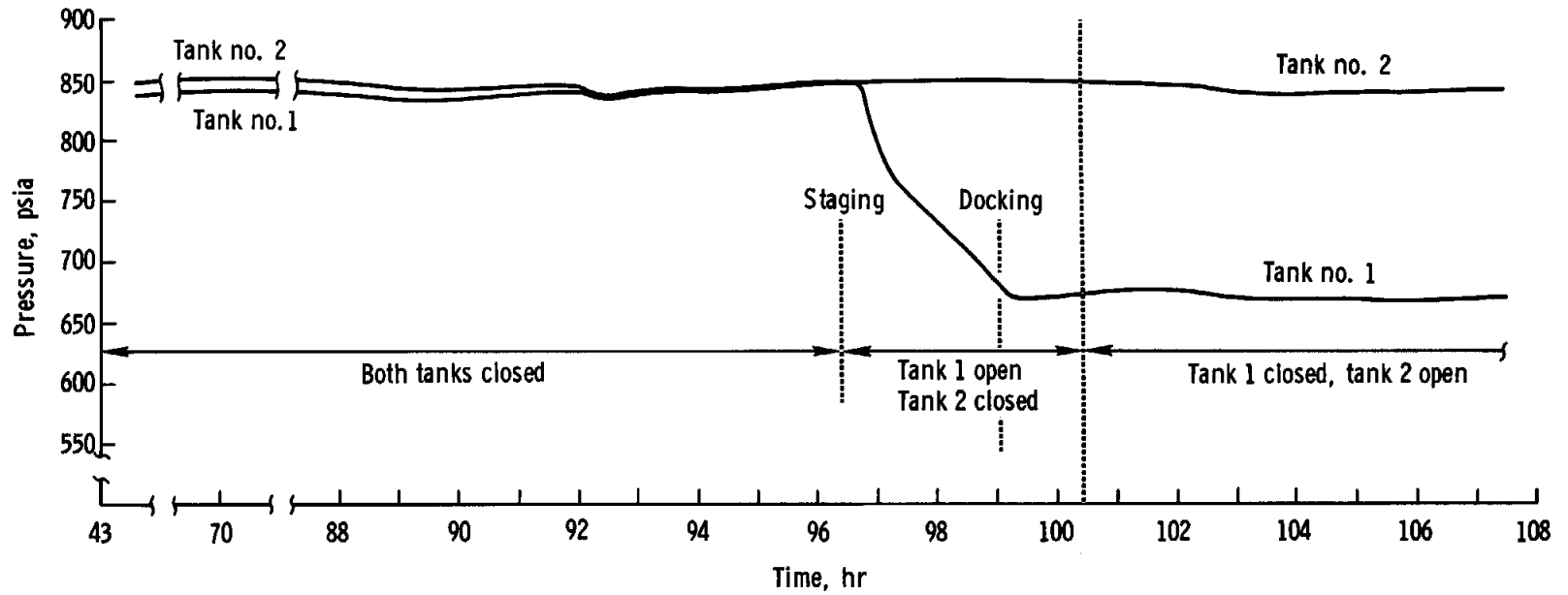
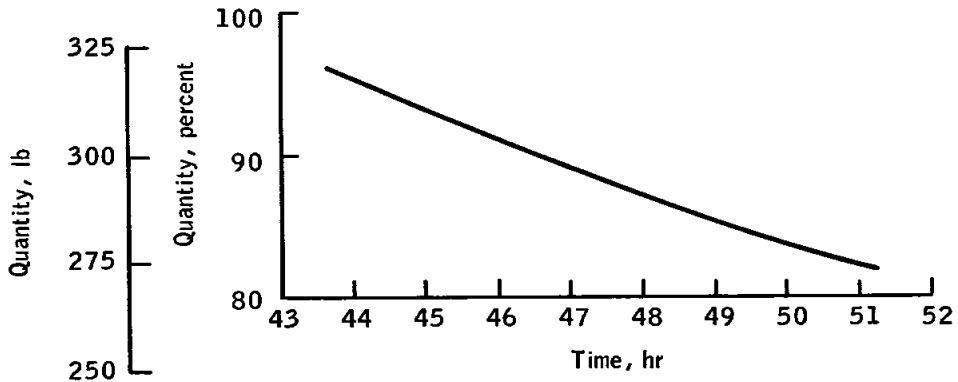
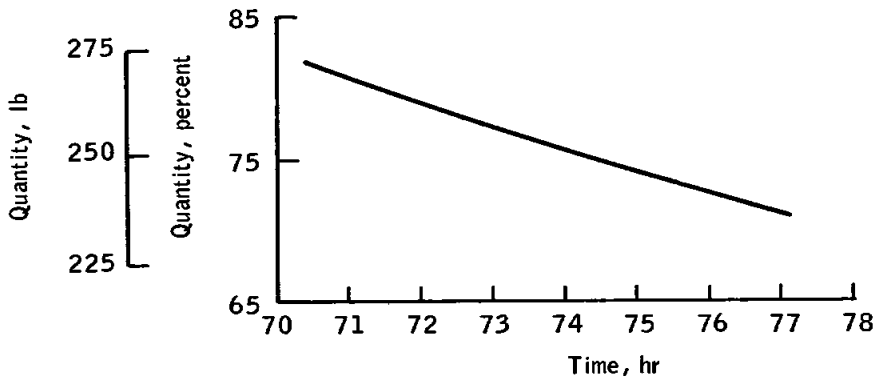


Figure 9.10-5. - Pressure history of ascent oxygen tanks.

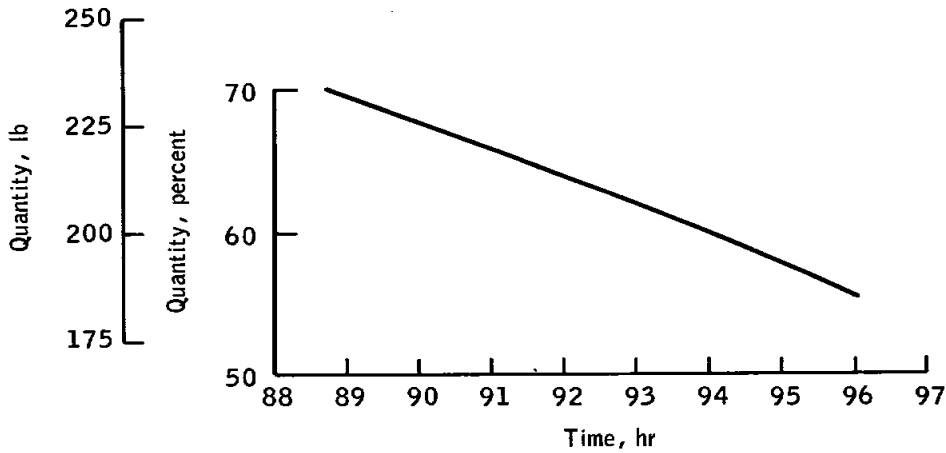
NASA-S-69-2066



(a) First manning.



(b) Second manning.



(c) Third manning.

Figure 9.10-6.- Water consumption.

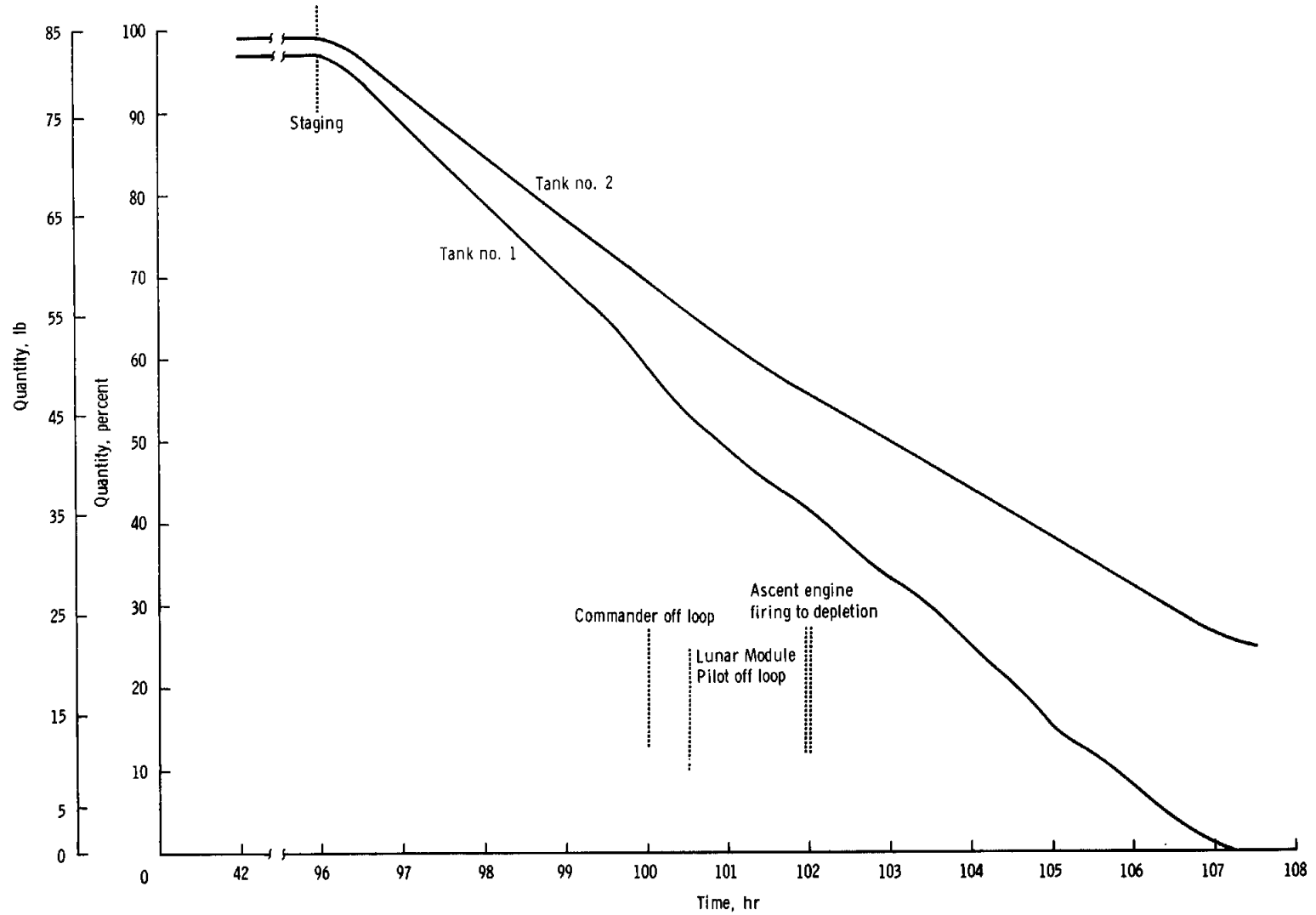


Figure 9.10-7. - Water consumption from ascent stage tanks.

## 9.11 CREW STATION

### 9.11.1 Displays and Controls

The displays and controls functioned satisfactorily in all but the following areas:

The helium pressure/temperature indicator did not indicate properly when the supercritical helium pressure measurement was selected. All other measurements displayed on this indicator were satisfactory. Because of the failure mode, a malfunction of the transducer has been eliminated, thus indicating a problem in the wiring or interconnections.

The exterior tracking light operated normally until staging, when the crew reported the light was out and did not operate thereafter. After docking, the light switch was cycled several times. The resulting increase in power of about 5 amperes confirmed normal operation of the power supply and isolated the failure to the pulse forming network, high voltage cable, or flash head. See section 17 for further details.

### 9.11.2 Crew Provisions

All crew provisions were satisfactory. The crew stated that the quantity of utility towels was adequate and that the lunar module water dispenser was easier to drink from than the command module dispenser.

The pressure garment assemblies were worn for all lunar module operations. The gloves and helmet were not worn during most of the lunar module manning. The pressure garment assemblies was pressurized for about 70 minutes. The Commander's helmet was badly scratched during operations in the rear of the lunar module. The extravehicular mobility unit maintenance kit was used to clean the helmets and the extravehicular visor assemblies. Operation of all extravehicular mobility unit components and accessories in the lunar module was nominal, except all attachment snaps separated from both helmet stowage bags. The bags, however, were stowed utilizing the Velcro on the base alone. The snaps are necessary only for the launch phase of the mission. Subsequent use of the bags with Velcro strip for retention is adequate. Checkout of the extravehicular mobility unit is discussed in section 4.

The lunar module window shades were apparently overheated by the window heaters, causing the shades to uncurl. The heaters will not be operated with the shades deployed on future flights.

The reticle pattern on the optics system was too dim and caused difficulties during docking; this problem is discussed in section 17.

## 9.12 RADAR

The radar system performed satisfactorily. The rendezvous radar performed within acceptable limits, and acquisitions were accomplished at ranges between 2000 feet and 80 miles in both the automatic and normal modes. During the rendezvous operation, the radar was operated over a range of 260 feet to 98.85 miles. The Commander reported a decrease in radar signal strength from approximately 2.6 volts to a low of 1.6 volts at 4 or 5 minutes prior to terminal phase initiation. After that time, the voltage returned slowly to the higher level. Calculation of the signal strength for the particular attitude changes which occurred at that time agree with the observed signal strength changes reported by the crew.

The performance of the landing radar during the self-test was within nominal limits. The landing radar was monitored during the 100-percent-throttle descent engine firing, as well as during two firings with the antenna tilted. Telemetry data and crew observation indicated that the frequency trackers continued to sweep during the test and did not lock onto spurious returns. Examination of power spectral density plots for the first descent engine firing revealed random pulses of approximately 50 Hz of 0.1-second duration on the telemetered velocity and altimeter channels. These spikes occurred before, during, and after the descent engine firing. Power spectral density plots for the other descent engine firings will be analyzed when available, and the results will be reported in a supplemental report.

## 9.13 CONSUMABLES

The usage of all lunar module consumables is summarized in this section. Electrical power consumption is discussed in section 9.3.

## 9.13.1 Descent Propulsion System Propellants

The total descent propulsion system propellant loadings and consumption values were as follows: (The loadings were calculated from readings and measured densities prior to lift-off.)

	<u>Fuel, lb</u>	<u>Oxidizer, lb</u>
Loaded	6 977	11 063
Consumed (estimated)	4 127	6 524
Remaining at separation	2 850	4 539

## 9.13.2 Ascent Propulsion System Propellants

The total ascent propulsion system propellant loading and consumption values were as follows: (The loadings were determined by weighing the off-loaded propellants and measured densities prior to lift-off.)

	<u>Fuel, lb</u>	<u>Oxidizer, lb</u>
Loaded	1 626	2 524
Consumed prior to ascent stage separation	31	59
Consumed by reaction control system	22	44
Total consumed at oxidizer depletion	1 558	2 524
Total remaining at oxidizer depletion	68	0

A portion of the reaction control system propellants was supplied from the ascent system propellant tanks during lunar module staging and the ascent firing to depletion. Ascent propellant was used by both system A and system B during 21 seconds of the staging maneuver and by system B only during the ascent firing to depletion. A summary of reaction control system propellant usage from the ascent propulsion system tanks is included in the following table:

	<u>Oxidizer, lb</u>	<u>Fuel, lb</u>	<u>Total, lb</u>
Lunar module staging	20.1	9.9	30.0
Ullage	17.0	8.4	25.4
Firing to depletion	<u>29.1</u>	<u>14.3</u>	<u>43.4</u>
Total	66.2	32.6	98.8

### 9.13.3 Reaction Control System Propellants

The propellant utilization and loading for the lunar module reaction control system, including manifolds, were as follows: (Consumption was calculated from telemetered helium tank pressure histories using the relationships between pressure, volume, and temperature.)

	<u>Fuel, lb</u>	<u>Oxidizer, lb</u>
<u>Loaded</u>		
System A	108	209
System B	108	209
<u>Consumed</u>		
System A	76	146
System B	50	95
<u>Remaining at last data</u> <u>transmission from lunar module</u>		
System A	32	63
System B	58	114

Note: Interconnects on system B were opened at about 100:49:00. The system A consumption during the ascent firing to depletion is based on the onboard propellant and quantity measuring device. The interconnects on both system A and B were opened during the staging maneuver from 96:16:12 to 96:16:35.

## 9.13.4 Oxygen

The oxygen quantities loaded at lift-off and consumed were as follows: (Consumption values are based on telemetered data.)

<u>Loaded</u>	<u>Oxygen, lb</u>
Ascent stage	
Tank 1	2.36
Tank 2	2.37
Descent stage tank	47.71
<u>Consumed</u>	
Ascent stage at last data transmission	
Tank 1	0.58
Tank 2	0
Descent stage tank at separation	19.08
<u>Remaining</u>	
Ascent stage at last data transmission	
Tank 1	1.78
Tank 2	2.37
Descent stage tank at separation	28.63

## 9.13.5 Water

The water quantities loaded and consumed were as follows: (Consumption values are based on telemetered data.)

<u>Loaded</u>	<u>Water, lb</u>
Ascent stage	84.8
Descent stage tank	322.1
<u>Consumed</u>	
Ascent stage through last data transmission	64.0
Descent stage tank at separation	135.2
<u>Remaining</u>	
Ascent stage at last data transmission	20.8
Descent stage at separation	186.9



Apollo 9 flight crew

Commander James A. McDivitt, Command Module Pilot David R. Scott, and Lunar Module Pilot Russell L. Schweichart.

10.0 FLIGHT CREW

## 10.1 FLIGHT CREW PERFORMANCE SUMMARY

The flight crew for Apollo 9 were J. A. McDivitt, Commander; D. R. Scott, Command Module Pilot; and R. L. Schweikart, Lunar Module Pilot. Their performance was excellent throughout the mission in accomplishing checkout, separation, and rendezvous of the lunar module, demonstration of extravehicular capability, and management of spacecraft systems while docked and undocked.

## 10.2 PILOTS' REPORT

### 10.2.1 Preflight Activities

The Apollo 9 mission was conducted according to a basic flight plan conceived 2-1/2 years previously; the crew was initially assigned at that same time. The preflight activities were divided into three major periods. During the first period, the crew became familiar with the flight hardware and worked closely with the major manufacturers in the manufacturing and checkout of the spacecraft. During the second period, the crew completed the details of the flight plan and produced an acceptable set of flight procedures that provided optimum use of the available flight time and covered all reasonable contingencies. During the last period, the crew concentrated almost entirely on training and integrating planned orbital operations into the ground simulation system.

During preflight training, three command module simulators and two lunar module simulators were assigned to the Apollo 9 crew. Efforts to integrate each command module simulator with an associated lunar module simulator became very time-consuming and were not very effective from a crew-training standpoint. The first completely integrated simulations using the Mission Control Center, the lunar module simulator, and the command module simulator were performed less than 2 months prior to the scheduled launch. Because of the difficulties encountered in integrating such a complex system, activities during these 2 months were very frustrating at times but eventually proved to be the most valuable of all the training activities. At the time of launch, the crew believed the spacecraft, the flight plan, the inflight procedures, and the integrated air-ground procedures were ready for flight.

### 10.2.2 Powered Flight

The lift-off sequence began when the blockhouse communicator began the countdown 15 seconds before lift-off. He called ignition at minus 5 seconds, when the engine ignition was actually visible on the television monitor, and lift-off at T minus 0. Some noise and vibration were apparent at ignition. The nature of this vibration changed slightly at lift-off and some slight acceleration was felt. Immediately after lift-off, there was some vibration within the spacecraft, and the rate needles vibrated at a high frequency up to about 1 deg/sec in all three axes. The yaw, roll, and pitch programs all began and ended at the appropriate times.

At approximately 50 seconds, the noise and vibration within the vehicle increased as the launch vehicle entered the region of maximum

dynamic pressure. The noise and vibration levels remained reasonably high throughout this region, then decreased to very low levels for the remainder of powered flight. During the region of maximum dynamic pressure, the maximum indicated angle of attack was approximately 1 degree. Cabin pressure was relieved with an obvious, loud noise. Inboard engine cutoff occurred on time. Subsequently, a very slight chugging was felt for a short time but damped out rapidly.

Separation of the first stage proved to be quite a surprise. At engine shutdown, the acceleration felt in the couches changed very abruptly from positive to negative, and the Command Module Pilot and Lunar Module Pilot went forward against their restraint harnesses. The crew expected a decrease in acceleration to near zero but not a change to negative (see section 8.1).

Second-stage ignition was normal, and all five engines ignited together. The escape tower was jettisoned on time without abnormal occurrence. At second-plane separation, a dull thud was felt in the spacecraft. Steering was initiated with the normal 1 deg/sec rate. Second-stage flight continued within nominal limits until at approximately 1 minute before shutdown, some very slight longitudinal oscillations were felt in the spacecraft. The magnitude of these oscillations appeared to build very slowly until shutdown but remained low and were of no concern to the crew.

The staging to the S-IVB and ignition was very mild. At steering initiation, the S-IVB went gradually to its guidance attitude, and the remainder of the launch into orbit was nominal. At S-IVB shutdown, the command module computer gave a resultant orbit of 103 by 89.5 miles, which was later refined by the ground to 103.9 by 102.3 miles.

Throughout the launch, the Command Module Pilot used the information displayed from the computer to calculate the launch vehicle trajectory. This information was of great value to the crew, since it provided them with an onboard estimate of their situation. These onboard calculations agreed very closely with the information relayed from the ground.

The noise within the spacecraft was somewhat less than the crew had anticipated. As a result of the Apollo 8 debriefing, the crew was prepared to operate without communications throughout first-stage flight. However, the noise environment within the spacecraft was such that the crewmen were able to communicate with each other and with the ground throughout the entire flight profile. As expected, the period of greatest noise level within the spacecraft was from 50 seconds to 2 minutes, near the region of maximum aerodynamic pressure.

In addition to the noise generated in the spacecraft by the launch vehicle, a considerable amount of noise was encountered on the S-band receiver from approximately 3 to 6 minutes after lift-off. The Lunar Module Pilot finally turned his volume control down so the noise would not interfere with his own operations within the spacecraft.

The only anomaly during the launch phase that affected the crew was loss of the onboard display of service propulsion helium pressure at lift-off. The service propulsion system is a required system for high altitude aborts, and prior to reaching these high altitudes, the crew obtained confirmation from the ground that the service propulsion system was operating properly.

### 10.2.3 Transposition, Docking, and Separation

Command and service module separation.- The series of operations required to extract the lunar module from the S-IVB commenced with the S-IVB/spacecraft maneuver to the inertial docking attitude at 2:34:00. Preflight-calculated gimbal angles in the spacecraft platform were correct, and Mode-3 error needles were therefore nulled. All systems were checked prior to separation, and all onboard indicators were nominal. Shortly after sunrise, the command and service modules were separated from the S-IVB with the associated pyrotechnics report and attendant acceleration. The attitude-hold control mode from the computer was used to take advantage of jet-selection logic. The preplanned 3-second reaction control maneuver did not produce the expected velocity, and an additional 2 seconds of thrust were added to increase the indicated separation velocity to 0.6 ft/sec.

Transposition.- At 15 seconds after separation, control was switched to the stabilization and control system to utilize pure control-axes rotational maneuvers, and a 180 degrees pitch-up maneuver was initiated to visually acquire the S-IVB. Mode-2 error needles were called to display the nominal docking attitude. The S-IVB became visible through the hatch window after approximately 70 degrees of rotation. At the completion of the pitch maneuver, translational alignment was very good. Range was approximately 60 feet; however, the pitch attitude was 10 degrees below the nominal docking attitude. The command and service modules were then rolled left 60 degrees to align with the lunar-module docking target.

Docking.- An attempt to align the spacecraft at this time was unsuccessful because of a lack of translation capability to the left. A noticeably higher closing rate with the S-IVB was also noticed. The propulsive venting was visible on both sides of the forward part of the S-IVB.

A control mode evaluation was made by switching through all stabilization and control system modes, reloading the digital autopilot, and reconfiguring the AUTO RCS SELECT  $\pm$ Y thruster switches from manual B to manual A, all to no avail. During this time, the spacecraft was maneuvered aft and right, then yawed left and translated forward across the front of the S-IVB to a position left of the S-IVB.

Approximately 10 minutes after separation, both the primary and secondary propellant isolation valves in quad C and the secondary valves in quad D were discovered to be closed. This condition caused the velocity and attitude discrepancies during separation and transposition noted earlier. After the valves were opened, all control modes returned to normal. The spacecraft was aligned properly with the lunar module target, and Mode-2 error needles were verified as null. Docking was accomplished by utilizing the autopilot up to a distance of 15 feet; then SCS MIN DEADBAND, LOW RATE was used because it was the tightest control mode available. Physical contact was made at a velocity of 0.07 ft/sec, capture occurred immediately, and control was switched to computer FREE mode.

Estimation of spacecraft attitude using the crewman optical alignment sight was very difficult during the last 15 feet of closure because of an almost complete washout of the reticle against the bright white background of the lunar module target. However, the standoff cross and Mode-2 error needles provided adequate cues for alignment.

Post-contact dynamics were mild, no large oscillations were evident, and all essential motion was terminated in approximately 10 seconds. At that time, the spacecraft had drifted up (pitch down) approximately 3 degrees and left (yaw right) 1 degree relative to the null position on the standoff cross. The spacecraft was realigned to zero offset in pitch and yaw using the minimum impulse mode of the stabilization and control system.

When rates were damped to zero, retraction was initiated and physical closure was evident immediately. The retraction cycle was completed in about 8 seconds, as indicated by the audible and physical sensation of the docking latch engagement. A firm joining of the two vehicles had unquestionably taken place. No post-latching dynamics were apparent. Subsequent inspection revealed that all 12 latches had engaged properly.

Throughout the exercise, the S-IVB remained a very stable base, and with the exception of the venting acceleration, no S-IVB motion was detectable. The magnitude of the propulsive venting was greater than expected. Very little forward thrust was necessary to null the initial separation velocity; and subsequent station-keeping and docking maneuvers were performed using aft thrust almost exclusively.

Expenditure of propellant was higher than anticipated because of the control-mode evaluation and troubleshooting, the higher-than-expected S-IVB propulsive venting, and the necessity of remaining near the S-IVB with only 5 degrees of translation freedom. With all reaction control engines active, all control modes were excellent and had been well represented in the simulator.

Spacecraft separation.- The pressure in the two vehicles was equalized to 4.0 psi through the tunnel hatch valve in approximately 5 minutes, conforming almost exactly to preflight calculations. Prior to separation, the command module cabin pressure had been increased to 5.7 psi manually. The connection of the lunar module electrical umbilical proceeded as planned.

Spacecraft separation from the S-IVB was performed on time and was verified by visual observation of the lunar module withdrawal relative to the adapter ring on the S-IVB. Five seconds after separation, a 3-second aft thrust using all four forward firing thrusters was applied to insure adequate clearance for the autopilot controlled maneuver to the final separation attitude.

The final separation maneuver lasted 6 seconds, applying aft thrust using the forward firing thrusters, and was initiated at 3 minutes after spacecraft separation. This maneuver provided adequate separation and continuous visual observation of the S-IVB during the preparation for and ignition of the first S-IVB restart firing. Prior to the S-IVB restart firing, the spacecraft was traveling above and aft of the S-IVB, but at the firing moved to slightly below and approximately 1500 feet behind the S-IVB.

#### 10.2.4 Command and Service Module Propulsion Maneuvers

The eight major service propulsion maneuvers consisted of docked and undocked firings. All firings except two were initiated on the thrust-A valves with the thrust-B valves turned on 3 seconds later; the first and sixth firings were too short to require this backup. In general, there was a significant difference in acceleration as the spacecraft weight decreased. The first firing was performed with the spacecraft at a total weight of approximately 90 000 pounds, while the eighth firing (deorbit maneuver) was performed with a spacecraft weight of approximately 22 000 pounds. In each case, the start was sharp and brisk, the thrust level increased slightly when the thrust-B valves were turned on, and the thrust terminated quickly at shutdown.

The first five firings were performed in the docked configuration. The first and fourth firings were conducted using nominal procedures.

The second and third firings were used to conduct the stroking test (deliberate oscillation of the service propulsion engine gimbals in pitch). The second firing was performed with a 40-percent amplitude stroke, while the third firing was performed with a 100-percent amplitude stroke. The purpose of these two tests was to establish the inflight bending response of the combined vehicles to a control system input. Prior to the start of the stroking test, some combined-vehicle maneuvering had been accomplished in the acceleration-command mode of the reaction control system. These acceleration-command inputs had actually created in the combined vehicles an oscillation that transferred from one axis to another. When the acceleration-command input was made in pitch, vehicle oscillations were first evident in pitch, then in yaw as the pitch oscillations decreased, and then back in pitch (see section 8.6 for further discussion of these oscillations). With this kind of response, there was some doubt as to the ability of the vehicle to complete the stroking test as planned.

In each stroking test, the stroke was initiated 1 minute after ignition to provide ample time for the initial start transients to subside. The test during the second firing resulted in a 0.1 to 0.2 deg/sec vehicle pitch-oscillation, which also coupled into yaw and back into pitch and damped in approximately 5 seconds. For the third firing, the test resulted in pitch oscillations of approximately 0.2 to 0.3 deg/sec with a similar coupling response. The amplitude of vehicle body rates was approximately half that observed on the hardware evaluator in Downey, California. The oscillations that resulted from the 100-percent stroking test damped in approximately 10 seconds. The vehicle response during these tests was considerably less than expected, especially after considering the dynamic response to acceleration-command inputs.

The third service propulsion firing was also used to evaluate manual thrust-vector control in the docked configuration using rate command. The test was initiated with 45 seconds of firing time remaining, and switchover from the guidance system to the stabilization and control system was accomplished with the control switch. While the spacecraft was under primary guidance control, the autopilot had allowed the vehicle roll attitude to drift to the 5-degree deadband limit. At switchover, there was a rapid roll transient as the stabilization and control system brought the vehicle back to a zero-roll attitude. At the completion of this initial transient, the guidance system error needles were almost full scale in both yaw and pitch. The attitude excursions were reduced to zero for the remainder of the firing. The service propulsion engine gimbals were deliberately trimmed to the values indicated at the beginning of the firing so that there would be a resultant trim offset at the time of takeover. The values that were set on the trim thumbwheels were 1.1 degrees in pitch and 0.2 degree in yaw. Just prior to takeover, the engine had actually trimmed to 1.9 degrees in pitch and to 0.6 degree in yaw. The rotational hand controller proved to be somewhat more sensitive than noted on the mission simulator. However, the needles could be nulled without difficulty but

did tend to start moving immediately thereafter. The entry monitor system was used to perform an automatic shutdown of the engine. The displayed residuals were 2.7, 2.1, and 2.6 ft/sec in X, Y, and Z, respectively. As a result of this test, it can be concluded that, with moderate initial gimbal mistrims and attitude errors, manual thrust-vector control can provide steering comparable to the other control modes.

The fifth service propulsion maneuver was performed after the docked descent propulsion system firing. Since the descent engine firing applied approximately 6-1/2 minutes of negative acceleration to the service propulsion propellant retention cans, there was some concern that this acceleration would cause these cans to be voided of propellants and fill with helium. Ignition proved normal, and during the course of this firing, there were no physiological sensations nor chamber pressure indications that would show any abnormal operation of the service propulsion engine. Before flight, it was believed that a firing of this duration in the docked configuration would probably result in a large cross-axis velocity at shutdown. The cross-axis velocity actually observed at shutdown was 11.6 ft/sec.

The undocked firings were all nominal. The only item of note was the sixth firing, a 1.4-second, 38.8-ft/sec, minimum-impulse firing. The performance during this firing was excellent, with the largest velocity residual in any axis being 1.2 ft/sec. In summary, the eight service propulsion firings were performed in a satisfactory manner through the spacecraft weight regime of 90 000 to 22 000 pounds in both the docked and undocked configurations.

#### 10.2.5 Lunar Module Checkout

Lunar module activities.- After the tunnel was cleared of hardware, ingress into the lunar module was accomplished without incident. The upper hatch dump valve had been positioned in the dump position prior to launch, and there was no pressure differential across the hatch during ingress.

The two inboard aft restraint cables were used to aid in body positioning for the initial vehicle power-up and checkout. These restraints were satisfactory; however, access to the audio center controls was marginal because the transfer umbilical limited body motion.

Entry status check and electrical power activation were performed with no problems. The low taps on the descent batteries maintained sufficient bus voltage until it became necessary to switch to the high taps when about two-thirds of the circuit breakers had been activated.

Glycol pump activation was clearly audible, but the water separator light was not verified as planned. An excessive wait was required for the water separator to coast down to the limit where the caution and warning system would be activated.

Following activation of the communications system, the Lunar Module Pilot transferred to the lunar module environmental control system and the Commander transferred between the vehicles and also connected to this system.

The mission activities were about 1 hour behind the flight plan at this time, so certain systems checks were eliminated to insure adequate time for the more essential checks required prior to the docked descent engine firing. The checks eliminated were as follows: regulator, daylight telescope star visibility, S-band steerable antenna, S-band backup voice, and S-band conference. Except for the S-band steerable antenna check and the S-band conference check, the deleted items were all accomplished either fully or in part at a later time.

Upon deployment of the lunar module landing gear, a slight shock or short series of shocks was felt, and the landing gear indications were normal.

The portable life support system was donned for the communication and relay checks. The donning was found to be considerably easier than anticipated, and keeping the entire backpack from contacting the spacecraft switches and controls was no problem. Some difficulty was experienced in locking the battery into the portable life support system because of the complex design of the locking mechanism.

The docked platform alignment procedure worked very smoothly, and excellent alignments were achieved on each occasion.

The accelerometer bias check was satisfactory, although an error in loading the observed bias necessitated the reloading of three erasable memory locations.

The reaction control system pressurization and cold- and hot-fire checks were accomplished as planned. Reaction control thruster activity was quite audible during the hot-fire check, although positive identification with more than one thruster firing was not possible.

The thrust buildup for the docked descent engine firing was very smooth, as was the throttle-up to 40 percent. No engine noise was noticed and vibration during the firing was below the detectable level. The vertical reaction control engines had been deactivated, and there was no thruster activity associated with the firing subsequent to ullage. The

descent propulsion fuel and oxidizer tank pressures began to drop shortly after ignition, but within several seconds after automatic throttle-up to the fixed throttle point, the pressures returned to normal. During the firing, several small pieces of what was assumed to be insulation were seen moving out and below the descent stage. None were larger than about 6 inches in diameter. Throughout the firing, steering was very good, and the light for the gimbal drive assembly did not come on.

As the throttle-down point was approached, a low-amplitude oscillation developed, primarily in roll. The oscillation appeared to be non-divergent and was assumed to be a propellant-slosh phenomenon. The amplitude and frequency of this oscillation (several tenths of a deg/sec and less than 2 Hz) were detectable both on the rate needles and also as lateral body sway.

During the manual throttling portion of the firing, the engine responded both smoothly and rapidly to commanded throttle inputs.

After the docked descent engine firing, the spacecraft was powered down and sublimator dryout was initiated. The crew remained on the suit circuit longer than expected following termination of water flow to the sublimator. However, no excessive humidity was noted in this circuit during the next activation.

During final closeout, a very loud and sharp noise was generated as the cabin repressurization valve was moved from the automatic to the closed position, but the ground controllers verified that the noise was normal.

Command module activities.- Tunnel clearance (including hatch, probe, and drogue removal and stowage) and closeout (reinstallation of these items) were each performed four times during the flight. No procedural or mechanical difficulties were experienced. The configuration and operation of these components were excellent. The checklist mounted on the tunnel wall was a valuable aid during the mechanical tunnel operations.

Tunnel clearance was accomplished in approximately 5 to 7 minutes. One man operation was most efficient with the lower equipment bay open to facilitate movement of the components to temporary stowage locations. Control of the large masses in zero gravity was easy and reliable. The hatch was stowed in the open hatch bag under the left couch, the probe under the right couch seat pan, and the drogue over the seat pan and probe.

Tunnel closeout required approximately 20 minutes, including the 10 minutes required for probe preload and hatch-integrity check. The maximum force required to ratchet the probe was less than 50 pounds, and

no restraint straps were necessary since the center couch and tunnel wall provided adequate support. Alignment and procedural markings were excellent and clearly visible even though tunnel lighting was dim.

The only problem encountered during tunnel operations was the location and stiffness of the suit oxygen umbilicals. These umbilicals completely engulf the tunnel envelope, and when the pressure suit is worn, the hoses excessively restrict mobility. Manipulating the tunnel components around and between the hoses was annoying and time-consuming.

Support of the lunar module checkout consisted of maneuvering the combined vehicles to proper attitudes for optics evaluations, communication checks, platform alignments, abort guidance calibrations, and the initial attitude for the docked descent engine firing. Control modes from both the computer and the stabilization and control system were utilized in a variety of deadbands, and all produced excellent results. The most useful modes were autopilot for automatic 3-axis maneuvers, stabilization and control system with limit cycle for tight deadband holding, and stabilization and control system minimum impulse for gimbal-lock avoidance during drifting flight.

The necessity for monitoring to avoid gimbal lock seemed to occur an abnormally high percentage of the time. The command module platform was aligned out of plane in preparation for the docked descent engine firing, and because some force evidently tended to align the X-axis of the combined vehicles into the orbital plane, there was a repeated tendency for the spacecraft to approach gimbal lock during drifting flight. This condition required more propellant and time to correct than had been anticipated. Most of the time, the lunar module tended to be closest to the earth.

The technique for monitoring of the docked descent engine firing was satisfactory and provided useful information to the lunar module crew during the firing. The technique also confirmed the equality of the two guidance systems and gave some preview of solution comparisons between the two computers.

#### 10.2.6 Extravehicular Activity

Lunar module.- Because of illness of the Lunar Module Pilot, the plan for extravehicular activity was modified. The restricted operation was to include simultaneous depressurization of both spacecraft, with the Lunar Module Pilot operating on the portable life support system but connected to the lunar module environmental control system instead of the oxygen purge system for backup life support. No extravehicular operation outside the spacecraft was planned.

As preparations for this plan proceeded, however, considerable improvement in mobility was evidenced by the Lunar Module Pilot, and a more ambitious plan became possible. Consideration was given to performing the entire preplanned activity; however, it had already been decided for the crew to awaken 1 hour earlier on the following day to insure meeting the planned rendezvous timeline. Therefore, a 45-minute extravehicular operation was incorporated in the plan.

During initial checkout of the oxygen purge system, the heater-circuit test lights on the Commander's unit were intermittent. This malfunction did not affect the dual extravehicular transfer capability, and no change in plans was necessary.

Preparations for extravehicular activity proceeded according to the checklist. Handling of the extravehicular mobility unit within the cabin was again found to be quite easy. Communications proved to be excellent. The Lunar Module Pilot was not only able to conduct reliable two-way voice with the command module but was also able to receive direct VHF voice from the network prior to egress. The dump-valve filter was used during cabin depressurization, since there was considerable debris floating within the cabin. Some difficulty was experienced in gaining access to the forward hatch handle and dump valve. The absence of gravity and the bulk of the combined suits and extravehicular mobility unit required cooperative action by both crewmen to place and maintain the Commander in a position to open the hatch. No visor fogging or discomfort was noted by the Lunar Module Pilot during this time. Following the hatch opening, the pump and feedwater were activated in the portable life support system, and within about 3 minutes, the Lunar Module Pilot could detect a cooling effect.

Throughout the extravehicular activity, the portable life support system was kept at the minimum-cooling level and suit comfort was good. The extravehicular crewman's hands were warm, but not uncomfortably so. Mobility and body control were very good and considerably improved over that experienced in the airborne simulations in a KC-135 and during water immersion tests. Communications were very good, with the exception of confusion generated by the delay time in the command module VOX dropout. This characteristic caused many simultaneous transmissions, with a resultant squeal and loss of communication. Visibility throughout the extravehicular activity was excellent.

During extravehicular operations, the Commander exposed his suited upper body to space and observed rather rapid heating of the intravehicular gloves. The Commander's partial egress was made to evaluate the thermal and visual effectiveness of what were essentially internal space-suit components. The ultraviolet-stabilized helmet protector admitted a relatively high light level, but this level was not unacceptable for contingency operations from the command module.

The activities during and after ingress were all nominal. The television transmission was accomplished about 1 hour after ingress with apparently good results. The translunar bus circuit breakers were discovered inadvertently closed following tunnel closeout and necessitated an extra ingress into the lunar module.

Command module.- Activities in the command module in support of the extravehicular activity consisted of evaluating procedures and techniques utilized to insure efficient extravehicular transfer from the lunar module to the command module. The initial configuration of the command and service modules and final preparations for hatch opening and depressurization were of primary interest.

Each time the lunar module was manned and the tunnel hardware installed, the command module was configured for an extravehicular transfer to the point where a minimum of procedural operations were required to depressurize the command module and open the hatch to receive the Lunar Module Pilot. However, this initial configuration still provided a comfortable and efficient environment for sustained periods of one-man operation. The configuration was also designed to enable the Command Module Pilot to maneuver the command and service modules within the proximity of a tumbling lunar module and retrieve the lunar module crew in a free-space transfer.

The initial transfer preparations after installation of the tunnel hatch consisted of disconnecting and storing the L-shaped bag and center couch, configuring the left- and right-hand couch struts, disconnecting the counterbalance and preparing the jackscrews on the side hatch, routing the suit umbilicals for post-ingress availability, securing all loose equipment, and configuring for one-man communications. The total effort required approximately 50 minutes and was accomplished without difficulty.

Final preparations for hatch opening consisted of donning the helmet and gloves, configuring the environmental control system, performing a suit-circuit integrity check, and depressurizing the command module. These operations and opening the side hatch required approximately 10 minutes.

Cabin depressurization through the side-hatch vent valve required 3 minutes. The hatch required about 40 pounds of force to open fully and tended to remain in any position in which it was placed.

Movement within the open hatch and center couch envelope and in and out of the left couch was easy. No restraints other than the environmental control hoses were utilized or required, and no difficulties were encountered. The service module thermal samples were retrieved without fully extending the suit hoses.

The attitude of the spacecraft was established manually by visually orienting the side hatch relative to the sun and uncaging the gyros for minimum rate, maximum deadband, and 6-engine attitude hold. The interior of the open side hatch was exposed directly to the sun, but there was no sun shafting on the interior of the command module.

The environment within the standard suit worn by the Command Module Pilot was comfortable at all times, and no visor fogging occurred. An extravehicular visor assembly was utilized, but subsequent evaluation of the stabilized helmet shield indicated that it would be adequate during an actual transfer. An extravehicular glove was worn on the right hand and an intravehicular glove on the left. No temperature extremes were encountered with the intravehicular glove. Since manual spacecraft control capability with the extravehicular glove is marginal, the intravehicular gloves are considered superior to the extravehicular gloves for all command module operations.

At the completion of one dayside pass, the side hatch was closed with little effort (less than 50 pounds of pull). No temperature extremes were noted. The hatch seal appeared normal.

Command module repressurization to 2.1 psi with the oxygen repressurization package required approximately 4 minutes, including a hatch integrity check. Complete repressurization to 5 psi using lunar module oxygen through the tunnel hatch valve and recharging the surge tank to about 700 pounds required an additional 15 minutes. All times and pressures were comparable to those experienced in preflight chamber operations.

All the command and service module systems and procedures utilized throughout the extravehicular operation are considered excellent and will adequately support any extravehicular transfer envisioned at this time.

#### 10.2.7 Rendezvous

The rendezvous was a complex integrated exercise involving the ground controllers and the two spacecraft in both the docked and undocked configurations. This report will discuss the rendezvous in two separate sections. The first will deal with lunar module activities and the second with command module activities. Refer to section 5 for a complete discussion of the rendezvous performance results.

Lunar module.- The key to the successful completion of the rendezvous was adhering to the nominal timeline. On the previous 2 days, lunar module operations started late, and the time lost was difficult to make up. Because of the critical nature of the rendezvous timeline, the

crew began operations 1 hour earlier than required by the flight plan. However, the activities in the command and service modules progressed according to the flight plan, and entry into the lunar module occurred approximately 1 hour early. Lunar module activities also progressed smoothly, and the crew remained well ahead of the timeline.

Undocking began at the proper time. When the probe was extended, the two spacecraft separated until the probe had reached full extension. At this time, the relative motion stopped abruptly, and it was obvious that the capture latches were still engaged. After the probe control switches in the command module were recycled, the latches released and the lunar module separated from the command module. At that time, the lunar module abort guidance system was selected, and the spacecraft was maneuvered so that the Command Module Pilot could visually inspect the lunar module exterior. At the completion of these maneuvers, the lunar module began active station-keeping. Abort guidance system operation was good in the pulse and attitude-hold mode but was poor in rate command. The 20-deg/sec scaling in rate command caused overcontrolling, and a fixed rate could not be selected and held. This high sensitivity provided very poor control for orbital operations.

Immediately after the service module reaction control separation maneuver, the rendezvous radar was activated and a radar check was performed with excellent results.

At the completion of the radar test, the spacecraft was maneuvered to point the telescope at Sirius and a platform alignment was begun. Sirius, which was approximately 90 degrees from the sun, was clearly visible in daylight, and all five pairs of marks were made before sunset. It was possible to identify both Canis Major and Orion before the sun set. The second set of marks was performed on Acrux, and the resultant torquing angles were quite small, indicating the initial docked alignment was good. Since this docked alignment is quite accurate and can be accomplished quickly without the use of reaction control propellants, this technique should be used on later flights.

When the alignment was completed, the spacecraft was maneuvered manually to the attitude for the phasing maneuver. Upon reaching this attitude, the flight control switches were placed in the automatic mode of the abort guidance system. This control mode performed adequately both prior to and during powered flight with small post-firing residuals. After a smooth ignition, some engine roughness was noticed at approximately 20 percent during the manual throttle-up. When the throttling was stopped, the roughness stopped, and the throttle-up to 40 percent was continued without incident.

Immediately after the phasing maneuver, the radar was locked onto the command module. Main lobe lock-on was verified visually, and the resultant data were allowed to update the state vectors. All terminal phase initiation solutions for a post-phasing abort agreed closely, and a GO decision was made to bypass this abort maneuver. The second platform alignment was performed without incident completely in the dark. Again, the torquing angles were low. Radar acquisition was achieved prior to the point of closest approach, and the crew was able to verify an acceptable miss distance. The maneuver to the insertion maneuver attitude was accomplished with primary guidance in the automatic mode at 2 deg/sec. This control mode proved to be satisfactory for all automatic maneuvers performed throughout the spacecraft weight regime. The insertion maneuver at 10 percent throttle was nominal. In the docked configuration, there was considerable thruster activity when maneuvering to remove the Y- and Z-axis residuals.

When targeting the computer for the coelliptic sequence initiation maneuver, the second apsidal crossing was used. At 14 minutes before initiation of the maneuver, the final computation of the maneuvers was made, and the computer gave an answer that was obviously incorrect. The computer was retargeted using the first apsidal crossing, and the solution agreed very closely with that of the ground. The maneuver was performed using four-thruster plus-X reaction control thrustings. Staging was performed shortly after thrusting began. There was a loud bang and a cloud of small pieces of debris, typical of pyrotechnic separations, but no large attitude excursions. When vehicle control was assured, the ascent propellant interconnect was opened, and ascent propellants were used through the reaction control system for most of the maneuver.

Radar lock-on was achieved shortly after the coelliptic sequence initiation. Main lobe lock-on was verified using a chart of range versus signal strength. At that time, the command module was no longer able to observe the lunar module tracking light, and it became apparent that the light had failed. Radar tracking and the calculation of the maneuver solution progressed normally. The constant delta height maneuver was a 4-second firing of the ascent propulsion system under primary guidance control. The firing was satisfactory, with very low residuals. Ignition and shutdown were abrupt, and the noise level was not objectionable for a firing of this duration.

During the period between the constant delta height and terminal phase initiation maneuvers, automatic radar updating of the primary guidance system was again used. In addition, manual updating of the abort guidance system using radar data was also accomplished. The radar updates into the abort guidance system appeared within a short time to bring the range and range-rate data into good agreement with the radar data. However, it also appeared that the abort guidance range and range-rate information degraded much more rapidly in flight than it did in the simulator.

The pulse mode was used for control of the spacecraft during the greatest portion of coasting flight and for all radar updates. It proved to be an excellent control mode and responded in a manner very similar to that in the mission simulator. Once again, all of the available solutions were in close agreement. The lunar module primary guidance solution was used, as it was in all other maneuvers that were calculated onboard. At approximately 5 minutes before terminal phase initiation, the only apparent discrepancy in radar operation occurred. The signal strength on the automatic-gain-control meter slowly dropped from approximately 2.5 to 1.6, then slowly returned to 2.5 in approximately 3 minutes. This discrepancy was later attributed to non-optimum attitudes. The impulse at terminal phase initiation was applied in the plus-Z direction using the aft firing thrusters, and the radar stayed locked on throughout the maneuver.

The midcourse corrections were quite small and were performed as calculated. Residuals were easily reduced to within 0.1 ft/sec. The first braking gate had been set at a range of 6000 feet with a velocity limit of 30 ft/sec. No braking was required at that point, but thrust was required at the remaining gates. At approximately 2 miles, the command and service modules became visible as a blunt crescent. When braking was complete, automatic attitude maneuvers were performed using different rates and deadbands. In all cases, vehicle response was satisfactory.

The command and service modules rolled 60 degrees, and the lunar module, as the active vehicle, pitched over 90 degrees to begin the docking maneuver. It became apparent that the brightness of the reticle in the crewman optical alignment sight was not great enough to be seen against the mirror-like surface of the command and service modules. The Command Module Pilot talked the Commander in to a range of 4 or 5 feet. At this point, the Commander could see the reticle and completed the docking. The lunar module thrust in a plus-X direction at physical contact, and capture was achieved. The Command Module Pilot then manually retracted the probe, and docking was complete.

Command and service modules.- The function of the command and service modules during the rendezvous was to remain in an active navigational status and to be prepared to perform a major propulsive maneuver at any point in the rendezvous to maintain nominal relative motion between the vehicles. In general, this requirement implied mirror-image maneuvers with ignition at 1 minute after the planned lunar module ignition time. Additionally, the command and service modules had to provide the correct radar transponder orientation relative to the lunar module when the radar was active, coordinate major maneuvers with network, and remain current on lunar module status at all times.

The procedures and techniques for the command and service modules were designed to enable efficient one-man operations that would insure proper control modes and attitudes, optimum utilization of onboard navigational capability, and maximum coverage of systems status. The latter task was almost completely delegated to network flight controllers through telemetry based on the capability demonstrated during simulations. This relief proved to be a valuable asset, enabling the Command Module Pilot to devote maximum time to guidance, navigation, and control.

Tunnel clearance prior to lunar module separation was as previously described except that the probe was also preloaded according to the tunnel checklist, with no difficulty. The 12 docking latches were released and cocked with little effort. Two latches initially appeared to obtain the complete preload after only one stroke. However, after a number of recycles, they operated normally, and inspection after redocking revealed that all 12 latches had automatically engaged.

Undocking was initiated on time according to the standard procedure. However, on the first two cycles of the EXTEND/RELEASE switch, the capture latches failed to release even though both probe indicators read properly with the switch in correct position. Subsequent movement of the switch to RETRACT and then back released the capture latches, and the lunar module disconnected.

Station-keeping and lunar module inspection were performed as planned, except for the descent engine inspection, which was eliminated to insure an on-time separation maneuver. Visual inspection of landing gear downlocks confirmed that each could be verified from the command module by their geometrical configuration. The separation maneuver was nominal and was performed on time. The subsequent platform alignment, calibration of the crewman optical alignment sight, and lunar module tracking were performed according to the timeline with no difficulty. Automatic tracking of the lunar module using the rendezvous navigation program at these close ranges appeared smoother and more accurate than in simulations.

The initial evaluation of the one-man operation utilizing automatic control and optics and the preflight navigation schedule indicated the entire system was performing better than expected. Post-phasing rate drive was smooth; engine firings were not noticeable after the initial entry from each group of marks; auto-optics pointed the sextant within 1 degree of the lunar module; the lunar module was clearly visible both day and night; onboard computer programs operated as expected; and the terminal phase initiation solutions in both spacecraft agreed very closely throughout the exercise.

After initial evaluation, the spacecraft was retained under primary guidance control throughout the remainder of the rendezvous and performed in an excellent manner. The only manual maneuvers executed were attitude changes to properly orient the transponder at the completion of major lunar module maneuvers to avoid exit from the thrusting computer program prior to its normal completion. Manual control was required because of a known deficiency in the related software.

During daylight, the lunar module was visible in the sextant as a definite scaled image even at the maximum daylight range of approximately 70 miles. The lunar module tracking light, when operational, was also visible through the sextant during daylight. Relative sun position did not affect visibility through the sextant at any time. However, reflections from the prism joint on the scanning telescope completely obscured the lunar module at certain times (for example, 20 minutes prior to terminal phase initiation).

The command and service modules were prepared to support each major lunar module maneuver according to preflight established guidelines. Adequate time was available to coordinate lunar module tracking requirements, maneuver to the firing attitude, check spacecraft systems, start and check gimbal motors, and be prepared for ignition at least 2 minutes prior to the command and service module ignition time.

Communications were adequate to maintain cognizance of lunar module status at all times, except for the 10-minute period prior to and just after coelliptic sequence initiation when the relative orientation of the two spacecraft precluded direct communications. Voice communication with network was adequate during this period. Network coordination and support of both vehicles was superior throughout the rendezvous, and there was never any confusion or doubt as to the status of either vehicle. Ground-calculated maneuvers were timely and accurate. Interruptions were minimal, and response to requests was immediate.

As described in section 5, the primary function of the command module during a lunar module rendezvous is to provide backup maneuver solutions so that "mirror image" impulses could be applied in the event of a lunar module contingency. The only potential problem which affected command module operations during the rendezvous was the failure of the tracking light at lunar module staging. Because of this outage, onboard optical navigation was not possible for approximately 1 hour, during which two major lunar module maneuvers were to be performed. However, lunar module data were entered into the computer, and automatic rate drive of the command module was maintained throughout this period to insure correct transponder orientation. Onboard state vector extrapolation was so precise that visual sighting of the ascent stage was made 5 minutes after the constant differential height maneuver using automatic pointing of the optics. The ascent stage was only 0.5 degree from the sextant optical axis. After

a nominal mark sequence, comparisons of range and range rate with lunar module data showed exact agreement in range and to within 5 percent in range rate. A tabulation of rendezvous solutions from all sources is given in table 5-IV, which exemplifies the excellent agreement of command module backup computations. The diastimeter, securely mounted at the window, provided accurate and readily accessible range data during the last 3 miles.

During the switch-configuring operation prior to the final lunar module docking, the EXTEND/RELEASE switch produced incorrect indications. However, recycling the switch resulted in the correct indications.

The lunar module active docking was well within the capture boundary. After aligning the spacecraft with minimum impulse, retraction was accomplished using the secondary retract system. The latching of the docking rings was accompanied by a loud noise and obvious rigid joining of the two vehicles.

Monitoring of the docking with the lunar module as the active vehicle indicated that in all cases, docking would be easier, more accurate, and less time-consuming if the command and service modules were the active vehicle.

#### 10.2.8 Post-Rendezvous Orbital Activities

Alignments.- All alignments prior to service propulsion maneuvers were accomplished satisfactorily according to checklist procedures, with coarse alignment requiring 10 minutes and fine alignment 5 minutes. The pre-maneuver star-attitude check was normally within 2 degrees. A fine alignment using the scanning telescope alone was only slightly less accurate than with the sextant. The option to align using a planet was performed for the first time using Jupiter, and the alignment was accurate and repeatable. A relatively accurate platform alignment was obtained using the crewman optical alignment sight, and subsequent improvement with sextant sightings was less than 0.1 degree. Calibration of this sight was repeatable after removal and replacement in the mount. The gyro display coupler was aligned successfully using the scanning telescope and minimum-impulse control with the south star set, and agreement with the platform was within 1.4 degrees after a 180-degree attitude maneuver.

Landmark tracking.- The roll/yaw landmark tracking technique was evaluated, and although the procedures were good, results were minimal because of cloud cover and the high earth orbital line-of-sight rates. In-plane platform alignment was satisfactory, and the times of acquisition and closest approach are both considered necessary. A rather surprising discovery was the capability to take landmark sightings using

the sextant in the medium-resolved control mode at 10-second intervals. The scanning telescope was used for target acquisition. Extrapolation to the lunar orbit case with the additional use of the automatic digital autopilot rate-drive about the X-axis indicate this to be a very efficient method of landmark tracking, either with the lunar module or during one-man command module operations.

Earth photography experiment.- The photography experiment (earth terrain) was completed successfully. The equipment was well designed, easy to install, and simple to operate. The requirement to maintain vertical pointing of the cameras during the photography sequence was completed both manually and automatically. The manual technique of maneuvering in minimum impulse using a special orbital rate display was acceptable but inferior to the autopilot rate drive. This experiment provided an ideal opportunity to evaluate the capability of the autopilot to rotate the spacecraft about any axis at any specified rate, while attitude holding in the other two axes. In this case, exact orbital rate about the Y-axis was selected utilizing a nominal alignment. This technique produced excellent results; the rate drive was smooth and efficient and the spacecraft attitudes were precise. Procedures used were in accordance with the checklist.

Passive thermal control.- Another application of the autopilot rate drive capabilities was verified in a passive thermal control exercise. Checklist procedures were used to initiate a 0.1 deg/sec roll rate about the X-axis. The attitude deadband was then increased in steps to a maximum of 25 degrees without affecting the roll rate. The technique was reliable, simple, and apparently very efficient. The deadband change was accomplished by merely changing one erasable location in the computer.

Visual sightings.- The Pegasus satellite was observed visually twice; acquisition was based on gimbal angles and time provided by the network. The diastimeter was utilized in the left rendezvous window mount to acquire and track the satellite. On one sighting, the Pegasus was observed through the crewman optical alignment sight in the right rendezvous window.

The lunar module ascent stage was automatically acquired and manually tracked through the sextant after the ascent propulsion maneuver to depletion. State vectors of both vehicles were uplinked by the network. The ascent stage orbit at the time was 3761 by 127 miles. Pointing accuracy using the digital autopilot was good enough to acquire initial contact at a range of 2500 miles approximately 16 minutes before reaching closest approach. Continuous visual tracking was possible for a 6-minute period from a range of 716 miles to 800 miles, during which time marks were made at 1-minute intervals to update the lunar module state vector. The final sighting was made at a range of 2700 miles against an earth background.

### 10.2.9 Retrofire, Entry, and Landing

Preparation for retrofire started somewhat earlier than required by the flight plan. The telescope shaft drive had been malfunctioning for the first 5 days. To allow time to compensate for a possible failure and still insure an aligned platform, the first alignment was planned such that there would be at least three night-side passes prior to retrofire. However, the telescope did not malfunction, and the initial alignment in-plane was completed some 5 or 6 hours before retrofire. The crew then completed entry stowage. The major portion of the stowage had been completed the previous day, and only a few unstowed items remained. This terminal portion of the stowage took approximately 1 hour.

During the systems check prior to retrofire, it was discovered that the entry monitor system had a potential problem. During the checks of the scroll drive system, it was noted that the scribe operated properly on the test patterns but would not scribe through the scroll film when slewed to the entry pattern. All other deorbit preparations were normal.

A number of checks were performed prior to retrofire and during entry to assure the crew that the spacecraft was in the proper attitude and that the guidance and navigation system was performing properly. The first of these checks was the deorbit attitude check, a 12-minute series of attitude verifications. Since retrofire would occur approximately at sunrise, the crew checked the spacecraft attitude one orbit before retrofire to determine whether they could actually see the horizon. During these checks, it was found that poor horizon lighting at sunrise precluded making exact attitude checks during this period. However, the crew was able to verify the deorbit attitude by performing a sextant star check one orbit prior to retrofire.

Retrofire was nominal, with the velocity residuals very low and the firing time as expected. After retrofire, all the checks in the command module were completed, and command module/service module separation occurred as planned. The command module was then flown to entry attitude using the window markings and the horizon.

A series of guidance checks was started at 0.05g. At that time, the out-the-window view and the attitude error needles on the flight director attitude indicator agreed very closely and indicated that the guidance and control system was steering the spacecraft to the proper attitude. The time of 0.05g calculated by the guidance computer compared closely with that sent by the ground.

At 0.2g, the downrange error was within 15 miles of that provided by the ground and was a GO condition. The first steering command was given when the downrange error dropped to 6 miles, still a GO condition. From

command module/service module separation until 0.05g, the spacecraft was flown in the pulse control mode. At 0.05g, spacecraft control was turned over to the primary guidance system for the remainder of entry.

As the entry began, it became apparent that the entry monitor system would not scribe through the emulsion on the film. The Commander could obtain range potential from the entry monitor system scroll and compare this with the range to go. It was a crude scheme but did give some assurance to the crew that the guidance system was steering properly. The maximum value indicated by the g-meter during entry was 3.2g. At the time a velocity of 1000 ft/sec was reached, the onboard displays indicated a range-to-go of 1.1 miles.

The drogues were deployed automatically and appeared to be normal. The main parachutes were deployed automatically, but initially it appeared that only two parachutes were out. As they filled with air and went to the reefed position, it became apparent that there were three normal parachutes. After they were disreefed, the Commander saw one small hole in one parachute and later three small holes in either the same parachute or another one.

The spacecraft landed within seconds after the altimeter passed through the corrected altitude. The landing was not particularly hard, the parachutes were released immediately after touchdown, and the spacecraft remained in the stable I position. Postlanding equipment operated properly, and the uprighting bags were not deployed, since the swimmers had the flotation collar around the spacecraft before the time these bags were to be deployed. After the spacecraft flotation collar was in place, the hatch was opened and the crew egressed into two waiting life rafts. The crew was then picked up by a helicopter and flown to the aircraft carrier, which was then only a few hundred yards away.

#### 10.2.10 Lunar Module Systems

The primary guidance, navigation, and control system performed flawlessly throughout the mission. Docked operations were satisfactory, and no difficulty was experienced in performing the docked platform alignments. The alignment optical telescope performed well, although some difficulty in achieving satisfactory focus was noted. The star and reticle did not appear to focus simultaneously and some parallax was noted. However, on two of the three alignments with the telescope, a star angle difference of less than 0.01 degree was obtained.

The abort guidance system performed satisfactorily, except that the data entry and display assembly operator error light illuminated many times and had to be cleared, and the caution and warning light remained

on throughout the rendezvous. Manual attitude control in the abort guidance system was judged as too sensitive to controller inputs for orbital work.

The landing radar was hardwired to operate in either the self-test mode or in conjunction with the computer spurious noise test. No spurious lock-ons were observed during any of the firings, and the self-test was normal on all occasions.

The rendezvous radar functioned normally throughout the flight. The antenna temperature remained below the expected level throughout the rendezvous, and the signal strength was equal to or greater than expected for all ranges.

The descent propulsion system functioned smoothly throughout the flight, with only two exceptions. The first was a decrease in the fuel and oxidizer tank pressures for the first 30 seconds of the docked descent propulsion maneuver. This problem cleared itself shortly after the guidance controlled throttle-up, and no further action was required by the crew. The second discrepancy was a short period of roughness during the manual throttle-up to 40 percent during the phasing maneuver. When throttling was interrupted, the engine stabilized and the throttle-up was continued. It was assumed by the crew that a bubble of helium gas had been ingested by the engine. All engine starts were very smooth, and no noise or vibration was noted by the crew during descent engine firings. The ascent system interconnect was employed for the coelliptic sequence initiation maneuver and functioned properly except that one of the ascent-feed indicators stuck momentarily.

No unusual observations were made concerning the reaction control system. Although all thruster firings were clearly audible, it is not certain whether cues were detected during sustained thrusting or only during the on/off transient periods.

The atmosphere revitalization section performed satisfactorily except for the high level of cabin noise. The primary noise source was the cabin fans, although the glycol pumps and suit fans also contributed. The noise level was high enough to cause objectionable interference on the intercom when the crew had helmets off. Another minor problem was encountered in replacing the primary lithium hydroxide canister cover. The mechanical design of this cover is such that a very small initial misalignment causes the cover to bind and close improperly. There were no persistent odors and no objectionable humidity or temperature conditions.

The oxygen supply and cabin pressure control section performed normally. Cabin dump and repressurization were satisfactory, except for the longer-than-normal depressurization time caused by the dump-valve

filter, which is used to protect the valve from debris floating within the cabin. Another disturbing factor was the loud report generated by positioning the cabin repressurization valve from AUTO to CLOSE. This report was subsequently confirmed as a normal occurrence.

The water management system performed normally. One interesting disclosure was that, with the bacterial filter installed, flow rates were much greater in orbit than those experienced at 1g during simulations.

The only observed abnormality of the heat transport section was the illumination of the glycol caution light caused by activation of the development flight instrumentation. This discrepancy was apparently an electromagnetic interference effect, since the glycol temperature indicated a step increase/decrease as instrumentation power was cycled.

The problem which most affected crew operation in the communications system was the loss of the Lunar Module Pilot's push-to-talk capability on the rendezvous day. This loss necessitated the use of VOX for all the Lunar Module Pilot's transmissions. In general, communications throughout the lunar module activity period were good. However, because of the multiplicity of configurations and conditions experienced in earth orbit, it is difficult to establish reasons for the several instances of degraded communications.

Although instrumentation was generally good, the response of the glycol temperature readout to tape recorder activation was disconcerting, and the bias and hysteresis characteristics of the rate indicators were objectionable.

When the window heaters were used with the shades deployed, the spacecraft windows tended to get very hot under direct solar impingement. The window temperature became so high that the window shades lost their design roll-up characteristics and required special handling.

The pallet retention handle on the aft bulkhead did not function properly. It was impossible to lock the pallet on the back wall, and special handling was required.

The restraint system functioned as designed; however, the total force was too high. A reduction by a factor of 2 to 3 would be more desirable.

#### 10.2.11 Command and Service Module Systems

Guidance platform operation appeared to be nominal throughout the flight once the proper X-axis accelerometer bias compensation was loaded

after launch. Accelerometer bias checks and compensations were performed exclusively by the network, and this procedure was accurate and efficient without inflight coordination. The computer operated properly except when keyboard inputs were apparently not recognized by the internal program. This discrepancy occurred once when the autopilot configuration was changed and again when the autopilot was deactivated (section 17 contains a discussion of this problem).

The autopilot control of the spacecraft was excellent in all six configurations, and only five relatively minor deficiencies were noted. Manual rate command is discrete rather than proportional, and the 4 deg/sec rate is somewhat high in either automatic or manual maneuvering; 2-deg/sec would be more useful. A preset 0.2-degree attitude deadband would enable optimum use of the autopilot during docking, although this capability is available by an erasable entry through the keyboard. Pure single-axis rotational maneuvers in acceleration or rate command are not available. The pre-entry autopilot mode appears to be very inefficient. Minimum impulse control is not available through the rotational hand controllers. Other than these minor discrepancies, the autopilot is the optimum control device for performing the entire lunar mission; with the rate drive capabilities demonstrated during the earth terrain experiment, the autopilot has great potential for earth orbital operations. Techniques such as adjacent-quad attitude hold, three-quad automatic maneuvers, and passive thermal control are important for propellant management and should be expanded in concept for use on future flights.

The optical system could be modified in a number of areas to improve operations, although it performed in a very satisfactory manner. The scanning telescope shaft drive stuck a number of times during the first 5 days because a pin was lost from the drive mechanism. Other noted discrepancies are inherent design deficiencies, some of which have been reported on previous flights. The prism joint on the exterior of the telescope produces a wide band of light across the center third of the view field because of reflected external light. The sextant exhibited an apparent increase in the manual drive deadband at the end of the flight. The image of scenes through the landmark line-of-sight while tracking targets or landmarks through the star line-of-sight is annoying. The reticle was fuzzy at all illumination levels, whereas the telescope reticle was sharp and clear. The quick disconnect feature of the eyepieces is excellent; however, the focus and eyeguard portion of the eyepieces tended to rotate because of vibration and had to be retained with tape.

Certain stars (e.g., Acrux and Regor) could be identified in the sextant during daylight navigation sightings because of their known relationship to adjacent secondary stars. With star charts for the sextant field of view applied to identification, translunar navigation would be immensely improved under adverse lighting conditions.

The stabilization and control system is excellent, and the many existing capabilities were very useful throughout the flight, particularly in coordinating and assisting in lunar module checkout and in reaction control propellant management. The limit cycle function appeared very effective during attitude hold, both docked and undocked. Six-thruster attitude hold also worked very well.

The entry monitor system failed to scribe an acceleration/velocity trace during entry and was ineffective in providing a backup entry ranging capability. The velocity counter in this system performed almost perfectly for all maneuvers.

The service propulsion system performed very well. However, the gaging system was questionable because of the erratic behavior experienced on long firings and the number of sensor warnings which resulted from the indicated unbalance. However, preliminary investigation indicates the possibility of a difference in the actual inflight operation compared with the expected operation based on preflight simulation.

With the exception of the unexplained closure of three sets of propellant isolation valves prior to initial docking, the reaction control system performance was nominal. Preflight propellant usage budgets were inaccurate because of the incomplete timelines and maneuver requirements defined at the time the budgets were calculated. Integrated mission simulation data should be used to evaluate and plan preflight propellant utilization.

Because of the periodically high condenser-exit temperatures, fuel cell 2 required more inflight attention than expected. The onboard management of cryogenic hydrogen pressure to preclude bothersome warning indications was a problem throughout the flight. Caution and warning limits were within the normal operating range of the system and required considerable manual switching of the automatic system to provide adequate periods of warning-free operation.

Environmental control system operation was very good, except for numerous minor discrepancies. The manual surge-tank valve did not open the surge tank until it had been rotated approximately 30 degrees beyond the ON position. The amount of gas in the potable water system was unacceptable and was a constant detriment to the operational timeline and to crew health. Water from the area of the environmental control unit collected in the center of the aft bulkhead during service propulsion maneuvers. The expected sequential numbers could not be found on the lithium hydroxide canisters. Too many operations were required to dump waste water. The primary evaporator was deactivated after the first day, and the radiators were adequate for the remainder of the mission. The radiator flow control automatically switched to valve 2 during a rest

period for no apparent reason, but subsequent recycle to valve 1 after power-up allowed continuation with no further problem.

In the communications systems, the S-band transponder was switched to secondary unit midway through the flight at network request. The VHF B frequency, used by other agencies, should be the exclusive frequency to prevent crew wake-up during rest periods when VHF is being used for network monitoring. Range aircraft often have considerable background noise and should be on call only during initial mission phases. The VOX delay at the completion of transmissions is too long, causing confusion and preventing rapid sequential transmissions among vehicles. The timing on lunar module VOX circuits is far superior.

The S-band high-gain antenna operation was evaluated during the passive thermal control exercise as the spacecraft passed over Carnarvon and Hawaii. The antenna did not return to the manually set reacquisition angles after Carnarvon passage; however, it did slew to the proper angles at Hawaii signal loss. The signal strength fell from almost maximum to zero in both cases. Tracking was smooth with constant lock-on during both passes. Network control and operation of the onboard data storage equipment through the use of real-time commands was satisfactory and saved considerable crew time and effort.

Because of the great number of mechanical systems in the command and service modules, a complete discussion of their operation, both inflight and in training, is not possible. Documentation explaining these systems to the crew and their operation in all modes is inadequate. The operation of the tunnel hardware was excellent. The side hatch worked very well, particularly during extravehicular operations. However, gearbox shear pin markings are inadequate; the markings show the shear pin to be at some position but not which position. Side hatch operation would be considerably more efficient with a checklist attached near the hatch. The foldable couch was a definite asset during the flight. Center couch removal was simple and efficient.

## 11.0 BIOMEDICAL EVALUATION

This section is a summary of Apollo 9 medical findings and anomalies, based upon preliminary analyses of biomedical data. A more comprehensive evaluation will be published in a supplemental report.

During this mission, the three crewmen accumulated 723 man-hours of space flight experience, including approximately 47 minutes of extravehicular activity by the Lunar Module Pilot. Physiological data were obtained simultaneously from all three crewmen at three independent sources, the command module, the lunar module, and the extravehicular mobility unit. As in Apollo 8, symptoms of motion sickness were experienced during adaptation to the space environment.

The Apollo 9 crewmen also participated in a series of special medical studies designed to assess changes incident to space flight. In general, the physiological changes observed after the mission were consistent with those observed in earlier missions.

From the viewpoint of crew health and safety, a preliminary analysis of the data indicates that the lunar module and the extravehicular mobility unit provided habitable environments.

### 11.1 BIOINSTRUMENTATION PERFORMANCE

The Command Module Pilot's sternal electrocardiogram signal was degraded at about 87 hours of flight. The baseline shifted frequently, and the signal-conditioner output was intermittently blocked; however, the quality of his impedance pneumogram signal was excellent. The problem was corrected inflight when the Command Module Pilot replaced his sternal electrocardiogram lead with a spare set. The data quality was good, and no further problems developed.

The Commander's axillary impedance-pneumogram signal and the Lunar Module Pilot's sternal electrocardiogram signal were each lost at different times later in the mission. In the Lunar Module Pilot's case, the signal was restored when the electrode paste was replenished, and the loose sensor was reapplied to the skin. In the Commander's case, the wire was demated and remated and the signal was restored.

Temperature-sensitive indicator tape, used to measure the maximum temperatures of the dc-dc converters, indicated temperatures of 120° F for the converters used for the Commander and Command Module Pilot and 125° F for that of the Lunar Module Pilot. These temperatures were less than the predicted maximum for the converters. The electrocardiogram

data received through the portable life support system during extravehicular activity were occasionally degraded by small noise, however this was insignificant when compared to the preflight expected interference.

## 11.2 PHYSIOLOGICAL DATA

The average heart rates during waking hours were 87 beats/min for the Commander, 78 beats/min for the Command Module Pilot, and 69 beats/min for the Lunar Module Pilot. The standard deviations for the heart rates were 17, 28, and 28 beats/min, respectively. Prior to and during launch, significant increases in heart rate were recorded for the Commander and the Command Module Pilot, while the Lunar Module Pilot's heart rate was only slightly over his average value (fig. 11-1). The heart rate changes during major mission events are presented in table 11-I. The average heart rates during major mission events were 96, 79, and 67 beats/min, respectively.

## 11.3 MEDICAL OBSERVATIONS

Preflight illness.- Three days before the scheduled Apollo 9 launch, the Commander reported symptoms of general malaise, nasal discharge, and stuffiness. These common cold symptoms were not present on the physical examination performed the previous day. The Commander was treated symptomatically and his temperature remained normal throughout the course of his illness. Two days before the scheduled launch, the Command Module Pilot and the Lunar Module Pilot also became ill with common colds and were treated symptomatically. However, because the symptoms persisted, the launch was postponed for 3 days. The crew responded rapidly to rest and therapy and were certified fit-for-flight the day prior to the rescheduled launch.

Lift-off and powered flight.- The Commander and Command Module Pilot demonstrated the characteristic heart-rate responses to lift-off and to the acceleration of powered flight. The Commander's and Command Module Pilot's heart rates at lift-off were 121 and 82 beats/min, respectively, and changed insignificantly throughout powered flight. The Lunar Module Pilot's heart rate, 72 beats/min, was the lowest ever observed at lift-off. After 3 minutes of flight, however, his heart rate had increased to 96 beats/min.

Weightlessness and intravehicular activity.- Following orbital insertion, all crewmen noted the characteristic feeling of fullness of the head described on previous missions. This sensation was of short duration.

Apollo 9 was the second consecutive mission in which the crew experienced symptoms of motion sickness during adaptation to the space environment. The Command Module Pilot reported that, when first leaving the couch to make a platform alignment in the lower equipment bay, he recognized the need to perform all head movements slowly. He did not, however, experience nausea or vomiting as a result of these activities. After several days of flight, the Command Module Pilot reported that he felt no unusual effect from rapid, unguarded head movements.

As a prophylactic measure against motion sickness, the Lunar Module Pilot took one Marezine tablet at 3 hours before lift-off and a second tablet at 1-1/2 hours after orbital insertion. Nevertheless, he experienced a mild dizziness when leaving his couch the first day and when turning his head rapidly. The dizziness did not seem to interfere with performance of his duties and was controlled without medication. However, he definitely had to restrict head movements to forestall the onset of motion sickness. He was most comfortable when executing all movements slowly and turning at the waist instead of the neck. Nausea did not accompany the dizziness produced by head movements.

After donning his pressure suit for transfer to the lunar module, the Lunar Module Pilot was sitting quietly in the lower equipment bay when he vomited suddenly. The vomiting was spontaneous and without warning. He was, however, able to retain the vomitus in his mouth long enough to use a disposal bag effectively. About 4 hours later, the Lunar Module Pilot vomited a second time shortly after transfer to the lunar module. The second vomiting was preceded by nausea. Aspiration of vomitus did not occur on either occasion. Just prior to the second vomiting, the Lunar Module Pilot was engaged in activities which required considerable movement within the lunar module.

In the postflight medical debriefing, the Lunar Module Pilot could not recall whether, after having vomited the first time, he had experienced any particular relief. Immediately following the second vomiting, he did feel much better and noted a rapid and marked improvement in his capability to move freely. The residual symptom was loss of appetite and an aversion to the odor of certain foods. Until the sixth day of the mission, he subsisted exclusively on liquids and freeze-dehydrated fruits.

In the postflight medical debriefing, both the Command Module Pilot and the Lunar Module Pilot described momentary episodes of spatial disorientation. These episodes were experienced when they donned their pressure suits early in the mission. The Command Module Pilot reported that, after he had closed his eyes, doubled up, and thrust his head through the neck ring of the suit, he was unable to differentiate up or down for several seconds. The brief spatial disorientation also produced what he described as a queasy feeling, which lasted for about 2 minutes;

however, he did not experience vertigo. When the Lunar Module Pilot donned his suit, he reported a definite sensation of tumbling for several seconds. Although he did not experience nausea or vertigo, he did feel the need to remain still for several minutes.

Crew reports.- The integrated radiation dose received and the estimated sleep quantity obtained during each sleep period were reported by the crew daily. The total radiation dose received by each crewman during the flight was about 0.2 rem. This dosage is medically insignificant. The crew's sleep estimates are presented in the following table.

Flight day	Sleep time, hr		
	Commander	Command Module Pilot	Lunar Module Pilot
1	2	6	7
2	6	7	7
3	7	7	7
4	5	5	5
5	8	8	8
6	8	7.5	8.5
7	9	9	8.5
8	7	6.5	6.5
9	7.5	7.5	6.5
10	6	7.5	8
Total	65.5	71.0	72.0

In addition to daily radiation and sleep information, the crew also reported all medications taken inflight. Afrin (nasal spray) was used periodically by all crewmen, but the exact amounts were not recorded. The following oral medications were consumed during the mission:

Drug	Number of units taken		
	Commander	Command Module Pilot	Lunar Module Pilot
Actifed (decongestant)	5	0	5
Aspirin (headache)	4	0	0
Marezine (motion sickness)	0	0	2
Seconal (sleep)	0	0	7

Direct medical consultations.- The first medical consultation was held after about 40 hours of flight. The Lunar Module Pilot was given

the heart-rate limits, determined from a preflight ergometry study, for controlling his extravehicular activities. The second medical consultation pertained to the Lunar Module Pilot's motion sickness. The crew reported that the potable water from the command module water dispenser contained about 60-percent hydrogen gas and 40-percent water and was causing the crew some abdominal distress. The crew was advised to drink from food bags filled with water instead of drinking directly from the water gun.

The final medical consultation was held after 54.5 hours of flight. The Lunar Module Pilot was reported as still not feeling well but had experienced no further vomiting. Neither the Commander nor the Lunar Module Pilot had eaten any solid food during the day. The Lunar Module Pilot reported he had experienced no symptoms of motion sickness so long as he remained still. He was advised to take a Marezine tablet 1 hour before donning his pressure suit for the reduced extravehicular activity.

Extravehicular activity.- On the morning of the fourth day, the Lunar Module Pilot's symptoms of motion sickness had significantly subsided, and he felt completely recovered. At about 71 hours, a decision was made to perform a modified extravehicular activity that would allow the Lunar Module Pilot to exit the lunar module and remain on the lunar module forward platform during one daylight pass. The transfer to the command module hatch was deleted because of the time constraints. The Lunar Module Pilot was able to perform his extravehicular activities without difficulty.

During the extravehicular period, the Lunar Module Pilot's heart rate ranged from 66 to 88 beats/min, with an average of 75 beats/min. His metabolic rate was determined with excellent correlation using three independent techniques, as follows:

Method	Total Btu produced
Heart rate	520
Liquid cooling garment thermodynamics	523
Oxygen bottle pressure decay	497

The work rate during the extravehicular activity was about 600 Btu/hr. A total of 1170 Btu were removed by the portable life support system during the 110-minute period of use. Calculations of Btu produced during the 47-minute period of extravehicular activity are listed in the previous table. Compared to the extravehicular activity during the Gemini Program, this work load was exceedingly light.

Work/rest cycles.- This mission was the first in which all three crewmen slept simultaneously. A definite improvement over the previous two flights was observed in the estimated quantity and quality of sleep. The lack of postflight fatigue was correspondingly evident during the physical examination on recovery day. It should be further recognized, however, that crew work load during the last 5 days of flight was significantly lighter than on previous missions.

The flight plan activities for the first half of the mission resulted in excessively long work periods for the crew, and the time allocated for eating and sleeping was inadequate. Crew performance, nonetheless, was outstanding. Departures from the crew's normal circadian periodicity also contributed to some loss of sleep during this time. The crew experienced a shift in their sleep periods, which varied from 3 to 6 hours from their assumed Cape Kennedy sleep time.

Inflight exercise.- As in previous Apollo missions, inflight exercise was solely for maintenance of the crew's relaxation, and a calibrated exercise program was not planned. The crewmen were unable to use their inflight exerciser for the first 7 days of flight because of their heavy workload. On the eighth day the clip which attached the rope to the webbing of the exerciser failed, terminating exercise. In the post-flight medical debriefing, the crew stated that the exerciser became too hot to touch during only mild exercise.

#### 11.4 PHYSICAL EXAMINATIONS

Preflight examinations were conducted at 30, 14, and 4 days prior to the original launch day. (The preflight illness and 3-day launch postponement have been previously discussed.) A cursory physical examination was performed on the morning of flight, and a comprehensive physical examination was completed after recovery.

The crewmen experienced no nausea or vomiting while awaiting recovery after landing. They were fully alert and exuberant aboard the recovery helicopter and were able to walk in a well coordinated manner aboard the recovery ship.

The recovery day physical examinations were accomplished in approximately 4 hours. All planned postflight medical procedures were conducted, with the exception of collecting sputum for Beta-fiber analysis. As stated, the crewmen appeared much less fatigued than those for Apollo 7 and Apollo 8.

During the lower-body negative pressure tests aboard the recovery ship, moderate cardiovascular deconditioning was observed in all crewmen.

The test on the Lunar Module Pilot was terminated prematurely because of presyncopal symptomatology (slight faintness associated with a decrease in blood pressure and heart rate). The Commander developed presyncopal symptoms just as his test was completed. All cardiovascular responses returned to normal within 2 days after recovery.

The crewmen tolerated the ergometry tests well, but each demonstrated the characteristic initial elevation of heart rate. The ergometry responses returned to normal within approximately 24 hours.

The only significant postflight medical finding was a mild bilateral inflammation caused by pressure differences in the Commander's middle ear cavities (bilateral barotitis media). This condition responded rapidly to decongestant therapy and cleared after 2 days.

Changes in body weights are shown in the following table.

Time	Weight, lb		
	Commander	Command Module Pilot	Lunar Module Pilot
Preflight	158.75	178.25	159.13
Recovery day	153.5	172.5	153.0
Day after recovery	156.25	181.0	157.25

Four days after recovery, the Lunar Module Pilot developed an upper respiratory infection with a secondary bacterial bronchitis. He was treated with penicillin and was well 7 days later. The etiology of the primary infection was determined to have been a type-B influenza virus.

The Commander developed a mild upper respiratory syndrome 8 days after recovery. He was treated symptomatically and recovered 4 days later. The etiology in this case was also a type-B influenza virus.

TABLE 11-I.- HEART RATES DURING MAJOR FLIGHT EVENTS

Event	Heart rate, beats/min											
	Commander				Command Module Pilot				Lunar Module Pilot			
	Mean	Standard deviation	High	Low	Mean	Standard deviation	High	Low	Mean	Standard deviation	High	Low
Prelaunch	87	10.1	105	75	65	14.5	80	55	61	10.5	70	50
Launch	115	13.8	145	70	99	20.2	135	70	71	18.8	95	50
Command and service module/S-IVB separation	114	16.0	176	69	122	7.9	127	117	72	14.3	88	41
Spacecraft ejection from S-IVB	98	19.4	166	77	80	12.2	100	52	71	11.2	84	56
First service propulsion maneuver	100	13.0	108	94	80	22.0	148	56	71	12.7	106	61
Second service propulsion maneuver	81	16.5	98	45	101	18.9	145	56	80	31.5	163	53
Third service propulsion maneuver	100	16.2	147	74	77	15.9	119	57	69	19.1	123	47
Fourth service propulsion maneuver	91	12.1	122	73	62	11.0	89	50	67	15.8	108	55
Docked descent propulsion engine firing	88	10.2	103	72	69	17.4	150	57	*	*	*	*
Fifth service propulsion maneuver	90	10.0	98	73	62	16.3	110	45	57	10.0	72	49
Extravehicular activity	90	18.0	105	85	95	20.0	115	75	67	14.0	85	55
Rendezvous insertion maneuver (descent engine)	97	8.6	108	89	59	8.6	66	50	61	10.7	84	54
Seventh service propulsion maneuver	88	9.4	96	79	60	11.9	89	52	58	12.0	91	49
Eighth service propulsion maneuver (deorbit)	104	10.6	110	79	78	15.0	82	59	68	13.8	82	54

\*No data available.

NASA-S-69-2068

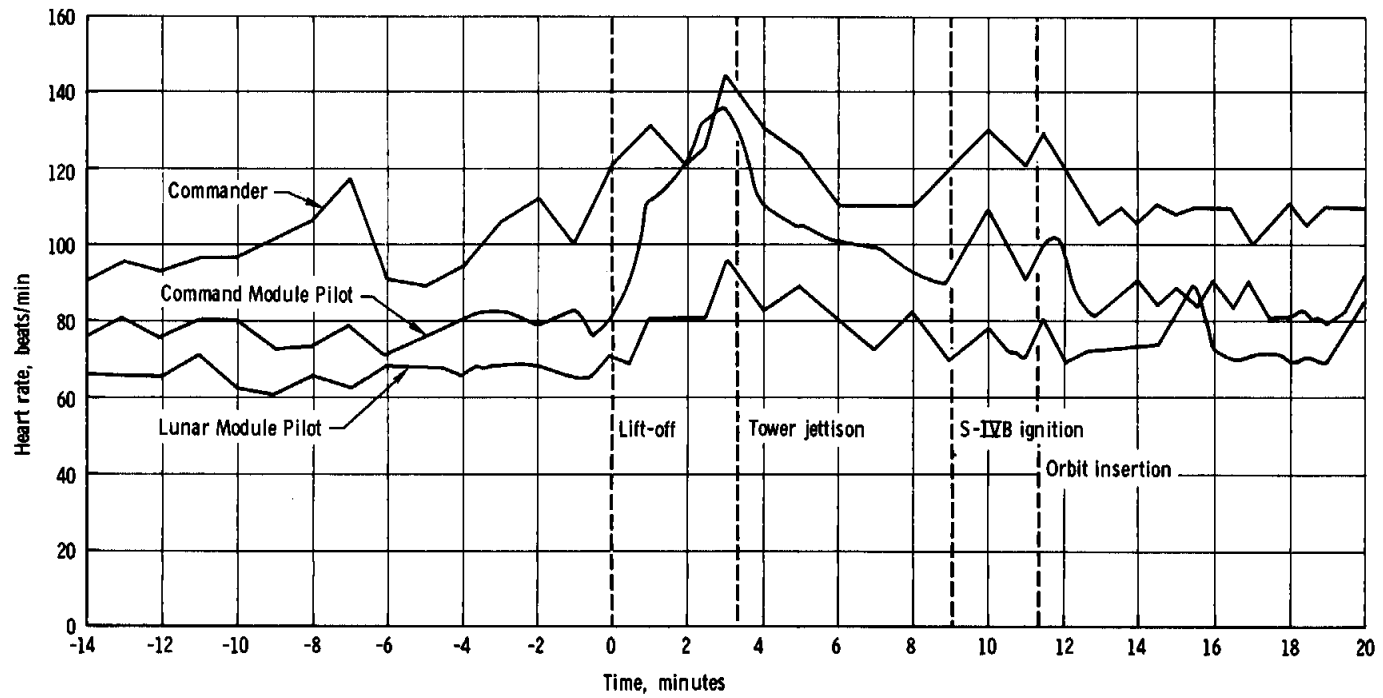


Figure 11-1.- Heart rates prior to and during launch.

## 12.0 FOOD AND WATER

### 12.1 FOOD

This section contains a discussion of the problems reported by the crew with regard to preparation and eating of the inflight food.

The types of foods used in Apollo missions are a development from previous manned space programs. As with other spacecraft components, the food and its containers have always been subject to weight and volume constraints. In addition, the food must be flight qualified to many of the same specifications (temperature, pressure, humidity, mechanical stress, and handling) as for other onboard hardware. As a result of these limitations, departure from ordinary, table-type foods was made, beginning with Project Mercury.

The most practical type of space food was found to be the freeze-dried variety which could be reconstituted with water inflight. This food type is low in both weight and volume, is stable without refrigeration, can be readily packaged, and can withstand the stresses and environmental conditions of space flight. However, preparation of these meals requires cutting the package, measuring the required water, kneading the mixture, and waiting for the rehydration process to be completed.

Another variety of food is that made in bite sizes. These foods do not require reconstitution with water since they are rehydrated in the mouth with saliva or small amounts of ingested water. The bite-size foods are usually prepared with a special coating to prevent crumbling before eating. For Apollo 8 and 9, special wet-pack foods were also added to the flight menu for variety, improved taste, and a closer similarity to conventional food. Both of these food types are more convenient than the freeze-dried meals because of the minimum preparation time.

In Gemini and Apollo, with design missions of up to 14 days and with power systems that produce potable water as a by-product, the weight and volume savings provided by freeze-dried foods are appreciable. However, concern for certain contamination in this water has led to chlorination procedures which, at best, detract from the intended taste of rehydrated foods. In addition, a higher-than-expected hydrogen gas content was noted in the water supplied by the fuel cells in Apollo 9.

### 12.1.1 Preflight Preparation

Prior to flight, each crewman was provided with a 4-day supply of flight food for menu evaluation and selection. Acceptability of the foods was reported as good, and no problems were anticipated. Flight menus were then established to provide each crewman with adequate nutrients to meet basic physiological requirements. No foods were included in the final flight menus which had been rejected during the preflight evaluation. However, conflicting crew activities and a crowded schedule precluded a thorough evaluation, familiarization, and selection of flight menus.

The flight menu provided approximately 2500 kilocalories per man per day, which was in excess of the daily requirement to allow for residual food adhering to the packages. Fruit-flavored beverage powders were fortified with calcium lactate to bring the available daily calcium up to 1 gram per man per day. Since maintenance of proper body hydration had proved to be a problem in previous flights, each man was provided with 120 grams of beverage powder per day, compared with 60 grams for the Gemini missions.

The 4-day menu cycle is outlined in table 12.1-I. In addition, each crew member was provided with special thermostabilized wet-pack foods, which included three servings each of ham and potatoes, beef and potatoes, and turkey and gravy. All wet-pack meals are eaten cold; the turkey and gravy could be eaten with a spoon, but the other two items were best eaten using the fingers.

### 12.1.2 Inflight Effectiveness

The crew reported that many of the rehydratable foods presented a monotonous flavor and a grainy texture. The flavor and texture can be affected by incomplete rehydration of the food. Proper rehydration requires that a specific volume of water be thoroughly mixed with the food for a specific period of time. If either of these requirements is violated, food flavor and texture are compromised. For example, cornflakes with the proper amount of water are good; add too much water and they taste like cornflakes and water; add too little water and the texture is grainy and unpalatable. The flavor of any chlorine in the water further degrades the taste.

In the command module water, excessive hydrogen gas (60 to 70 percent by volume) from the fuel cells resulted in a greatly reduced transfer of liquid from the water dispenser to the food packages and inhibited complete rehydration of the food. Since the packages were expanded by the gas, the addition of water was further impeded. Satisfactory separation of the gas from the food inside the package was impossible.

The reported distaste of the command module water (see section 12.2) undoubtedly affected the flavor of reconstituted foods, and the crew reportedly used rehydratable food and beverages to dilute the unsatisfactory flavor of the water. The potable water is also known to contain acceptable traces of ionic and gaseous contaminants which alter the flavor of rehydrated food.

The crew found the following rehydratable foods to be more acceptable:

- a. Fruit flavored beverages
- b. Fruit cocktail and peaches
- c. Puddings
- d. Salad/meat items
- e. Beef and vegetables
- f. Chicken and vegetables

These items seemed to be liked best because of their color and texture. The crew believed that if the salt and spice content of these food could have been varied, the flavors would have been even more acceptable.

The wet-pack foods were most accepted by the crew because:

- a. they are not affected by the taste of potable water
- b. They have a familiar taste, texture, and appearance
- c. They require no elaborate preparation.

The main disadvantage of the wet-pack foods is that the texture and taste of some of the food constituents normally eaten hot, such as gravy and potatoes, are not as palatable when they are cold.

As a substitute for some of the bite-size foods, dried fruits such as peaches, apricots, and apples, which require no special processing, have been approved and will be included in future flight menus. The resilience and texture of these items permits them to withstand the mechanical stresses and environmental extremes of space flight, but still remain tasteful and non-hazardous to the teeth. Their natural color and consistency are retained to present a more familiar and appetizing appearance and taste than the bite-size foods.

### 12.1.3 Postflight Evaluation

Examination of returned foods and packaging as well as data from the inflight food log revealed the average daily consumption provided

approximately 1750 kilocalories of energy per man, representing an average daily deficit of 500 kilocalories per man. This deficit is considered to be a normal variation for the mission duration involved. Food menus should be designed to meet psychological as well as physiological needs of the flight crew. That is, foods should be a motivating force to the crew, rather than a source of irritation as reported in Apollo 9. The food should look good, taste good, feel familiar, and be easy to prepare, as well as being nutritious.

Bite-size foods are either compressed or freeze-dried products with a special coating to inhibit crumbling. The main technical problems associated with the design and fabrication of these foods are in maintaining sufficient strength to withstand the mechanical stresses encountered in shipping and flight, yet soft enough to chew without injury to the teeth. In general, the crew found the bite-size items to be too dry and therefore undesirable. These foods are designed to have an average moisture content of only 2 or 3 percent and are intended to be rehydrated in the mouth with natural saliva or with small quantities of potable water when saliva is inadequate.

## 12.2 WATER

The inflight water consumption was not recorded, but body weights and physical examinations indicated the crew was in a state of negative water balance at the time of landing. The crew complained about the excessive gas content and the bad taste of the water in the command module. In contrast, the lunar module water was quite acceptable.

### 12.2.1 Command Module Water

Prior to flight, the command module water system was loaded with water containing 10 mg/liter of residual chlorine. The system was soaked for about 13 hours, flushed, and filled with non-chlorinated, de-ionized, microbially filtered water. Three hours before lift-off, the system was chlorinated using inflight equipment and procedures.

The crew complained of the excessive hydrogen content (60 to 70 percent by volume) in the potable water from the fuel cells. In addition, the water was found to be somewhat distasteful. Although the exact times of all inflight chlorinations cannot be determined, it is known that some of the scheduled inflight chlorinations were missed; in one instance, two sequential chlorinations scheduled for early in the flight were not performed because of a very busy schedule. The reduction in chlorinations would add to the unpalatability of the water because of micro-organisms present. However, dissatisfaction with a chlorine taste for the first

30 minutes to 1 hour after purification has been reported in previous flights. Therefore, to reduce the effect of chlorination, the purification schedule was changed from early morning to just prior to initiation of crew sleep periods.

Analysis of potable water samples obtained about 40 hours after the last inflight chlorination showed a free-chlorine residual of 1.0 mg/liter in the hot-water food-preparation port and 2.0 mg/liter in the cold water port. Although no micro-organisms were cultured from the potable water samples taken 30 hours after the final inflight chlorination, effective bacteriocidal concentration of free chlorine cannot be assured in the potable water system when the interval between chlorinations becomes greater than 24 hours.

Chemical analysis of water from the hot water port showed that the nickel concentration had increased from 0.18 mg/liter 2 days before launch to 2.97 mg/liter on the day after recovery. Although this value is significantly greater than the originally specified allowable limit, no adverse effects were detected on the crew during the immediate post-flight medical evaluations. The nickel concentration is derived from leaching of the brazing alloys used in the fabrication of the hot-water heater. For the mission durations planned for Apollo, the nickel concentration is of no immediate concern and no corrective action is required.

Because of the objectionable taste of the water and the smaller increments metered from the water dispenser, the crew usually elected to take drinking water from the cold-water tap on the food reconstitution panel. Although gas was still present from this source, the concentration of distasteful organic and metallic compounds was considerably reduced. In particular, the cold water tap does not receive water which has contacted the neoprene hose to the water dispenser; therefore, this water does not become contaminated by the leached organic salts.

#### 12.2.2 Lunar Module Water

Prior to flight and after the initial sterilization, the lunar module water system was loaded with microbially filtered, de-ionized water, which had been iodinated to a residual of 13 mg/liter in the ascent stage tank and 10 mg/liter in the descent stage tank. The preflight iodine residual was 2.3 mg/liter in the descent stage tank when final test samples were obtained on February 28, 1969. The iodine depletion rate dictated that the crew would have to utilize the water microbial filter which was stored in the lunar module. In contrast to the command module potable water, the crew found the taste of the lunar module water to be good and used it at every opportunity.

TABLE 12-I.- MENU CYCLE

	<u>Days 1, 5, 9*</u>	<u>Days 2, 6, 10</u>	<u>Days 3, 7, 11</u>	<u>Days 4, 8</u>
Meal A	Peaches Bacon squares Cinnamon toasted bread cubes Grapefruit drink Orange drink	Grapefruit drink Canadian bacon and apple- sauce Brownies Sugar coated cornflakes Grape drink	Fruit cocktail Bacon squares Cinnamon toasted bread cubes Cocoa Orange drink	Sausage patties Bacon squares Peaches Cocoa Grape drink
Meal B	Salmon salad Chicken and gravy Toasted bread cubes Sugar cookie cubes Cocoa	Tuna salad Cinnamon toasted bread cubes Pineapple-grapefruit drink Chicken and vegetables Pineapple fruitcake	Cream of chicken soup Beef pot roast Butterscoth pudding Grapefruit drink Toasted bread cubes	Pea soup Chicken and gravy Cheese sandwiches Grapefruit drink Bacon squares
Meal C	Beef and gravy Beef sandwiches Chocolate pudding Orange-grapefruit drink Cheese cracker cubes	Spaghetti with meat sauce Banana pudding Grapefruit drink Beef bites Bacon squares	Beef hash Chicken salad Turkey bites Graham cracker cubes Orange drink	Shrimp cocktail** Beef and vegetables Cinnamon toasted bread cubes Date fruitcake Orange-grapefruit drink

\*Day 1, meals B and C only.

\*\*Spaghetti and meat sauce substituted for shrimp cocktail for Lunar Module Pilot on Day 4 only.

## 13.0 PHOTOGRAPHY

Apollo 9 photography is divided into two categories, operational and scientific. The operational coverage was concerned with spacecraft and launch vehicle operations, and the scientific photography involved both the multispectral terrain experiment and general hand-held camera exposures. This photography was generally very good, particularly because the flight plan lent itself to good photography. With two separated manned vehicles during a portion of the mission, the first complete pictures of both spacecraft in orbit were possible. During extravehicular activity, photography was obtained to evaluate crew operations with the extravehicular mobility unit. Relatively light activity periods during the latter half of the mission also afforded an opportunity to obtain good photography of the earth terrain. Availability of propellant and ground planning made it possible to get photographs of greater scientific value than on any previous flight.

Seven modified Hasselblad cameras were onboard for photography, four for the S065 experiment and three for general photography. Almost 1400 frames of 70-mm film were exposed, and 584 of these were with the cameras provided for the S065 experiment. The hand-held, target-of-opportunity photographs were all taken with SO-368 film. Sixteen 140-foot magazines (approximately 2200 feet) of 16-mm film were used for vehicle-to-vehicle photography, interior pictures, and ground-track exposures. Three of these magazines contained SO-168 film for interior photographs, and the remainder contained SO-368 film.

### 13.1 OPERATIONAL PHOTOGRAPHY

The operational photography included transposition, docking, and ejection; the S-IVB restart at 1000 feet separation; lunar module docking target motion during stroking tests; drogue removal and tunnel operations; extravehicular activity; undocking and inspection; rendezvous, docking, and lunar module jettison; ascent engine firing to depletion; command module interior photography; water dumps showing the formation of ice crystals; and entry, showing the ionization sheath and parachute deployment. The operational photography includes data on the condition of the spacecraft after being exposed to the launch and space environment and permitted a detailed postflight inspection of the separated vehicles and the crew procedures, especially during extravehicular activity.

## 13.2 MULTISPECTRAL TERRAIN EXPERIMENT

The one formal Apollo 9 experiment, designated S065, was the Multispectral Terrain Photography Experiment. The objectives were (1) to determine the extent to which multi-band photography in the visible and near-infrared region from orbit may be effectively applied to the earth resources disciplines, and (2) to obtain simultaneous photographs with four different film/filter combinations from orbit to assist in defining future multispectral photographic systems. As an adjunct to the formal photographic experiment, hand-held target-of-opportunity coverage was planned and conducted on a time-available basis.

The photographic results were excellent, and quality and subject material exceeded that of any previous orbital mission. This mission concluded the Apollo earth orbital flight series in support of the Earth Resources Program, and the excellent photographic results were timely in support of future program planning. The primary reasons for the excellent exposures are discussed in the following paragraphs.

The flight plan provided about 4 consecutive days for this experiment. Therefore, many areas under cloud cover during one pass could be photographed at a later time. In addition, ample time was available for the crew to plan and set up the experiment.

The orbital inclination of 33.6 degrees late in the flight permitted vertical and near-vertical coverage of many areas never before photographed from space. Of particular interest are the Appalachian and Ouachita Mountains, the eastern coastal plain, and the Piedmont Plateau.

The availability of sufficient reaction-control propellants permitted the crew to orient the spacecraft whenever necessary for vertical and near-vertical coverage, whereas, photography during previous missions was often constrained to periods of free drifting flight. The crew was also able to use effectively the orbit-rate mode of attitude control; therefore, a relative orientation with respect to the earth's surface could be maintained and image motion minimized.

The spacecraft windows were as free of inflight contamination as on any previous U.S. manned mission, a condition of immense importance to a scientifically rigorous photography experiment. In addition, the infrared-reflective coating on the hatch window was removed prior to flight.

During the flight, operation of a science support room at the Manned Spacecraft Center permitted continuous evaluation, planning, and updating of photography by experiment investigators. Information on weather conditions, sun angle, ground-track coverage, and status of earth resources aircraft was available in this support room for the investigators and the flight crew.

### 13.2.1 Camera System

The equipment used for the S065 experiment consisted of four modified Hasselblad cameras installed in the hatch window. These cameras were commonly boresighted and triggered by the crew with a manually timed shutter release. The film/filter combinations were Panatomic X film with red (25A) and green (58) filters, infrared black-and-white film with a red (89B) filter, and Ektachrome Infrared with a Wratten 15 filter.

### 13.2.2 Photographic Targets

The targets for the experiment were primarily in the United States, with typical sites being Phoenix, Yuma, Houston, and Los Angeles. Additional primary sites were in the Mexico City area, and several secondary sites were in Africa along the ground track of the Apollo 6 mission, from which the S0121 experiment photography provides comparative results. To allow for adverse weather and lighting conditions, many more targets were specified than could be photographed with the available film.

### 13.2.3 Experiment Results

From the four different cameras, 584 frames were exposed representing 127 complete photographic sets. Approximately 93 frames were taken over relatively cloud-free land areas, as well as obscured and partially obscured areas. Coast-to-coast coverage of parts of the southern United States, as well as parts of southern Mexico and Central America, was obtained. The test area specifically designated for oceanographic and meteorological studies was photographed with partial sets, including color infrared.

Terrain photography.- Except for some cloud cover, all terrain photography was of very good to excellent quality. A few frames of northern Chihuahua, Mexico, appear slightly over-exposed, probably because of the high albedo of the desert and the high sun angle. Several of the target sites, including those in the Imperial Valley (see fig. 13-1) and near Phoenix (see fig. 13-2), were photographed from orbit at about the same time photographs were being taken from NASA earth resources aircraft. A wide variety of terrain was covered by the photographs, including the Colorado, Yuma, Sonora, and Chihuahua deserts, many mountain ranges, the High Plains, the Mississippi Valley (see fig. 13-3), the southern Appalachians, the southeast Piedmont region, and the coastal plains along the Gulf of Mexico and the Atlantic Ocean. Several major cities in the United States were photographed; including San Diego, southern Los Angeles, Phoenix, Birmingham, and Atlanta.

The value of the multispectral photography was increased by the skill and initiative demonstrated by the crew in taking nearly simultaneous pictures with the hand-held 70-mm camera containing S0-368 film. This photography with the hand-held camera will be used to compare the effectiveness of the four multispectral film/filter combinations with the results obtained from standard color film used during previous orbital flights.

Pending a detailed analysis by the experiment investigators and user agencies, the following preliminary conclusions are available regarding the relative effectiveness of the four film/filter combinations.

The color infrared film with a Wratten 15 filter provided the best combination of photographic information and resolution of the four film/filter configurations. With this film, rapid discrimination between geological features, such as water, vegetation, and rock or soil, is possible (for an example see fig. 13-1). Of the three black-and-white film combinations, the Panatomic-X film with a red (25A) filter produced the best tone differentiation, contrast, and resolution (figs. 13-4 and 13-5); however, the best discrimination between types of vegetation and the ability to reconstitute color imagery (compare figs. 13-3 and 13-5) were possible with the infrared film using a red (89B) filter. The Panatomic-X film with a green (58) filter was the least effective of the four film combinations and yielded a lower variation in shades of gray (see fig. 13-2) and less resolution than those obtained with the same film but with the red filter. These conclusions are based strictly on an initial observation of transparencies and film prints, and a thorough analysis of photographic results is to be completed. Preliminary results of this analysis will be published in June, 1969, in a Science Screening Report, with the final results documented in a formal report due for publication in the latter half of 1969.

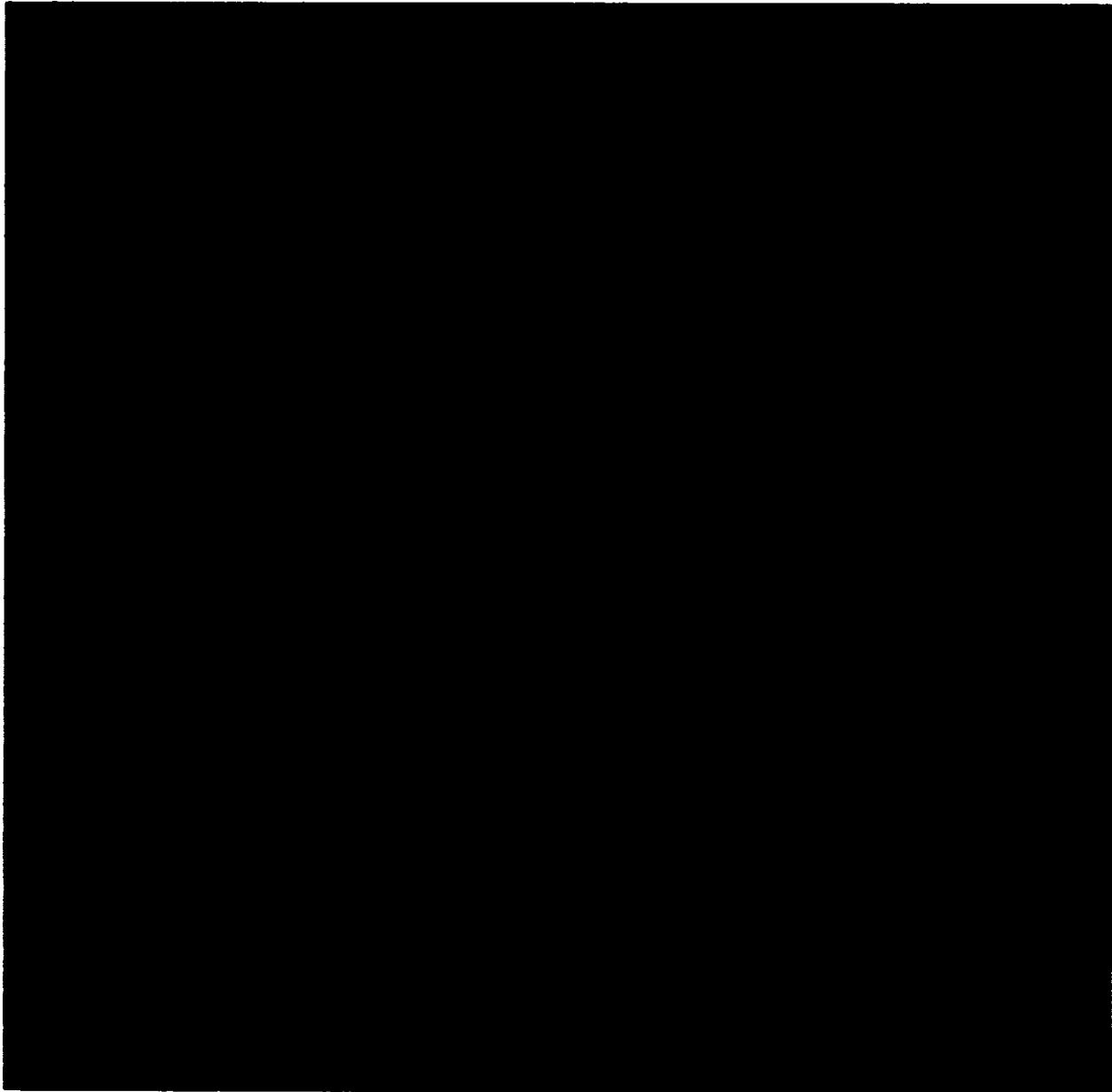
Meteorological photography.- A significant portion of the photography contained meteorological information, ranging from clouds in the foreground of geological and general terrain targets to specific meteorological phenomena. Preliminary inspection of the results indicates a greater value for meteorological applications than was obtained during any previous manned orbital mission. This success can be attributed to the inclusion of a bracketed camera system, an improved system for defining meteorological targets on a real-time basis, and maintenance of a detailed photography log by the crew.

Where suitable overlap exists, the photographs can be used for stereoscopic cloud-height determination. Of most immediate value is a series of photographs taken over the trade-wind belt in an area of prime interest (see fig. 13-6). These cloud photographs will permit a detailed comparison with simultaneous weather-satellite coverage of the same area. Several magazines of 16-mm film were taken of meteorological phenomena, and these can also be used for stereoscopic cloud-height determination.

Hand-held photography.- Although no formal terrain or meteorology experiments for a single, hand-held camera were scheduled, a number of targets of opportunity were included in the flight plan and updated periodically by the photographic support room. The crew obtained a remarkably large number of high-quality hand-held pictures using the SO-368 film. These results will be very useful in the study of all earth resources disciplines and meteorology, as well as for comparative purposes in support of the SO65 photography. Typical frames from the hand-held target-of-opportunity series are presented in figures 13-7 to 13-9 showing coverage of the Phoenix, Houston, and Cape Hatteras areas. Figure 13-10 is a photograph showing cumulonimbus cloud formations of significant meteorological interest.

13-6

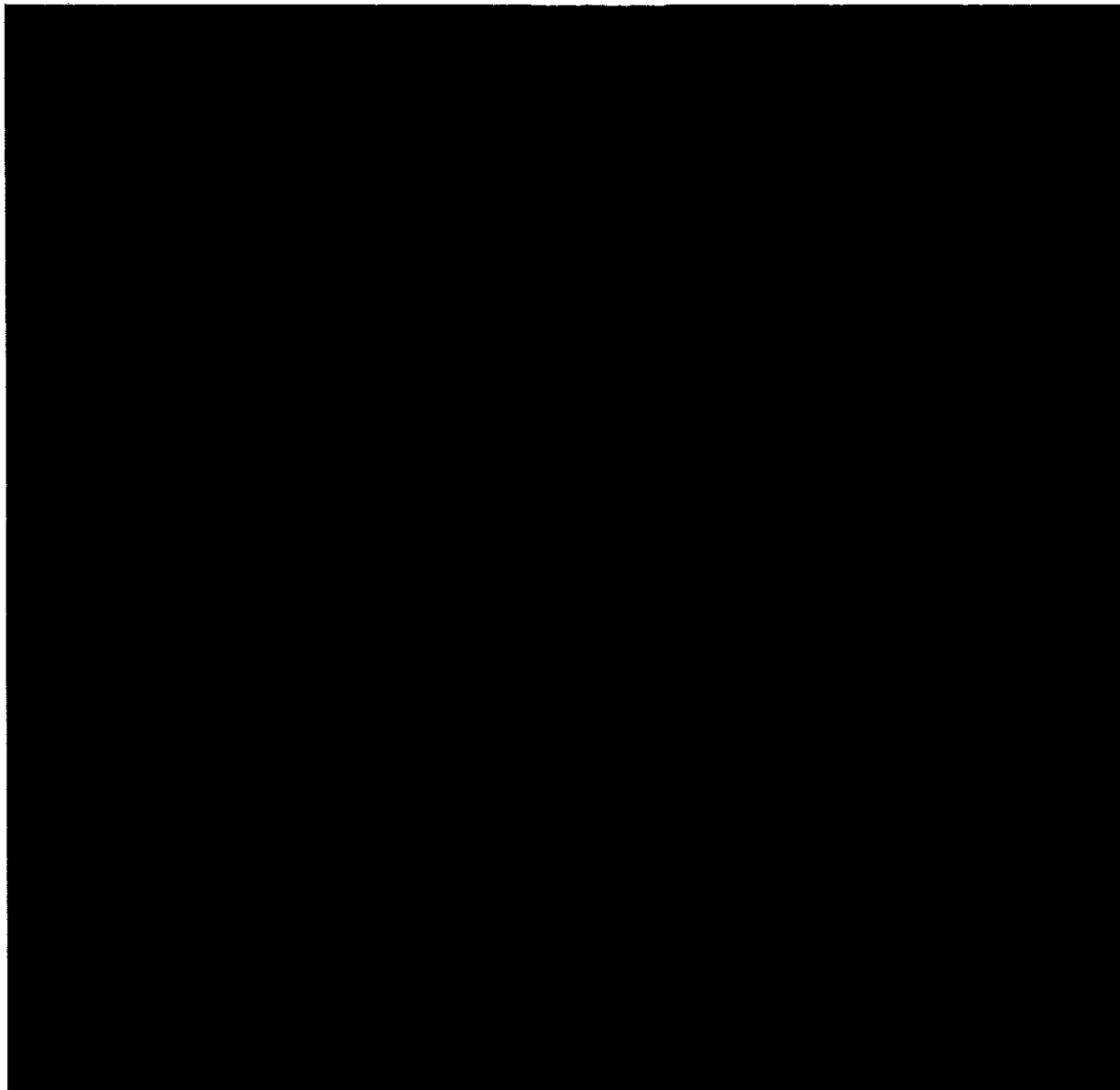
NASA-S-69-2069



Cultivated fields representing different crop types  
distinguished by varying shades

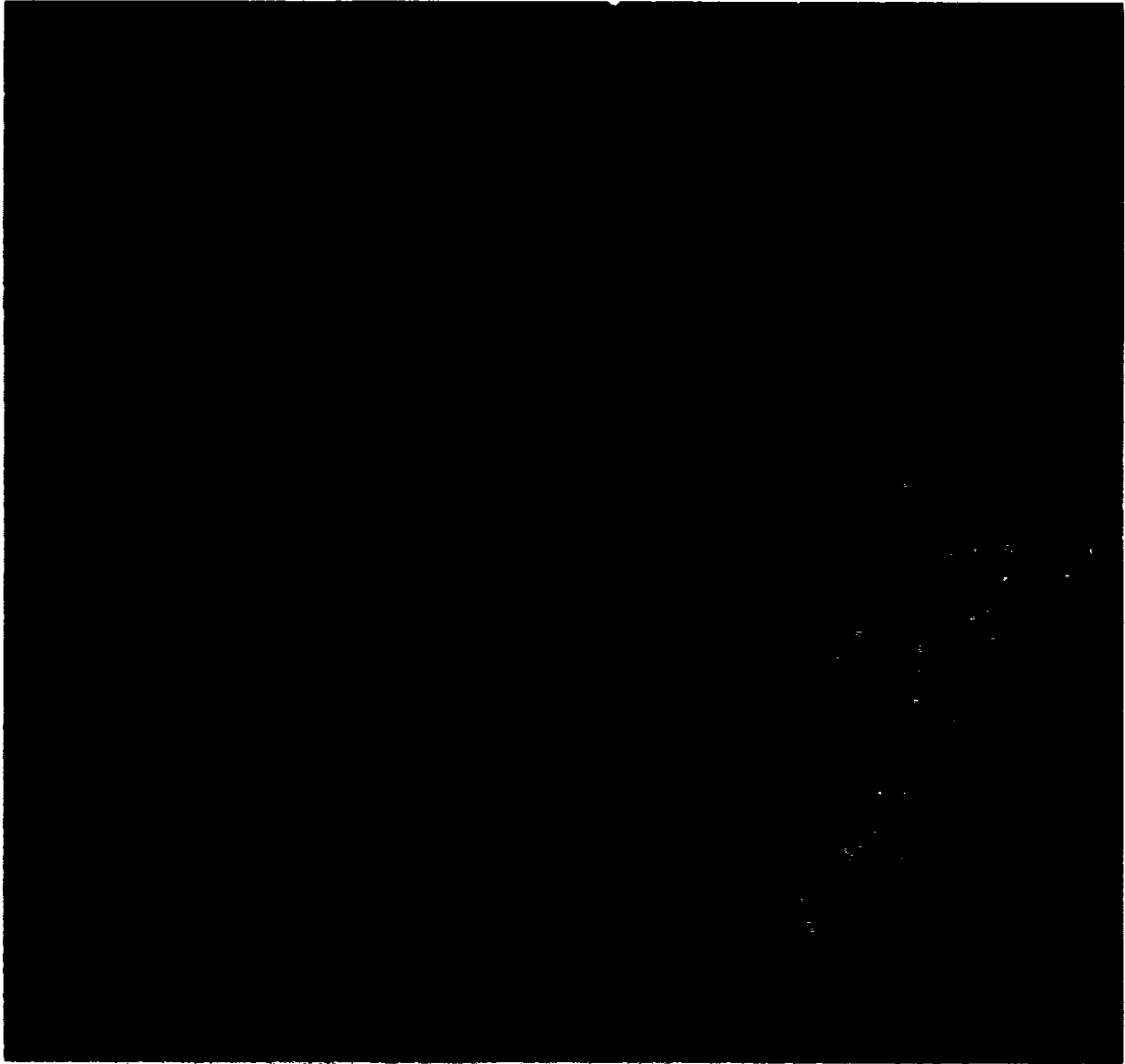
Figure 13-1.- Imperial Valley of California and Mexico and Colorado River.

NASA-S-69-2070



Size and patterns of fields as well as urban areas easily recognized.

Figure 13-2.- Phoenix, Arizona, Gila River, snow-capped mountain peaks north of city.



Old meander scars and oxbow lakes indicate former channels of Mississippi River.

Figure 13-3.- Mississippi River and associated flood plain  
in Mississippi, Arkansas, and Louisiana.

NASA-S-69-2072



Observe excellent discrimination between water, vegetation and dark rock/soil.

Figure 13-4.- Long Beach, California, Pacific Ocean,  
and Coastal Mountain ranges.

13-10

NASA-S-69-2073



Meandering Mississippi River in the upper right corner and the major road network visible in Monroe, Louisiana at lower left.

Figure 13-5.- Western part of Mississippi River flood plain in Arkansas and Louisiana.

NASA-S-69-2074



Oceanic cumulus clouds arranged in bands paralleling the easterly trade-wind flow.

Figure 13-6.- Western Atlantic Ocean near 22 degrees North Latitude.

13-12

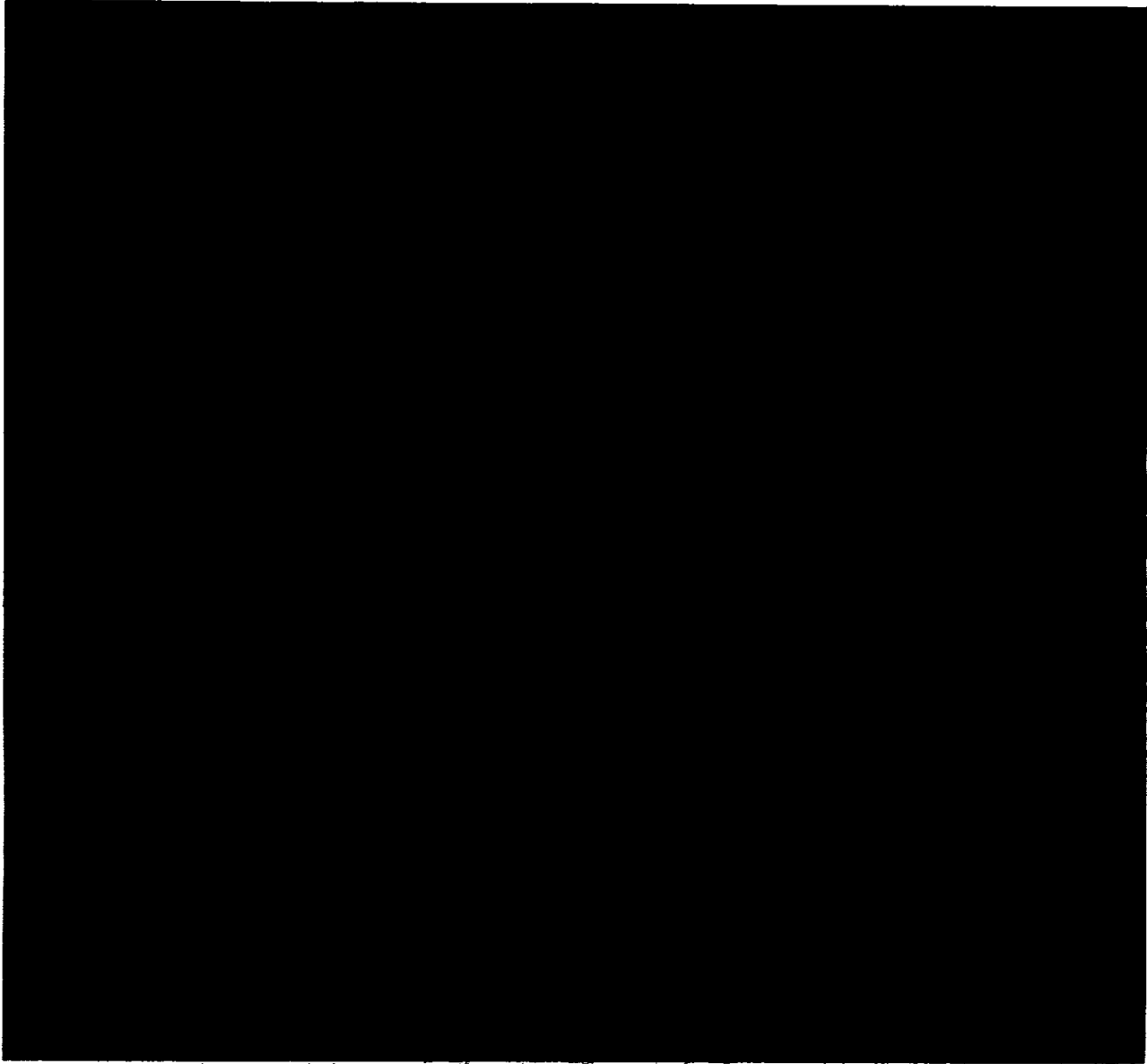
NASA-S-69-2075



Road network and urban areas show distinctly.

Figure 13-7.- Phoenix, Arizona, and Gila River under cumulus and cirrus clouds.

NASA-S-69-2076



Sediment flow into Galveston Bay can be observed as well as the major road network of Houston. Cirrus clouds.

Figure 13-8.- View of Texas Gulf Coast showing Houston, and Galveston Bay.

13-14

NASA-S-69-2077



Outflow of rivers into the Atlantic shows extent of sediment discharge. Cumulus clouds over Atlantic.

Figure 13-9.- North Carolina, Atlantic Ocean, Cape Lookout, Cape Hatteras, Pamlico and Albemarle Sounds.

NASA-S-69-2078

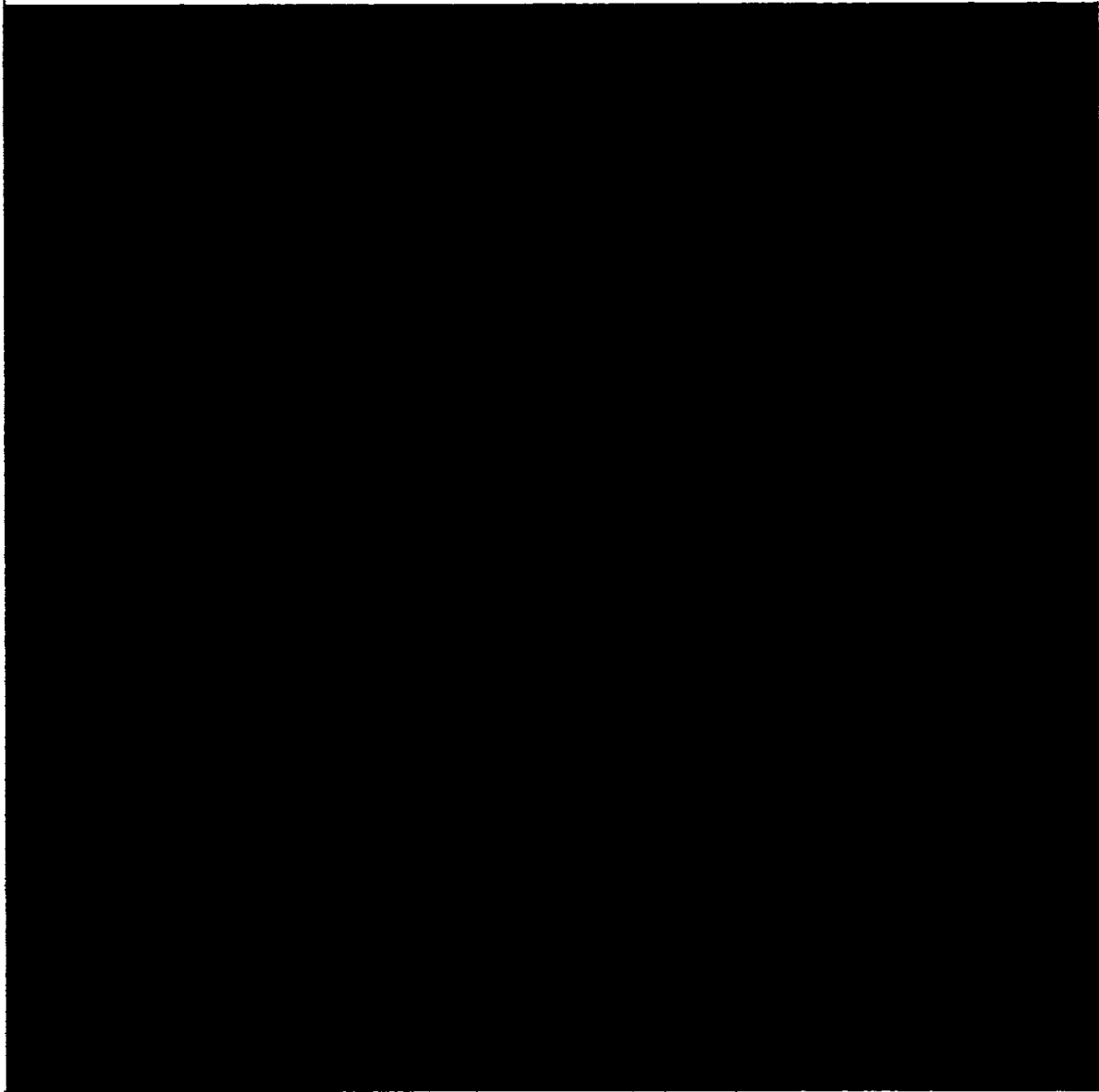


Figure 13-10.- Cumulonimbus cloud with central turret of high vertical development over southwestern Venezuela.

14.0 MISSION SUPPORT PERFORMANCE

## 14.1 FLIGHT CONTROL

This section of the report is based upon real-time observations and may not agree with the final data analyses in other sections of the report.

## 14.1.2 Powered Flight

Lift-off was at 16:00:01.07 G.m.t. on March 3, 1969. At approximately 0:03:49, the crew reported that the onboard display of service propulsion helium tank pressure was indicating zero. The Mission Control Center advised that the telemetered pressure was valid. The onboard display remained at zero for the entire mission, and the telemetered pressure was valid. At 0:08:26, all digital data were lost from the launch vehicle computer, preventing use of the instrument unit vectors as a launch trajectory data source. All other launch vehicle functions were essentially nominal during the launch phase. The S-IC engine thrust chamber pressures were 10 to 20 psia lower than expected, and the S-IC firing was long by approximately 3 seconds. The S-II firing was nominal. The S-IVB firing was long by approximately 6 seconds, apparently caused by a requirement to compensate for the performance of the S-IC.

Shortly after S-IVB cutoff at 0:11:04, discrepancies were noted in the data sources for the orbit go/no-go decision. The cutoff vectors all indicated "go"; however, the cutoff velocity varied up to 40 ft/sec and the flight-path angle up to 0.5 degree. Also, the mission operations computer and the dynamic standby computer processed different answers. The crew reported an orbit of 103.2 by 88.5 miles; however, the orbit computed on the ground varied according to data sources as follows:

Data source	Apogee, miles	Perigee, miles
Initial vector by Real Time Computer Complex	121.9	72.7
Bermuda S-band	107	98.9
Goddard Space Flight Center	103.3	99.8
Canary Island	103.9	102.3

Later, it was indicated that the Real Time Computer Complex had used two different vectors to determine the orbit. The cutoff vector from USNS Vanguard was used in the mission operations computer, but the cutoff vector from the Bermuda station was used in the dynamic standby computer. After incorporation of the Canary Island and Tananarive tracking data, the orbit was verified at 106.4 by 102.6 miles.

## 14.1.3 Orbital Phase

After insertion and orbital trajectory verification, it was apparent that the orbital solution by the command module computer was approximately 25 ft/sec low in velocity. The problem was determined to be a bias error of 0.038 ft/sec/sec in the X-axis accelerometer. This bias was corrected on the second day of the mission.

At approximately 0:30:00, a master alarm indicated low pressure in hydrogen tank 1. Thereafter, the master alarm sounded each time the hydrogen pressure neared the activation point of the heaters. To avoid interruptions of crew rest periods, the pressure in both tanks was allowed to decrease during activity periods to below 200 psia, then the fans in one tank were operated to cause a slight pressure increase during the rest period. On two occasions, the pressure was increased to the upper end of the operating range and then allowed to decrease, but in both instances the crew rest period was interrupted by the master alarm.

The crew reported that during the docking maneuver, the spacecraft had no left-translation capability. In the course of troubleshooting the service module reaction control system, it was discovered that the primary and secondary propellant isolation valves for quad C were closed, and the secondary propellant isolation valves in quad D were also indicated to be closed. The crew operated the switches to the open position, and no further problems were reported.

The primary glycol evaporator functioned normally during launch and the first day in orbit. The evaporator was turned off and reactivated on the second day at about 24 hours. When the radiator outlet temperature reached the level for evaporator operation to begin, the evaporator had dried out as indicated by an increase in evaporator outlet temperature and a decrease in steam pressure. The evaporator was then reserviced and shut off until entry cold soak. The radiator outlet temperature was sufficiently low that evaporative cooling was not required for equipment cooling nor for crew comfort.

During the second service propulsion firing, repeated master caution and warning indications occurred, apparently because of an unbalanced condition in the propellant utilization and gaging system at ignition. The E-stroker (engine gimbaling) test at half amplitude was initiated as soon as the starting transients had been damped. The maximum rates during the test were 0.1 deg/sec, and these were essentially damped out within 5 seconds of stroker termination. No cross coupling was noted in either the pitch or the yaw axis. The propellant utilization and gaging system tracked properly during the firing, and at cutoff, the indications were 69.25 percent oxidizer and 69.4 percent fuel. The oxidizer unbalance was approximately 500 pounds high.

A "go" was given at 42:37:00 for crew transfer to the lunar module; however, the crew advised that they were behind on the schedule. At 43:19:00, the Lunar Module Pilot was reported to be transferring to the lunar module. At 44:05:00, the Commander initiated the transfer. At that time, the crew was about 50 minutes behind in the flight plan, and all communications tests were cancelled except for the lunar module secondary S-band check and the two-way relay with television.

At approximately 45:40:00, the Commander indicated that the Lunar Module Pilot had been sick on two occasions, and the crew was behind in their timeline. For these reasons, the extravehicular activity was planned to be restricted to one daylight pass and included only the opening of the hatches of the command module and the lunar module. Further, the Lunar Module Pilot was to remain connected to the environmental control system hoses. The portable life support system was to be connected in a normal fashion, and the environmental control system would supply any backup requirements.

On numerous occasions, the scanning telescope in the command module stuck at 64 degrees of shaft rotation. However, the crew used a special tool to manually free the telescope when necessary, and they continued to use the optics normally. This problem did not affect any significant mission activity.

Ignition for the first lunar module descent propulsion firing occurred at 49:41:33. Engine performance appeared normal until the crew throttled up to 40 percent thrust and then to full throttle. During the first 35 seconds, the fuel and oxidizer inlet and tank pressures dropped very rapidly to lows of 179 and 180 psia for fuel and oxidizer, respectively. Also, a warning light indicated that the regulator manifold pressure was below 218.1 psia. Shortly after the full throttle position was reached, the pressure increased to nominal values, and the firing appeared to be normal thereafter. Also, approximately 5 minutes into the firing, the crew reported some slight oscillations. During the second descent engine firing at approximately 93:49:00, the crew reported that the descent engine was a little rough when throttling through the 20 percent thrust region and that they had let it stabilize before throttling up to 40 percent. The data indicate that the thrust chamber pressure was steady during the 20 percent thrust region. (Editor's note: Chamber pressure did reflect rough combustion but stabilized before increased thrust was again commanded.)

At 50:31:00, the descent oxidizer tank pressure was higher than expected (up to 253 psia).

On the fourth day, the Commander and Lunar Module Pilot transferred to the lunar module for the extravehicular activity. The communications tests were again cancelled to allow the crew sufficient preparation time.

The guidance and navigation system was not powered up; instead, the stabilization and control system would be used to hold attitude in maximum deadband. The limit cycle switch was turned off to preclude excessive thruster firings. At 71:53:00, the Commander assessed the Lunar Module Pilot's condition as excellent, and with Mission Control Center concurrence, the extravehicular activity was extended to one daylight pass on the lunar module platform. At 73:04:00, the lunar module forward hatch was opened, and the Lunar Module Pilot egressed into the foot restraints.

After the two crewmen had returned to the command module and the tunnel hardware had been installed, the current measurement indicated that the translunar bus tie circuit breakers were closed. With these breakers closed, the amount of current provided the lunar module from the command and service modules could not be determined. At 78:09:00, the Lunar Module Pilot returned to the lunar module and opened the translunar bus tie circuit breakers.

The descent propulsion helium pressure was 759 psia at 70:26:00 and 48 minutes later was 751 psia. This decrease apparently resulted from a leak.

For the rendezvous activities on the fifth day, the two crewmen transferred to the lunar module without their helmets or the transfer umbilical. This, combined with early crew preparation, greatly reduced transfer time. The crewmen were in the lunar module an hour ahead of the schedule but returned to the nominal timeline by 90:40:00.

When the spacecraft was powered up on the fifth day, the fuel cell 2 condenser exit temperature increased to 179° F, where it stabilized. Also, on the ninth day, this temperature increased slightly, then returned to the normal range.

At 85:55:00, an automatic switchover to the secondary proportioning valve occurred in the primary glycol loop; the primary radiator outlet temperature had increased to 51° F prior to the switchover. No other abnormal indications were present within the primary glycol system, and it was returned to the primary proportioning valve. The system operated satisfactorily for the remainder of the mission.

At approximately 93:00:00, the hydrogen tank motor switch failed to close at the nominal pressure, although the hydrogen tank 1 heaters were in automatic. The crew placed hydrogen tank 2 heaters in automatic but without favorable results. At approximately 101:25:00, the pressure in both hydrogen tanks started increasing and failed to stop at the nominal level. The problem was concluded to be an intermittent failure in the hydrogen motor switch or switch circuit.

During the crew rest period on the fifth day, battery A bus voltage decreased at an unexpected rate. During the next activity period, high battery A currents were observed (up to 2.0 amperes). The flight and postlanding battery A circuit breaker was found closed. This breaker was opened, and the condition was not observed again.

The Command Module Pilot could not see the lunar module tracking light after staging; however, when the lunar module was in daylight, it could be tracked with the command module optical alignment system. Subsequent tests showed the tracking light drew proper current when the switch was on.

When the sixth firing of the service propulsion system was attempted at 121:48:00, the spacecraft computer failed to command the reaction control system +X translation for propellant settling. A corrected load, with the proper configuration, was put into the computer, and approximately 90 minutes later, the +X translation was obtained and the firing was successful.

During the landmark tracking exercise at approximately 143 hours, a computer program alarm was caused by a coupling-display-unit high rotation rate. This alarm resulted from the yaw/roll technique of landmark tracking causing rates greater than 0.6 deg/sec, one of the criteria which inhibit coupling display unit transient effects.

As a result of the problem that occurred during the first three service propulsion firings, an investigation had revealed that the fuel capacitance probe for a short time indicated considerably more fuel than was actually in the tanks. The spike was enough to indicate a critical unbalance and to activate the caution and warning system. The primary system also performed erratically at crossover, and again the caution and warning system sensed a large unbalance. After crossover, the oxidizer storage tank did not indicate empty on the primary system, and since the comparator network sums the storage and sump tank probe outputs before comparing oxidizer to fuel, the system again indicated an unbalance.

To provide an additional exercise of the propellant utilization and gaging system, the seventh service propulsion firing was increased to 25 seconds duration. However, the servo gains for the fuel and oxidizer readouts are different in the primary system, and the fuel was considerably higher than it should have been. This masked any fuel spiking caused by capillary action near the beginning of the firing. The oxidizer storage tank was still not indicating empty.

Throughout the mission, the weather in the western Atlantic recovery areas was very poor, but the forecasts had been for considerable improvement prior to the end of the mission. However, the weather conditions deteriorated, and the forecast for the time of landing was for winds of approximately 23 knots and wave heights of 6 to 8 feet. Although within the recovery limits, these conditions were very undesirable. The forecast further indicated that the area south of the nominal recovery zone would have favorable weather with winds light and variable and wave heights of 2 to 3 feet. Therefore, the deorbit maneuver was delayed by one revolution to permit the spacecraft to land in this area.

#### 14.2 NETWORK PERFORMANCE

The Mission Control Center and the Manned Space Flight Network were placed on mission status for Apollo 9 on February 14, 1969. Overall mission support by the Mission Control Center, including the Real Time Computer Complex, and the Manned Space Flight Network was good, and hardware, communications, and computer support was excellent, with no major data losses attributed to these systems. Telemetry, tracking, and command support was particularly reliable. The few failures had minimal impact on Mission Control Center operations. Air-to-ground communications were generally good; however, some problems were experienced as a result of procedural errors.

At orbital insertion, the orbits determined by the mission operations computer and by the dynamic standby computer in the Real Time Computer Complex did not agree. The discrepancy was attributed to a slight out-of-synchronization of less than 1 second between the two processors. Consequently, the mission operations computer began orbit processing with an erroneous insertion state vector and the dynamic standby computer began processing using S-band data from Bermuda. The dynamic standby computer orbit was determined to be more accurate, and this computer was selected as the mission operations computer.

Air-to-ground communication uplink were lost during a portion of the extravehicular activity. This failure was due to the stations being configured for S-band uplink only, while the crew had the S-band volume down. The stations were improperly configured because of a misinterpretation of a teletype message from the network controller.

The only significant data loss occurred during the first two revolutions, when launch vehicle data from all stations went to zero because of an erroneous bit in the instrument unit air-to-ground downlink. Data was restored during the second revolution.

Command operations were excellent throughout the mission. Although remote site computers experienced some faults and looping conditions, these failures had no significant impact on mission operations.

No significant tracking coverage, either S-band or C-band, was lost because of tracking system failures or procedural problems. During launch, between 0:01:00 and 0:06:25, Merritt Island and Bermuda tracking ~~data~~ indicated periodic loss of lock, bad angles, bad range rate, and generally intermittent track. After the spacecraft antenna configuration was changed from B OMNI to D OMNI, the tracking problem cleared. In addition, at the 85-foot S-band stations, difficulties were experienced in acquiring valid 2-way ranging with the lunar module while operating at a nominal 2-kilowatt power output. As a result, all 85-foot antenna stations were instructed to operate at 500 watts and to increase the power as necessary to maintain 2-way lock; no additional problems were experienced.

Several ground communications outages were experienced without significant data loss except for the time Goddard Space Flight Center switched from the on-line communications processor to the standby processor. This procedural error caused a loss of high-speed tracking data for about 10 minutes.

### 14.3 RECOVERY OPERATIONS

The Department of Defense provided recovery forces commensurate with the probability of a spacecraft landing within a specified area and with any special problems associated with such a landing. The recovery force deployment was very similar to that for Apollo 7 and is detailed in table 14-I.

#### 14.3.1 Command Module Location and Retrieval

The first recovery force contact with the spacecraft occurred at 1651 G.m.t. March 13, 1969, by the McCoy radar aircraft. Approximately 6 minutes later, recovery beacon and voice contacts were made by separate aircraft. At 1658 G.m.t., the spacecraft was sighted as it descended on the main parachutes, and it landed at 1701 G.m.t. (241 hours, 54 seconds elapsed time). The landing point was latitude 23 degrees 12.5 minutes north and longitude 67 degrees 56.5 minutes west as determined by a loran fix and a Tacan bearing taken from a helicopter at the point of landing.

The spacecraft remained in a stable I flotation attitude, and the swimmers and flotation collar were deployed approximately 6 minutes after landing. After collar installation, the flight crew egressed and were retrieved by helicopter. The crew arrived aboard the prime recovery ship U.S.S. Guadalcanal 49 minutes after landing. The main parachutes were not recovered, but the apex cover was retrieved. The command module was hoisted aboard the recovery ship 2 hours 12 minutes after landing.

The flight crew departed the recovery ship by helicopter at 1500 G.m.t., March 14, 1969, and arrived in Eleuthera, in the Grand Bahama Islands at 1630 G.m.t. The crew was then transferred by aircraft to Houston.

The following is a chronological listing of significant events during the recovery operation.

<u>Time, G.m.t.</u>	<u>Event</u>
1651	Radar contact by aircraft
1657	Recovery beacon contact by recovery aircraft on 243.0 MHz; VHF voice contact by recovery helicopter on 296.8 MHz
1658	Visual sighting of command module from recovery helicopter
1701	Command module landed
1707	Swimmers and flotation collar deployed
1714	Flotation collar installed and inflated
1727	Command module hatch opened
1745	Flight crew aboard helicopter
1750	Flight crew aboard ship
1913	Command module retrieved

The weather conditions, as reported by the U.S.S. Guadalcanal at 1913 G.m.t., were as follows:

Wind direction, deg true	200
Wind speed, knots	9
Air temperature, °F	79
Water temperature, °F	76
Cloud cover	2000 scattered 9000 broken
Visibility, miles	10
Wave height (swells)	7 feet
Wave direction, deg true	340

### 14.3.2 Recovery Equipment Performance

All recovery equipment performed normally with the following exceptions.

During the crew retrieval operation, difficulty was encountered in maintaining the life rafts in an upright position because of gusting from the helicopter. In one instance, one of the rafts overturned while one of the crew was transferring to another raft. This problem will be remedied on future missions by properly securing and weighting the rafts.

Improper recovery techniques resulted in two of the crew momentarily entering the water during helicopter pickup. Proper emphasis on recovery training will preclude this problem from recurring after future flights.

Before command module retrieval, it was necessary for the swimmers to recycle the hatch latching mechanism before closing the hatch, since the initial attempt to latch the hatch was unsuccessful. The reason for this discrepancy is not known.

During spacecraft retrieval, the fitting which secures one end of the lifting cable on the crane failed and jammed in the pulley mechanism, rendering the crane inoperative. A mobile backup crane was used to complete spacecraft retrieval. At the time of the failure, the command module fell back into the water, and the resulting impact on the flotation collar caused the sea anchor attachment to come loose. Prior to future missions, cranes will be static load tested and visually inspected while in port, and periodically during the flight prior to command module retrieval.

The first surface-to-air retrieval operation, for press film, was completed as scheduled. During the second operation, however, the container of biomedical samples was not successfully retrieved because the line connecting the container and the balloon snapped. The line had not yet been fully engaged by the aircraft, and the reason for the failure was considered to be a defective line.

### 14.3.3 Direction Finding Equipment

The following is a summary of the electronic contacts made by the recovery forces after entry and before visual sighting.

<u>Aircraft</u>	<u>Time of first contact G.m.t.</u>	<u>Range, miles</u>	<u>Type receiver</u>
McCoy Radar	1651	236	Radar
Kindley Rescue 1	1657	158	AN/ARD-17
Recovery 1 (SH-3D)	1657	15	Sarah
Recovery 2 (SH-3D)	1657	13	Sarah
Recovery 3 (SH-3D)	1657	1	Sarah
Air Boss (SH-3D)	1657	4	Sarah

#### 14.3.4 Command Module Postrecovery Inspection

The following is a summary of discrepancies noted during the post-recovery inspection. All other aspects of the spacecraft were normal.

- a. The edge around the top of the tunnel had been damaged during the retrieval operations.
- b. The wires for the interphone were severed in several places, apparently during the retrieval operation.
- c. Both VHF antennas were destroyed during the retrieval operation.
- d. The heat shield had several small dents caused by contact with the ship's catwalk during retrieval. There also were some vertical dents caused by the flotation collar positioning cables.
- e. Bubbles were noticed in the liner of the plus-Y roll thrusters.
- f. The hatch window had a 1-inch wide film deposit around its perimeter. The two rendezvous windows had a light "rainbow-like" film over most of their surfaces. Both side windows had a light film deposit around their perimeters.
- g. It was necessary to recycle the hatch latching mechanism before closing and latching the hatch, because the initial attempt to latch the hatch was unsuccessful. When the hatch was initially reopened, the shear pin was found to be extended.

#### 14.3.5 Command Module Deactivation

The command module was offloaded at the Norfolk Naval Air Station on March 16, 1969. The Landing Safing Team began evaluation and deactivation at 1600 G.m.t. Inspection of the command module indicated that all of the normally activated pyrotechnics had operated. The remainder of the pyrotechnics were safed by removal of the electrical connectors and the installation of caps. The reaction control system propellants had been dumped by the crew during descent, and the remaining quantities were not measurable. Gas samples taken during deactivation indicated that the reaction control system tanks and plumbing had been properly cleaned.

Deactivation was completed on March 19, 1969. The command module was received at the contractor's facility in Downey, California, on March 21, 1969.

TABLE 14-I.- RECOVERY SUPPORT

Landing area	Maximum retrieval time, hr	Maximum access time, hr	Support		Remarks
			Number	Unit	
Launch site	--	1/2	1	HH-3E	Helicopter which provided short access time to landing point for 3-man pararescue team. Carry launch site recovery commander.
			2	HH-53C	Heavy-lift helicopter which provided short access time to landing point for 3-man pararescue team. Provide command module uprighting capability.
			2	LVTR	Amphibious vehicle which provided surf command module retrieval capability.
			1	LCU	Landing craft utility which provided deep water retrieval capability.
			2	K-501 fire suppression kit	Provide fire suppression capability.
			1	ATF	USS Paiute, salvage ship which provided deep water salvage capability
Launch abort	24 Sector A	4	1	LPH	USS Guadalcanal, landing platform helicopter
			5	SH-3D	Helicopters, three recovery, each with a 3-man swim team, one photographic, and one air traffic control
	48 Sector B		1	ATF	USNS Vanguard, Apollo instrumentation ship
			1	AKA	USS Algol, attack cargo ship
			3	HC-130H	Fixed wing search and rescue aircraft, each with a 3-man pararescue team
Primary	8	2	1	LPH	Primary recovery ship, USS Guadalcanal, redeployed from launch abort station.
			5	SH-3D	Helicopters, three recovery, each with a 3-man swim team, one photographic and one air traffic control.
			2	EC-121	McCoy radar aircraft
			2	HC-130	Fixed wing search and rescue aircraft, each with a 3-man pararescue team.
			8	HC-130	Fixed wing search and rescue aircraft, each with a 3-man pararescue team; includes three supporting launch abort area.
Secondary	24	6	8	HC-130	Fixed wing search and rescue aircraft, each with a 3-man pararescue team; includes three supporting launch abort area.
West Atlantic			1	LPH	USS Guadalcanal redeployed from launch abort station.
Mid-Pacific			2	DD	USS Nicholas and USS Cochrane
West Pacific			1	DD	USS Mason
East Atlantic			1	AKA	USS Algol redeployed from launch abort station.
Contingency	--	18	16	HC-130	Fixed wing search and rescue aircraft, each with a 3-man pararescue team, including eight supporting the four recovery zones.
TOTALS: Fixed wing aircraft - 18; helicopters - 5; ships - 7 (including the USNS Vanguard).					

## 15.0 ASSESSMENT OF MISSION OBJECTIVES

The primary objectives for the Apollo 9 mission are defined in reference 7 and were as follows:

1. Demonstrate crew/space vehicle/mission support facilities performance during a manned Saturn V mission with command and service modules and lunar module.
2. Demonstrate lunar module/crew performance.
3. Demonstrate performance of nominal and selected backup lunar-orbit rendezvous mission activities, including:
  - a. Transposition, docking, and lunar module withdrawal
  - b. Intervehicular crew transfer
  - c. Extravehicular capability
  - d. Service propulsion system and descent propulsion system firings
  - e. Lunar module active rendezvous and docking.
4. Spacecraft consumables assessment.

Detailed test objectives defining the tests required to fulfill the primary mission objectives are defined in reference 8. These detailed test objectives are listed in table 15-1 and referenced to the primary objectives discussed previously.

The data presented in other sections of this report are sufficient to verify that the primary mission objectives were met. However, in three cases, portions of detailed test objectives were not met. These objectives and their significance are discussed in the following paragraphs.

### 15.1 LUNAR MODULE S-BAND COMMUNICATION PERFORMANCE

The following functional tests were not accomplished:

1. Signal combination 7; Carrier, voice/biomedical extravehicular mobility unit, 1.6 kbps telemetry
2. Signal combination 8; Carrier, backup voice/extravehicular mobility unit/biomedical, 1.6 kbps telemetry

The planned tests were not completed because of timeline constraints. These frequency combinations will not be demonstrated on the lunar orbit mission. The failure to accomplish these tests does not impose constraints on subsequent missions or on the hardware. Initial planning indicated that frequency mode 7, in low power, would be adequate for lunar stay communications. A recent review of circuit margins indicates that the optimum prime lunar stay mode would be similar to mode 7, only using high power with the erectable or steerable antenna. A functional demonstration of frequency combination 8 (backup mode) should be included on the first lunar landing mission during checkout prior to the first surface exploration.

The lunar module steerable antenna functional test was deleted during the mission. The planned investigation of the antenna tracking capability in both the manual and automatic modes was not attempted because of timeline constraints. Successful completion of the lunar orbit mission objective - Lunar Module Communications at Lunar Distance (Mission Objective P16.10) will demonstrate the steerable antenna modes.

#### 15.2 SPACECRAFT/NETWORK S-BAND/VHF COMPATIBILITY

The functional test of voice relay from network to command module by VHF and from command and service modules to lunar module by S-band was not completed. Time constraints prevented the actual demonstration of the planned test.

#### 15.3 EXTRAVEHICULAR ACTIVITY

The principal portion of this detailed test objective was the donning and checkout of the operation of the extravehicular mobility unit depressurizing the spacecraft, and evaluating the hatch operation. A secondary portion of the objective, that of extravehicular activity, included egress from the lunar module, transfer to and return from the command module hatch using translation aids and retrieval of thermal samples.

All the principal portions of the objectives were accomplished. The extravehicular transfer capability was successfully demonstrated during the extravehicular activity, which was abbreviated because of a minor in-flight illness experienced by the Lunar Module Pilot on the preceding day. Even though a complete extravehicular transfer was not accomplished, sufficient data were obtained to demonstrate crew life support.

In addition, the degree of proficiency necessary for transfer while maintaining the desired body control using the translation aids, was also demonstrated. As a result of this demonstration, this portion of the objective was also considered successful.

TABLE 15-1.- DETAILED TEST OBJECTIVES

Number	Description	Primary objectives supported*	Completed
P1.23	Command and service module autopilot stability margin	3	Yes
P1.24	Command and service module platform alignment accuracy	3, 4	Yes
P1.25	Platform orientation determination/visibility	3	Yes
S1.26	Orbital navigation/landmark tracking	3, 4	Yes
P2.9	Guidance, navigation, and control system/manual thrust vector control takeover	3	Yes
S7.29	Exhaust effects/command and service module	1	Yes
P11.5	Lunar module platform inflight alignment	2	Yes
M1.6	Lunar module primary guidance, navigation, and control system/digital autopilot and descent propulsion thrust performance	2	Yes
P11.7	Primary guidance, navigation, and control system attitude/translation control**	2, 4	Yes
P11.10	Primary guidance, navigation, and control system and guidance, navigation, and control system performance	2, 3	Yes
P11.14	Primary guidance, navigation, and control system control of ascent propulsion firing	2, 4	Yes
P12.2	Abort guidance inflight calibration and performance	2	Yes
P12.3	Abort guidance/control electronics attitude/translation control	2, 4	Yes
P12.4	Abort guidance delta V capability using descent propulsion system	2, 4	Yes
S13.10	Ascent propulsion system firing to propellant depletion	2	Yes
M3.11	Long-duration ascent propulsion system firing	2	Yes
M3.12	Descent propulsion firing effects and primary propulsion/vehicle interactions	2, 3	Yes
M4	Lunar module environmental control system performance	2, 4	Yes
M5.3	Lunar module electrical power system performance	2, 4	Yes
P16.4	Rendezvous radar tracking performance	2, 3	Yes
P16.6	Landing radar self-test	2	Yes
M6.7	Landing radar/structure/plume	2	Yes
P16.19	Rendezvous radar/reaction control system plume impingement/corona effects	2	Yes
M7.9	Landing gear deployment/thermal	2	Yes
M17.17	Lunar module environmental and propulsion thermal effects	1, 2	Yes
M7.18	Lunar module structural integrity	1	Yes
P20.21	Lunar module/Manned Space Flight Network S-band communication performance	1, 2	Partially
P20.22	Lunar module/Manned Space Flight Network/extravehicular activity S-band/VHF compatibility	1, 2, 3	Partially
P20.24	Command and service module active docking	3, 4	Yes
P20.25	Lunar module ejection from adapter	3	Yes
P20.26	Lunar module/command and service module undocking	2, 3	Yes
P20.27	Lunar module rendezvous	2	Yes
P20.28	Lunar module active docking	2, 3, 4	Yes
P20.29	Lunar module jettison	2	Yes
P20.31	Support facilities performance	1	Yes
S20.32	Crew activities evaluation (command and service modules/lunar module)	1, 2	Yes
P20.33	Command and service module single crewman rendezvous capability	3	Yes
P20.34	Intravehicular crew transfer	2, 3	Yes
P20.35	Extravehicular activity	3	Yes
S20.37	Descent engine plume effect	2, 3	Yes
S20.120	Command and service module/lunar module electromagnetic compatibility	3	Yes
Functional tests added during the mission			
Command and service module intravehicular transfer, unsuited			
Tunnel clearing, unsuited			
Command module platform alignment, program 52, in daylight			
Command module platform alignment, program 52, using planet (Jupiter)			
Digital autopilot orbital rate, pitch and roll			
Backup gyro display coupler alignment of stabilization and control system			
Window degradation photography			
Satellite tracking, ground inputs			
Command and service module high-gain S-band antenna reacquisition test			
Passive thermal control cycling at 0.1 deg/sec at three deadbands: $\pm 10$ deg, $\pm 20$ deg, $\pm 25$ deg			

\*See page 15-1 for primary objectives.

\*\*Proportional rate control not exercised.

## 16.0 LAUNCH VEHICLE SUMMARY

Launch vehicle performance was within the preflight-predicted dispersion envelopes. All test objectives were accomplished, except that the scheduled liquid oxygen and hydrogen dump after the S-IVB third firing was not achieved. The performance of most launch vehicle systems was nominal, and no major failures occurred.

All first stage flight performance parameters were within the predicted 3 sigma limits, but the thrust was lower than predicted as evidenced by low velocity and altitude at the end of S-IC thrusting. First stage thrust at center engine cutoff was approximately 2.29-percent lower than predicted. Preliminary analysis indicates that the low thrust resulted mostly from lower-than-predicted engine sea-level performance, and higher fuel density than used in the prediction.

First stage thrust reduced to standard inlet conditions at 36.5 seconds was 1.21-percent lower than predicted. This was primarily the result of the use of erroneous tag values in the prediction due to an error in measuring specific gravity and combustion pressures in preflight engine firing tests. Also there was a thrust bias variation between the Saturn V flights and the acceptance test firings.

Low-frequency (16 to 19 Hz) oscillations occurred in the engine parameters during the latter portion of S-II powered flight and damped out shortly before cutoff. These oscillations were similar to, but appeared to be somewhat more severe than, those observed on Apollo 8. Initial oscillations in the engine parameters occurred intermittently over several short time intervals in the center engine liquid oxygen pump inlet pressure beginning at 482 seconds. These short periods of oscillation were also detected in the center engine crossbeam and liquid oxygen sump accelerometers at 482 and 487 seconds, respectively. Continuous oscillation buildup at these locations began at approximately 497 seconds and damped out at approximately 531 seconds.

Center-engine thrust-chamber pressure oscillations began at approximately 500 seconds, peaked at 506 seconds (predominant frequency 16.9 Hz), and damped out at 531 seconds. The peak-to-peak amplitude of chamber pressure oscillations at 506 seconds was about 80 psi, as compared to 60 to 70 psi maximum peak-to-peak oscillations observed in the center engine chamber pressure on Apollo 8. During the oscillation period, 16 to 19 Hz oscillations were also evident in the chamber pressure measurements on the outboard engines.

The liquid oxygen net positive suction pressure was maintained at a high level during the latter portion of powered flight by a liquid-oxygen-tank step pressurization sequence. Higher net positive suction pressure, as provided on Apollo 9, apparently is not a factor in eliminating the low-frequency oscillation. The cause of the low-frequency oscillations has not yet been conclusively identified. The problems appears to be associated with inflight liquid-oxygen levels.

The purpose of the third S-IVB firing was to demonstrate restart capability after an 80-minute coast and to demonstrate performance related to a failure of both chilldown systems. Normally, the engine requires liquid oxygen and liquid hydrogen chilldown to condition the pumps prior to the engine start command. To simulate a chilldown system failure, after the chill pumps were spun up, the chilldown shutoff valves were closed. An attempt was then made to restart the S-IVB engine under the simulated failure condition. A ground command initiated a 51.6-second fuel lead to condition the thrust chamber and fuel pump inlet. At the opening of the start tank discharge valve, the resulting fuel-pump inlet conditions were well within the start and run limits, indicating adequate conditioning of the fuel pump inlet. Due to the absence of chilldown, the liquid oxygen pump inlet conditions were outside the start limits and this condition is related to the abnormal performance seen on the third firing.

The abnormal propellant quality and the cold hardware conditions at the opening of the start tank discharge valve could have been the source of abnormal start condition which was noted throughout the third firing. Early engine injector development testing indicated that thrust chamber pressure oscillations could occur as a result of excessive chilling of the thrust chamber and injector.

At 0.62 second after the engine start command, a 100-psid spike was noted in the gas generator chamber pressure. Due to slow response time of the instrumentation, the magnitude of the pressure spikes cannot be measured, however, correlation with a close-coupled transducer during the engine gas generator development testing indicated the actual pressure may be as high as 5000 psid. This pressure could "blow out" the gas generator spark plugs or severely damage the combustor. One hypothesis at this time is that the erratic behavior of the engine area ambient and thrust chamber jacket temperature measurements was caused by hot gases escaping from the gas generator.

At 50 seconds after the opening of the start tank discharge valve, the engine pneumatic regulator pressure dropped to zero. At this time, it is believed that the high-vibration levels which accompany thrust chamber pressure oscillations caused the helium control solenoid valve to fail closed. After engine pneumatic regulator pressure was lost, the accumulator pressure decayed to a level insufficient to keep the augmented

spark igniter liquid oxygen valve, gas generator valve, and liquid oxygen and fuel bleed valves fully open. The gas generator valve left the open position 93 seconds after the opening of the start tank discharge valve. The liquid oxygen bleed valve opened 6 seconds later, thus bypassing liquid oxygen flow back to the liquid oxygen tank and resulting in an engine chamber pressure decrease of 200 psid 98 seconds after the opening of the start tank discharge valve. At 141 seconds after the opening of the start tank discharge valve, the liquid hydrogen bleed valve opened resulting in an additional 50 psid decrease in chamber pressure.

The S-IVB engine cutoff was initiated at 242.433 seconds after the opening of the start-tank discharge valve by a timed cutoff. The engine cutoff transient was unusual due to the drop in performance during the firing and resulted in a very low chamber pressure at cutoff. Because of the low closing pressure required by the main oxidizer valve and main fuel valve, there was sufficient accumulator pressure to close these valves at cutoff. The cutoff transient total impulse was 43 718 lbf-s predicted as compared to 46 891 lbf-s from actual engine data.

## 17.0 ANOMALY SUMMARY

This section contains a discussion of the significant anomalies from the Apollo 9 mission. All other discrepancies are discussed in the systems performance sections of this report.

### 17.1 COMMAND AND SERVICE MODULES

#### 17.1.1 Propellant Isolation Valve Closures

Following separation from the S-IVB, the crew reported a control problem which had lasted for about 12 minutes during the transposition period. The crew first noticed a lack of capability for translation to the left. The position indicator flags for the quad C primary and secondary propellant isolation valves and the quad D secondary valves were in the "barber pole" or closed position (fig. 17-1). The valves were opened and the system performed normally thereafter. These valves had been opened during final checks prior to launch, were verified to be open during orbital insertion checks by the crew, and again were verified during a cursory examination of the panel after the Commander and the Command Module Pilot exchanged seats prior to separation from the adapter.

The isolation valve magnetically latches open and is spring-loaded to the closed position. The valves are controlled by momentary switches, located on panel 2, which are spring-loaded to center-off. The four isolation valves in each quad are controlled by one switch (fig. 17-1). The quad C and D switches are adjacent to each other, and normally all four primary and secondary valves are opened or closed simultaneously. The closed indication in quad D for the secondary valves only required that either one or both of the secondary valves be closed, but neither of the primary valves. Tests have demonstrated that it is possible to strike the switch momentarily so that only one of the four valves is closed, but this occurrence has only been demonstrated once in two hundred attempts. Each switch is guarded by a wicket which extends slightly beyond the switch to minimize inadvertent actuation; however, since the switch is spring-loaded to center, inadvertent actuation could go undetected.

Propellant usage data (fig. 17-2) showed that all four quad C valves were closed and that quad D was performing normally before the crew reopened the propellant isolation valves. Propellant may be supplied from either the primary or secondary tanks, and only the valve indicator for the secondary tank was in the "barber pole" position for quad D. Closure of only one of the secondary valves is sufficient to cause the indication (fig. 17-1).

The following possibilities could explain the valve closures:

a. Momentary, inadvertent switch actuation by the crew - This is not likely, as the two crewmen checked the panel after they exchanged seats.

b. Momentary switch closure caused by contamination - No particulate contamination was found in the switches.

c. Induced electrical transients - This has been discounted because of the power level required to operate the solenoids.

d. Reduced latching force - The propellant isolation valves in the command module reaction control system are identical to those in the service module system. To determine whether the magnetic latching force of the valves could have been deteriorated, the valves on command modules 103 and 104 and those from several ground tests were checked. Results compared favorably with original acceptance test data on those particular valves.

e. Valve closure caused by mechanical shock at separation of the command and service modules from the adapter - Shock tests were performed on several isolation valves and on an assembled quad. These tests were conducted to determine the shock load required to close the valves and to determine the effect of the shock loads encountered during the separation sequence. A cross section of the valve is shown in figure 17-3. The results of the individual valve tests indicate that 80g with an onset rate of about 11 milliseconds could cause a valve to close. The shock at the valve resulting from the pyrotechnic charges used to separate the command and service modules from the adapter has been estimated to be between 180 and 260g with an onset rate between 0.2 and 0.5 millisecond. Shock loads from 120 to 670g with onset rates ranging from 0.12 to 1.8 milliseconds failed to cause the valves to close during the test on the assembled quad. Apollo 7 and 8, with the same pyrotechnic and structural configuration, did not have the problem.

Results of the investigation have been inconclusive as to the cause of the valve closures. However, the possibility of a valve closure still exists, and since the hardware was not detrimentally affected, the flight procedures have been modified to verify isolation valve indications after exposure to shock environments.

This anomaly is closed.

### 17.1.2 Scanning Telescope Shaft Drive Problem

The scanning telescope shaft stuck intermittently during the first 5 days of the mission, and the mechanical counter shaft became inoperative on the second day of the mission.

The counter malfunction was caused by the pin on the "tenths" drum dropping out (fig. 17-4) and eventually jamming the gear. One revolution of the counter shaft results in the pin engaging a geneva gear which is meshed to the "units" drum of the counter. If the pin is missing, the "tenths" drum will rotate but, the "units" drum will not be engaged through the geneva mechanism, resulting in no movement of the degree indicators of the counter. The intermittent sticking of the shaft was caused by the loose pin from the counter lodging between the split anti-backlash gear on the shaft resolver. Repeated operation of the manual adjust screw with the universal tool eventually wedged the pin between the anti-backlash gears, providing proper mesh of the gear train; this, in turn, freed the telescope shaft and enabled proper freedom of motion. Detailed tolerance measurements of the failed unit show that all parts conformed to the drawings and specifications with the exception of the hole on the "tenths" drive hub. The hole, which should have retained the pin, was out of tolerance. Figure 17-4 shows the pin/hole interface specification dimensions for this assembly. The hole dimension of the failed part was +0.00032-inch oversize in diameter, resulting in a hole diameter of 0.03992 inch. The pin diameter was measured to be 0.03992 inch. The specification requires an interference fit of 0.0002 to 0.00011 inch. Dynamic load analysis of the counter and a tolerance study of the pin/hole interface indicates that the design is adequate. The failure was the result of an out-of-tolerance hole on the drive hub of the "tenths" drum. Repeated impact by the geneva mechanism resulted in the pin slipping from the hole sufficiently to come into contact with the pinion gear on the counter shaft. Impact by the pin on the pinion gear resulted in the pin dislodging from the drive hub.

The counter design is common to both the command module and the lunar module optics. As a corrective action, the counter on the command module for Apollo 10 have been replaced with a counter that has been properly inspected. The counters on subsequent command modules and lunar modules will be replaced with inspected counters.

This anomaly is closed.

### 17.1.3 Loss of Automatic Cryogenic Hydrogen Pressure Control

During the flight, the automatic pressure control system in the hydrogen tanks failed. The logic of the control system (fig. 17-5) is such that the pressure switches in both tanks must close in order for the heaters to be activated; however, opening of only one pressure switch will deactivate the heaters. The first indication of failure was noted at 93 hours, shortly after the initial undocking, when the heaters were not automatically activated (fig. 17-6). At approximately the time of the final lunar module undocking, all hydrogen tank heaters came on and pressurized the tanks to about 270 psia, which required that the heaters be turned off manually.

As a result of the automatic pressure control system failure, the hydrogen pressure was controlled using the manual mode throughout the remainder of the mission.

Since the first failure (failure to turn on) would have required one pressure switch to fail open and the second failure (failure to turn off) would have required that both pressure switches fail closed, the switches can be ruled out. The most probable cause for the failures was an intermittent open-circuit condition in the motor control circuit (including the power line, ground, and the terminal board for 16-gage pins) resulting from the undocking shock (see fig. 17-5). Sixteen-gage terminal boards have been the source of intermittent contact in other circuits during ground tests.

No corrective action will be taken for Apollo 10, since the tank pressures can be controlled manually by either the heaters or the fans if the automatic system fails.

This anomaly is closed.

### 17.1.4 Erroneous Docking Probe Indications

During initial undocking, the Command Module Pilot placed the probe-extend/release-retract switch to extend/release, and the vehicles began to separate, indicating release of the probe-extend latch. However, the vehicles did not physically unlatch until the third attempt. Indications are that the switch was not held in position long enough for a separating force to effect physical separation.

The second discrepancy occurred prior to the lunar module docking maneuver, when the Command Module Pilot placed the switch in the retract position in preparation for docking. In this position, the display showed "barber pole," indicating that the probe was not cocked for docking. This is further evidence that the extend/release-retract switch

was not actuated for a sufficient time to allow the docking probe to fully extend. Cycling the docking mechanism produced the proper gray display indication.

The design will allow the latches not to cock during undocking if the release motors are not energized sufficiently long for the latches to spring back to proper attitude for cocking. The system returns to the uncocked (latches-locked) configuration which exists when docked. This action has been verified in ground tests and visual analysis of the mechanism.

The Apollo Operations Handbook has been changed to include the requirement for holding the extend/release-retract switch in the extend/release position until physical separation.

This anomaly is closed.

#### 17.1.5 Uplink Commands Not Accepted

Beginning about 109 hours, the spacecraft/ground command system malfunctioned. This condition existed until the crew cycled the up-telemetry command/reset switch at approximately 118:45, restoring normal operation.

During the period from 109:00 to 118:45, 55 real-time commands were attempted. For over 50 percent of the attempts, the command system was inoperative due to one or more of the following conditions: ground station uplink modulation was turned off; ground station decommutator was out-of-lock; and up- and down-RF signal strengths were marginal or too low.

Any of these conditions would contribute to the discrepancy. However, no explanation exists for the remainder of the commands to which the spacecraft did not respond.

A spacecraft problem could have been caused by the spacecraft wiring, a spacecraft switch (up-telemetry command/reset), the updata link, or an interface stimulus. Analysis of postflight tests conducted indicates the following results:

- a. Spacecraft wiring continuity/resistance tests have uncovered no problem.
- b. Spacecraft switch operation and contact resistance were measured, and no problems were identified.
- c. The updata link has completed bench checkout, functional test, acceptance thermal tests, and acceptance vibration test with all performance parameters nominal.

d. The updata link was operated with a signal-to-noise ratio below the specification level of 8 dB for 17 000 messages with no rejects. The updata link was successfully operated with an input signal as low as 50 millivolts (normal input 1 volt) with no problem identified.

pecial low-voltage tests resulted in "hanging up" the updata link program counter. It was necessary to lower the 28 V dc input voltage to 15.3 volts and vary the voltage above and below that point. When the voltage was reduced below the critical voltage and then brought back up, the low-voltage detector failed to send a reset signal to the programmer. The vehicle address flip-flop circuit was set in the wrong state and inhibited the program counter. This prevented the updata link from accepting commands until the dc power was turned off and back on, which reset the counter.

A review of the spacecraft bus voltages did not reveal a power voltage characteristic of this nature and it is most unlikely that the updata link supply voltage during flight could have assumed the necessary conditions to "hang up."

A comprehensive review of spacecraft data, plus postflight testing of flight hardware and detailed analysis of the total spacecraft command system has not identified a specific cause for the flight program. However, if the malfunction should recur, the up-telemetry command/reset switch shall be recycled to restore operation.

This anomaly is closed.

#### 17.1.6 Entry Monitor System Failure

The entry monitor failed to scribe during entry. Postflight testing of the scroll assembly has determined that the environmental seal contained a gross leak. The leak was detected around the base of one of the four scribe glass adjustment screw cups and was estimated to be of the order of 1.0 cc/sec. The leaking screw cup showed evidence of physical damage, indicating possible unit mishandling after the last leak test.

Analysis of the scroll after removal from the unit disclosed that the unit scribed properly for the first flight test pattern. It failed to scribe at the start of the pre-entry flight test pattern and began scribing again during the last half of the pattern. Scribing of the film was proper down to the initial set position of the first entry pattern but scribing failed from that point through entry until just prior to drogue deployment.

Through use of special lighting and photographic techniques, photographs of the scroll revealed that the acceleration/velocity drive assembly which holds the stylus for scribing the film functioned properly and would have indicated the proper entry pattern if the scribing had worked properly. The scribe coat became hard during flight such that the stylus failed to scribe.

The scroll is susceptible to moisture and subsequent slow drying of the moisture causes a hardening of the film coat. The scroll was probably moisturized when ambient air leaked into the unit prior to lift-off. During flight, the cabin pressure was reduced to 5 psia, providing a slow vacuum dry as the moist air was expelled from the unit. After soaking for 10 days at 5 psia, the scribe coat hardened, causing the failures to scribe.

Postflight analysis also revealed contamination on the stylus holder and bushing; the contamination, found to be Lock-tite used on the keeper screw of the stylus holder, caused a 2- to 3-second lag in the stylus response.

Corrective action will be implemented on command module 106 and subsequent, as follows:

- a. Glyptol will be used instead of Lock-tite on the keeper screw.
- b. The stylus spring load will be increased to 11 (+1, -0.5) ounces.
- c. The dimension of the stylus holder and bushing will be verified.
- d. Acceptance tests will be performed to verify repeated scribing.

This anomaly is closed.

#### 17.1.7 Indicated Service Propulsion Propellant Unbalance

During the third firing of the service propulsion engine, there were eight master alarms from the propellant utilization and gaging system indicating an excessive propellant unbalance (fig. 17-7).

All the master alarms are explainable. The first alarm was caused by propellant level in the capacitive measuring tube not reaching the settled level as soon as expected after start-up. The next five alarms, shown in figure 17-7, resulted from an electrical zero bias in the oxidizer measuring circuit after storage tank depletion. Thus, continuous alarms on the primary gaging system caused the crew to switch to the auxiliary system, which employs point sensors at discrete levels in the tanks.

A legitimate unbalance caused an alarm during the auxiliary system operation, as noted. Also, switching back to the primary system resulted in another alarm, which reflected not only the oxidizer storage tank bias but a legitimate unbalance.

Master alarms and caution and warning indications from the propellant utilization and gaging system are not required. Consequently, these functions have been cut from the system for spacecraft 106 and subsequent, as shown in figure 17-8. A procedural change in the zero adjustment to minimize the electrical zero bias has been implemented. Also, the extended time for gaging stabilization will be brought to the attention of crews of subsequent flights.

This anomaly is closed.

#### 17.1.8 Unexplained Master Alarms

A master alarm without a caution and warning annunciator occurred coincident with docking. No input was identified as being in the range of the caution and warning system at that time. The fact that the alarm did not occur at physical contact but during the hard docking rules out static discharge between the two vehicles and indicates a shock-sensitive condition. The master alarm system is very sensitive to trigger signals and requires only a 5-microsecond pulse to initiate an alarm. The caution and warning lights require a continuous input to illuminate. A shock-sensitive intermittent condition in one of 69 inputs could trigger the alarm.

During the Apollo 10 docking tests at the launch site, three unexplained master alarms occurred. Data review revealed that accelerations were occurring in the vehicle coincident with each master alarm. Review of data procedures, voice tapes, and troubleshooting of suspect transmitter circuits revealed no condition that would cause the master alarms. Therefore, a recurrence is likely during the Apollo 10 mission.

Numerous master alarms were noted during the mission and in all except three cases, they have been satisfactorily explained. The cause of these master alarms at the following times cannot be determined.

- a. During the first docking at 3:02:00
- b. During the deorbit maneuver at 240:31:20.472
- c. Following drogue deployment at 240:55:45.472.

The caution and warning unit was removed from the spacecraft and postflight tests were conducted. The results of this testing indicated

that none of the caution and warning input limits had shifted to an out-of-tolerance condition. Thermal, vibration, and shock tests on the unit do not show a shock-sensitivity or input-limit shift.

There are no data available to indicate that a caution and warning unit malfunction was the cause for the unexplained master alarms. These master alarms can only be explained by external inputs to the caution and warning system caused by such items as intermittent wiring, shock sensitive transducers, or system transients.

This anomaly is closed.

#### 17.1.9 Fuel Cell 2 Condenser Exit Temperature

The condenser exit temperature for fuel cell 2 was outside the normal range (155° to 165° F) on numerous occasions but did not exceed 200° F. This condition was similar to that observed on Apollo 7. Analysis shows that the travel of the secondary coolant regenerator bypass valve (see fig. 17-9) was restricted between approximately 4- and 10 percent bypass between 88 and 191 hours. The condenser exit temperature remained within normal operating limits at all loads after 191 hours. However, the loads after that time were relatively high, requiring normal bypass valve modulation between 8 and 19 percent.

Previous ground tests and analysis of coolant drained from vibration and flushing operations of other spacecraft show that coolant loop contamination buildup in the valve caused the restricted travel of the bypass valve. This contamination is present in the form of gelatinous phosphates and/or solid particles.

Analysis indicates that two fuel cells can support spacecraft electrical loads even if one or both have sticking secondary bypass valves. Additionally, the block I valve, which is less susceptible to contamination, will be incorporated in spacecraft 110 and subsequent.

This anomaly is closed.

#### 17.1.10 Docking Spotlight Failed

The Command Module Pilot reported during the lighting check prior to rendezvous that the docking (exterior) spotlight on the service module did not operate. Photographs of the vehicle during rendezvous showed that the light did not deploy. The circuit breaker for deploying the light was open at launch, as specified, to prevent inadvertent deployment, and the breaker had not been closed prior to the attempt to deploy the light (the crew checklist did not include closure of the breaker).

Other circuits powered through this breaker were either redundant or were not used until later in the mission. Later, the breaker was closed for operation of the crewman optical alignment sight in the right-hand position, and the sight operated properly.

The crew checklist has been changed to include closing of the circuit breaker prior to spotlight deployment.

This anomaly is closed.

#### 17.1.11 Interior Floodlight Anomalies

The crew reported three anomalies associated with the interior floodlights.

Functional postflight testing disclosed that only the primary lamp in the right-hand lower equipment bay floodlight failed. The failure analysis showed total erosion of the cathode. Also, the failed lamp had a mechanical bond failure that could have contributed to the cathode failure by causing cathode breakage. Breakage will result in total erosion. Erosion can also be caused by lamp contamination, the effects of electrical starting characteristics, and the operation of the lamp at lower voltage. By operating the lights in the full-bright configuration, the effect of cathode erosion is reduced. Procedures have been incorporated to insure that this is done in ground tests and in flight.

The floodlight on the right-hand head rest reportedly overheated and emitted a burning odor. Functional testing of the light indicated normal operation, and inspection did not disclose any visual evidence of overheating. A thermal rise test showed that the hottest point on the assembly, under stabilized temperatures, was the lens. The following temperatures were recorded during the testing:

Single lamp - 130° F at 5 psia; 170° F at 0.0001 torr

Dual lamp - 170° F at 5 psia; 200° F at 0.0001 torr

During the test, an odor was detected and attributed to touch-up paint applied to the light. A note has been added to the Apollo Operations Handbook that the floodlights will be hot and that operation should be in a single-lamp configuration.

The failure of the secondary lamp on the left-hand head rest was caused by a broken wire in the command module.

These anomalies are closed.

## 17.1.12 Computer Response to Manual Entries

The crew reported two occasions in which the computer did not receive and act upon data entered through the display and keyboard assembly. The first case involved a digital autopilot configuration change before the sixth service propulsion maneuver. The data required to incorporate the intended change were keyed into and displayed on the display and keyboard assembly. Depression of the ENTER key was reported, but the autopilot configuration did not change. The second case occurred during a spacecraft power-down period when Verb 46 ENTER, which deactivates the autopilot, was unsuccessful. The two occurrences are different in that different failure or procedural error characteristics would be required to produce the reported symptoms. A depression of the ENTER key transmits a 5-bit keycode to the computer, which then takes appropriate action corresponding to the data previously keyed into and displayed on the display and keyboard assembly. At the same time, the computer causes the display and keyboard assembly to blank or change to the next display if under program control. Depression of the ENTER key will not blank the display and keyboard assembly unless the proper keycode is received by the computer. Depression of other keys may blank all or part of the display, depending on the situation (that is, a CLEAR key blanks the data registers, a VERB key blanks the verb display, and a PROCEED key will blank or change to the next display). All require proper receipt of information and action by the computer.

In the first case, the depression of the PROCEED key instead of an ENTER would have caused the symptoms and results reported. In the second case, if a Verb 46 was keyed in, only another VERB key depression would have blanked the display and keyboard assembly without entering the data. Another possibility would be entry of a verb which causes no action at all or an action which is undetectable. Possible verbs which fit this category are V45E, V47E, V56E, V66E, V76E, and V86E.

In summary, the failures cannot be associated with hardware failures because the computer did in fact blank the displays, but procedural errors of the type discussed could have caused the failure conditions noted.

This anomaly is closed.

## 17.1.13 Surge Tank Shutoff Valve

The repressurization of the surge tank required an excessive length of time. Nominal repressurization was achieved when the crew repositioned the tank shutoff valve. During the systems debriefing, the crew stated that they believed no mechanical problems existed with the valve but that

the decal marking was misaligned with the valve detent position. Post-flight, the valve positions were checked and found to be misaligned by 20 degrees. Spacecraft 106 has been checked for proper alignment.

This anomaly is closed.

#### 17.1.14 Docking Ring Separation Charge Holder

One docking ring separation charge holder was deformed and out of its channel, extending several inches beyond the periphery of the external tunnel structure (fig. 17-10). Such a configuration might foul or cut the nylon suspension lines during parachute deployment. Hence, corrective action was deemed necessary for spacecraft 106 and subsequent.

The docking ring is jettisoned by a shaped charge. This charge is embedded in two semicircular steel charge holders which are approximately 1/4 inch square in cross section. One end of each holder is pinned to tunnel structure; the other end is free but is held in place by the docking ring geometry (fig. 17-11). Backup rings form the channel to enclose the assembly and to provide reactive resistance during shaped charge detonation. The charge holders have laminated brass shim stock bonded to the outboard periphery so that a very close fit can be obtained during installation by peeling off the required amount of lamination. The assembly performs its function of cutting the docking ring; however, after the docking ring has been cut and has moved from the backup ring channel, the free end of the charge holder has nothing to prevent its coming out of the channel except the cantilever "spring action" of the pinned end, which is rather weak.

Qualification test firings were conducted on a fixture oriented such that the docking ring was on top. Consequently, gravity counteracted any tendencies of the charge holder to come out of the backup ring channel. In spite of this, however, charge holders did come out and stay out on several of these tests. Because the charge holders curled inward when they come out on these occasions, a problem was not recognized to exist. It is not known whether the outboard distortion of the Apollo 9 charge holder occurred during flight or during recovery operations. The latter is suspected, however, inasmuch as there is no heat discoloration on either the holder or shim stock as would be expected from the entry environment.

A retention spring design (fig. 17-12) has been installed on spacecraft 106 to retain the charge holders in the backup ring channel. Two springs are installed for each charge holder. The torsion springs are preloaded against the outboard surface of the docking ring; when the docking ring moves out of the channel, the springs swing across the channel

to capture the charge holders. Prior to spacecraft 106 installation, the design was successfully tested with the docking ring in an inverted position such that gravity would aid the charge holders from being captured. After the initial test which detonated the charge and severed the ring, the docking ring was refitted and mechanically withdrawn more slowly to simulate the slow separation of command module and lunar module. During one of two such tests, all springs captured the charge holders; during the other test, each charge holder was captured by one of its two springs. For the springs that did not capture, it is reasoned that the charge holder was following the severed docking ring too closely for the retainer spring to wedge between them. Analysis has shown that springs are positioned on each charge holder such that the holder will always be retained by one of the two springs.

This anomaly is closed.

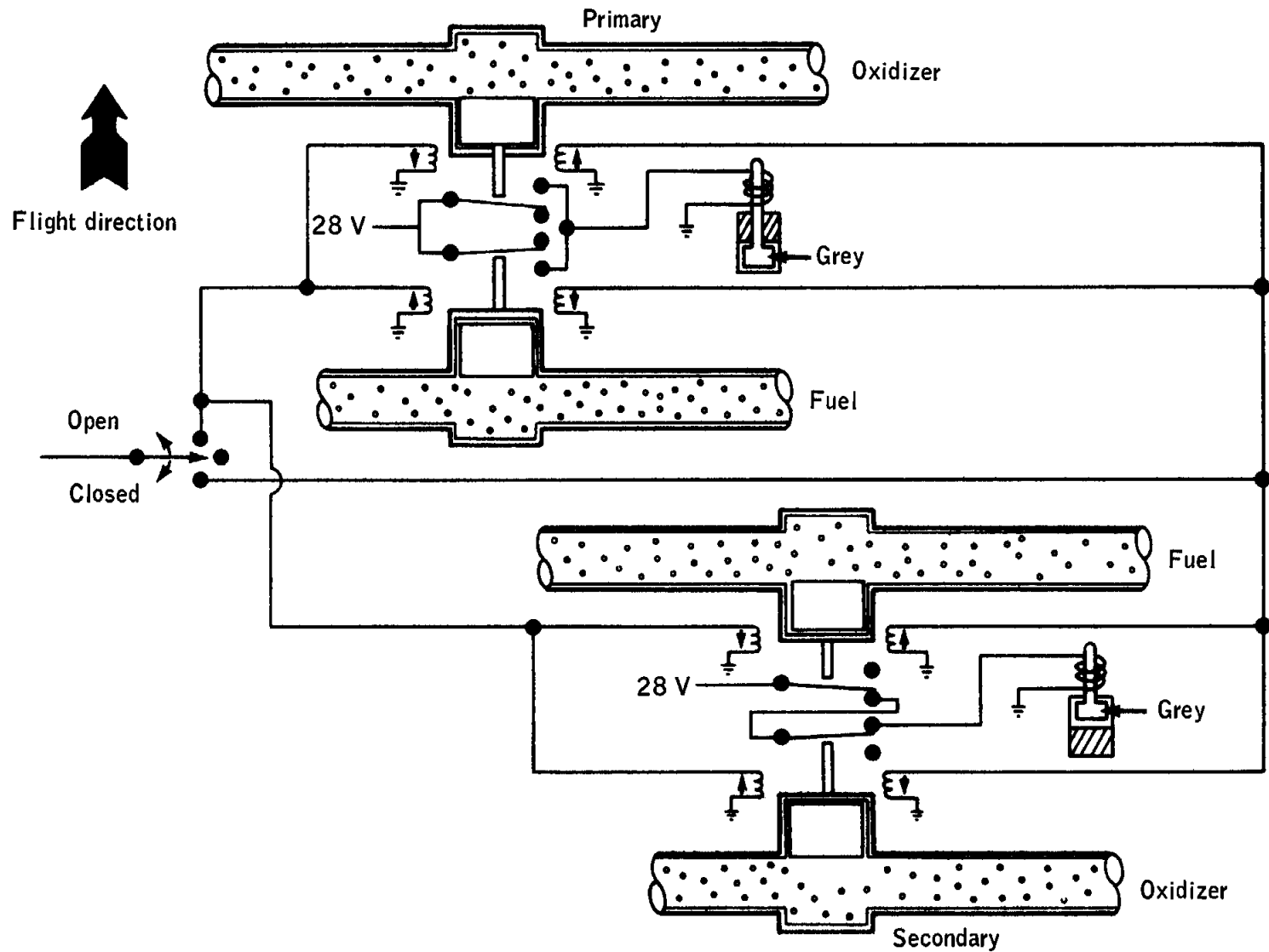


Figure 17-1.- Reaction control isolation valve.

NASA-S-69-2080

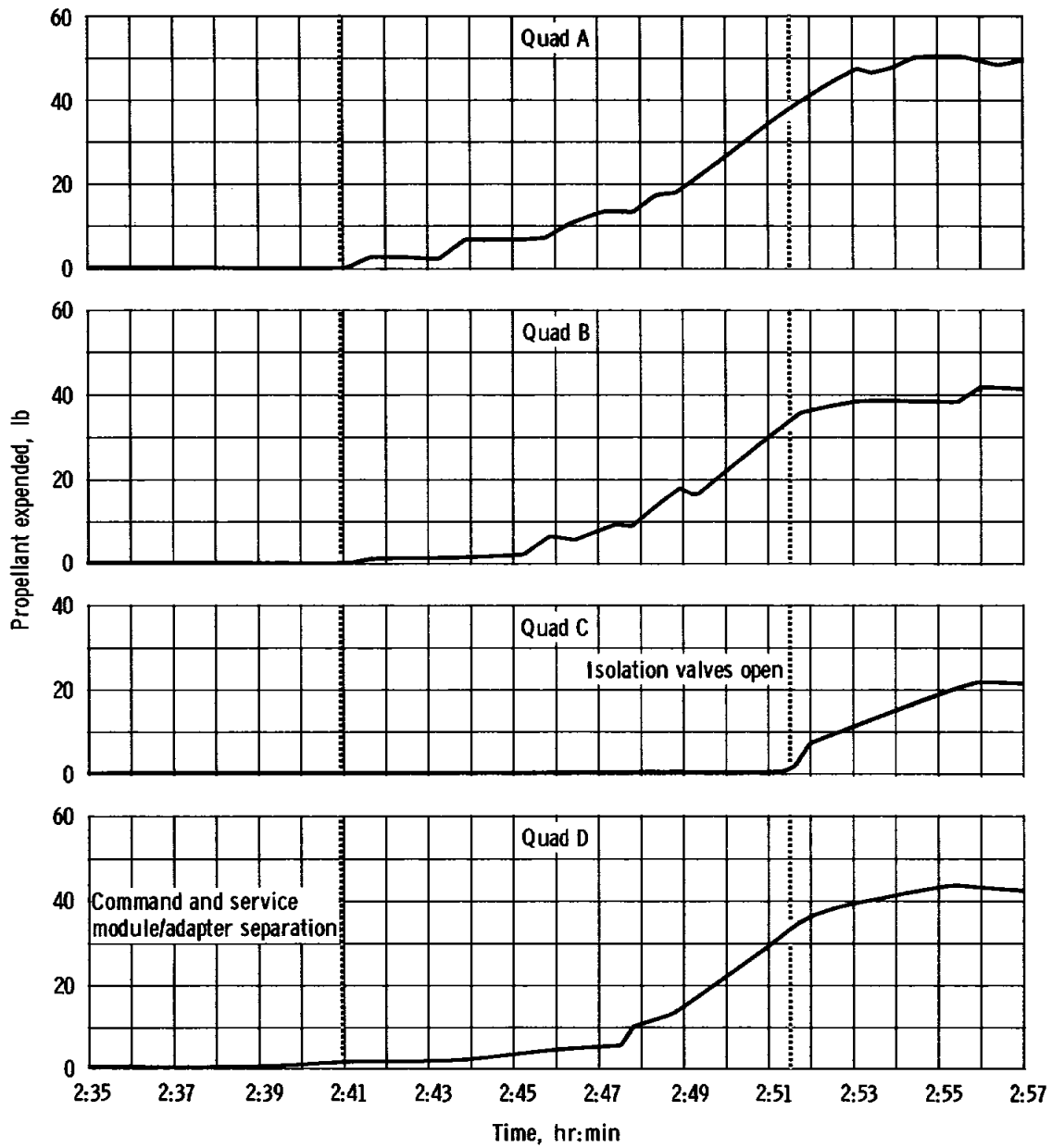


Figure 17-2. - Propellant expended showing inactivity of quad C.

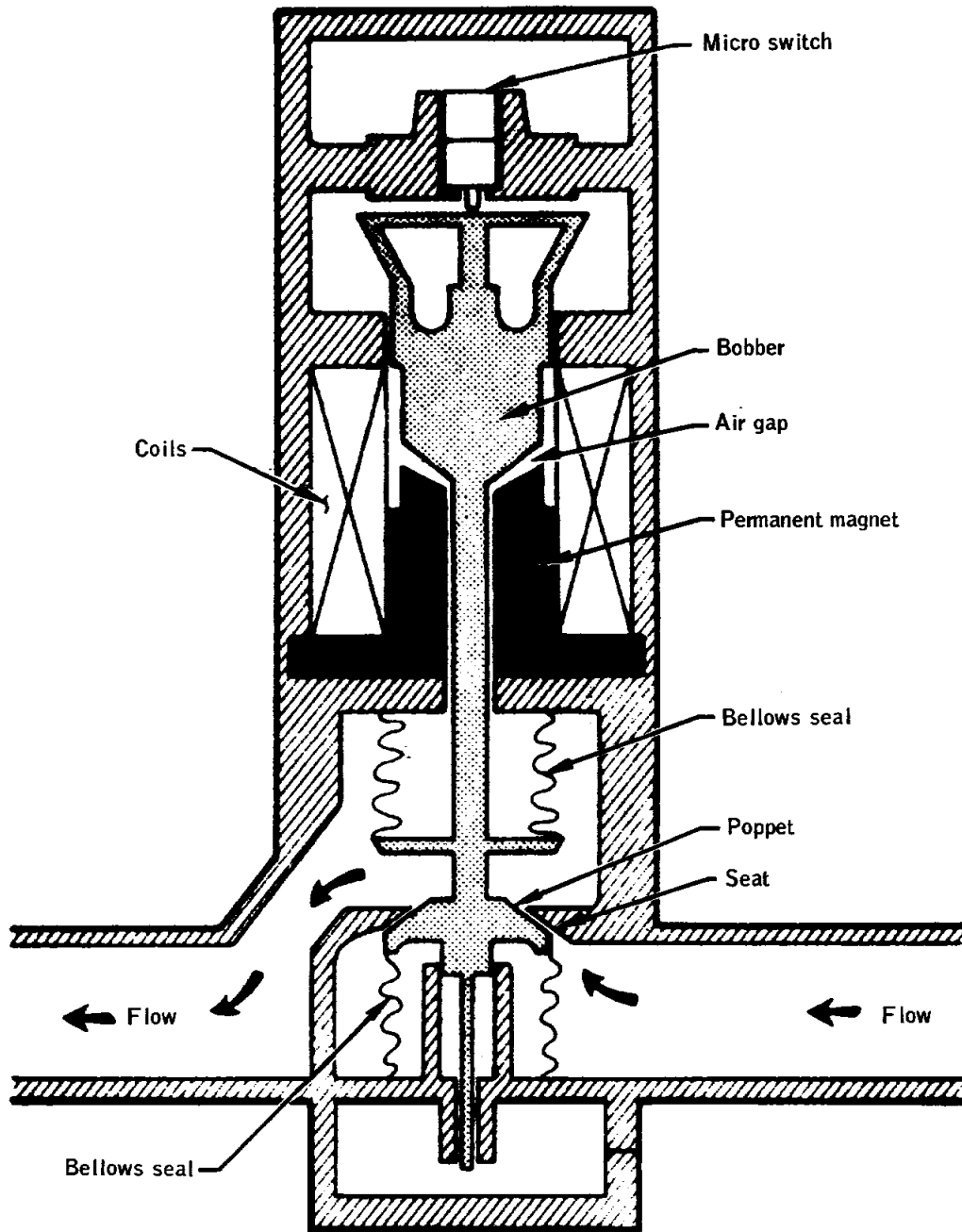


Figure 17-3.- Cross section of reaction control system isolation valve.

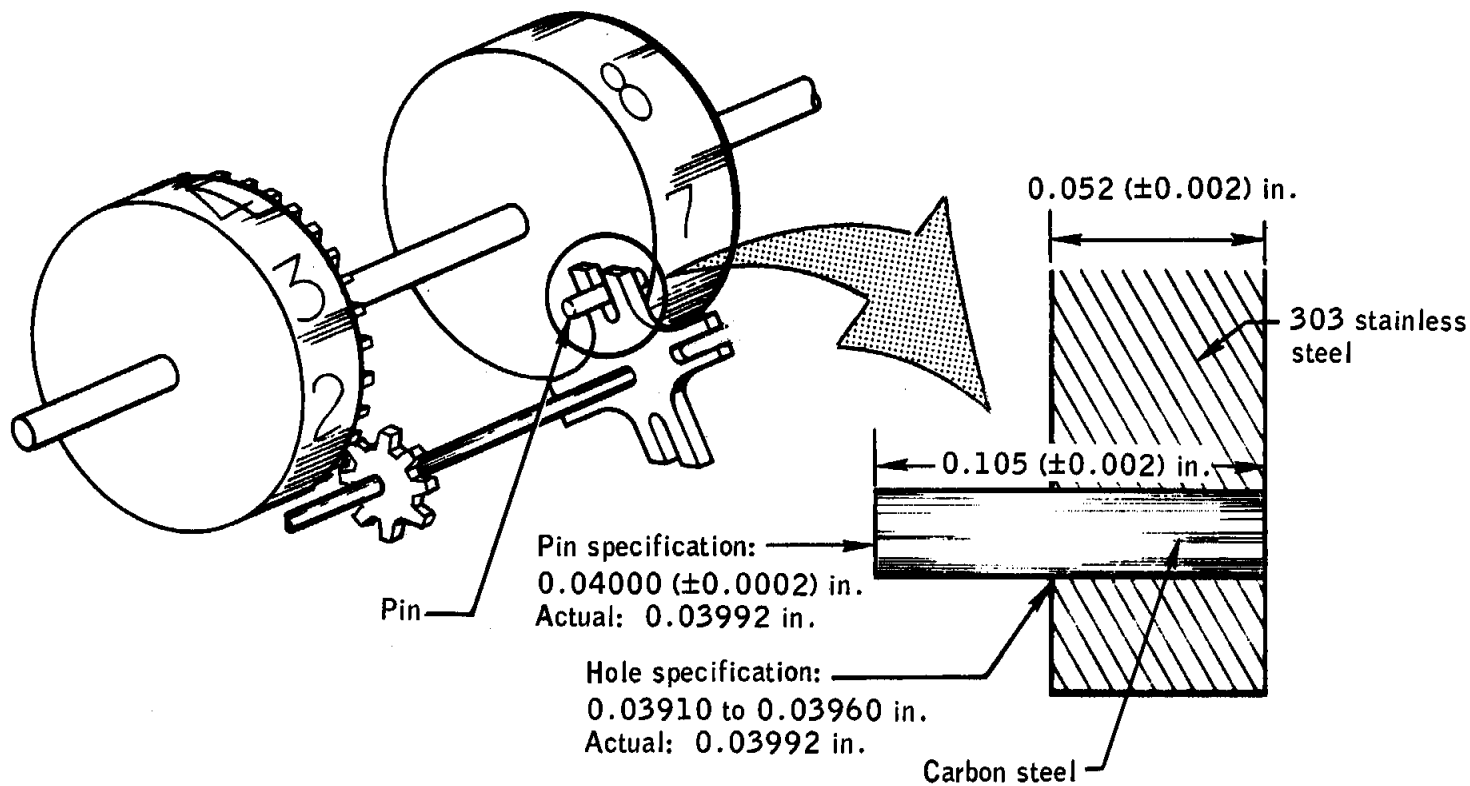


Figure 17-4.- Scanning telescope counter.

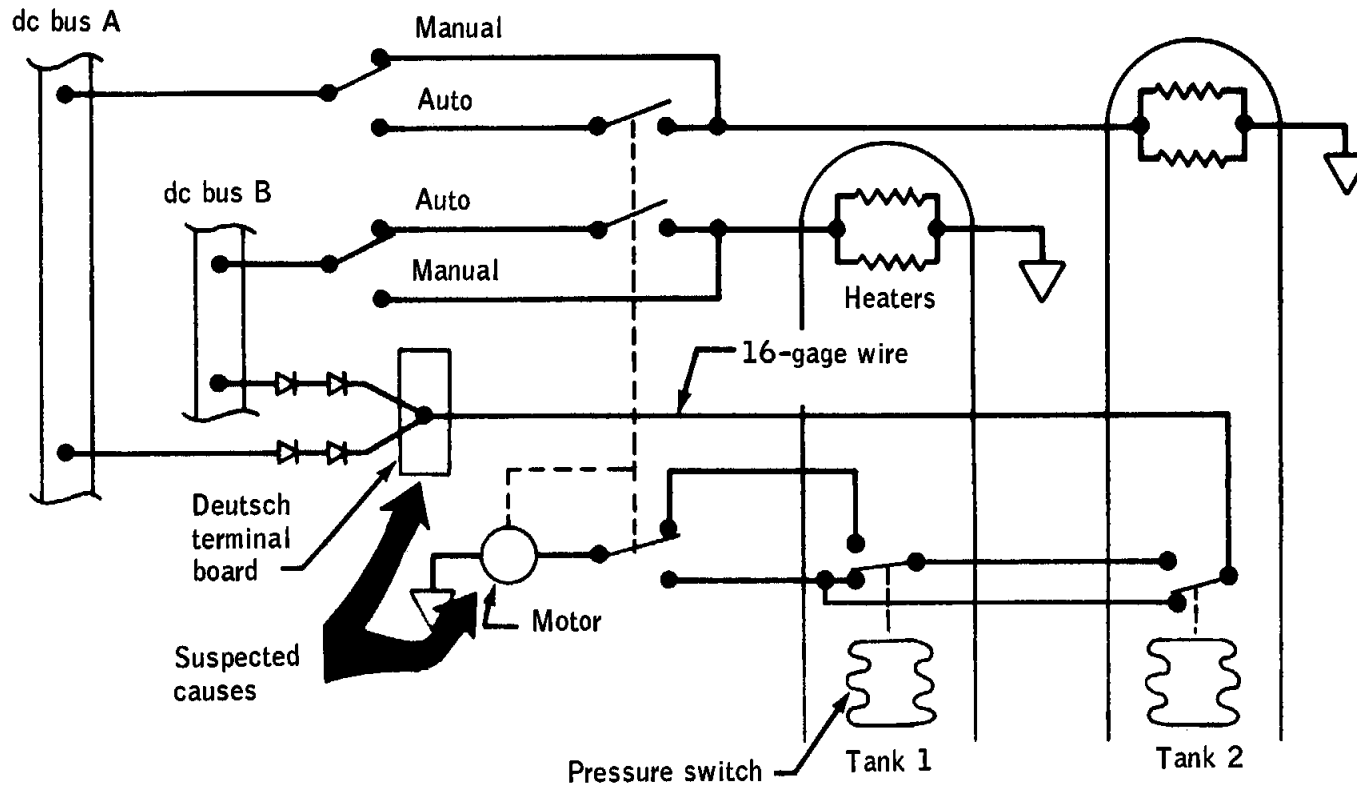


Figure 17-5.- Hydrogen tank pressure control.

NASA-S-69-2084

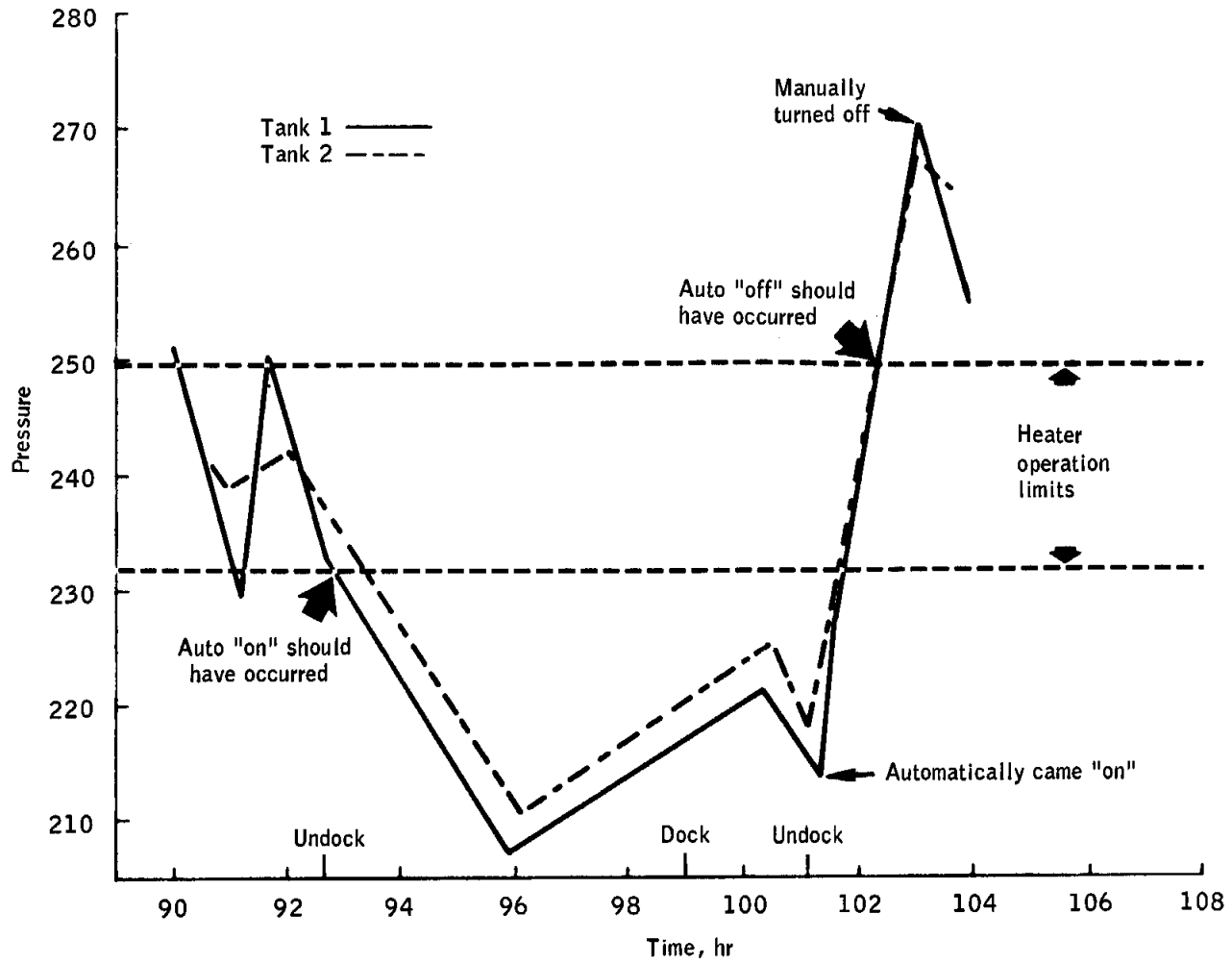


Figure 17-6.- Hydrogen tank pressure - heater operation.

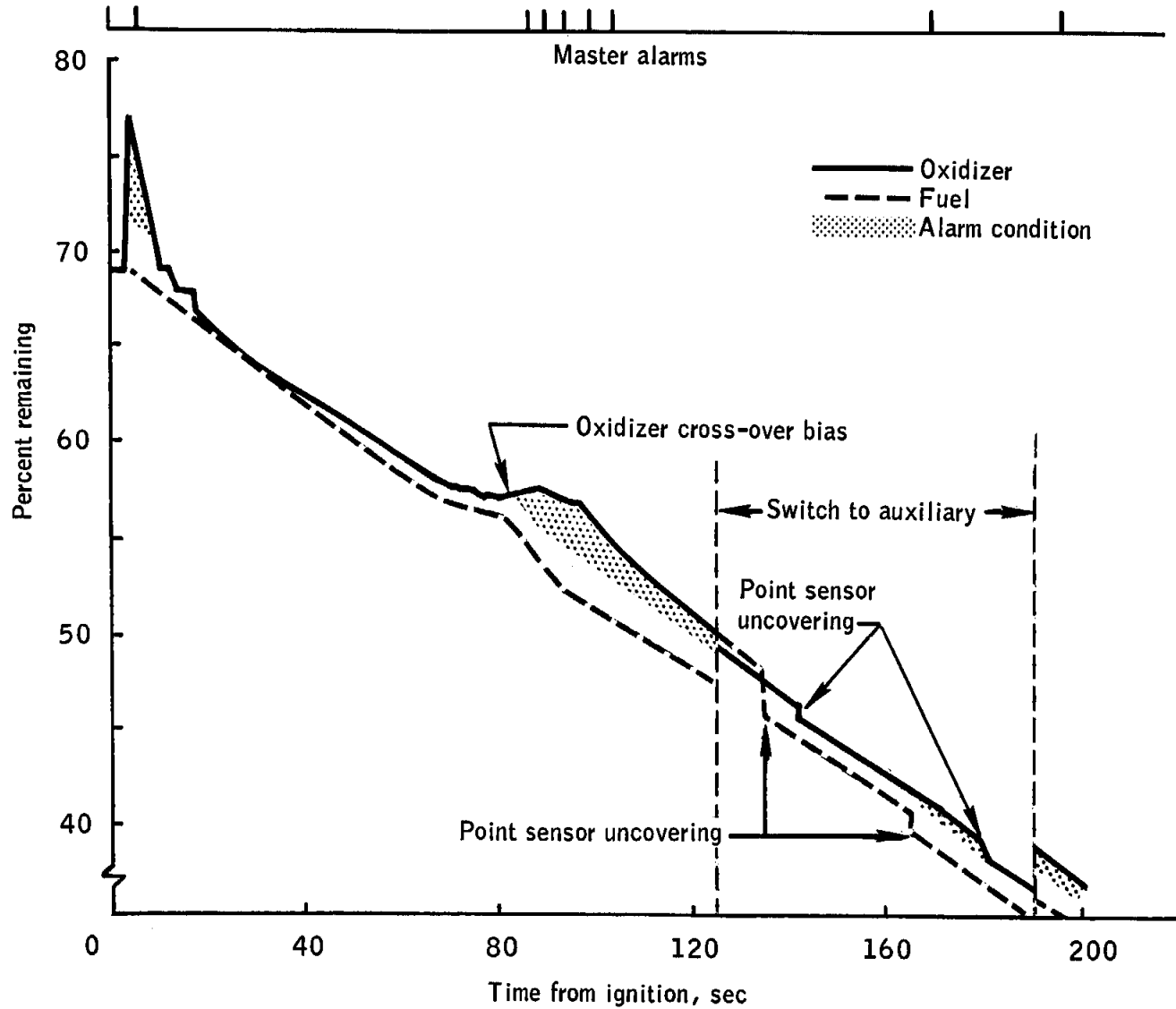


Figure 17-7.- Service propulsion system propellant quantities.

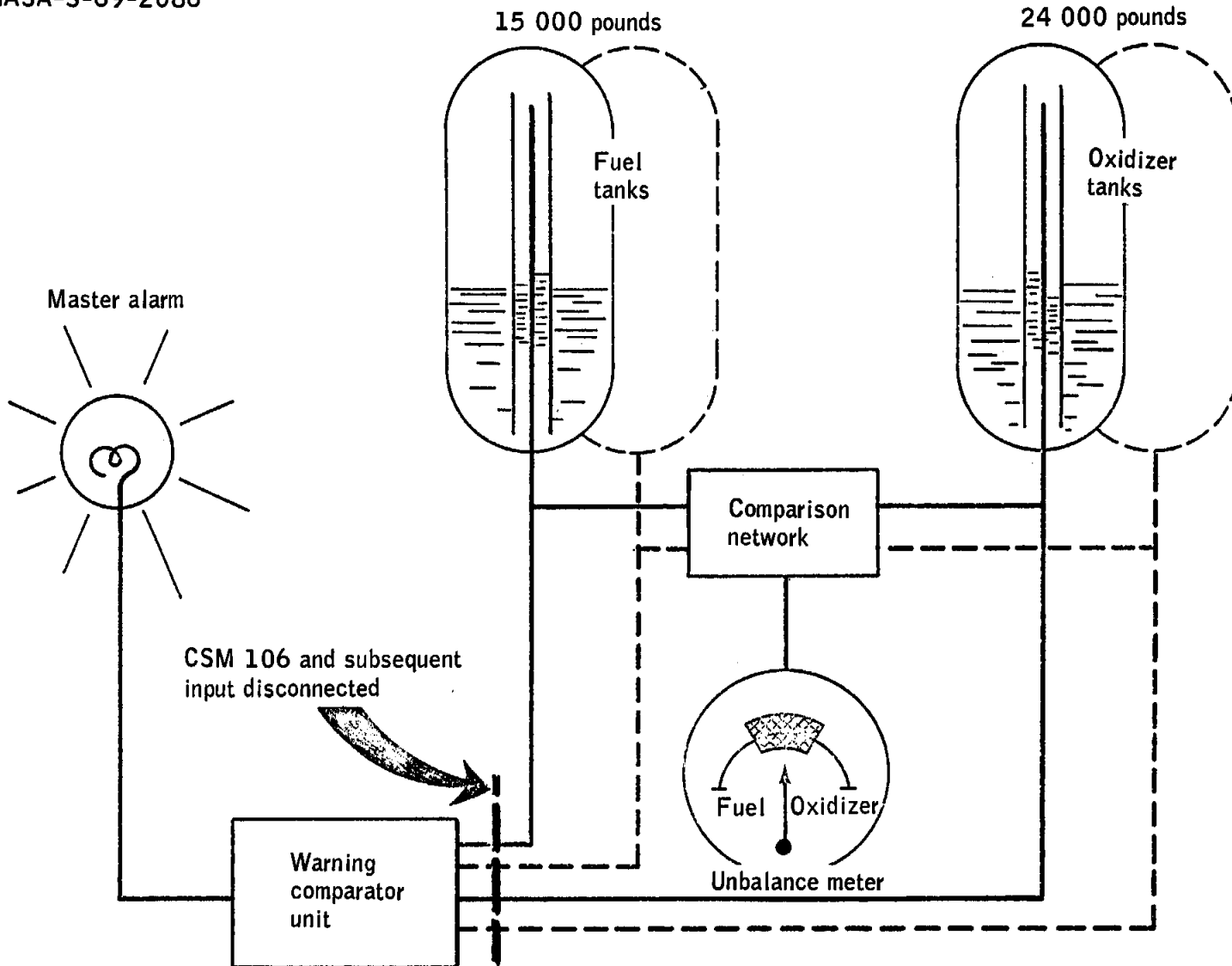


Figure 17-8.- Primary propellant utilization system circuit.

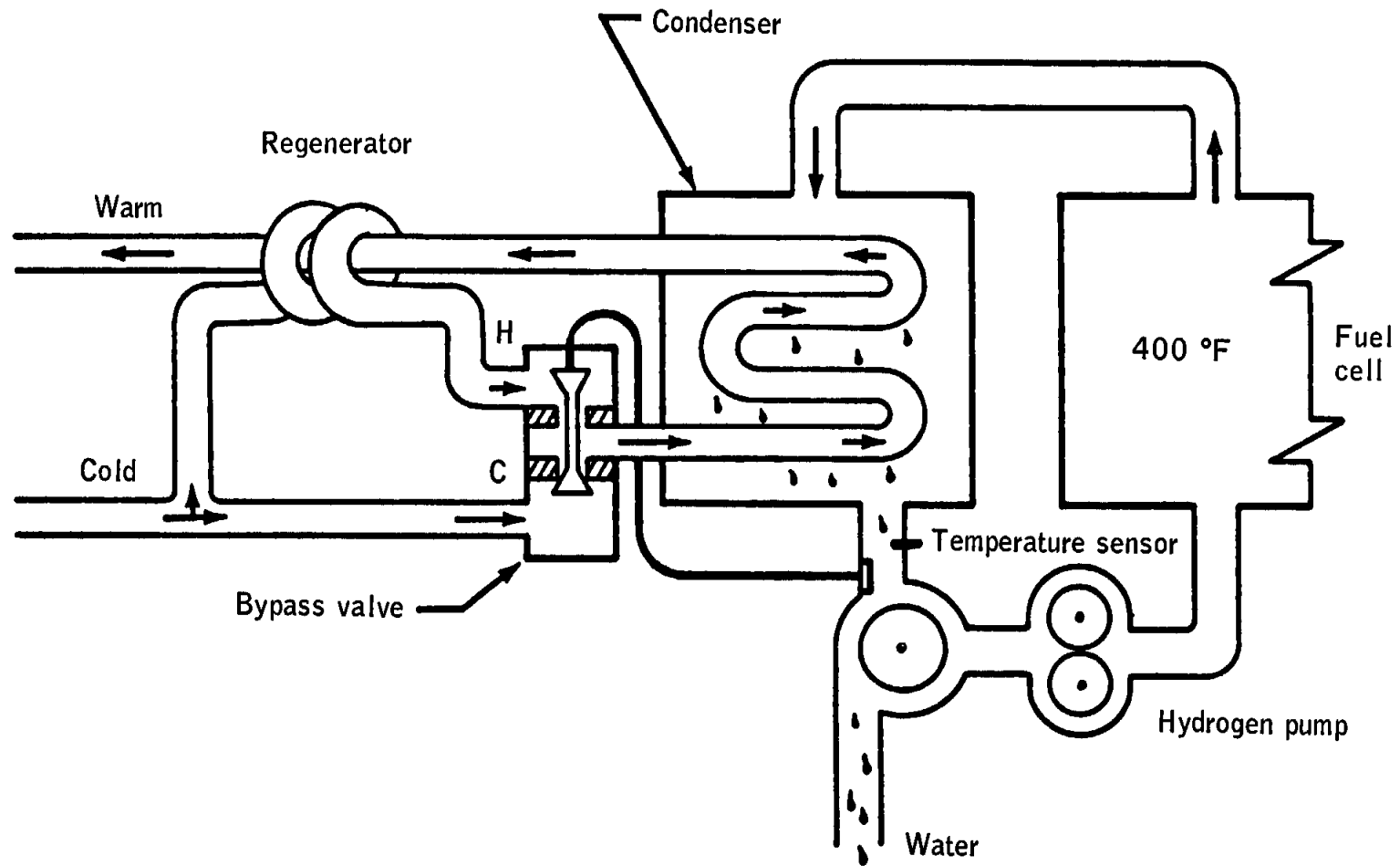


Figure 17-9.- Condenser system.

NASA-S-69-2088

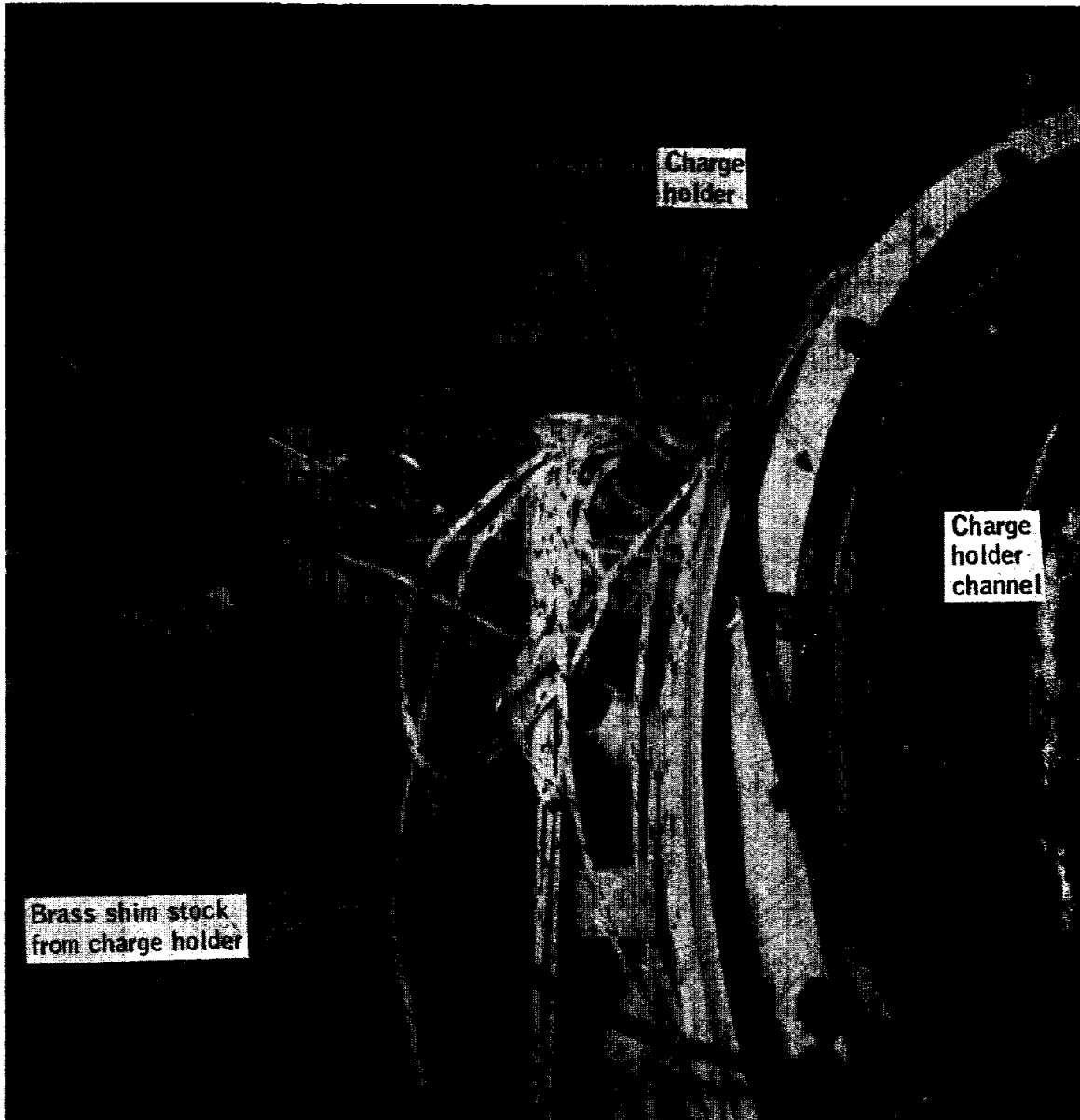


Figure 17-10.- Top of tunnel structure after recovery.

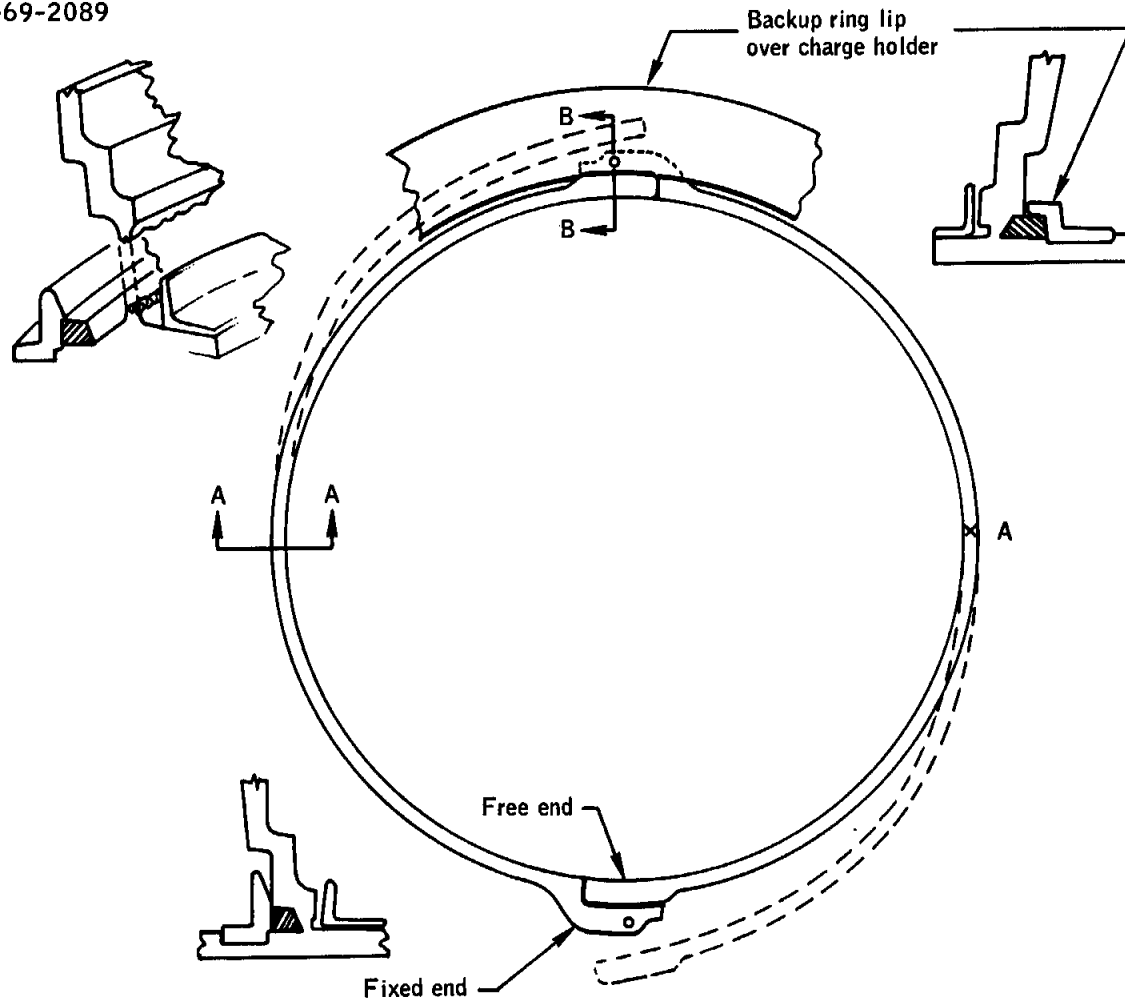


Figure 17-11.- Shaped charge holder.

NASA-S-69-2090

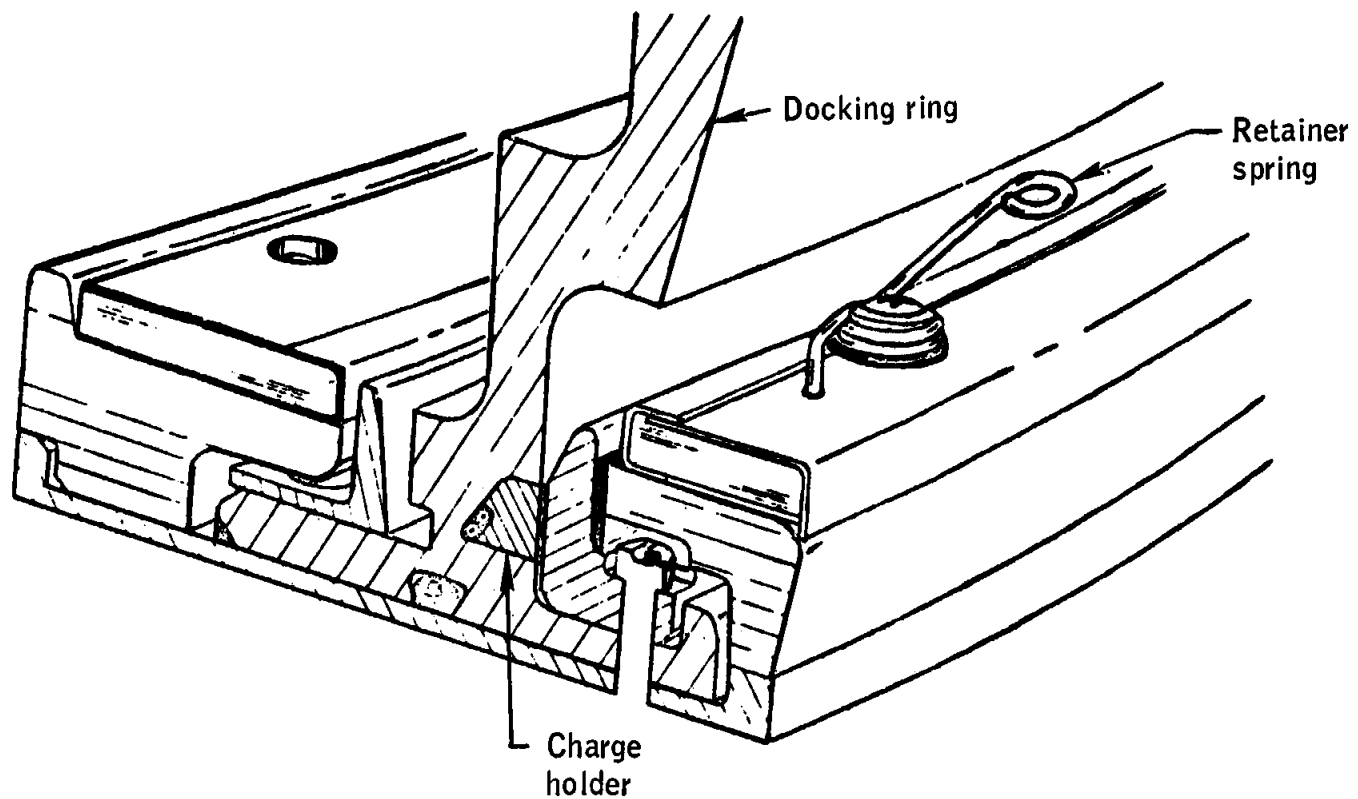


Figure 17-12.- Charge holder retainer spring.

(This page intentionally left blank)

## 17.2 LUNAR MODULE

### 17.2.1 Descent Propulsion Regulator Manifold Pressure Drop

During the first 35 seconds of the docked descent engine firing, the regulator outlet manifold pressure decreased from 235 to 188 psia. The regulator should have regulated at 247 psia. During the same period of time, the supercritical helium tank pressure decreased from 743 to 711 psia, indicating some helium flow from the tank (fig. 17-13). The helium, however, flowed through the bypass rather than the tank heat exchanger. If it had flowed through the heat exchanger, the tank pressure would have increased rather than decreased. These conclusions are also substantiated by the helium system temperatures (fig. 17-14).

The supercritical helium tank outlet temperature dropped after ignition, indicating helium was flowing out of the tank. No data are available for the heat exchanger inlet temperature for the first 35 seconds of the firing because the measurement was pegged at the high end ( $-65^{\circ}$  F). The heat exchanger outlet temperature during the same time period showed a gradual decay. It should have dropped off-scale low ( $-210^{\circ}$  F) within a few seconds of the start of engine firing if the helium had been flowing through the tank heat exchanger. Approximately 35 seconds after engine ignition, the regulator inlet temperature showed a rapid decrease. Both the inlet and outlet temperatures of the internal heat exchanger experienced a similar drop in temperature. The combination of temperatures recorded at this time indicates a sudden surge of relatively cold helium through the system. Following the initial surge, temperatures approached the anticipated operating temperatures of the system. The temperature data indicate that the internal heat exchanger was initially blocked (fig. 17-15). At approximately 35 seconds after engine ignition, the blockage cleared and allowed the regulator outlet manifold pressure to rise to the proper operating level.

After the supercritical helium servicing at the launch complex, the quick-disconnects for tank fill and vent are purged with helium to insure that the quick-disconnects are warm and dry before being disconnected and capped. The purge helium was supplied from the same regulator that normally maintains the manifold pressure above 5 psig.

During the Apollo 9 servicing, the pressure must have dropped to zero, thus allowing air to be drawn into the manifold. A postlaunch calibration check of the ground support equipment, which monitored the manifold pressure, showed that the gage was indicating 2 psia when the actual pressure monitored was zero psig. The air condensed out in the supercritical helium tank heat exchanger, thus lowering the pressure, and causing more air to be drawn into the manifold. Tests have shown

that dropping the manifold pressure to zero for a minimum time (between 15 and 30 minutes) will allow air to be drawn through the manifold into the tank heat exchanger, where it will freeze and block the heat exchanger. The freezing process transfers heat into the supercritical helium tank, causing a pressure rise of about 90 psi, very similar to what occurred during the Apollo 9 top-off (fig. 17-16). If no air were introduced, the tank pressure would be expected to increase 10 psi/hr or less.

The ground support equipment has been modified for Apollo 10 and subsequent to isolate the purge system from the manifold pressure control system. Further, continuous pressure recording with proper scaling will be employed on the manifold (fig. 17-17). Servicing procedures using the new ground support equipment configuration have been satisfactorily demonstrated.

This anomaly is closed.

#### 17.2.2 Supercritical Helium Pressure Decay

The pressure in the supercritical helium tank for the descent propulsion system began decaying at 2.9 psi/hr immediately after shutdown of the first descent engine firing and continued to decay until staging. Because of heat transfer into the tank, the pressure normally should always increase under no-flow conditions (fig. 17-18). Calculations showed that a leak of about 0.1 lb/hr would have caused the 2.9 psi/hr pressure decay rate.

Tests were performed with a leak introduced at the squib valve and at the solenoid valve just upstream of the tank helium regulator. A 0.1 lb/hr leak lowered the temperature upstream of the squib valve to minus 70° F (230° F higher than the high end of the flight measurement) duplicating the flight temperature indications. The leak introduced at the solenoid valve caused no rise in tank pressure, indicating that the leaking helium flowed through the bypass rather than through the supercritical helium tank heat exchanger. Calculations showed that this occurred because the test vehicle was in a one-g field. Vehicle configuration in a 1g field places the internal heat exchanger below the bypass orifice and the routing resembles a "U"-tube arrangement with the bypass orifice at the top (fig. 17-19). The leakage flow rate would have to be great enough to force the head of cold and dense helium out of the heat exchanger rather than through the bypass. Analysis indicates that if the leaking helium had flowed through the heat exchanger, the pressure in the storage tank would have risen at a rate of about 6 psi/hr. The flight results, which shows a pressure decay rather than rise, compared with ground test data indicate that the leak was upstream of the heat exchanger.

A failure of an internally brazed squib valve was found during drop tests of Lunar Module 2 at the Manned Spacecraft Center. The failure was a crack in the brazing material which was thin in the failed area. The time of the failure cannot be ascertained; however, it most likely was caused by the shock of the squib firing to pressurize the ascent propulsion system.

The Apollo 9 supercritical helium squib valve, like the Lunar Module 2 squib valve, differed from the Apollo 10 configuration in that the valve fittings were internally brazed, which prevented inspection of the joint. The Apollo 10 descent propulsion high-pressure squib valve is externally brazed (fig. 17-20), allowing inspection of the braze.

Except for the Apollo 5 mission (LM-1), which had no indication of helium leakage, the flight configuration of helium tank, squib valve, bimetallic fitting, and associated plumbing had not previously been tested together for the launch and boost vibration, squib valve firing shock, and thermal shock environments. A test has since been completed which showed the Apollo 10 configured components from the tank to the fuel heat exchanger have sufficient strength margin for the flight environment.

Two specimens with externally brazed valves and one specimen with an internally brazed valve were subjected to the following tests:

- a. Apollo 10 launch and boost vibration (0.24-inch double amplitude, 6-Hz sine dwell for 10 seconds)
- b. Cold flow including squib valve firing
- c. Descent propulsion firing vibration
- d. Overstress vibration
  1. 0.275-inch double amplitude, 6-Hz sine dwell for 10 seconds
  2. 0.55-inch double amplitude, 6-Hz sine dwell for 10 seconds.

The highest stress levels were in the tubing just upstream of the squib valve. At this location, the Apollo 10 launch and boost vibration produced a strain of 0.002 in./in. The squib firing and cold flow produced 0.0015 in./in., and the overstress (0.275-inch double amplitude) produced 0.0055 in./in. The yield strength of the tubing material is 35 000 psi, resulting in a strain of 0.003 in./in., and the ultimate is 75 000 psi, which produces 0.5 in./in.; therefore, the overstress environment (0.275-inch) resulted in some yielding. In the vibration environment of 0.55-inch double amplitude, 6 Hz sine dwell, the externally brazed specimen failed (see figure 17-20) after 3 minutes 20 seconds, and the

internally brazed specimen failed after 7 minutes 30 seconds. The failures were in the external tubing, not in the braze joints.

The squib valve and associated plumbing have adequate strength to survive the expected flight environment for Apollo 10 and subsequent. The leak experienced during Apollo 9 was probably caused by a defective braze that was internal to the squib valve and could not be inspected.

On the Apollo 10 descent propulsion system, the ambient-helium start-bottle squib valve, the oxidizer-tanks compatibility squib valve, and the two squib valves which are fired to depressurize the propellant tanks on the lunar surface are internally brazed. The latter two valves will not be fired in Apollo 10. If the ambient start bottle squib valve leaks a sufficient amount that a decay in supercritical helium tank pressure results between the first and second descent engine firings, the solenoid latch valves upstream of the regulators will be closed to conserve supercritical helium. The valve would only leak that helium trapped between the solenoid latching valves and the quad check valves downstream of the regulators.

If the oxidizer tank compatibility squib valve leaks, the oxidizer tank could be depressurized, or if the solenoid latch valves were closed, helium supplied from the supercritical helium tank to maintain the oxidizer tank pressure could leak out of this system. This valve has had RTV potting placed inside external clamps, which will prevent leakage if the brazes crack (fig. 17-20).

This anomaly is closed.

### 17.2.3 Tracking Light Failure

The tracking light failed shortly after lunar module staging. Possible causes are high-voltage breakdown in the flash head assembly, breakdown in the high-voltage cable, component failure in the electronics package, or high-voltage breakdown in the pulse-forming network. Based on failure history, breakdown in the pulse-forming network is considered the most likely.

Tests have been completed which show that the Apollo 10 tracking light configuration can withstand the vibration, shock, vacuum, and thermal stress of the mission. This configuration differs from the Apollo 9 in that it contains an arc-suppressing capacitor and has successfully completed a thermal vacuum acceptance test. A modified tracking light with increased reliability will be available for Apollo 11. The Apollo 11 unit has a pulse-forming network and flash head that have been modified to eliminate voltage breakdown in the flight environment.

This anomaly is closed.

#### 17.2.4 Push-to-Talk Switches Inoperative

The Lunar Module Pilot's push-to-talk switches (fig. 17-21), located on the umbilical and on the attitude control assembly, were inoperative at about 89 hours. The Lunar Module Pilot used the VOX mode for transmission for the remainder of lunar module operations. Failure of both switches is not probable. The common path on either side of the switches includes switch contacts on the audio section, connectors, and diodes in the signal processor assembly. The problem was probably caused by a discontinuity (broken wire) in the common wire to the parallel push-to-talk switches.

The push-to-talk mode of communication is isolated from the VOX mode of communication. In addition, switching the backup push-to-talk mode will bypass most of the common wiring where the failure may have occurred.

The operating procedures have been changed to include malfunction troubleshooting procedures that can be used to circumvent this type of problem.

This anomaly is closed.

#### 17.2.5 Abort Guidance Warning Light

During the third manning, a caution and warning alarm occurred when the abort guidance system was activated. During the previous mannings, no alarm had occurred when the abort guidance system was operated.

The caution and warning indication indicates one of the following conditions:

- a. The abort sensor assembly 12-volt power supply voltage is out of limits.
- b. The abort sensor assembly 28-volt power supply voltage is out of limits.
- c. The abort sensor assembly ac power supply voltage is out of limits.
- d. The abort electronics fails a self-test.
- e. An overtemperature exists in the abort electronics assembly.

A separate instrumentation measurement indicated that the temperature of the abort electronics assembly was not near the warning level. Also, the abort guidance system was successfully calibrated in flight, indicating that the power sources were functioning properly.

The specification limits for alarms and the operating specification limits of the parameters have sufficient range that an out-of-specification condition would have caused a malfunction of the abort guidance system.

The caution and warning trip levels are measured in each vehicle at the launch site. Also, the output parameters for each abort electronics assembly and the transfer functions for each signal conditioner electronics assembly are measured on the bench.

The most likely cause of the anomaly was either a shorted or broken wire between the abort electronics assembly and the signal conditioner electronics assembly (26-gage wires with seven splices), a shorted or broken wire between the signal conditioner electronics assembly and the caution and warning electronics assembly, a failure within a signal conditioner electronics assembly, or a failure in the caution and warning system.

This anomaly is closed.

#### 17.2.6 Binding of Forward Hatch

The crew reported that when the forward hatch was opened for extravehicular activity, it tended to bind on top and had to be pushed downward to be opened. The potential hatch interference points that could have caused the binding are shown in figure 17-22.

An inspection of the Apollo 10 lunar module showed that the vehicle front-face insulation blankets, above and around the hatch opening, protrude below the vehicle fixed structure shielding, although 0.250-inch clearance should exist in this area. This protrusion was in the path of and interfered with the hatch shield lip. Note also in the figure that an area that should have had 0.175-inch clearance, was 0.08 inch. Similar conditions probably existed on Apollo 9. Corrective action for Apollo 10 and subsequent will be to extend the top hatch shield to the hatch structure, as shown in figure 17-22, and the hatch will be trimmed to increase the 0.08-inch clearance to 0.125-inch minimum clearance.

This anomaly is closed.

#### 17.2.7 Failure of Forward Hatch Door Stop

The forward hatch would not stay open for extravehicular activity.

The door stop (snubber), shown in figure 17-23, is attached to the forward hatch door and is designed to ride against Velcro patches on the

floor, thereby holding the door open. The allowable tolerance between the door and the floor indicates that under worst-case conditions, a 0.040-inch clearance can exist between the snubber and the Velcro.

No change will be made for Apollo 10 since it is not planned to open the door. A redesigned snubber, shown in figure 17-23; will be used for Apollo 11 and subsequent.

This anomaly is closed.

#### 17.2.8 High Cabin Noise Level

The excessive noise in the lunar module cabin during helmets-off operation, reported by the crew, was caused primarily by operation of the cabin fans, glycol pumps, and suit compressors. One crewman improvised ear pieces to provide some noise reduction. The crewman who did not wear the ear pieces was most aware of the noise level.

Noise measurements made on a vehicle with the glycol pumps and suit compressors operating indicated that the glycol pumps caused the highest noise level. The pumps couple acoustic energy into the glycol lines and then to the pressure vessel at the penetration points. The pressure vessel then amplifies this energy.

To reduce the overall noise level in the cabin, a change to the operating procedures specifies use of only one cabin fan when cooling is required. In addition, the Apollo 10 crewmen have been fitted and trained with ear pieces which will reduce the noise approximately 10 dB.

For missions subsequent to Apollo 10, sleep in the lunar module is required, and modifications are being tested, such as flexible couplings between the glycol pumps and the bulkhead and Beta padding around the suit compressors (see figs. 17-24 and 17-25).

This anomaly is closed.

#### 17.2.9 Structural Contact at S-IC Shutdown

Axial accelerometer data from the minus Z descent propellant tank (fig. 9.1-8) indicate that the lateral loads introduced at shutdown of the launch vehicle first stage (S-IC) probably caused the helium diffuser flange to contact the sheet metal flange of the upper deck (fig. 17-26). However, this contact had no detectable effect on any system or vehicle performance.

Analysis of the Apollo 10 configuration using static-firing data from the Apollo 10 first stage and the Apollo 10 mass indicates that the lateral loads on the minus-Z oxidizer tank will be about 50 percent less than experienced on Apollo 9. The X-axis accelerations on the tank are estimated to be 30-percent less than the Apollo 9 measured values.

This anomaly is closed for Apollo 10.

For Apollo 11 and subsequent, an evaluation of the integrity of the tank, plumbing, and structure is being conducted.

#### 17.2.10 Data Entry and Display Assembly Operator Error Light

The CLEAR pushbutton on the data entry and display assembly was routinely activated at the end of each entry or display operation to clear the address and display registers. Frequently during the mission, this procedure resulted in illumination of the operator error light. When this occurred, four or five depressions of the CLEAR pushbutton were often required before the operator error light would remain extinguished, although it would go out temporarily while the button was depressed.

A simplified diagram of the CLEAR pushbutton logic circuit is shown in figure 17-27. The pushbutton contains two microswitches which are designed to activate within 30 milliseconds of each other after the button is depressed. The CLEAR pushbutton microswitches issue discrettes to the data entry and display assembly and to the abort electronics assembly. The data entry and display assembly discrete extinguishes the operator error light directly as shown and also sets the clear flip-flop. The clear flip-flop issues a logic "one" to an "and" gate as shown and to other internal logic. The abort electronics assembly discrete is used in program control for several operations which include setting the shift discrete shown in the figure to "zero."

When the pushbutton is released, the direct command to extinguish the operator error light is removed, and if the shift discrete is zero and no other error inputs are present, the light will stay out. If the electronics assembly discrete was not issued, as is suspected in this case, the shift discrete would not be set to "zero" by the program and the light would come on again when the button was released.

A review of the Apollo 9 system test history revealed two preflight occurrences similar to those experienced in flight. One was at the vendor before acceptance, the other during checkout at the launch site.

Apollo 10, 11, and 12 system test histories have been researched, and no evidence of any other pushbutton discrepancies has been found. One occurrence of a failure to CLEAR was found on the qualification unit; however, the suspected cause was failure to depress the button completely. The CLEAR pushbutton and one other on the unit have been disassembled without finding contamination or any other mechanism which could have caused the symptoms. In addition, two of the eight pushbuttons which were part of the pushbutton qualification program have been disassembled, and no discrepancies were found.

As can be seen in the exploded view of the pushbutton switch in the figure, if one of the switch leaves were slightly bent, contact with one of the microswitch buttons may have not been completed. Another possibility is a small piece of contamination which occasionally prevented depression of one of the microswitches by restricting the leaf motion.

No change will be made for Apollo 10. For Apollo 11 and subsequent, the CLEAR, HOLD, ENTER, and READOUT microswitches will be modified by connecting the switches with a jumper as shown in figure 17027. Thus, either of the switches will activate the functions instead of requiring both switches.

This anomaly is closed.

#### 17.2.11 Rough Descent Engine Throttling

During the second descent engine firing, the engine was rough at about 27-percent throttle for a few seconds, then settled out and operated smoothly during the remainder of the firing. The data during the rough period show a rise in the oxidizer interface pressure, followed by a rise in the fuel interface pressure; both subsequently returned to normal pressure. During this time period, the engine chamber pressure fluctuated, causing the roughness.

Tests have shown that with helium deliberately introduced into the propellant lines, the interface pressures increase as the gas passes the throttle assembly, because the throttled area operates at cavitating pressures. The variation of interface pressures and the bleeding of helium into the injector results in fluctuations in the engine chamber pressure. These test results match very closely the flight data during the engine roughness (fig. 17-28).

Helium from the propellant tanks could enter the propellant lines under certain conditions of lateral and/or rotational accelerations. The hole size of the screen in the zero-g can was selected so that propellant surface tension at the screen would retain propellant against the 4-inch

propellant head within the zero-g can itself. During lateral and rotational accelerations, the actual propellant head includes the 114 inches of connecting line between the two parallel tanks (see fig. 17-29). Helium ingestion requires that the zero-g can be uncovered and that lateral or rotational accelerations be present. This was highly probable with the 60-percent ullage volume present in Apollo 9 propellant tanks prior to the second descent engine firing. However, if helium should be introduced into the line, the engine would fire roughly sometime during the first several seconds of the firing. In any event, tests have demonstrated that ingestion of helium into the engine in this manner has no detrimental effect on the system.

This anomaly is closed.

#### 17.2.12 Ascent Propulsion System Regulator Outlet Pressure

At the start of the second ascent engine firing, the regulated helium pressure to the propellant tanks decreased from 186 psia to 176 psia and remained at that level throughout the major portion of the firing. Normal operating pressure should have been 184 psia. At 290 seconds into the firing, the pressure increased to approximately 179 psia and remained at that level until oxidizer depletion.

Figure 17-30 shows the helium supply pressure and regulator outlet pressure during this firing. Also presented are the regulation bands of each of the helium regulators as well as the pressure at which they were regulating during checkout at the launch site. The class I primary is normally the controlling regulator. As shown in figure 17-30, the regulator outlet pressure was 8 to 10 psi lower than nominal class I primary regulated pressure during most of the firing.

Because the step-up in regulated pressure near the end of the firing was essentially instantaneous, it suggests that the class I primary regulator was operating at that time (if multiple failures are ignored). In all probability, only the class II primary regulator was controlling up to that point in the firing. The malfunction of the class I regulator was, therefore, not of a nature that would cause permanent inability to regulate under flow demand. Note also that the lock-up pressure of the system before and after the firing corresponded to the class I lock-up pressure, which further substantiates this point.

At this time, the most likely conditions which could have caused the indicated malfunction of the class I regulator (see fig. 17-31) was contamination of the regulator. This contamination could have caused a restriction in the feedback line from the pilot poppet to the slave piston. Tests have shown that a regulator band shift can result by reducing the

orifice size at the possible restriction point shown on the figure. A reduction from 0.062 inch to 0.016 inch will reduce the regulated pressure to 177 psia. Binding of the main piston due to contamination is an additional possibility. This malfunction could cause a reduction in the outlet pressure of the class I primary regulator sufficient to allow the class II regulator to control.

The likelihood that contamination caused the indications is increased by the fact that the solenoid latching valve in the primary helium regulator leg was replaced at the launch site. Normal procedures required backflowing through the regulators during the replacement process to keep out contamination. The external gas source is filtered; however, there is no filter in the flight system to prevent contamination of the regulators due to backflow. Contamination of a regulator has occurred as a result of this procedure in at least one prior instance in the Apollo Program.

Additional testing has been performed at White Sands Test Facility on a test vehicle and at Manned Spacecraft Center on a component level. The purpose of these tests is to determine regulator malfunction modes which will explain the pressure profiles seen in flight. Preliminary data from these tests have been used in arriving at the conclusions discussed above, but a final assessment of the anomaly requires a detailed review and analysis of the test data.

This anomaly is open pending that assessment.

NASA-S-69-2091

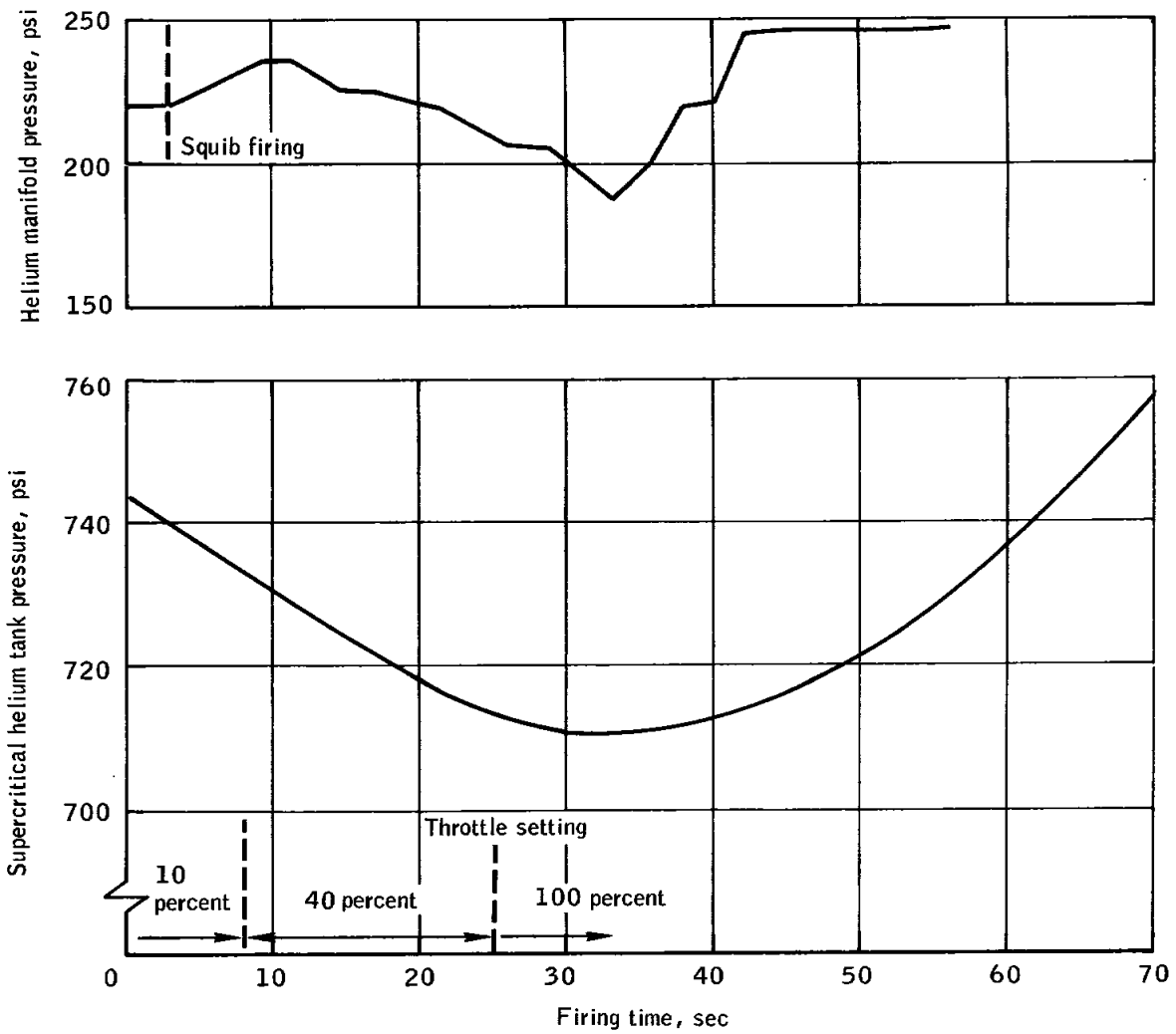


Figure 17-13.- Supercritical helium tank blockage data.

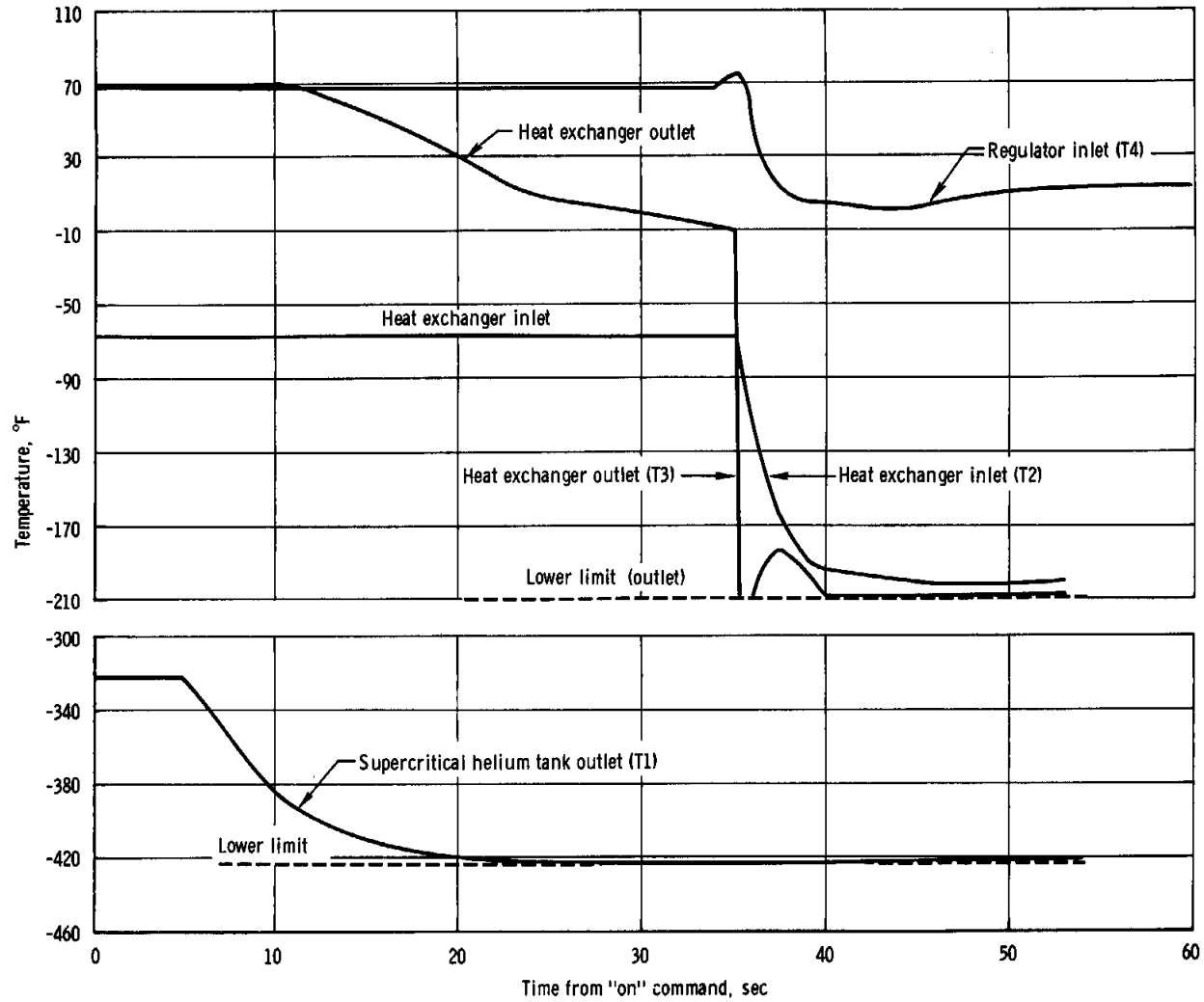


Figure 17-14. - Supercritical helium system temperatures during initial portion of first firing.

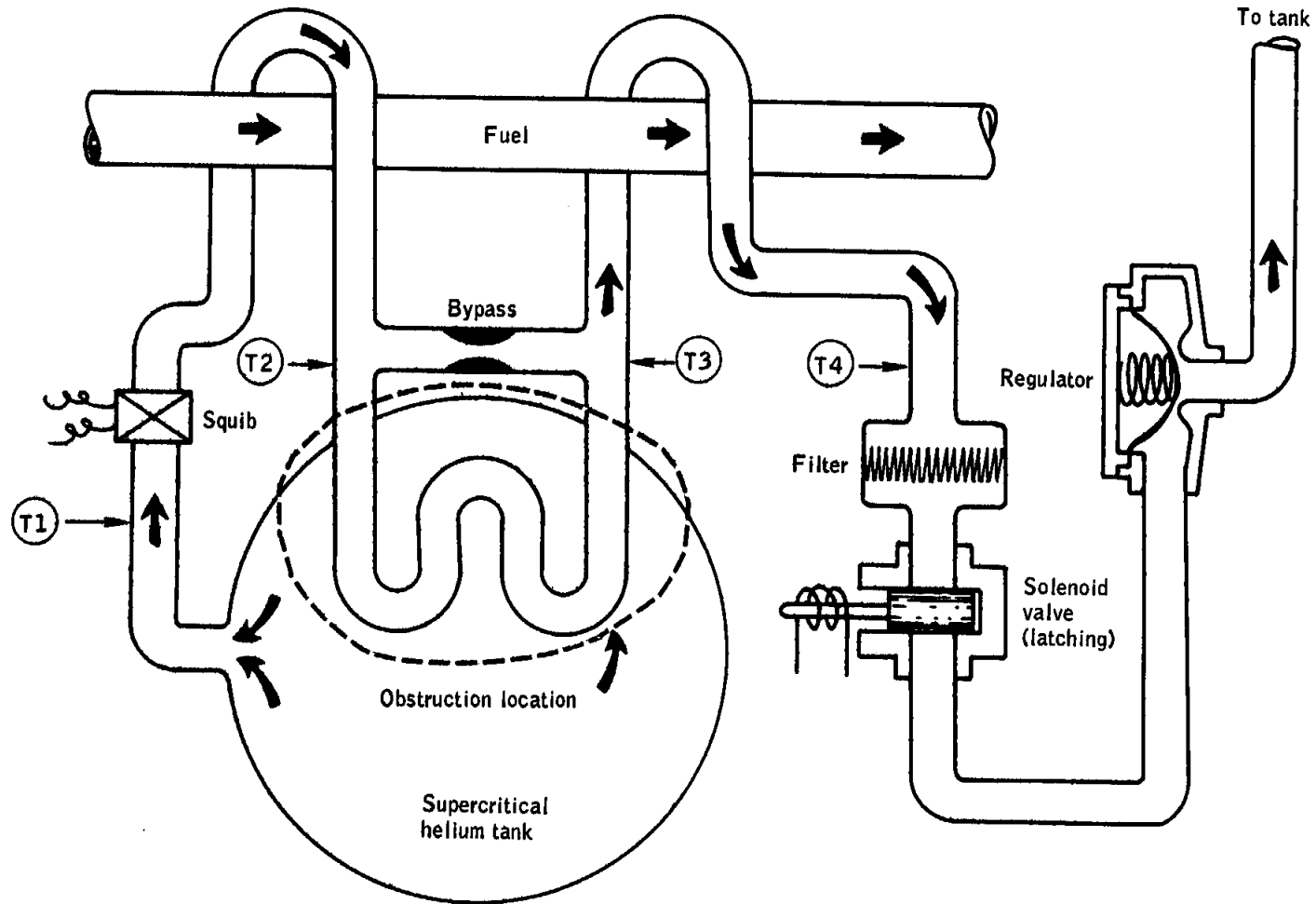


Figure 17-15.- Supercritical helium system.

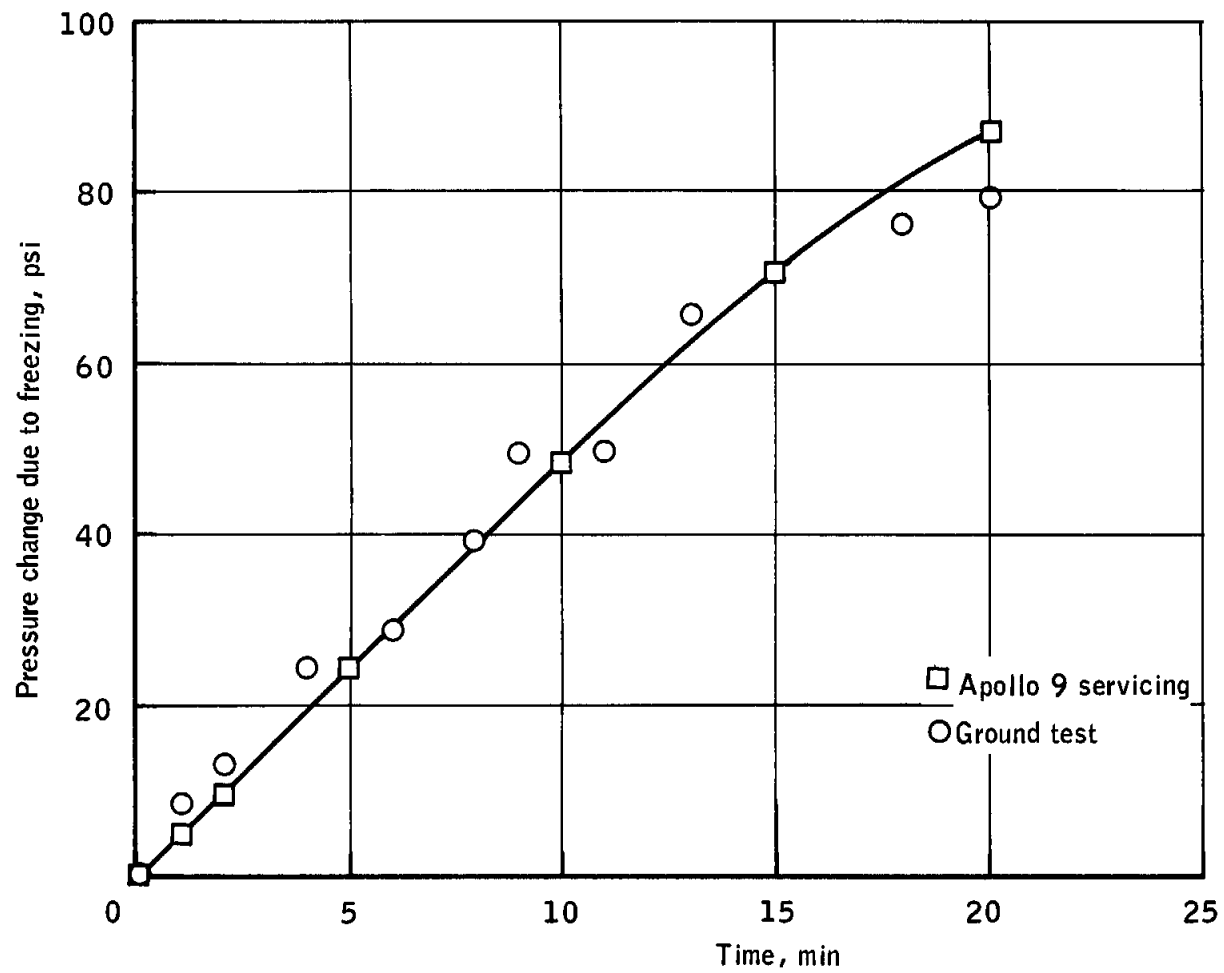


Figure 17-16.- Supercritical helium tank pressure rise.

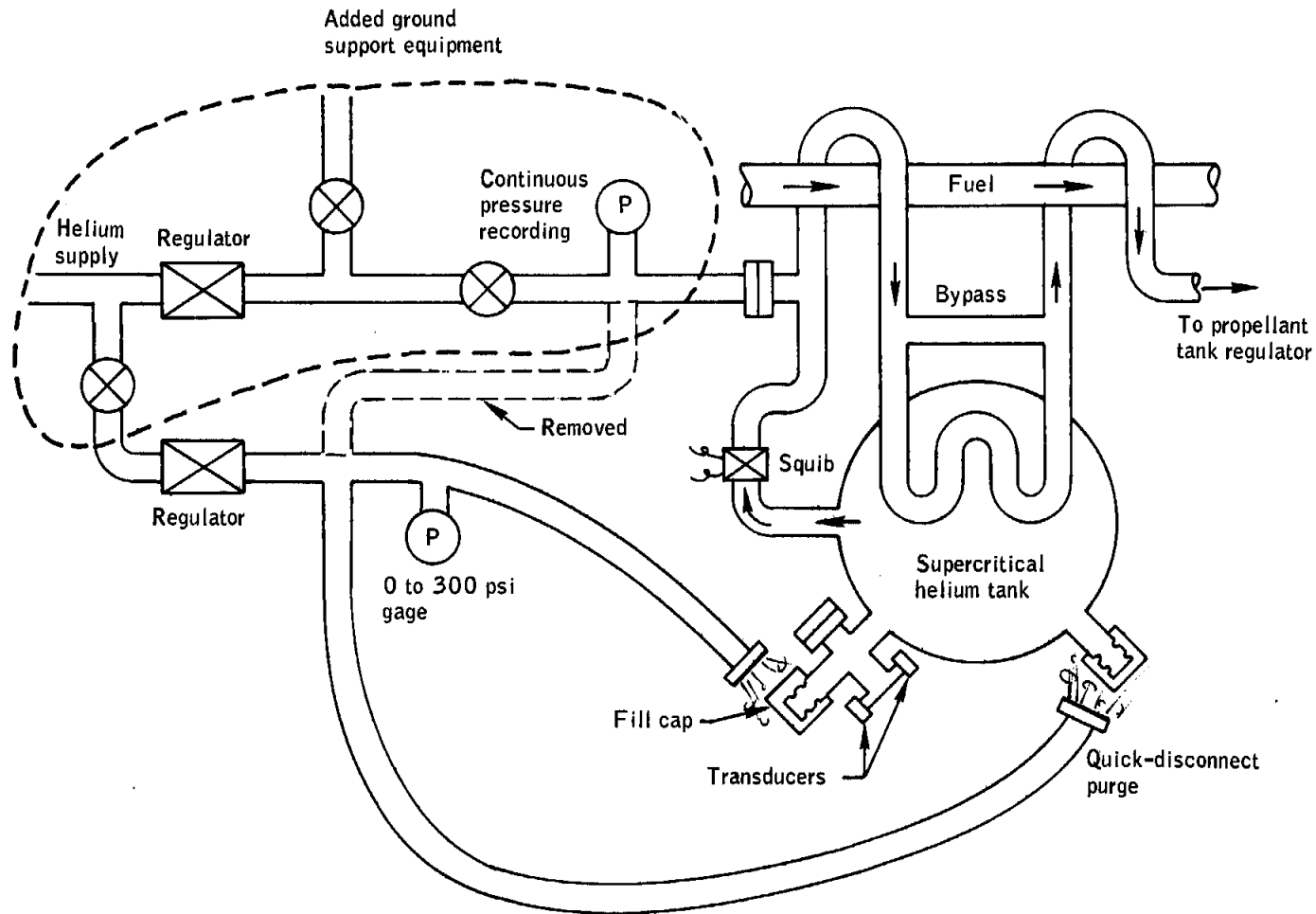


Figure 17-17.- Supercritical helium servicing ground support equipment configuration.

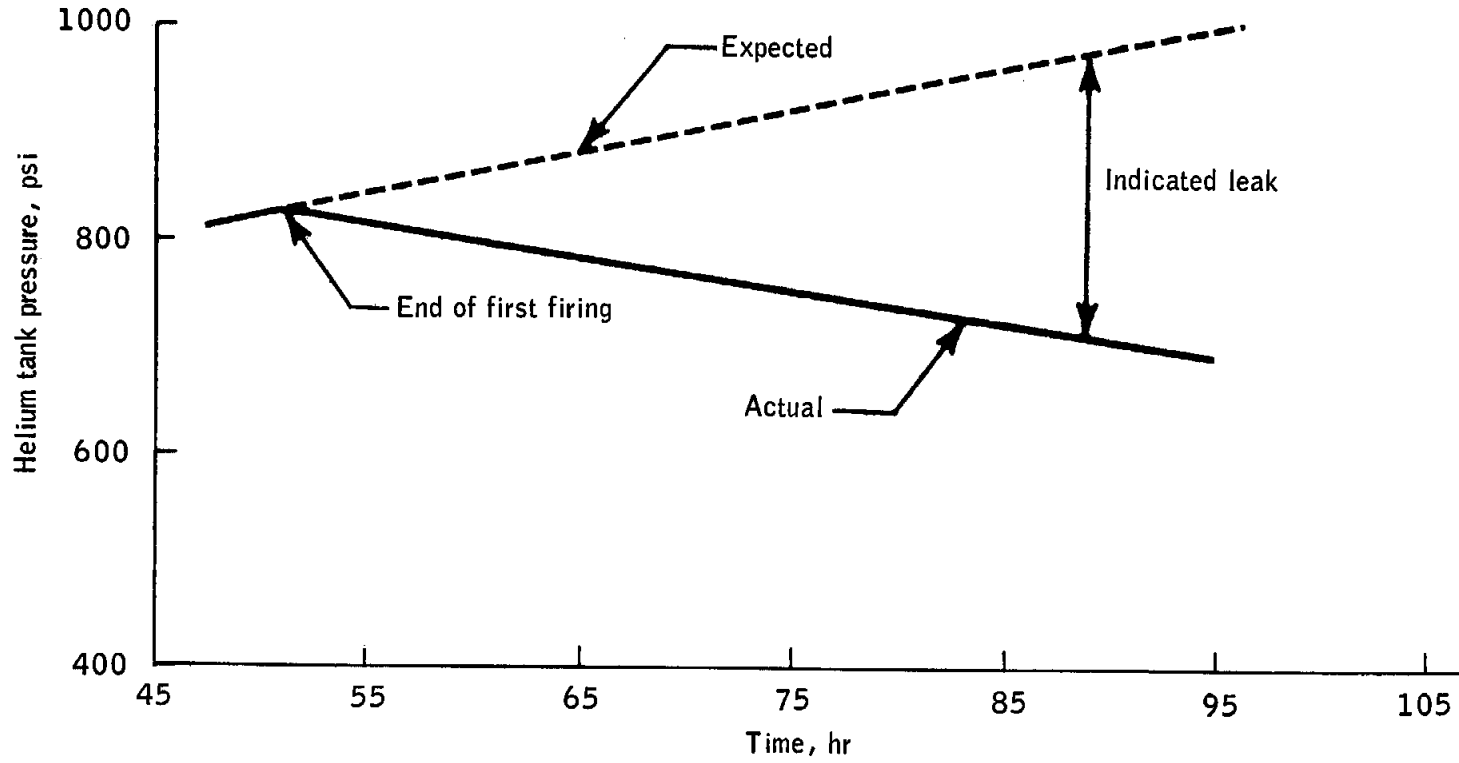


Figure 17-18.- Supercritical helium pressure decay.

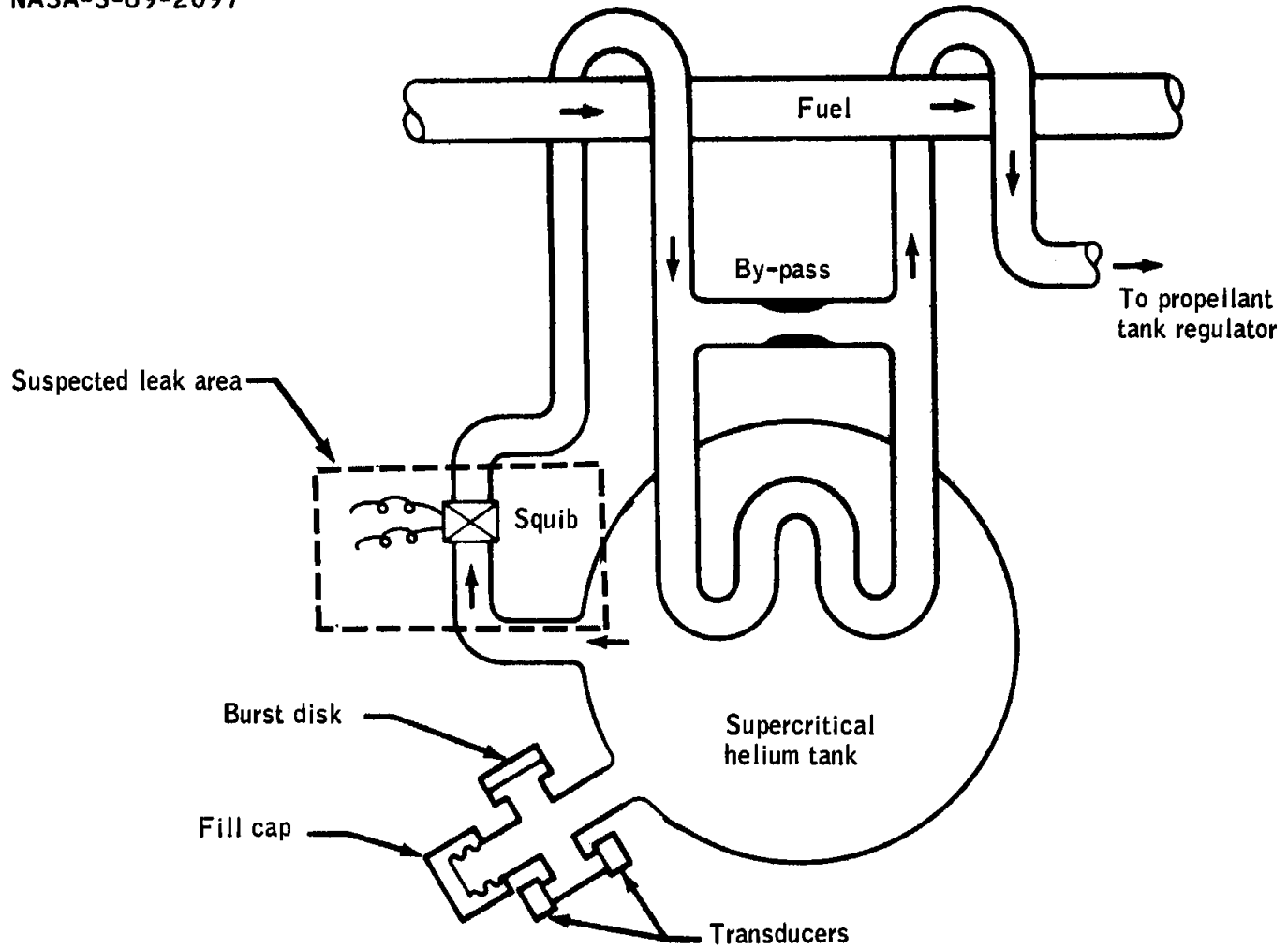


Figure 17-19.- Supercritical helium pressure suspected leak area.

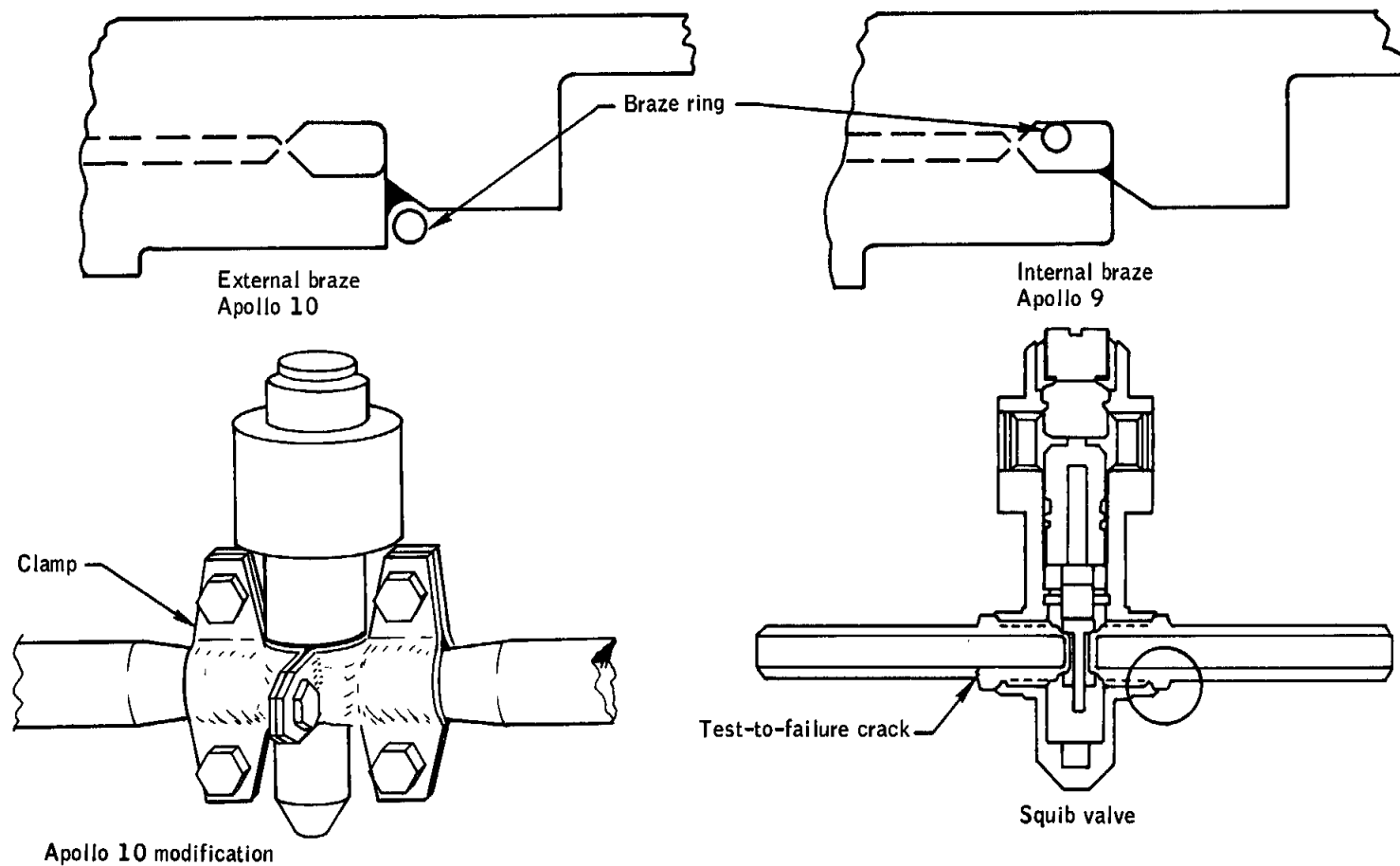


Figure 17-20.- Supercritical helium squib valve configuration.

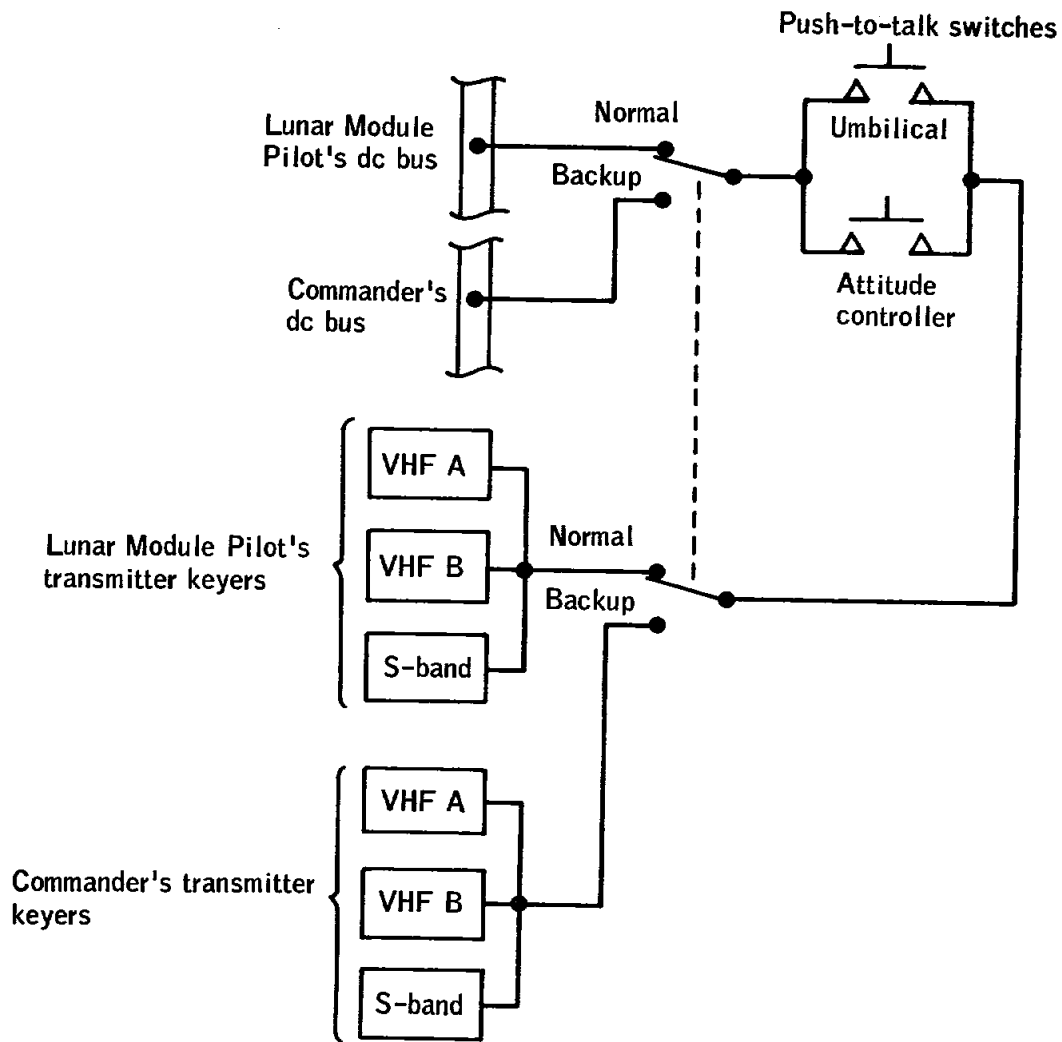


Figure 17-21.- Push-to-talk switch circuits.

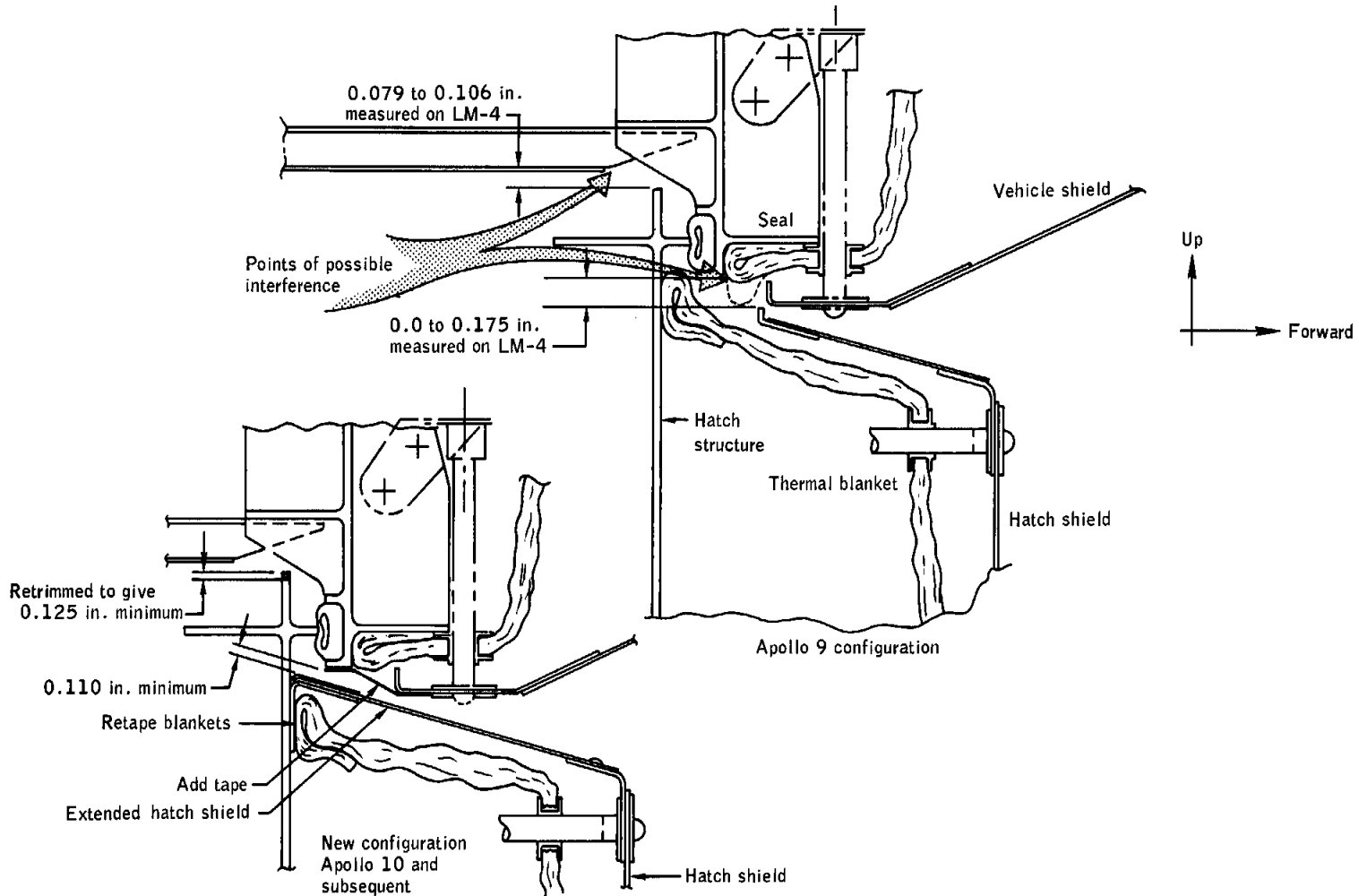


Figure 17-22.- Potential hatch interferences.

17-48

NASA-S-69-2101

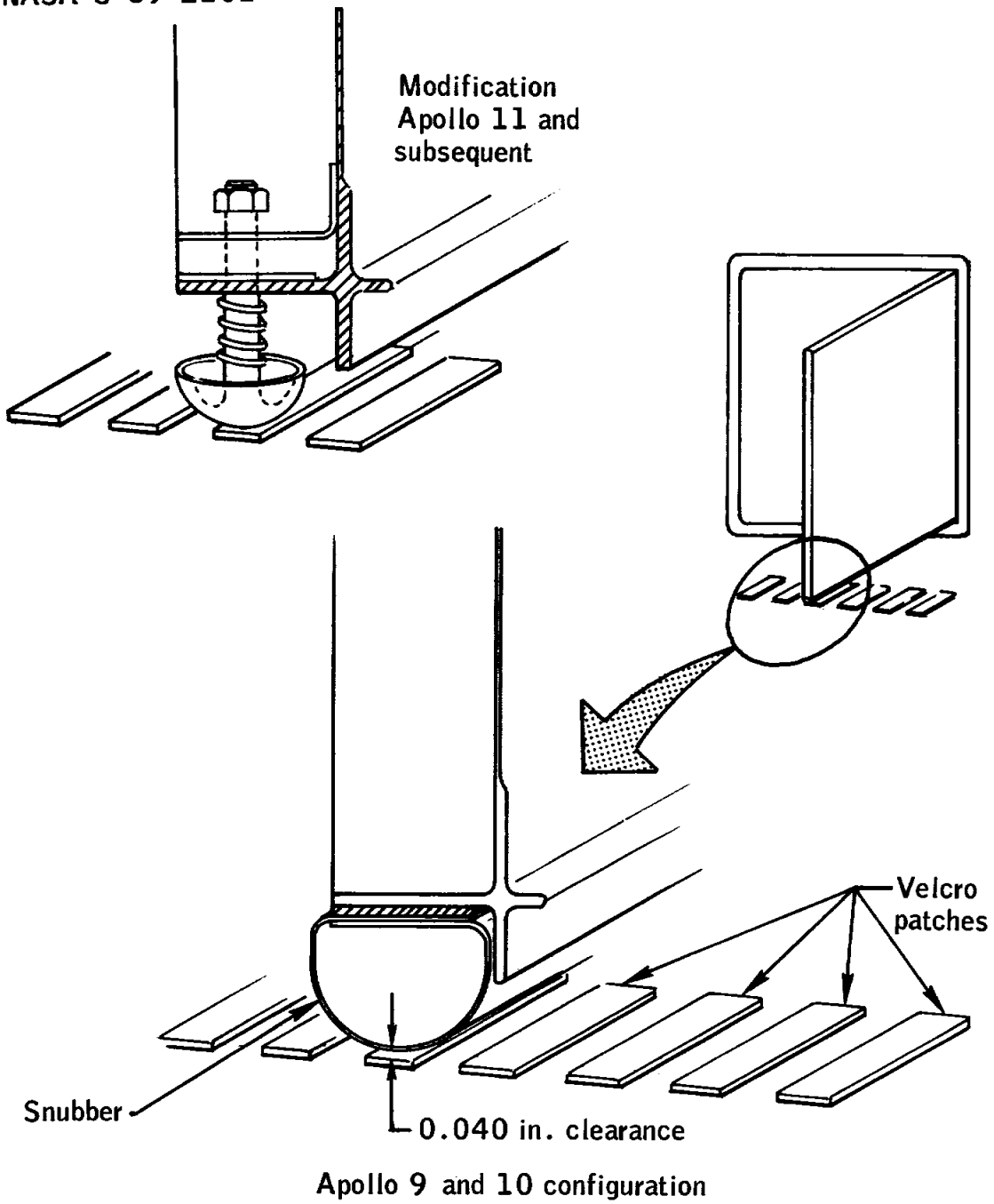


Figure 17-23.- Forward hatch snubber.

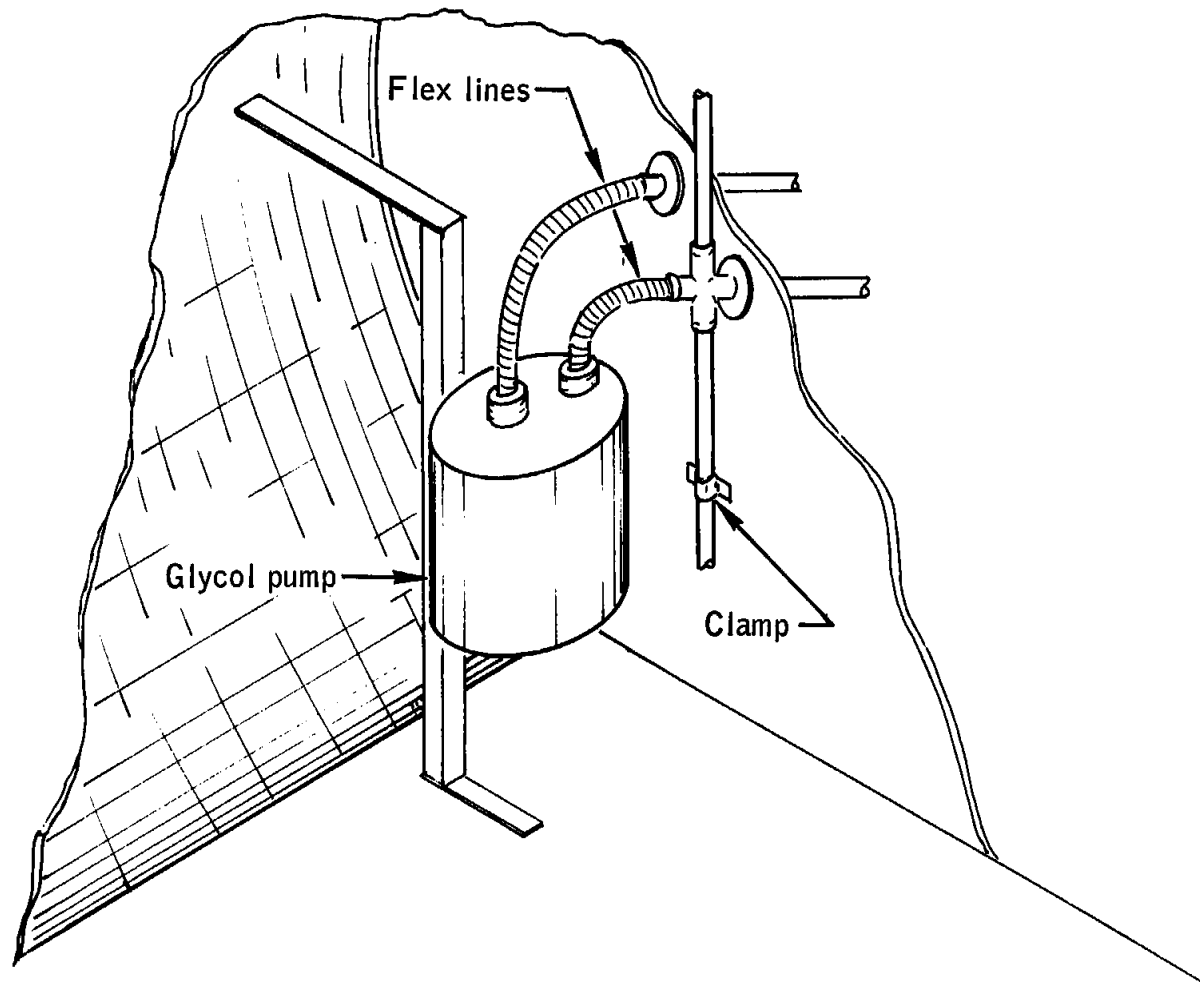


Figure 17-24.- Glycol pump noise suppression modification.

NASA-S-69-2103

17-50

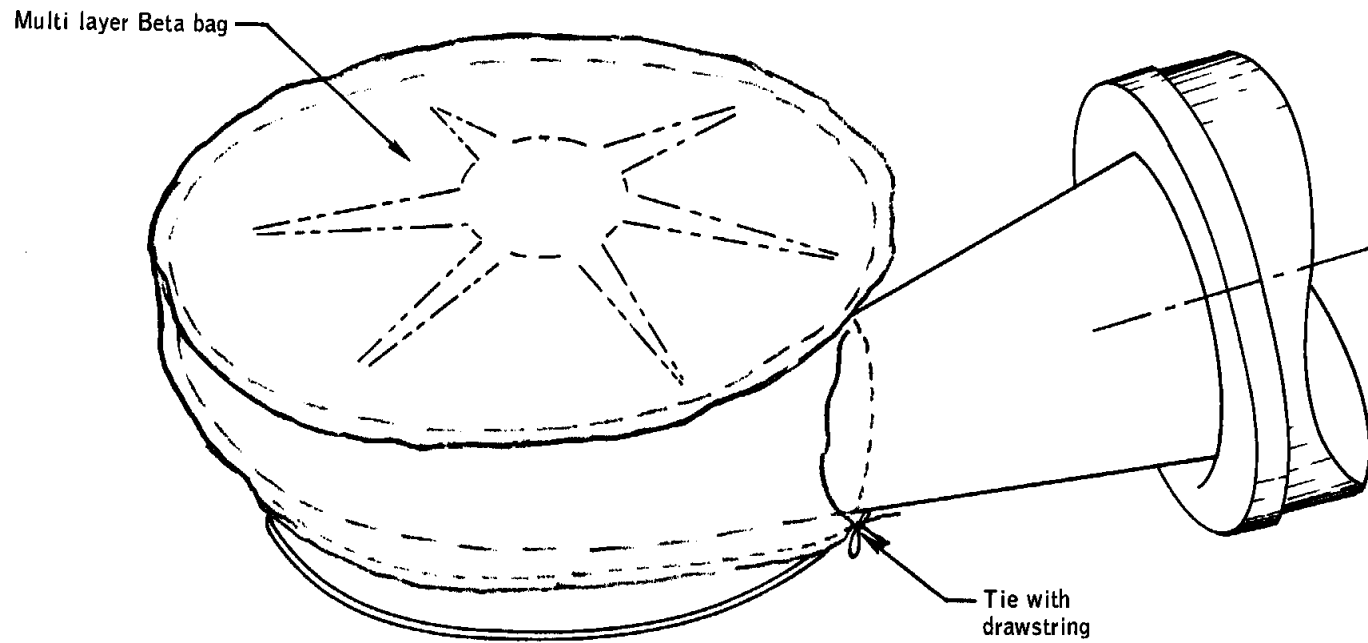


Figure 17-25.- Suit fan noise attenuation modification.

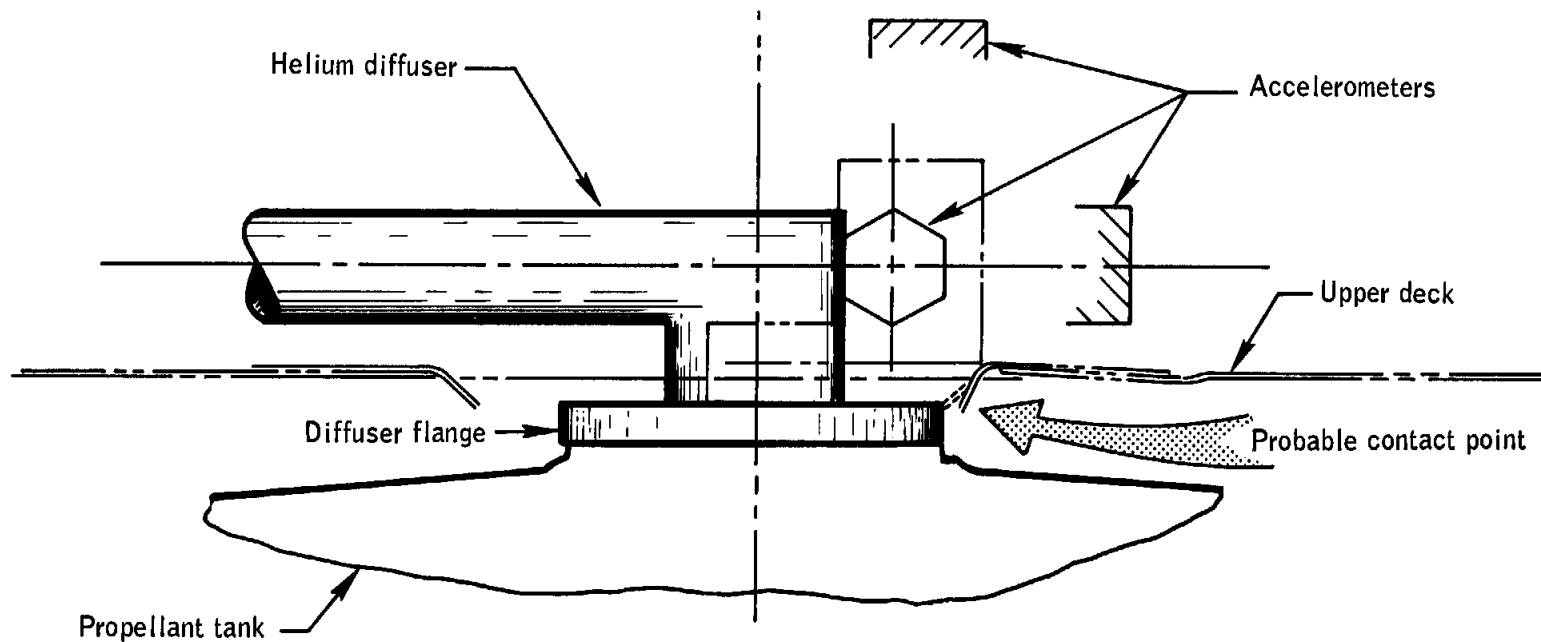


Figure 17-26.- Probable tank-to-upper-deck contact point.

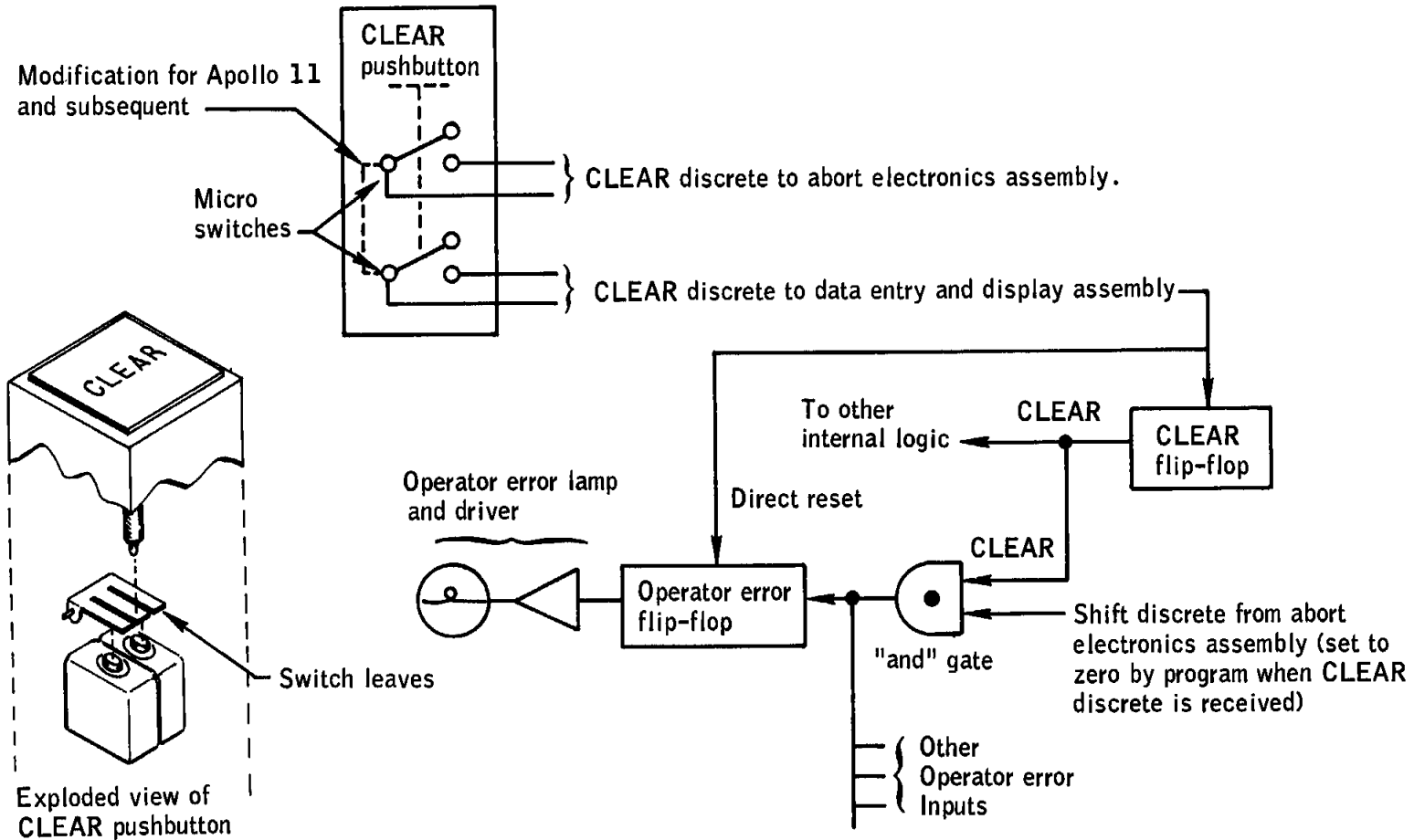


Figure 17-27.- Simplified data entry and display assembly operator error light circuit.

NASA-S-69-2106

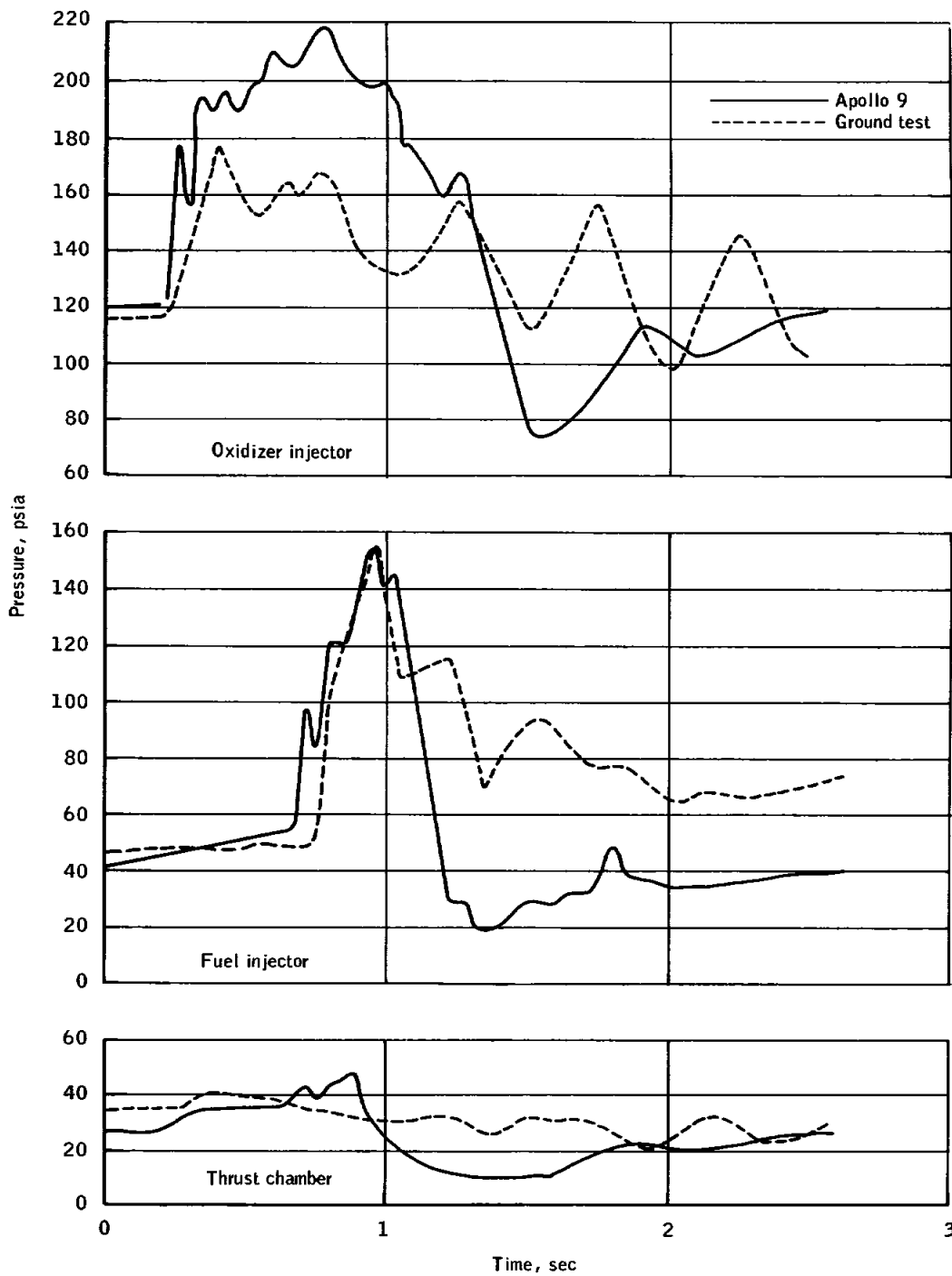


Figure 17-28.- Comparison of roughness during second descent engine firing and ground tests.

17-54

NASA-S-69-2107

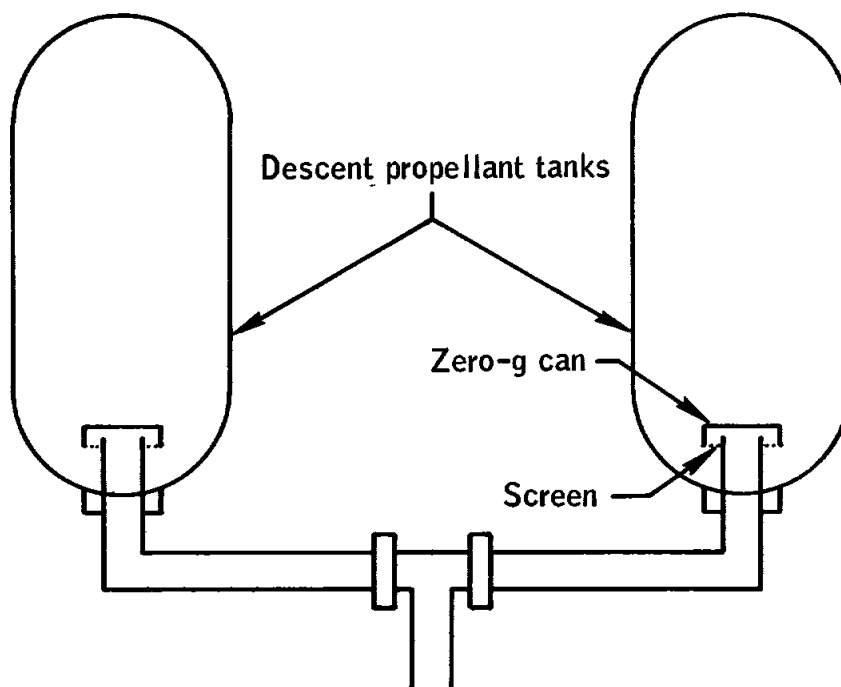


Figure 17-29.- Descent propellant tank manifolding.

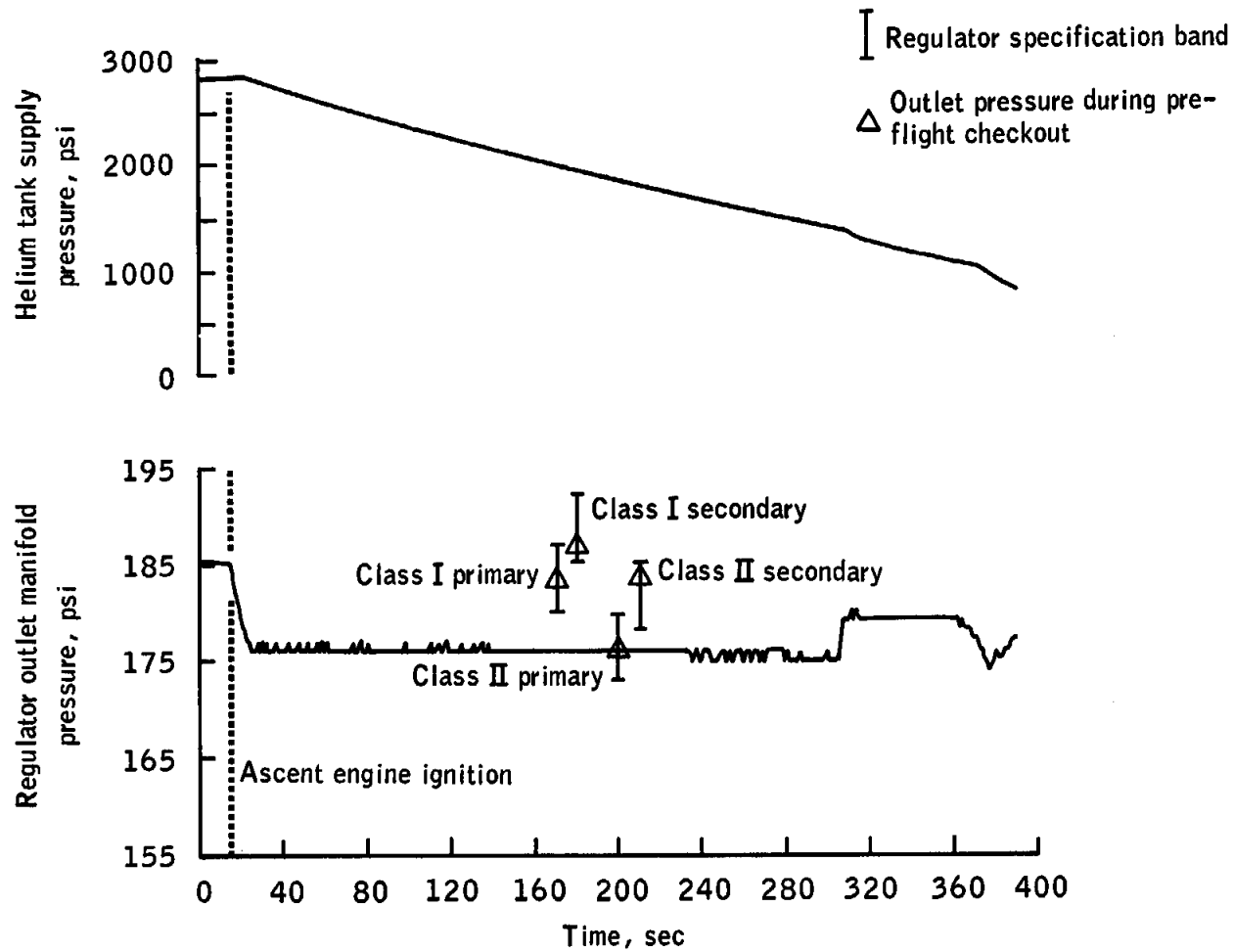


Figure 17-30.- Helium tank and regulator outlet pressures during ascent engine firing to depletion.

17-56

NASA-S-69-2109

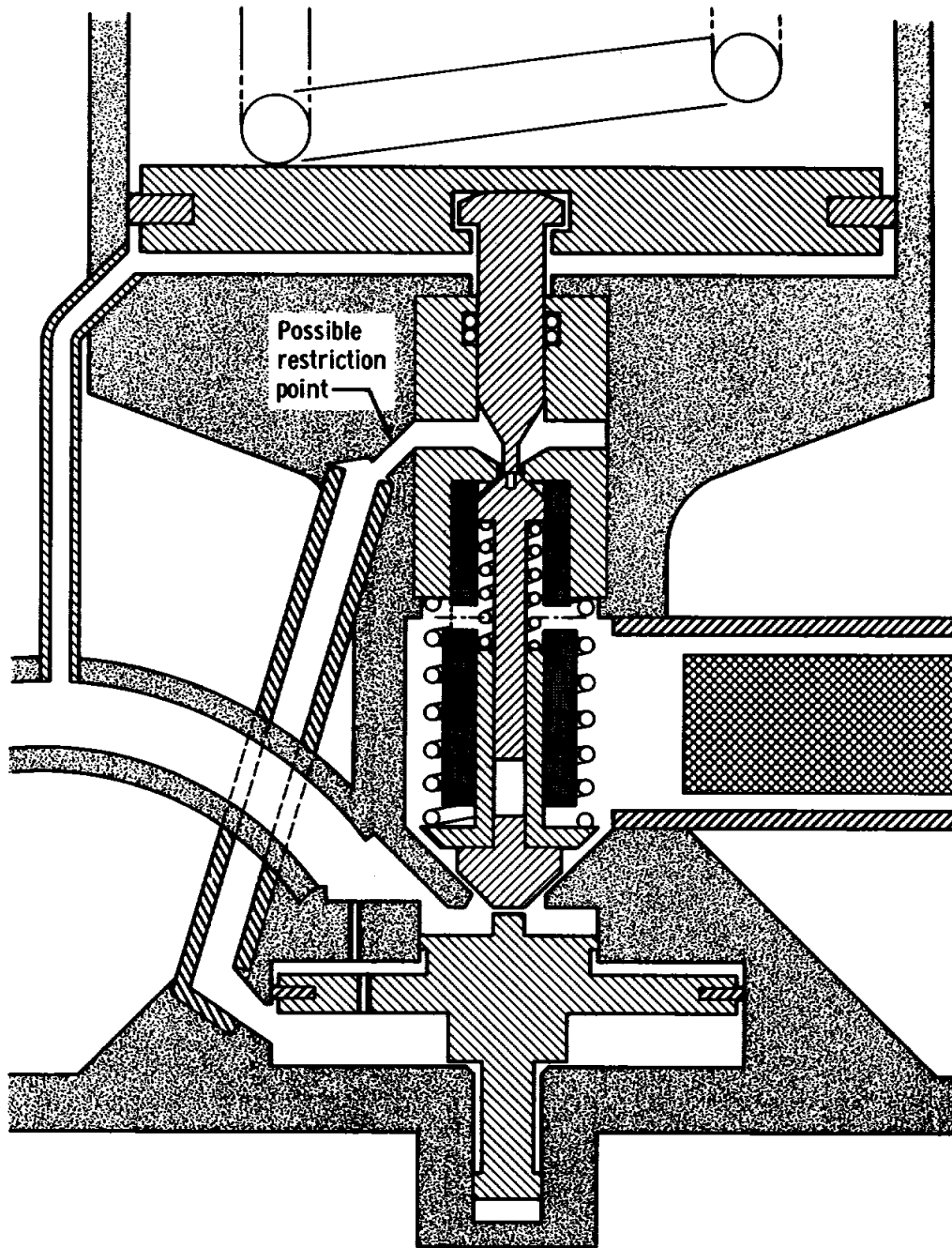


Figure 17-31. - Cross section of ascent propulsion system regulator.

### 17.3 GOVERNMENT-FURNISHED EQUIPMENT

#### 17.3.1 Air Bubbles in Liquid Cooled Garment

When the Lunar Module Pilot removed his liquid cooled garment after completing the extravehicular activity, he noted many air bubbles entrained in the liquid tubes.

The preflight procedure for charging the portable life support system has been eliminated as a possible source of air inclusion into the system. The air most probably entered the system when the portable life support system was being connected to the liquid cooled garment in the pressurized lunar module cabin. Because of the location of the coolant make-up line for the portable life support system, air is ingested through the sublimator into the coolant loop (fig. 17-32) whenever the total pressure in the liquid cooled garment is less than that in the portable life support system. The amount of air bubbles observed also corresponded roughly to the amount experienced in ground tests whenever the liquid cooled garment had been connected to the portable life support system after having been out of its storage bag, and detached from the life support system for 24 hours. The portable life support system has been redesigned to eliminate this problem for the Apollo 11 hardware (fig. 17-32). This change will relocate the make-up line to the upstream side of the water shutoff and relief valve, and any pressure make-up will be replenished with water instead of gas.

This anomaly is closed.

#### 17.3.2 Stowage of Oxygen Purge System Pallet

At the time the crew attempted to restow the oxygen purge system pallet, the locking pin could not be inserted through the lunar module bulkhead structure all the way into the pallet. The difficulty was caused by the location of the hole in the bulkhead bracket, interference by adjacent structure, poor lighting conditions, and awkward angle of insertion.

The Apollo 9 mission was the only one on which this kind of pallet will be used and, also, is the only mission on which the oxygen purge system will be stowed in this location. On Apollo 10 and subsequent, the oxygen purge system units are located in the sample return container stowage area in the midsection, where lighting and alignment access are adequate. Also, a more easily operated ball-detent locking pin will be used.

This anomaly is closed.

### 17.3.3 Lighting for Crewman Optical Alignment Sight

During docking, the brightness of the background of the sunlit command module "washed out" the reticle image of the crewman optical alignment sight in the lunar module. This problem was caused by:

a. The neutral density filter which was housed in the barrel assembly to limit the brightness of the reticle image so that fifth-magnitude stars could be seen with the sight at night.

b. The excessive illumination of the lunar module docking window by high specular reflection from the command module surface because of the attitude of the two vehicles relative to the sun and earth during the docking maneuver.

For Apollo 10 and subsequent missions, the neutral density filter will be replaced by a diffuser glass; in addition, an external snap-on filter will be provided to cover the open end of the barrel when required. This will provide two ranges of reticle illumination intensity:

a. Without the filter - Zero to between 500 and 800 foot-lamberts for use against a bright background of up to 10 000 to 16 000 foot-lamberts.

b. With the filter - Zero to between 50 and 80 foot-lamberts for a darker background and for fainter targets.

For docking on Apollo 10 and subsequent missions, it is planned that the lunar module and command module will be oriented for illumination by the diffused reflected light from lunar or earth albedo, and in contingency cases, the passive spacecraft will roll to reduce the glare.

Based on sun angles during Apollo 9 docking, the background against the lunar module alignment sight increased to more than 10 000 foot-lamberts. A background of 1600 foot-lamberts would have "washed out" the 80 foot-lambert reticle. During the last 10 feet of the docking maneuver, the command module surface came within the shadow of the lunar module structure, reducing the background glare so that the lunar module reticle could be seen.

This anomaly is closed.

### 17.3.4 Oxygen Purge System Light

The checkout light on the Commander's oxygen purge system operated erratically during the flight and failed to come on during preparations for rendezvous. An examination of all possible conditions that could have caused the failure indicates that the main power switch actuator

mechanism did not close the switch. The following changes were incorporated into the actuator mechanism (fig. 17-33) for Apollo 10 and subsequent:

- a. Change type of Teflon insert material in the flexible cable
- b. Change to a swivel joint in the flexible cable at the oxygen purge system interface
- c. Increase cam rise on switch actuator cam
- d. Bond switch actuator cam to slide
- e. Bond switch in place after adjustment.

This anomaly is closed.

#### 17.3.5 Temporary Loss of Communications

The commander reported one loss of communications while using the lightweight headset, and one loss while using the communications carrier. No hardware discrepancies were noted during postflight checks of the lightweight headsets and associated cables, control heads, and adapters (see fig. 17-34). The communication carriers and the commander's suit harness were also tested with associated cables and control heads and operated properly.

The airlock sleeves on the T-adapters were loose (see fig. 17-34) during mating and demating of the connectors for the postflight tests. Subsequent checks of the spacecraft showed a loose airlock sleeve on the bulkhead connector that mates with the commander's umbilical. Considering the worst case connector insert, pins, and airlock sleeve tolerances, an airlock sleeve loosened by one turn could cause loss of communications. During previous ground tests, loss of communications has been encountered because of improper mating of the lightweight headset connector to the suit harness and/or the T-adapter.

The most probable cause of the commander's loss of communication was either a loose airlock sleeve on one of three connectors, or an improper mating of the lightweight headset connector to the suit harness and T-adapter.

For Apollo 10 and subsequent, the airlock sleeves will be torqued to between 45 and 50 inch-pounds and loctite will be applied to secure the sleeves to the connector.

This anomaly is closed.

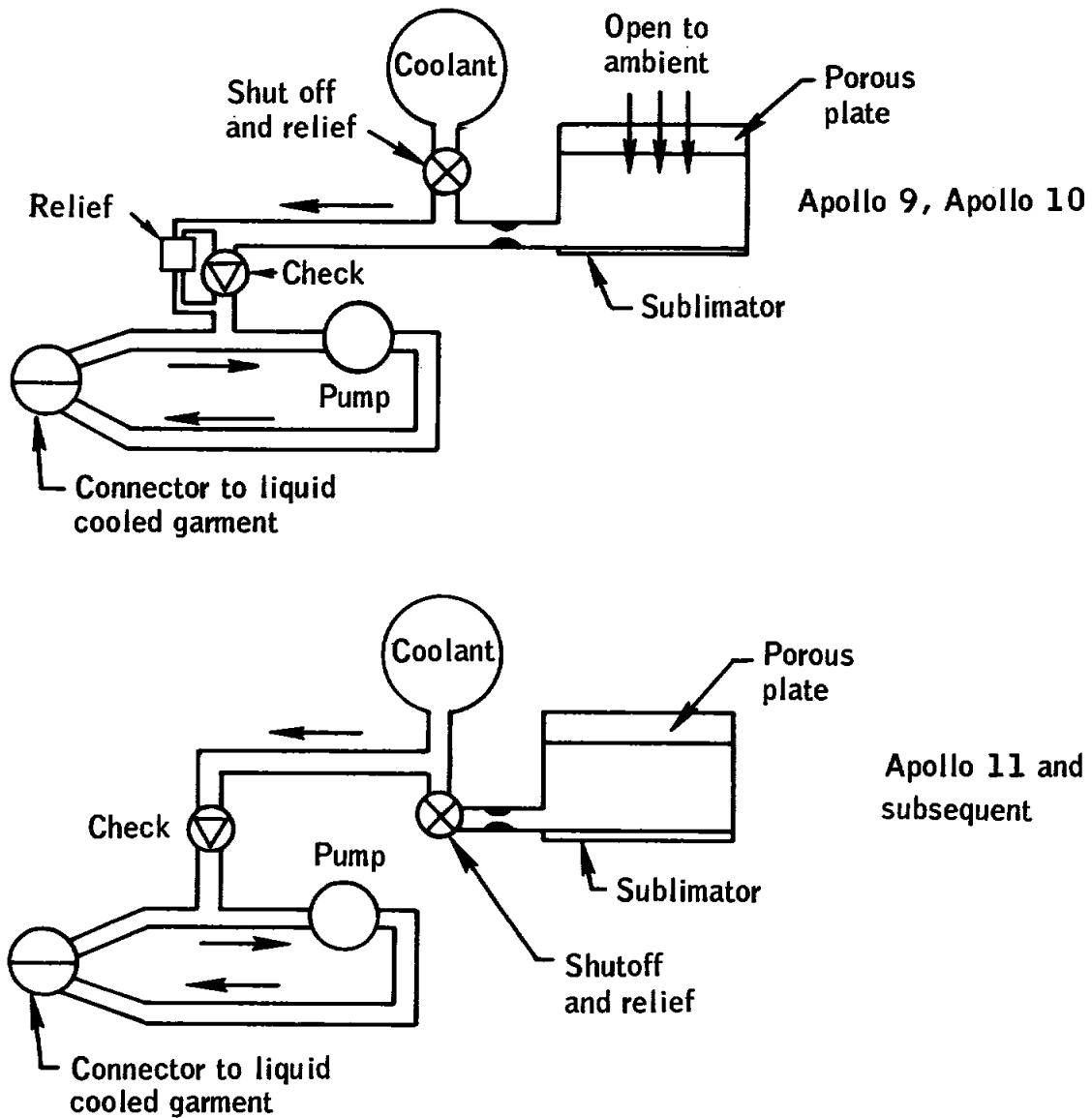


Figure 17-32.- Air in liquid cooled garment at time of connection to portable life support system.

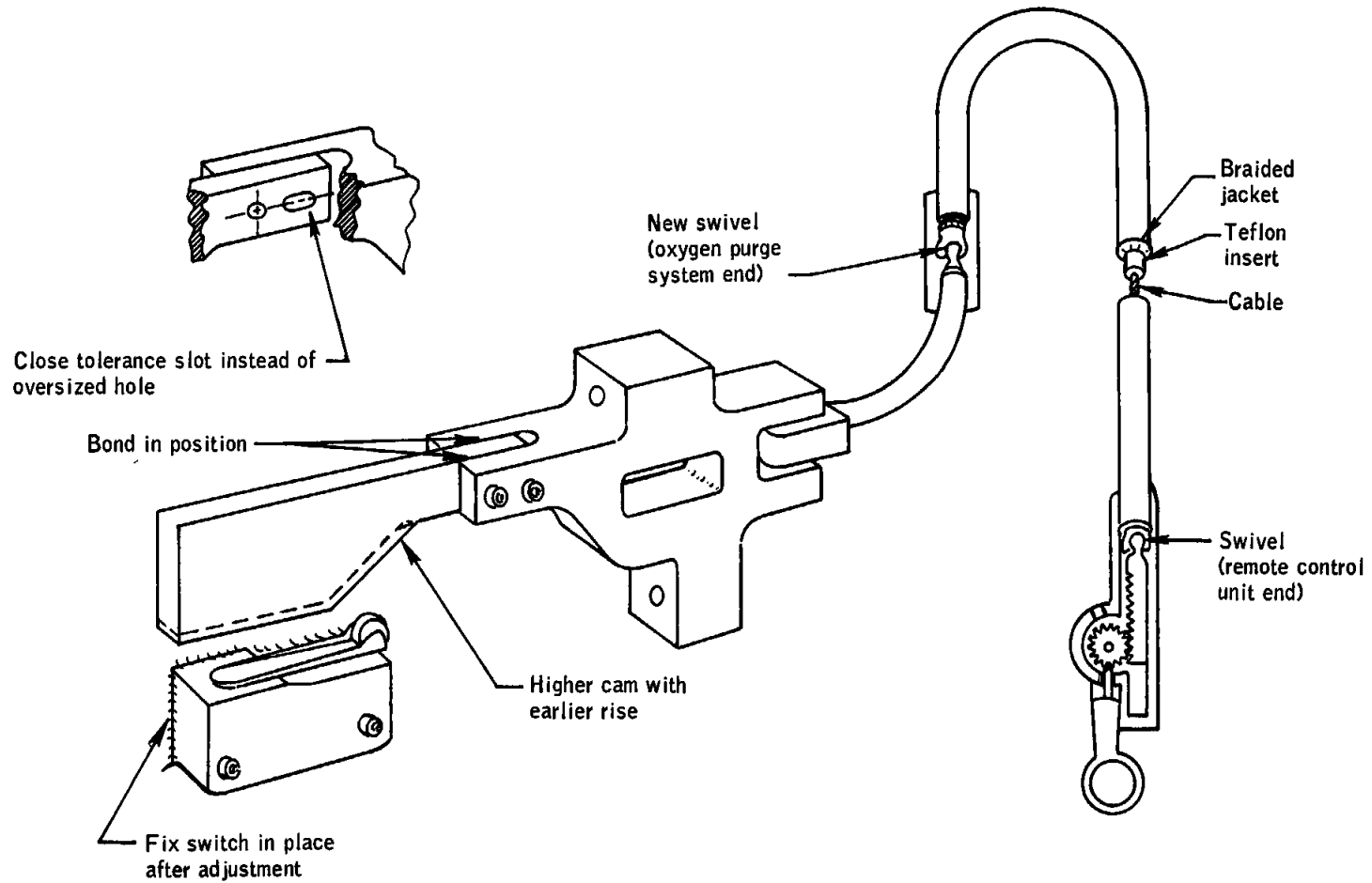


Figure 17-33.- Oxygen purge system heater power switch actuator mechanism changes for Apollo 10.

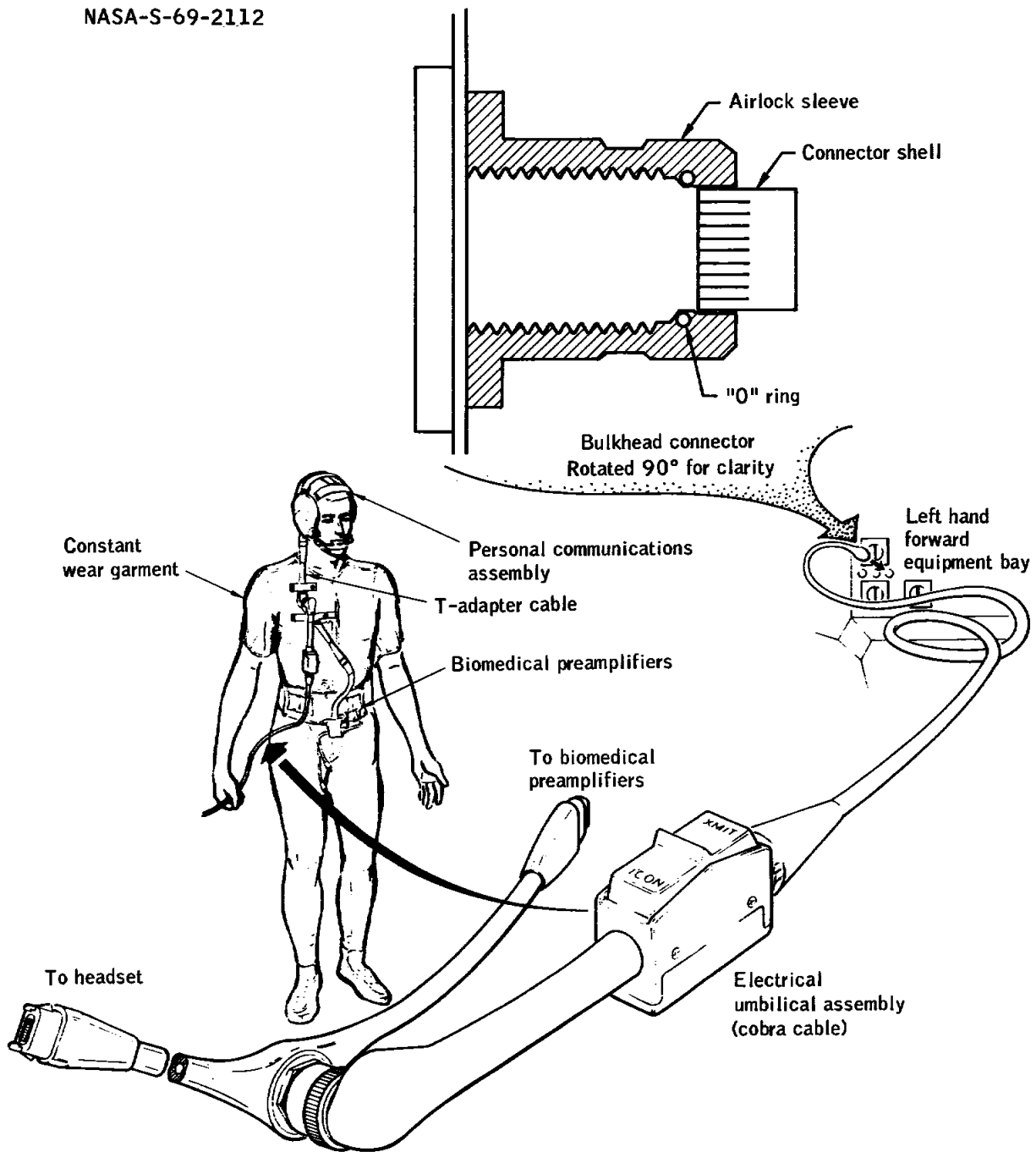


Figure 17-34.- Sectional view of airlock sleeve on connector shell.

## 18.0 CONCLUSIONS

Based on the results and observations of the Apollo 9 mission, the following conclusions are drawn from the information contained in this report.

1. The onboard rendezvous equipment and procedures in both spacecraft provided the required precision for rendezvous operations to be conducted during the lunar landing mission. The command and service module computations and preparations for mirror-image maneuvers were completed on time by the Command Module Pilot.

2. The functional operation of the docking process of the two spacecraft was demonstrated. However, the necessity for proper lighting conditions for the docking alignment aids was illustrated.

3. The performance of all systems in the extravehicular mobility unit was excellent throughout the entire extravehicular operation. The results of this mission, plus satisfactory results from additional qualification tests of minor design changes, will provide verification of the operation of the extravehicular mobility unit on the lunar surface.

4. The extent of the extravehicular activity indicated the practicality of extravehicular crew transfer in the event of a contingency. Cabin depressurization and normal repressurization were demonstrated in both spacecraft.

5. Performance of the lunar module systems demonstrated the operational capability to conduct a lunar mission, except for the steerable antenna which was not operated and for the landing radar which could not be fully evaluated in earth orbit. None of the anomalies adversely affected the mission. The concepts and operational functioning of the crew/spacecraft interfaces, including procedures, provisioning, restraints, and displays and controls, are satisfactory for manned lunar module functions. The interfaces between the two spacecraft, both while docked and undocked, were also verified.

6. The lunar module consumable expenditures were well within predicted values, demonstrating adequate margins to perform the lunar mission.

7. Gas in the command module potable water supply interfered with proper food rehydration and therefore had some effect on food taste and palatability. Lunar module water was acceptable.

8. Orbital navigation of the command and service modules, using the yaw-roll control technique for landmark tracking, was demonstrated and

reported to be adequate. The star visibility threshold of the command module scanning telescope was not definitely established for the docked configuration; therefore, platform orientation using the sun, moon, and planets may be required if inertial reference is inadvertently lost during translunar flight.

9. Mission support, including the Manned Space Flight Network, adequately provided simultaneous ground control of two manned spacecraft.

## APPENDIX A - VEHICLE DESCRIPTIONS

The Apollo 9 space vehicle consisted of a block II configuration spacecraft and a Saturn V launch vehicle (AS-504). The spacecraft comprised a launch escape system, command and service modules (no. 104), a spacecraft/launch-vehicle adapter, and a lunar module (LM-3). All components except the lunar module were similar to those for Apollo 8, and only the major differences are discussed. The Apollo 9 lunar module was configured for manned capability. Although there were a number of structural and systems similarities between the Apollo 5 (LM-1) and the Apollo 9 lunar module, a baseline description is presented for the manned vehicle configuration.

The extravehicular mobility unit used for Apollo 9 was composed of the pressure garment and extravehicular visor assemblies, the extravehicular gloves, the portable life support system, the remote control unit, and the oxygen purge system. The pressure garment assembly is discussed in section A.1.9 and the other components in section A.2.8.

### A.1 COMMAND AND SERVICE MODULES

#### A.1.1 Structural and Mechanical Systems

A docking and transfer system was added to the forward hatch area of the command module; combined with the female docking assembly in the lunar module, this system permitted rigid docking of the two spacecraft and provided for transfer of the crew. The docking assembly (fig. A.1-1) included a docking probe, docking ring and associated seals, and automatic docking latches. A rigid docking configuration was achieved when the probe engaged the drogue in the lunar module and the lunar-module tunnel ring activated the 12 automatic latches. This latching action effected a pressure-tight seal, and the pressure on each side of the closed tunnel hatches was equalized through a valve. Should one of the automatic latches have failed to function, the crew could have manually closed this latch. Once a rigid dock was performed and pressures equalized, the command module forward hatch was removed, the latches verified, and the probe and drogue assembly dismantled and stowed. The lunar module hatch was then opened to permit crew transfer.

An additional change was to pre-cure the RTV sealant and other materials in the area surrounding the center (hatch) and two side windows of the command module. In the previous two missions, outgassing from the RTV sealant resulted in window contamination and associated optical degradation.

### A.1.2 Sequential Events Control System

The sequential events control system was modified to accommodate combined spacecraft functions involving the lunar module. These functions were docking following transposition, ejection of the docked spacecraft from the S-IVB, separation of the lunar module from the command module, docking of the lunar module to the command module, and jettisoning of the lunar-module ascent stage (fig. A.1-2).

### A.1.3 Communications

In the communications system, the S-band power amplifier was modified to eliminate diode failures caused by the proximity of a high voltage wire by re-routing the wire.

The VHF/AM transceiver was modified by adding certain resistors to decouple the output stages of the receivers, thus minimizing the audio distortion when the two receivers were operating simultaneously.

The capability of simultaneous biomedical data transmission from all three crewmen was incorporated in the telemetry system, rather than the time-sharing configuration of Apollo 8.

The lightweight headsets for use during unsuited operations were electrically equivalent to those for Apollo 7 and 8. However, the microphone amplifier was mechanically relocated from the head area to the connector area to reduce the mass of the assembly worn on the head. This change permitted improved retention of the assembly on the head while in orbit.

The television camera was deleted, and a new configuration (see section A.2.6) stored in the lunar module prior to launch.

### A.1.4 Environmental Control System

An additional overboard water dump nozzle was incorporated in the waste management system to accommodate battery venting without backflow into the waste management system. With the new configuration, oxygen bleed and water dumping was accomplished through the urine dump nozzle, and an interconnect was provided between the two overboard nozzles in the event one had become inoperative. Each nozzle was fitted with a temperature transducer and heating element to prevent freezing at the outlet.

The glycol temperature controller incorporated 100-percent quality-controlled parts, a revised synchronous circuit for added reliability,

and a change from a pulsed to a continuous-drive signal for the back-pressure control valve.

#### A.1.5 Service Propulsion System

The configuration of the bipropellant valve was changed, and the new material from which the valve piston was constructed limits the valve to a lower temperature limit of 40° F. A temperature measurement was added to monitor this parameter.

Fiberglass brackets were used on the propellant-utilization valve to thermally isolate the valve from the surrounding structure.

Inlet filters were added to both the oxygen and the fuel helium check valves to prevent valve contamination.

#### A.1.6 Reaction Control Systems

The major changes to the reaction control systems were in the service module. A helium isolation valve was added immediately upstream of the secondary fuel tank (fig. A.1.-3) and a change was made in the four propellant isolation valves. These valves were changed from a primary and a secondary control-switch configuration to a single switch function such that all four valves in each quad were controlled from a single switch, even though independent flags for the primary and the secondary valves were maintained.

#### A.1.7 Instrumentation

The flight qualification instrumentation, including the flight qualification recorder, modulation packages, commutators, and transducers, were deleted.

#### A.1.8 Pyrotechnics

There were no changes to the pyrotechnic devices except for items added to accommodate the lunar module docking function. The docking-ring separation system, which had a full-circle pyrotechnic charge that severed the docking ring, was added for vehicle separation from the lunar module, and the probe-retract system was added with a single bridgewire initiator to release pressure and to effect retraction of the docking probe.

## A.1.9 Crew Provisions

The only major change to the crew provisions was in the pressure garment assembly for the Lunar Module Pilot to accommodate extravehicular activity. Other items of a minor nature are also discussed.

The Apollo 9 pressure garment assemblies were identical to that worn during the Apollo 8 mission except that the Apollo 9 Lunar Module Pilot wore a liquid cooling garment instead of the constant wear garment. The liquid cooling garment was worn next to the skin under the pressure garment assembly and was made of nylon-Spandex knitted material to provide perspiration absorption and heat transfer from the crewman's body. The garment provided a continuous flow of temperature-controlled water from the portable life support system (see section A.2.6) through a network of polyvinyl chloride tubing stitched to the inside surface of the open-mesh fabric garment. The coolant water was warmed by the crewman's body heat and returned through the outlet channel of the multiple water connector. The liquid cooling garment could have removed heat at a maximum rate of 2000 Btu/hr for a 15-minute period or a continuous rate of 1700 Btu/hr. Evaporative cooling could also have been provided by the oxygen supply in the portable life support system through the inner chifon liner fabric of this garment.

A urine collection and transfer adapter was added to permit urine dumping after doffing the pressure garment assembly.

A thermal sample tether was added to allow the Command Module Pilot to retrieve the thermal samples mounted on the outer surface of the command and service module. A hook was attached to the D-ring on the thermal sample assembly for this purpose, and the samples were to be sequentially released and retrieved.

A docking target was added on the command module as the primary visual aid to assist in lunar module docking. The target consisted of a green electroluminescent base plate with a protruding red target and was mounted in the right-hand rendezvous window. The Lunar Module Pilot was to align on this target using the crewman optical alignment sight. A target adapter was included to mount the target in the window.

Couch restraint straps were provided to hold the center couch in the stowed position to facilitate intravehicular activity.

A stowage container was provided to stow the forward hatch under the left couch after removal, and straps were added to retain the docking probe after removal.

## A.1.10 Displays and Controls

The displays and controls in the command module were modified by having a light added to illuminate the exterior of the command module hatch area during extravehicular activities. This light was mounted on the end of a boom-assembly that extends when the boost protective cover is removed. The light provided an intensity of 0.5 foot-candle directed 45 degrees to the spacecraft longitudinal axis (fig. A.1-4).

A docking light was added to illuminate the passive vehicle while station keeping and for final docking maneuvers within a 50- to 500-foot range. This light was mounted on the fairing interface between the command and service modules and was to be deployed, using a hot-wire initiator, for forward illumination along the longitudinal axis (fig. A.1-5).

A beacon light was provided as a backup in the event of rendezvous radar failure during lunar module rendezvous. The light was to emit at a rate of approximately 60 bursts/min with an intensity of 120 beam-candle-seconds and a beamwidth of 120 degrees. The light was designed to be seen by an unaided viewer at 60 miles or with a telescope at 160 miles (fig. A.1-6).

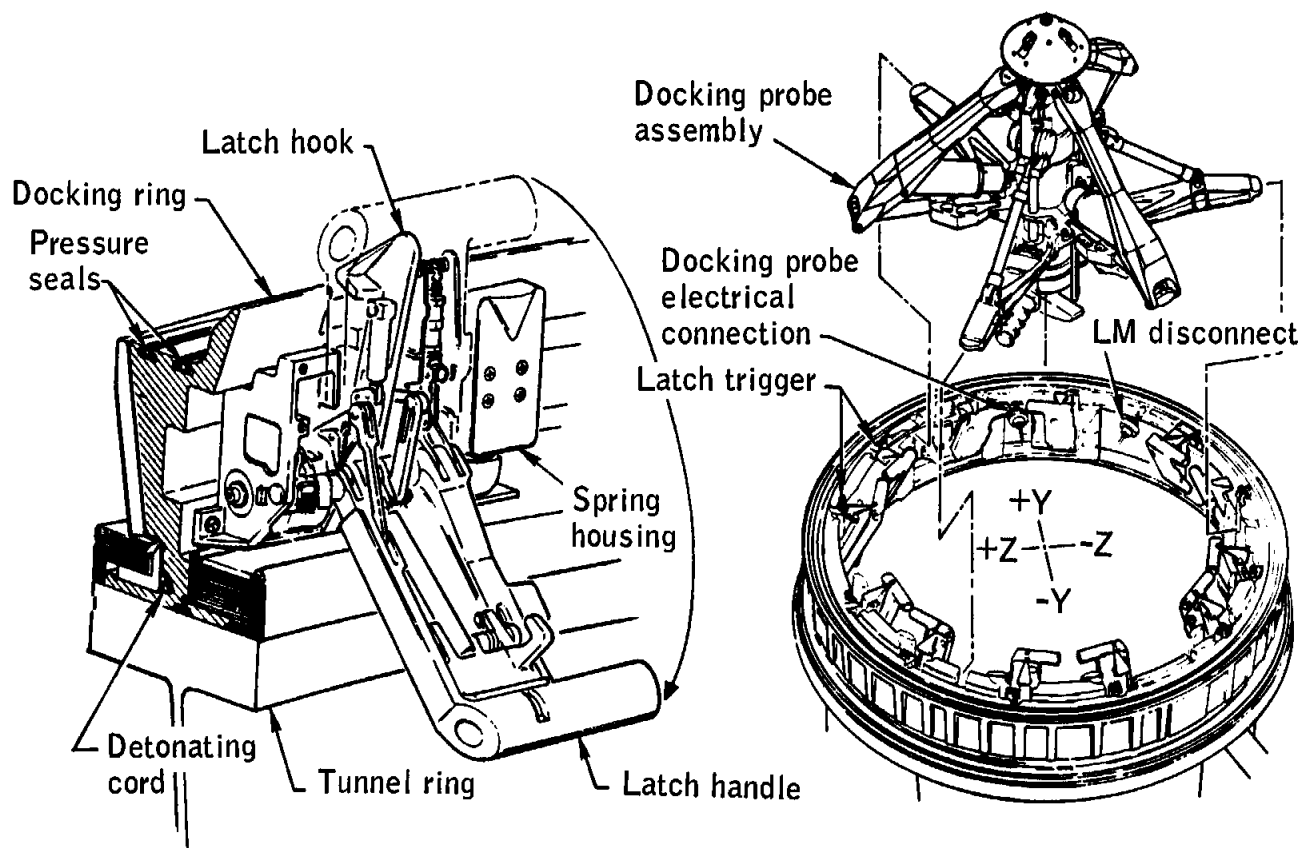


Figure A.1-1.- Command module docking assembly.

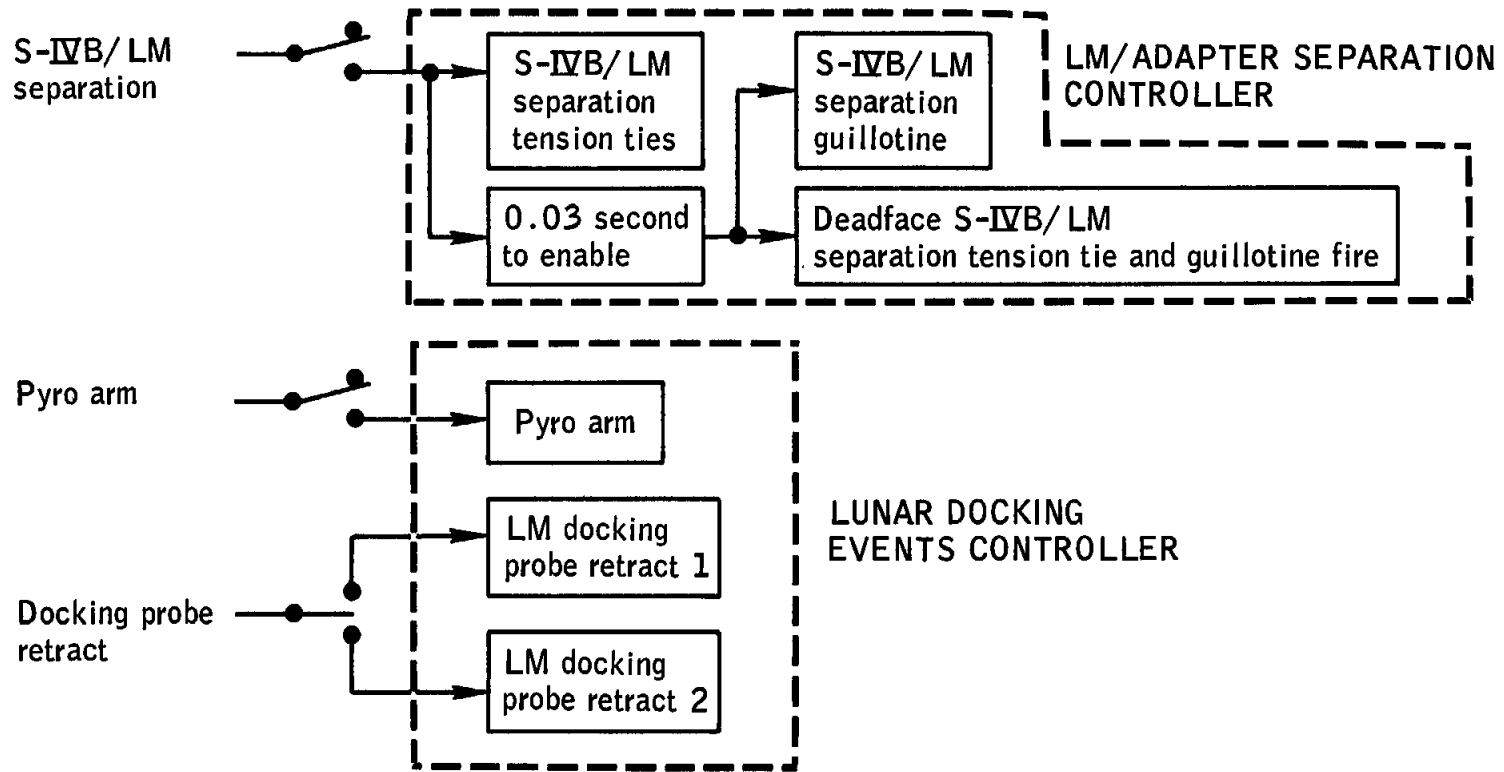


Figure A.1-2.- Sequential events control system additions for lunar module control.

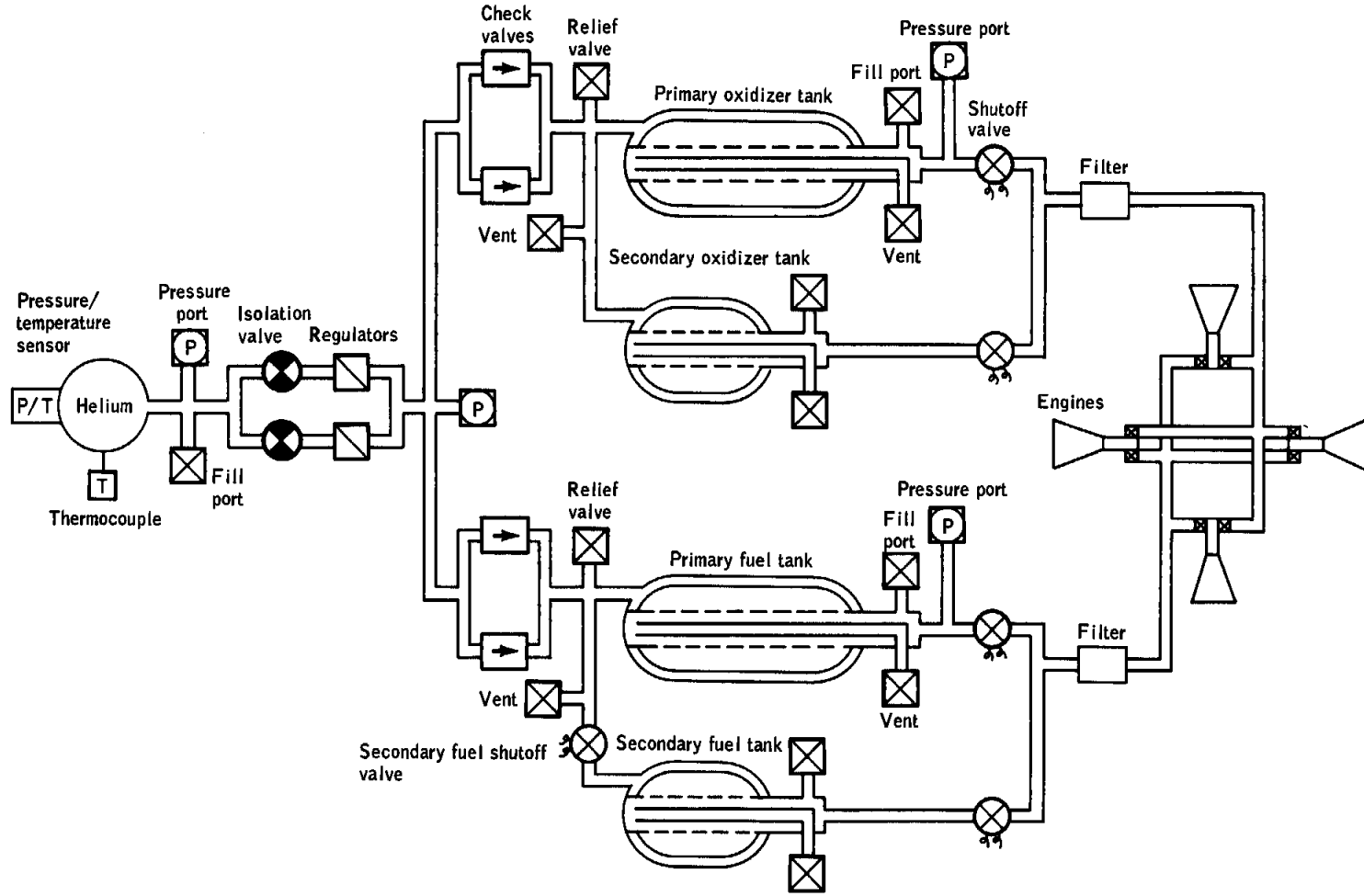
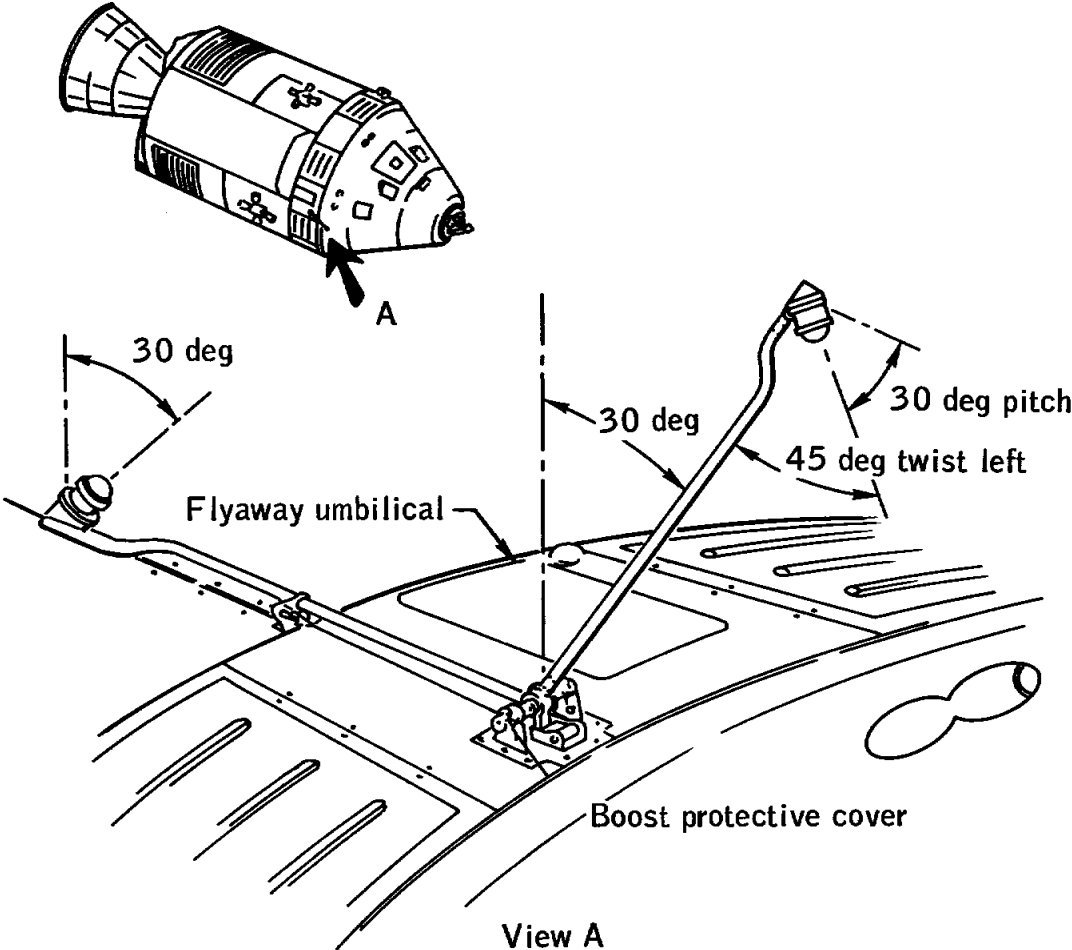


Figure A.1-3.- Service module reaction control system.

NASA-S-69-2116



A.1-4.- Extravehicular activity floodlight.

A-10

NASA-S-69-2117

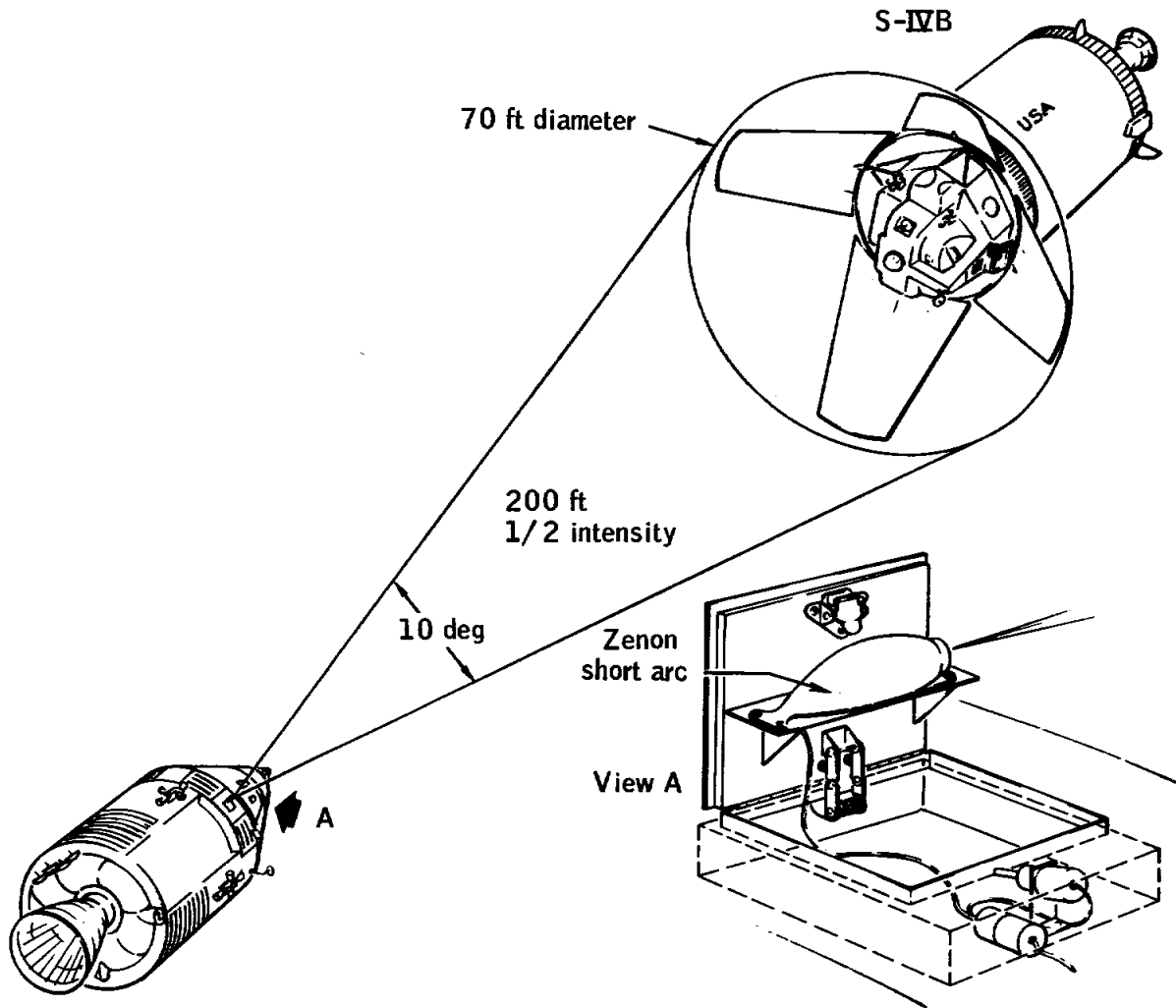


Figure A.1-5.- Exterior spotlight.

NASA-S-69-2118

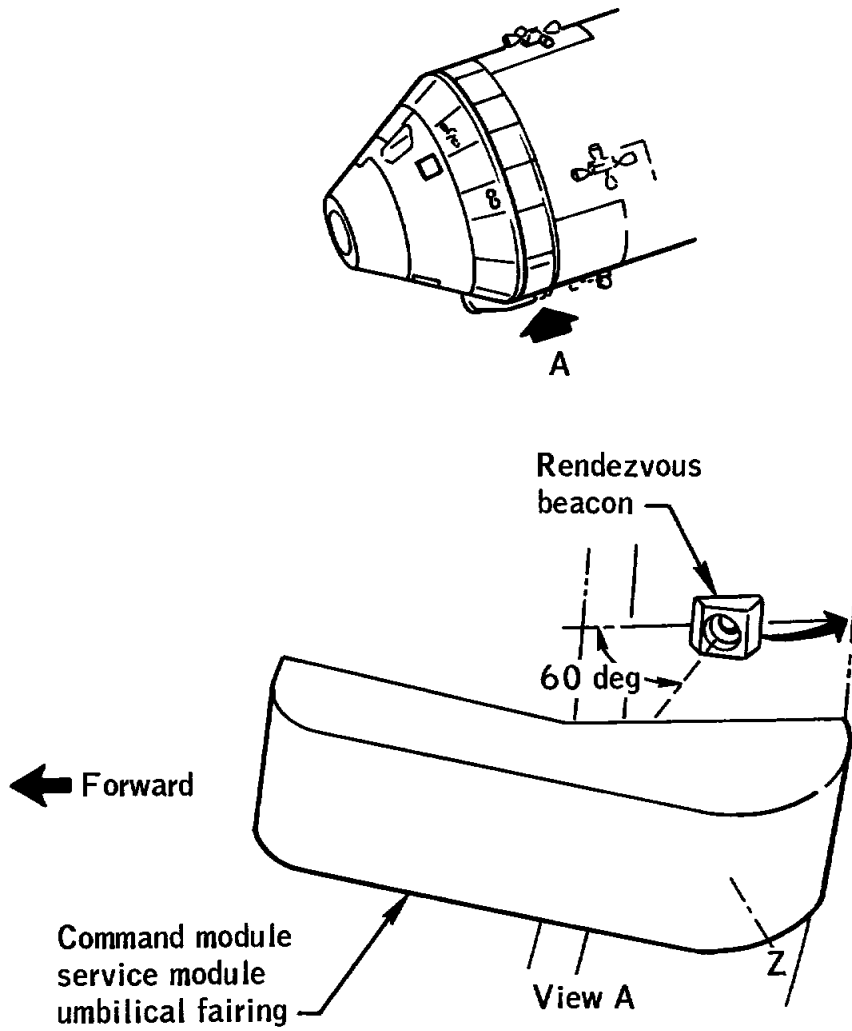


Figure A.1-6.- Rendezvous beacon light.

## A.2 LUNAR MODULE

The lunar module is designed to land two men on the lunar surface, then return them to the lunar-orbiting command and service module. The lunar module consists of an ascent and a descent stage (fig. A.2-1) and has the dimensions shown in figure A.2-2. The mass properties of LM-3 at launch and at separation of the ascent and descent stages are listed in section A.5. The various vehicle systems are described in the following paragraphs.

## A.2.1 Structures and Mechanical Systems

Ascent stage.- The ascent stage structure (fig. A.2-3) consisted of a crew compartment, a midsection, an aft equipment bay, tanks, and equipment mountings.

Crew compartment: The crew compartment was a cylindrical structural shell 92 inches in diameter, of semimonocoque construction, and composed of aluminum alloy chemically milled skins and machined longerons. The front face assembly incorporated two triangular windows and the egress/ingress hatch. Two structural beams extending up the forward side supported the structural loads applied to the cabin.

Midsection: The midsection structure consisted of a ring-stiffened semimonocoque shell constructed similar to the crew compartment. The lower deck provided the structural support for the ascent engine and the upper deck provided support for the docking tunnel and docking hatch. A drogue was provided in the tunnel to accommodate docking with the command module. The midsection also contained the ascent engine and the propellant storage tanks.

Aft equipment bay: The main supporting structure of the aft equipment bay consisted of tubular truss members fastened to the minus Z27 bulkhead. The vertical box beams of the equipment rack assembly contained integral coldplates for cooling electronic equipment.

Thermal shield support: Aluminized Kapton and Mylar thermal blankets formed into various sizes and shapes were secured to standoffs on the outer surface of the structure. In the midsection and aft equipment bay areas, where the thermal shield could not be attached directly to the primary structure, aluminum tubular framework was installed. The thermal shield was attached to this framework by standoffs similar to those in the crew compartment. The base heat shield protected the entire bottom of the ascent stage from the staging pressures and temperatures.

Descent stage.- The descent stage primary structure (fig. A.2-4) was aluminum alloy and was composed of chemically milled webs, extruded and milled stiffeners, and capstrips. The structure consisted of two pairs of parallel beams arranged in a cruciform, with structural upper and lower decks. The ends of the beams were closed off by bulkheads. The outrigger truss assemblies consisted of aluminum alloy tubing and were attached at the ends of each pair of beams. The five compartments formed by the descent stage basic beam assemblies housed the major components of the descent propulsion system. The base heat shield protected the entire bottom of the descent stage from the temperatures experienced during the descent engine firings.

Landing gear.- The landing gear is of the cantilever type (see fig. A.2-5); it consists of four leg assemblies connected to outriggers that extend from the ends of the descent stage structural beams. The legs extend from the front (+Z), rear and both sides of the lunar module. Each leg assembly consists of a primary strut, a footpad, two secondary struts, an uplock assembly, two deployment and downlock mechanisms, a truss assembly, and a lunar-surface sensing probe. A ladder is affixed to the forward leg assembly.

#### A.2.2 Thermal Control

Except for the electronics equipment, thermal control was provided by a passive system consisting of propellants, structures, insulation, and thermal control coatings. Thermal control of the electronic equipment was provided by coldplates, a part of the environmental control system. The large thermal mass of the propellants and structure was enclosed by multilayer radiation superinsulation to reduce the heat loss. This superinsulation was a composite of 30 layers of 0.5-mil aluminized Kapton (H-film) sheets on the ascent stage and a composite of 16 and 11 layers of aluminized Kapton and aluminized Mylar, respectively, on the descent stage (except where ascent plume protection was required). Additional thermal shielding was located outboard of the insulation on both stages and provided protection from micrometeoroids and from reaction control thruster plume impingement.

The ascent stage thermal shielding consisted of aluminum panels varying in thickness from 0.004 to 0.032 inch plus added localized external layers of nickel foil/Inconel mesh insulation, depending on the calculated local heating rates for lunar module and service module reaction control system plume impingement. The descent stage thermal shielding consisted of localized panels made up of alternate layers of nickel foil and Inconel mesh (separator) and an outer sheet of 1.25-mil Inconel; all external to the basic 27-layer blanket. These panels provided a high-temperature radiative barrier, whereas the aluminum panels on the ascent stage absorbed the heat of maximum engine firing conditions.

Thermal control coatings were painted on the exterior of the thermal shielding and on externally exposed structure to maintain vehicle temperatures.

Thermal protection was also provided on the exterior bottom of the ascent stage and the upper exterior surface of the descent stage for protection during an ascent stage engine firing. This protection consists of the 25-layer radiation superinsulation and several outboard layers of 0.5-mil aluminized Kapton plus two outer layers of 5-mil aluminized Kapton.

The base heat shield thermally insulated the bottom of the descent stage during engine firings and thermal soak back. This insulation is a composite of alternate layers of nickel foil and Fiberfrax. In the area of the descent stage tank bays, 2 layers of 5-mil H-film were added and 15 layers of H-film were substituted for Mylar.

### A.2.3 Pyrotechnics

The two independent pyrotechnic electrical systems, A and B, were mutually redundant. Each system (fig. A.2-6) consisted of the following:

- a. Four explosive bolts and four explosive nuts for separating the ascent and the descent stage structures
- b. Three circuit interrupters for deadfacing electrical circuits prior to staging
- c. An umbilical guillotine for severing the ascent/descent stage umbilical
- d. Pyrotechnic valves for pressurizing propellants in the reaction control, ascent and descent propulsion systems; for isolating the helium from propellants in the ascent and descent propulsion systems; and for dumping fuel in the descent propulsion system (The control power for the reaction control A system was from the Commander's bus and for the B system was from the Lunar Module Pilot's bus. Firing power for the pyrotechnic devices was supplied by a separate pyrotechnic battery for each system).
- e. A landing gear uplock and cutter assembly for deploying each of the landing gear legs.

Separation of the spacecraft /launch-vehicle adapter from the lunar module was initiated by signals from the command module through lunar module wiring to the adapter.

#### A.2.4 Electrical Power

The electrical power system consisted of the following components.

Descent stage batteries.- Four silver-zinc batteries (400 amp-hr, 28 V dc) supplied power to the descent stage dc buses. The initial high-voltage of a fully charged battery required taps at the output of 17 and 20 cells to maintain the bus voltage within specification limits, depending on the discharge state of the batteries.

Ascent stage batteries.- Two silver-zinc batteries (310 amp-hr, 28 V dc) supplied power to the ascent stage dc buses and were used in parallel with the descent stage batteries during all undocked descent propulsion maneuvers.

Electrical control assembly.- Electrical control assemblies (two in ascent stage and two in descent stage) provided protection and control of the batteries. In the event of an overcurrent (200 amps) a current-sensing system within the control assemblies would have automatically disconnected the affected battery. Reverse current greater than 10 amperes, for more than 6 seconds, would have been indicated by the current sensing devices through PCM data. In the ascent stage, two contactors allowed selection of either battery to feed either or both of the dc buses. With the batteries selected in the normal position (for example, control assemblies 3 and 4 on figure A.2-7), overcurrent protection would be provided.

Relay junction box.- External and internal power control was provided by the relay junction box. At staging, this junction box and the deadface relays deadfaced the main power cables between the ascent and descent stages. Before launch, the launch umbilical tower latching relay, controlled from the ground support equipment, connected external power to the lunar module electrical loads.

DC buses.- The two dc buses were connected electrically by the cross-tie wire system and circuit breakers.

Inverters.- The 400-Hz 117 V ac power was supplied from one of two solid-state 350 V-amp inverters (fig. A.2-8).

Power transfer provisions.- When the two spacecraft were docked, power from the command and service modules could be provided to the lunar module for the guidance and control system gyro heaters, and radar antenna heaters, and the abort guidance system gyro heaters.

## A.2.5 Instrumentation

Operational instrumentation.- The operational instrumentation system (fig. A.2-9) consisted of sensors, a signal conditioning electronics assembly, a caution and warning electronics assembly, a pulse code modulation and timing electronics assembly and a data storage electronics assembly (voice tape recorder) (fig. A.2-10).

Signal conditioning.- Electrical output signals from select instrumentation sensors were conditioned to the proper voltage and impedance levels within the signal conditioning electronics assembly. Other signals were preconditioned and not processed by the signal conditioning electronics assembly, and these, together with event information in the form of bilevel inputs, were routed to the pulse-code-modulation and timing electronics assembly. Signals from critical parameters were also routed to the logic elements of the caution and warning electronics assembly, which in turn controlled displays and warning lights.

Pulse code modulation and timing.- The pulse-code-modulation and timing electronics assembly sampled the incoming analog and bilevel information according to a pre-programmed matrix. The individual sampling rates were determined by the frequency response of the parameter being measured and intelligence desired. An analog-to-digital converter translated signal voltages into eight-bit words which gave a resolution of one part in 254. Bilevel inputs, such as an "on" or an "off" event, were converted to a bit state (one or zero) in the digital multiplexer section. Eight events could be represented in an eight-bit word. Each frame contained 128 eight-bit words, and 50 frames of PCM data were transmitted per second. Synchronization and timing signals to other spacecraft systems and a serial time code for mission elapsed time were also generated within the assembly. The words representing the converted analog signals, event functions, and time were stored in the output registers and were read-out serially into the bit stream. The bit stream modulated both the S-band and the VHF telemetry transmitters.

Data storage.- The data storage electronics assembly was a single speed, four-track, magnetic tape recorder used to record crew communications simultaneously with mission time to provide a time reference during playback.

Development flight instrumentation.- The development flight instrumentation (figs. A.2-11 through A.2-13) supplemented the operational instrumentation in certain areas. There were three distinct operational phases for the development flight instrumentation: from lift-off to first intravehicular transfer, from transfer to ascent/descent stage separation, and from staging to the conclusion of lunar module operations. All instrumentation switching was effected manually except that a timer was used to terminate development flight instrumentation 3 minutes after lift-off.

Five development flight instrumentation measurements were commutated into the operational PCM system. Eight operational measurements were transmitted both by the FM/FM link and by the operational PCM.

The FM composite outputs from modulation packages were routed to 10-watt VHF FM transmitters. A fifth VHF transmitter was used to transmit the operational PCM signals simultaneously with PCM signals on S-band. The RF transmitter outputs were routed to the UHF/VHF scimitar antenna (fig. A.2-11). Launch phase measurement signals were transmitted through two scimitar antennas mounted on the adapter.

#### A.2.6 Communications

The communications systems (fig. A.2-14) provided the necessary RF links between the lunar module and the Manned Space Flight Network, the command module, and the extravehicular crewman.

The communications systems included all S-band, VHF, and signal-processing equipment necessary to transmit and receive voice and tracking and ranging data and to transmit telemetry, television, and emergency keying. Voice communications between the lunar module and the network were provided by both the S-band and VHF transceivers and between the lunar module and the command module and extravehicular crewman by the VHF transceivers. Telemetry, ranging, and tracking data were transmitted to the network through the S-band equipment. Also included for Apollo 9 was a UHF command system to receive signals in a modulated serial digital format, and to update the guidance computer. This system also armed the ascent stage engine for a firing to depletion.

Voice operations.- All voice communications, including the relay of command module communications through the lunar module, were controlled from the audio-center of the signal processor. The audio center served as the common acquisition and distribution point for voice signals to the headsets and from the microphones and permitted selection of all modes of operation.

Data operations.- Data were transmitted to the network in PCM and analog form. The PCM data were derived from transducer signals, converted to digital form, and routed serially to the communications system for transmission to either the network or the command module. The PCM data were transmitted through the S-band system at either a high bit rate (51.2 kbps) or a low bit rate (1.6 kbps). When the lunar module was not in communication with the network, the PCM data were transmitted by the 259.7 MHz transmitter at the low-bit rate to the command module and recorded for later retransmission to the Manned Space Flight Network. Analog data from biomedical sensors were also transmitted to the network using the S-band system.

S-band transceiver.- The S-band transceiver had a nominal power output of 0.75 watt and consisted of two identical phase-locked receivers, two phase modulators with driver and multiplier chains, and a frequency modulator. The receivers and phase modulators provided the ranging, voice, emergency-keying, and telemetry transmit/receive functions. The frequency modulator provided for transmission of television signals, telemetry and biomedical data, and voice. The operating frequencies of the S-band equipment were 2282.5 MHz (transmit) and 2101.8 MHz (receive).

S-band power amplifier.- When additional transmitting power was required, the S-band output was amplified by the S-band amplifier, which consisted of two selectable amplitrons, each having a power supply and an input/output isolator. When a power amplifier was selected, the S-band transmitter output was amplified to a nominal output power of 18.6 watts through the primary stage or 14.8 watts through the secondary stage.

Very high frequency transceiver.- The VHF transceiver consisted of two receivers, two transmitters, and a diplexer. One transceiver provided a 296.8-MHz channel (channel A) and the other a 259.7-MHz channel (channel B) for simplex or duplex voice communications. Channel B also transmitted PCM data at the low bit rate and received biomedical data from an extravehicular crewman. The transmitter used a keyed on-off carrier-type amplitude modulation and delivered 3.8 watts average RF power at the diplexer output.

Signal processor assembly.- The signal processor assembly provided the interface between the various communications electronics and processed all voice and biomedical signals. This assembly consisted of an audio center for each of the two crewmen and a premodulation processor. The premodulation processor provided signal modulation, mixing, and switching in accordance with selected modes and permitted a relay of command module transmissions to the network. The pulse code modulation data were routed to a bi-phase modulator in the premodulation processor, which controlled the phase of the 1.024-MHz telemetry subcarrier. Each logic-level change of the PCM data changed the telemetry subcarrier phase by 180 degrees. The 1.024-MHz and 1.25-MHz subcarriers were generated from two 512-kHz clock signals provided by the instrumentation system.

Backup voice transmission was accommodated using the S-band system by routing the low-pass filter output directly to a speech-processing network linked directly to the narrow-band phase modulation input of the S-band equipment. Received voice signals were routed through the premodulation processor to the microphone and headset volume control circuits in the audio centers. The VHF channel B input had high- and low-pass filters to separate voice and extravehicular mobility unit data.

The premodulation processor accepted hardline biomedical data from each crewman and, by external control, selected either of these sources

for S-band transmission. The phase modulation (PM) mixing network processed the outputs of the 1.024- and 1.25-MHz channels (a composite of voice, biomedical data, telemetry data, and extravehicular mobility unit data). These outputs were then supplied to the selected S-band phase modulator for transmission to the network. The frequency modulation mixing network processed the outputs of the 1.024-MHz data channel and a composite of voice and biomedical and extravehicular-unit data, all on the 1.25-MHz subcarrier. These outputs were then supplied to the S-band frequency modulator for transmission. FM video, PM ranging, backup voice, and emergency key signals were not processed through the mixing networks but were supplied directly to the selected modulator for base-band modulation.

Audio centers.- Two identical audio centers, one for each crewman provided individual selection, isolation, and amplification of audio signals received and transmitted by the communications system. Each audio center contained a microphone amplifier, headset amplifier, voice circuit, diode switches, volume control circuits, and isolation pads. Audio signals were routed to and from the VHF-A, VHF-B, and S-band systems and the intercommunications bus through the audio centers. The intercommunications bus, common to both audio centers, provided hardline communications between the astronauts.

Antenna equipment.- The antenna equipment consisted of two S-band inflight antennas, an S-band steerable antenna, and two VHF antennas (fig. A.2-15). The S-band inflight antennas, one forward and one aft, were omnidirectional and together covered 90 percent of the directional sphere. The S-band steerable antenna was a 26-inch-diameter parabolic reflector with a point source feed that consisted of a pair of cross-sleeved dipoles over a ground plane. This antenna, operated either manually or automatically, provided for coverage of 150 degrees in azimuth and 330 degrees in elevation. Once the antenna was positioned manually within the capture cone, it could be operated in the automatic mode. The VHF antennas, one on each side of the lunar module top structure, operated in the 259.7- to 296.8-MHz range.

Space-suit communications.- The space-suit communications were used to transmit and receive voice communications and to transmit biomedical and extravehicular mobility unit data during extravehicular activity. This communications system was an integral part of the portable life support system worn by the extravehicular crewman. The system transmitted on 259.7 MHz for relay to the network through the lunar module, and the received frequency was 296.8 MHz. The telemetry data transmitted by this system included suit pressure, oxygen supply quantity, suit water temperature, suit-water inlet and outlet temperature difference, sublimator water pressure, battery current and voltage, and crewman's electrocardiogram.

Television.- The television system was of a different design than used on the two previous missions. The camera was of the lunar mission configuration, with an 80-degree wide-angle lens and a 35-degree lunar-day lens. Depth of focus for the wide angle lens was from 20 inches to infinity and for the lunar-day lens from 11 feet to infinity. The camera had a 10-frame/sec scanning mode, similar to the Apollo 7 and 8 camera configuration, and a low-scan mode of 0.628 frame/sec. The camera could televise scenes of low-light intensity.

#### A.2.7 Radar Systems

The lunar module radar system consisted of two separate units, one for landing and one for rendezvous operations.

Landing radar.- The landing radar consisted of the antenna and electronics assemblies, (fig. A.2-16). The lunar mission design was modified for Apollo 9 as follows: tracker lock-on discrete links were severed and the signals simulated; the frequency deviation control line was severed; the altitude scale-factor line was severed; the blanking signal line from the frequency modulator to the RF tracker was severed; and the inputs to the three velocity computers were wired so that only one frequency tracker would be accepted. Also for Apollo 9, two of the velocity beam channels and the altimeter beam channel were to be monitored and both antenna positions exercised to determine whether spurious signals were rejected.

Rendezvous radar.- The rendezvous radar consisted of antenna and electronics assemblies (fig. A.2-16) and was locked coherently to the transponder mounted on the command and service modules (fig. A.2-16(c)). The rendezvous radar, when operated in the various modes, provided angle, digital range, digital range-rate, and line-of-site angular-rate information. This information was supplied to the primary and abort guidance computers as well as to the display panel.

#### A.2.8 Displays and Controls

The display panels provided the switches, meters, circuit breakers, dials, and indicators through which the crew controlled the spacecraft and monitored its performance. All controls were designed to be operated by crewmen while wearing gloves and were of four basic types: toggle switches, rotary switches, potentiometers, and push-button switches. Critical switches had guards incorporated to avoid inadvertent actuation.

All displays were designed for easy identification and readability and consisted of five basic types: analog meters, digital meters, tape meters, event indicators, and indicating lights. The indicating lights were part of the caution and warning system to signal malfunctions or

out-of-tolerance conditions. Displays which indicated mission and event time were included. The time displays could be reset, stopped, and any digit could be changed at will.

Lighting was provided by exterior and interior lights. The external lighting included a tracking light, five docking lights, and a self-illuminating docking target. Interior lighting consisted of integral panel and display lights, backup floodlights, electroluminescent lights, and general ambient lighting to illuminate the cabin and the controls and displays.

#### A.2.9 Guidance and Control

The guidance and control systems (fig. A.2-17) consisted of a primary guidance and navigation system, an abort guidance system, and a control electronics section.

Primary guidance and navigation.- The primary guidance, navigation and control system consists of the sensing, data processing, computational, control, and display devices necessary to accomplish spacecraft navigation and guidance. The system's primary task is to obtain lunar module orientation, position, and velocity data; and thereby, calculate any steering and thrust commands necessary to fulfill the lunar module flight objectives.

The system's navigation function consists of determining the location of the lunar module and calculating pertinent trajectory information related to the present location and predicted locations so that the guidance function can be performed.

The guidance function interrelates the navigation function to the flight control function. Navigation information is employed to determine what commands should be issued to maintain desired flight control. A velocity to be gained concept results from a comparison of the actual velocity and the velocity required. Steering equations are used which force the difference between the actual velocity and the velocity to be gained to zero by issuing the appropriate commands to the flight control subsystems. In addition, a fully manual piloting task is available by the crew's use of navigational displays.

The functional subsystems contained within the primary guidance, navigation and control system are the inertial subsystem, optical subsystem, and computer subsystem.

The inertial subsystem senses lunar module acceleration and changes in attitude and provides incremental velocity and attitude data to the computer subsystem. The inertial subsystem sensor is the inertial

measurement unit which consists of a stable member mounted in a three-degree-of-freedom gimbal system. Three gyroscopes and three accelerometers are mounted on the stable member. Each gyroscope has a stabilization loop associated with it for maintaining the stable member nonrotating with respect to inertial space. Thus, each stabilization loop maintains one axis of an orthogonal reference system; whereby, the spacecraft yaw, pitch, and roll orientation is definable. The lunar module orientation is measured by the stabilization loops producing signals proportional to the changing orientation of the gimbals relative to the stable member. The three accelerometers are pendulous mass unbalance devices with each maintaining one axis of another orthogonal system parallel to the gyro orthogonal system. Hence, each accelerometer and its associated accelerometer loop permits measurement of changes in velocity along its axis relative to the inertial reference frame.

The optical subsystem provides directional data of a selected target to the lunar module guidance computer. Consisting of the alignment optical telescope, its primary function is to provide star sighting data for insertion into the computer system to establish an accurate reference frame for inertial measurement unit alignment.

The computer subsystem performs data processing, storing and monitoring; maintains a time standard; performs computational programs; provides central control ability; and performs limited malfunction diagnosis. The subsystem consists of the lunar module guidance computer and the display and keyboard.

The display and keyboard is the interface device between the crewman and the lunar module guidance computer. It permits the crewman to enter data into the computer and to receive data from the computer.

The lunar module guidance computer processes data from the other lunar module subsystems and from the crew to solve navigation and guidance equations. The computer performs a control function by issuing command pulses to the inertial subsystem, radar subsystems, and flight control subsystems. Malfunction diagnosis is performed by monitoring certain operational discrettes and issuing appropriate discrettes to the caution/warning subsystem when an irregularity occurs. The computer also supplies timing signals to synchronize and control primary guidance, navigation and control system operations.

Coupling data unit.- The coupling data unit converts angular data and transfers the data between major assemblies of the guidance and control system. The coupling data unit contains the following five channels for processing these data.

- a. One channel for the rendezvous radar
- b. One channel for the rendezvous radar trunnion axis
- c. One channel for each of the three gimbal axes of the inertial measurement unit.

The two channels used with the rendezvous radar provide interfaces between the antenna and the lunar module guidance computer. The computer calculates digital antenna position commands before acquisition of the command and service modules. These signals are converted to analog form by the coupling data unit and applied to the antenna drive mechanism to aim the antenna toward the command and service modules. Tracking-angle information is converted to digital form by the coupling data unit and applied to the computer.

The three coupling data unit channels used with the inertial measurement unit provide interfaces between this unit and the computer, and between the computer and the abort guidance system. Each inertial measurement unit gimbal angle transmitter resolver provides its channel with analog gimbal-angle signals that represent lunar module attitude. The coupling data unit converts these signals to digital form and supplies them to the computer. The computer uses these signals to calculate attitude or translation commands and routes the commands, through the control electronics section, to the proper engine. The coupling data unit converts the steering-error signals to 800-Hz analog signals and applies them to the flight director attitude indicator. Inertial measurement unit coarse and fine alignment commands generated by the computer are coupled to the inertial measurement unit through the coupling data unit.

The pulse torque assembly supplies input to, and processes outputs from, the inertial components in the inertial measurement unit. The pulse torque assembly contains all the pulse-torquing electronics for the accelerometers and gyros.

The power and servo assembly contains electronic equipment in support of the primary guidance and navigation, power supplies for the generation of internal power required by the primary guidance and navigation system, servo-mechanisms for the ground support equipment, and inertial subsystem moding logic used during inertial measurement unit operate turn-on.

Abort guidance.- The abort guidance system was a strapped-down inertial system with the inertial sensors rigidly mounted with respect to the vehicle, rather than mounted on a stabilized platform. The abort guidance provides independent backup for the primary guidance. If a mission must be aborted, and the primary system is not functioning properly, abort guidance is used to control the lunar module.

The abort guidance system is used to determine the lunar module trajectory required for a coelliptic rendezvous sequence to establish a safe parking orbit. It controls attitude, navigation, and guidance. Rendezvous from the abort point can be accomplished automatically under abort guidance control, or by the flight crew using displayed data. When the abort guidance system is used, the control electronics section functions as an autopilot and uses abort guidance input signals and manual control signals to control vehicle attitude and translation.

Control electronics.- The control electronics section controls vehicle attitude and translation about, and along, the three orthogonal axes. The control electronics processes and routes command signals to fire the 16 thrusters of the reaction control system. The attitude and translation control signals originate either automatically from primary or abort guidance or are manually provided by the flight crew. The control electronics also processes on and off commands for the ascent and the descent engines and controls the direction of the descent engine thrust vector.

#### A.2.10 Reaction Control

The reaction control system (fig. A.2-18) was composed of two parallel, independent systems, system A and system B. Each system contained identical components with the associated valves and plumbing necessary to deliver and control the propellants to the reaction control engines. Normally both systems were operated together. The arrangement of the engines was such that rotational control in all axes was provided when either system was deactivated.

All pressurization (helium) components, propellant tanks, main shutoff valves, and propellant-servicing quick-disconnect couplings were arranged into an independent module for each system. Sixteen identical 100-pound thrust engine assemblies (thrusters) were arranged in clusters of four and mounted on four equally spaced outriggers around the ascent stage. System A and system B each included an oxidizer tank having a capacity of 206 pounds nitrogen tetroxide and a fuel tank having a capacity of 103 pounds of Aerozine 50.

Fuel and oxidizer are loaded into bladders within the propellant tanks and into the manifold plumbing that extends from the tanks through the normally open main shutoff valves and the normally open cluster isolation valves leading to the thruster pairs. Before separation of the lunar module from the command and service modules, the thrusters are heated to their operating temperature, and the helium isolation squib valves are fired. Gaseous helium, reduced to a working pressure, enters the propellant tanks and forces the fuel and oxidizer to the thrusters. The propellants are blocked at the thruster by normally closed fuel and oxidizer

valve assemblies which are actuated by a thruster-on command. As the valve assemblies open, the propellants are routed through the thruster injector into the combustion chamber, where they impinge and ignite. A malfunction in the system can be isolated and the affected thrusters made inoperative by manually closing cabin switches. Each switch is connected to a fuel and an oxidizer valve so that each propellant supply is shut off simultaneously.

#### A.2.11 Descent Propulsion

The descent propulsion system (fig. A.2-19) consisted of a liquid-propellant rocket engine, two fuel tanks, two oxidizer tanks, and the associated propellant pressurization and feed components. The engine was throttleable between thrust levels of 1050 and 10 500 pounds. The engine was mounted in the center compartment of the descent stage through a gimbal ring arrangement which allowed gimbaling within  $\pm 6$  degrees to provide trim in pitch and roll.

Pressurization.- The propellant tanks were pressurized by helium stored supercritically in a cryogenic vessel. Squib valves isolated the supercritical helium supply until the initial engine start. After activation of the valves, the supercritical helium passed through the first loop of a two-pass fuel/helium heat exchanger located in the engine fuel feed line. The warmed helium was routed back through a heat exchanger inside the cryogenic vessel where heat was transferred to the supercritical helium remaining in the vessel, thereby maintaining the pressure. The helium was then routed through the second loop of the fuel/helium heat exchanger before passing to a regulator which reduced the pressure to a suitable level, approximately 235 psi, for introducing into the tanks.

The descent propulsion system also had an ambient helium tank containing approximately 1 pound of usable helium to pre-pressurize the propellant.

The supercritical helium tank squib valve was fired 1.3 seconds after engine start. This delay, in conjunction with the pre-pressurization, established fuel flow through the heat exchangers prior to helium flow and prevented fuel freezing. A pressure relief valve in each helium supply line prevented tank over-pressurization; a burst disk upstream of each relief valve prevented helium leakage during normal operation.

Propellants and feed.- The descent engine used hypergolic propellants. The fuel was a mixture of 50 percent hydrazine and 50 percent unsymmetrical dimethylhydrazine, and the oxidizer was nitrogen tetroxide. Each pair of oxidizer tanks and each pair of fuel tanks were manifolded into a common discharge line. Total propellant capacity was 17 800 pounds.

The propellant tanks were interconnected by a double crossfeed piping arrangement to maintain positive pressure balance across the helium and the propellant portions of the tanks. A capacitance- and resistance-type quantity gaging system and low level sensors provided propellant quantity information during thrusting.

The fuel and oxidizer were piped directly into the flow control valves and then into a series-parallel ball valve assembly controlled by four actuators. After ENGINE ARM had energized the solenoid-operated pilot valves, fuel was introduced into the valve actuators and caused the ball valves to open, allowing propellant flow to the injector. For engine shutdown, the solenoid-operated pilot valves were de-energized, the spring-loaded actuators closed the ball valves, and residual fuel from the actuator cavities was vented overboard.

Engine.- Engine controls, mounted integral to the injector end, included a gimbal ring, a variable-area injector, flow control and shutoff valves, and a throttle actuator. The thrust chamber consisted of a composite ablative-cooled nozzle (area ratio 16:1) and a crushable radiation-cooled nozzle extension (area ratio 49:1). The ablative components were encased in a titanium shell and jacketed in a stainless steel foil and glass wool composite thermal blanket.

The mechanical throttling scheme utilized variable-area, cavitating-venturi, flow-control valves mechanically linked to a variable-area injector. This scheme permitted separation of the propellant flow control and propellant injection functions so that each could be optimized without compromising the other. Two separate flow-control valves metered the fuel and oxidizer simultaneously. The throttling was controlled by an electrical linear servo actuator powered by three mutually redundant dc motors. Throttling between 10 and 60 percent was achieved through hydraulic decoupling; movement of the pintle would reduce the venturi exit pressure to the vapor pressure of the propellant, inducing cavitation. The valves then functioned as cavitating venturis, and downstream pressure fluctuations did not affect the flow rates.

The injector consisted of a faceplate and fuel manifold assembly with a coaxial feed tube and a movable metering sleeve. Oxidizer entered through the center tube and exited between a fixed pintle and the bottom edge of the sleeve. Fuel was introduced into an outer race, and the fuel aperture was an annular opening between the side contour and the injector face. As the metering sleeve moved, both propellant apertures changed in area and maintained close-to-optimum injection conditions at any thrust level.

A lunar-configuration dump system was added and consisted of a squib and solenoid valve in series but arranged in parallel with the propellant tank relief valves. This system is employed in both the fuel and oxidizer tanks so that, on the lunar surface, the tanks can be relieved from the pressure increase caused by thermal soakback.

#### A.2.12 Ascent Propulsion

The ascent propulsion system (fig. A.2-20) consisted of a restartable pressure-fed liquid propellant rocket engine and a propellant and pressurization storage system. The ascent engine was fixed-mounted and developed a constant thrust of 3500 pounds.

Propellant and feed.- The engine used hypergolic propellants. The fuel was a mixture of 50 percent hydrazine and 50 percent unsymmetrical dimethylhydrazine, and the oxidizer was nitrogen tetroxide. Propellant flow to the engine was controlled by an injector, two trim orifices, four electromechanical flow control actuators, and eight propellant shutoff valves. The valve package assembly consisted of eight shutoff valves, which were series-parallel redundant, in both the fuel and oxidizer feed lines. Each fuel-oxidizer pair was simultaneously opened or closed on a common crankshaft by a hydraulic actuator that used fuel as the actuating medium.

The engine consisted of a structural shell with mounts and ablative material in the thrust chamber and in the nozzle extension for cooling. The ablative material for the combustion chamber and nozzle throat, to the region where the expansion ratio was 4.67, was a refrasil phenolic backed with an insulator of asbestos phenolic. The nozzle utilized high silica modified phenolic for ablative material for the extension from the regions of expansion ratio of 4.6 to 45.6. The combustion chamber and nozzle extension were bonded together and wrapped with fiberglass for structural support. The combustion chamber and throat were encased in an aluminum alloy casing, which served primarily as a mounting surface for engine components.

The injector assembly consisted of propellant inlet lines, a fuel manifold inlet screen, an oxidizer manifold inlet screen, a fuel manifold, an oxidizer manifold, and an injection orifice plate assembly. The injector was a fixed-orifice type with a 1-3/4 inch Y-shaped baffle and acoustic cavities to dampen any induced combustion disturbances. The injector used a pattern of unlike-doublet orifices to obtain a high combustion efficiency with high percentages of axial and canted fuel film cooling flow. The baffle was bipropellant dump cooled and used 45 unlike impinging orifices, 3 oxidizer showerhead orifices at the center, and 6 fuel showerhead (2 at each leg end) orifices.

There were two propellant storage tanks (titanium) for the ascent propulsion system, one for oxidizer and one for fuel. The tanks were spherical and had a combined capacity of approximately 5000 pounds of propellant. Each tank was equipped with a helium diffuser at the inlet to provide even pressurization at the helium/propellant interface. A propellant retention device is located at the tank outlet of each tank. These devices allowed unrestricted propellant flow from the tank to the engine under normal pressurization but would not allow reverse flow of propellant from the outlet line back into the tank under zero g conditions or at the maximum negative g-load expected. The propellant tanks did not have a quantity gaging system but did have low-level sensors to monitor propellant quantities when propellants were depleted to a level equivalent to approximately 10 seconds of firing time.

The outflow from each tank was divided into two paths. The main path passed through a trim orifice and a filter to the engine shutoff valve. The other path led to normally closed solenoid valves interconnecting the ascent and reaction control propellant systems. Opening these valves would permit the use of ascent propellants by the control engines.

Pressurization.- The gaseous helium that was used for pressurization of the propellant feed system was stored in two tanks at approximately 3500 psi and ambient temperature. A normally closed squib valve in the line immediately downstream of each storage tank isolated the helium supply until the initial ascent engine start.

Each parallel helium flow path contained a filter to trap any debris resulting from squib valve actuation. After the filter, each helium flow path contained a normally open latching solenoid valve and two pressure regulators or reducers. The upstream regulators in each flow path were set to a slightly lower pressure than the downstream regulators, and the two series regulators in the primary flow path were set to a slightly lower pressure than their corresponding regulators in the redundant flow path. The pressure settings of the four regulators varied from 172 psi to 194 psi with the primary-path controlling regulator set at approximately 184 psi. In normal operations, the upstream regulator in the primary flow path was the controlling element. Downstream of the pressure reducers, the helium flow paths were manifolded together and then divided into two separate tank pressurization paths, each having a quadruple check valve and two isolation squib valves.

#### A.2.13 Environmental Control System

Atmospheric revitalization section.- The atmosphere revitalization section (fig. A.2-21) consisted of cabin-recirculation and suit-circuit assemblies. The suit circuit assembly consisted of two suit fans, two

water separators, two heat exchangers for cooling and heating, one sublimator used during secondary loop operation, carbon-dioxide and odor removal cartridges, valves for closed- and open-loop operation, and crew isolation valves for low pressure protection. The suit-circuit assembly served as a complete atmosphere revitalization system, in that it removed moisture, carbon dioxide, and noxious odors and provided for heating and cooling. Centrifugal water separators removed excess moisture that normally condenses during the cooling phase of the transfer loop. The cabin recirculation assembly consisted of two fans and a heat exchanger for heating and cooling.

Pressurization.- The oxygen-supply and cabin-pressure-control section (fig. A.2-22) consisted of one descent and two ascent oxygen tanks, two demand regulators, a high-pressure oxygen-control assembly, a portable life support system fill valve, two cabin dump valves, and a cabin pressure switch. This section stored the gaseous oxygen required by the environmental control system and maintained cabin and suit pressurization by supplying oxygen in sufficient quantity to replenish losses from crew metabolic consumption and cabin leakage. This section also provided emergency pressurization in the event of a cabin puncture, protected the cabin against overpressurization, and enabled the crew to intentionally depressurize and repressurize the cabin, as well as provided for oxygen refill of the portable life support system.

Water management.- The water management section (fig. A.2-23) consisted of a water tank in the descent stage and two smaller tanks in the ascent stage, water pressure regulators, and various flow valves. This section stored and distributed the water required for refilling the portable life support system, fire fighting, crew consumption, and evaporative cooling. In addition, this section provided for utilization of the condensed water vapor removed from the suit-circuit assembly.

Thermal control.- The heat transport section (fig. A.2-24) consisted of primary and secondary heat transport loops. The primary loop consisted of two pumps, an accumulator, cold plates, filter, temperature control valves, one sublimator, and one regenerative heat exchanger. The primary loop provided active thermal control for all cold-plated electronic equipment in conjunction with the cooling provided by the cabin and suit ventilating gases. The secondary loop consisted of a pump, filter, accumulator, and sublimator. This loop would have provided thermal control of the electronic equipment necessary for a lunar-module-active rendezvous with the command module, if the primary loop had failed.

#### A.2.14 Crew Provisions

The major crew provisions carried onboard are described in the following paragraphs.

Extravehicular mobility unit.- The extravehicular mobility unit (fig. A.2-25) consisted of a visor, gloves, a portable life support system, a remote control unit, an oxygen purge system, and a pressure garment assembly. The complete extravehicular mobility unit weighed approximately 182 pounds.

Visor.- The extravehicular visor assembly provided visual attenuation and thermal and meteoroid-impact protection during activity outside the spacecraft. This assembly consisted of a polycarbonate shell, polycarbonate plastic visor, and plexiglass visor. The inner visor provided for meteoroid protection, and the outer visor allowed only 10 percent transmittance of infrared rays, 20 percent of light at 4000 to 7000 angstroms, and 0.1 percent of ultraviolet light from 2000 to 3200 angstroms. A soft protective cover was provided to prevent damage to the visor when not in use.

Gloves.- The extravehicular gloves were intravehicular gloves modified with a thermal layer of multilaminate fabric. Additional layers of insulating material covered the palm area. A metal woven fabric, coated with silicone to reduce slippage, was included in the palm area and the inner finger area to provide abrasion resistance. The outer cover, similar to a gauntlet, extended to the forearm to provide thermal protection for the wrist disconnect.

Portable life support.- The portable life support system (see figure A.2-26) contained the expendable materials and the communication and telemetry equipment required for extravehicular operation. The system supplied oxygen to the pressure garment assembly and cooling water to the liquid-cooled garment and removed solid and gas contaminants from returning oxygen. The portable life support system, attached with a harness, was worn on the back of the suited crewman. The total system contained an oxygen ventilating circuit, water feed and liquid transport loops, a primary oxygen supply, a main power supply, communication systems, displays and related sensors, switches, and controls. A cover encompassed the assembled unit and the top portion supported the oxygen purge system.

The remote control unit was a display and control unit chest-mounted for easy access. The controls and displays consisted of a fan switch, pump switch, space-suit communication-mode switch, volume control, oxygen quantity indicator, and oxygen purge system actuator.

The oxygen purge system provided oxygen and pressure control for certain extravehicular emergencies and was mounted on top of the portable life support system. The system was self-contained, independently powered, and nonrechargeable. It was capable of 30 minutes of regulated ( $3.7 \pm 0.3$  psid) oxygen flow at 8 lb/hr to prevent excessive carbon dioxide buildup and to provide limited cooling. The system consisted of

two interconnected spherical 2-pound oxygen bottles, an automatic temperature-control module, a pressure regulator assembly, a battery, oxygen connectors, and the necessary checkout instrumentation. The oxygen purge system provided the hard mount for the VHF antenna.

Crewman restraint.- Each of the two crewman restraint systems consisted of a set of spring-loaded cable and pulley assemblies. The system attached to hard points located at the waist level on the pressure garment assembly and afforded a stable standing position while facing and working at the consoles.

Crewmen optical alignment sight.- The crewman optical alignment sight was a collimator device, similar to an aircraft gunsight, consisting of a lamp with intensity control, reticle, barrel-shaped housing, combiner glass, and a 28-volt dc power receptacle. The sight had two functions, to provide line-of-sight, range, and range-rate information during the docking and to provide a backup alignment for the alignment optical telescope. The alignment sight for the lunar module was different from that of the command module in that the brightness control was rotated 90 degrees around the barrel.

Waste management system.- The waste management system consisted of two small and two large urine collection assemblies, one of which was installed prior to launch while the remaining three were stowed. This system could not be dumped overboard.

Window shades.- Window shades were provided to darken the cabin interior for viewing instruments during direct sun illumination. The shades were made of a flexible material capable of being rolled up and restrained when not in use. When the shades were deployed they were held in place with Velcro strips located along the edges of the windows and shades. The shades were semi-translucent, transmitting less than 10 percent of the incident light.

Beta fabric containers.- Beta fabric containers were used for stowage of miscellaneous crew equipment. The principal stowage areas were on the right- and left-hand sides of the cabin, and an interim stowage area was over the front center console.

Extravehicular waist tethers.- Extravehicular waist tethers were used as required for restraint. In addition, a 25-foot lifeline and equipment assembly was provided for safety purposes during the Apollo 9 extravehicular activity. An additional hook was provided as part of this assembly to facilitate transfer of cameras between the extravehicular crewman and the Command Module Pilot.

Miscellaneous.- In addition to these items, the following crew provisions were included: a metal mirror, an eye patch, an emergency wrench, a canister retrieval bag, a medical package, defecation collection devices, and two types of water dispenser, one capable of fire fighting and the other with a bacteria filter.

NASA-S-69-2119

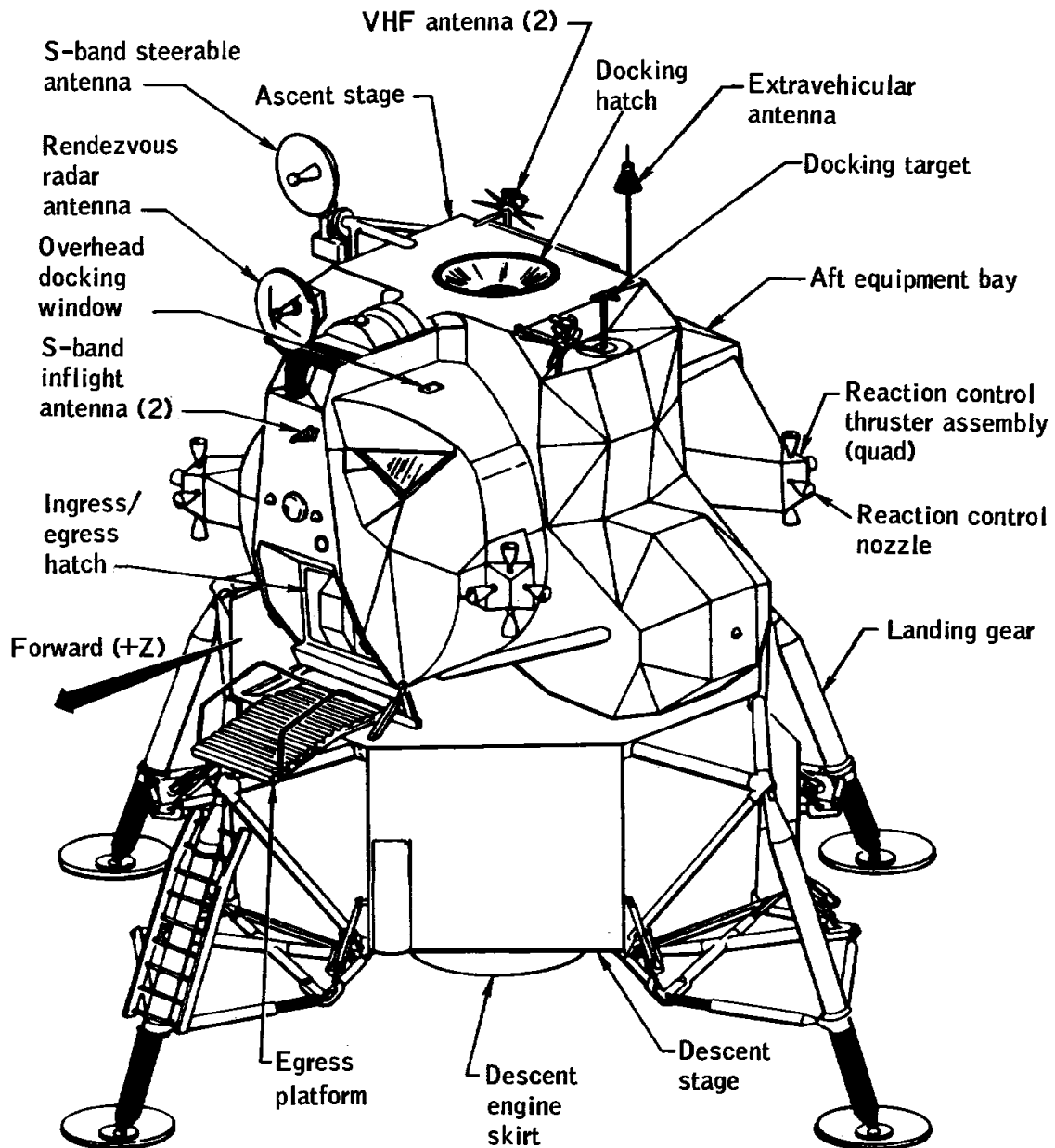


Figure A.2-1.- LM vehicle.

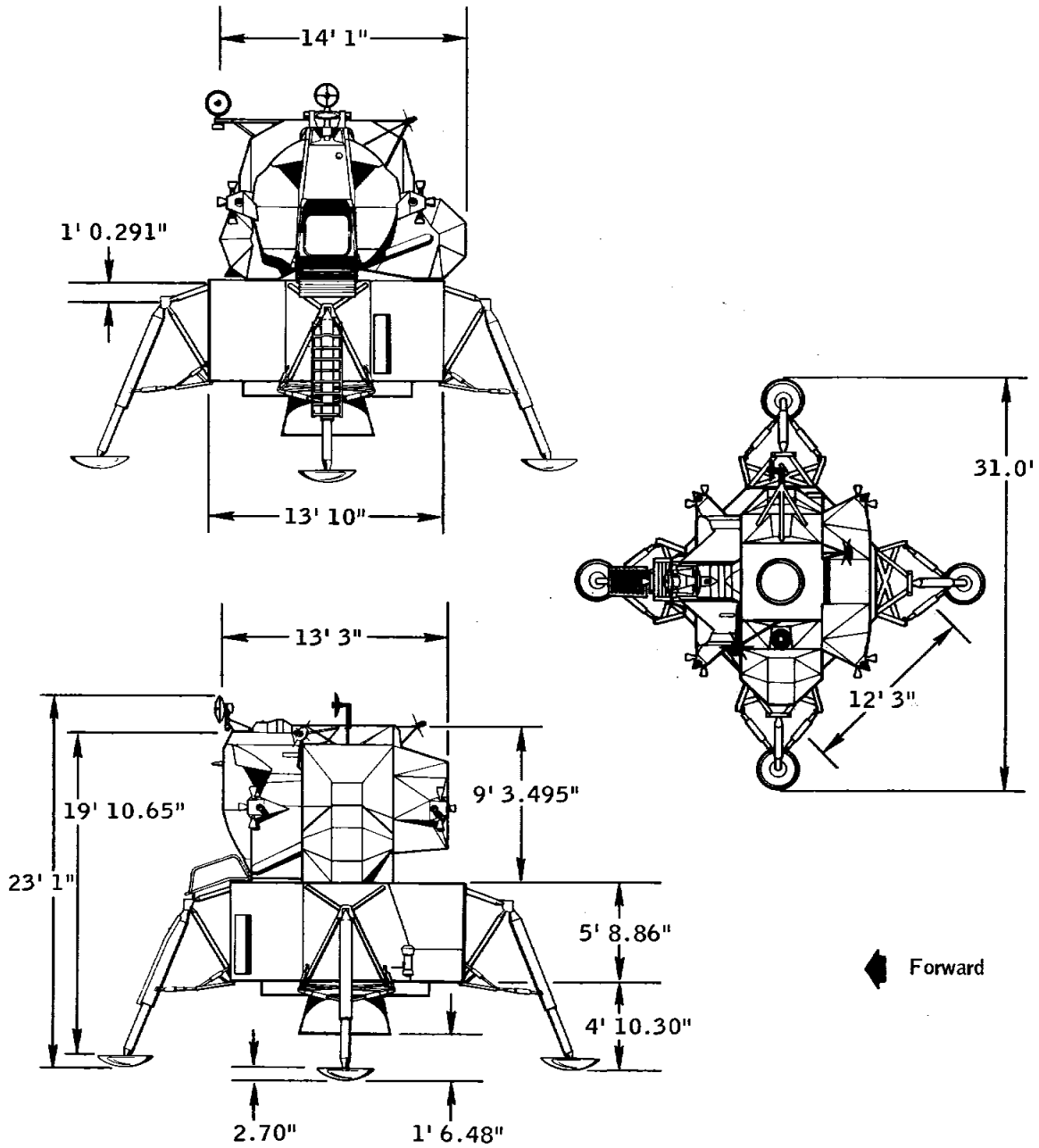


Figure A.2-2.- LM-3 overall dimensions.

NASA-S-69-2121

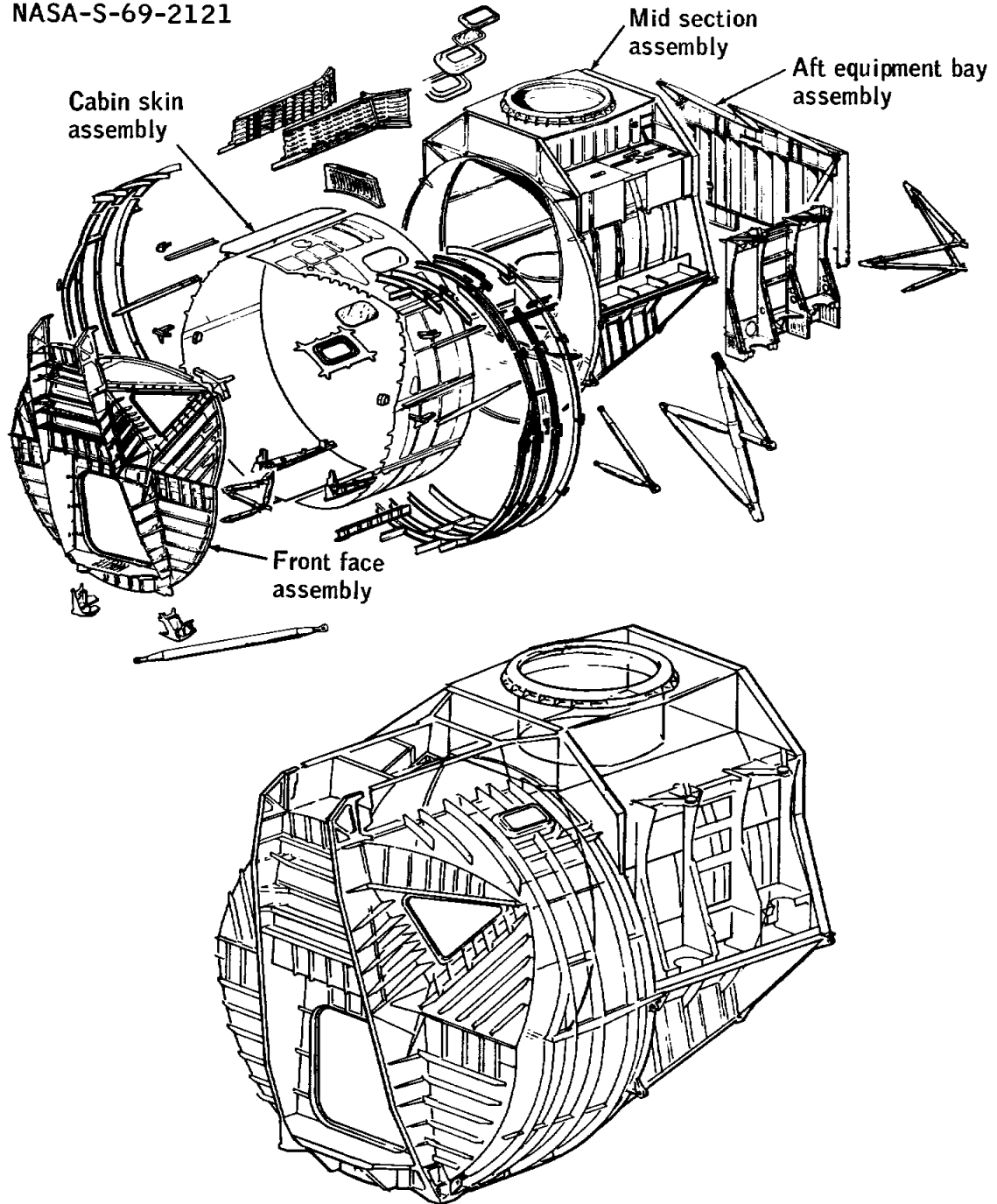


Figure A.2-3.- Ascent stage structure .

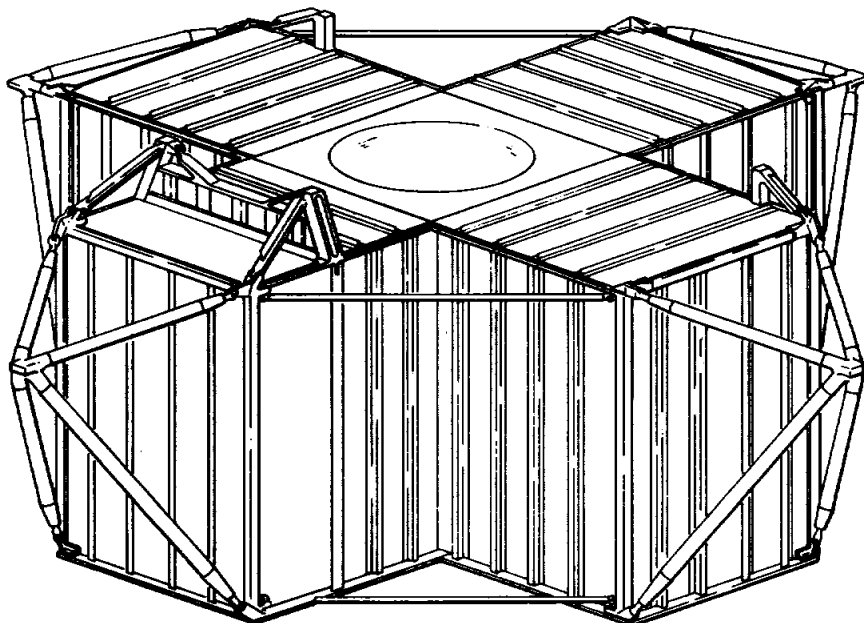
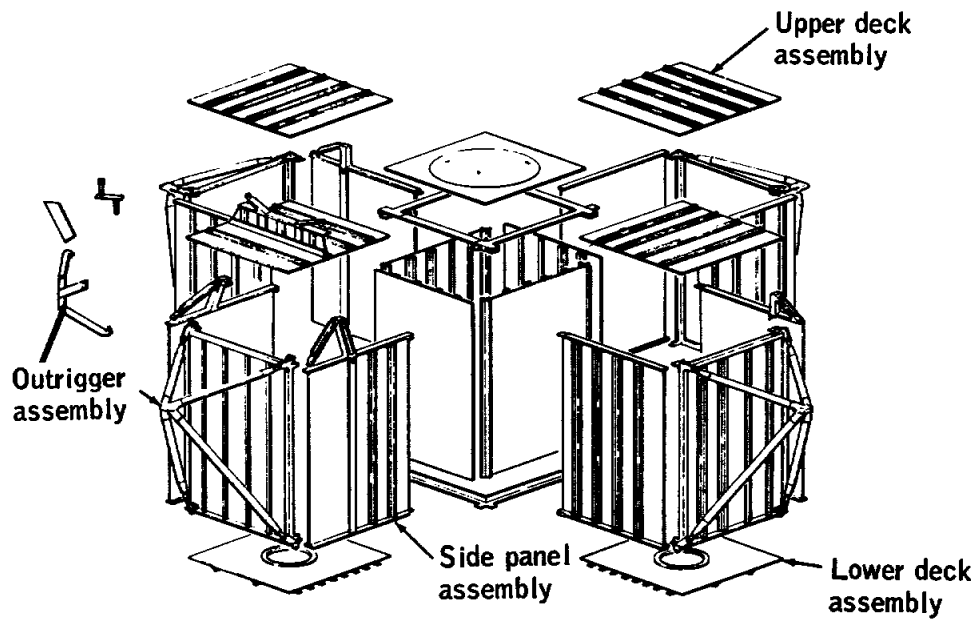


Figure A.2-4.- Descent stage structure.

NASA-S-69-2123

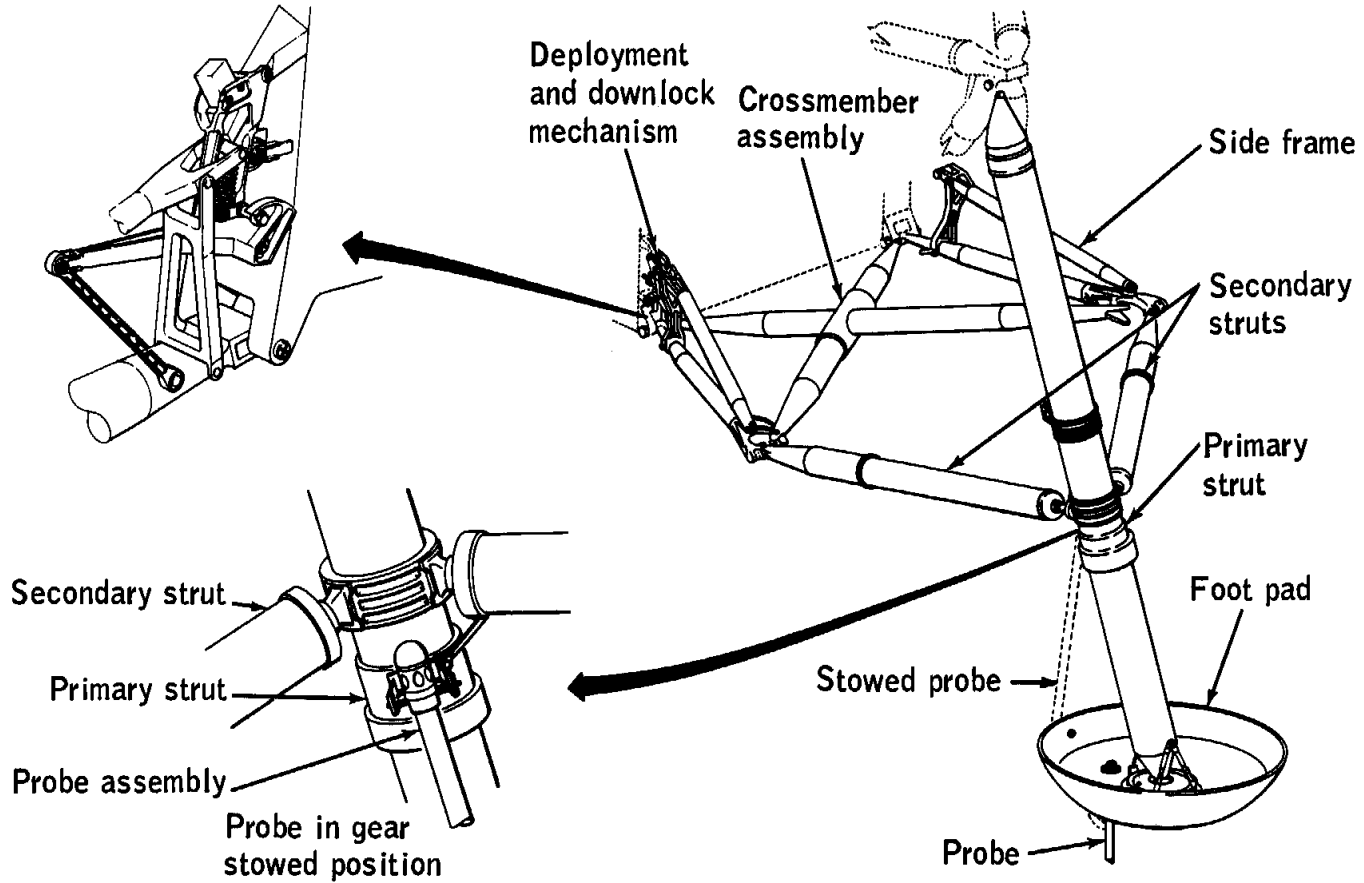


Figure A.2-5.- Landing gear.

NASA-S-69-2124

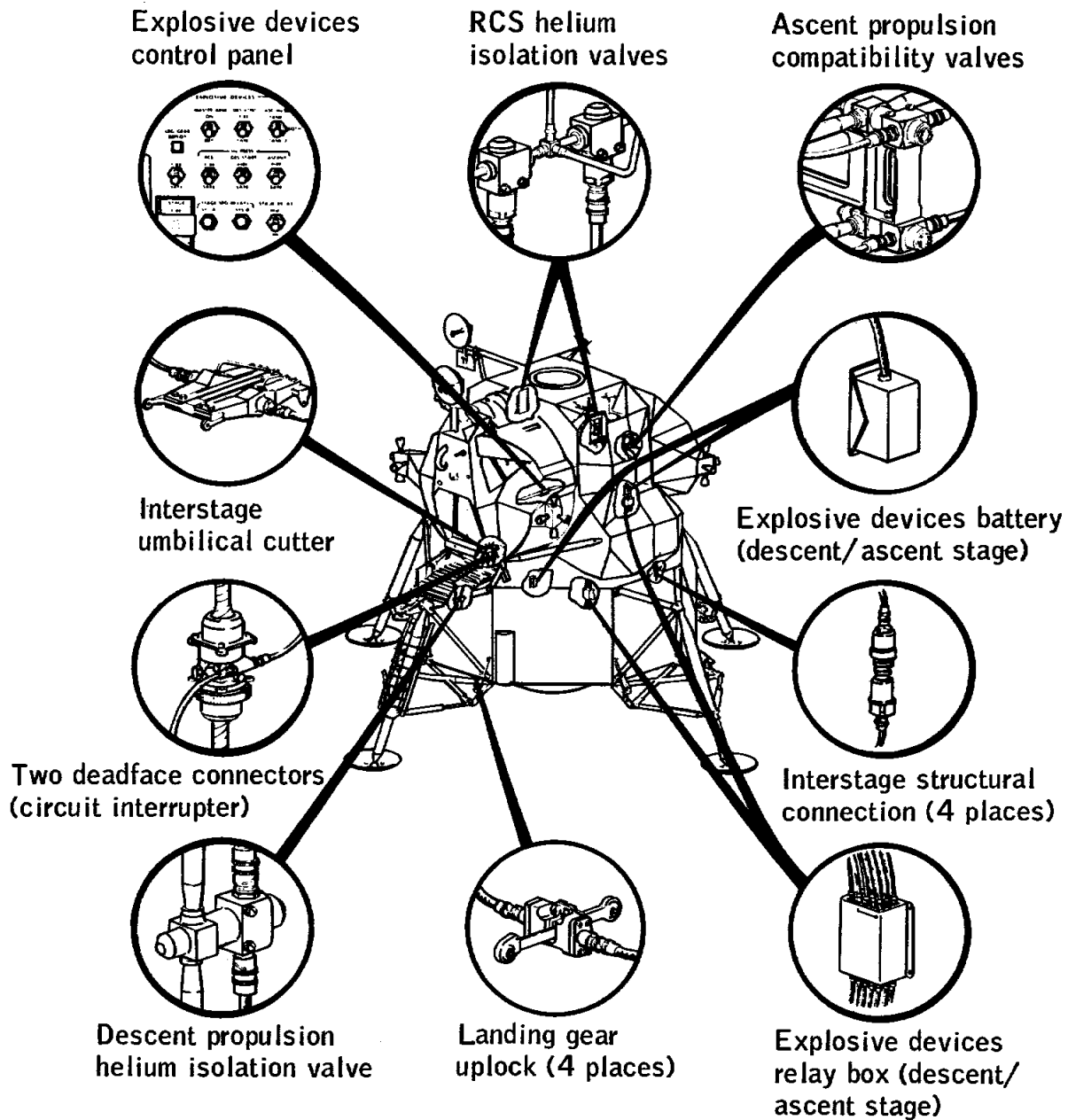


Figure A.2-6.- Explosive devices - component location.

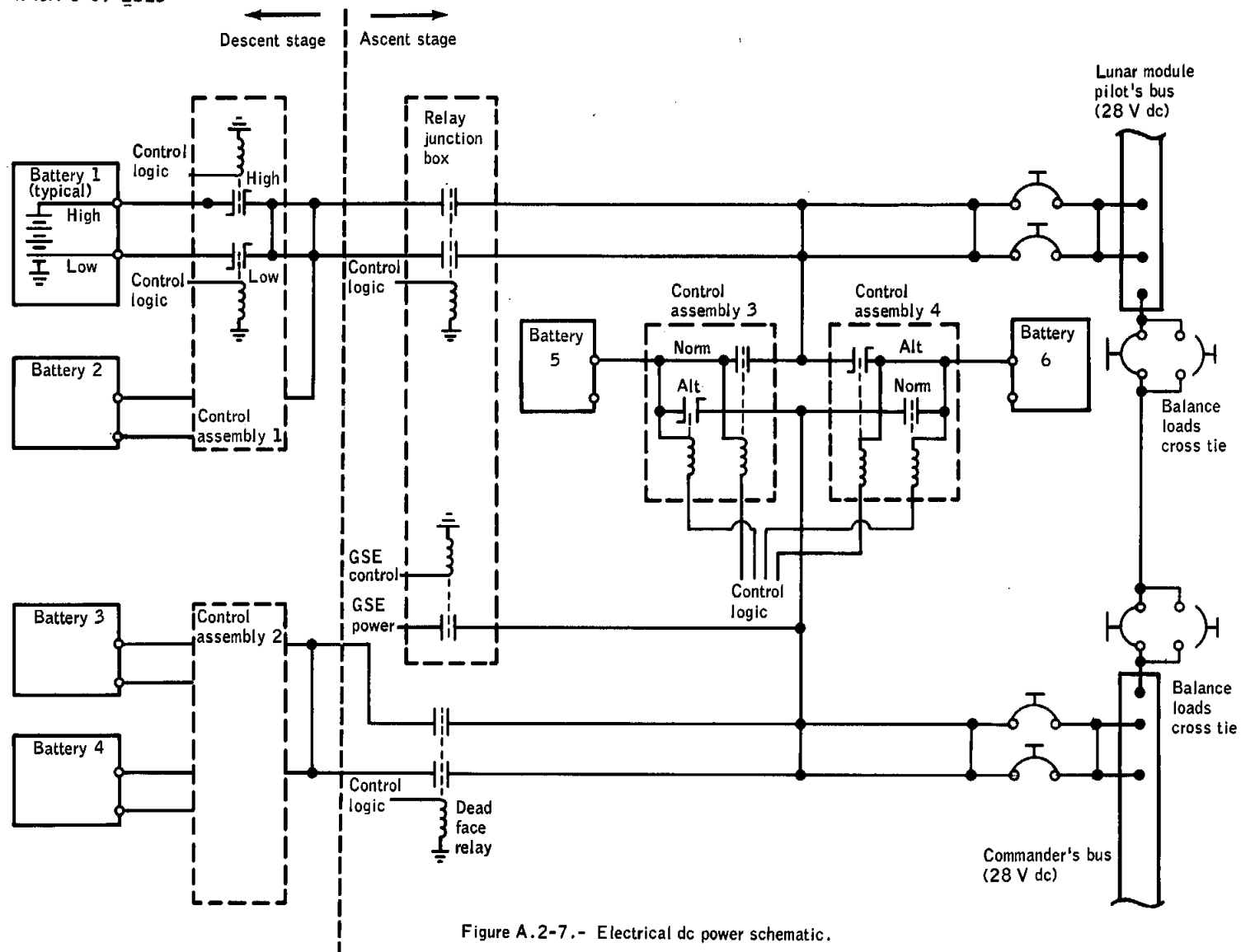


Figure A.2-7.- Electrical dc power schematic.

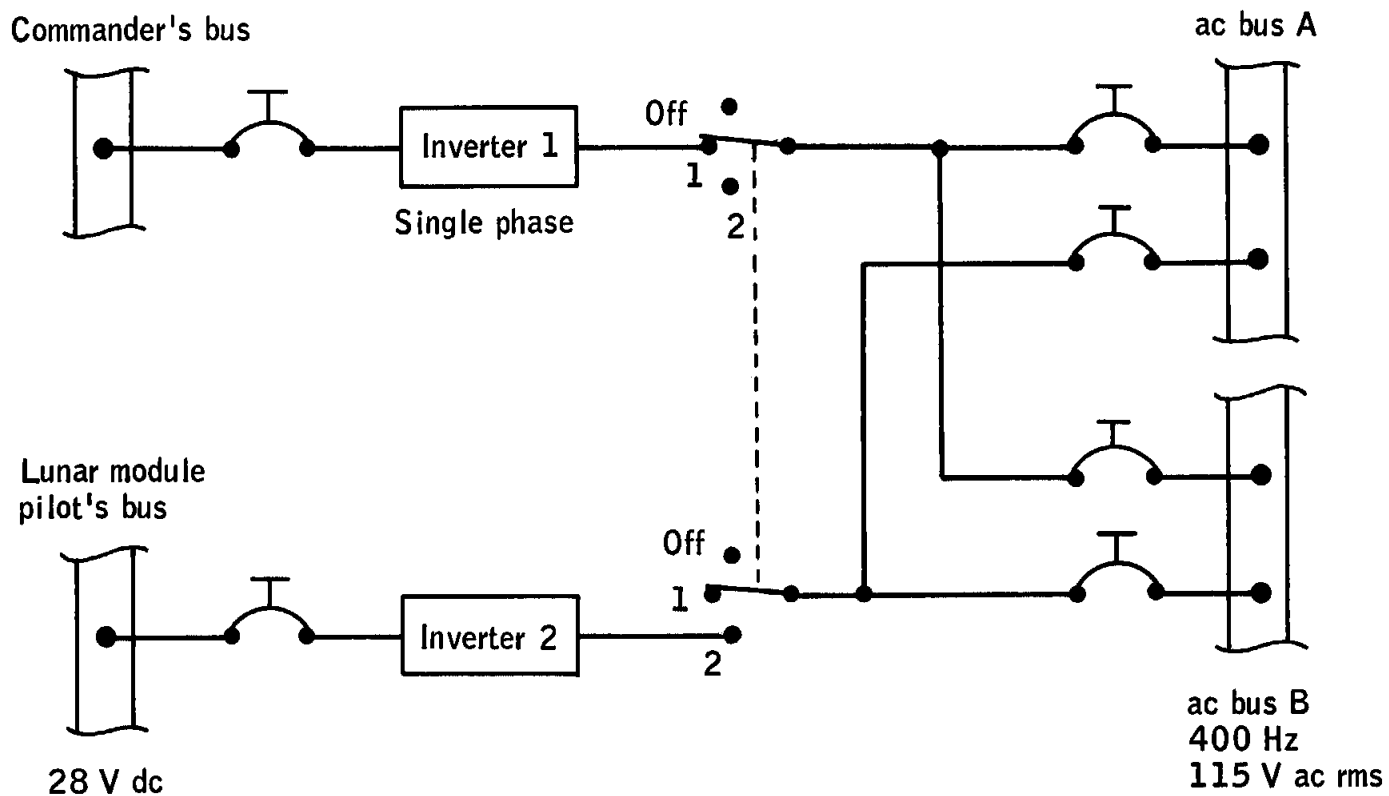


Figure A.2-8.- Electrical ac power schematic.

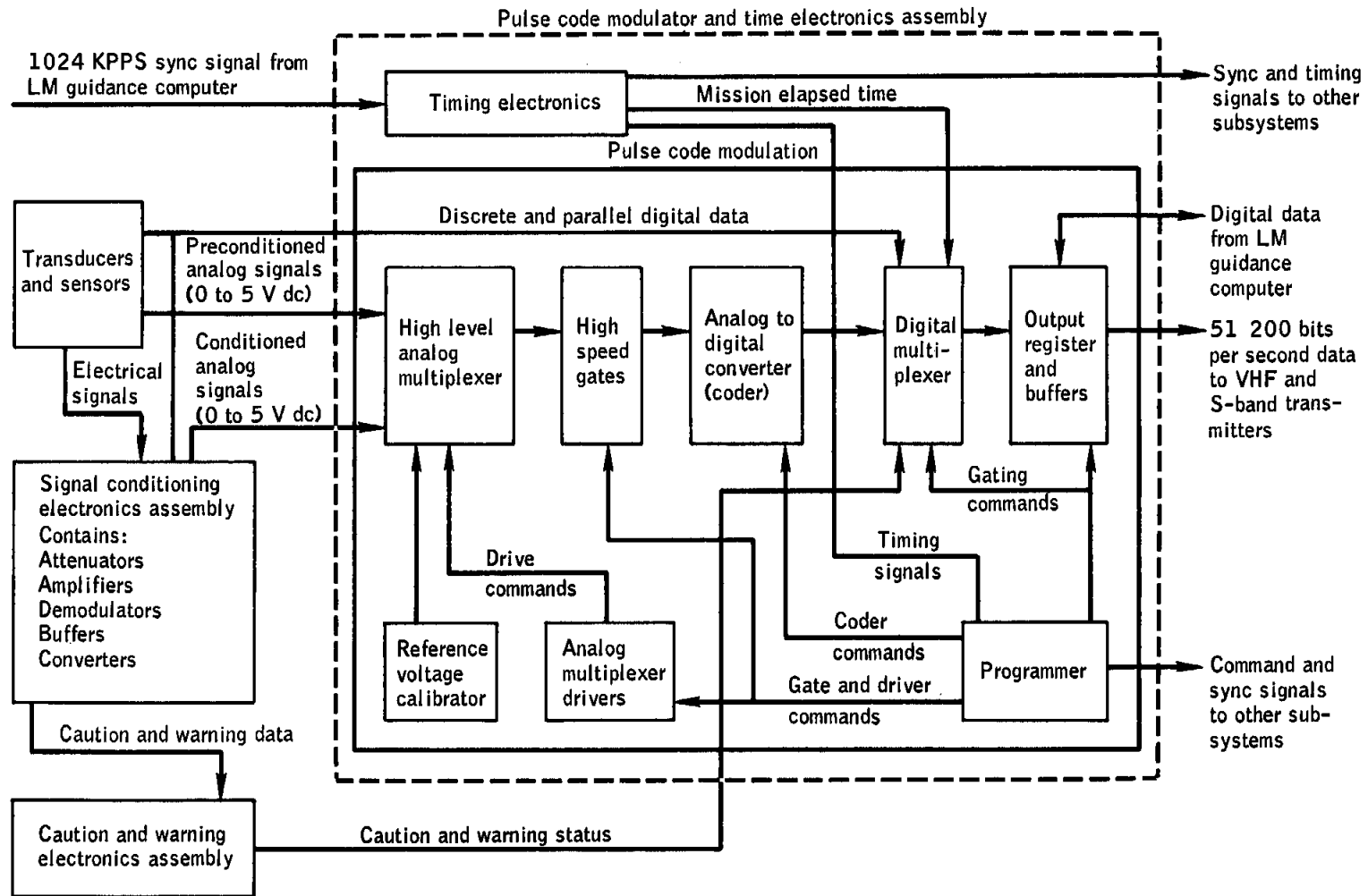


Figure A.2-9.- Operational instrumentation functional block diagram.

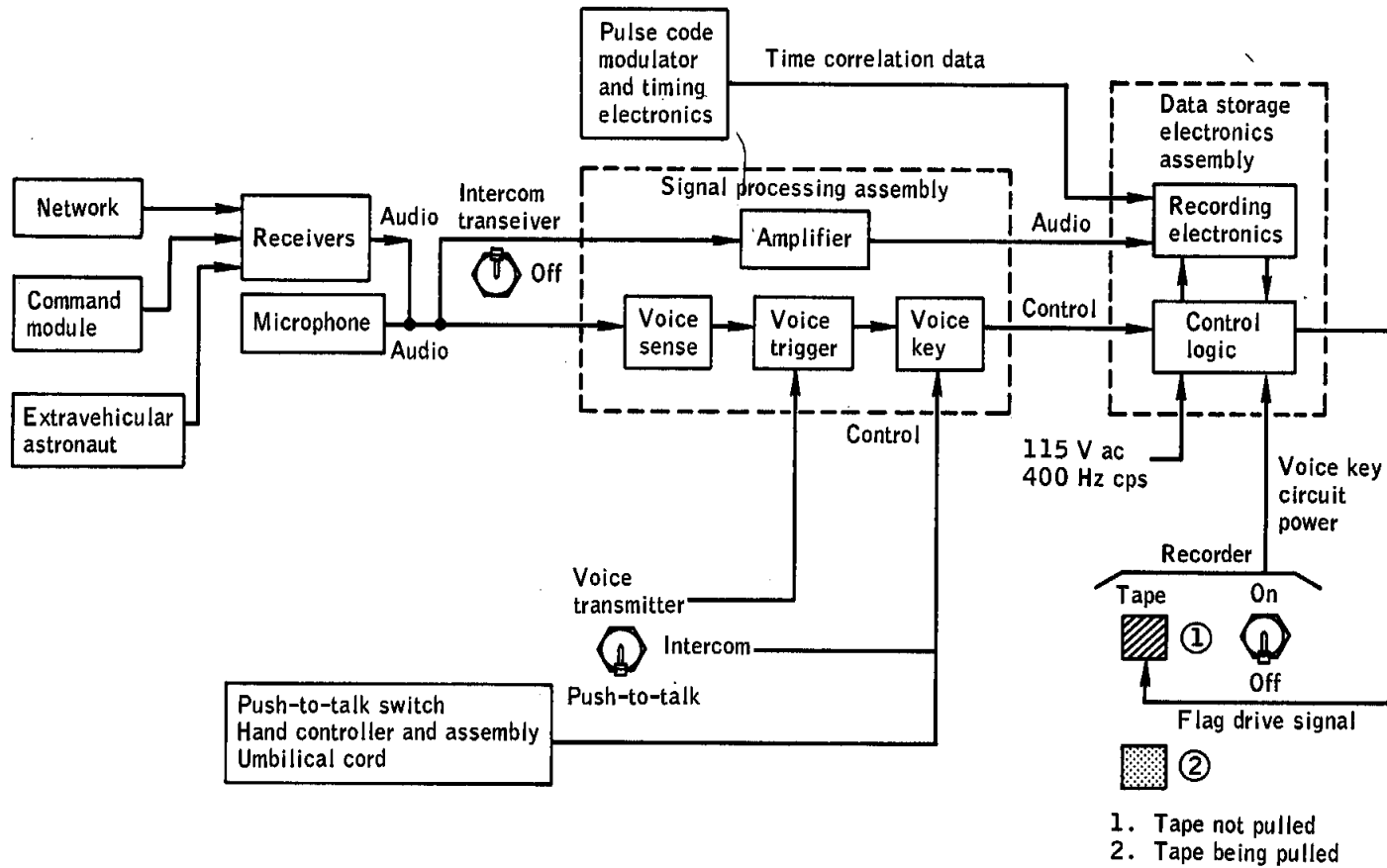


Figure A.2-10.- Data storage electronics assembly functional schematic.



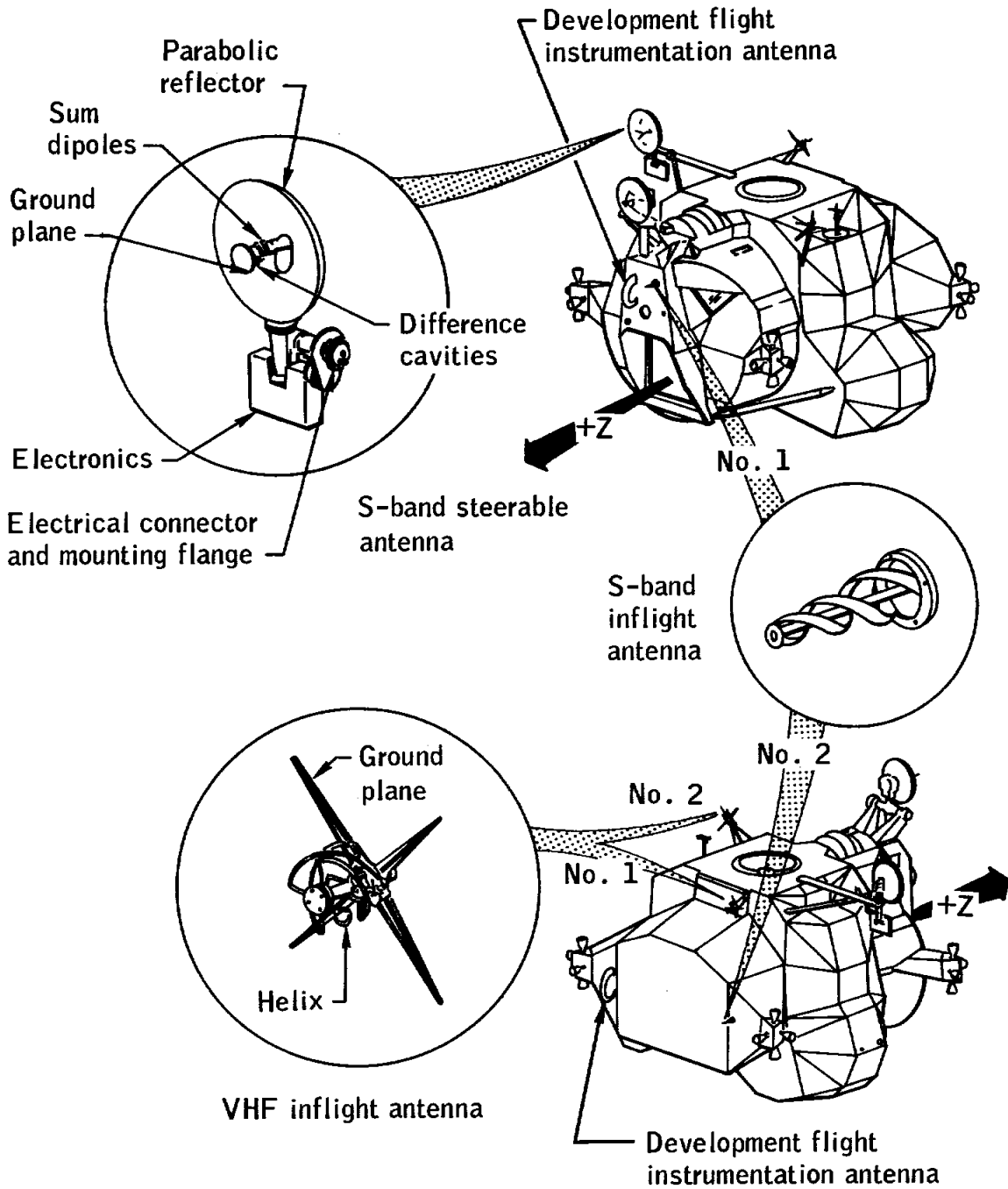
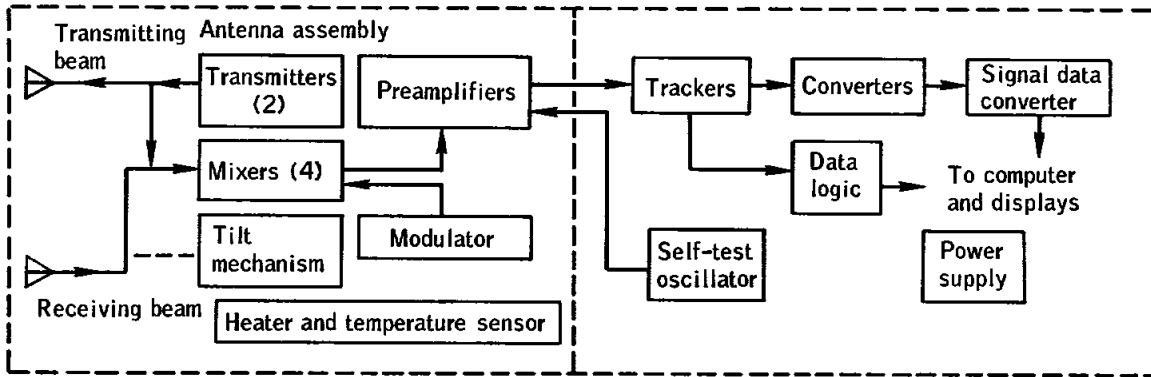
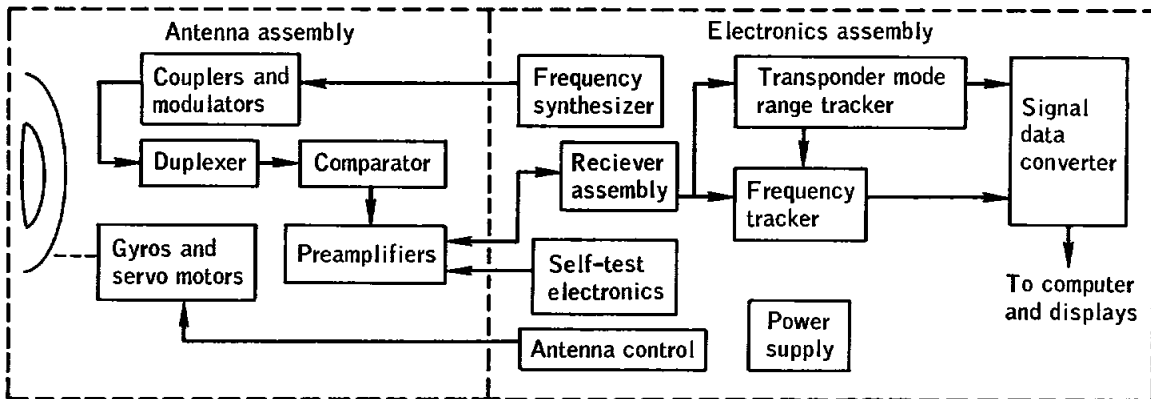


Figure A.2-15.- Communications subsystems - antennas.

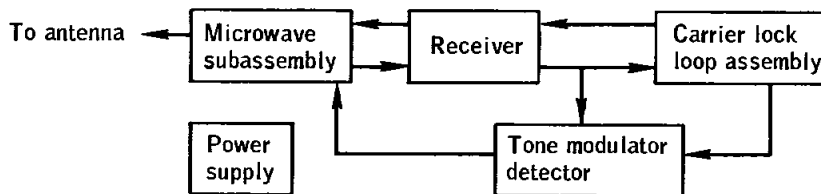
NASA-S-69-2134



(a) Landing radar.



(b) Rendezvous radar.



(c) Rendezvous radar transponder.

Figure A.2-16.- Radar systems functional block diagrams.

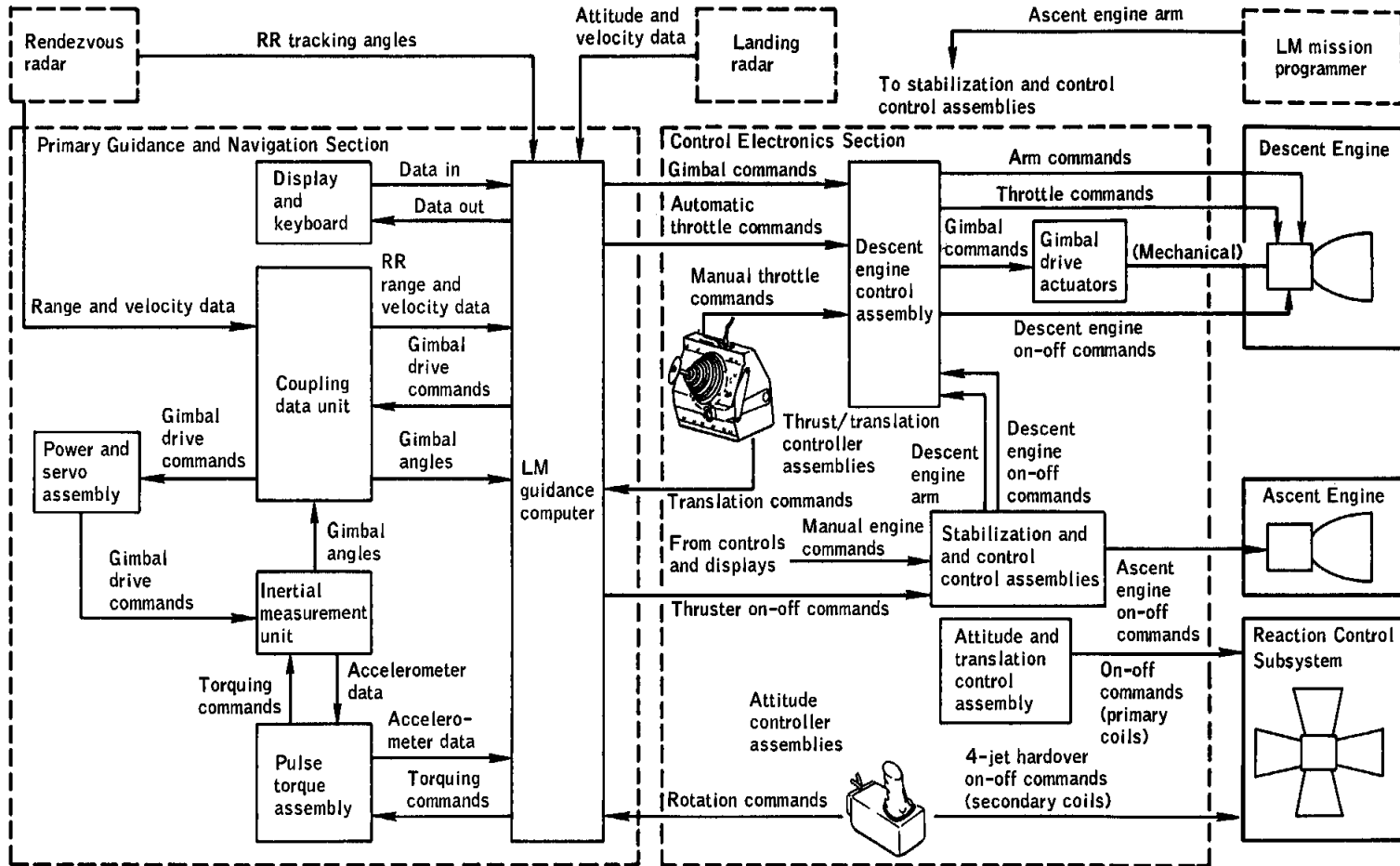


Figure A.2-17.- Primary guidance path - simplified block diagram.

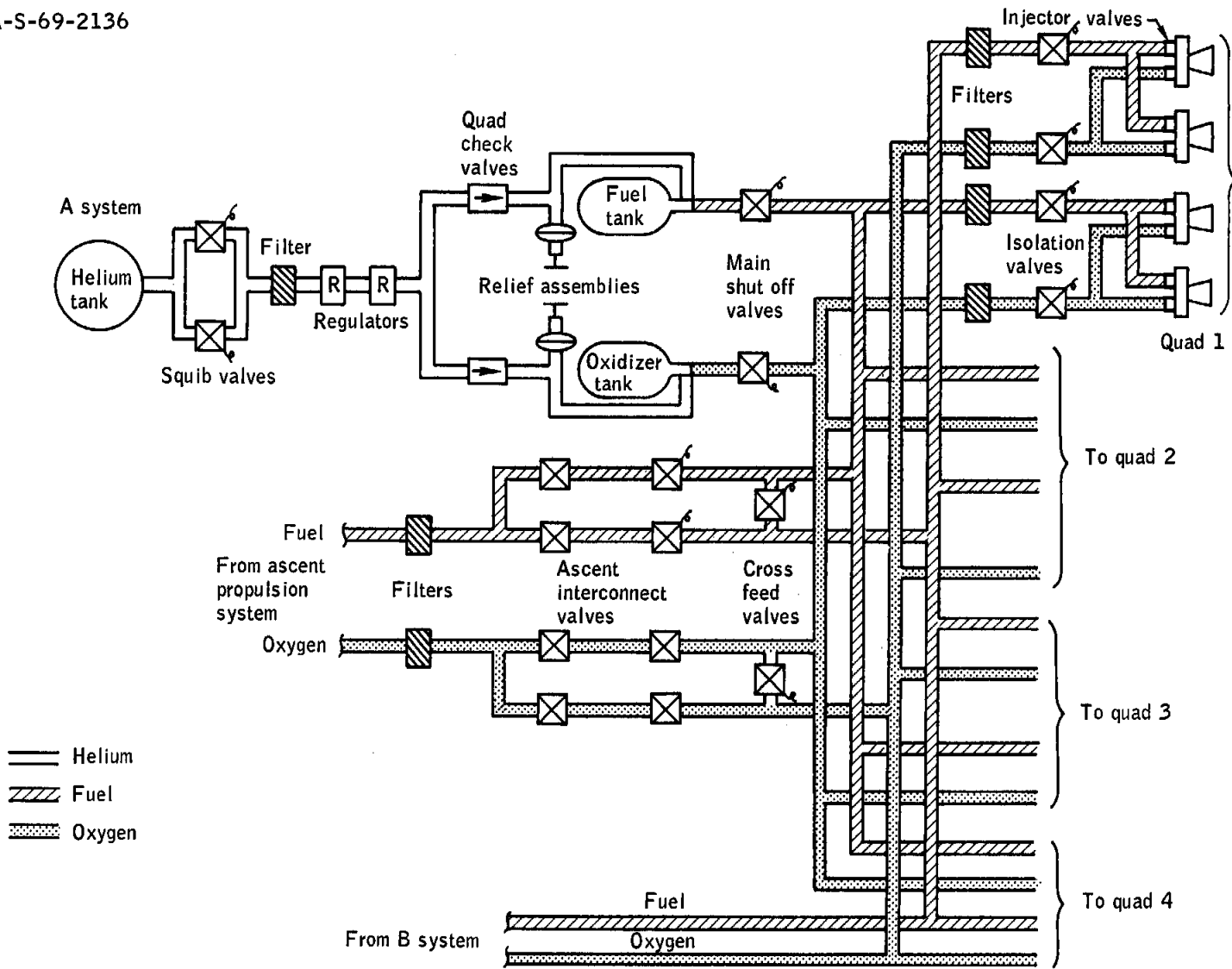


Figure A.2-18.- Reaction control system.

A-50

NASA-S-69-2137

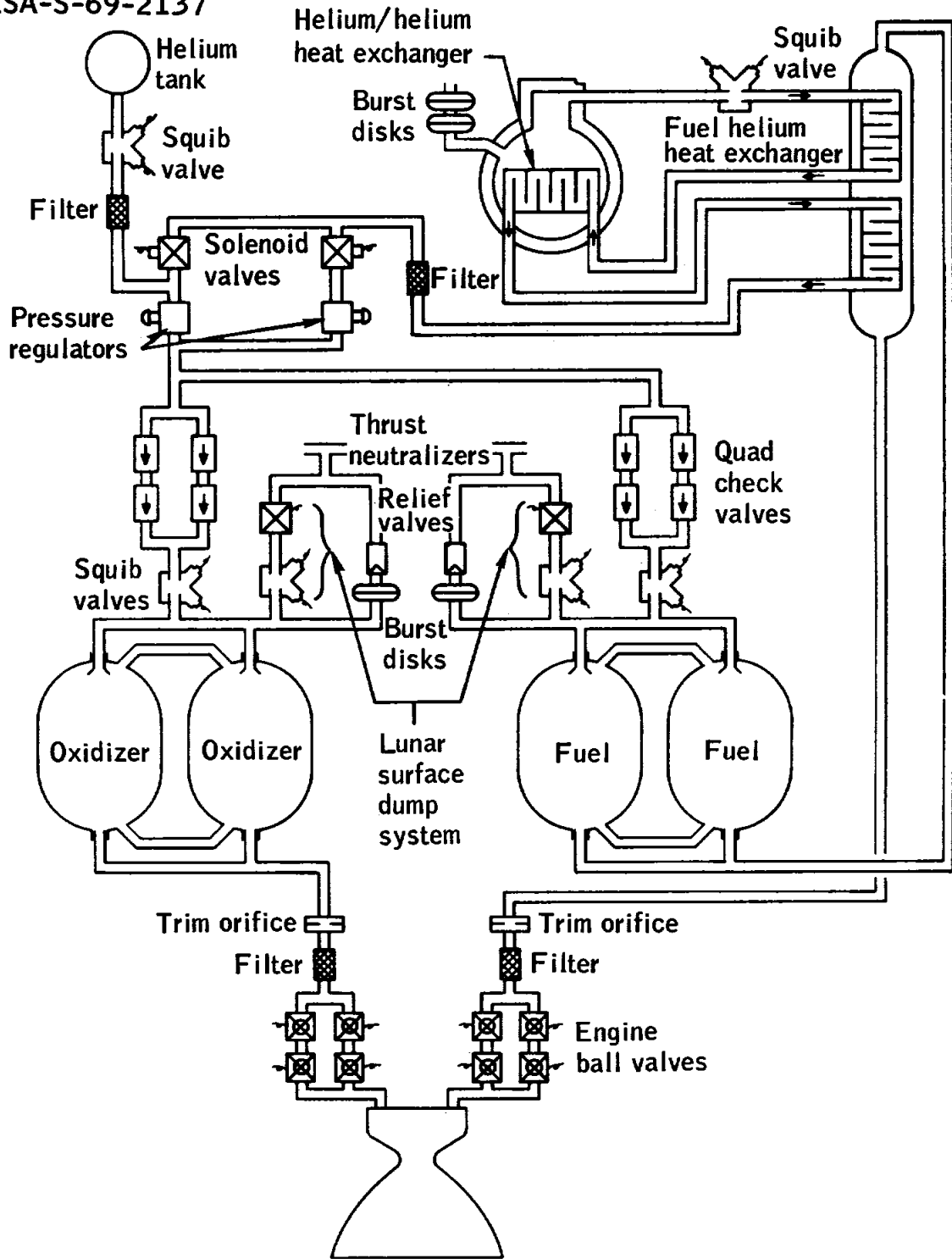


Figure A.2-19.- Descent propulsion system schematic.

NASA-S-69-2138

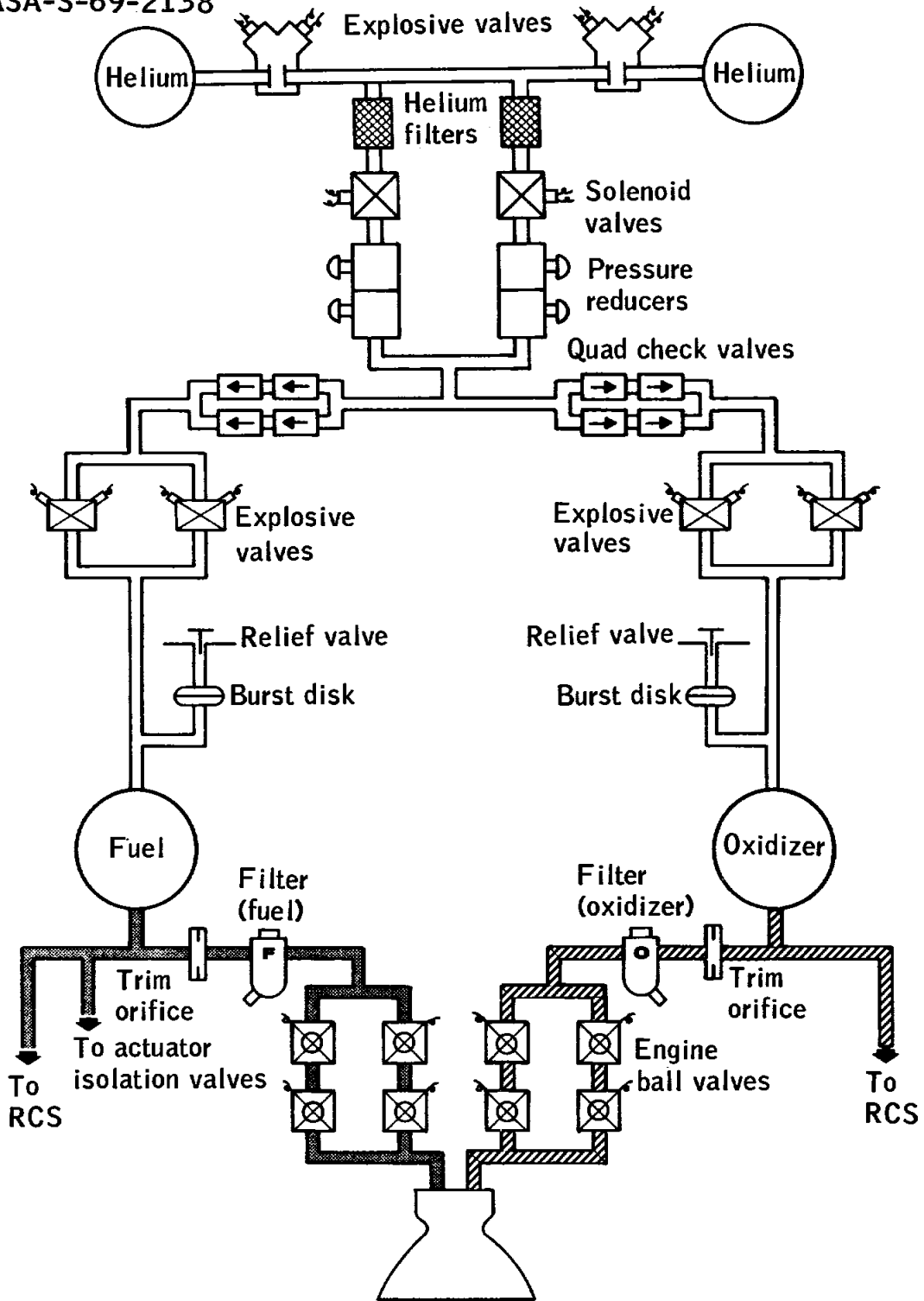


Figure A.2-20.- Ascent propulsion system schematic.

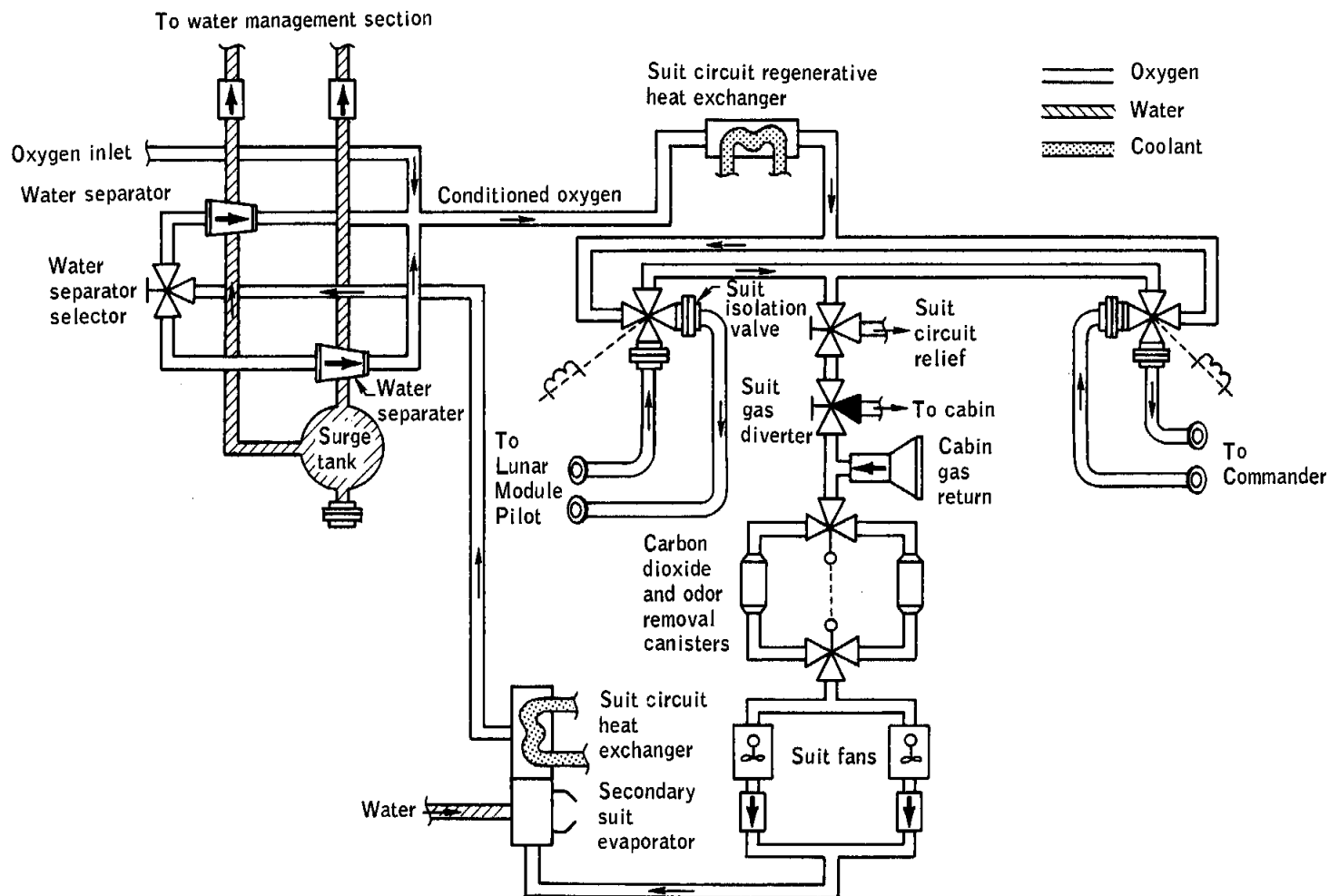


Figure A.2-21.- Atmosphere revitalization section of the environmental control system.

NASA-S-69-2140

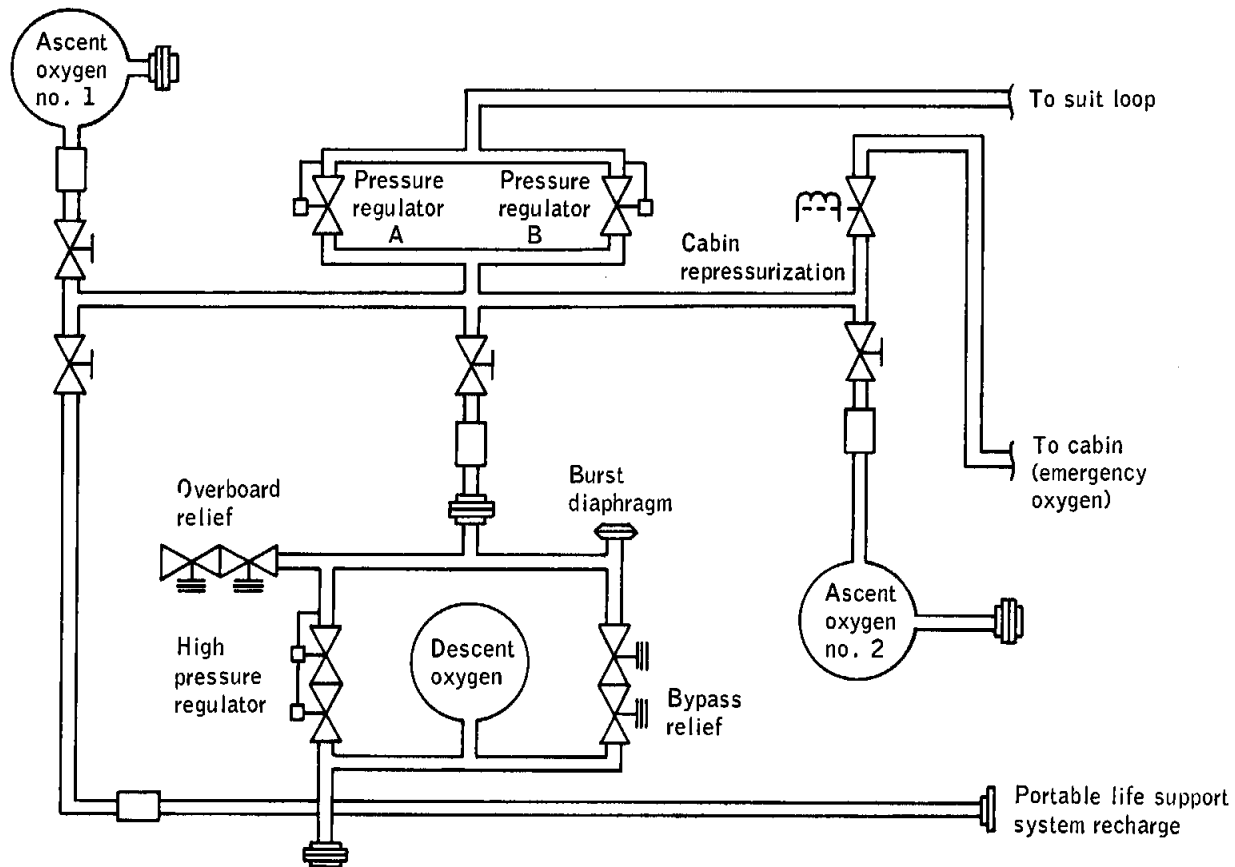


Figure A.2-22.- Oxygen supply and cabin pressure control section of the environmental control system.

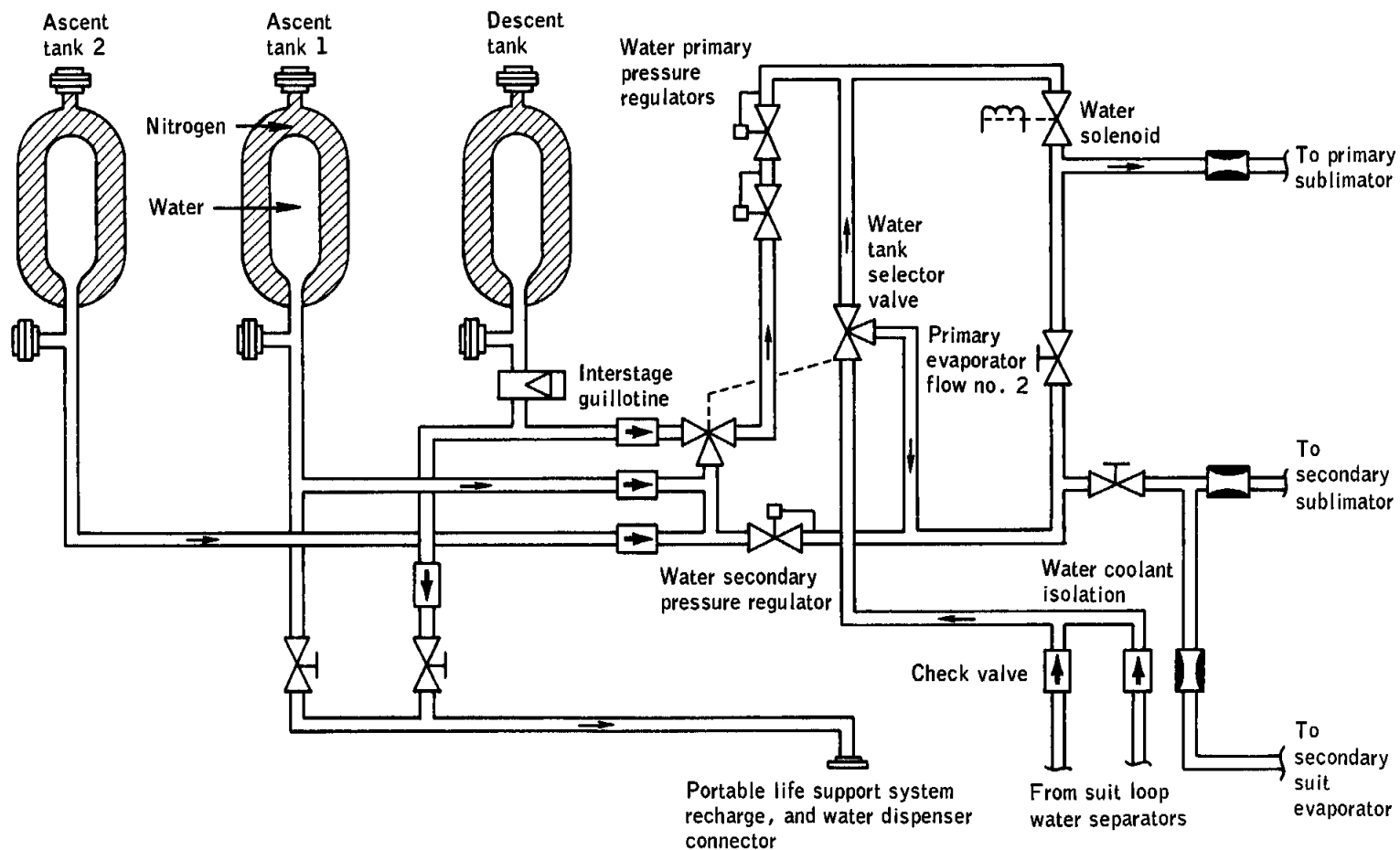


Figure A.2-23.- Water management section of the environmental control system.

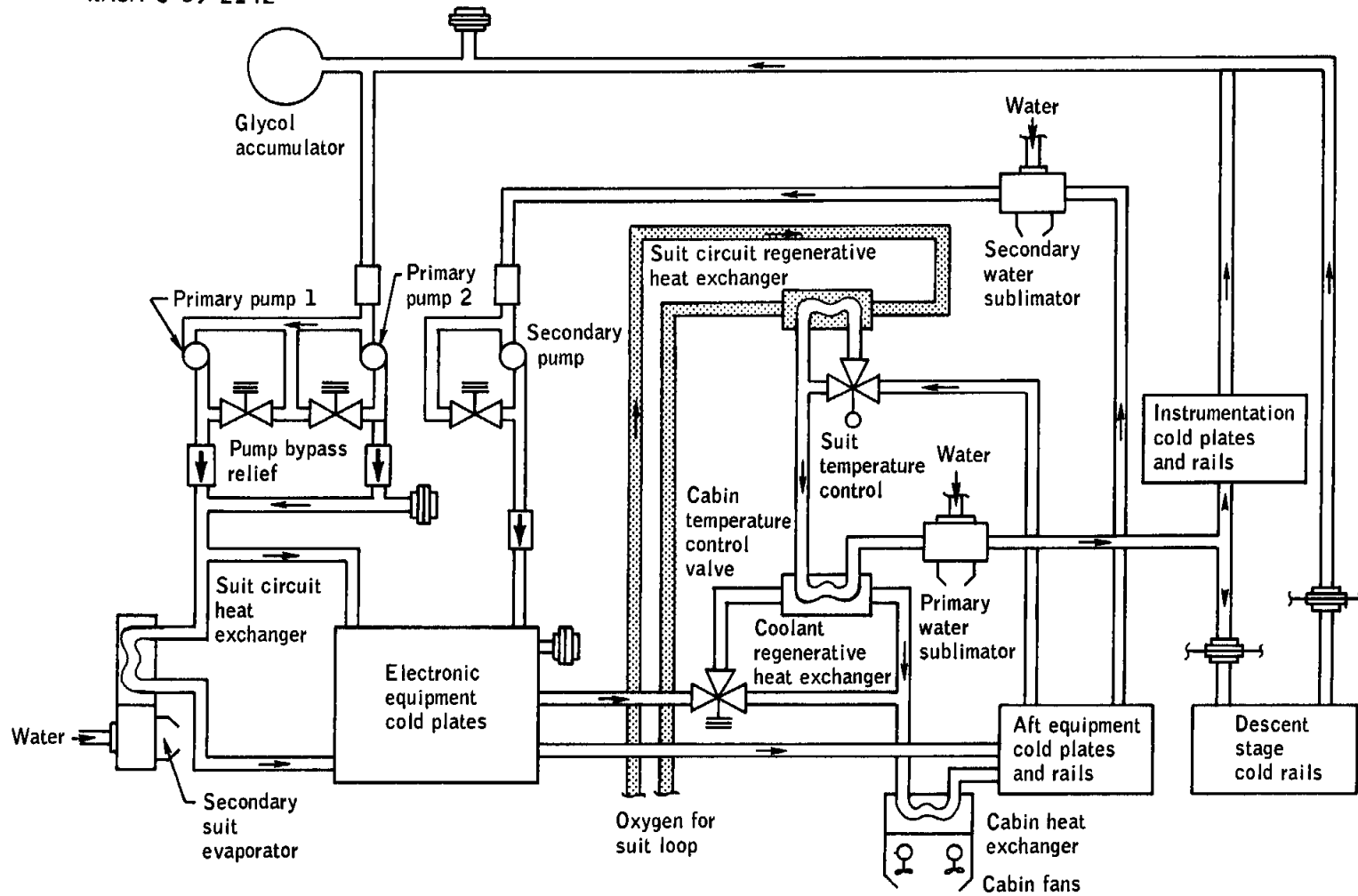


Figure A.2-24.- Heat transport and cold plate sections of the environmental control system.

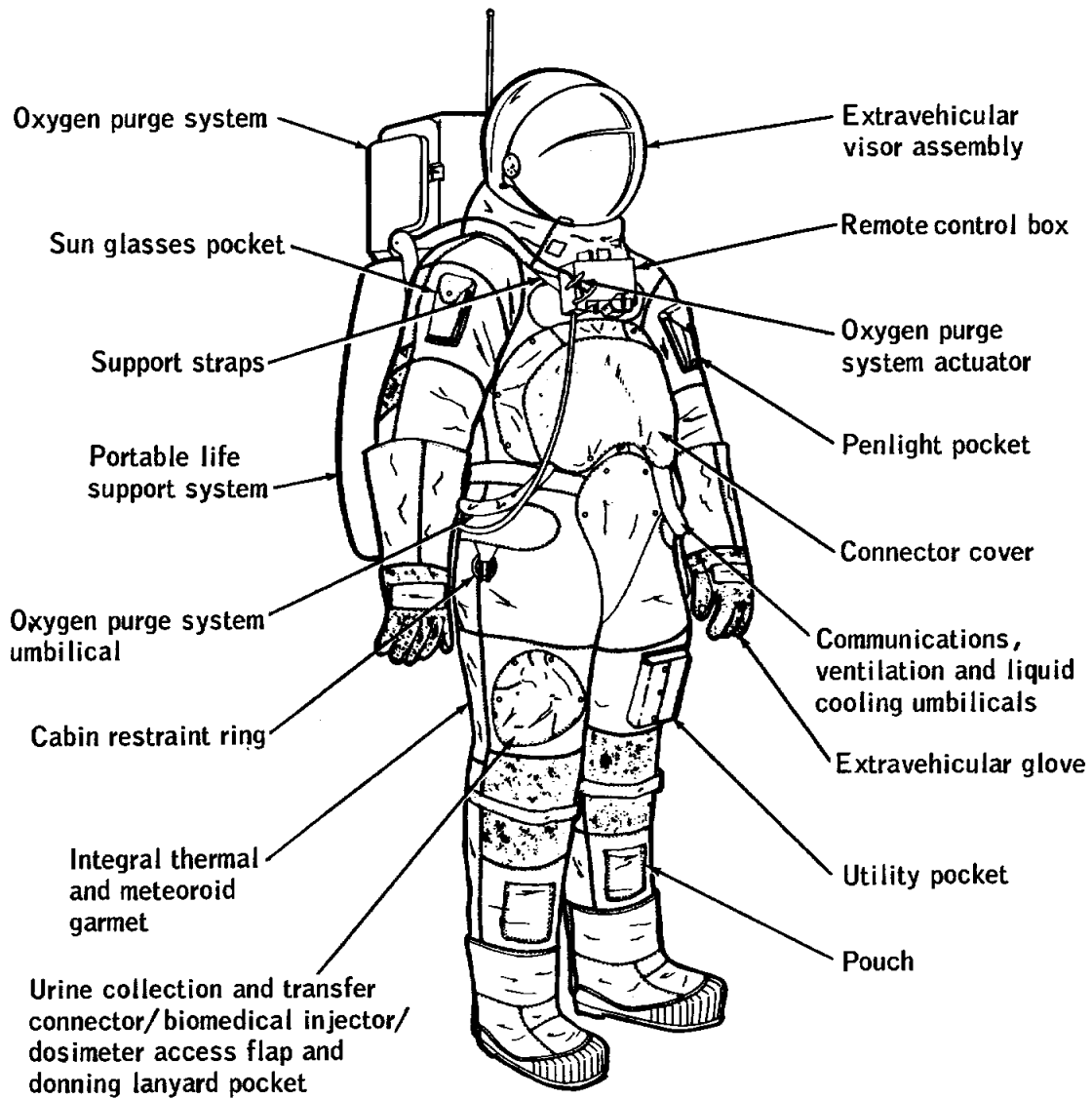


Figure A.2-25.- Extravehicular mobility unit.

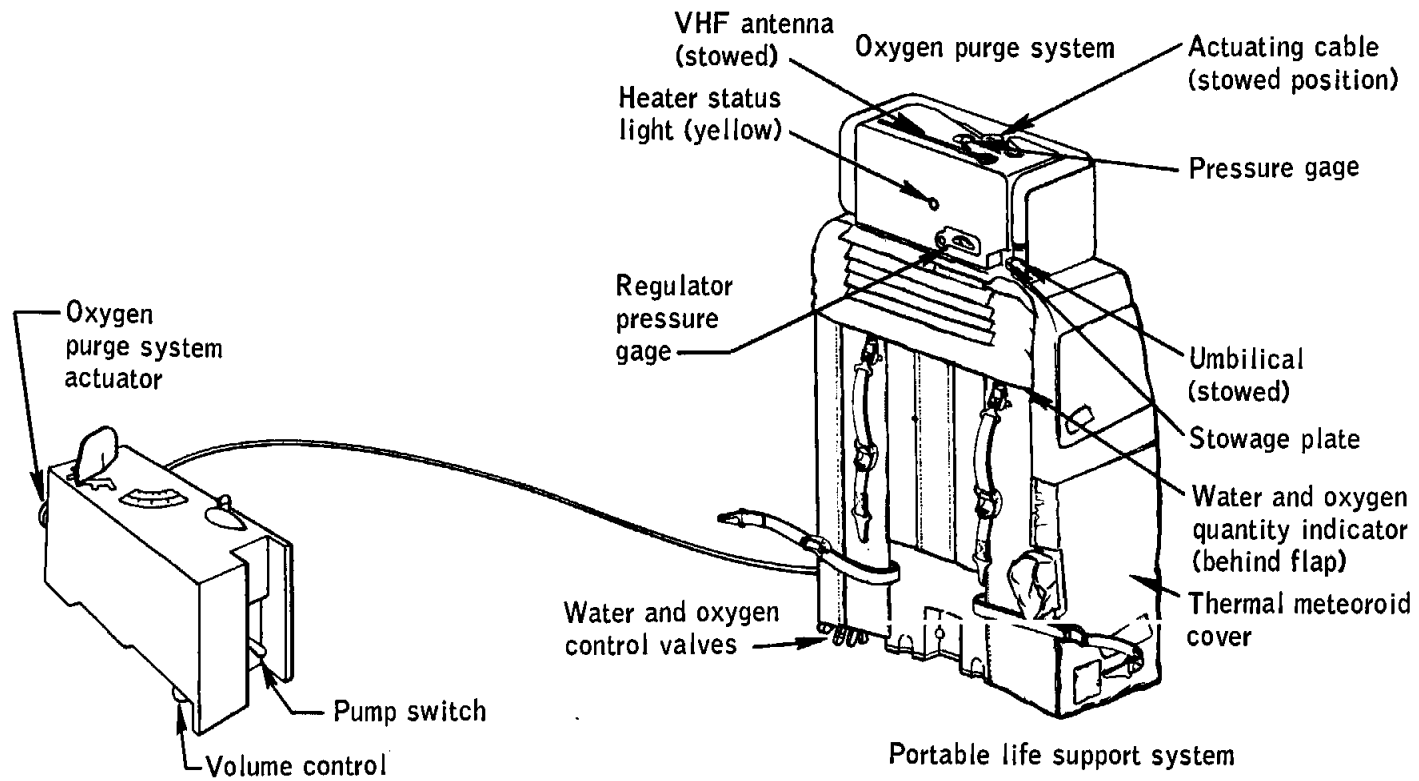


Figure A.2-26.- Portable life support system.

### A.3 SPACECRAFT/LAUNCH-VEHICLE ADAPTER

The two major changes to the spacecraft/launch-vehicle adapter from the Apollo 8 configuration were the deletion of the launch-vibration instrumentation pickups and the addition of lunar-module separation sequence controllers. The instrumentation was deleted as unnecessary because the adapter has been fully qualified. The sequence controllers were added to accommodate the combined spacecraft ejection function.

## A.4 LAUNCH VEHICLE DESCRIPTION

Launch vehicle AS-504 was the fourth in the Saturn V series and the first to carry a lunar module. The Apollo 9 configuration was very similar to that for Apollo 8, and the more significant differences between the two vehicles are described in the following paragraphs.

In the first (S-IC) stage, the inner cone of the F-1 engine chamber was removed to produce a slight increase in specific impulse and yet reduce weight. To improve specific impulse and combustion stability, the fully qualified thrust-chamber injector for the F-1 engine was incorporated. Maximum propellant was loaded with minimum ullage volume to increase payload capability. As a secondary precaution against the vehicle exceeding maximum acceleration limits, the length of the standpipe in the center-engine liquid oxygen delivery system was increased by approximately 35 inches. Other weight reduction items on this stage included the replacement of the liquid-oxygen tank stepped skins with tapered skins, reduction in the web thickness of the cantilever baffle, removal of 72 radial stiffeners, scalloping of the Y-rings, and reduction of the chord cross-sectional areas near the helium bottles.

To reduce weight on the second (S-II) stage, a lightweight structural design was incorporated on the forward and aft skirts, the propellant tanks, the thrust structure, and the interstage. The nominal propellant load was increased from 930 000 pounds to 975 000 pounds to increase payload capability, and to minimize propellant residuals at engine cutoff, the time delay between receiving a dry indication from the liquid oxygen low-level sensors and sending an engine cutoff command was changed from zero to 1.5 seconds. To improve efficiency of propellant control, the Apollo 9 vehicle had a closed-loop propellant utilization system rather than the open-loop configuration used on Apollo 8. Increased Saturn-V payload capability was provided by uprated J-2 engines, which had a nominal thrust increase from 225 000 to 230 000 pounds.

The third (S-IVB) stage did not use the anti-flutter kit flown on Apollo 8. To eliminate propulsive relief venting during separation of the command and service modules from the S-IVB and during initial command module/lunar module docking, the pressure settings for the liquid oxygen vent-and-relief valve and for the non-propulsive-vent latching valve were revised. To reduce post-ignition thrust shifts, the flow baffle in the propellant-utilization valve was rotated 30 degrees.

In the instrument-unit environmental control system, seven heaters were replaced by cold plate thermal isolators. Also, the methanol/water accumulator was enlarged from 189 to 374 cubic inches to provide the capability for an earlier fill operation during countdown.

## A.5 MASS PROPERTIES

Spacecraft properties for the Apollo 9 mission are summarized in table A.5-I. These data represent the conditions as determined from postflight analyses of expendable loadings and during the flight. Variations in spacecraft mass properties are determined for each significant mission phase from lift-off through landing. Expendables usage is based on reported real-time and postflight data as presented in other sections of this report. The weights and center-of-gravity of individual modules were measured prior to flight, and the inertia values were calculated. All changes incorporated after the actual weighing were monitored, and the mass properties were updated.

TABLE A.5-1.- MASS PROPERTIES

Event	Weight, lb	Center of gravity, in.			Moment of inertia, slug-ft <sup>2</sup>			Product of inertia, slug-ft <sup>2</sup>		
		X <sub>A</sub>	Y <sub>A</sub>	Z <sub>A</sub>	I <sub>XX</sub>	I <sub>YY</sub>	I <sub>ZZ</sub>	I <sub>XY</sub>	I <sub>XZ</sub>	I <sub>YZ</sub>
Combined Spacecraft										
Lift-off	104 099	845.0	2.6	3.5	62 778	1 135 836	1 141 954	820	8 679	2878
Earth orbit insertion	95 231	802.9	2.8	3.8	61 917	682 876	689 039	3052	10 724	2867
Command and service modules at trans- position	59 085	933.0	4.0	6.1	31 593	74 526	79 304	-1826	-245	2497
Docking	91 055	1039.9	2.6	4.3	51 620	511 585	516 064	-7378	-7 252	3543
First service propulsion firing	91 011	1039.9	2.6	4.2	51 578	511 441	515 930	-7385	-7 248	3556
Coast	90 666	1040.4	2.6	4.2	51 398	510 434	515 072	-7379	-7 195	3506
Second service propulsion firing	90 602	1040.4	2.7	4.2	51 350	510 251	514 909	-7404	-7 163	3523
Coast	83 375	1052.1	2.6	3.7	47 565	475 765	483 556	-7272	-5 738	2466
Third service propulsion firing	83 365	1052.1	2.6	3.7	47 556	475 711	483 501	-7276	-5 735	2468
Coast	64 715	1092.1	0.9	3.5	38 026	367 172	370 809	-3525	-4 675	865
Fourth service propulsion firing	64 673	1092.2	0.9	3.5	37 984	366 903	370 543	-3531	-4 675	875
Coast	62 805	1098.2	0.6	3.5	37 032	350 147	352 871	-2750	-4 848	761
Command and service modules at first descent engine firing (docked)	30 175	976.8	1.1	6.7	16 791	37 259	40 328	101	-383	-158
Combined spacecraft at first descent engine firing (docked)	62 675	1111.8	0.9	3.5	38 256	292 111	294 829	-769	-5 328	693
Coast	52 345	1084.1	1.1	4.1	31 681	237 215	239 232	-425	-4 033	1316
Fifth service propulsion firing	52 262	1063.9	0.8	4.2	31 457	265 384	267 411	-2402	-3 091	1405
Coast	49 386	1074.8	0.2	4.4	29 986	242 360	242 976	-1198	-3 431	1236
Rendezvous separation	49 105	1076.2	0.7	4.3	29 918	241 610	242 223	-760	-3 604	1190
Command and service modules at lunar module docking	26 895	961.3	0.2	7.2	14 938	50 438	52 162	-1103	156	-215
Combined spacecraft after docking (lunar module manned)	36 828	1018.9	0.8	4.7	21 056	126 602	127 345	-563	-2 935	477
Combined spacecraft after crew transfer	36 824	1017.7	0.5	4.8	20 990	125 186	125 958	-788	-2 714	516
Command and service modules after lunar module jettison	27 139	961.5	0.2	7.0	15 021	50 156	51 904	-1100	62	-212
Sixth service propulsion firing	27 069	961.6	0.3	6.9	15 979	50 091	51 856	-1107	66	-197
Coast	26 987	961.9	0.2	6.9	14 937	49 936	51 660	-1090	57	-201
Seventh service propulsion firing	26 831	962.1	0.3	6.8	14 825	49 809	51 553	-1112	86	-166
Coast	26 831	962.7	-0.4	7.1	13 959	46 014	46 944	-724	-118	-253
Eighth service propulsion firing	24 953	969.1	-0.2	7.0	13 824	45 820	46 775	-758	-68	-209
Coast	24 183	972.7	-0.6	7.2	13 423	43 557	44 137	-550	-177	-248
Command module/service module separa- tion	24 183	972.6	-0.6	7.1	13 424	43 506	44 081	-560	-171	-245
Command module after separation	12 259	1041.0	-0.3	5.7	5 800	5 075	4 606	29	-390	16
Entry interface	12 257	1041.0	-0.3	5.7	5 799	5 074	4 606	29	-390	16
Mach 10	12 149	1041.2	-0.3	5.6	5 720	4 987	4 538	29	-382	16
Drogue deployment	11 839	1039.8	-0.3	5.7	5 654	4 766	4 322	30	-364	16
Main parachute deployment	11 758	1039.5	-0.3	5.9	5 638	4 708	4 279	30	-339	16
Landing	11 094	1037.8	-0.1	4.9	5 441	4 301	3 969	18	-308	36
Lunar Module										
Lift-off	32 132	184.7	0.7	-0.2	20 001	24 022	25 736	-167	446	344
Command module transposition and docking	32 130	1235.9	0.1	0.7	19 996	25 372	25 117	-307	369	913
First descent engine firing (docked)	32 500	185.7	0.7	0.4	21 333	25 096	26 666	-177	699	325
Rendezvous separation	22 066	192.6	1.3	0.7	14 716	20 766	23 790	-229	664	300
Second descent engine firing	22 030	192.5	1.3	0.8	14 695	20 704	23 717	-231	662	298
Coast	21 702	193.1	1.3	0.8	14 488	20 458	23 569	-234	660	298
Third descent engine firing	21 640	192.9	1.3	0.8	14 453	20 356	23 449	-236	658	295
Coast	21 548	193.0	1.3	0.8	14 395	20 293	23 399	-237	657	295
Ascent stage at staging	10 216	244.2	-0.6	3.0	6 123	3 588	5 395	49	180	-14
Constant delta height maneuver	10 157	244.1	-0.6	3.0	6 091	3 575	5 354	49	180	-13
Terminal phase initiation	10 099	244.1	-0.7	3.0	6 058	3 567	5 314	49	181	-13
Docking	9 932	243.5	-0.7	3.1	5 976	3 515	5 195	49	184	-7
Ascent stage unmanned	9 685	243.2	-0.5	2.0	5 858	3 543	5 270	57	107	-4
Ascent stage after firing to depletion	5 616	256.7	-0.9	3.5	3 079	2 959	1 938	101	51	1

APPENDIX B - SPACECRAFT HISTORIES

The history of command and service module (CSM 104) operations at the manufacturer's facility, Downey, California, is shown in figure B-1, and the operations at Kennedy Space Center, Florida, in figure B-2.

The history of the lunar module (LM-3) at the manufacturer's facility, Bethpage, New York, is shown in figure B-3, and LM-3 operations at Kennedy Space Center, Florida, in figure B-4.

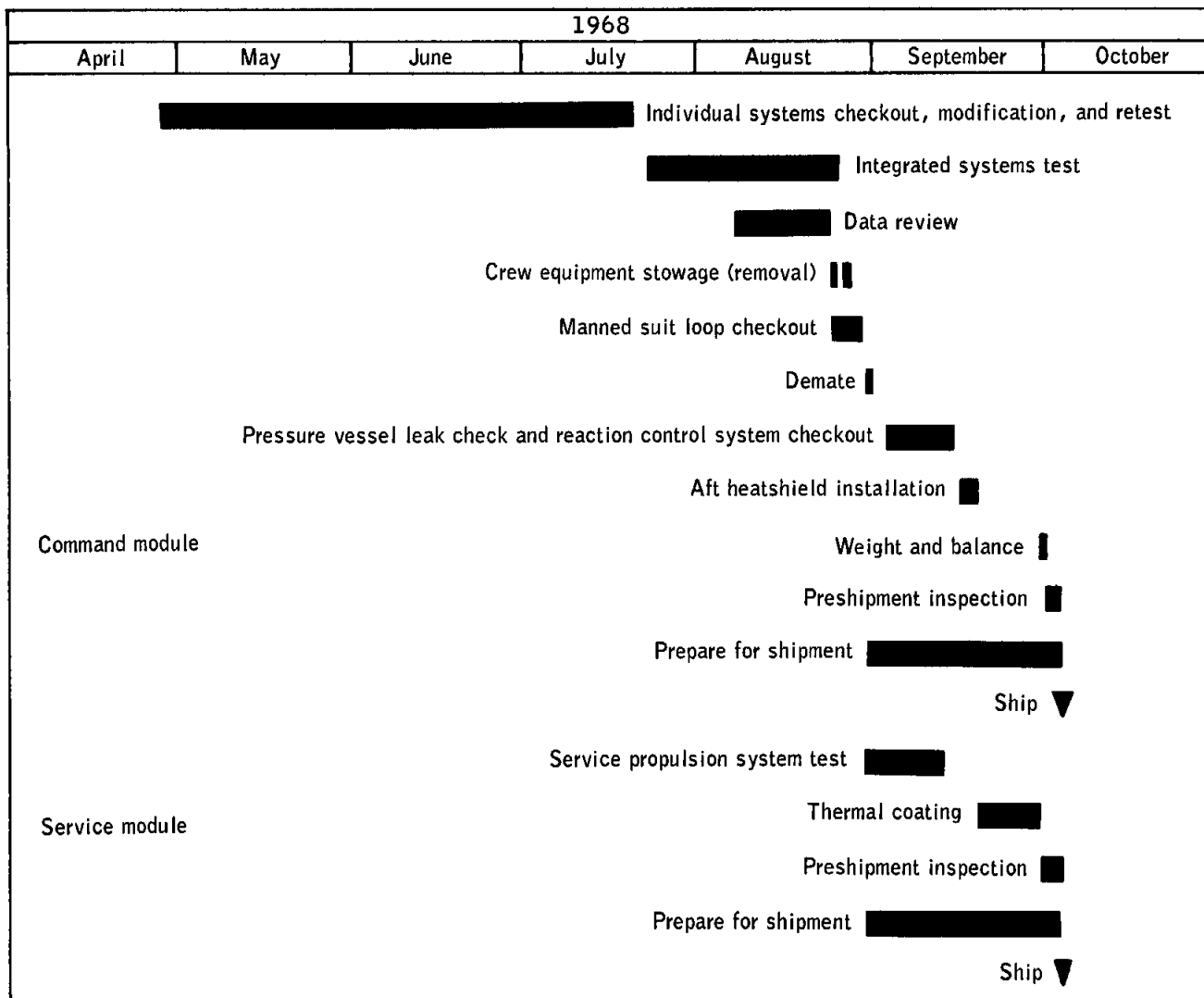


Figure B-1.- Factory checkout flow for command and service modules at contractor facility.

NASA-S-69-2146

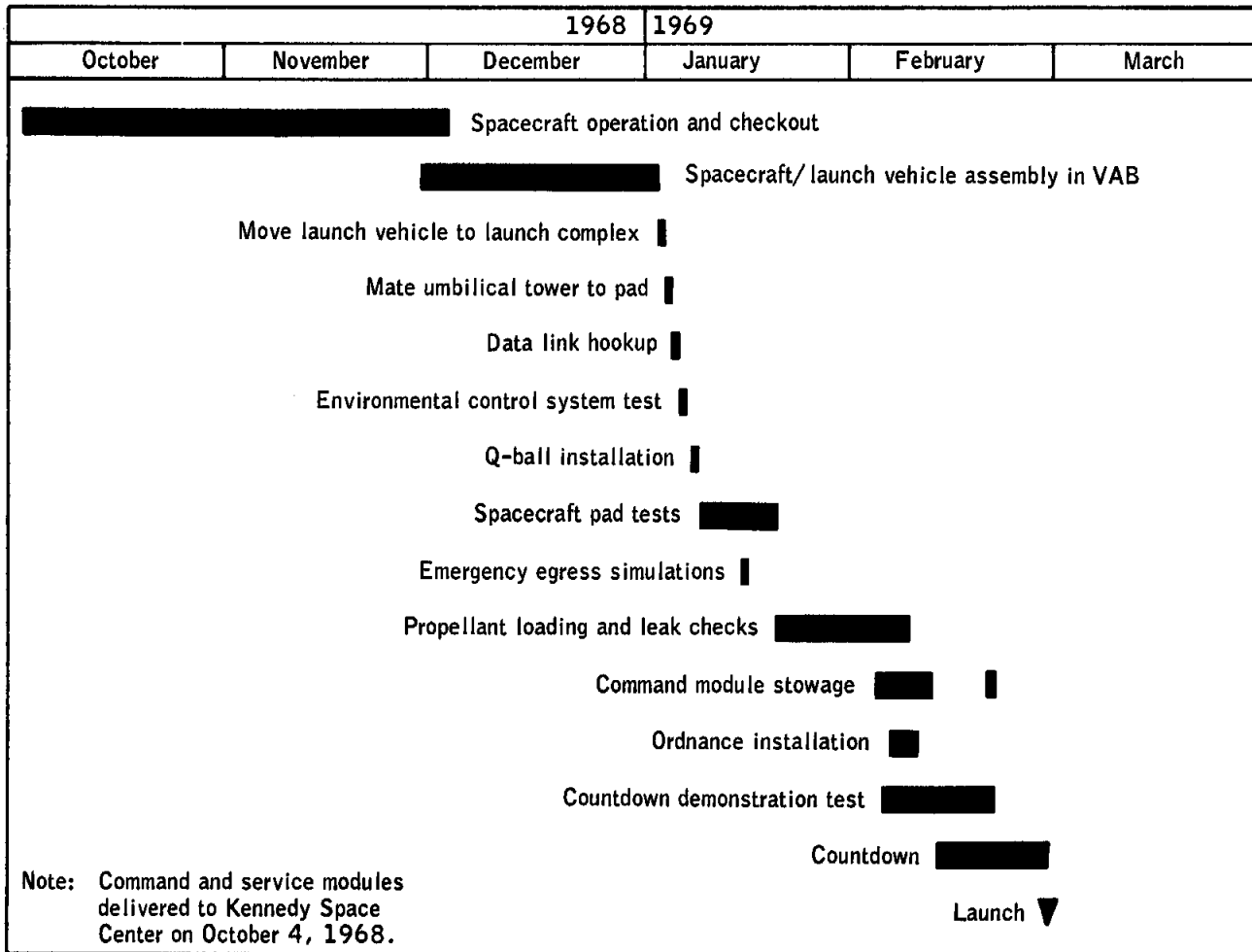


Figure B-2.- Spacecraft checkout history at Kennedy Space Center.

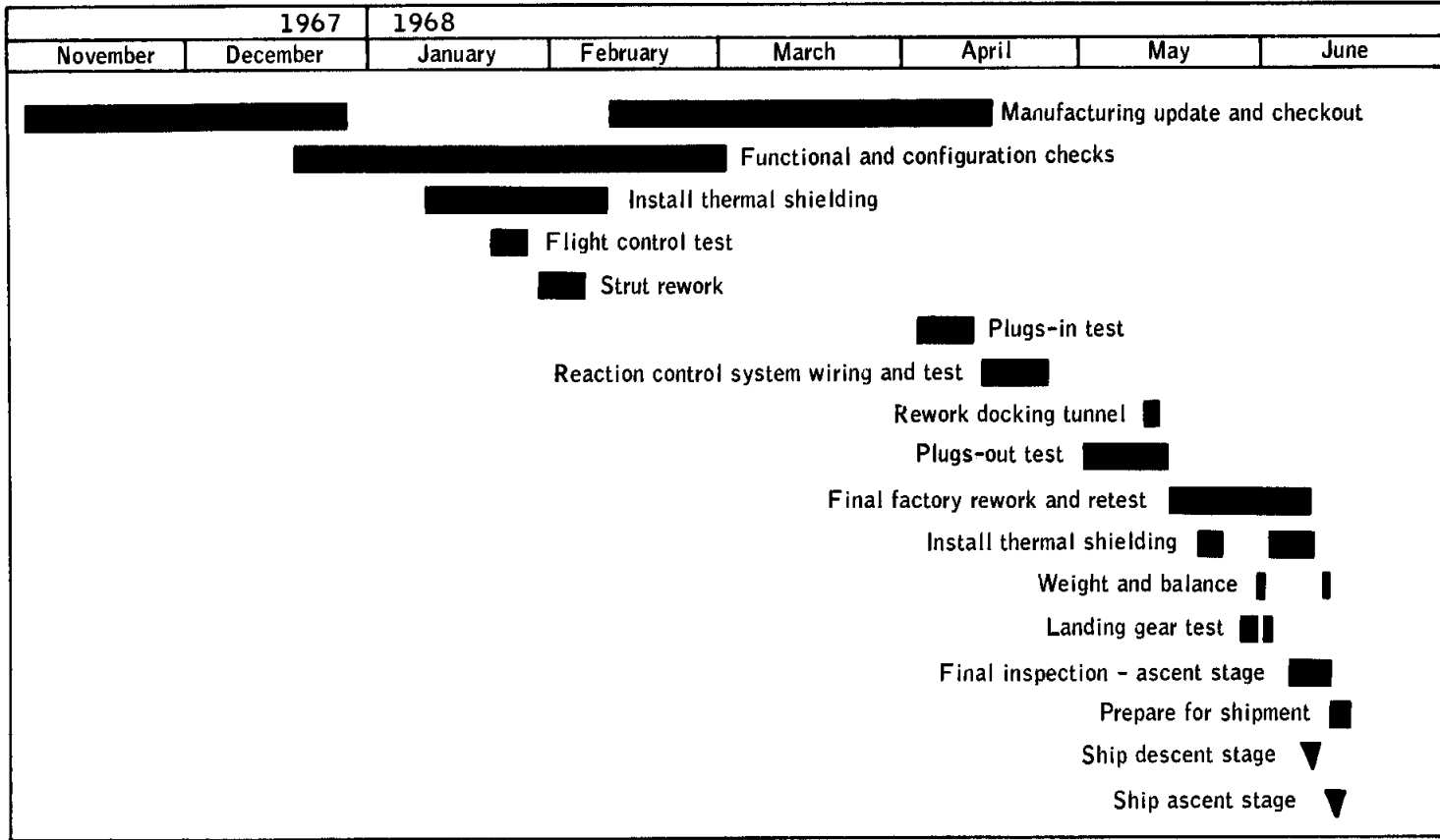


Figure B-3.- Factory checkout flow for lunar module at contractor facility.



APPENDIX C - POSTFLIGHT TESTING

The command module arrived at the contractor's facility in Downey, California, on March 20, 1969, after reaction control system deactivation and pyrotechnic safing in Norfolk, Virginia. Postflight testing and inspection of the command module for evaluation of the inflight performance and investigation of the flight irregularities were conducted at the contractor's and vendors' facilities and at the Manned Spacecraft Center in accordance with approved Apollo Spacecraft Hardware Utilization Requests (ASHUR's). The tests performed as a result of inflight problems are described in table C-I and discussed in the appropriate systems performance sections of this report. Tests being conducted for other purposes in accordance with other ASHUR's and the basic contract are not included.

TABLE C-I.- POSTFLIGHT TESTING SUMMARY

ASHUR no.	Purpose	Tests performed	Results
Displays and Controls			
104017	To investigate the failure of the VHF AM squelch potentiometer	Perform failure analysis	Improper handling during panel assembly and galling of a bearing increased knob torque.
104018	To investigate the unexplained caution and warning master alarm at docking	Perform a functional and shock test of the caution and warning unit	Not complete
104030	To investigate operation of the toggle switches and circuit associated with the quad C and D propellant isolation valves	Check the command module control to the quad C and D isolation valves. Remove switches for X-ray examination, vibration, shock, and resistance tests	The control circuit was verified proper. X-ray examination and resistance test showed no discrepancy.
104041	To investigate failure of the spotlight	Perform command module circuit integrity test	Circuits were normal.
104042	To investigate the floodlight failure	Perform a circuit check and remove floodlights for functional test and failure analysis	All lamps worked properly except for the lower equipment bay right-hand primary lamp which failed because of cathode erosion. The left-hand couch arm secondary circuit did not operate because of a broken wire.
104044	To investigate the reported misalignment of toggle switches	Check the alignment of the switches in the command module and after the panels are removed	The alignment check showed three switches exceeded 5 deg and less than 10 deg
104056	To investigate the reported overheating of an interior floodlight	Measure the stabilized temperature of a floodlight at vacuum and at 5 psi	With both the primary and secondary circuits on and the pressure at 5 psi, the lens temperature was 160° F and case temperature was 130° to 135° F. At vacuum, the lens reached 190° F, and the lamp thermal circuit breakers opened.
104065	To verify the integrity of the data storage equipment forward/rewind switch	X-ray examination; measure resistance and operating force	Tested satisfactory
104505	To verify the integrity of the up-telemetry command switch	X-ray examination; measure resistance and operating force	Tested satisfactory
Communications and Instrumentation			
104020	To investigate the failure of the service propulsion system helium tank pressure reading	Check the command module circuit and display meter	The circuit and meter functioned properly
104021	To investigate the failure of the update link to respond to commands	Perform a functional test	Lowering of power supply voltage to 15.3 V causes improper set of vehicle address, which does not reset until input power is cycled off, then back on.

TABLE C-I.- POSTFLIGHT TESTING SUMMARY - Concluded

ASHUR no.	Purpose	Tests performed	Results
Guidance and Navigation			
104015	To investigate the scanning telescope shaft drive problem	Perform failure analysis	The pin from the "tenths" drum of the counter drive mechanism was found wedged in a split gear on the drive shaft of the one speed resolver in the telescope gear box.
Docking Probe			
104503	To investigate the erroneous "barber pole" indication of lunar module capture when vehicles were separate	Check continuity from the plug that connected the docking probe to the display panel; X-ray the docking probe switch	Circuit checks were proper and switch normal in all aspects
Crew Station			
104012	To determine any performance degradation of the lunar module crewman optical alignment sight	Perform reticle light intensity test	Performance was normal
104031	To investigate the failure of the inflight exerciser	Perform failure analysis	A D-ring on one of the hand straps opened
104040	Evaluate difficulty in stowing and extending the Y-Y strut, window shade fit, and the loose arm rest	Function the Y-Y struts, check the window shade fit, and inspect/function the arm rest	A jamming condition could exist on the Y-Y strut, but by proper orientation, it could be freed. If the shades are not carefully installed, interference will result between the shade and the latch. Arm rest position slot and pin were out of tolerance.
104043	To investigate failure of lightweight headset	Perform failure analysis	Operation satisfactory
104049	To investigate failure of 16-mm camera and fuse	Perform failure analysis	Camera operated properly.
104068	To determine if crewman's microphone circuits are intermittent.	Perform functional test on crewman's personal communication equipment	Not complete
Reaction Control System			
104501	To investigate propellant isolation valve latching forces	Determine minimum opening and closing voltages of system 1 and 2 propellant isolation valves.	Voltage not degraded from acceptance test.

TABLE C-I.- POSTFLIGHT TESTING SUMMARY - Continued

C-4

ASHUR no.	Purpose	Tests performed	Results															
Communications and Instrumentation																		
104023 Rev. 1	To determine the cause of preflight calibration shift of carbon dioxide sensor	Perform calibration	Contamination found in sensor; but shift still present after unit cleaned.															
104038	To determine the cause of lack of communications between the crew and the swimmers	Perform a circuit check	The intercom circuit was verified from the audio center to the umbilical interface connector on the top deck. Both wires in the swimmers' umbilical were severed in two places.															
104039	To investigate communication difficulty between the command and service modules and the lunar module	Measure the Commander's audio center VOX release time	The VOX release time was in specification.															
Environmental Control System																		
104019	To evaluate contamination in the water system filters	Determine the quantity and composition of yellow contamination in the filters	Approximately 0.4 mg. of nickel compound was found.															
104036	To investigate the malfunction of cabin fan 1	Determine winding resistance and fan temperature in stalled condition	Inspection showed cabin fan stalled because of ingestion of a small piece of Velcro. The winding resistance was normal. Stalled power measured 70 watts; nominal running power is 22 watts. The temperatures on the housing and the motor case were:  <table style="margin-left: auto; margin-right: auto;"> <thead> <tr> <th><u>Time, min</u></th> <th><u>Housing</u></th> <th><u>Motor</u></th> </tr> </thead> <tbody> <tr> <td>0</td> <td>77° F</td> <td>77° F</td> </tr> <tr> <td>5</td> <td>125° F</td> <td>141° F</td> </tr> <tr> <td>20</td> <td>193° F</td> <td>210° F</td> </tr> <tr> <td>50</td> <td>213° F</td> <td>233° F</td> </tr> </tbody> </table>	<u>Time, min</u>	<u>Housing</u>	<u>Motor</u>	0	77° F	77° F	5	125° F	141° F	20	193° F	210° F	50	213° F	233° F
<u>Time, min</u>	<u>Housing</u>	<u>Motor</u>																
0	77° F	77° F																
5	125° F	141° F																
20	193° F	210° F																
50	213° F	233° F																
104037	To determine the cause of slow oxygen surge tank pressurization	Perform leak test and check flow rates at incremental valve positions	All flow rates were satisfactory and no measurable leakage. Examination showed the panel marking 30 deg off from the actual full-open position.															
104059	To investigate the reported difficulty in actuating the suit circuit return check valve	Measure force required to open and close the valve	Force to open valves was 23 lb; closing force was 21 lb, which is in specification															
Batteries																		
104502 104016	To investigate the cause of abnormal charging of battery B inflight	Perform battery charger voltage/current calibration and measure circuit impedance; charge batteries using the flight charger	All measurements were proper; battery charging was acceptable.															

APPENDIX D - DATA AVAILABILITY

Table D-I is a summary of the data made available for system performance analyses and anomaly investigations. Although the table reflects only data processed from Network magnetic tapes, Network data tabulations and computer words were available during the mission with approximately a 4-hour delay. For additional information regarding data availability, the status listing in the Central Metric Data File, building 12, MSC, should be consulted.

TABLE D-1.- COMMAND AND SERVICE MODULE DATA AVAILABILITY

Time, hr:min		Rev.	Range station	Bandpass tabs or plots	Bilevels	Computer word tabs	Special programs	O'graphs or Brush recorder	Comments
From	To								
-00:02	+00:09			X					ALDS data
-00:01	+00:09	1	CIF	X	X		X	X	
+00:00	04:06			X		X			MSFN data
00:01	00:07	2	MILA			X		X	Dump, high bit rate
00:02	00:15	1	BDA		X			X	
01:53	02:52	2	TEX	X		X	X	X	Dump, low bit rate
02:48	02:56	2	HAW	X	X		X	X	
02:56	03:03	2	RED	X	X	X	X	X	
02:56	02:58	2	TEX	X	X	X			Dump, high bit rate
03:00	03:07	2	GDS	X	X			X	
03:00	03:10	2	GYM		X	X		X	
03:01	03:02	3	BDA	X					Dump, high bit rate
03:03	03:14	2	TEX	X	X		X	X	
03:06	03:16	3	MILA		X			X	
03:10	03:19	3	BDA		X			X	
03:21	03:49	4	ANG	X		X			Dump, low bit rate
03:54	04:08	4	CRO		X			X	
04:06	04:23	5	GYM	X		X	X		Dump, low bit rate
04:06	07:58	5	RED	X		X			Dump, low bit rate
04:19	10:48			X		X			MSFN data
04:31	04:42	3	GDS		X			X	
04:39	04:51	4	MILA		X			X	
04:58	05:09	4	ACN		X			X	
05:55	06:05	4	HAW		X		X	X	
07:50	09:05	6	HAW	X		X			Dump, low bit rate
09:18	10:38	7	HAW	X					Dump, low bit rate
11:00	18:00	12	MER	X					Dump, low bit rate
12:13	16:04			X		X			MSFN data
17:17	12:55	10	ACN	X					Dump, low bit rate
15:32	17:36	12	CYI	X					Dump, low bit rate
16:06	20:13			X		X			MSFN data
18:01	18:26	18	MILA	X					Dump, low bit rate
18:39	19:03	13	CYI	X					Dump, low bit rate
19:49	19:53	13	CRO					X	
19:55	20:02	13	HSK					X	
20:34	24:02			X		X			MSFN data
21:19	21:28	14	CRO		X			X	
21:29	21:36	14	HSK		X			X	
22:02	22:09	14	TEX		X			X	
22:03	22:14	15	MILA	X	X	X	X	X	
22:04	22:17	15	BDA	X	X	X		X	
22:10	22:14	15	ANG		X		X	X	
22:11	22:20	15	VAN		X		X	X	
22:27	22:54	15	CRO	X		X			Dump, low bit rate
23:09	23:36	15	TEX	X		X			Dump, low bit rate
23:12	27:53			X		X			MSFN data
23:34	23:39	15	GYM		X			X	
23:37	23:49	16	MILA		X			X	
24:09	25:05	16	GYM	X		X			Dump, low bit rate
25:06	25:14	16	GDS		X			X	
25:10	25:18	16	TEX		X			X	
25:13	25:24	17	MILA	X	X	X	X	X	
25:18	25:25	17	BDA	X	X	X		X	
25:22	25:32	17	VAN				X		
25:36	26:35	17	TEX	X		X			Dump, low bit rate
26:32	26:41	17	HAW		X			X	
26:39	26:48	17	RED		X			X	
26:42	26:53	17	GYM		X			X	
26:51	26:58	18	MILA		X			X	
28:10	31:45			X		X			MSFN data

TABLE D-I.- COMMAND AND SERVICE MODULE DATA AVAILABILITY - Continued

Time, hr:min		Rev.	Range station	Bandpass tabs or plots	Bilevels	Computer word tabs	Special programs	O'graphs or Brush recorder	Comments
From	To								
28:18	28:28	18	GDS	X	X	X		X	
28:24	28:31	18	TEX		X		X	X	
32:04	34:51			X		X			MSFN data
36:13	39:41			X		X			MSFN data
40:52	43:37			X		X			MSFN data
44:11	44:24	28	HSK		X			X	
44:20	44:36	28	MER		X			X	
44:32	47:38			X		X			MSFN data
45:34	45:49	29	HSK				X		
45:58	46:14	29	MER				X		
46:22	46:31	29	TEX				X		
47:29	49:20			X		X			MSFN data
47:58	48:09	30	TEX		X			X	
48:01	48:12	31	MILA		X			X	
48:07	48:14	31	BDA		X			X	
48:09	48:20	31	VAN		X			X	
48:15	48:28	31	CYI		X			X	
48:52	49:04	31	CRO		X			X	
49:00	49:11	31	HSK		X			X	
49:02	49:10	31	HTV		X		X	X	
49:20	52:18			X		X			MSFN data
49:25	49:37	31	RED		X			X	
49:31	49:40	31	GDS		X			X	
49:40	49:47	32	MILA		X			X	
49:44	49:50	32	BDA		X			X	
49:47	49:55	32	VAN		X			X	
49:51	50:04	32	CYI		X			X	
52:34	56:04			X		X			MSFN data
52:42	52:47	33	RED		X			X	
52:44	52:52	33	GDS		X			X	
52:52	53:00	34	MILA		X			X	
52:55	53:10	34	ANG		X			X	
53:55	54:07	34	GWM		X			X	
54:05	54:12	34	TEX	X		X			Dump, low bit rate
54:10	54:19	34	HAW		X			X	
54:17	54:20	34	RED		X			X	
54:22	54:29	34	GYM		X	X		X	
54:23	54:36	34	TEX	X	X		X	X	
56:06	59:06			X		X			MSFN data
56:54	63:50			X		X			MSFN data
64:19	68:15			X		X			MSFN data
68:20	72:18			X		X			MSFN data
71:46	71:54	45	RED		X				
72:47	76:01			X		X			MSFN data
73:01	73:19	47	MILA	X		X			Dump, low bit rate
73:19	73:29	46	RED		X			X	
73:22	73:34	46	GYM		X			X	
73:29	73:40	47	MILA		X			X	
73:33	73:43	47	BDA		X			X	
73:36	73:49	47	VAN		X			X	
73:44	73:55	47	CYI		X			X	
73:50	74:22	47	CRO	X		X			Dump, low bit rate
75:19	76:18	48	MILA	X		X			Dump, low bit rate
76:31	79:40			X		X			MSFN data
79:42	82:46			X		X			MSFN data
84:14	87:33			X		X			MSFN data
85:00	85:53	54	MER	X					Dump, low bit rate
85:34	85:44	54	GWM	X					
85:51	86:01	54	MER	X					
88:06	92:15			X		X			MSFN data

TABLE D-I.- COMMAND AND SERVICE MODULE DATA AVAILABILITY - Continued

Time, hr:min		Rev.	Range station	Bandpass tabs or plots	Bilevels	Computer word tabs	Special programs	O'graphs or Brush recorder	Comments
From	To								
91:23	92:37	59	CYI	X		X			Dump, low bit rate
92:33	92:45	59	ANG		X		X	X	
92:36	95:56			X		X			MSFN data
92:40	92:50	59	VAN		X		X	X	
92:59	94:06	60	VAN	X		X			Dump, low bit rate
93:41	93:53	59	MER		X		X	X	
94:29	95:31	60	TEX	X		X	X		Dump, low bit rate
94:56	95:04	60	CRO					X	
95:15	95:26	60	MER		X			X	
95:28	95:37	60	RED		X			X	
95:38	95:51	61	MILA		X			X	
95:43	100:21			X		X			MSFN data
95:48	95:58	61	VAN		X			X	
95:56	97:08	61	TEX	X		X	X		Dump, low bit rate
97:00	97:12	61	RED		X			X	
97:22	97:32	62	VAN		X			X	
97:28	97:39	62	CYI		X			X	
97:33	98:30	62	GDS	X		X	X		Dump, low bit rate
97:35	101:52			X		X			MSFN data
98:04	98:14	62	CRO		X				
98:28	98:40	62	HAW		X			X	
98:35	98:45	62	RED		X			X	
98:46	98:59	63	MILA		X			X	
98:50	99:00	63	BDA		X		X	X	
98:54	99:05	63	VAN		X		X	X	
99:02	100:05	63	GDS	X		X	X		Dump, low bit rate
99:15	103:31			X		X			MSFN data
100:35	101:25	64	GWM	X		X			Dump, low bit rate
101:18	101:25	64	GWM				X		
101:22	101:35	64	GWM		X	X		X	
101:25	106:29			X		X			MSFN data
101:32	103:35		RED	X		X	X		Dump, low bit rate
108:39	108:45	69	ACN	X					
108:43	110:01	75	TEX	X		X			Dump, low bit rate
109:17	109:27	69	GWM	X					
109:33	109:44	69	MER	X					
110:08	110:19	70	ACN	X				X	
110:49	111:02	70	GWM	X					
111:07	111:18	70	MER	X					
112:26	112:33	71	GWM	X					
112:41	112:52	71	MER	X					
112:43	115:57			X		X			MSFN data
113:20	113:31	72	CYI	X					
113:27	113:34	72	MAD	X					
114:16	114:23	72	MER	X					
114:42	114:55	73	ANG	X					
114:49	114:59	73	VAN	X					
114:57	115:07	73	MAD	X					
115:32	115:41	73	CRO	X					
115:40	115:47	73	HSK	X					
115:57	119:31			X		X			MSFN data
116:16	116:24	74	MILA	X					
116:21	116:34	74	VAN	X					
116:28	116:38	74	CYI	X					
117:04	117:14	74	CRO	X					
117:13	117:22	74	HSK	X					
117:23	117:36	74	MER	X					
117:52	118:01	75	BDA	X					
117:55	118:07	75	VAN	X	X				
118:02	118:14	75	CYI	X					

TABLE D-I.- COMMAND AND SERVICE MODULE DATA AVAILABILITY - Concluded

Time, hr:min		Rev.	Range station	Bandpass tabs or plots	Bilevels	Computer word tabs	Special programs	O'graphs or Brush recorder	Comments
From	To								
118:38	118:49	75	CRO	X					
118:48	118:55	75	HSK	X					
119:31	124:31			X		X			MSFN data
121:22	122:13	77	TEX	X		X			Dump, low bit rate
123:21	123:33	78	CRO	X	X	X	X	X	
124:58	127:10			X		X			MSFN data
125:50	130:09			X		X			MSFN data
132:16	135:34			X		X			MSFN data
136:22	140:08			X		X			MSFN data
139:59	144:01			X		X			MSFN data
143:59	148:03			X		X			MSFN data
148:13	150:26			X		X			MSFN data
150:44	152:04	96	HAW	X		X			Dump, low bit rate
152:01	152:12	96	HAW		X				
152:03	155:37			X		X			MSFN data
152:16	153:10	97	HAW	X	X				Dump, low bit rate
154:17	160:01			X		X			MSFN data
160:35	164:21			X		X			MSFN data
164:21	168:20			X		X			MSFN data
166:54	167:41	106	GYM	X		X			Dump, low bit rate
168:57	171:29			X		X			MSFN data
169:35	169:46	107	TEX	X	X	X	X	X	
172:06	176:00			X		X			MSFN data
176:12	183:56			X		X			MSFN data
184:00	187:53			X		X			MSFN data
187:40	191:32			X		X			MSFN data
192:09	193:56			X		X			MSFN data
193:07	193:15	122	CRO				X		
193:33	193:45	122	HAW				X		
193:44	195:51			X		X			MSFN data
195:20	195:35	123	GDS		X	X		X	
195:25	195:35	123	TEX		X	X		X	
195:29	195:38	124	MILA		X	X		X	
196:34	200:08			X		X			MSFN data
198:52	204:03			X		X			MSFN data
202:15	208:07			X		X			MSFN data
208:08	212:07			X		X			MSFN data
211:53	214:27			X		X			MSFN data
214:40	216:32			X		X			MSFN data
216:32	223:19			X		X			MSFN data
223:19	229:57			X		X			MSFN data
230:42	234:04			X		X			MSFN data
233:35	237:40			X		X			MSFN data
237:43	240:37			X		X			MSFN data
239:57	240:09	151	CRO		X		X		
240:22	240:34	151	HAW	X	X	X	X	X	
240:31	241:01			X	X	X	X	X	Onboard recorder

TABLE D-II.- LUNAR MODULE DATA AVAILABILITY

Time, hr:min		Rev.	Range station	Bandpass tabs or plots	Bilevels	Computer words	Special programs	O'graphs or Brush recorder	DFI strip-charts
From	To								
-00:01	+00:03	1	MILA				X		X
+44:03	44:12	28	CRO	X	X			X	X
44:11	44:22	28	HSK	X	X			X	
44:23	44:33	28	MER	X	X				X
44:52	45:00	29	ANG	X	X	X	X		
44:58	45:05	29	VAN	X	X			X	X
45:04	45:11	29	CYI	X	X			X	
46:00	46:11	29	MER	X	X				
46:24	46:29	29	TEX	X	X				
46:26	46:34	30	MILA		X				
46:30	46:37	30	BDA		X				
46:41	46:48	30	CYI		X				
47:15	47:27	30	CRO		X				
47:23	47:35	30	HSK		X	X		X	
47:37	47:47	30	MER		X	X		X	
47:57	48:03	30	GYM	X	X	X	X	X	
47:59	48:06	30	TEX	?	?	?	?	?	?
48:03	48:10	31	MILA		X	X	X	X	
48:06	48:14	31	BDA	X	X	X	X	X	X
48:11	48:18	31	VAN	X	X	X	X	X	X
48:17	48:25	31	CYI	X	X	X	X	X	X
48:52	49:04	31	CRO		X	X		X	
49:00	49:11	31	HSK		X	X		X	
49:09	49:18	31	HTV	X	X	X		X	
49:17	49:20	31	MER		X	X		X	
49:27	49:35	31	RED	X	X	X	X	X	
49:32	49:40	31	GYM	X	X	X	X	X	
49:36	49:43	31	TEX	X	X	X	X	X	X
49:40	49:46	32	MILA	X	X	X	X	X	X
49:43	49:50	32	BDA	X	X	X	X	X	X
49:47	49:55	32	VAN	X	X	X	X	X	
49:53	50:02	32	CYI		X	X	X	X	
50:30	50:41	32	CRO	X	X	X		X	X
50:37	50:46	32	HSK	X	X	X	X	X	
50:46	50:55	32	HTV	X	X	X	X	X	X
50:58	51:05	32	HAW	X	X	X		X	
51:04	51:11	32	RED	X	X			X	
51:09	51:16	32	GYM	X	X	X		X	
51:12	51:19	32	TEX	X	X			X	
70:23	70:25	44	TEX		X				
72:00	72:08	46	BDA						X
72:05	72:13	46	VAN	X	X			X	X
72:11	72:19	46	CYI	X	X			X	
72:48	72:54	46	CRO	X	X			X	
75:13	75:19	48	VAN		X				X
75:25	75:32	48	ACN		X				X
75:41	75:46	48	TAN		X				X
75:55	76:03	48	CRO						X
76:35	76:43	48	TEX						X
76:39	76:47	49	MILA						X
76:43	76:48	49	BDA						X
88:43	88:48	56	GWM	X	X				
89:00	89:06	56	MER	X	X	X			
89:39	89:46	57	CYI	X	X	X			
89:44	89:49	57	MAD		X	X			
90:35	90:40	57	MER	X	X	X		X	
91:02	91:09	58	ANG		X	X			
91:09	91:13	58	VAN	X	X	X		X	
91:13	91:20	58	CYI		X	X	X	X	
91:16	91:23	58	MAD	X	X	X	X	X	

TABLE D-II.- LUNAR MODULE DATA AVAILABILITY - Continued

Time, hr:min		Rev.	Range station	Bandpass tabs or plots	Bilevels	Computer words	Special programs	O'graphs or Brush recorder	DFI strip-charts
From	To								
91:50	91:55	58	CRO		X	X		X	
91:57	92:04	58	HSK	X	X	X			
92:09	92:15	58	MER		X	X			
92:35	92:43	59	ANG	X	X	X	X	X	
92:41	92:48	59	VAN	X	X	X	X	X	
92:47	92:54	59	CYI	X	X	X	X	X	
93:30	93:38	59	HSK		X	X	X	X	
93:42	93:50	59	MER	X	X	X	X	X	X
94:04	94:10	59	TEX		X	X	X	X	
94:06	94:14	60	MILA	X	X	X	X	X	
94:10	94:18	60	BDA		X	X	X	v	
94:14	94:22	60	VAN		X	X	X	X	
94:21	94:29	60	CYI		X	X	X	X	
94:23	94:30	60	MAD		X	X	X	X	
94:57	95:03	60	CRO		X	X	X	X	
95:04	95:12	60	HSK		X	X	X	X	
95:16	95:24	60	MER	X	X	X	X	X	
95:30	95:35	60	RED	X	X	X	X	X	
95:34	95:41	60	GYM	X	X	X	X	X	
95:36	95:44	60	TEX	X	X	X	X	X	X
95:40	95:48	61	MILA	X	X	X	X	X	y
95:44	95:52	61	BDA	X	X	X	X	X	
95:48	95:56	61	VAN	X	X	X	X	X	
95:55	96:03	61	CYI	X	X	X	X	X	
96:15	96:23	61	TAN	X	X	X	X	X	
96:31	96:38	61	CRO	X	X	X	X	X	
96:38	96:45	61	HSK		X	X	X	X	
96:47	96:52	61	HTV		X	X	X	X	
97:03	97:10	61	RED	X	X	X	X	X	X
97:08	97:15	61	GYM		X	X	X	X	X
97:11	97:18	61	TEX		X	X	X	X	
97:15	97:22	62	MILA	X	X	X	X	X	
97:17	97:25	62	BDA		X	X	X	X	
97:22	97:30	62	VAN		X	X	X	X	
97:30	97:35	62	CYI	X	X	X	X	X	
97:49	97:56	62	TAN		X	X	X	X	
98:19	98:27	62	HTV		X	X	X	X	
98:30	98:38	62	HAW		X	X	X	X	
98:37	98:44	62	RED	X	X	X	X	X	
98:41	98:49	62	GYM		X	X	X	X	
98:45	98:52	62	TEX	X	X	X	X	X	X
98:48	98:56	63	MILA	X	X	X	X	X	X
98:51	98:59	63	BDA	X	X	X	X	X	X
98:56	99:02	63	VAN	X	X	X	X	X	X
99:24	99:29	63	TAN	X	X	X	X	X	
99:39	99:46	63	CRO	X	X	X	X	X	
100:04	100:11	63	HAW	X	X	X	X	X	
100:12	100:17	63	RED	X	X	X	X	X	
100:15	100:23	63	GYM	X	X	X	X	X	
100:18	100:26	63	TEX	X	X	X	X	X	
100:22	100:30	64	MILA	X	X	X	X	X	
100:27	100:35	64	ANG	X	X	X	X	X	
100:42	100:48	64	ACN	X	X	X	X	X	X
101:13	101:18	64	CRO		X	X	X	X	X
101:24	101:32	64	GWM		X	X	X	X	X
101:39	101:45	64	HAW		X	X	X	X	X
101:49	101:57	64	GYM		X	X	X	X	X
101:52	102:00	64	TEX	X	X	X	X	X	X
101:57	102:04	65	MILA	X	X	X	X	X	X
102:00	102:17	65	ANG	X	X	X	X	X	X

TABLE D-II.- LUNAR MODULE DATA AVAILABILITY - Concluded

Time, hr:min		Rev.	Range station	Bandpass tabs or plots	Bilevels	Computer words	Special programs	O'graphs or Brush recorder	DFI strip-charts
From	To								
102:00	103:08	65	ACN	X	X			X	X
103:02	103:44	65	CRO		X			X	X
104:45	104:51	65	GYM	X	X			X	
104:48	104:55	65	TEX	X	X			X	
104:56	105:22	66	ANG	X	X			X	X
106:04	106:36	66	TAN	X				X	
106:34	107:48	66	TAN	X				X	
107:10	107:22	66	GWM	X	X			X	
107:34	107:48	66	RED	X				X	
107:42	108:05	67	ANG	X	X			X	X
108:05	108:47	67	ANG	X				X	
108:46	109:00	67	ANG	X				X	
110:10	110:18	67	GWM	X	X			X	
110:33	111:02	67	MER	X				X	
110:59	111:31	68	ANG	X				X	
111:28	112:15	68	ANG	X				X	
111:59	112:44	68	MAD	X				X	

APPENDIX E - SUPPLEMENTAL REPORTS

Supplemental reports will be issued to provide information that was not available at the time of publication of this report. The titles and publication date of these supplements have not yet been determined but will be published in an addendum within 30 days after publication of this report.

#### REFERENCES

1. Scientific and Technical Information Division, National Aeronautics and Space Administration, Washington, D.C.: "Ground Control and Monitoring of Rendezvous." Gemini Summary Conference, February 1-2, 1967, Manned Spacecraft Center, Houston, Texas. NASA-SP-138, February 1-2, 1967.
2. \_\_\_\_\_: "Onboard Operations for Rendezvous." Gemini Summary Conference, February 1-2, 1967, Manned Spacecraft Center, Houston, Texas. NASA-SP-138, February 1-2, 1967.
3. Manned Spacecraft Center, Houston, Texas: Analysis of Terminal Phase Rendezvous Lighting. MSC Internal Note CF-R-69-6, March 5, 1969.
4. \_\_\_\_\_ Apollo Mission D Spacecraft Operational Trajectory, Vol. I, Mission Profile. MSC Internal Note 68-FM-284, December 2, 1968.
5. \_\_\_\_\_ LM Rendezvous Procedures D Mission, Revision A. (no number) January 31, 1969.
6. Marshall Space Flight Center, Huntsville, Alabama: Saturn V Launch Vehicle Flight Evaluation Report AS-504 Apollo 9 Mission. MPR-SAT-FE-69-4, May 4, 1969.
7. Office of Manned Space Flight, National Aeronautics and Space Administration, Washington, D.C.: Mission Requirements, D-type Mission, (LM Evaluation and Combined Operations). SPD 8-R-005, January 21, 1969.

APOLLO SPACECRAFT FLIGHT HISTORY

(Continued from inside front cover)

<u>Mission</u>	<u>Spacecraft</u>	<u>Description</u>	<u>Launch date</u>	<u>Launch site</u>
Apollo 4	SC-017 LTA-10R	Supercircular entry at lunar return velocity	Nov. 9, 1967	Kennedy Space Center, Fla.
Apollo 5	LM-1	First lunar module flight	Jan. 22, 1968	Cape Kennedy, Fla.
Apollo 6	SC-020 LTA-2R	Verification of closed-loop emergency detection system	April 4, 1968	Kennedy Space Center, Fla.
Apollo 7	CSM 101	First manned flight; earth-orbital	Oct. 11, 1968	Cape Kennedy, Fla.
Apollo 8	CSM 103	First manned lunar orbital flight; first manned Saturn V launch	Dec. 21, 1968	Kennedy Space Center, Fla.
Apollo 9	CSM 104 LM-3	First manned lunar module flight; earth orbit rendezvous; EVA	Mar. 3, 1969	Kennedy Space Center, Fla.